NCHRP Web Document 65 (Project 24-11)

Geofoam Applications in the Design and Construction of Highway Embankments

Prepared for:

National Cooperative Highway Research Program

TRANSPORTATION RESEARCH BOARD
OF THE NATIONAL ACADEMIES

Submitted by:

Timothy D. Stark
David Arellano
Department of Civil and Environmental Engineering
University of Illinois at Urbana-Champaign
Urbana, Illinois

John S. Horvath
Scarsdale, New York

Dov Leshchinsky
ADAMA Engineering, Inc.
Newark, Delaware

July 2004

ACKNOWLEDGMENT

This work was sponsored by the American Association of State Highway and Transportation Officials (AASHTO), in cooperation with the Federal Highway Administration, and was conducted in the National Cooperative Highway Research Program (NCHRP), which is administered by the Transportation Research Board (TRB) of the National Academies.

THE NATIONAL ACADEMIES

Advisers to the Nation on Science, Engineering, and Medicine

The **National Academy of Sciences** is a private, nonprofit, self-perpetuating society of distinguished scholars engaged in scientific and engineering research, dedicated to the furtherance of science and technology and to their use for the general welfare. On the authority of the charter granted to it by the Congress in 1863, the Academy has a mandate that requires it to advise the federal government on scientific and technical matters. Dr. Bruce M. Alberts is president of the National Academy of Sciences.

The **National Academy of Engineering** was established in 1964, under the charter of the National Academy of Sciences, as a parallel organization of outstanding engineers. It is autonomous in its administration and in the selection of its members, sharing with the National Academy of Sciences the responsibility for advising the federal government. The National Academy of Engineering also sponsors engineering programs aimed at meeting national needs, encourages education and research, and recognizes the superior achievements of engineers. Dr. William A. Wulf is president of the National Academy of Engineering.

The **Institute of Medicine** was established in 1970 by the National Academy of Sciences to secure the services of eminent members of appropriate professions in the examination of policy matters pertaining to the health of the public. The Institute acts under the responsibility given to the National Academy of Sciences by its congressional charter to be an adviser to the federal government and, on its own initiative, to identify issues of medical care, research, and education. Dr. Harvey V. Fineberg is president of the Institute of Medicine.

The **National Research Council** was organized by the National Academy of Sciences in 1916 to associate the broad community of science and technology with the Academy's purposes of furthering knowledge and advising the federal government. Functioning in accordance with general policies determined by the Academy, the Council has become the principal operating agency of both the National Academy of Sciences and the National Academy of Engineering in providing services to the government, the public, and the scientific and engineering communities. The Council is administered jointly by both the Academies and the Institute of Medicine. Dr. Bruce M. Alberts and Dr. William A. Wulf are chair and vice chair, respectively, of the National Research Council.

The **Transportation Research Board** is a division of the National Research Council, which serves the National Academy of Sciences and the National Academy of Engineering. The Board's mission is to promote innovation and progress in transportation through research. In an objective and interdisciplinary setting, the Board facilitates the sharing of information on transportation practice and policy by researchers and practitioners; stimulates research and offers research management services that promote technical excellence; provides expert advice on transportation policy and programs; and disseminates research results broadly and encourages their implementation. The Board's varied activities annually engage more than 5,000 engineers, scientists, and other transportation researchers and practitioners from the public and private sectors and academia, all of whom contribute their expertise in the public interest. The program is supported by state transportation departments, federal agencies including the component administrations of the U.S. Department of Transportation, and other organizations and individuals interested in the development of transportation.
www.TRB.org

CONTENTS

CHAPTER 4 PAVEMENT SYSTEM DESIGN

CHAPTER 5 EXTERNAL (GLOBAL) STABILITY EVALUATION OF GEOFOAM EMBANKMENTS

CHAPTER 6 INTERNAL STABILITY EVALUATION OF GEOFOAM EMBANKMENTS

CHAPTER 7 DESIGN EXAMPLES

CHAPTER 8 GEOFOAM CONSTRUCTION PRACTICES

CHAPTER 9 GEOFOAM MQC/MQA

CHAPTER 10 TYPICAL DESIGN DETAILS FOR EPS-BLOCK EMBANKMENTS

Acknowledgments

The research herein was conducted under NCHRP Project 24-11 titled "Guidelines for Geofoam Applications in Embankment Projects." The research was conducted from 6 July 1999 to 31 August 2002. Dr. Timothy D. Stark and Mr. David Arellano, Professor and Graduate Research Assistant, Department of Civil and Environmental Engineering (CEE), University of Illinois at Urbana-Champaign (UIUC), Dr. John S. Horvath, Consulting Engineer and Professor, Department of Civil Engineering, Manhattan College, and Dr. Dov Leshchinsky, President of ADAMA Engineering, Inc. and Professor, University of Delaware, were the principal investigators for the project.

The project consisted of two phases. The objective of Phase I was to review, document, and synthesize the 25 years of worldwide experience of using EPS-block geofoam in lightweight fill applications and develop an interim design guideline and standard. The first phase consisted primarily of a literature review which formed the basis of Chapters 1, 2, 8, 9, 11, Appendices A, C, and D. Dr. Horvath was the lead investigator for Phase I of this project and the primary author of the interim project report. Mr. Arellano also had significant input to Phase I and the interim report. Phase I covered nine months and utilized 25 percent of the project budget as required by the NCHRP contract.

The objective of Phase II was to develop a comprehensive design methodology for geofoam in lightweight fill applications including the development of design charts to optimize both technical performance and cost and update the interim design guideline and standard developed in Phase I. The major results of Phase II are included in Chapters 2, 3, 4, 5, 6, 7, 10, 11, 12, 13, Appendices B, E and F. Dr. Stark was the lead investigator for Phase II and Mr. Arellano had significant input to Phase II. Phase II covered twenty-nine months and consumed the remaining 75 percent of the project budget.

The main text of the report was prepared at the UIUC but it was reviewed by all the principal investigators. Other research assistants in the CEE at the UIUC contributing to the project and report include Erik J. Newman, Andy Garza, Perry L. Stover, and Timothy Frank. These research assistants assisted with the external and internal stability analyses (Newman and Stover), laboratory testing (Newman and Frank), and figure and report preparation (Newman, Garza, and Frank). The typing and editing was performed by Martha Thompson and is also gratefully acknowledged.

The review panel for N.C.H.R.P. Project 24-11 consisted of Mr. David V. Jenkins (Chair, Washington State D.O.T.), Dr. Michael Mathioudakis, P.E. (AASHTO Monitor, New York State D.O.T.), Dr. Richard Berg (Member, Frost Associates), Dr. Manoj B. Chopra, P.E. (Member, University of Central Florida), Mr. Colin A. Franco, P.E. (Member, Rhode Island D.O.T.), Ms. Susan Herrenbruck (Member, Foamed Polystyrene Alliance), Dr. Thomas W. Kennedy, P.E. (Member, University of Texas- Austin), Mr. Thomas E. Polacek, P.E. (Member, Pennsylvania D.O.T.), Mr. James E. Shannon (Member, Hunstman Corporation), Mr. Riyad M. Wahab, P.E. (Member, Illinois D.O.T.), Mr. Jerry A. DiMaggio, P.E. (FHWA Liaison, Federal Highway Administration), Mr. Albert DiMillio (FHWA Liaison, Federal Highway Administration), Mr. Jay Jayaprakash (TRB Liaison, Transportation Research Board), Mr. Timothy G. Hess, P.E. (N.C.H.R.P. Staff, Transportation Research Board), and Mr. Keaven M. Freeman, (N.C.H.R.P. Staff, Transportation Research Board).

The assistance of several state departments of transportation, the EPS Molders Association, as well as others in the private sector in providing cost and other relevant information is noted with gratitude. The technical assistance of Mr. Paul E. Arch of NOVA Chemicals, Inc. for providing information relative to EPS manufacturing and Mr. Donald D. Oglesby of Hanson Professional Services Inc. for providing information relative to design was particularly useful and is appreciated. Wisconsin EPS, Inc. of Fond du Lac, WI provided EPS block samples and Seaman Corporation of Cornelius, NC provided geomembrane samples for the

interface shear strength testing and are gratefully acknowledged. Finally, all of the individuals who responded to the geofoam usage survey conducted for this project are also gratefully acknowledged.

Abstract

This report is a comprehensive document that provides both state-of-the art knowledge and state-of practice design guidance for the use of geofoam in roadway embankments and bridge approaches. This document presents a design guideline or procedure as well as an appropriate material and construction standard, both in AASHTO format. It is anticipated that this document will encourage greater and more consistent use of EPS-block geofoam in roadway embankments. The ultimate benefit of this is an optimization of both the technical performance as well as cost of EPS-block geofoam embankments. It is anticipated that designers will be more willing to consider EPS-block geofoam as an alternative for construction of embankments over soft ground using the design methodology and construction standard presented herein. The research has confirmed that EPS-block geofoam can provide a safe and economical solution to problems with construction of roadway embankments on soft soils. This report is designed to produce a single source of information on the present knowledge of geofoam usage in roadway embankments.

GUIDELINES FOR GEOFOAM APPLICATIONS IN EMBANKMENT PROECTS

SUMMARY

Construction of roadway embankments on soft foundation soils, such as peats or soft clays, has long been problematic. The two main approaches for coping with the problem is to improve the engineering properties, e.g., shear strength and compressibility, of the foundation soils or reduce the weight of the embankment and thus the load applied to the problematic foundation soils. Because of the uncertainty involved in using ground improvement techniques, DOTs and other owners have been increasingly using lightweight fills to reduce the weight of the embankment. The level of uncertainty involved in ground improvement techniques, e.g., quantifying the increase in foundation shear resistance, is high relative to the use of lightweight fill because strengthening of the foundation can be difficult to control and the soil strata may not be known accurately. In addition, the improvement in the engineering properties of the foundation soils must be verified prior to embankment construction to ensure satisfactory performance. Conversely, the properties and geometry of man-made lightweight fills, e.g., geofoam, are well defined which provides more confidence and less uncertainty in its use than foundation improvement techniques. The reduced uncertainty is mainly caused by the fill being so light that it does not stress the foundation and thus the need to accurately know the soil strata and engineering properties is significantly reduced or eliminated.

There are a large number of potential lightweight fill materials available. However, EPS-block geofoam usage has been increasing for a number of reasons including it exhibits the lowest density/unit weight and thus the smallest impact on the soft foundation soils, exhibits consistent material properties because it is manufactured, is easy and fast to construct even in adverse weather conditions, results in decreased maintenance costs as a result of less settlement from the

low density of EPS-block geofoam, alleviates the need to acquire additional right-of-way to construct flatter slopes because of the low density of EPS-block and/or the use of a vertical embankment, applies less lateral stress to bridge approach abutments, can be used over existing utilities which reduces or eliminates utility relocation, and exhibits excellent durability. EPS-block geofoam has been used as lightweight fill worldwide since at least 1972, which corresponds to a road project in Norway. The use of EPS-block geofoam in the U.S.A. for the lightweight fill application dates back to at least the 1980s although at least two conceptual U.S. patents for the use of plastic foams as lightweight fill were issued in the U.S.A. in the early 1970s. Since the Norwegian roadway project in 1972, the Japanese constructed their first lightweight fill project in 1985. Approximately ten years later, geofoam usage in Japan comprises approximately 50 percent of the worldwide usage. In the U.S. approximately 10 percent of annual sales of block molded EPS is now used in the geofoam market versus none approximately ten years ago.

Objectives of the Report

Despite the continuing worldwide use of EPS-block geofoam, a specific design guideline or design procedure for its use as lightweight fill in roadway embankments was unavailable. Therefore, there was a need in the U.S.A. since the mid 1990s to develop a formal and detailed design document for use of EPS-block geofoam in routine practice. The purpose of this report is to fill this void with a comprehensive document that provides both state-of-the-art knowledge and state-of-practice design guidance for engineers. This document presents a design guideline as well as an appropriate material and construction standard, both in AASHTO format. It is anticipated that this document will encourage greater and more consistent use of EPS-block geofoam in roadway embankments. The ultimate benefit of this is an optimization of both the technical performance as well as cost of EPS-block geofoam embankments. It is anticipated that designers will be more willing to consider EPS-block geofoam as an alternative for construction of embankments over soft ground using the design methodology and material and construction standard presented herein.

Organization of Report

The report is divided into two parts. The first part of the report, which consists of thirteen chapters, is concerned with the design of EPS-block geofoam roadway embankments. Chapter 1 provides an overview and history of the use of EPS-block geofoam for roadway embankments and discusses appropriate terminology. Chapter 2 presents a summary of the engineering properties that are necessary to implement the proposed design methodology, such as, modulus, elastic limit stress, Poisson's ratio, and interface shear resistance. Chapter 3 provides an overview of the design methodology developed herein for embankments on soft soil incorporating EPS-block geofoam. The design methodology consists of the following three main parts: pavement system design (Chapter 4), external stability evaluation (Chapter 5), and internal stability evaluation (Chapter 6). All three of these considerations are interconnected and must be considered for each geofoam embankment. Chapter 3 also includes the background for the "Provisional Design Guideline" that is included in Appendix B. Chapter 4 presents the pavement system design module that utilizes both flexible or rigid pavement systems. Chapter 5 presents the external stability considerations, e.g., bearing capacity, settlement, static and seismic slope stability, hydrostatic uplift, translation due to water and wind, that should be evaluated when utilizing an EPS-block geofoam embankment. Finally, Chapter 6 presents the internal stability issues, e.g., static and seismic sliding between the EPS blocks, load bearing capacity of the blocks, sliding due to water and wind, and EPS durability that should be considered. Chapter 7 presents design examples that demonstrate the design methodology outlined in Chapter 3 and detailed in Chapters 4, 5, and 6 for a traditional trapezoidal embankment that can be used by design engineers to facilitate design of their projects. The key feature in Chapters 4, 5, and 6 is the inclusion of design charts that can be used to obtain an optimal design for a geofoam embankment on soft soil. Chapters 8, 9, and 10 discuss geofoam construction practices, MQC/MQA testing, and design details, respectively. These chapters provide the background for understanding the "Provisional Standard" included in Appendix C. Chapter 11 provides a

summary of several case histories that have successfully incorporated EPS-block geofoam into roadway embankments and slope stabilization applications. Chapter 12 provides cost information to allow a cost estimate for the geofoam embankment to be prepared during the design phase so that an optimal geofoam design can be selected. The designer can then use this optimal geofoam design to perform a cost comparison with other soft ground construction techniques. Finally, Chapter 13 presents areas of future research for EPS-block geofoam for roadway embankments.

The second part of the report is composed of six appendices. Appendix A describes a geofoam usage survey that was developed and distributed during this study and also presents the responses to the survey. Appendix B presents the provisional design guideline for EPS-block geofoam embankments that is outlined in Chapter 3. Appendix C presents the provisional standard for the use of EPS-block geofoam, which should facilitate DOTs in specifying, and thus contracting for the use of geofoam in roadway embankments. Appendix D presents an extensive bibliography of all references encountered during this study that relate to EPS-block geofoam. Finally, Appendix E presents a glossary of the terms used in the report and Appendix F provides conversion factors that can be used to convert between Système International d'Unités (SI) and inch-pound (I-P) units.

The key products of the research are the provisional design guideline in Appendix B and the provisional material and construction standard in Appendix C. Designers that desire a quick overview of the design process and/or a recommended material and construction standard can utilize Appendix B and C.

Both the Système International d'Unités (SI) and inch-pound (I-P) units have been used in this report. SI units are shown first and I-P units are shown in parentheses within text. Numerous figures are included for use in design. Therefore, only SI units are provided in some of the figures to avoid duplication of figures. Additionally, in some cases figures have been reproduced that use either all SI or all I-P units. These figures have not been revised to show both sets of units. However, Appendix F presents factors that can be used to convert between SI and I-

P units. The one exception to the dual SI and I-P unit usage involves the quantities of density and unit weight. Density is the mass per unit volume and has units of kg/m^3 (slugs/ft^3) and unit weight is the weight per unit volume and has units of kN/m^3 (lbf/ft^3). Although density is the preferred quantity in SI, unit weight is still the common quantity in geotechnical engineering practice. Therefore, the quantity of unit weight will be used herein except when referring to EPS-block geofoam. The geofoam manufacturing industry typically uses the quantity of density with the SI units of kg/m^3 but with the I-P quantity of unit weight with units of lbf/ft^3. Therefore, the same dual unit system of density in SI and unit weight in I-P units will be used when referring to EPS-block geofoam.

Concluding Comments

The research has amply confirmed that EPS-block geofoam can provide a safe and economical solution to problems with construction of roadway embankments on soft soils. This report is designed to produce a single source of information on the present state-of-the-art knowledge of geofoam usage in roadway embankments. It is important to recognize, that although much progress has been made in the use of geofoam in roadway embankments since the early 1970s, our understanding of all aspects of the behavior and cost/benefits, especially the intangible benefits, of EPS-block geofoam for embankment construction is not complete. For example, there are unanswered questions about the creep characteristics of EPS-block geofoam, seasoning times required prior to shipment, and appropriate testing to determine the small-strain stiffness of EPS blocks for use in the design methodology presented herein. It is anticipated that the information documented herein will serve as a guide to initiate technical advances that will lead to even more efficient designs and increased usage of geofoam in roadway embankments.

CHAPTER **1**

INTRODUCTION

Contents

GENERAL

Although there are many lightweight fill materials than can be and have been used for embankments, geofoam has experienced an increase in usage over the last decade. It is estimated by the geofoam industry that approximately 10 percent of annual U. S. sales of block-molded EPS is for the geofoam market, i.e., civil engineering applications, while ten years ago the U. S. geofoam market was non-existent. Another indication of increased geofoam usage is that geofoam usage in Japan started in 1985 and by 1995 the Japanese usage accounted for one-half of all geofoam usage worldwide. The Japanese usage suggests that provided proper technical support of EPS geofoam is available, the potential for significant growth is high. The main

objective of this report is to present the necessary technical information to facilitate usage of EPS-block geofoam in roadway embankments.

Geofoam is any material or product that has a closed-cell structure that was created either in a fixed plant or in situ by an expansion process (*1*). Although most geofoam materials are polymeric (plastic) in composition, other materials such as Portland cement concrete (PCC) or glass have been and are used. Geofoam is now recognized as a type or category of geosynthetic in the same way as geogrids, geomembranes and geotextiles. Despite the fact that there are numerous geofoam materials and products, decades of worldwide use have demonstrated that block-molded expanded polystyrene (EPS) is the geofoam material of choice in lightweight fill applications. Therefore, this report focuses on EPS-block geofoam.

Benefits of utilizing an EPS-block geofoam embankment include: (1) ease and speed of construction, (2) placement in adverse weather conditions, (3) possible elimination of the need for preloading, surcharging, and staged construction, (4) decreased maintenance costs as a result of less settlement from the low density of EPS-block geofoam, (5) alleviation of the need to acquire additional right-of-way to construct flatter slopes because of the low density of EPS-block and/or the use of a vertical embankment because of the block shape of EPS, (6) reduction of lateral stress on bridge approach abutments, (7) use over existing utilities which reduces or eliminates utility relocation, and (8) excellent durability. In a soil removal and replacement situation without the use of surcharging, the use of EPS-block geofoam may result in cost savings compared to other types of lightweight fill materials and conventional fill materials because the density of geofoam is $1/10^{th}$ to $1/30^{th}$ of the density of foamed concrete, $1/55^{th}$ to $1/145^{th}$ of the in-place density of boiler slag, and $1/100^{th}$ of the density of conventional granular fill material. Thus, the lower density of EPS-block geofoam may alleviate the costs of soft soil removal (which include the attendant disposal problems and costs) and the possible need for an excavation support system, excavation widening, and temporary dewatering.

EPS-block geofoam is unique as a lightweight fill material, with a density that is only about 1 percent of the density of traditional earth fill materials yet sufficiently strong to support motor vehicles, trains, airplanes, lightly loaded buildings, and the abutments of small bridges. The extraordinarily low density of EPS-block geofoam results in significantly reduced gravity stresses on underlying soil foundations as well as reduced inertial forces during seismic shaking. In addition, geofoam is extremely easy and quick to place in all types of weather. On many projects, the overall immediate and long-term benefits and lower construction cost of using EPS-block geofoam more than compensate for the fact that its material unit cost is greater than that of traditional earth fill materials.

This chapter provides an overview of soft ground treatment methods and lightweight fills, which includes a history of geofoam development and a summary of the current state of practice of designing with geofoam.

SOFT GROUND TREATMENT METHODS

If either the allowable bearing capacity of the underlying soft foundation soil is too low and/or the estimated settlement of the proposed embankment is too large, the geotechnical engineer traditionally must either select a suitable ground treatment or improvement procedure or recommend use of an elevated structure supported on deep foundations if an alternative route is not possible. Roadway construction techniques over soft ground have a long history. The earliest known roads built over organic soils are found in England. These roads consist of planks and are estimated to be between 4000 and 4800 years old (*2,3*). Roads supported on wood piles have been discovered in roads constructed over the entire Roman territory during the period of 300 BC to AD 400 (*3*).

A summary of various soft ground treatment alternatives that have been used for highway embankments in the United States can be found in (*4*). These alternatives are also summarized in

Table 1.1 (terminology has been updated in some cases). As indicated in Table 1.1, these treatment alternatives can be categorized into the following treatment approaches (*4,5*):

- Reducing the applied load,
- Replacing the problematic materials with more competent materials,
- Increasing the shear strength and reducing compressibility of the problematic materials,
- Transferring the loads to more competent layers via a deep foundation system,
- Reinforcing the soft soil and/or the embankment, and
- Providing lateral stability.

The deep foundation alternative is typically the most expensive alternative so most efforts to date have focused on the other alternatives. The strategies for designing with the various soft ground treatment methods, except for the use of deep foundations, can be divided into two methods, each representing a different philosophical approach. The first method is to utilize conventional soil for the embankment and to increase the shear strength and compressibility of the soft foundation soil. The second method is to utilize a lightweight fill embankment to reduce the load applied by the embankment to the soft ground to prevent overstressing of the soft ground, which could lead to a bearing capacity failure or to unacceptable settlement. The basis for each method is to satisfy the following equations for the ultimate limit state (ULS) and serviceability limit state (SLS) respectively:

ULS: resistance of embankment to failure > embankment loads producing failure (1.1a)

SLS: estimated deformation of embankment ≤ maximum acceptable deformation (1.1b)

The first soft ground treatment design method is based on increasing the resistance and stiffness of the overall embankment system (embankment material and natural foundation soil) to resist the applied loads and limit deformations to an acceptable level as required by Equations

(1.1a) and (1.1b). This is traditionally accomplished by employing a ground improvement technique that collectively increases the shear strength and reduces the compressibility of the overall system but primarily the soft foundation soil. As noted in Table 1.1, improvement techniques include preloading, surcharging, staged construction, accelerated consolidation through installation of prefabricated vertical (wick) drains, electroosmosis, excavation and replacement, use of stone or lime columns or other replacement techniques, and the placement of geosynthetic reinforcement within the base of the embankment soil. Geometric methods that result in overall improvement of the embankment system, e.g. flattening side slopes of the embankment and/or adding toe berms, are also included in this group. The overall use of ground improvement techniques is addressed in (*4*).

Because ground improvement has been a popular geotechnical design tool for decades, there has been significant research into existing and new methods. The subject of ground improvement is the topic of a current (as of early 2000) U.S. Federal Highway Administration (FHWA) technology transfer initiative titled Demonstration Project 116. The current state of ground-improvement technology is well summarized in the manuals (*6*) prepared for and distributed to participants in the workshops held as part of Demonstration Project 116.

Less prevalent is the alternative soft ground treatment design approach to satisfying Equations. (1.1a) and (1.1b) which involves reducing the load applied by the embankment. This involves replacing the soil fill material within the embankment with a lighter material and accepting the natural resistance (strength and compressibility) of the existing soft foundation soil. The use of this concept may yield a more technically effective and more cost efficient embankment because expensive ground improvement techniques do not have to be employed for the foundation soil. This is important because there is uncertainty involved in using ground improvement techniques. For example, the level of uncertainty involved in increasing the foundation shear resistance is high relative to the use of lightweight fill because strengthening of the foundation can be difficult to control and the soil strata may not be known accurately. In

addition, the change in engineering properties should be verified prior to embankment construction to ensure satisfactory performance. Conversely, the properties and geometry of man-made lightweight fills, e.g., geofoam, are well defined which provides more confidence and less uncertainty in its use than foundation improvement techniques. The reduced uncertainty is mainly caused by the fill being so light that it does not stress the foundation and thus the need to accurately know the soil strata is eliminated. By design, lightweight fill materials have unit weights (0.1 to 17 kN/m³ (0.8 to 109 lbf/ft^3) less than that of soil and rock (20.4 kN/m³ (130 lbf/ft^3)) so the resulting gravity or seismic forces from the lightweight fill materials are significantly less than those from normal earth materials.

Table 1.1. Soft Ground Treatment Methods (modified from (*4*)).

The following factors should be considered in evaluating the different types of soft ground foundation treatment alternatives (*4,7*):

- The operating criteria for the embankment, e.g., stability requirements, allowable total and rate of settlement, level of maintenance, etc. This will establish the level of improvement required in terms of soil properties such as strength, modulus, compressibility, etc.;
- The area, depth, and total volume of soil to be treated or improved;
- Soil type and its initial properties;
- Availability of construction materials;
- Availability of equipment and required skills;
- Environmental factors such as waste disposal, erosion, water pollution, and effects on adjacent facilities and structures;
- Local experience and preference;
- Time available; and
- Cost.

As indicated in the above factors, the type of soft ground treatment that is selected will depend on the tolerable settlement of the embankment or bridge approach system. Post-construction settlements as much as 0.3 to 0.6 m (1 to 2 ft) during the economic life of a roadway are generally considered tolerable provided that the settlements are uniform, occur slowly over a period of time, and do not occur next to a pile-supported structure (*8*). If post-construction settlement occurs over a long period of time, any pavement distress caused by settlement can be repaired when the pavement is resurfaced. Although rigid pavements have under gone 0.3 to 0.6 m (1 to 2 ft) of uniform settlement without distress or objectionable riding roughness, flexible pavements are usually selected where doubt exists about the uniformity of post-construction settlements and some states utilize a flexible pavement when predicted settlements exceed 150 mm (6 in.) (*8*). Tolerable settlements of bridge approach embankments depend on the type of structure, location, foundation conditions, operational criteria, etc (*4*). The following references are recommended for information on tolerable abutment movements: (*9-12*).

TYPES OF LIGHTWEIGHT FILLS

As summarized in (*4*) and also discussed in (*13*), there are a large number of potential lightweight fill materials available. The most significant aspect of lightweight fill materials is their range in density which can vary from as little as 1 percent to as much as 70 percent of the density of soil or rock. There is also a significant range in material costs, engineering properties, and construction costs so the technical and economic benefit of using lightweight materials can vary widely. Of course, lightweight fill materials can be used in combination with ground improvement techniques for the foundation soil. However, experience indicates that on most projects it is most cost effective to use either one technology or the other.

Various categories have been used to classify lightweight fill materials. Categories used in (*13*) include lightweight fill materials with inherent compressive strength (EPS-block geofoam, foamed concrete geofoam) and granular lightweight fills (wood fiber, blast furnace slag, fly ash,

boiler slag, expanded clay or shale, shredded tires). Lightweight fill categories used in (*14*) include artificial fills (foam plastics and foamed concrete geofoams) and waste materials (shredded tires and wood chips). Lightweight fills are categorized in (*15*) as traditional light material (wastes from the timber industry such as sawdust and bark, wastes from the production of building blocks of cellular concrete, and expanded clay aggregate) and super-light fill (EPS-block geofoam). Table 1.2 provides a summary of the common types of lightweight fills.

As indicated in Table 1.2, there is a significant range in density/unit weight, specific gravity, and costs, so the technical and economic benefit of using lightweight fill materials can vary widely. Chapters 11 and 12 herein present additional cost information for EPS-block geofoam. Factors that influence cost of the various types of lightweight fills include quantity required for the project, transportation costs, availability of materials, contractor's experience with the product, placement or compaction costs, and specialty items, e.g., anchor plates for EPS-blocks or separator geosynthetics for wood fibers, that may be required (*13,16*). Additionally, the cost of using some waste materials will be dependent on the availability of federal or state government incentive or rebate programs. The lightweight fill types indicated in Table 1.2 are arranged by density/unit weight and it can be seen that EPS-block geofoam clearly has the lowest density/unit weight and specific gravity.

Table 1.2. Summary of Various Lightweight Fill Materials (*13*).

EPS-BLOCK GEOFOAM

Geofoam is any manufactured material created by an internal expansion process that results in a material with a texture of numerous, closed, gas-filled cells using either a fixed plant or an in situ expansion process (*1*). Geofoam materials include polymeric (plastic), glass (cellular glass), and cementitious foams (*19*). Because geofoam encompasses a variety of materials and products, it is necessary in practice to state the specific geofoam material and product being discussed. This is also consistent with what is required for other types of

geosynthetics. For example, when specifying a geotextile it is necessary to state the polymer, manufacturing technique (woven or non-woven), and desired weight or mass per unit area of the geotextile, and possibly whether it is calendered.

Most geofoam materials are polymeric with polystyrene foams being the most common. The two types of polystyrene foam are expanded polystyrene (EPS) and extruded polystyrene (XPS). They are collectively referred to by the American Society for Testing and Materials (ASTM) D 578 (*20*) as "rigid cellular polystyrene" (RCPS). EPS is a polymeric foam that is inherently white in color and can be found in some familiar consumer products such as coffee cups and cushion packaging.

EPS and XPS are differentiated based on the manufacturing process. EPS is manufactured by a two-stage process. The first stage consists of pre-expansion of the polystyrene solid resin beads into a cellular sphere with numerous closed cells by heating with steam. The expanded polystyrene beads are referred to as pre-puff. The second stage consists of further expansion of the pre-puff by heating with steam within a fixed-wall mold. The pre-puff fuses during this additional expansion process. On the other hand, XPS is manufactured by expanding the polystyrene solid resin beads and shaping the cellular product in a continuous process using an extruder. The final XPS has the appearance of a uniform texture of closed cells whereas the EPS product has the appearance of individual, fused particles. XPS is typically molded as thin planks or panels whereas EPS is typically molded as prismatic blocks. Thus, the preferred or more representative name for an EPS product is *EPS-block geofoam*. Further discussion on the manufacturing processes is included in Chapter 2 herein and in (*1*).

Although the generic use of the term geofoam is relatively new (it was used for a proprietary EPS product in Alaska starting in the late 1970s but has been in generic use worldwide only since the early 1990s), foam materials have been used in geotechnical applications, including in the U.S.A., since the early 1960s. Thus, there is a published historical record of use of the term geofoam that exceeds almost all other type of geosynthetics. Based on

this record, the predominant geofoam material used successfully from a technical and cost perspective as lightweight fill in road construction is EPS.

There are two additional terminology issues that need to be clarified before proceeding. First, because EPS-block geofoam is and has been the predominant geofoam material and product for many years, there is a tendency in current U.S. practice to simply use the term "geofoam" as a synonym for "EPS-block geofoam". Because there are so many recognized different geofoam materials and products (e.g., there is a brand of foamed portland-cement concrete that uses "geofoam" in its registered tradename), this synonymous relationship does not, in fact, exist and should be avoided to prevent potential errors, problems, or claims relative to supplying the appropriate geofoam material and product on a project.

Second, it is common in colloquial speech in the U.S.A. to refer to all polymeric foams as *styrofoam*. This is incorrect because Styrofoam® is the registered trademark and tradename of a line of XPS foam products manufactured by The Dow Chemical Company. Therefore, indiscriminate and incorrect use of the word styrofoam should be avoided in practice to prevent potential errors, problems, or claims relative to supplying the correct geofoam material and product for a project. A simple yet useful rule is to note that Styrofoam is always colored blue. Thus, the use of the word styrofoam must be restricted to those times when the blue-colored XPS product manufactured by The Dow Chemical Company is specifically intended. This would not likely occur when geofoam is used as lightweight fill for a road but might occur when geofoam is used as thermal insulation for a road pavement. Thus, Styrofoam usage might occur in road construction so diligent use of correct geofoam terminology is important in road construction.

FUNCTIONS

Geofoam is a type or category of geosynthetic. Depending on the particular geofoam material and product, geofoams can provide a wide variety of geosynthetic *functions*. Each of these functions may have numerous potential applications. With one exception, geofoam

functions do not duplicate those provided by other types of geosynthetics. A complete discussion of geofoam functions and applications is given in (*1*).

As with most types of geosynthetics, geofoams can provide a wide variety of functions including thermal insulation, lightweight fill, compressible inclusion, fluid transmission (drainage), damping, and structural. Also, as with other geosynthetics, the design by function approach is the most effective means of designing with geofoam. Design by function is based on initially selecting the function(s) required in a project and then selecting the geofoam product that will satisfy the function(s) most cost effectively (*19,21*).

Although the focus of the present study is on the geofoam function of *lightweight fill* and the specific application of this function is roadway embankments, the fact that geofoams provide other functions, even if not intended or not necessarily desired in a particular project, should be considered in design of lightweight fills for roads. These other functions include structural and thermal insulation.

HISTORY OF GEOFOAM

A comprehensive history of the various applications of geofoam is provided in (*1*). However, a general overview is presented here. Foam materials have been used in geotechnical applications since the early 1960s initially for the function of thermal insulation (*19*). The date and location of the first use of geofoam as lightweight fill is not known. EPS-block geofoam has been used as lightweight fill worldwide since at least 1972, which corresponds to a road project in Norway. The use of EPS-block geofoam in the U.S.A. for lightweight fill dates back to at least the 1980s although at least two conceptual patents for the use of plastic foams as lightweight fill in earthworks are known to have been issued in the U.S.A. in the early 1970s. Dr. Edward J. Monahan, P.E. indicates that he invented the geofoam function of lightweight fill circa 1970 (*1,22*) as part of his weight-credit concept (*1,23,24*) and through his U.S. patents in 1971 and 1973 (*1,25,26*).

In the early 1970s, XPS was used for a bridge approach fill in Pickford, Michigan. In (*1*) it is suggested that the Norwegian Road Research Laboratory (NRRL) developed the concept of using geofoam in general circa 1960 including use as lightweight fill circa 1970. Since a road project in 1972, the NRRL has utilized EPS blocks on hundreds of projects (*27,28*). The first lightweight fill project in Japan occurred in 1985. Approximately ten years later, an independent assessment found that geofoam usage in Japan comprised approximately 50 percent of the worldwide usage. Geofoam usage in Japan has largely been limited to the use of EPS-block geofoam. Significant research and development of the use of EPS-block geofoam has been performed in Japan for lightweight fill and seismic loading applications (*19*). Although XPS has been used to a limited extent as lightweight fill in the U.S.A., Japan, and the United Kingdom, geofoam applications worldwide have shown that XPS is not cost effective for use in lightweight fill applications (*1*), and consequently, the predominant geofoam material used as lightweight fill in road construction is EPS-block geofoam.

EPS-block geofoam is mentioned in (*4*) (although not identified as a geofoam material as the term was not in generic use at that time) and is included in the FHWA Demonstration Project 116 manuals (*13*). However, its use for roads in the U.S.A. increased dramatically during the 1990s, largely as a result of technology transfer initiatives by Prof. John S. Horvath, Ph.D., P.E. of Manhattan College in New York City (his first of many publications on the subject appeared in 1990) as well as marketing and geotechnical-engineering conference displays by EPS molders beginning in 1993. To date, EPS-block geofoam has been successfully used as a lightweight embankment fill material for roads ranging from Interstate highways to two-lane residential streets. It has also been successfully used as a lightweight fill for landslide repairs.

CURRENT STATE OF PRACTICE

The use of lightweight fill materials including EPS-block geofoam for roadway embankments as an alternative to ground improvement increased during the 1990s due to four significant reasons. First, the overall time for construction is typically much shorter and less

uncertain when lightweight fills are used rather than a foundation soil or ground improvement method. The shorter construction time results from the simplicity of placing the blocks and the ability to place the blocks in adverse conditions. Second, lightweight fills produce relatively small undrained (initial) and consolidation settlements whereas traditional ground improvement methodologies, such as preloading, typically produce relatively large undrained and consolidation settlements. While these settlements may not affect the final road, they can negatively affect adjacent property, roads, bridges, buildings, utilities, etc. However, it is important to note that the use of lightweight fill materials will not reduce the magnitude of secondary (creep) compression settlement that will occur without an embankment. The magnitude of secondary consolidation settlement is a function of the properties of the underlying soft foundation soil only, and is thus independent of the external stresses applied to the foundation soil. Third, lightweight fills decrease maintenance costs because of less settlement. Fourth, the durability of EPS-block geofoam has been proven by projects completed in the 1970s.

In consideration of these benefits, the typically higher unit cost of lightweight fill materials (a "negative" cited in (*4*) which was prepared in the late 1980s) is usually more than offset by savings when overall project costs are considered. An increase in use of lightweight fill materials for road construction is reflected in the fact that they have been emphasized by various governmental transportation agencies. The U.S. Federal Highway Administration (FHWA) has developed Demonstration Project 116, Ground Improvement Methods, to enhance the acceptance and implementation of ground improvement methods by the transportation community. Lightweight fills have been incorporated in this FHWA project as a method of ground improvement by reducing the applied load (*13*). This project consists of workshops and seminars. On the international level, the Permanent International Association of Road Congresses (PIARC) has issued a document (*29*) describing the use of various lightweight fill materials for different applications in road construction. Both the FHWA and PIARC references address material properties, design considerations, general standards related to the construction, environmental

considerations, if any, and value engineering of lightweight fill material. However, neither reference recommends or presents a detailed and comprehensive design procedure or a combined material and construction standard.

Various countries have developed general design guidelines and manuals to aid in the design of an embankment on soft soil incorporating EPS-block geofoam. These countries include France (*30*), Germany (*31,32*), Japan (*33*), Norway (*34-37*), and the United Kingdom (*38*). Other national efforts are currently known to be under development, e.g., NNI (the Dutch standards organization) through CROW (the Dutch standards organization dealing specifically with civil engineering) is currently preparing a document titled "Guideline for Design and Installation of EPS as Geofoam". The first monograph dedicated to geofoam discusses the concepts for analyzing and designing EPS-block geofoam fills (*1*). An outline-type manual with a general guideline specification has even appeared in the United States (*13*). However, these design guidelines and manuals do not provide a comprehensive design procedure that makes selection of a cost-effective design practical and reliable.

OBJECTIVES OF THE REPORT

Despite the extensive and continuing worldwide use of EPS-block geofoam, including in the U.S.A., specific design guidelines for its use as lightweight fill in roadway embankments is currently unavailable. Therefore, there was a need in the U.S.A. since the mid 1990s to develop formal and detailed design documents for use of EPS-block geofoam in routine practice. These documents would include both design guidelines as well as appropriate material and construction standard, both in the American Association of State Highway and Transportation Officials (AASHTO) format. The purpose of these design documents would be to encourage wider as well as more consistent use of EPS-block geofoam in roadway embankments. The ultimate benefit of these guidelines would be an optimization of both the technical performance as well as cost of EPS-block geofoam embankments.

The purpose of this report is to provide a comprehensive document that provides both state-of-the-art knowledge and state-of-practice design guidance for engineers. It is anticipated that designers will be more willing to consider EPS-block geofoam as an alternative for construction of embankments over soft ground using the design methodology and standard presented herein.

REPORT ORGANIZATION

The purpose of this report is to provide those who have primary involvement with roadway embankment projects, including the following four groups: end users, manufacturers, contractors, and owners, with both state-of-art knowledge and state-of-practice design guidance for use of EPS-block geofoam. The end users include engineers who perform the design and develop specifications; EPS block molders who manufacture the product; and construction contractors who install the product. To understand the technical basis for the design methodology and standard presented in the report, knowledge of the geotechnically relevant properties of block-molded EPS, e.g., modulus, compressive strength, Poisson's ratio, and interface shear resistance, is required (Chapter 2). Chapter 3 provides an overview of the design methodology developed herein for embankments on soft foundation soil incorporating EPS-block geofoam. The design methodology consists of the following three main parts: pavement system design (Chapter 4), external stability evaluation (Chapter 5), and internal stability evaluation (Chapter 6). All three of these considerations are interconnected and must be considered for each geofoam embankment. Chapter 3 also includes the background for the "Provisional Design Guideline" that is included in Appendix B. Chapter 4 presents the pavement system design module that yields typical flexible or rigid pavement systems that can be constructed over EPS-block geofoam. Chapter 5 presents the external stability considerations, e.g., bearing capacity, settlement, static and seismic slope stability, hydrostatic uplift, translation due to water and wind, that should be evaluated when utilizing an EPS-block geofoam embankment. Finally, Chapter 6 presents the internal stability issues, e.g., seismic sliding between the EPS blocks, sliding due to water and

wind, load bearing capacity of the blocks, and durability, that should be considered. Chapter 7 presents design examples that demonstrate the design methodology outlined in Chapter 3 and implemented in Chapters 4, 5, and 6 for a roadway embankment that can be used by design engineers to facilitate design of their projects. The key feature in Chapters 4, 5, and 6 are the inclusion of design charts that can be used to obtain a technically optimal design for a geofoam embankment on soft foundation soil.

Chapters 8, 9, and 10 discuss geofoam construction practices, MQC/MQA testing, and design details, respectively. These chapters provide the background for understanding the basis of the "Provisional Standard" included in Appendix C. Chapter 11 provides a summary of several case histories that have successfully incorporated EPS-block geofoam into roadway embankments and slope stabilization applications. Chapter 12 provides cost information to allow a cost estimate to be prepared during the design phase so that an optimal geofoam design can be selected. The designer can then use this optimal cost-based design to perform a cost comparison with other soft ground construction techniques. Finally, Chapter 13 presents recommended areas of future research.

Both the Système International d'Unités (SI) and inch-pound (I-P) units have been used in this report. SI units are shown first and I-P units are shown in parentheses within text. Numerous figures are included for use in design. Therefore, only SI units are provided in some of the figures to avoid duplication of figures. Additionally, in some cases figures have been reproduced that use either all SI or all I-P Units. These figures have not been revised to show both sets of units. However, Appendix F presents factors that can be used to convert between SI and I-P units. The one exception to the dual SI and I-P unit usage involves the quantities of density and unit weight. Density is the mass per unit volume and has units of kg/m^3 ($slugs/ft^3$) and unit weight is the weight per unit volume and has units of kN/m^3 (lbf/ft^3). Although density is the preferred quantity in SI, unit weight is still the common quantity in geotechnical engineering practice (*39*). Therefore, the quantity of unit weight will be used herein except when referring to EPS-block

geofoam. The geofoam manufacturing industry typically uses the quantity of density with the SI units of kg/m^3 but with the I-P quantity of unit weight with units of lbf/ft^3. Therefore, the same dual unit system of density in SI/unit weight in I-P units will be used when referring to EPS-block geofoam.

REFERENCES

1. Horvath, J. S., *Geofoam Geosynthetic*, , Horvath Engineering, P.C., Scarsdale, NY (1995) 229 pp.
2. MacFarlane, I. C., ed., *Muskeg Engineering Handbook*, University of Toronto Press, Toronto, Canada (1969) pp.
3. Sasaki, H., "A historical review of foundation treatment techniques for embankments over peat deposits." *Symposium on Recent Developments in Ground Improvement Techniques,*29 Nov.-3 Dec. 1982, Asian Institute of Technology, Bangkok, (1985) pp. 533-542.
4. Holtz, R. D., "Treatment of Problem Foundations for Highway Embankments." *NCHRP Synthesis 147,* Transportation Research Board, Washington, D.C. (1989) 72 pp.
5. Broms, B. B., "Problems and Solutions to Construction in Soft Clay." *Proceedings of the Sixth Asian Regional Conference on Soil Mechanics and Foundation Engineering*Singapore, Vol. II (1979) pp. 3-38.
6. Elias, V., Welsh, J., Warren, J., and Lukas, R., "Ground Improvement Technical Summaries." *Publication No. FHWA-SA-98-086,* 2 Vols, U.S. Department of Tranportation, Federal Highway Administration, Washington, D.C. (1999) .
7. Mitchell, J. K., "Soil Improvement - State-the-Art Report." *Proceedings of the Tenth International Conference on Soil Mechanics and Foundation Engineering*Stockholm, Vol. 4 (1981) pp. 506-565.
8. "Treatment of Soft Foundations for Highway Embankments." *NCHRP Synthesis 29,* Transportation Research Board, Washington, D.C. (1975) 25 pp.
9. "Bridge Approach Design and Construction Practices." *NCHRP Synthesis of Highway Practice 2,* Transportation Research Board, Washington, D.C. (1969) 30 pp.
10. Wahls, H. E., "Shallow Foundations for Highway Structures." *NCHRP Synthesis of Highway Practice 107,* Transportation Research Board, Washington, D.C. (1983) 38 pp.
11. Moulton, L. K., GangaRao, H. V. S., and Halvorsen, G. T., "Tolerable Movement Criteria for Highway Bridges." *FHWA/RS-85/107,* Federal Highway Administration, Washington D.C. (1985) .
12. Moulton, L. K., "Tolerable Movement Criteria for Highway Bridges." *FHWA-TS-85-228,* Federal Highway Administration, Washington, D.C. (1986) 93 pp.
13. Elias, V., Welsh, J., Warren, J., and Lukas, R., "Ground Improvement Technical Summaries." *FHWA-SA-98-086,* Vol. 2, 2 Vols, U.S. Department of Transportation, Federal Highway Adminstration, Washington, D.C. (1999) .
14. Monahan, E. J., *Construction of Fills*, 2nd ed., John Wiley & Sons, Inc., New York, N.Y. (1994) 265 pp.
15. Flaate, K., "The (Geo) Technique of Superlight Materials." *The Art and Science of Geotechnical Engineering At the Dawn of the Twenty-First Century: A Volume Honoring Ralph B. Peck,* E. J. Cording, W. J. Hall, J. D. Haltiwanger, J. A.J. Hendron, and G. Mesri, eds., Prentice Hall, Englewood Cliffs, N.J. (1989) pp. 193-205.
16. Harbuck, D. I., "Lightweight Foamed Concrete Fill." *Transportation Research Record 1422,* Transportation Research Board, Washington, D.C. (1993) pp. 21-28.

17. "Processed Blast Furnace slag, The All-Purpose Construction Aggregate." *Bulletin No. 188-1,* National Slag Association (1988) .
18. Upton, R. J., and Machan, G., "Use of Shredded Tires for Lightweight Fill." *Transportation Research Record 1422,* Transportation Research Board, Washington, D.C. (1993) pp. 36-45.
19. Horvath, J. S., "Geofoam and Geocomb: Lessons from the Second Millennium A.D. as Insight for the Future." *Research Report No. CE/GE-99-2,* Manhattan College, Bronx, NY (1999) 24 pp.
20. ASTM D 578-95, "Standard Specification for Rigid, Cellular Polystyrene Thermal Insulation." Vol. 04.06, American Society for Testing and Materials, West Conshohocken, PA (1999) .
21. Koerner, R. M., *Designing with Geosynthetics*, 4th, Prentice Hall, Upper Saddle River, N.J. (1998) .
22. Monahan, E. J., "editorial letter." *Geotechnical Fabrics Report*, Vol. 11, No. 3 (April 1993) p. 4.
23. Monahan, E. J., *Construction of and on Compacted Fills*, , John Wiley & Sons, New York, N.Y. (1986) .
24. Monahan, E. J., "Weight-Credit Foundation Construction Using Artifical Fills." *Transportation Research Record No. 1422,* Transportation Research Board, Washington, D.C. (1993) pp. 1-4.
25. Monahan, E. J., "Floating Foundation and Process Therefor." *U.S. Patent No. 3,626,702* (1971).
26. Monahan, E. J., "Novel Low Pressure Back-Fill and Process Therefor." *U.S. Patent No. 3,747,353* (1973).
27. Aabøe, R., "Long-term performance and durability of EPS as a lightweight fill." *Nordic Road & Transport Research*, Vol. 12, No. 1 (2000) pp. 4-7.
28. Aabøe, R., "Evidence of EPS long term performance and durability as a light weight fill." Preprint Paper, *Transportation Research Record No. 1736,* Transportation Research Board, Washington, D.C. (2000) .
29. "Matériaux Légers pour Remblais/Lightweight Filling Materials." *Document No. 12.02.B,* PIARC-World Road Association, La Defense, France (1997) 287 pp.
30. "Utilisation de Polystyrene Expanse en Remblai Routier; Guide Technique." Laboratoire Central Ponts et Chaussées/SETRA, France (1990) 18 pp.
31. "Merkblatt für die Verwendung von EPS-Hartschaumstoffen beim Bau von Straßendämmen." Forschungsgesellschaft für Straßen- und Verkehrswesen, Arbeitsgruppe Erd- und Grundbau, Köln, Deutschland (1995) 27 pp.
32. "Code of Practice; Using Expanded Polystyrene for the Construction of Road Embankments." BASF AG, Ludwigshafen, Germany (1995) 14 pp.
33. "Design and Construction Manual for Lightweight Fill with EPS." The Public Works Research Institute of Ministry of Construction and Construction Project Consultants, Inc., Japan (1992) Ch. 3 and 5.
34. "Guidelines on the Use of Plastic Foam in Road Embankment." Public Roads Administration, Road Research Laboratory, Oslo, Norway (1980) 2 pp.
35. "Expanded Polystyrene Used in Road Embankments - Design, Construction and Quality Assurance." *Form 482E,* Public Roads Administration, Road Research Laboratory, Oslo, Norway (1992) 4 pp.
36. "Material Requirements for Expanded Polystyrene Used in Road Embankments." *Form 483E,* Public Roads Administration, Road Research Laboratory, Oslo, Norway (1992) 2 pp.
37. "Quality Control of Expanded Polystyrene Used in Road Embankments." *Form 484E,* Public Roads Administration, Road Research Laboratory, Oslo, Norway (1992) 4 pp.

38. Sanders, R. L., and Seedhouse, R. L., "The Use of Polystyrene for Embankment Construction." *Contractor Report 356,* Transport Research Laboratory, Crowthorne, Berkshire, U.K. (1994) 55 pp.
39. Holtz, R. D., and Kovacs, W. D., *An Introduction to Geotechnical Engineering*, , Prentice Hall, Englewood Cliffs,NJ (1981) 733 pp.

Category	Alternative	Variations of Method
Reducing the load	Reduced-stress method	Lightweight Fill: bark, sawdust, peat, fuel ash, slag, cinders, scrap cellular concrete, low-density cellular concrete geofoam, expanded clay or shale (lightweight aggregate), expanded polystyrene geofoam, shells, shredded tires.
Replacing the problem materials by more competent materials	Removal of problem materials and replacement by suitable fill	Complete excavation, partial excavation, displacement of soft materials by embankment weight assisted by controlled excavation, displacement by blasting.
Increasing the shear strength and reducing compressibility of the problem materials	Stabilization of soft foundation materials by consolidation	By surcharge only, by surcharge combined with vertical drains, by surcharge combined with pressure relief wells or vertical drains along toe of fill.
	Consolidation with paving delayed (stage construction)	Before paving, permit consolidation to occur under normal embankment loading without surcharge, accept post-construction settlements.
	Chemical alteration and stabilization	Lime and cement columns, grouting and injections, soil mixing, electro-osmosis, thermal, freezing, organic.
	Physical alteration and stabilization; densification	Dynamic compaction, blasting, vibrocompaction and vibro-replacement, sand compaction piles, stone columns, water.
Transferring the loads to more competent layers	Supported on deep foundations	Drilled shafts, driven piles
Reinforcing the embankment and/or its foundation	Reinforcement	Mechanically stabilized earth walls, reinforced soil slopes, soil nailing, geotextiles and geogrids, fascines, Wager short-sheet piles, anchors, root piles (minipiles).
Providing lateral stability	Berms; flatter slopes	

Lightweight Fill Type	Range in Unit Weight, kN/m^3 (lbf/ft^3)	Range in Specific Gravity	Approximate Cost, $/m^3 ($/yd^3)	Source of Costs
EPS (expanded polystyrene)-block geofoam	0.12 to 0.31 (0.75 to 2.0)	0.01 to 0.03	35.00 - 65.00 (26.76 - 49.70)(2)	Supplier
Foamed portland-cement concrete geofoam	3.3 to 7.6 (21 to 48)	0.3 to 0.8	65.00 - 95.00 (49.70 - 72.63)(3)	Supplier, (*16*)
Wood Fiber	5.4 to 9.4 (34 to 60)	0.6 to 1.0	12.00 - 20.00 (9.17 - 15.29)(1)	(*17*)
Shredded tires	5.9 to 8.8 (38 to 56)	0.6 to 0.9	20.00 - 30.00 (15.29 - 22.94)(1)	(*18*)
Expanded shales and clays	5.9 to 10.2 (38 to 65)	0.6 to 1.0	40.00 - 55.00 (30.58 - 42.05)(2)	Supplier, (*16*)
Boiler slag	9.8 to 17.2 (62 to 109)	1.0 to 1.8	3.00 - 4.00 (2.29 - 3.06)(2)	Supplier
Air cooled blast furnace slag	10.8 to 14.7 (69 to 94)	1.1 to 1.5	7.50 - 9.00 (5.73 - 6.88)(2)	Supplier
Expanded blast furnace slag	Not provided	Not provided	15.00 - 20.00 (11.47 - 15.29)(2)	Supplier
Fly ash	11 to 14.1 (70 to 90)	1.1 to 1.4	15.00 - 21.00 (11.47 - 16.06)(2)	Supplier

Notes: These prices correspond to projects completed in 1993 - 1994. Current costs may differ due to inflation.

(1) Price includes transportation cost.

(2) FOB (freight on board) at the manufacturing site. Transportation costs should be added to this price.

(3) Mixed at job site using pumps to inject foaming agents into concrete grout mix.

CHAPTER **2**

RELEVANT ENGINEERING PROPERTIES OF BLOCK-MOLDED EPS

Contents

BACKGROUND

Introduction

This chapter presents an overview of the engineering properties of EPS. A knowledge of the physical, mechanical (stress-strain-time-temperature), and thermal properties of block-molded EPS is required to understand the basis for past design methodologies as well as to understand the recommended design methodology that is summarized in Chapter 3 and incorporated in the provisional design guideline in Appendix C.

The properties of block-molded EPS of interest for the function or application of lightweight fill include:

- physical,
- mechanical (stress-strain-time-temperature), and
- thermal.

These properties are discussed subsequently. However, the EPS block molding process can significantly influence the quality and other performance aspects of EPS-block geofoam to include the physical, mechanical, and thermal properties. Therefore, a knowledge of the key elements of the molding process is useful and is initially discussed.

Manufacturing (Molding) EPS

Overview

There are two distinct steps involved in manufacturing (molding) EPS:

- A manufacturer called a *resin supplier* produces the raw material that is formally called *expandable polystyrene* but colloquially referred to as *beads* or *resin*. Expandable polystyrene consists of fine to medium sand-size spherical particles of solid polystyrene with a naturally occurring petroleum hydrocarbon, almost always pentane (Japan is the only known country where an alternative, butane, is used routinely), mixed in as a *blowing agent*. The expandable polystyrene may also contain other additives that are discussed subsequently. Most resin suppliers are large, multi-national chemical companies with a broad range of products.
- A manufacturer called a *molder* buys the expandable polystyrene and, in a multi-stage process, transforms it into expanded polystyrene (EPS). The final EPS products are broadly categorized as either being prismatic blocks (block-molded EPS) or some type of custom shape (shape-molded EPS). *Block molders* traditionally were relatively small, privately, locally owned businesses serving a relatively limited geographical area. This is changing in the U.S.A. to ownership by larger corporations with multiple plant locations. Although there are still more than approximately 100 block molders, no one molder serves the entire country.

EPS blocks can be used for a wide variety of purposes and applications, one of which is EPS-block geofoam. In the U.S.A. at present, EPS-block geofoam is most often marketed by and purchased directly from a local block molder although sale through distributors who handle other geosynthetics and/or construction products as well as large retail chains selling construction materials is becoming more common. Practices vary widely in this regard at the present time, even within a given area where one molder might sell directly to an owner and a competitor will only sell through a distributor. End users should be aware of the fact that purchasing EPS-block

geofoam through a distributor generally results in a greater unit cost for the product because of distributor markup for their overhead and profit. In many cases, there is no value added by a distributor. In typical road construction in the U.S.A. at the present time, EPS-block geofoam is purchased by the general contractor from a molder or a distributor.

Block Molding

Manufacturing EPS-block geofoam is basically a two-step process. The first step is called *pre-expansion* of the expandable polystyrene. The expandable polystyrene (a.k.a. beads, resin) raw material is placed into a large container called a *pre-expander* and then heated with steam. The steam causes the blowing agent that is dissolved in each bead of expandable polystyrene to phase change into a gas and expand the polystyrene in the process to approximately 50 times its initial volume, a diameter increase of the order of three to four times. The expanded spheres of polystyrene is colloquially referred to as *pre-puff*. Each pre-puff particle contains numerous closed cells with about 98 percent of the total volume consisting of gas-filled voids. Initially, the gas is a mixture of the residual blowing agent and air. The density of the pre-puff can be varied within certain limits which will affect the density of the final product. As will be discussed subsequently, the density of EPS-block geofoam can be an important and useful index property.

The pre-puff is then moved to temporary storage in large fabric bags to allow it to stabilize thermally and chemically. After several hours of storage (the overall quality of the final product is sensitive to storage time), the pre-puff is placed into a mold which is essentially a closed steel box that is rectangular parallelepiped in shape. Steam is injected into the sealed mold and this simultaneously resoftens the polystyrene and causes some further expansion of the pre-puff. As a result, the spheres of pre-puff fuse thermally and distort somewhat in shape to more of a polyhedral shape to fill most of the void spaces between the originally spheroidal pre-puff particles. The block is then released from the mold and allowed to "season", i.e. stabilize thermally (dimensional changes of the block occur during cooling) and chemically (residual blowing agent remaining in the cells of the EPS outgasses and is replaced by air). The block also

dries during this seasoning period as a relatively significant amount of water vapor and liquid (which can artificially increase the apparent density of the EPS) that is condensed steam from molding remains in the block at the end of molding. The duration of the seasoning can vary widely from hours to weeks depending on the desired stability of the final product. A minimum seasoning time of three days (72 hours) at ambient room temperature is recommended and will be discussed subsequently in the "Flammability" section of this chapter. Seasoning is often accelerated by short-term storage in a room with temperatures that are elevated relative to ambient conditions within the molding plant. However, not all EPS molders in the U.S.A. have such storage rooms. At the end of the seasoning period, a block can be trimmed, cut, or used as desired.

There has been insufficient study to date to be able to quantify the effects of time and temperature on the mechanical and thermal properties of EPS-block geofoam. The primary reasons for the lack of data is primarily due to the numerous variables related to seasoning, including time and temperature, that affect the mechanical and thermal properties of EPS. For example, in (*1*) it is suggested that resin type and molding technique affect the rate of pentane emissions. The issue of pentane emissions is further discussed in the "Flammability" section of this chapter. The recommended seasoning requirement of three days (72 hours) is based primarily on safety concerns related to the outgassing of residual pentane blowing agent and is based on an assessment of the little industry information available on this subject. Thus, the seasoning recommendation represents the state of knowledge at this time and no further quantitative information can be provided.

The final EPS product has the visual texture of individual, fused particles (the former pre-puff particles, each of which is still roughly spherical in shape). Because of this, EPS was, and sometimes still is, occasionally referred to in literature as *molded expanded polystyrene* or *molded-bead expanded polystyrene* although these terms are typically not used in current U.S. practice. This macrofabric of EPS is also the reason that it has been and still is sometimes referred

to colloquially as *beadboard*, a term that the EPS industry in the U.S.A. appears to deprecate because of an-often negative connotation associated with this term.

There is a variation of the above manufacturing procedure that is worth mentioning. The above process is the typical process when the molder is using 100 percent virgin raw material (expandable polystyrene). However, EPS molding always generates some in-plant scrap or waste material. Consequently, to reduce their costs for both waste disposal as well as raw material purchase, most block molders in the U.S.A. try to reuse at least some of this scrap. This is accomplished by grinding it up into pieces that are generally sand-size to produce what is called *regrind*. The regrind is mixed in with virgin pre-puff during the final block molding process. Because the regrind has long since lost any residual pentane, it does not react the same way as virgin pre-puff during the final molding process. Therefore, block-molded EPS containing regrind will, all other variables being equal, have poorer properties (the mechanical properties which are the ones of greatest importance in geofoam applications as lightweight road fill are particularly affected) than block-molded EPS made with 100 percent virgin prepuff. For example, the percentage of regrind, if any, can affect the compressive properties of block-molded EPS, especially the design-critical initial tangent Young's modulus, E_{ti} (*2,3*). The effect of increasing regrind content on the small strain stiffness is further discussed in the "Compression" section of this chapter. The degradation in mechanical properties occurs gradually as the relative proportion of regrind is increased.

Below are several reasons why regrind negatively affects the quality of the finished EPS-block geofoam that were provided in (*4*):

- The grinding process tears and crushes the original cellular structure of the EPS. Torn and crushed cells have much lower stiffness than the intact cells in virgin prepuff.
- Regrind has long since lost all of its hydrocarbon blowing agent. As a result, during the final molding process it does not soften and fuse together in the same

way that virgin prepuff does so that the overall bead fusion of the finished EPS is poorer than if all virgin prepuff were used. The resulting new EPS with regrind has a more crumbly texture.

- All EPS is inherently white regardless of density and flame retardancy. It is thus possible that regrind of incorrect density and/or material that is not flame retardant may be mixed in and compromise the density and/or flame retardancy of the new EPS.
- If post-consumer regrind is used, plastic foams other than EPS may be mixed in and further contaminate the new EPS.

The final quality (in terms of geotechnical relevant mechanical properties in particular) of an EPS block is influenced by numerous factors and procedures at each of the above steps of the manufacturing process, including what percentage, if any, of regrind is used. However, an appropriate material standard for EPS-block geofoam does not have to explicitly address any of the quality issues at intermediate stages of manufacturing, including maximum allowable regrind content. Rather, it is sufficient to specify minimum quality parameters for the final product and then leave it to the molder to take appropriate measures at each step in the manufacturing process to ensure that final quality parameters are met.

PHYSICAL PROPERTIES AND ISSUES

Introduction

The physical properties of EPS-block geofoam can be thought of as being conceptually similar to the traditional index properties of soil (description, classification, particle size, Atterberg Limits, etc.) and thus useful, within a certain context, during the design process. Soil index properties are those properties that are used to classify or discriminate among the different kinds of soil in a given category (*5*). A material property is a good index property if the property is simple to express, e.g., numerical values, measurement is quick, measurement is simple, measurement is reproducible, and property is significant, i.e., property is a measure of or

correlates with a significant engineering property of soils (*6*). Density and fusion are two key index properties of EPS-block geofoam. However, other physical properties, such as block dimensions, color, flammability, durability, and environmental effects, can also affect cost, design, or construction.

Density

As noted previously, it is possible to manufacture EPS blocks within a range of densities, primarily through controlling the density of the pre-puff created during the first stage of manufacturing (the pre-expansion process). The overall range in EPS density possible is between approximately 10 to 100 kg/m^3 (0.62 to 6.24 lbf/ft^3) although for practical purposes the range available for lightweight fill applications is much smaller, of the order of 16 to 32 kg/m^3 (1.0 to 2.0 lbf/ft^3).

The relevance of EPS density is that the density of EPS-block geofoam can be a very useful index property only if the EPS meets certain minimum quality parameters. Assuming that the appropriate quality standards are met, density of EPS-block geofoam has been shown to correlate well with both geotechnical relevant mechanical and thermal properties. For example, compression behavior in general exhibits a primary dependency on EPS density. Therefore, EPS-block geofoam density can be used as an index property to estimate some mechanical and thermal properties provided the EPS meets a set of minimum standards, such as those specified in the provisional American Association of State Highway and Transportation Officials (AASHTO) standard included in Appendix C.

There are several additional issues regarding the density of EPS-block geofoam. First, a given production run of EPS blocks will always exhibit some variability of final product density from block to block, even if appropriate manufacturing quality controls are being employed. This simply reflects inherent variability in the EPS manufacturing process and can easily be checked by weighing each block to determine its nominal (average) density.

Second, there will be density variations (called *density gradients* in the industry) within every block, also a result of inherent variability in the EPS manufacturing process. Density gradients up to approximately ±10 percent relative to some nominal (average) value are often given in the literature as typical. In addition, it is generally assumed that densities are largest at the center of a block and smallest at the edges. However, with molding equipment currently in use it appears that neither of these statements is universally true any more. Density gradients can, in fact, exceed ±10 percent (the range appears to increase with increasing average density of the block) and can potentially have complex patterns of variation. Thus the density of a relatively small specimen cut from a block can be significantly different than the gross density of the entire block. This is significant because the compressive behavior of block-molded EPS is most dependent on density (*7-11*). The density of specimens cut from a block can be determined in accordance with ASTM D 1622 (*12*). The use of a hot-wire cutter may yield more consistent density values than the use of a fine-tooth band saw because a hot-wire cutter produces a cleaner and smoother surface than a fine-tooth band saw.

Third, most block molders in the U.S. are set up to manufacture EPS to five standard densities specified in the ASTM standard used for this purpose (*13*). Thus it is always most cost effective to develop a design based on these densities whenever possible. It is important to note that this ASTM standard is written from the perspective of specifying minimum acceptable values of product density and several other parameters. This has apparently led to certain misconceptions within the EPS industry regarding product quality. These misconceptions are discussed in Chapter 9.

Several issues need to be noted with regard to measuring block density which is generally viewed as being a trivial measurement:

- For relatively freshly molded EPS, density is sensitive to time to outgassing of both residual pentane blowing agent as well as moisture from condensed steam.

Therefore, the date of molding for the block from which a test specimen is obtained should always be recorded as part of the test data.

- Density can be affected by absorbed atmospheric moisture. Therefore, density should be determined immediately prior to testing and only after an appropriate seasoning protocol (referred to *aging and conditioning* in the EPS industry). A typical protocol essentially requires a minimum of 40 hours under standard laboratory conditions (*13*).

Fusion

Another index of overall EPS quality is called *fusion*. This refers to the thermal fusion between pieces of prepuff (and regrind when used) that occurs during the second stage of manufacturing (final block molding). Experience and testing indicates that fusion does not so much influence the mechanical and thermal properties as it does the overall durability and robustness of the finished product. Tensile loading is an indicator of EPS fusion. However, flexural strength correlates well with tensile strength and can also provide an indirect indicator of EPS fusion. Both tensile and flexural testing are discussed subsequently as part of the "Mechanical Properties" section of this chapter.

Block Dimensions

The dimensions of an EPS block do not affect its geotechnical engineering properties. However, other design issues such as product unit cost (including delivery to a job site) and in situ block layout are influenced by block dimensions.

The dimensions of an EPS block are governed primarily by the mold used during manufacturing. There is no standard mold size used worldwide or even within the U.S.A. so some variation between molders must be expected. However, there is an overall trend, at least within the U.S.A., toward using molds that produce somewhat larger blocks (primarily with respect to the smallest (thickness) and largest (length) dimensions) than in the past. Where possible, it is generally desirable to try to use EPS blocks in their full as-molded size, assuming that the blocks

meet certain dimensional quality criteria for straightness, etc. Although it is possible to factory cut a seasoned block into a smaller size, such cutting can add significantly to the unit cost of the final EPS-block geofoam product.

For many years, the typical dimensions of EPS-block geofoam available in the U.S.A. were 610 x 1,220 x 2,440 mm (24 x 48 x 96 in.). The first trend that developed during the 1990s was toward longer blocks, typically 4,880 mm (192 in.) in length. More recently, the trend has been toward thicker blocks, with the thickness dimension increasing from 610 mm (24 in.) to between 760 and 1,000 mm (30 and 39 in.) depending on the particular mold used. Thus, many EPS blocks currently produced in the U.S.A. are almost square in cross-section. Fortunately, in most lightweight fill applications, it is possible to use these larger blocks for at least most of the fill. However, some factory and field cutting of blocks is generally necessary on every project.

There are basically two ways to deal with the variability in dimensions of EPS-block geofoam (keep in mind that there are more than 100 EPS block molders in the U.S.A.):

- Select a supplier (molder or distributor) of the EPS-block geofoam during the design phase of a project and determine what is the standard block size available from that supplier. The design professional of record for the project then develops the explicit block layout for the project and this information is shown on the design drawings.
- The design professional produces design drawings that show the overall geometry and dimensions of the desired mass of EPS-block geofoam, as well as specifies certain key conceptual elements of the block layout (minimum number of layers, overall geometry of each layer, etc.). The construction contractor on the project is then required to submit shop drawings depicting the actual block dimensions and layout proposed for use. These shop drawings are typically prepared by the EPS molder and would be reviewed and approved per the normal process used for years in many other aspects of engineered construction.

The first alternative is generally not feasible for government projects such as road construction. In addition, experience in the latter part of the 1990s has indicated that more and more EPS block molders in the U.S.A. are developing the capability to provide shop drawings so this alternative is proving to be feasible in practice.

Color

EPS is inherently white in color although it is possible, for a cost, to tint it another color during the manufacturing process. There is no technical merit or benefit in geofoam applications to a color other than white. The only benefit would be for product identification and marketing purposes.

Although EPS-block geofoam of a color other than white is sold in several countries (e.g. certain proprietary products are brown in Canada and pink in the United Kingdom), such products are not known to be available in the U.S.A. This is perhaps partially due to the fact that the most common and obvious colors (blue, green, pink and yellow) have already been used and legally identified (through registered trademark) with extruded polystyrene (XPS) products that are manufactured in the U.S.A.

What has seen sporadic use in the U.S.A. is for a molder to stencil or otherwise mark some or all blocks of EPS-block geofoam with their name or a logo for product identification or marketing purposes. Such markings can also have a technical benefit to identify (by using different colors for the markings) EPS blocks of different density shipped to the same project site (this is done in the U.K. for example). More common, however, for cost reasons, is the use of simple color markings to identify EPS blocks of different density shipped to the same project site.

Flammability

Flammability of a polymeric material such as polystyrene is often measured or expressed by its *oxygen index* (OI). The OI is the minimum relative proportion (expressed as a percent) of oxygen in some mixture of gases that is required to support continuous combustion. Air at sea level contains approximately 21 percent oxygen so if a material has an OI less than 21 percent it

will burn freely in air until all the material is consumed provided there is an initial ignition source. If the OI of the material is greater than 21 percent, it will not support continuous combustion after initial ignition (this is generally referred to as being *self extinguishing*) although it may still melt as well as support combustion if an ignition source is continuously present.

Polystyrene has an OI of 18 percent which means that normal EPS is inherently flammable. However, it is possible to incorporate an inorganic, bromine-based chemical into the expandable polystyrene raw material used to manufacture EPS so that final block product is flame retardant and self extinguishing. Such raw material is referred to as *modified* bead or resin. EPS made with modified bead can still melt, however, at a temperature between approximately +150 and +260°C (300° and 500°F) although +95°C (200°F) is generally recommended as a maximum working value. In the U.S.A., ASTM specifications (*13*) for flame-retardant EPS call for a minimum OI of 24 percent which is 3 percent greater than the OI of air. It is of interest to note that flame-retardant EPS cannot be identified visually nor are any other physical, mechanical or thermal properties affected by the bromine additive.

In general, flame-retardant EPS block reportedly may cost up to 10 percent more than EPS block that is not flame retardant because of higher raw-material costs. Therefore, on a global basis, use of flame-retardant EPS block for geofoam applications has not been universal and should never be assumed. For example, in Norway which pioneered the use of EPS-block geofoam as lightweight fill in 1972, flame-retardant EPS-block geofoam is reportedly rarely specified. However, in some countries such as the U.S.A., it has become routine to supply only flame-retardant EPS-block geofoam. There are at least two reasons for this. First, whenever ASTM C 578 is used as a material specification, only flame-retardant material will be supplied. Second, if a molder uses normal or regular (non-flame-retardant) raw material, it will contaminate the various components of the manufacturing equipment (mold, etc.) and thus potentially compromise a subsequent manufacturing run of flame-retardant EPS. Thus, most molders find it easier to simply always manufacture flame-retardant EPS block.

There is another flammability issue separate from the inherent flammability of the EPS block. It is related to the outgassing of the blowing agent used in the manufacturing process. The blowing agents used for EPS, primarily pentane but butane in some countries (chiefly Japan), are inherently flammable and potentially explosive. In addition, the blowing agents are heavier than air and tend to pool or settle around a block as opposed to freely dispersing into the atmosphere. After an EPS block is released from the mold during the second and final stage of manufacturing, the closed cells within the fused pre-puff will still contain some blowing agent. The remaining blowing agent will naturally outgass from the cells and be replaced by air within a relatively short period of time. The exact duration of this outgassing process depends on many factors, especially temperature, but the duration is usually on the order of days. However, based on available published information (*14*) as well as anecdotal information obtained by personal communication with both resin suppliers and block molders in the U.S.A., an interim recommendation of three days of seasoning at ambient room temperature is proposed.

As discussed in (*15*), there was a lightweight fill project in Japan where the EPS blocks were being delivered to the job site and reportedly placed with very little seasoning time after molding due to project needs (this is not uncommon and is known to have occurred on several projects in the U.S.A.). On this specific project in Japan, the outgassed butane blowing agent accumulated in the joints between blocks and was ignited in situ by some on-site ignition source (welding or flame cutting of metal that was unrelated to the geofoam usage or even personal tobacco smoking).

Durability

The overall durability of EPS-block geofoam encompasses a range of issues. Flammability was addressed separately in the preceding section as it is primarily a manufacturing issue and not directly related to post-manufacturing durability. Considered in this section are the external factors related to construction and the in situ environment that may affect the physical, mechanical, or thermal properties of EPS-block geofoam after it leaves the molding plant. The

effect of EPS-block geofoam on the in situ environment is discussed separately in the following section.

In general, EPS-block geofoam has proven to be a very robust geosynthetic product, much more problem-free on the whole compared to many other types of geosynthetics where there is a potential for significant physical damage to and detrimental chemical changes within the geosynthetic during and after construction. EPS is inherently non-biodegradable and will not dissolve, deteriorate, or change chemically in the ground and ground water. Although EPS will absorb some ground water over time, the product will not change dimensionally and its mechanical properties are unaffected. The EPS will, however, lose some of its thermal efficiency which is irrelevant per se to most lightweight fill applications.

EPS provides no nutritive food source to any living organism or animal. However, certain burrowing insects such as termites and carpenter ants have been found to either tunnel through EPS or nest in it. This has only been observed for relatively thin (of the order of several tens of millimeters thick) geofoam panels used as thermal insulation in residential construction where there is an abundance of dead wood. There is no known case in the world where insect damage has been detected for EPS-block geofoam used as lightweight fill. There was an active discussion of this topic at Session 6 of the International Symposium on EPS Construction Method (*EPS Tokyo '96*) that was held in Tokyo, Japan in 1996 and reported in the final report (*16*) for this symposium.

It is worth noting that an inorganic chemical additive with the tradename *Timbor* was developed in the U.S.A. toward the end of the 20th century for EPS. The reported benefit of this additive is that it acts as a deterrent to insect infestation of block-molded EPS. The use of this additive in EPS block is proprietary and is available only from certain EPS block molders in the U.S.A. and Puerto Rico at the present time. EPS block manufactured with this additive is marketed under various tradenames including *Bug Block-R*™, *Perform Guard*®, *Teps*™ and possibly others. Some design professionals have elected to specify EPS-block geofoam treated

with *Timbor* for lightweight fill applications. The additive does not affect any of the geotechnical relevant physical, mechanical or thermal properties of the EPS. Specifiers of this additive should, however, be aware of the fact that requiring this additive in EPS-block geofoam will, in most parts of the U.S., restrict the number of molders who can bid on and supply a project. Because of this elimination of competition plus the inherent cost of the additive itself, the unit cost of the EPS blocks would be expected to be higher, possibly significantly so, than otherwise. However, it is not possible to quantify the likely relative cost increase because there are many intangible business issues involved.

There are relatively few conditions against which EPS-block geofoam needs protection. When exposed to ultraviolet (UV) radiation from sunlight, the surface of an EPS block will turn yellow in color and become somewhat brittle and chalky. However, this process takes from months to years to develop and is limited to the surface (degradation does not progress into the block) so it is only necessary to protect EPS-block geofoam from long-term UV radiation. Relatively brief exposure such as during construction is not a problem.

There are relatively few liquids that will dissolve EPS. The only ones likely to be encountered in lightweight fill geofoam applications are fuels such as gasoline and diesel fuel. The need and design methodology for dealing with this potential exposure is discussed in detail as part of separation materials in Chapter 4.

Environmental Effects

Environmental effects related to EPS-block geofoam fall into several categories. First, regarding the material itself, polystyrene is not inherently harmful or hazardous. Solid polystyrene is used for eating utensils and food containers, and EPS is used for beverage containers (the ubiquitous white foam coffee cup is a shape-molded EPS product) as well as food packaging. The blowing agents used to manufacture EPS are naturally occurring hydrocarbons, not a synthetic fluorocarbon-family gas which is used as a blowing agent for most other plastic foams. Thus, there are no gases that are potentially harmful to the Earth's upper-atmosphere

ozone layer that are associated with manufacturing EPS. Furthermore, because the cells within EPS are completely filled with air within a few days after molding, there is no concern about long-term outgassing of potentially toxic and hazardous gases as has been a problem with other types of plastic foam.

EPS will not interact in any way with the ground or ground water, and will not leach any chemical into the ground or ground water. If EPS is burned, either accidentally or intentionally as part of a waste-to-energy program, the products of combustion are primarily carbon dioxide and water. In addition, flame-retardant EPS (as would typically be used for lightweight fill geofoam in U.S. practice) will also emit traces of hydrogen bromide. The residual ash from burned EPS contains no heavy metals or other substances generally considered to be toxic or hazardous.

Note that the above comments regarding environmental impact of EPS only apply to "normal" EPS. Information concerning the impact(s), if any, associated with EPS treated with the insecticide noted above would have to be obtained from the proprietary supplier of such EPS.

MECHANICAL PROPERTIES

Introduction

The mechanical properties of EPS-block geofoam for the use as lightweight fill are important during the design because they affect both external and internal stability as well as pavement design. The mechanical properties of block-molded EPS primarily involve its stress-strain response under various modes and duration of loading. The temperature of the EPS can also affect the mechanical behavior but is generally a secondary issue. As noted previously, water absorption, if any, has no effect on the mechanical properties of the EPS. In particular, two distinct categories of mechanical properties that need to be addressed include:

- The properties of the EPS itself under vertical stress. This information is used during the internal stability assessment phase to determine the appropriate EPS density to support the applied dead- and live- loads as well as to provide equivalent soil property information for pavement design.

- The interface shear properties, both between EPS blocks as well as between EPS and dissimilar materials (both soil and non-soil). This information is used during external and internal stability assessment, particularly under conditions that produce lateral loading during an extreme event involving either wind, an unbalanced water head, or seismic loading.

Therefore, the compression and interface shear properties of EPS will be discussed. However, tension and flexure properties of EPS are also briefly discussed because both tensile and flexural loading tests can be useful manufacturing quality control and manufacturing quality assurance (MQC/MQA) tests. Although the thermal insulation function of EPS-block geofoam is not a primary concern for the function of lightweight fill, some knowledge of the geothermal properties of EPS is necessary to understand the issues of differential icing and solar heating that need to be considered during design of the pavement system.

Modern analysis and design methods for EPS-block geofoam as lightweight fill are based on explicit deformations of the geofoam mass. Therefore, the most important properties of block-molded EPS to test for are those related to the overall mechanical (stress-strain-time-temperature) behavior of an entire EPS block in compression as this is what will be loaded in the final embankment. However, given the typical dimensions of EPS blocks, precision testing of an entire block is not feasible on a routine basis although some testing of this nature is highly desirable as discussed subsequently. Therefore, any testing must be performed on specimens prepared from samples cut from blocks. Thus, there is always going to be some approximation or error involved in testing of such specimens, simply because what is being tested is not what is being placed in the actual fill. This approximation or error is not "fatal" or insurmountable. In fact, for most construction materials, whether natural (e.g., soil) or manufactured, only relatively small specimens relative to the final product are typically tested.

Compression

Introduction

Loading in unconfined uniaxial compression has been and remains the primary mode of loading for tests performed on EPS-block geofoam for both quality control and research purposes. This is because compression is by far the predominant mode of loading for EPS in load-bearing applications, including when used as lightweight fill. Thus, as indicated previously, the most important properties of block-molded EPS to test for are those related to the overall mechanical (stress-strain-time-temperature) behavior of an entire EPS block in compression as this is what will be loaded in the final embankment. Also, as indicated previously, blocks of EPS tend to have density gradients (variations) that are inherent in the manufacturing process. Therefore, the density of a relatively small specimen cut from a block can be significantly different than the gross density of the entire block and thus not representative of behavior of the entire block. This is significant as fundamental research has shown that the compressive behavior of block-molded EPS is most dependent on density (*7-11,16*).

Although research has been performed on the relative effect of specimen shape and dimensions on test results (*17*), studies where laboratory tests were performed on both small specimens and full-size blocks to evaluate the absolute difference in measured results is lacking. Additionally, there is also a lack of comparison between the deformation measurements of full-scale fills with calculated values. Both of these comparisons are required to better understand and predict the behavior of full size blocks.

Rapid Loading Testing

The primary variables to consider for rapid-loading tests are:

- test specimen shape,
- test specimen dimensions,
- test specimen age,
- use of strain versus stress controlled loading,
- loading rate,

- confining stress (if any) on the test specimen, and
- ambient temperature and relative humidity in the laboratory where the test is performed.

The effect of each of these variables on overall stress-strain behavior has been studied to varying degrees over the years. As a result, it is possible to draw some broad conclusions as to the relative effect of each of these variables. Although there is variation in practice for each of the above variables, there is a combination of variables that are most commonly used and thus can be viewed as the de facto standard against which other variations can be compared. The de facto standard is:

- Cube-shaped specimens 50 mm (2 in.) wide.
- Strain-controlled unconfined axial compression at a strain rate of 10 percent per minute.
- Standard laboratory conditions of approximately +23°C (73° F) and 50 percent humidity.

Using this combination of variables for reference, the observed variations in test variables and recommendations for practice are provided. As will be discussed, standardization currently does not exist for testing of EPS- block specimens. Standardization is recommended because test data from standardized testing procedures are needed in developing mathematical models for EPS behavior (*18*) and implementing the design methodology presented herein. Overall, there appears to be no compelling reason to deviate significantly from past practices until such time as fundamental research is performed to compare results between compression testing of full-size blocks versus relatively small laboratory test specimens. In an effort to develop guidelines for future testing, recommendations are provided for the following test variables to develop future standard test protocols.

- Specimen shape.

Observation: There has been a trend since about the 1980s toward occasional use of specimens that are right circular cylindrical in shape with dimensions similar to soil specimens used in triaxial tests, i.e. approximately 150 mm (5.9 in.) in height and 70 mm (2.75 in.) in diameter. Presumably this shape has been used to accommodate use of geotechnical laboratory testing equipment. Both the initial tangent Young's modulus and elastic limit stress for such specimens reportedly decrease compared to values measured using the de facto standard specimens (which would appear to be contradictory to the above statement that stiffness increases with increasing specimen size) (*19*). On the other hand, recent testing on cylindrical specimens of different dimensions (approximately 25 mm (1 in.) high and 60 mm (2.36 in.) in diameter which is similar to soil specimens used for oedometer (one-dimensional consolidation) tests showed no practical difference from the "standard" 50 mm (2 in.) cubes (*20*).

Recommendation: A square as opposed to circular cross-section is desirable to simplify trimming of test specimens from EPS samples taken from blocks. Care should be taken when preparing a test specimen, regardless of its shape and dimension. No surface of the specimen should include any portion of a face of the block from which the specimen sample was cut to avoid any localized edge effects. Experience indicates that a hot-wire cutter produces the cleanest and smoothest surfaces for test specimens so this method of cutting is recommended. The alternative using a fine-tooth band saw tends to leave a rougher surface.

- Specimen dimensions.

  Observation: Specimen thickness (height) appears to have relatively less influence than width on the compression test results. In general, as specimen dimensions increase so does the initial tangent Young's modulus, E_{ti}. Compression test results on 400 mm (16 in.) cubes and the typical 50 mm (2 in.)

cubes indicate that the larger specimens are approximately 50 percent stiffer compared to the smaller specimens at small strains (*17*). This suggests that an entire block might tend to behave stiffer than any small test specimen would indicate. However, this is speculative at this time and needs to be evaluated by detailed research. ASTM D 1621 (*21*) has been specified in the past for performing rapid-loading unconfined uniaxial compression tests. This test procedure allows the use of square or circular test specimens with a cross-sectional area ranging between 25.8 cm² (4 in.²) and 232 cm² (36 in.²). The specimen height can range from 25.4 mm (1 in.) to a maximum height no greater than the width or diameter of the specimen. Therefore, if cube-shaped specimens are utilized, specimens ranging in dimensions from 50 mm (2 in.) to 203 mm (8 in.) can be used per ASTM D 1621. One trend that appears to be developing in the EPS industry is to utilize specimens of increasing dimensions within the allowable ASTM D 1621 dimensions until the specimens meet the required compressive strength parameters. Therefore, it is recommended that determination of the uniaxial compression behavior between specimens of various sizes to full-size blocks be considered a high priority for future research.

Recommendation: The width of the specimen should be such that it can be accommodated by typical end platens used in geotechnical compression test machines. This suggests a 50 mm (2 in.) width which is just accommodated by the standard 71 mm (2.8 in.) diameter platen. With regard to specimen thickness (height), the thickest specimen possible should be used to increase the vertical displacement to achieve an axial strain of 1 percent. This is because the strain range of interest for most lightweight fill applications is focused on the region from 0 percent to 1 percent axial strain. The thicker the specimen the greater the precision in strain measurement for a fixed precision in deformation

measurement (as most test apparatus would be expected to have). In addition, any end effects are minimized with a thicker specimen. Of course, if the thickness-to-width ratio is too large inadvertent specimen buckling during testing could be a problem. Based on experience with triaxial compression tests on soils, a two-to-one height to width ratio should be used, which implies a 100 mm (3.9 in.) maximum specimen thickness.

A research project should be initiated to evaluate the possible switch to using test specimens that are 50 mm (2 in.) square in cross-section and 100 mm (3.9 in.) thick (high) with all other test variables unchanged. The measured properties of such specimens should be compared to those from 50 mm (2 in.) cubes for a range in EPS densities. In addition, there should be large-scale laboratory testing (most likely in a solid mechanics or structural engineering laboratory to be able to utilize large compression testing machines in an environment with the same temperature as a geotechnical laboratory) involving full-size blocks to compare the measured performance to that of both the 50 mm (2 in.) and 100 mm (3.9 in.) thick specimens.

- Specimen age.

  Observation: This variable has not been explored in any systematic or extensive research program. Assuming that the specimen is at least several days old so that the effects of molding have disappeared, there are indications that specimen age has no influence (*17*). There are some indications based on testing of EPS-block geofoam that had been in the ground for approximately 24 years that there was no significant difference in material behavior from that measured prior to installation (*22*). This also suggests excellent long-term durability of EPS-block geofoam.

Recommendation: A minimum specimen age is desirable to ensure that the test specimen has undergone at least most of its seasoning and facilitate comparison of test results. Based on informal discussions with EPS block molders in the U.S.A., it appears that for the pentane blowing agent content and mold sizes in common use, a minimum age of three days is sufficient.

- Strain rate.

  Observation: Not surprisingly for a polymeric material such as EPS, strain rate has a profound effect on the measured stress-strain behavior. The de facto standard rate of 10 percent per minute appears to be at the high end of the range used in past research. Rates one or more orders of magnitudes lower have been used at various times and by various researchers. It appears that stress-strain behavior under relatively small strains (the range of interest in lightweight fill applications) is most affected by strain rate (*17*), with the initial tangent Young's modulus either increasing or decreasing as strain rate is increased or decreased, respectively.

  Recommendation: There appears to be no compelling reason not to use a strain rate of 10 percent per minute for axial compression tests on EPS geofoam.

- Specimen confining stress.

  Observation: A relatively few number of researchers (e.g., (*23,24*)) have tried to emulate "true" triaxial compression testing of soils by subjecting right-circular-cylindrical specimens of EPS to an isotropic confining stress prior to increasing the axial stress. There does not appear to be any benefit from doing so as the horizontal confining stresses in roadway embankments are generally small in magnitude to the point of being negligible in most cases. In addition, there has been no systematic study that compares laboratory behavior of EPS and full-scale performance in lightweight fills to indicate that testing of EPS specimens that

includes a radial confining stress provides a more accurate estimate of EPS mechanical behavior.

Recommendation: There appears to be no compelling reason not to use unconfined compression tests to measure the compressive strength and initial tangent Young's modulus.

- Temperature.

  Observation: The vast majority of testing of EPS has been at the normal ambient laboratory temperature of +23°C ± (73°F±). Thus there has been relatively little study of the effect of temperature on the mechanical properties of EPS in the small-strain range of interest for lightweight fill applications and only slightly more testing of the effects at larger strains. However, existing data suggests stiffer geofoam behavior with decreasing temperature and softer behavior with increasing temperature compared to the de facto standard laboratory conditions. For example, data in (*25*) indicates that the initial tangent Young's modulus is either unchanged or slightly larger in magnitude under lower than ambient laboratory temperatures. Based on the present knowledge, there is insufficient information to incorporate temperature into any analysis or design procedure for EPS-block geofoam as lightweight fill.

  Recommendation: There appears to be no compelling reason not to use ambient conditions typical of most laboratories (+23°C ± (73°F±) and 50 percent ± humidity).

Compatibility with MQC/MQA Testing. If possible without compromising the goals of either research or manufacturing quality control and assurance testing, specimen and test parameters for the two areas of testing should be the same for both simplicity and comparison of results.

Monotonic. The most commonly performed test on EPS specimens involves strain-controlled compression loading at a relatively rapid rate, typically 10 percent per minute, with the load applied in a monotonically increasing fashion until a desired strain level is reached. Figure 2.1 illustrates the typical stress-strain response from such a test that was performed on a 50 mm (2 in.) cubic specimen and a strain rate of 10% per minute to an unusually large strain level (approximately 90 percent) to illustrate the entire range of EPS compression behavior. The test was performed on a block-molded EPS specimen with a density of 21 kg/m^3 (1.3 lbf/ft^3). However, the stress-strain response for other densities are qualitatively similar (*18*). The primary item of note is that the EPS does not fail in the traditional sense of other solid materials used in construction (metals, concretes, wood) by a physical rupture of the material. Nor does the EPS behave like soil or other particulate materials where inter-particle slippage occurs and a steady state or residual strength develops at large strains. Rather, the EPS essentially crushes one dimensionally (Poisson's ratio of EPS is discussed in detail subsequently) back to its original solid polystyrene state, and the behavior is continuously work (strain) hardening in nature.

The stress-strain behavior of EPS shown in Figure 2.1 can be divided into the following four zones (*18*):

- Zone 1: initial linear response.
- Zone 2: yielding.
- Zone 3: linear and work hardening in nature.
- Zone 4: non linear but still work hardening in nature.

Figure 2.1. Stress-strain behavior of 21 kg/m^3 (1.3 lbf/ft^3) EPS block under rapid, strain-controlled, unconfined axial compression (*18,26*).

The limit of Zone 1, i.e., the initial linear stress-strain behavior, extends to strains between 1 percent and 1.5 percent with the larger strain at the end of the linear region occurring with an increase in EPS density (*18*). An initial slightly curved, concave upward, response has

been observed within Zone 1 prior to the linear portion (*18*). However, it has been suggested that this curvature is the result of the testing equipment and procedures and not a fundamental characteristic of EPS (*18*). In particular, errors related to seating of the end platens due to surface irregularities of the test specimen introduced during trimming and mechanical slack in the loading system will introduce errors in the deformation measurements. These errors can be minimized by making deformation measurements directly on the test specimens with the use of extensometers (*18*). It is indicated in (*18*) that data in (*25*) suggests that the initial portion of the stress-strain curve is slightly curved, concave downward, in the 0 percent to 1 percent strain range even after correcting for seating effects. This appears to be similar to the small-strain behavior of soil. Research results in (*27*) suggest that behavior is linear only up to a strain level of about 0.5 percent.

In summary, the consensus that has evolved worldwide is that the stress-strain behavior of EPS-block geofoam is both linear and elastic up to a compressive strain of 1 percent. As a result, a new material parameter for EPS-block geofoam called the *elastic limit stress*, σ_e, has been suggested (*18*). This is defined as the compressive stress at 1 percent strain as measured in a standard rapid-loading compression test. Furthermore, the slope of the initial (approximately) linear portion of the stress-strain curve (see Zone 1) is defined as the *initial tangent Young's modulus*, E_{ti}.

As shown in Figure 2.2, for all practical purposes there is a linear empirical relationship between EPS density and E_{ti} assuming that the EPS is of appropriate quality (for the purposes of this proposal, material satisfying the provisional AASHTO standard included in Appendix C). The data shown in Figure 2.2 was obtained from (*17,28-31*) Equation (2.1) provides an average E_{ti} based on the data of Figure 2.2:

$$E_{ti} = 450\ \rho - 3000 \qquad \textbf{(2.1)}$$

where E_{ti} has units of kilopascals (kPa) and ρ = EPS density in kg/m^3.

From Hooke's law relation, $\sigma = (E_{ti})*(\varepsilon)$, where σ is the applied stress and ε is strain after stress application, Equation (2.1) can be extended to form an expression for the elastic limit stress at an axial strain of 1 percent that is sufficiently accurate for routine analysis and design purposes:

$$\sigma_e = (450\ \rho - 3000)*(0.01) = 4.5\ (\rho) - 30 \qquad \textbf{(2.2)}$$

where σ_e has units of kPa and ρ = EPS density in kg/m^3.

The data used to create Figure 2.2 and Equations (2.1) and (2.2) are based on testing relatively small specimens prepared from samples cut from full-size blocks of EPS. There is a lack of information at the present time concerning the stress-strain behavior of full-size EPS blocks although limited unpublished information suggests that full size blocks may be somewhat stiffer, i.e. have a larger initial tangent Young's modulus, than either Figure 2.2 or Equation (2.1) would imply.

Figure 2.2. Correlation between density and initial tangent Young's modulus for block-molded EPS (*18*).

Zone 2 of a typical stress-strain curve (see Figure 2.1) is called yielding. The zone of yielding is dependent on density and extends to strains between 3 percent and 5 percent (*18*). After the zone of yielding, the behavior is linear again. The radius of curvature inside the zone of yielding is dependent on the density of EPS but in general, the greater the density, the smaller (sharper) the radius of curvature and the smaller the strain at which linear post-yield behavior resumes (*18*).

Even though EPS loaded in compression does not fail in the traditional sense of a physical rupture and yielding occurs over a range of stresses, it has been and still is traditional nonetheless to define a material parameter called *compressive strength* of EPS, σ_c. Compressive strength of EPS is defined as the compressive stress at some arbitrary strain level. There is no universal agreement as to what this arbitrary strain level is. ASTM and most other standards organizations around the world define it as 10 percent so in this report the compressive strength

of EPS is given the notation σ_{c10}. This point on the stress-strain curve is shown in Figure 2.1. In Norway, where much of the early use of EPS-block geofoam occurred, the strain criterion used for σ_c is 5 percent.

Referring to Figure 2.1, it can be seen that there is nothing particularly noteworthy about a strain level of 10 percent (or 5 percent for that matter) other than that it occurs after a zone of initial yielding of the EPS. This is an important point because early geofoam design methods were based on compressive strength. In many ways, the use of a parameter called "strength" for EPS is unfortunate as it implies an ultimate condition (ULS type failure) involving material rupture. In fact, neither aspect is exhibited by EPS geofoam. Compressive strength increases linearly with increasing EPS density (*18*) and the following equation has been suggested (*18,32*):

$$\sigma_{c10} = 8.82\rho - 61.7 \quad \textbf{(2.3)}$$

where σ_{c10} = compressive strength using the 10 percent-strain criterion in kPa and

ρ = EPS density in kg/m^3.

As indicated previously, compressive strength occurs after a zone of initial yielding of the EPS and is defined at a strain level beyond the yield range. Therefore, a parameter called the "plastic stress" (σ_p) (*30*) or "yield stress" (σ_y) (*18*) has been proposed to define the stress corresponding to the onset of yielding. Figure 2.3 shows the definition of yield stress. The yield stress can be determined graphically or by the use of empirical equations. Graphically, the yield stress can be determined by forward extrapolation of the initial linear portion (Zone 1) and backward extrapolation of the post-yield linear portion of the stress-strain curve (Zone 3) as shown in Figure 2.3 (*18*). The stress at the intersection of the two lines is the yield stress. The following three empirical equations have also been suggested to estimate the yield stress (*18*):

$$\sigma_y = 6.41\rho - 35.2 \quad \textbf{(2.4)}$$

$$\sigma_y = 6.62\rho - 46.3 \quad \textbf{(2.5)}$$

$$\sigma_y = 6.83\rho - 48.4 \quad \textbf{(2.6)}$$

where σ_y = yield stress in kPa and

ρ = EPS density in kg/m^3.

Figure 2.3. Definition of yield (plastic) stress (*18*).

Figure 2.4 shows a comparison of the three empirical equations. Equation (2.4) was obtained from (*18,30*) and Equations (2.5) and (2.6) were obtained from (*18*). By definition the yield stress is less than the compressive strength. This is generally depicted in Figure 2.4 except for Equation (2.4) for low-density EPS. Thus, it is possible to estimate the yield stress from the recommended compression testing with sufficient accuracy in practice even if project-specific testing is not performed (*18*). In general, the magnitude of yield stress is approximately 75 percent of the magnitude of the compressive strength and the strain corresponding to the yield stress is approximately 1.5 percent, which is slightly greater than 1 percent which corresponds to σ_e, over a wide range of EPS densities (*18*).

Figure 2.4. Comparison of empirical relationships between yield stress and density for block-molded EPS (*18*).

As shown in Table 2.1, compressive strength varies with temperature (*18,32*).

The percentage (if any) of in-plant regrind and post-consumer recycled material and how it is fused into blocks may have varying affects on the compressive strength, elastic limit stress, and initial tangent Young's modulus in compression of block-molded EPS, especially the initial tangent Young's modulus (*2,3*). For example, tests have

Table 2.1. Compressive Strength Variation with Temperature (*18,32*).

revealed that EPS with an average density on the order of 16 kg/m^3 (1.0 lbf/ft^3) had virtually the same compressive strength with up to 50 percent regrind content yet the initial tangent Young's modulus was reduced by a factor of approximately two between samples with no regrind and 50

percent regrind (*33*). Figure 2.5 shows a qualitative description of the effect of regrind content on the small-strain region of the stress-strain region of EPS, which is the most critical region for load-bearing applications. Both the initial tangent Young's modulus and elastic limit stress decrease with increasing regrind content. However, the compressive strength is affected only slightly by regrind content.

Figure 2.5. Effect of regrind content on the stress-strain behavior of EPS-block geofoam (*4*).

Cyclic. For the purposes of this report, cyclic loading is defined as loads that are applied, removed, and reapplied in a fairly rapid and repetitive manner. Research to date indicates that as long as the maximum applied stress has a magnitude not exceeding the elastic limit stress, σ_e, there is:

- no plastic (permanent) strain upon stress removal and
- no degradation of the initial tangent Young's modulus with cyclic loading.

However, as shown in Figure 2.6, if the stress level goes beyond the elastic range there is both plastic deformation as well as a degradation of modulus. The latter can be seen by the progressive flattening of the unload-reload curves. Figure 2.6 is based on testing performed on a 50 mm (2 in.) cubical specimen with a density of 13 kg/m^3 (0.81 lbf/ft^3) subjected to rapid cycles of loading and unloading in the post-yield range, i.e., the applied stress exceeds the elastic limit stress (*18*). As shown in Figure 2.6, the average tangent Young's modulus of each unload-reload cycle is smaller than the initial tangent Young's modulus and decreases in magnitude with increasing strain. At very large strains, the unload-reload cycles become sharply curved as the EPS stiffens.

Figure 2.6. Cyclic load behavior for 13 kg/m^3 (0.81 lbf/ft^3) block-molded EPS (*18*).

The mechanical properties of EPS, including cyclic loading behavior, are dependent primarily on the shape of the polyhedra (*18,32*). As indicated in the manufacturing (molding)

section of this chapter, the pre-puff changes from spherical shape to a more polyhedral shape after the pre-puff is further expanded in the second step of the manufacturing process. Each face of a polyhedron represents a contact plane with an adjacent polyhedron. However, the contacts are not perfect and some void space may exist between polyhedra. Fusion between polyhedra occurs from the cooling of the softened polystyrene at these contact planes. Each polyhedron retains the numerous closed cells. The deformation of the polyhedra is elastic within the elastic range which is defined as axial strains up to approximately 1 percent. It is reported in (*18*) that research performed in (*31*) indicates that no change in the tangent Young's modulus occurred after 2 x 10^6 cycles of loading on a strain-controlled cyclic test between 0 percent and 1 percent strain on a specimen with a density of 20 kg/m^3 (1.25 lbf/ft^3). Beyond the elastic range, the cellular polyhedra undergo permanent shape change from polyhedral to ellipsoidal, with the short axis of the ellipsoids parallel to the direction of loading (*18*). This permanent change in shape is represented by plastic, non-recoverable, deformation and a lower tangent modulus.

In summary, cyclic loading, e.g., traffic loading, should not adversely impact the geofoam unless the maximum applied stress exceeds the elastic limit stress. These observations and conclusions concerning behavior under cyclic loads are based on testing relatively small specimens prepared from samples cut from full-size blocks of EPS. There is a lack of information at the present time concerning the cyclic loading behavior of full-size EPS blocks.

Poisson's Ratio. The following findings regarding the Poisson's ratio, ν, of EPS block are provided:

- Within the elastic range, ν is relatively small (of the order of 0.1) and often taken to be zero for practical design purposes, e.g. in the French national design manual (*34*). However, if a more accurate estimate of ν is desired, the following empirical relationship, which indicates that ν increases slightly with increasing EPS density, can be used:

$$\nu = 0.0056\,\rho + 0.0024 \quad \textbf{(2.7)}$$

where ρ = EPS density in kg/m^3. This equation is based on research performed in Japan (*19*).

- If an estimate of the coefficient of lateral earth pressure at rest, K_o, is desired, the following equation, which is valid for any elastic material, can be used:

$$K_0 = \frac{v}{1-v} \quad \textbf{(2.8)}$$

This means that under confined (at-rest) conditions horizontal stresses will be approximately one-tenth the vertical stresses, a fact that has been confirmed by full-scale case-history observations (*35*) and highlights a benefit of using EPS-block geofoam as backfill behind retaining structures.

- Beyond the elastic range, ν rapidly decreases to zero. For example, testing performed on EPS with a density of 20 kg/m^3 (1.25 lbf/ft^3) shows, ν decreases from 0.12 within the elastic range (strains between 0 percent and 1 percent) to 0.03 at a strain of 5 percent (*18,19*). In some tests necking of the test specimens (which implies a negative Poisson's ratio) has been observed (*32*).

The above observations and conclusions concerning Poisson's ratio are also based on testing relatively small specimens prepared from samples cut from full-size blocks of EPS. There is limited information available at the present time concerning the stress-strain behavior of full-size EPS blocks although case history observations, primarily in Norway, suggest that Poisson's ratio is indeed relatively small in magnitude compared to most other civil engineering materials.

Time-Dependent Behavior (Creep and Relaxation)

Introduction

Another area of research in recent years has been the time-dependent response of EPS-block geofoam to compressive loads. Five variables that affect the time-dependent behavior of EPS include density, stress, strain, time, and temperature (*18*). Only the time-dependent behavior

is discussed here. The temperature dependent behavior is discussed separately. Two time-dependent behaviors of EPS are:

- *Creep* which is the additional strain or deformation that occurs with time under an applied stress or load of constant magnitude.
- *Relaxation* which is the reduction in applied stress or load with time under a constant magnitude of strain or deformation.

For the function of lightweight fill, creep is the only time-dependent behavior of concern. Thus, relaxation will not be addressed here.

Testing

A review of published creep test results (*27,30,31,36-41*) performed for this study reveal a lack of a standard creep test method for geofoam. About the only common denominator in creep tests performed around the world to date is that they are almost always performed under ambient laboratory conditions of approximately +23°C (+73°F) and 50 percent humidity. In addition, there has been no direct comparison of creep tests performed using different combinations of test variables so an assessment of variable variation is impossible to conduct at the present time. It is recommended that a standard test method be developed for performing creep tests on EPS-block geofoam so creep models can be developed and reliably evaluated. The best that can be accomplished at this time is to discuss the test variations used in practice and make recommendations based on judgment and indirect comparative testing.

The primary variables that need to be considered for creep tests are:

- test specimen shape,
- test specimen dimensions,
- test specimen age,
- applied stress level,
- confinement of the test specimen,

- test duration, and
- ambient temperature in the laboratory where the test is performed.

Using the above list of variables for reference, the observed variations in test variables and recommendations for creep testing in practice are as follows:

- Specimen shape and dimensions. Specimen shapes that have been reported in the literature include a cube, right-circular cylinder, and disc. Cube-shaped specimens are typically 50 mm (2 in.) cubes. Right-circular cylinder specimens with heights of 38, 50, 200, and 300 mm (1.5, 2, 8, and 12 in.) and diameters of 76, 50, 100, and 150 mm (3, 2, 4, and 6 in.), respectively, have been utilized. Disc-shaped specimens typically replicate the dimensions of soil oedometer (one-dimensional consolidation) test specimens (i.e., 25 mm (1 in.) thick and 65 mm (2.5 in.) ± in diameter). Figure 2.7 shows creep test results from three different specimen sizes with a density of 20 kg/m³ (1.25 lbf/ft³) tested at a sustained stress of 20 kPa (417 lbs/ft²). These results as well as comparisons made from specimens tested at stresses of 30 and 50 kPa (625 and 1,045 lbs/ft²) indicate that disc shaped specimens may yield higher creep strains than cylindrical specimens.
- Specimen age. This has not been studied but it is desirable that all specimens in a given suite of tests (creep tests tend to be performed in groups or suites of tests on EPS of the same density and subjected to different stress levels) have the same age and, in fact, be prepared from samples taken from the same EPS block. As an absolute standard, it appears that the minimum specimen age of three days as for rapid-loading compression tests is appropriate for creep tests as well.

Figure 2.7. Comparison of laboratory compression creep test data for an EPS density of 20 kg/m^3 (1.25 lbf/ft^3) and applied stress of 20 kPa (417 lbs/ft^2) and the creep equations. (*42*)

- Applied stress level. This will be dependent on the stress that the EPS-block will be subjected to in the particular load-bearing application.
- Specimen confinement. When geotechnical oedometer equipment is used, tests have been performed both with and without the metal confinement ring although no direct comparison of results has been reported. Given the relatively small magnitude of the Poisson ratio of EPS under small strains, the results between the two test protocols are expected to be similar. However, the unconfined test is arguably more representative of actual conditions; should yield somewhat greater deformations (and thus be more conservative); is easier to perform; and removes concern over friction between the EPS specimen and ring. Thus, unconfined creep tests are recommended.
- Test duration. This parameter has seen the greatest variation in practice. Many early creep tests only lasted several hundred hours. It is now recognized that this is inadequate and can produce potentially misleading results as tertiary creep can be totally missed (*39*). As a result, 10,000 hours (approximately 13 months) is now considered to be the absolute minimum test duration with 15,000 hours (approximately 20 months) or more preferred (tests in excess of 19,000 hours (approximately two years) have been performed). The justification for these longer duration tests is that it is believed that the creep performance of EPS can only be projected for 30 times the creep test duration which is somewhat more generous than the factor of 10 suggested for polymeric geosynthetics in general (*43*). This suggests that creep test durations of at least 15,000 hours (20 months) is required using the extrapolation factor of 30 for a 50-year design life (which is not unreasonable for a geotechnical highway structure).

- Temperature. Little creep testing has been conducted at temperatures other than de facto standard laboratory conditions. Creep at temperatures greater than +23°C± (73°F±) has been found to accelerate with increasing temperature.
- Specimen Preparation. The same care in specimen preparation discussed previously for rapid-loading compression tests is recommended for creep tests.

The general time-dependent behavior of EPS is similar to other engineering materials and exhibits primary, secondary, and tertiary creep as shown in Figure 2.8. Creep tests on EPS-block geofoam are typically depicted as shown in Figure 2.9. However, experience indicates that the most useful way to portray creep-test data is by constructing a family of isochronous stress-strain relations for tests performed on EPS specimens of the same density. An isochronous curve is the estimated stress-strain behavior for a range of applied stresses for a specific duration of time. Figure 2.10 illustrates a typical family of isochronous stress-strain curves together with a portion of the standard rapid-loading compression test for comparison. However, the approximate stress-strain relation for the standard rapid loading compression test and the isochronous curves are not strictly comparable because they represent different loading conditions of sustained versus constantly changing load (*18,44*). Isochronous stress-strain curves for different durations of loading are useful in geotechnical applications where sustained loads are typically involved (*18*).

Figure 2.8. Regions of behavior in creep (*45*).

Figure 2.9. Results of typical unconfined axial compression creep tests on block-molded EPS (*18*).

Figure 2.10. Isochronous stress-strain curves for 23.5 kg/m^3 (1.47 lbf/ft^3) block-molded EPS based on unconfined axial compression creep tests (*18,26*).

Constitutive Modeling of the Stress-Strain-Time Behavior of EPS

Introduction. Two time-dependent stress-strain (creep) models that have been suggested for predicting the vertical strain or deformation of EPS blocks that occurs under an applied stress

include the general power-law equation and the Findley equation (*39*). An initial overview of the theory and application of both equations is presented. The total vertical strain predicted by these two equations consist of two components as shown below.

$$\varepsilon=\varepsilon_o+\varepsilon_c \quad \textbf{(2.9)}$$

where ε = total strain at some time period t after stress application,

ε_o = immediate strain upon stress application, and

ε_c = time-dependent strain (creep) at some time period t after stress application.

Based on the assumption that ε_o is linear-elastic and based on empirical relationships established through laboratory creep-test data, the Laboratoire Ponts et Chaussess (LCPC) derived the following General Power-Law equation for the total strain of EPS blocks (*30,39*):

$$\varepsilon=\left(\frac{\sigma}{E_{ti}}\right)+0.00209\left(\frac{\sigma}{\sigma_p}\right)^{2.47}\left(t^{\left\{-0.9\log_{10}\left[1-\left(\frac{\sigma}{\sigma_p}\right)\right]\right\}}\right) \quad \textbf{(2.10)}$$

where ε = total strain at some time period t after stress application (in decimal form, not as a percent),

σ = applied stress in kPa,

σ_p = plastic stress of EPS in kPa,

E_{ti} = initial tangent modulus in kPa, and

t = time in hours after stress application.

The LCPC established the following two empirical relationships based on laboratory testing to facilitate use of Equation (2.10):

$$\sigma_p = 6.41\rho - 35.2 \quad \textbf{(2.11)}$$

$$E_{ti} = 479\rho - 2875 \quad \textbf{(2.12)}$$

where σ_p = plastic stress in kPa,

E_{ti} = initial tangent modulus in kPa, and

ρ = EPS-block geofoam density in kg/m^3.

However, it was found in (*39*) that Equation (2.12) yields values of initial tangent modulus that are higher than typically reported in the literature. The consequence of using Equation (2.12) to estimate the initial tangent modulus is discussed subsequently. Equation (2.1), which is based on averaging other published relationships by (*18*) can also be used to estimate E_{ti}.

The Findley equation (*46,47*) is also used to predict the total time-dependent vertical strain of geofoam. The Findley equation has been modified by (*39*) based on creep test results that extend for nearly 19,000 hours (2.2 years) as shown below:

$$\varepsilon = 1.1\sinh\left(\frac{\sigma}{54.2}\right) + 0.0305\sinh\left(\frac{\sigma}{33.0}\right)(t)^{0.20} \qquad \textbf{(2.13)}$$

where ε = total strain at some time t after a stress application (in percent),

σ = applied stress in kPa, and

t = time in hours after stress application.

Equation (2.13) is based on three tests performed on 50 mm (2 in.) cube-shaped EPS specimens with a density of 20 kg/m^3 (1.25 lbf/ft³) at stresses of 30, 40, and 50 kPa (625, 835, and 1,045 lbs/ft²). Therefore, the modified Findley equation, i.e., Equation (2.13), is applicable to EPS block with a density of 20 kg/m^3 (1.25 lbf/ft³) subjected to stresses between 30 and 50 kPa (625 and 1,045 lbs/ft²). The applicability of Equation (2.13) at stress levels not between 30 and 50 kPa (625 and 1,045 lbs/ft²) is investigated herein to determine the potential benefit of refining Equation (2.13) so that it can be used for other stress levels. Both the general power-law and modified Findley equations will be compared with laboratory measured results on full-size EPS blocks to assess their accuracy.

Laboratory Creep Tests. As indicated previously, there is a lack of a standard creep test method for geofoam. Therefore, a qualitative, not quantitative, comparison is made between

published laboratory creep test results and the calculated strain values derived from the general power-law and modified Findley equations to assess the accuracy of these equations.

Figures 2.7 and 2.11 provide a qualitative comparison between various size EPS specimens with a density of 20 kg/m^3 (1.25 lbf/ft³) at stresses of 20 kPa (417 lbs/ft²) and 70 kPa (1,460 lbs/ft²) and the calculated results based on the general power-law and the modified Findley equations. The laboratory test results shown in these figures are limited to specimens with a density of 20 kg/m^3 (1.25 lbf/ft^3) and to stress levels of 20 kPa (417 lbs/ft²) and 70 kPa (1,460 lbs/ft²) because this is the density and stress range of EPS blocks that are used in the full-size block and full-scale model tests. Laboratory test data utilized in deriving the general power-law and modified Findley equations are not shown to provide non-bias comparisons. At the lower stress level of 20 kPa (417 lbs/ft²), see Figure 2.7, both equations predict strains that are in agreement with the measured values from cylindrical EPS specimens. However, the modified Findley equation predicts slightly larger strains than the general power-law equation. Neither equation predicts strains near the measured values obtained on a disc-shaped specimen at an applied stress of 20 kPa (417 lbs/ft²). A disc-shaped specimen is usually used when creep testing is performed with an oedometer, which is typically used to simulate one-dimensional compression of soils in the laboratory. At the higher stress level of 70 kPa (1,460 lbs/ft²), see Figure 2.11, the power-law equation and the modified Findley equation predict larger and smaller total strains, respectively, than the measured values. It is indicated in (*36*) that the creep test was performed with a standard consolidation test machine. Thus, it can be inferred that a disc-shaped specimen typically used in soil oedometer (one-dimensional consolidation) testing, which is typically on the order of 25 mm (1 in.) thick and 65 mm (2.5 in.) ± in diameter, was used.

The general power-law equation indicates a relationship between the time-dependent behavior of EPS and the plastic stress and initial tangent modulus, see Equation (2.10). Therefore, it is recommended that compressive strength tests be performed on similar specimens that will be used for creep testing so values of plastic stress and initial tangent modulus can be obtained from

the same test sample. It is also recommended that the elastic-limit stress be determined from compressive strength tests because, as will be discussed later, the elastic-limit stress may be a useful guide for estimating the onset of significant creep effects (*18*). It is also recommended that axial strain data be obtained immediately upon stress application and frequently for the first hour after load application to better estimate the immediate strain, $\varepsilon_{o,}$ (*39*). A good estimate of ε_o is critical to estimating the total strain because ε_o contributes more to the total strain than the creep-induced strain, ε_c.

Full-Size EPS Block Creep Test. A full-size block with a density of 20 kg/m^3 (1.25 lbf/ft^3) and dimensions of 1.5 m (4.9 ft) by 1 m (3.3 ft) by 0.5 m (1.6 ft) was loaded under a stress of 71 kPa (1,480 lbs/ft^2) for 61 days (*48*). A stress of 27 kPa (564 lbs/ft^2) was initially applied for four days. An additional stress of 19 kPa (397 lbs/ft^2) (total stress equal to 46 kPa (961 lbs/ft^2)) was applied for seven days and an additional stress of 25 kPa (522 lbs/ft^2) (total stress equal to 71 kPa (1,483 lbs/ft^2)) was applied for 50 days. The stress at the bottom of the block was

Figure 2.11. Comparison of compression laboratory creep test data for an EPS density of 20 kg/m^3 (1.25 lbf/ft^3) and applied stress of 70 kPa (1,460 lbs/ft^2) and the creep equations.

measured using seven pressure cells and an average pressure of 34, 55, and 79 kPa (710, 1,149, and 1,650 lbs/ft^2) was measured in the pressure cells for days 1 through 5, 5 through 12, and 12 through 62, respectively. These average stresses are used in calculating the vertical strains using the power-law and modified Findley equations.

Figure 2.12 shows a comparison between the calculated and measured total strains for compressive stresses of 34, 55, and 79 kPa (710, 1,149, and 1,650 lbs/ft^2). At the initial stress levels of 34 and 55 kPa (710 and 1,149 lbs/ft^2), both the general power-law and modified Findley equations predict total strains that are in agreement with the measured strains. At the largest stress of 79 kPa (1,650 lbs/ft^2), the power-law equation significantly overestimates the measured strains

and the modified Findley equation underestimates the measured strains. However, the modified Findley equation provides the best agreement with the measured values especially as the time, t, increases.

Full-Scale Model Creep Test. A full-scale model creep test was performed at the Norwegian Road Research Laboratory (*48,49*) to investigate the time-dependent performance of EPS-block geofoam. The test fill had a height of 2 m (6.6 ft) and measured 4 m (13.1 ft) by 4 m (13.1 ft) in plan at the bottom of the fill decreasing in area with height approximately at a ratio of 2 (horizontal) to 1 (vertical) to about 2 m (6.6 ft) by 2 m (6.6 ft) at the top of the fill. A load of 105 kN (23.6 kips) was applied through a 2 m (6.6 ft) by 1 m (3.3 ft) plate at the top of the fill resulting in an applied stress of 52.5 kPa (1,096 lbs/ft²). The fill consisted of four layers of full-size EPS blocks with dimensions 1.5 m (4.9 ft) by 1 m (3.3 ft) by 0.5 m (1.6 ft) and densities of 20 kg/m^3 (1.25 lbf/ft³).

Figure 2.12. Comparison of full-size EPS block creep test data and the creep equations for an EPS density of 20 kg/m^3 (1.25 lbf/ft³) and an applied stress of 34 kPa (710 lbs/ft^2) for days 1-5, 55 kPa (1,149 lbs/ft^2) for days 5-12, and 79 kPa (1,650 lbs/ft^2) for days 12-62.

The stress at the bottom of the fill was measured using four pressure cells. An average pressure of 7.8 kPa (163 lbs/ft²) was measured in the pressure cells during the 1,270 day test. Based on this average pressure measured at the bottom of the test fill and the stress of 52.5 kPa (1,096 lbs/ft²) applied at the top of the fill, the stress distribution within the EPS fill was approximately 1 (horizontal) to 1.8 (vertical). This is in agreement with a stress distribution of 1 (horizontal) to 2 (vertical), which is typically assumed in design calculations incorporating EPS-block geofoam structures. The measured stress distribution is slightly wider but still in agreement with 1 (horizontal) to 2 (vertical). Thus, the measured stress with depth is slightly less than the typically assumed stress distribution, which results in a slightly conservative design when a 1 (horizontal) to 2 (vertical) stress distribution is assumed. Therefore, it is recommended that a 1

(horizontal) to 2 (vertical) stress distribution be utilized in design calculations for EPS-block geofoam embankments.

Figure 2.13 shows a comparison of the total strain measured in the EPS blocks of the full-scale test fill and the calculated total strains based on the power-law and modified Findley equations. In calculating the total strains, the fill was divided into the same number of horizontal layers as EPS block layers used, four. The total strain of each layer was determined based on the average stress calculated at the middle of each block using the measured 1 (horizontal) to 1.8 (vertical) stress distribution. Thus, the stress used for each layer from top to bottom was 36.2, 20.4, 13.1, and 9.1 kPa (756, 426, 274, and 190 lbs/ft²). As indicated in Figure 2.13, both the general power-law and modified Findley equations underestimate the strains measured in the full-scale test fill. The power-law predictions are lower than the modified Findley predictions and thus the Findley equation provides the best agreement.

Figure 2.13. Comparison of full-scale model creep test data and the creep equations for an EPS density of 20 kg/m^3 (1.25 lbf/ft³).

Full-Scale Field Monitoring. A field monitoring program was implemented as part of the Løkkeberg bridge project built in Norway in 1989 (*48,49*). EPS blocks were used to construct a bridge approach embankment and to support the bridge foundation. Pressure cells were installed at various locations within the embankment and settlement monitoring rods were installed at four locations to measure the total settlement of the embankment and the vertical strains at various depths in the embankment. The height of the embankment is 4.5 m (14.7 ft). EPS blocks with an unconfined compressive strength of 240, 180, and 100 kPa (5,012, 3,759, 2,089 lbs/ft²), were used in the top 1.2 m (3.9 ft), middle, and bottom 2.1 m (6.9 ft) of the embankment, respectively. A 10 cm (3.9 in.) concrete slab was placed between the 180 and 100 kPa (3,759 and 2,089 lbs/ft²) blocks to further distribute the stresses within the 100 kPa (2,089 lbs/ft²) blocks.

Figure 2.14 shows the total vertical strain measured in the lowest block layer. The density of the bottom row of EPS blocks is 20 kg/m^3 (1.25 lbf/ft³) and the original thickness of the EPS

blocks is 0.6 m (2 ft). Three pressure cells were installed below the first row of blocks. An average pressure of 67 kPa (1,399 lbs/ft²) was recorded in the three pressure cells during the period that the vertical strain was being obtained from the settlement rods. As shown in Figure 2.14, the power-law and modified Findley equations significantly overestimate and underestimate the measured total strains, respectively. However, the total strains predicted by the modified Findley equation are again in better agreement with the measured values than the power-law equation.

Figure 2.14. Comparison of total vertical strain measured in the lowest EPS block layer of the field test fill and the general power-law and modified Findley equations.

Summary of Comparison of Measured and Calculated Values of Total Strain. For stresses between 10 and 55 kPa (209 and 1,149 lbs/ft²), both the power-law and modified Findley equations yield total strain values similar to or less than the measured values obtained on the full-size block and full-scale creep test fills. In general, the power-law equation predicts total strains smaller than the modified Findley equation for compressive stresses between 10 and 55 kPa (209 and 1,149 lbs/ft²). A similar observation was made in (*39*). In (*39*) it is suggested that the power-law equation predicts smaller total strains than laboratory measured values, especially for short time durations, because the test specimens used by the LCPC to derive the power-law equation yield larger values of initial tangent modulus than other specimens reported in the literature. This is apparent by comparing Equations (2.12) and (2.1). It is also suggested in (*39*) that the values of E_{ti} obtained from the LCPC relationship in Equation (2.12) are approximately 40 percent larger than the values from Equation (2.1), which is based on averaging other published relationships. In summary, the modified Findley equation is recommended to predict total vertical strains for compressive stresses between 10 and 55 kPa (209 and 1,149 lbs/ft²). Further refinement of the modified Findley equation for stresses outside the 30 to 50 kPa (627 and 1,044 lbs/ft²) stress range that was used in developing the equation may result in better predictions.

At larger compressive stresses of 67, 70, and 79 kPa (1,399, 1,462 and 1,650 lbs/ft²), the total strains determined by the power-law equation and the modified Findley equation significantly overestimate and underestimate, respectively, the measured full-size block and full-scale test fill values. The modified Findley equation provides better agreement than the power-law equation, especially as the elapsed time increases. Further refinement of the modified Findley equation for stresses outside 30 to 50 kPa (627 to 1,044 lbs/ft²) stress range that was used in developing the equation may result in better predictions. As noted in (*39*), the power-law equation may provide unusually high strain values at large compressive stresses, especially at longer durations of applied stress, because the power-law equation was developed from creep tests of insufficient duration. This results in greater strains because the total strains decrease with increasing elapsed time as shown in Figures 2.7 and 2.11 through 2.14.

The time-dependent behavior obtained on one layer of blocks in the full-scale field test is similar to the behavior obtained during the full-size block test. After a time equal to 1,440 hours (60 days), the difference in total strain measured was approximately 3.2 percent, with the full-size block test producing the larger total strain because the average total stress measured in the full-size block test was 79 kPa (1,650 lbs/ft²) compared to 67 kPa (1,399 lbs/ft²) for the full-scale field test. Therefore, it appears that creep tests based on a full-size EPS block may provide reasonable predictions of total vertical strain with time for full-scale projects utilizing EPS-block geofoam as lightweight fill. This reduces the need for constructing full-scale model test fills to develop time-dependent data and validate or modify existing creep models. Therefore, a standard test method could be developed either using a full-size block or comparing the results from smaller specimens with the results of full-size blocks.

At present, the general power-law and modified Findley equations do not provide a reliable estimate of the time-dependent total strains. Further research is required to either refine these expressions or develop new expressions based on other creep models. In particular, the power-law equation should be refined to include results from specimens with lower values of E_{ti}

and tests of longer duration. The modified Findley equation should be refined to include test results from compressive stresses outside the 30 to 50 kPa (627 to 1,044 lbs/ft²) stress range that was used to develop the relationship.

The results of the full-scale model test conducted at the Norwegian Road Research Laboratory indicates that the typically assumed 1 (horizontal) to 2 (vertical) distribution of compressive stresses through a geofoam embankment is reasonable, albeit slightly conservative because the measured stress showed a stress distribution of 1 (horizontal) to 1.8 (vertical), for design calculations.

Temperature – Dependent Behavior

Introduction. In general, the stress-strain behavior of polymeric materials, such as EPS-block geofoam, is temperature dependent (*50*). Available information suggests that very little creep testing of EPS block has been conducted at temperatures other than ambient in a typical laboratory environment (+23°C± (+73°F±). The limited testing at elevated (relative to typical laboratory) temperatures indicates that the behavior of EPS block is consistent with trends of polymeric materials in general, i.e. creep rates increase with increasing temperature. The data shown in Table 2.2 and discussed in (*18*) shows this trend.

Table 2.2. General Temperature-Dependent Behavior for EPS (*18*).

A likely reason for the lack of creep tests at elevated temperatures is the fact that most EPS-block geofoam applications were, until the 1990s, in relatively cool Northern Hemisphere locations where annual average air temperatures are of the order of +5°C (+41°F) to +15°C (+59°F) maximum. Creep at these temperatures would be expected to be somewhat less than at ambient laboratory temperatures and long-term case history observations (mostly from Norway) confirm that.

Constitutive Modeling of the Stress-Strain-Time-Temperature Behavior of EPS. The availability of a mathematical model for the stress-strain-time-temperature behavior for EPS is

currently unavailable. Such a model would be useful in practice to estimate creep behavior beyond the duration of creep tests. The variables of test duration and temperature are of particular interest for future improvements in test protocols. Consideration should be given to using time-temperature superposition procedures or a combination of both conventional testing procedures and time-temperature superposition procedures (stepped isothermal methods) to measure creep behavior. These alternate methods have been used to study creep behavior of other geosynthetic materials (*43*) and can accelerate acquisition of meaningful creep data. The resulting creep data could be used to develop a stress-strain-time-temperature mathematical model for EPS block. Such a model would enable better predictions of creep strains at temperatures other than the conventional laboratory ambient conditions.

Recommended Procedure for Considering Creep Strains

The current state of practice for considering creep strains in the design of EPS block embankments and bridge approaches is to base the design on laboratory creep tests on small specimens trimmed from the same EPS block that will be used in construction or to base the design on published observations of the creep behavior of EPS such as:

- If the applied stress produces an immediate strain of 0.5 percent or less, the creep strains, ε_c, will be negligible even when projected for 50 years or more. The stress level at 0.5 percent strain corresponds to approximately 25 percent of the compressive strength defined at a compressive normal strain of 1 percent or 33 percent of the yield stress.
- If the applied stress produces an immediate strain between 0.5 percent and 1 percent, the geofoam creep strains will be tolerable (less than 1 percent) in lightweight fill applications even when projected for 50 years or more. The stress level at 1 percent strain corresponds to approximately 50 percent of the compressive strength or 67 percent of the yield stress.

- If the applied stress produces an immediate strain greater than 1 percent, creep strains can rapidly increase and become excessive for lightweight fill geofoam applications. The stress level for significant creep strain corresponds to the yield stress which is approximately 75 percent of the compressive strength.

The approximate compressive strengths indicated above are based on empirical relationships. Compressive strength, which is dependent on the strain level, e.g., 5 percent or 10 percent, does not provide fundamental knowledge into the creep behavior of EPS because it is determined in a rapid load compression test (*18*). It should be noted that material stressed at or near the compressive strength will exhibit large creep deformations almost immediately (*18*). Therefore, to produce acceptable strain levels in lightweight fill applications, stress levels must be kept low relative to compressive strength. This is illustrated in Figure 2.10. Lower density EPS tends to creep more than higher density EPS at the same relative stress level defined as the same fraction of the yield stress or compressive strength with creep effects increasing significantly for EPS with a density equal to or less than 16 kg/m^3 (1 lbf/ft^3) (*18*).

In summary, the compressive stress at a vertical strain of 1 percent, i.e., the elastic-limit stress, appears to correspond to a threshold stress level for the development of significant creep effects and the field applied stresses should not exceed the elastic-limit stress until more reliable creep models are developed (*18*). Based on these observations, it is concluded that creep strains within the EPS mass under sustained loads are expected to be within acceptable limits (0.5 percent to 1 percent strain over 50 to 100 years) if the applied stress is such that it produces an immediate strain between 0.5 percent and 1 percent (*18*).

Tension

Although tensile loading generally does not occur when EPS block is used in geofoam applications, tensile loading is an important mode of loading for evaluating EPS fusion, a manufacturing quality parameter. Thus, tensile loading can be an important MQC/MQA test. However, tensile testing is not typically performed because of the difficulty in fabricating the

hourglass-shaped test specimens required for tensile testing per the ASTM C 1623 standard test method (*51*) and the availability of other types of tests (most notably flexure which is discussed subsequently) that essentially test for the same behavior and are easier to perform. Laboratory tests for tensile loading are performed at a standard speed of testing such that rupture occurs in 3 to 6 min. Tensile strength is defined as the tensile stress at which physical material rupture occurs.

Figure 2.15 illustrates the linear relationship between tensile strength and EPS density. Also shown for comparison is the relationship for compressive strength using the ASTM criterion of 10 percent strain. The tensile strength data shown in Figure 2.15 was obtained from (*52*) which did not indicate strain rate, specimen dimensions, or the magnitude of axial strain at which tensile failure occurred (*18*). No test data was located concerning long-term tensile behavior of EPS (*18*).

Flexure

Although tensile strength is the fundamental indicator of EPS fusion and thus a useful MQC/MQA parameter, the test itself is somewhat cumbersome as discussed in the previous section. As a result, flexural tests on beam-shaped specimens are typically performed for testing the tensile strength of EPS. The relevant ASTM standard, ASTM C 203 (*53*), test setup used is such to produce maximum bending moment and, therefore, maximum tension in the extreme bottom fiber of the EPS beam. A beam-type specimen on the order of 100 mm (4 in.) wide, and 300 mm (12 in.) long, and 25 mm (1 in.) thick is subjected to transverse load (*18*). However, the test method also provides recommended test specimen sizes based on the geometric setup of the test apparatus. As with other basic tests, the loading rate to failure (physical rupture of the EPS beam) is fairly rapid. The ASTM test method allows for some variation in strain rates (*18*). The flexural strength is defined as the calculated maximum-fiber stress at the time of rupture of the specimen (*18*). As can be seen in Figure 2.15, flexural strength correlates well with tensile strength which validates the assumption that flexural tests can be used routinely as a measure of bead fusion during the manufacture of EPS. No information is available regarding actual

specimen dimensions and strain rates used to obtain the data in Figure 2.15. No long-term test data is known to exist for the flexure mode of loading (*18*).

Figure 2.15. Strength of block-molded EPS in various test modes as a function of density (*18*).

Shear

Introduction

There are two modes of shear that are of interest:

- internal shear strength within a specimen of EPS and
- external shear strength (sliding resistance) between EPS blocks or between an EPS block and a dissimilar material (soil, other geosynthetic, etc.).

These modes of shear are discussed separately.

Internal

The internal shear strength of EPS is measured by loading a test specimen fairly rapidly until the maximum shear stress is reached, whether or not this stress produces a physical rupture of the test specimen. ASTM test method C 273 (*54*) addresses internal shear strength of geofoam. However, this standard test method addresses the testing of cores of structural "sandwiches" or composites (*18*). The correlation between shear strength of EPS block and EPS density is shown in Figure 2.15. The test values for shear strength were obtained by (*18*) from (*29*). Specimen dimensions and testing strain rate are not provided in (*18*). Because the shear strength of EPS block exhibits a correlation with compressive strength, experience indicates that the shear strength test is rarely performed in practice for either MQC/MQA or engineering design.

External

Introduction to External (Interface) Properties. Interface friction, primarily along horizontal surfaces, is an important consideration in external and internal stability assessments under horizontal loads such as wind, unbalanced water head, or seismic shaking. Thus, tests to

assess interface friction between the surface of EPS blocks and a variety of other materials is of interest in projects where significant horizontal design loads or internal sliding can occur. Two types of interfaces that are of interest for EPS-block geofoam in lightweight fill applications include an EPS/EPS interface and an EPS/dissimilar material interface.

EPS/EPS Interface. The interface friction between two pieces of EPS has been studied by a number of researchers (*19*). Unfortunately, the lack of a standard test method has meant that a range of test variables (specimen size, specimen preparation, smoothness of specimen surface, test setup, loading rate, etc.) have been used. In particular, a large effect on the EPS/EPS interface strength is the smoothness of the EPS surface. The smoothest surface is obtained from a relatively smooth molded face of a full-size block and the roughest from a piece of EPS cut from a block.

Although there is no standard method for EPS/EPS interface tests, the typical procedures that have been used involve placing two pieces of EPS in contact along a single horizontal surface; subjecting the contact to a vertical normal stress; then horizontally shearing one piece of EPS (typically the upper one) relative to the other while measuring the horizontal displacement and force required for movement, which is similar to direct shear testing (ASTM D 5321) in soils and geosynthetics testing.

Based on a review of existing shear strength data between two pieces of EPS (*19*), the shearing resistance can be defined adequately by the classical Coulomb (dry) friction equation:

$$\tau = \sigma_n * (\mu) = \sigma_n * (\tan\delta) \qquad \textbf{(2.14)}$$

where τ = interface shear resistance,

σ_n = applied normal stress on interface,

μ = friction coefficient = tan δ, and

δ = EPS/EPS interface friction angle.

When the interface shear resistance, τ, is plotted against normal stress, a linear relationship indicative of a classical Coulomb behavior is obtained. The data does not show a

post-peak strength loss and thus a residual interface friction angle is not reported. Previous testing also indicates that the value of δ is independent of EPS density because shearing occurs on the surface of the specimen, although the normal stress is assumed to be low enough that excessive deformation of the EPS did not occur (*19*).

Because of variations in specimen dimensions, displacement rate, roughness of the EPS surfaces, and other factors, a range in EPS/EPS interface friction angles have been reported. All reported values fall within the range between $\mu = 0.5$ to 0.7, with $\mu = 0.64$ the value reported in the most extensive and detailed published study to date that was performed in Japan (*19*). The corresponding values of δ are 27 degrees to 35 degrees with $\delta = 32$ degrees found for the Japanese study (*19*). For routine design, it is recommended that $\delta = 30$ degrees be used.

As indicated by Equation (2.14), shear stress is dependent on the applied normal stress. The normal stress that will act between blocks of EPS for lightweight fill applications will typically be small (*18*). Therefore, the corresponding shear resistance between blocks will also be small. Consequently, the use of mechanical connectors are sometimes required to increase the shear resistance between blocks. The use of mechanical connectors is discussed in Chapter 6.

In view of the lack of a standardized test protocol, it is recommended that the standard test method for geosynthetic interface friction, D 5321 (*55*) be adopted for determining the EPS/EPS interface friction. However, ASTM D 5321 allows other direct shear devices (ASTM D 3080 (*56*)) to be used for geosynthetic shear testing if the device yields similar results as the large-scale direct shear box. It should be further required that test specimens should be prepared so that shearing occurs only along the relatively smooth molded exterior surfaces of the EPS block to produce a conservative estimate of the interface friction angle. The surfaces of the EPS also should be free of any small indentations or projections that can be created by the walls of the steel block mold.

EPS/Dissimilar Material Interfaces. A significant gap in the published literature exists for interface friction values between EPS block and other materials likely to be encountered in lightweight fills such as planar geosynthetics (chiefly geotextiles and geomembranes) as well as poured-in-place portland cement concrete (PCC).

Two locations within the embankment where these dissimilar materials may be utilized include as a separation layer between the pavement system and the EPS blocks and as a separation layer between the EPS blocks and the natural foundation soil. The use of separation materials between the top of the EPS blocks and the overlying pavement system is discussed in Chapter 4. Materials that are sometimes utilized between the pavement system and the EPS blocks include a geotextile, geomembrane, a PCC slab, geogrid, geocell with soil or PCC fill, soil cement, and pozzolanic stabilized materials. Materials that are sometimes utilized between the EPS blocks and the natural foundation soil include granular material such as sand and geotextiles.

The only published data on interface friction with dissimilar materials involves EPS/sand interfaces and the results indicate that δ equals the Mohr-Coulomb angle of internal friction (ϕ) of the sand (*57,58*). Whether this is the peak or constant-volume (critical state) value of ϕ for the sand was not identified. However, it appears reasonable that the choice would depend on the relative magnitude of shear strain, with a peak value (which is stress dependent) appropriate for small strains and a constant-volume value (which is usually assumed to be stress independent) for large strains. For design purposes a peak value of the sand friction angle can be used because it is undesirable for the embankment to undergo large strains. A friction coefficient, μ, of 0.5 was reported for a sand with similar grain shape and gradation of Ottawa sand (*59*). This is equivalent to a friction angle of 27 degrees. An average friction angle of 33 degrees was obtained from interface shear strength tests performed between EPS and bedding sand tested over a stress range of 25 kPa (522 lbs/ft^2) to 40 kPa (835 lbs/ft^2) (*58*). In summary, the EPS/sand interface friction appears to range from 27 degrees to 33 degrees which is typical for the ϕ of a sand. In (*60*), it is

suggested that the friction coefficient between EPS blocks and soil is approximately 0.5 (δ=27 degrees). However, the type of soil was not indicated.

Various sliding situations may need to be evaluated during design depending on the types of materials that are placed, if any, between the EPS blocks and the natural foundation soil. For example, if a sand layer is placed between the EPS blocks and natural foundation soil, the friction between the EPS and sand as well as the sand and foundation soil will need to be considered. The interface friction angle between the sand and the underlying natural foundation soil will be dependent on the type of natural soil as well as type of sand. However, it is suggested that for preliminary design of retaining walls where well compacted sharp-grained sand or sand with gravel is placed between the foundation of a retaining wall and a natural silt or clay that a friction angle of 20 degrees can be assumed between the sand and the underlying silt or clay (*5*).

Because the use of an EPS-block geofoam embankment will typically be used over soft soils, the case of sliding occurring within the soft soil must also be considered. It is indicated in (*5*) that if the undrained shear strength, s_u, of the underlying soil is less than the frictional resistance beneath any part of a retaining wall base, sliding will occur by undrained shear within the soil at some distance below the base. Additional sliding cases will need to be considered if geosynthetics are used between the EPS blocks and the natural soil which can be measured using site specific interface shear testing.

Geosynthetic interface testing was conducted during this study to evaluate the interface shear resistance between EPS-block geofoam and a nonwoven geotextile and a gasoline containment (GC), i.e., gasoline resistant, geomembrane. These interfaces are common in EPS-block geofoam embankments and thus are considered in the internal stability analysis described in Chapter 6. Large-scale direct shear and torsional ring shear tests were conducted on EPS-block geofoam/nonwoven geotextile and EPS-block geofoam/GC geomembrane interfaces. The geosynthetics used in the interface shear testing are listed below.

- Geofoam: EPS-block geofoam with a unit weight of 20 kg/m^3 (1.25 lbf/ft^3). This geofoam was manufactured by Wisconsin EPS, Inc. in Fond Du Lac, Wisconsin.
- Nonwoven Geotextile: A nonwoven, polypropylene geotextile with a mass per unit area of 205 g/m^2 (6 oz/yd^2). This geotextile was manufactured by Polyfelt Americas of Atlanta, Georgia.
- Gasoline Containment (GC) Geomembrane: A minimum 0.76 mm (30 mils) thick, smooth tri-polymer alloy geomembrane that is manufactured by Seaman Corporation of Wooster, Ohio. The geomembrane can contain both diesel fuel and gasoline.

The shear testing was conducted to simulate the stress conditions in EPS-block geofoam embankments and thus three effective normal stresses were used for the testing, 12, 20 or 21, and 26 kPa (250, 426 or 436, 550 lbs/ft²). Therefore, at least three interface shear tests were conducted for each geotextile and geomembrane interface.

Interface Shear Testing Procedure

Large-scale direct shear and torsional ring shear tests were conducted on the geofoam interfaces. To facilitate the required testing, it is desirable to use a ring shear device instead of the large-scale direct shear box required by ASTM D 5321. ASTM D 5321 allows other shear devices to be used for geosynthetic shear testing if they yield similar results as the large-scale direct shear box. To investigate this substitution, large-scale direct shear tests were conducted on the same geofoam interfaces that were tested in the torsional ring shear device. The direct shear tests were performed in accordance with ASTM D 5321 using a 305 mm (12 in.) by 305 mm (12 in.) upper geosynthetic specimen that was sheared over a 305 mm (12 in.) by 356 mm (14 in.) lower geosynthetic specimen. The direct shear normal stresses are applied pneumatically and the same shear displacement rate 0.37 mm/min (0.0144 in./min) that was used for the ring shear tests

were used for the direct shear tests to avoid displacement rate-related discrepancies in the test results.

The successful use of a torsional ring shear apparatus to measure the shear strength of geosynthetic/geosynthetic and geosynthetic/soil interfaces is described in (*61-63*). The torsional ring shear apparatus is much easier to use than the large-scale direct shear box and allows: (a) unlimited continuous shear displacement to occur in one direction, resulting in the development of a true residual strength condition; (b) a constant cross-sectional area during shear; (c) minimal laboratory supervision; and (d) data acquisition techniques to be readily used. A modified Bromhead ring shear apparatus was used to measure the shear strength of the geofoam/geosynthetic interfaces. A modified specimen container was used to hold the bottom interface component in place. In tests on geosynthetic/geosynthetic interfaces, the knurled porous stone in the specimen container is replaced with a plastic insert to secure the appropriate geosynthetic. The insert is fastened to the specimen container using four screws. Specifically, an annular geofoam specimen with an inside and outside diameter of 40 and 100 mm (1.6 and 3.9 in.), respectively, is secured to the plastic insert using an adhesive. The other interface component is adhered to the top (loading) platen. The normal stress is applied by dead weight to the top platen, which sits on top of the specimen container. During shearing, the bottom interface component moves with respect to the stationary top interface component. All of the shear displacement values and shear displacement rates reported herein were calculated using a diameter of 70 mm (2.8 in.), which is the average diameter of the annular specimen.

Geofoam And Geosynthetic Specimen Preparation Procedure

The EPS-blocks were cut into square and annular shapes using a hot-wire cutter for the direct shear and torsional ring shear testing, respectively. The geofoam was always placed in the specimen container and the geomembrane or geotextile was secured to the top platen. The molded exterior surface was used as the shearing interface to produce an estimate of the field interface shear resistance.

The geomembrane specimens were cut from a geomembrane sheet using a hydraulic jack and steel die that is the same size and shape as the required specimen. An adhesive was used to secure the geomembrane specimen to a plastic insert that fits into the top platen of the direct shear box. The geofoam specimen was cut so that it fit into the 305 mm (12 in.) by 356 mm (14 in.) lower container. A thin coat of epoxy was used to adhere the geofoam and geomembrane to a plastic insert for the bottom specimen container and the top platen, respectively, of the torsional ring shear device. The epoxy was allowed to cure for 24 hours under a normal stress of 12 kPa (250 lbs/ft^2). The curing normal stress did not exceed the normal stress at which the tests were conducted and thus the specimens were normally consolidated at the time of testing. The curing normal stress aided bonding of the geosynthetics and minimized vertical displacement caused by the epoxy adhering procedure during testing. The geomembrane and specimen container/top platen were marked to ensure that the geomembrane did not slip during shearing.

The geotextile specimens were cut into square and annular shapes using scissors and/or a razor blade knife. The nonwoven geotextile specimens were secured to the top platen in the direct shear or torsional ring shear devices. To secure the geotextile in the direct shear box, the geotextile was wrapped around the edges of the upper platen and secured using a metal bar that is screwed into the top platen.

To secure the geotextile to the top platen in the torsional ring shear device, the geotextile was initially glued to a smooth high-density polyethylene (HDPE) geomembrane ring that was cut to the same size as the geomembrane specimen. The geotextile was cut in a circle with a diameter of approximately 160 mm (6.3 in.), which is larger than the outside diameter of the ring shear specimen (100 mm (3.9 in.)). A small circular hole (roughly 20 mm (0.8 in.)) was cut in the center of the geotextile specimen so that the centering pin of the ring shear apparatus was not interfered with. The HDPE geomembrane ring was then glued to the geotextile using a thin coat of epoxy. A 2-3 kg (4.4-6.6 lb) mass was placed on the geotextile/geomembrane ring to aid adhesion. After about 15 minutes of drying, the geotextile extending beyond the edge of the

geomembrane ring was cut so that eight wedges or flaps of geotextile that were equal in size and spacing remained. Epoxy was applied to the back of the smooth geomembrane and the eight geotextile wedges were folded over and adhered to the backside of the smooth geomembrane. The 2-3 kg (4.4-6.6 lb) mass was reapplied for roughly 45 minutes. This wrapping of the geotextile around the geomembrane ring prevented geotextile fibers from readily pulling out during shearing. This procedure was also used so epoxy did not contaminate the geotextile fibers that would be in contact with the geofoam and thus produce dubious values of shear resistance.

The geotextile/geomembrane ring system was secured to the top platen using a thin coat of epoxy. The side with the eight wedges was adhered to the top platen. The top platen with the attached geotextile specimen was then placed in the ring shear apparatus on top of the specimen container, to which the geofoam specimen was adhered. A sacrificial geotextile cushion was placed between the geofoam and geotextile so that there was no contact between the interface components before shearing. The epoxy was allowed to cure for 24 hours under a normal stress (12 kPa (250 lbs/ft^2)) that did not exceed the normal stress at which the test was to be conducted. The top platen and geotextile were also marked to ensure that the geotextile did not slip during shearing.

After allowing the epoxy to cure for 24 hours, the sacrificial geotextile was removed and the two interface components were placed in contact such that no relative displacement occurred between them prior to shearing. The ring shear apparatus was then loaded to the shearing normal stress using a load increment ratio of 1.0. Once the desired normal stress was applied, the interface system was allowed to equilibrate for about 20 minutes before shearing started.

Comparison of Large-Scale Direct Shear and Torsional Ring Shear Tests

Large-scale direct shear tests were conducted at one normal stress for comparison with results on the same interfaces tested in the torsional ring shear device. Figure 2.16 presents a comparison between the shear stress-displacement relationships obtained from the large-scale direct shear and ring shear tests on the geofoam/GC geomembrane interface at a normal stress of

21 kPa (436 lbs/ft²). It can be seen that both test procedures produce similar shear stress-displacement relationships up to a shear displacement of about 100 mm (3.9 in.). At this displacement, the direct shear test is stopped because the travel of the direct shear box is limited. However, this is enough shear displacement to measure the peak shear resistance and the peak friction angle. The direct shear and ring shear tests yielded peak friction angles of 53 and 56 degrees, respectively, for this normal stress. These friction angles are in agreement and a similar agreement was obtained for the geofoam/nonwoven geotextile interface. This agreement is expected because shearing occurred on the surface or outside of the EPS. As a result, the torsional ring shear device was used for the majority of the testing of the two geofoam interfaces.

The main difference between the ring shear and direct shear test methods is in the values obtained for the residual friction angle and shear displacement at the residual strength. The direct shear test terminates at a shear displacement of approximately 100 mm (3.9 in.) and, thus, the resulting friction angle does not correspond to a residual friction angle whereas the ring shear test was conducted until a constant minimum, i.e., residual, strength was reached.

In summary, it was assumed that the ring shear device yields similar results to the large-scale direct shear apparatus for the normal stresses and geomembrane and geotextile interfaces considered herein and could be used as a substitute for the direct shear apparatus as suggested in ASTM D 5321. The ring shear device was chosen because ring shear tests are easier and more cost effective to perform than large-scale direct shear tests. This is mainly due to the fact that a much larger specimen is required for the direct shear test.

Figure 2.16. Comparison of large-scale direct shear and torsional ring shear tests on geofoam/GC geomembrane interface at a normal stress of 21 kPa (436 lbs/ft^2).

Geofoam/GC Geomembrane Interface Test Results

Figure 2.17 presents a comparison between the shear stress-displacement relationships obtained from the ring shear tests on the geofoam/GC geomembrane interface at a normal stresses of 12.0, 21, and 26 kPa (250, 436, 550 lbs/ft²). It can be seen that the geofoam/geomembrane

interface exhibits a peak and residual strength at each of the three normal stresses. These three shear stress-displacement relationships were used to develop the peak and residual failure envelopes for this interface that are presented in Figure 2.18. It can be seen that the failure envelopes correspond to peak and residual interface friction angles of approximately 55 and 43 degrees, respectively. Therefore, the shear strength of the geofoam/GC geomembrane interface is extremely high, which is attributed to the bonding or sticking that was observed between the geomembrane and the surface of the EPS specimen.

Figure 2.17. Shear stress-displacement relationships for the geofoam/GC geomembrane interface at normal stresses of 12, 21, and 26 kPa (250, 436, 550 lbs/ft²).

Figure 2.18. Peak and residual failure envelopes for the geofoam/GC geomembrane interface at normal stresses of 12, 21, and 26 kPa (250, 436, 550 lbs/ft^2).

Geofoam/Nonwoven Geotextile Interface Test Results

Figure 2.19 presents a comparison between the shear stress-displacement relationships obtained from the ring shear tests on the geofoam/nonwoven geotextile interface at a normal stresses of 12, 20, and 26 kPa (250, 426, 550 lbs/ft²). It can be seen that the geofoam/nonwoven geotextile interface also exhibited a peak and residual strength at each of the three normal stresses. As shown in Figure 2.20, these three shear stress-displacement relationships correspond to peak and residual friction angles of approximately 25 and 18 degrees, respectively. The shear strength of the geofoam/nonwoven geotextile is significantly lower than the geofoam/GC geomembrane interface because the geotextile did not stick or bond to the geofoam. As a result, a geofoam/nonwoven geotextile interface is more critical than a geofoam/geomembrane interface for internal stability analyses.

Figure 2.19. Shear stress-displacement relationships for the geofoam/geotextile interface at normal stresses of 12, 20, and 26 kPa (250, 426, 550 lbs/ft^2).

Figure 2.20. Peak and residual failure envelopes for the geofoam/geotextile at

normal stresses of 12, 20, and 26 kPa (250, 426, 550 lbs/ft^2).

Summary of EPS Interface Strengths

The following conclusions are based on the data and interpretations of the interface friction data presented in this section:

- It is recommended that an EPS/EPS interface friction angle of 30 degrees be used for design
- It is recommended that an EPS/nonwoven geotextile interface friction angle of 25 degrees be used for design if the geotextile is the same or substantially similar to the geotextile used in this study.
- It is recommended that an EPS/GC geomembrane interface friction angle of 52 degrees be used for design if the geomembrane is the same or substantially similar to the GC geomembrane used in this study.
- Based on the results reported in (*58,59*) an interface friction angle of 30 degrees can be used for an EPS/sand interface for preliminary analysis.
- Site specific interface testing should be conducted to ensure that representative values of interface friction angle are being used for external and internal stability calculations. EPS interface friction tests can be conducted using ASTM standard test method D 5321. If preferred, the test results obtained herein suggest that torsional ring shear tests can be substituted for the large-scale direct shear tests specified in ASTM D 5321.

THERMAL PROPERTIES

Although the thermal insulation function of EPS-block geofoam is not a primary concern for the function of lightweight fill, some knowledge of the geothermal properties of EPS is necessary to understand the potential problems of differential icing and solar heating. These

problems are discussed in Chapter 4. The key aspects of the thermal behavior of EPS-block geofoam are:

- The coefficient of thermal conductivity of EPS block in the as-molded (dry) state varies with both EPS density and ambient temperature as shown in Figure 2.21. Thermal conductivity defines the rate of heat flow through the EPS. The smaller the coefficient of thermal conductivity, the more efficient the EPS is as a thermal insulator.

Figure 2.21. Coefficient of thermal conductivity, k, for dry, block-molded EPS (*18*).

- EPS block will absorb water with time once placed in the ground. The magnitude of absorbed water (which is traditionally expressed on a relative volume basis, not relative weight basis as for soil) can vary widely and is a function of many variables, with thickness of the piece of geofoam one of the more important variables. Therefore, it is not possible to give typical values or even a range of values for absorbed water that apply to EPS-block geofoam usage in roadway embankments. However, the coefficient of thermal conductivity is expected to increase with increasing water content, which means that the EPS loses some of its thermal efficiency with increasing water content.
- Overall, EPS-block geofoam is a very efficient thermal insulator compared to soil. A general rule is that dry EPS-block geofoam is 30 to 40 times more efficient thermally compared to soil, e.g. 1 mm (0.04 in.) of EPS will have the same thermal-insulation effect as 30 to 40 mm (1.2 to 1.6 in.) of soil.

REFERENCES

1. "Pentane Emissions during Processing." *Technical Bulletin N-840,* BASF Corporation, Jamesburg, New Jersey (1999) 4 pp.
2. Bartlett, P. A., "Expanded Polystyrene Scrap Recovery & Recycling." ARCO Chemical Company (undated) .
3. Bartlett, P. A., "Letter report to unnamed customer 11 September." ARCO Chemical Company, Newtown Square, PA (1986) .

4. Horvath, J. S., "Recycling is Good...But Not Necessarily When It Comes to Geofoam-Grade EPS," In Manhattan College-School of Engineering, Center for Geotechnology [website]. [updated 26 July 2001; cited 20 September2001]. Available from http://www.engineering.manhattan.edu/civil/CGT/T2olrgeomat1.html; INTERNET.
5. Terzaghi, K., Peck, R. B., and Mesri, G., *Soil Mechanics in Engineering Practice*, 3rd, John Wiley & Sons, Inc., New York (1996) .
6. Mesri, G., "Study Guide for C.E.E. 383 Fall 2000 Soil Mechanics and Soil Behavior Using Soil Mechanics in Engineering Practice by Terzaghi, Peck and Mesri." Department of Civil and Env. Engineering, University of Illinois at Urbana, Urbana (1999) .
7. Bartlett, P. A., "Density and Thermal Gradients in Billets and Their Effects on Physical Properties." Technical data bulletin published by the ARCO Chemical Company, Newtown Square, PA (undated) .
8. Bartlett, P. A., "Density and Thermal Gradients in Billets and Their Effects on Physical Properties." *Presented at the Meeting of the Society of the Plastics Industry*, (March 22, 1985) .
9. Sarlin, J., Järvelä, P., and Törmälä, P., "The Inhomogeneity Inside a Block of Expanded Polystyrene (EPS)." *Plastics and Rubber Processing and Applications*, Vol. 6, No. 1 pp. 43-49.
10. Throne, J. L., *Thermoplastic Foams*, , Sherwood Publishers, Hinckley, Ohio (1996) .
11. Sarlin, J., "Dependence of the strength and structure of expanded polystyrene on processing in the block molding method." *Plastics and Rubber Processing Applications*, Vol. 7, No. 4 (1987) pp. 207-214.
12. ASTM D 1622-88, "Standard Test Method for Apparent Density of Rigid Cellular Plastics." Vol. 08.01, American Society for Testing and Materials, West Conshohocken, PA (1999) .
13. ASTM D 578-95, "Standard Specification for Rigid, Cellular Polystyrene Thermal Insulation." Vol. 04.06, American Society for Testing and Materials, West Conshohocken, PA (1999) .
14. Coughanour, R. B., "Pentane Issue." *Presentation at the 16th Annual SPI Expanded Polystyrene Division Conference,*1988, San Diego, CA, .
15. Horvath, J. S., "Lessons Learned from Failures Involving Geofoam in Roads and Embankments." *Research Report No. CE/GE-99-1,* Manhattan College, Bronx, NY (1999) 18 pp.
16. "The Final Report of International Symposium on EPS Construction Method (in English and Japanese)." EPS Construction Method Development Organization, Tokyo, Japan (undated) 161 pp.
17. Eriksson, L., and Tränk, R., "Properties of Expanded Polystyrene-Laboratory Experiments." *Expanded Polystyrene as Light Fill Material; Technical Visit around Stockholm,*1991, Stockholm, (June 19, 1991) .
18. Horvath, J. S., *Geofoam Geosynthetic*, , Horvath Engineering, P.C., Scarsdale, NY (1995) 229 pp.
19. "EPS." Expanded Polystyrol Construction Method Development Organization, Tokyo, Japan (1993) 310 pp.
20. Geotech Systems Corporation, Unpublished commercial laboratory test data.
21. ASTM D 1621-94, "Standard Test Method for Compressive Properties of Rigid Cellular Plastics." Vol. 08.01, American Society for Testing and Materials, West Conshohocken, PA (1999) .
22. Frydenlund, T. E., and Aaboe, R., "Expanded Polystyrene - A Light Solution." *International Symposium on EPS Construction Method (EPS Tokyo '96)*, Tokyo, Japan (1996) pp. 31-46.

23. Preber, T., Bang, S., Chung, Y., and Cho, Y., "Behavior of Expanded Polystyrene Blocks." *Transportation Research Record No. 1462,* Transportation Research Board, Washington, D.C. (1994) pp. 36-46.
24. Athanasopoulos, G. A., Pelekis, P. C., and Xenaki, V. C., "Dynamic Properties of EPS Geofoam: An Experimental Investigation." *Geosythetics International*, Vol. 6, No. 3 (1999) pp. 171-194.
25. Duskov, M., "Materials Research on Expanded Polystyrene Foam (EPS)." *Report 7-94-211-2,* Delft University of Technology, Delft, The Netherlands (1993) .
26. Horvath, J. S., "Discussion: Status of ASCE Standard on Design and Construction of Frost Protected Shallow Foundations by L.S. Danyluk and J.H. Crandell." *Journal of Geotechnical and Geoenvironmental Engineering*, , (1999) .
27. Duskov, M., "EPS as a Light-Weight Sub-Base Material in Pavement Structures," Doctor of Engineering thesis, Delft University of Technology, Delft, The Netherlands (1998).
28. "Earthwork; Soil Stabilization." *SPEC-DATA ® Section 02200,* AFM® Corporation, Excelsior, Minn. (1994) 4 pp.
29. "Styropor®; Construction; Highway Construction/Ground Insulation." BASF, AG, Ludwigshafen, Germany (1991) 12 pp.
30. Magnan, J.-P., and Serratrice, J.-F., "Propriétés mécaniques du polystyréne expansé pour ses applications en remblai routier." *Bulletin Liaison Laboratoire Ponts et Chaussées*, , No. 164 (1989) pp. 25-31.
31. van Dorp, T., "Expanded Polystyrene Foam as Light Fill and Foundation Material in Road Structures (preprint paper)." *The International Congress on Expanded Polystyrene: Expanded Polystyrene- Present and Future,* Milan, Italy (1988) .
32. "Styropor®; Processing; Measurements/Tests." *Technical Information Bulletin No. 0-220e,* BASF AG, Ludwigshafen, Germany (1990) 4 pp.
33. Horvath, J. S., Personal Communication.
34. "Utilisation de Polystyrene Expanse en Remblai Routier; Guide Technique." Laboratoire Central Ponts et Chaussées/SETRA, France (1990) 18 pp.
35. Kutara, K., Aoyama, N., and Takeuchi, T., "Earth Pressure Test of Retaining Wall Using EPS as Back-filling Material." *Technical Reports of Construction Method Using Expanded Polystrol,* Expanded Polystyrol Construction Method Development Organization, Tokyo (1989) .
36. "Design and Construction Manual for Lightweight Fill with EPS." The Public Works Research Institute of Ministry of Construction and Construction Project Consultants, Inc., Japan (1992) Ch. 3 and 5.
37. Negussey, D., and Jahanandish, M., "Comparison of some engineering properties of expanded polystyrene with those of soils." *Transportation Research Record*, Vol. 1418, (1993) pp. 43-48.
38. Zou, Y., and Leo, C. J., "Laboratory Studies on the Engineering Properties of Expanded Polystyrene (EPS) Materials for Geotechnical Applications." *2nd International Conference on Ground Improvement Techniques: 8-9 October 1998,*1998, Singapore, pp. 581-588.
39. Horvath, J. S., "Mathematical Modeling of the Stress-Strain-Time Behavior of Geosythetics Using the Findley Equation: General Theory and Application to EPS-Block Geofoam." *Research Report No. CE/GE-98-3,* Manhattan College, Bronx, N. Y. (1998) .
40. Sun, M. C.-W., "Engineering Behavior of Geofoam (Expanded Polystyrene) and Lateral Pressure reduction in Substructures," M.S. thesis, Syracuse University, Syracuse (1997).
41. Wu, Y., "An Investigation of Long-Term Deformation Behavior of EPS Block Under Static & Repeated Loads," M.S. thesis, South Dakota School of Mines and Technology, Rapd City (1996).

42. Duskov, M., and Scarpas, A., "Three-Dimensional Finite Element Analysis of Flexible Pavements with an (Open Joint in the) EPS Sub-Base." *Geotextiles and Geomembranes*, Vol. 15, No. 1-3 (1997) pp. 29-38.
43. Sandri, D., Thornton, J. S., and Sack, R., "Measuring geosynthetic creep: three methods." *Geotechnical Fabrics Report*, No. August (1999) pp. 26-29.
44. Chambers, R. E., "Behavior of Structural Plastics." Chapter 2, *Structural Plastics Design Manual,* ASCE, New York (1984) pp. 134-251.
45. Goodman, R. E., *Introduction to Rock Mechanics*, 2nd, John Wiley & Sons, New York (1989) 562 pp.
46. Findley, W. N., and Khosla, G., "An equation for tension creep of three unfilled thermoplastics." *SPE Journal*, Vol. 12, No. 12 (1956) pp. 20-25.
47. Findley, W. N., "Mechanism and mechanics of creep of plastics." *SPE Journal*, Vol. 16, No. 1 (1960) pp. 57-65.
48. Aabøe, R., "Deformasjonsegenskaper og spenningsforhold i fyllinger av EPS (Deformation and stress conditions in fills of EPS)." *Intern Rapport Nr. 1645,* Public Roads Administration (1993) 22 pp. Norwegian.
49. Aabøe, R., "Long-term performance and durability of EPS as a lightweight fill." *Nordic Road & Transport Research*, Vol. 12, No. 1 (2000) pp. 4-7.
50. Koerner, R. M., *Designing with Geosynthetics*, 4th, Prentice Hall, Upper Saddle River, N.J. (1998) .
51. ASTM D 1623-78, "Standard Test Method for Tensile Adhesion Properties Of Rigig Cellular Plastics." Vol. 08.01, American Society for Testing and Materials, West Conshohocken, PA (2001) .
52. "Styropor®; Construction; Highway Construction/Ground Insulation." *Technical Information Bulletin No. 1-800e,* BASF AG, Ludwigshafen, Germany (1993) 12 pp.
53. ASTM C 203-99, "Standard Test Methods for Breaking Load and Flexural Properties of Block-Type Thermal Insulation." Vol. 04.06, American Society for Testing and Materials, West Conshohocken, PA (1999) .
54. ASTM C 273-00, "Standard Test Method for Shear Properties of Sandwich Core Materials." Vol. 15.03, American Society for Testing and Materials, West Conshohocken, PA (2001) .
55. ASTM D 5321-92, "Standard Test Method for Determining the Coefficient of Soil and Geosynthetic or Geosynthetic and Geosynthetic Friction by the Direct Shear Method." Vol. 04.09 (II), American Society for Testing and Materials, West Conshohocken, PA (2001) .
56. ASTM D 3080-98, "Standard Test Method for Direct Shear Test of Soils Under Consolidated Drained Conditions." Vol. 04.08, American Society for Testing and Materials, West Conshohocken, PA (2001) .
57. Jutkofsky, W. S., "Geofoam Stabilization of an Embankment Slope, A Case Study of Route 23A in the Town of Jewett, Greene County." Geotechnical Engineering Bureau, New York State Department of Transportation, Albany (1998) 42 pp.
58. Bartlett, S., Negussey, D., Kimble, M., and Sheeley, M., "Use of Geofoam as Super-Lightweight Fill for I-15 Reconstruction (Paper Pre-Print)." *Transportation Research Record 1736,* Transportation Research Board, Washington, D.C. (2000).
59. Jutkofsky, W. S., Sung, J. T., and Negussey, D., "Stabilization of an Embankment Slope with Geofoam." *Transportation Research Record 1736,* Transportation Research Board, Washington, D.C. (2000) pp. 94-102.
60. Refsdal, G., "Frost Protection of Road Pavements." *Frost Action in Soils - No. 26,* Committee on Permafrost, ed., Oslo, Norway (1987) pp. 3-19.

61. Stark, T. D., and Poeppel, A. R., "Landfill Liner Interface Strengths From Torsional-Ring-Shear Tests." *ASCE Journal of Geotechnical Engineering*, Vol. 120, No. 3 (1994) pp. 597-615.
62. Stark, T. D., Williamson, T. A., and Eid, H. T., "HDPE Geomembrane/Geotextile Interface Shear Strength." *ASCE Journal of Geotechnical Engineering*, Vol. 122, No. 3 (1996) pp. 197-203.
63. Eid, H. T., and Stark, T. D., "Shear Behavior of an Unreinforced Geosynthetic Clay Liner." *Geosythetics International*, Vol. 4, No. 6 (1997) pp. 645-659.

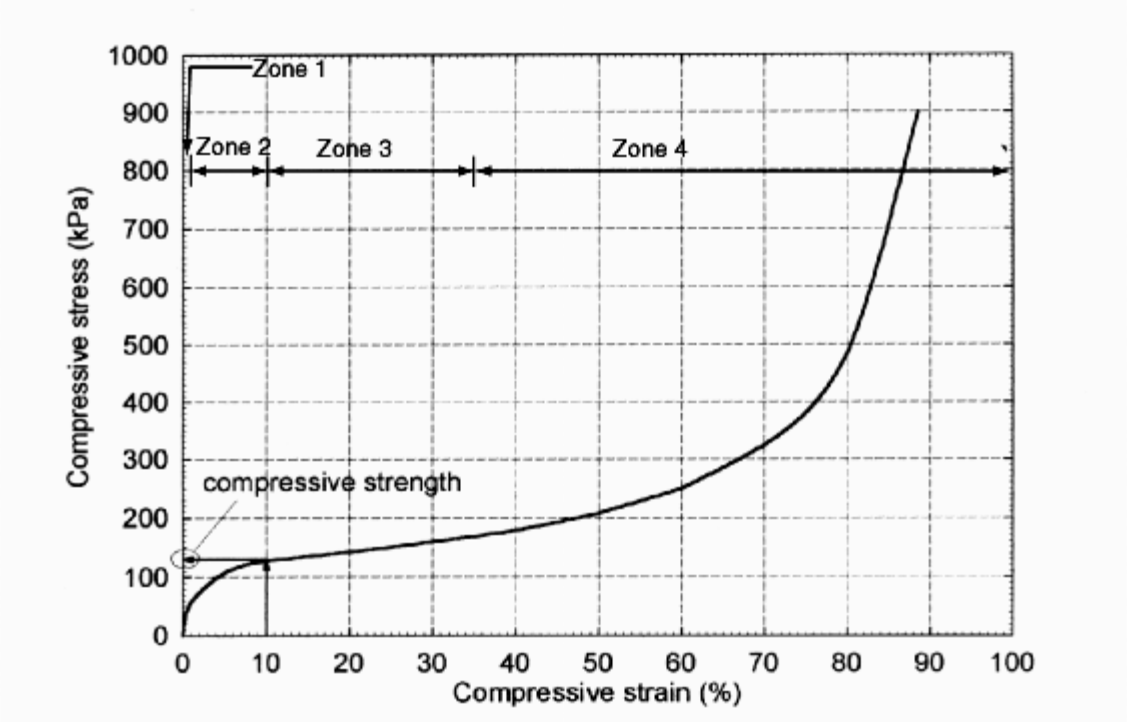

FIGURE 2.1 PROJ 24-11.doc

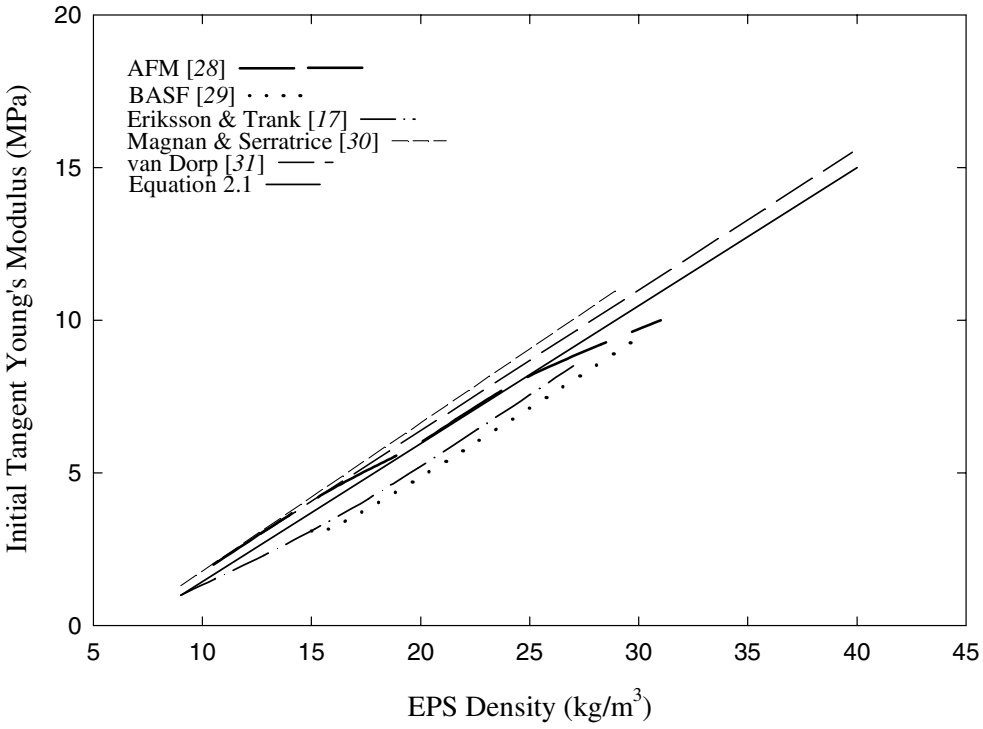

FIGURE 2.2 PROJ 24-11.doc

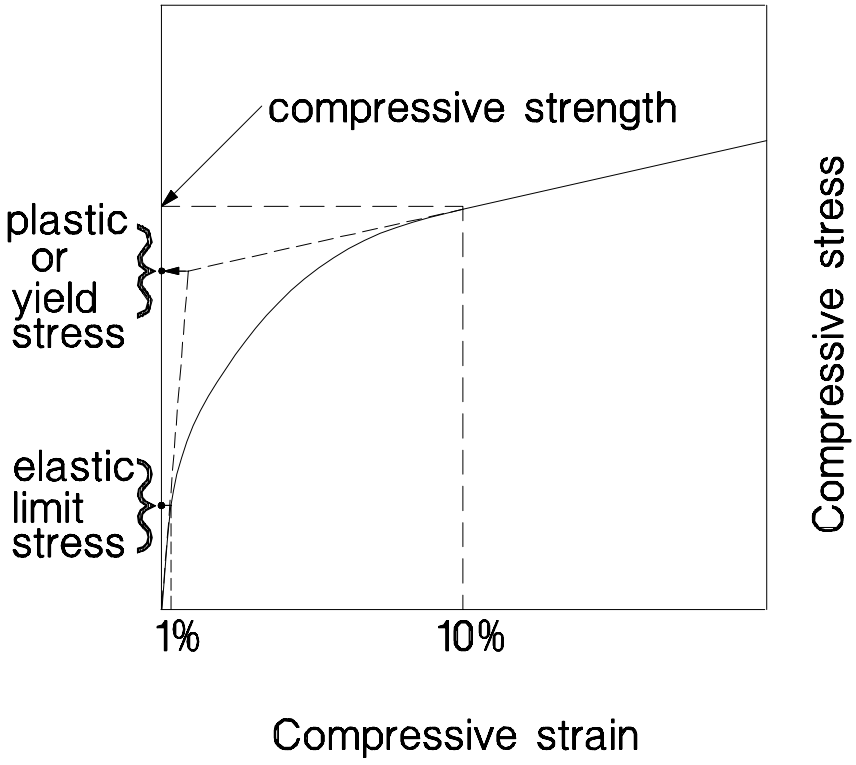

FIGURE 2.3 PROJ 24-11.doc

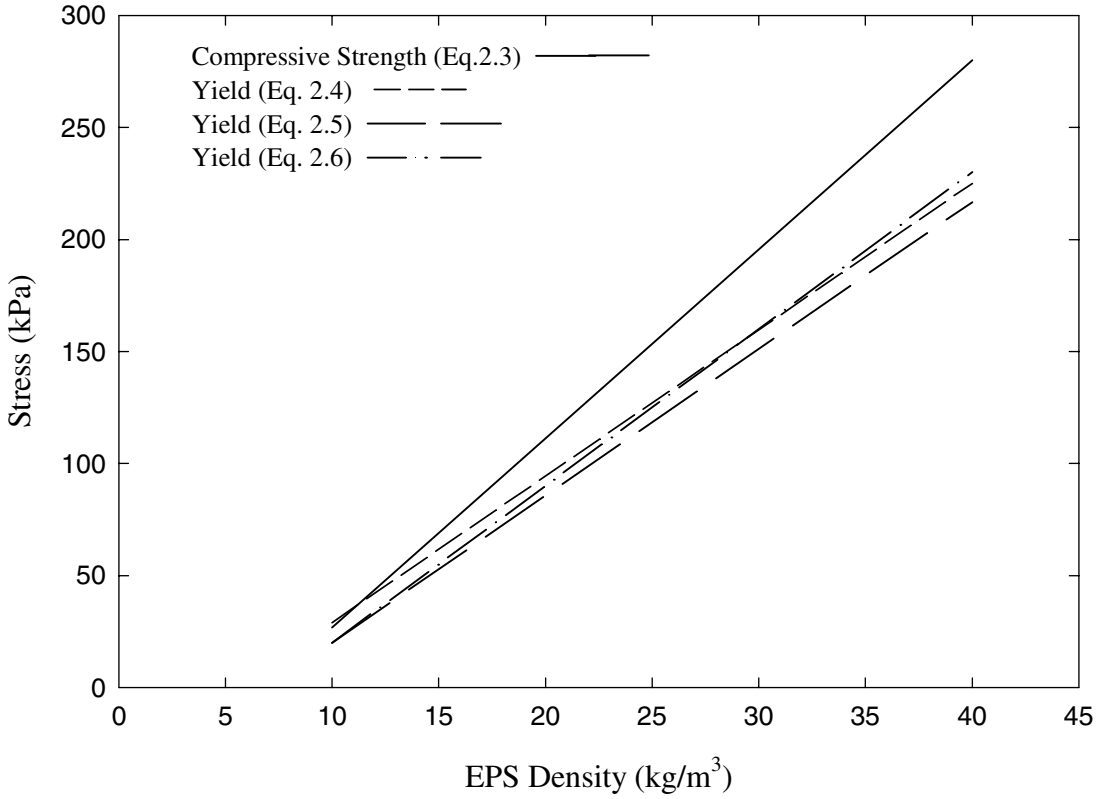

FIGURE 2.4 PROJ 24-11.doc

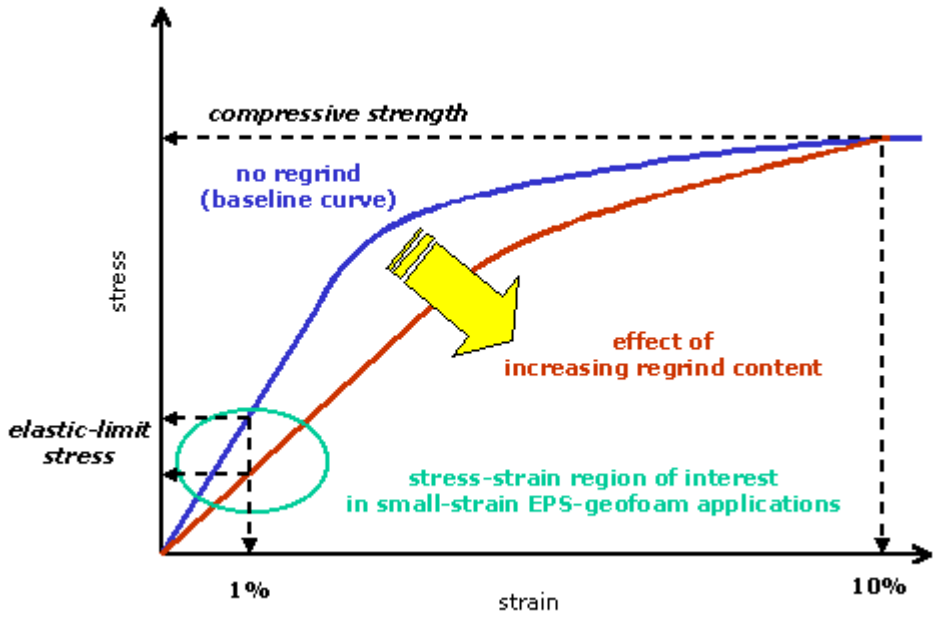

FIGURE 2.5 PROJ 24-11.doc

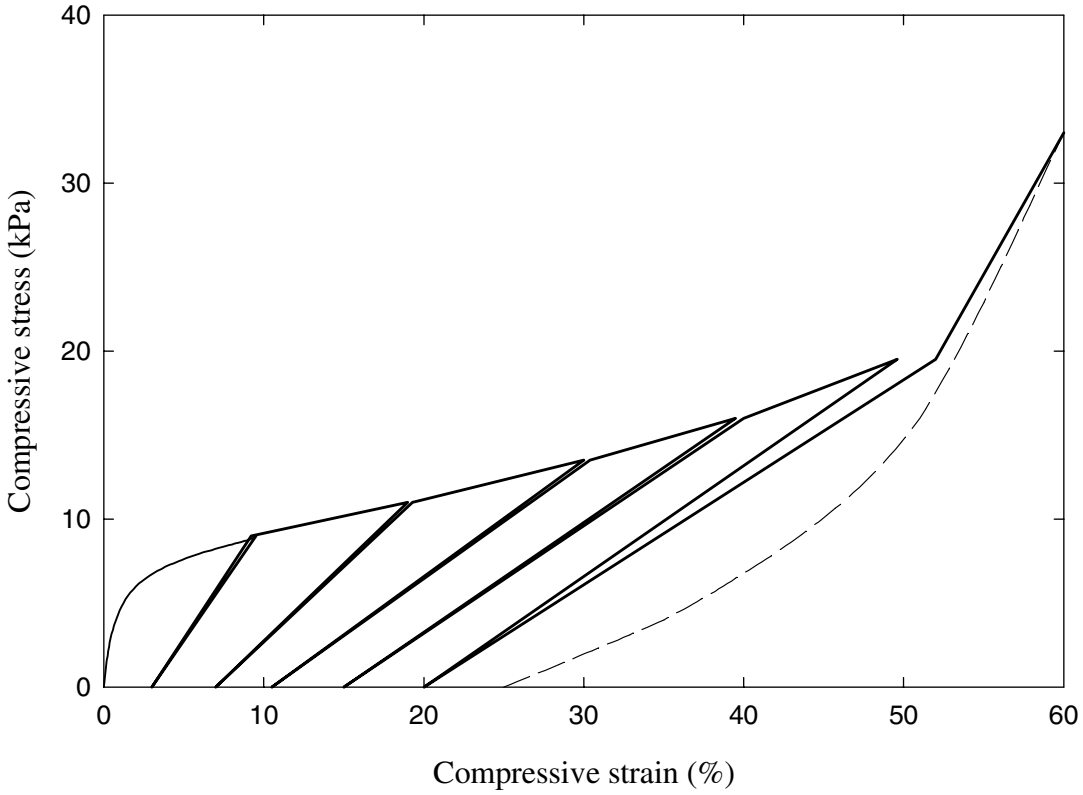

FIGURE 2.6 PROJ 24-11.doc

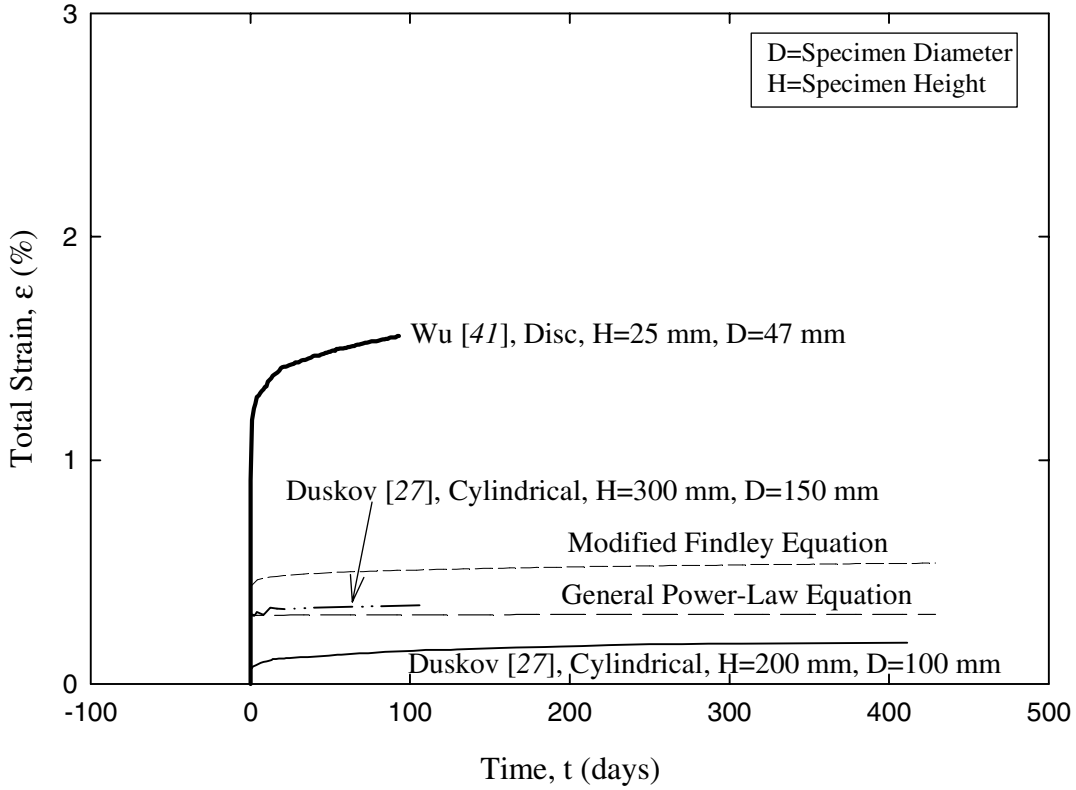

FIGURE 2.7 PROJ 24-11.doc

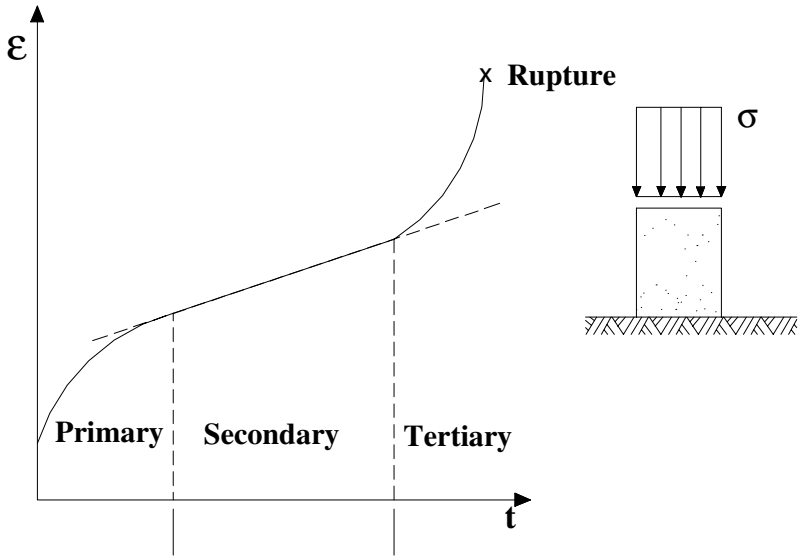

FIGURE 2.8 PROJ 24-11.doc

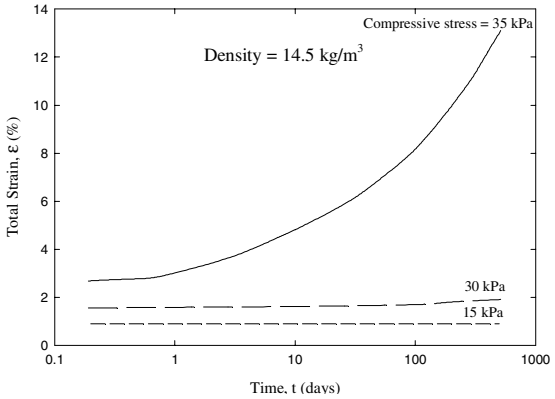

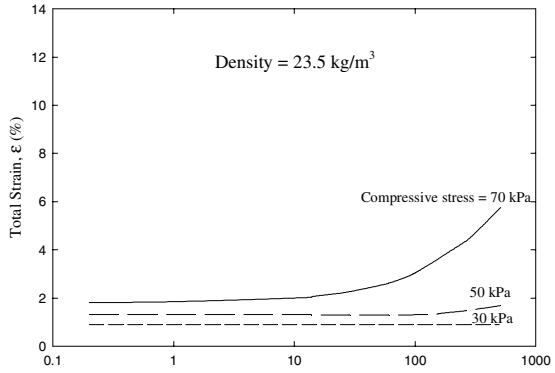

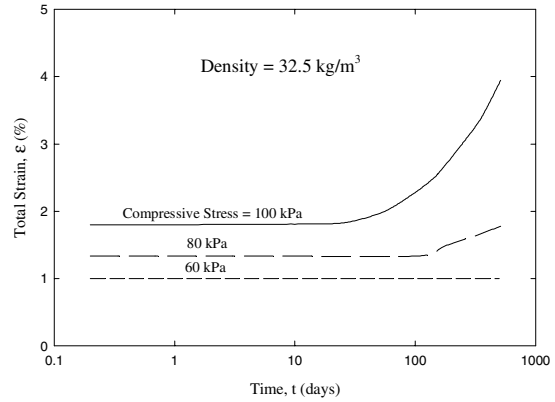

FIGURE 2.9 PROJ 24-11.doc

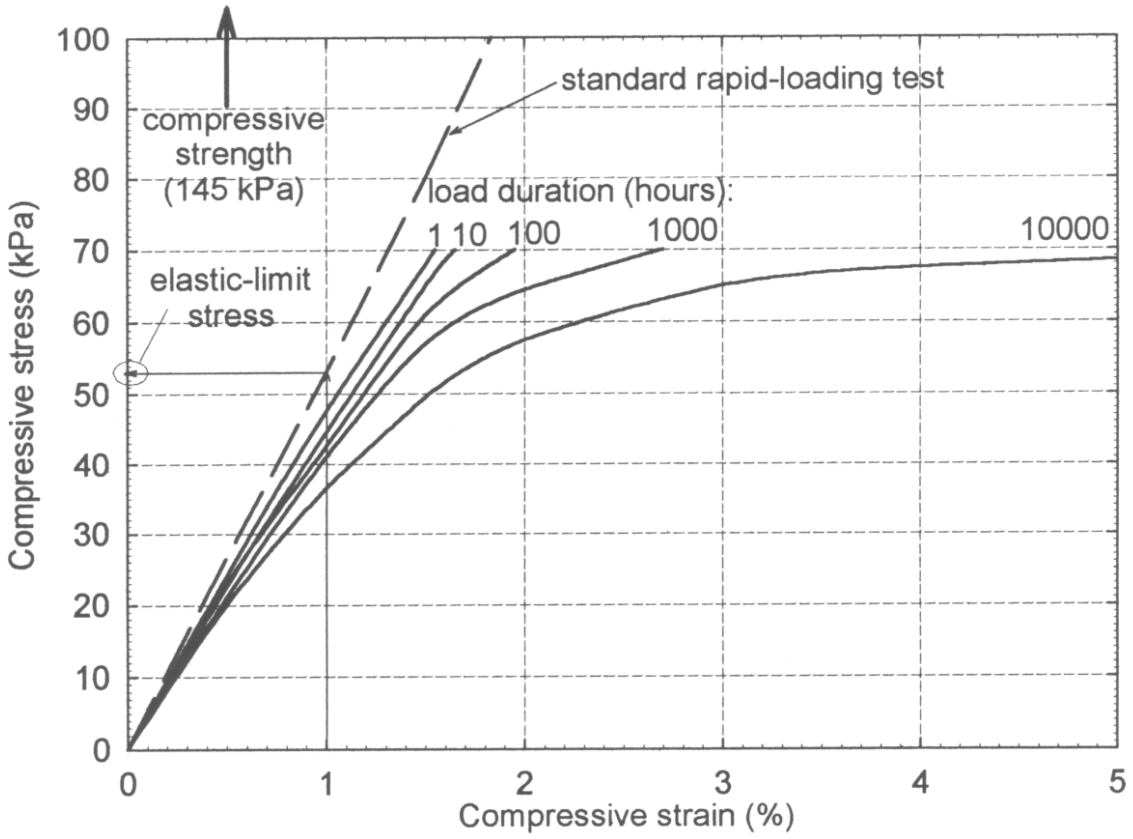

FIGURE 2.10 PROJ 24-11.doc

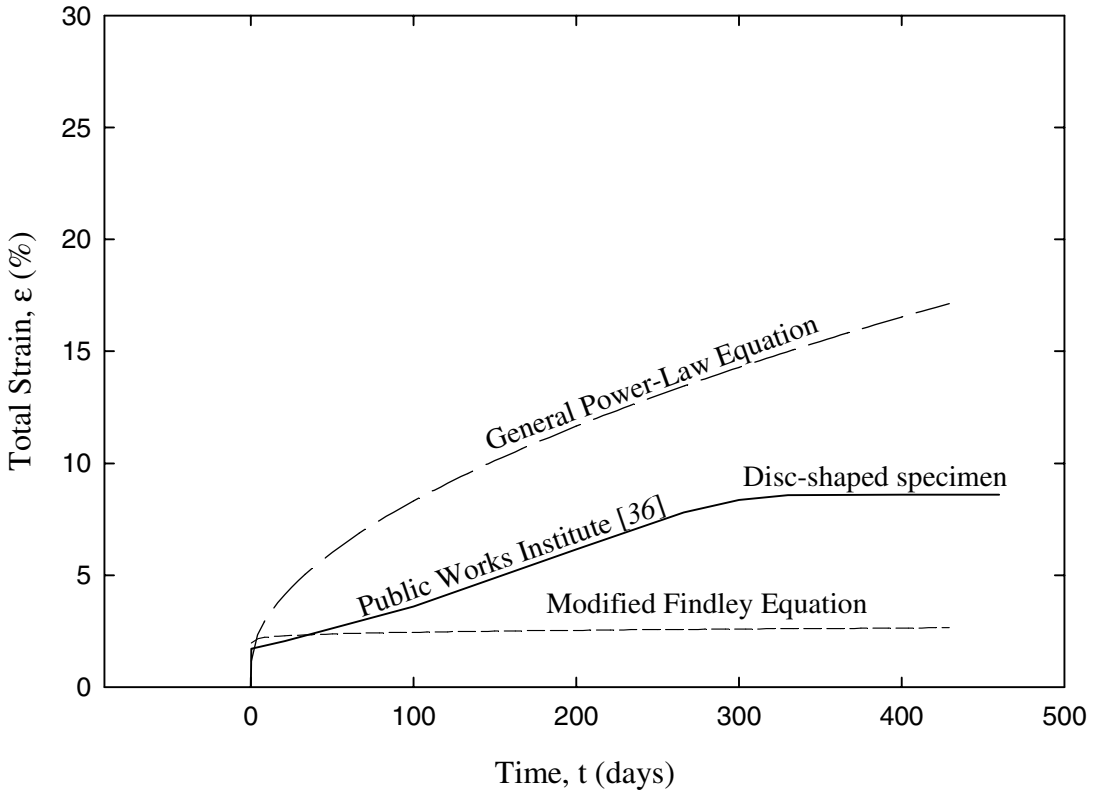

FIGURE 2.11 PROJ 24-11.doc

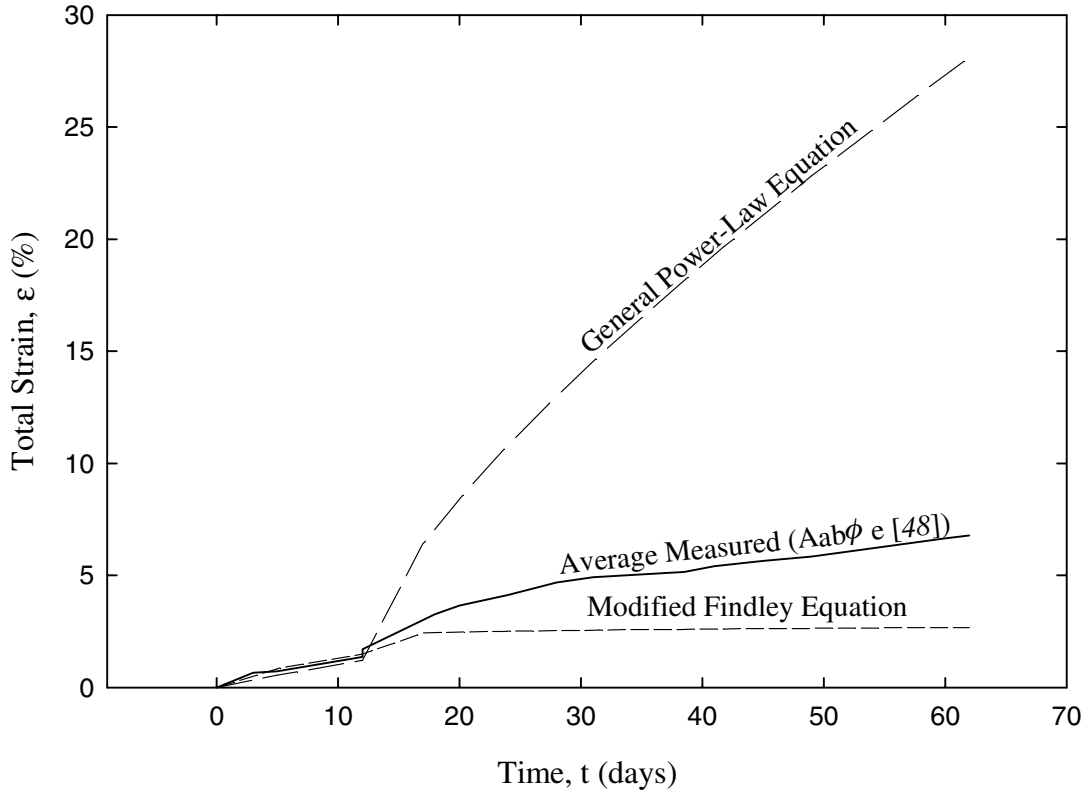

FIGURE 2.12 PROJ 24-11.doc

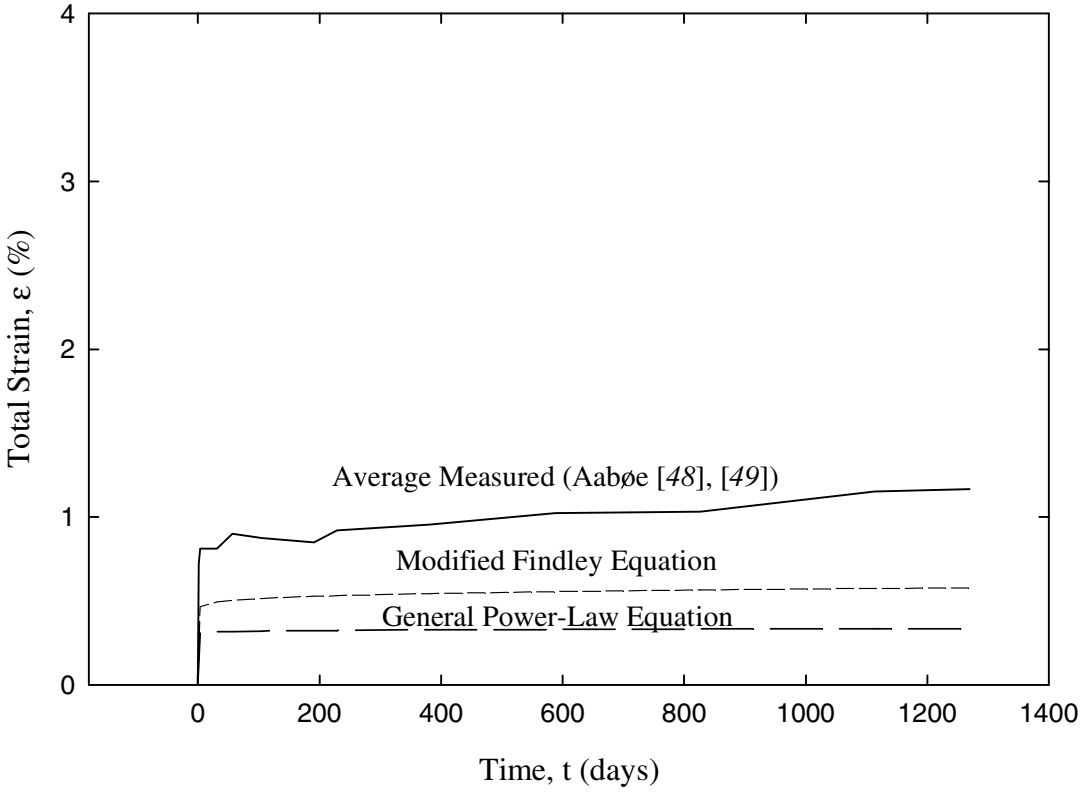

FIGURE 2.13 PROJ 24-12.doc

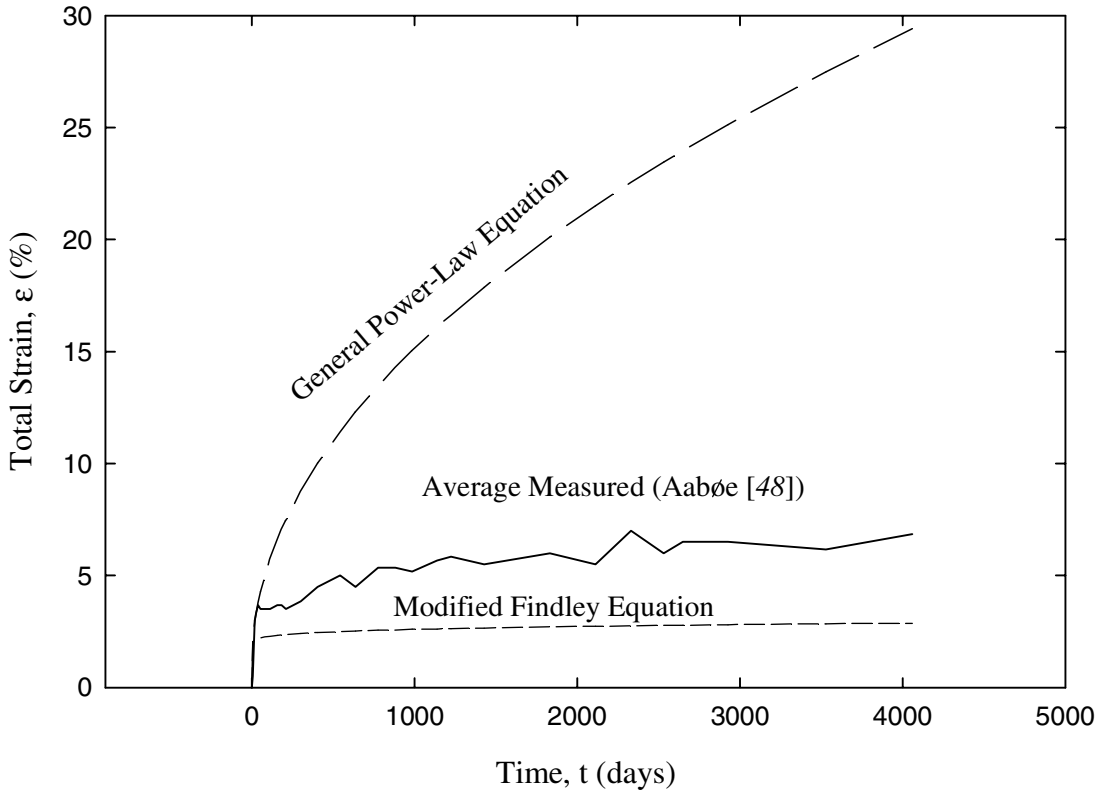

FIGURE 2.14 PROJ 24-11.doc

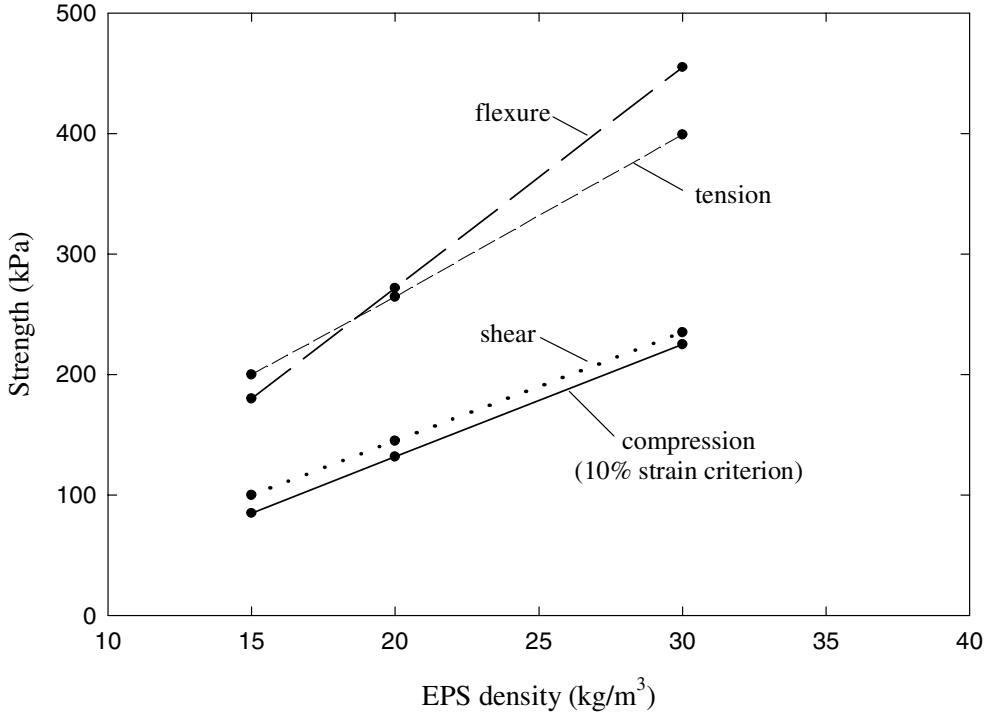

FIGURE 2.15 PROJ 24-12.doc

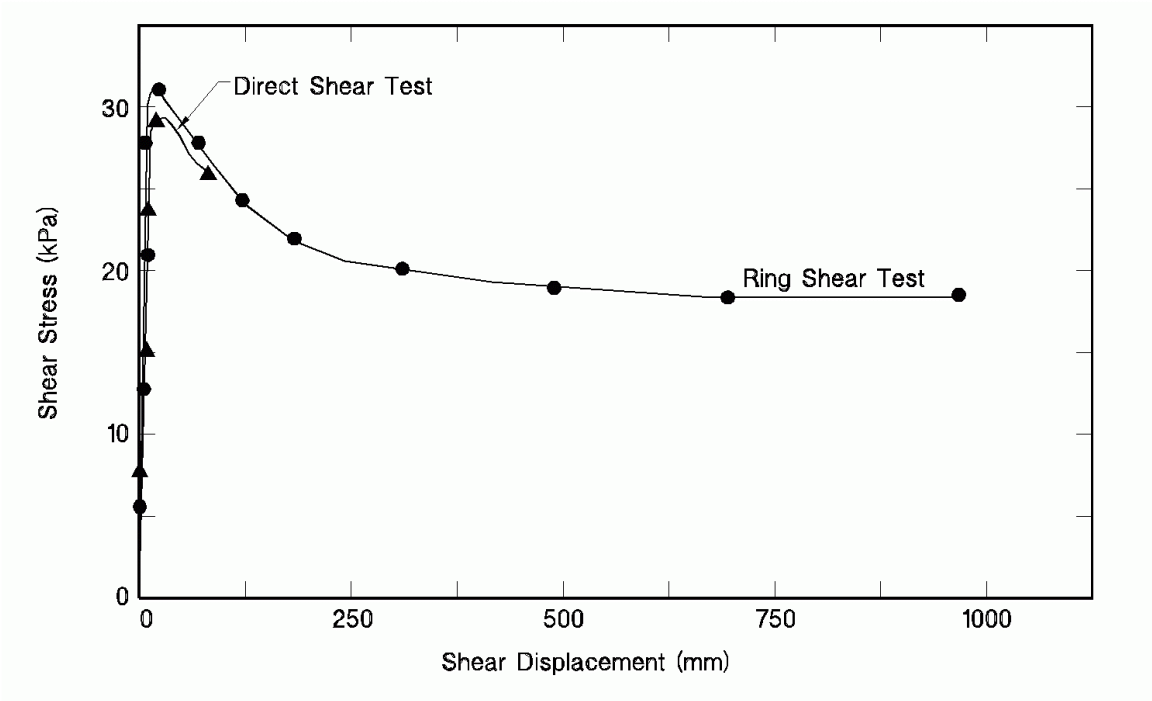

FIGURE 2.16 PROJ 24-12.doc

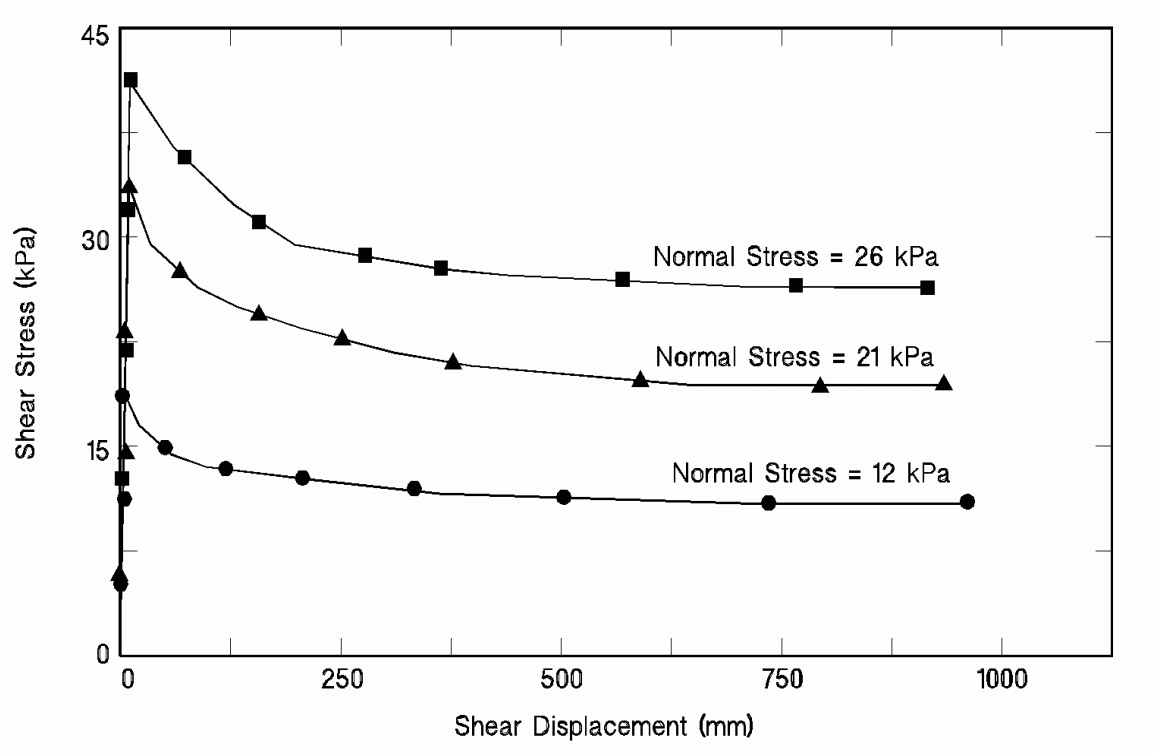

FIGURE 2.17 PROJ 24-12.doc

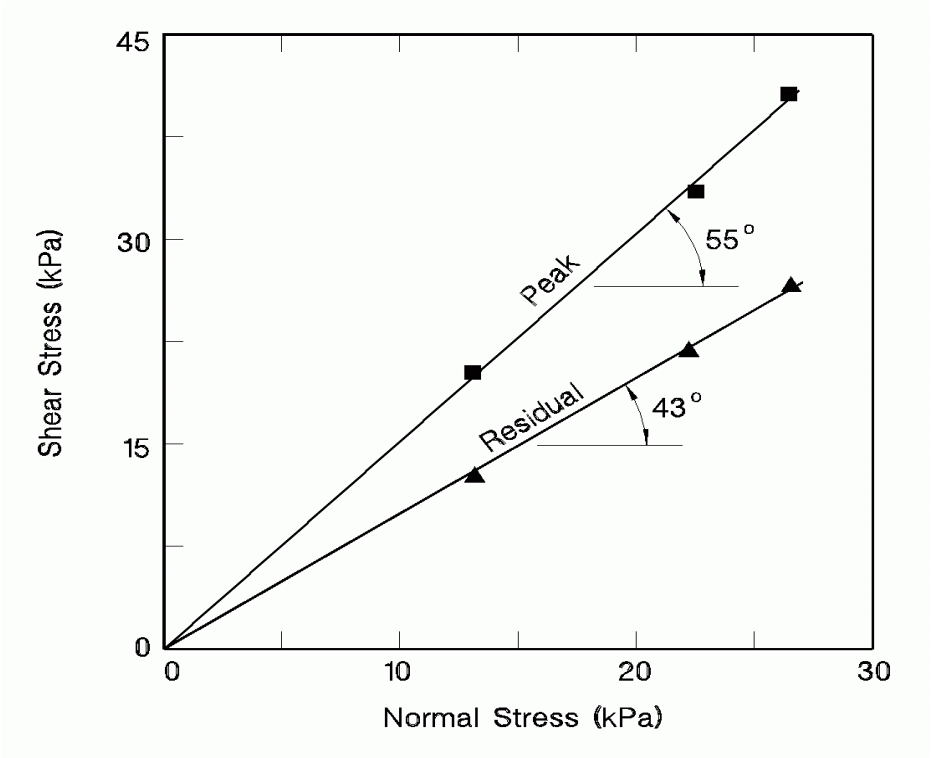

FIGURE 2.18 PROJ 24-12.doc

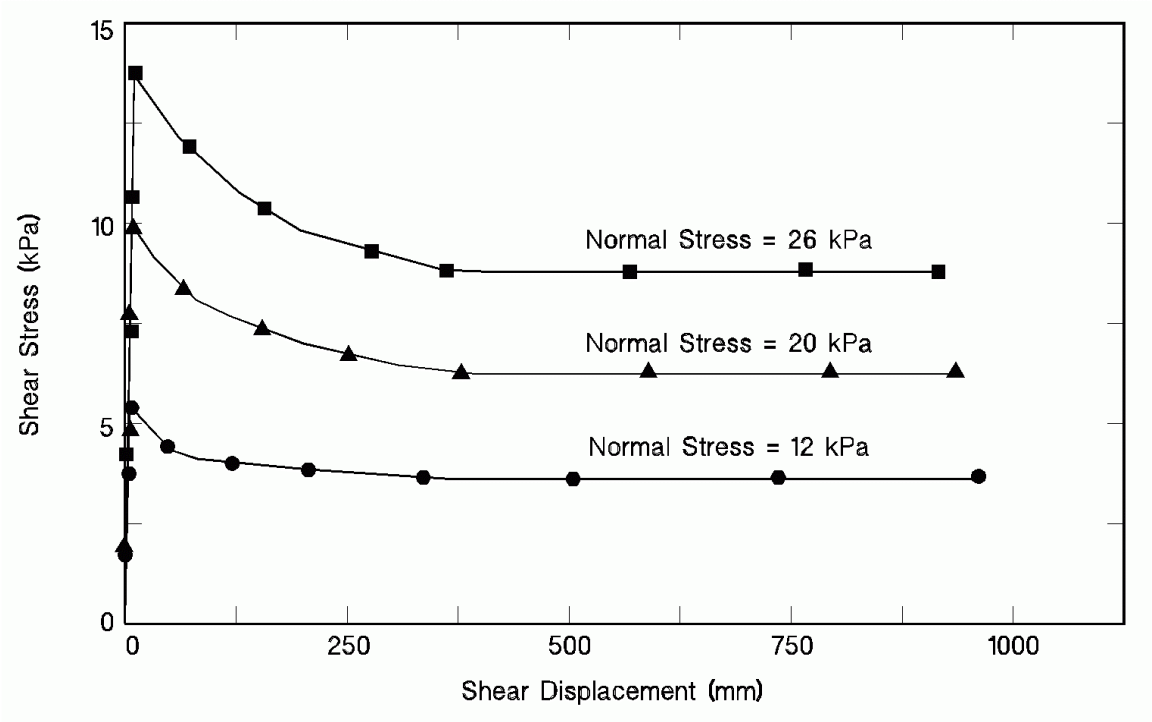

FIGURE 2.19 PROJ 24-12.doc

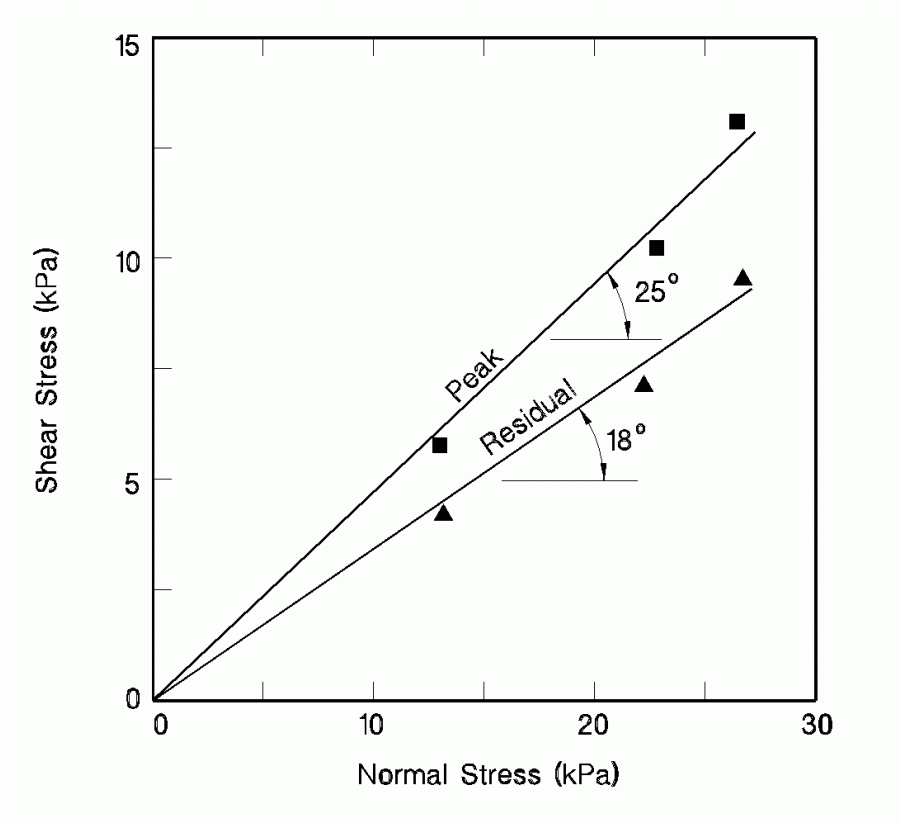

FIGURE 2.20 PROJ 24-12.doc

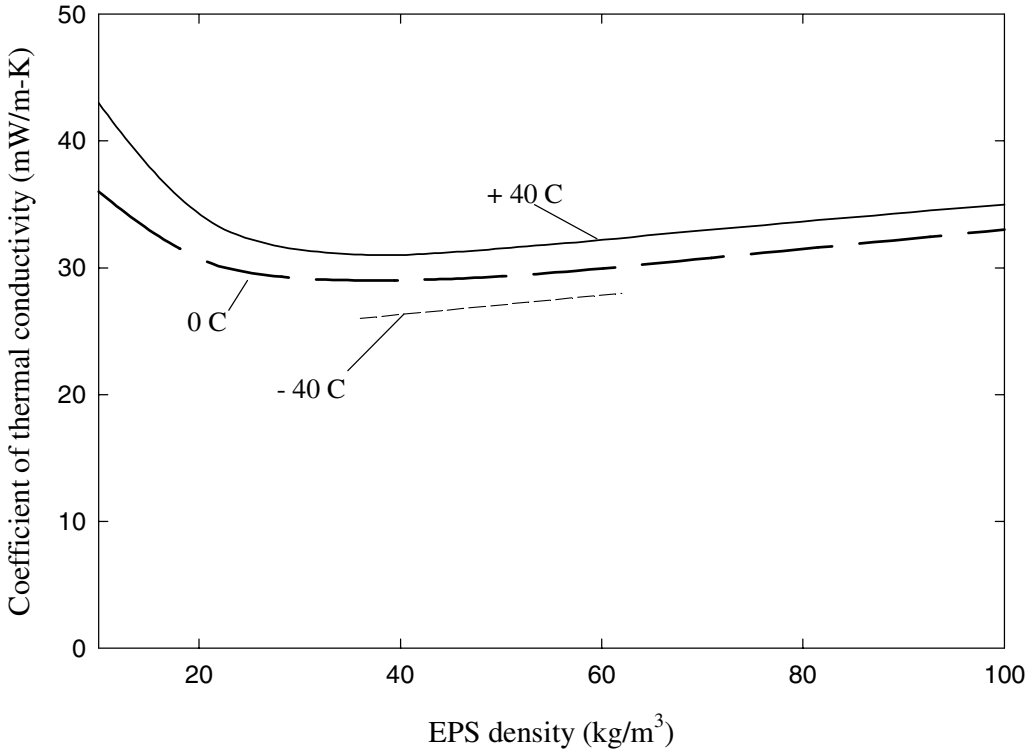

FIGURE 2.21 PROJ 24-12.doc

Temperature Range	Rate of Change	Comment
less than 0°C (+32°F)	0%	Remains approximately constant
+23°C (+73°F) to 0°C (+32°F)	+7% per 10°C (18°F)	Increases linearly with decreasing temperature
+23°C (+73°F) to +60°C (+140°F)	-7% per 10°C (18°F)	Decreases linearly with decreasing temperature

Note: EPS does not become brittle even at -196°C (-321°F).

EPS melts between +150°C (+302°F) and +260°C (+500°F).

Density	Temperature	Stress	Duration	Strain	Strain Increase
20 kg/m^3 (1.25 lbs/ft^3)	+23 °C (+73°F)	30 kPa (626 lbs/ft²)	2,400 hours (approx. 3 months)	0.8%	0%
	+60 °C (+140 °F)			1.5%	88%
	+23 °C (+73 °F)	40 kPa (835 lbs/ft²)	2,400 hours (approx. 3 months)	1.1%	0%
	+60 °C (+140 °F)			3.25%	195%

CHAPTER **3**

DESIGN METHODOLOGY

Contents

INTRODUCTION

Despite the worldwide use of EPS-block geofoam, a specific design guideline for its cost-effective use as lightweight fill in roadway embankments is unavailable. Therefore, the overall objective of this research was to develop a consistent design methodology to optimize both the technical performance and cost through the development of a comprehensive design guideline including design and analysis procedures for the use of EPS-block geofoam in road embankments over soft ground. This chapter presents detailed background information on the design methodology incorporated in abbreviated form in the provisional design guideline included in Appendix B. The recommended design methodology is based on an assessment of existing technology and literature as well as findings of the research performed during this study.

The chain link analogy applied to geotechnical design in Figure 3.1 is used to illustrate the general design approach for the design of embankments over problem foundations (*1,2*). The geotechnical design system is compared with each link representing a design stage, e.g., sampling, testing, analysis, and application of tolerable criteria, anchored to previous experience of similar structures in the project area. The key point of the analogy is that the system is only as strong as its weakest link. If any link, or if the anchorage is insufficient, failure may occur. The second point of the analogy is that if each design stage or link is performed using usual geotechnical engineering practices, designers can "build with confidence or BWC." The recommended design methodology and design guideline for the use of EPS - block geofoam in roadway embankments focuses on the analysis (design) link in the chain. As a result, if the other links are not performed satisfactorily, e.g., sampling or testing, use of the design methodology presented herein will not guarantee satisfactory performance.

Figure 3.1. The geotechnical "system". BWC = Build With Confidence (*1,2*).

Lightweight fill embankments are typically placed over soft saturated soils that are normally or at best slightly overly consolidated. Soft soil ground conditions as defined in the provisional design guideline is a soil subgrade that is compressible and has relatively low shear strength. Design and construction of embankments over soft ground is based on avoiding failure during construction by providing adequate stability and limiting postconstruction settlement to desirable amounts (*3*). The term "failure" as used in the provisional design guideline is a *loss of function*. Failure or loss of function may occur as either a *serviceability failure* (the *serviceability limit state*, SLS) or a *collapse failure* (the *ultimate limit state*, ULS). An embankment over soft soil may experience a serviceability failure due to excessive total or differential settlement that develops over time and which produces premature failure of the pavement system. Premature failure of the pavement system may include an uneven and often cracked pavement surface that may require frequent repaving and possibly other maintenance. An embankment over soft soil may experience a collapse failure through either a rotational (slope stability), lateral spreading, or bearing capacity failure mechanism. The collapse failure may involve at least partial, if not total, collapse.

The overall design goal is to satisfy the following equations for the ULS and SLS respectively:

ULS: resistance of embankment to failure > embankment loads producing failure **(3.1)**

SLS: estimated deformation of embankment ≤ maximum acceptable deformation **(3.2)**

The extent that resistance exceeds loads in Equation (3.1) is interpreted as representing the "safety" incorporated into the design. Thus, the "safety" or *factor of safety* (FS) is defined as

$$FS = \frac{\sum \text{resistances of embankment to failure}}{\sum \text{embankment loads producing failure}} \quad \textbf{(3.3)}$$

In the traditional Allowable Stress Design (ASD) method, the actual service loads are used in the design and safety is incorporated by using a single factor of safety applied to the ULS mechanism (e.g. slope stability) being investigated. The more modern Load and Resistance Factor Design (LRFD) method, safety is incorporated through the use of separate factors applied to simultaneously increase service loads and reduce material strengths or resistances. At the time this report was finalized (2002), geotechnical design practice in the U.S.A. was still in the early stages of transitioning from ASD to LRFD although road design is on the forefront of this transition with LRFD methodologies incorporated into various American Association of State Highway and Transportation Officials (AASHTO) design standards. It appears that refinements to LRFD methodologies are still required before they will be embraced for geotechnical design (*4*). At the present time, design of earthworks incorporating EPS-block geofoam are only designed deterministically using service loads and the traditional Allowable Stress Design (ASD) methodology with safety factors. Regardless of whether ASD or LRFD is used, the SLS assessment reflected in Equation (3.2) is always performed using service loads.

The common strategy for selecting a soft ground treatment alternative has been to use the traditional approach of satisfying Equations (3.1) and (3.2) by utilizing normal soil for the embankment. This means that the resistance and stiffness of the embankment and soft soil foundation must be increased artificially to be able to resist the loads with acceptable deformations. This is accomplished by employing one or more soft ground treatment techniques that collectively increase the strength and reduce the compressibility of the overall system (primarily the existing soft foundation soil but also the embankment soil itself to some degree). Chapter 1 presents an overview of soft ground treatment methods.

Less prevalent is the alternative approach to satisfying Equations. (3.1) and (3.2) of reducing the embankment loads. This involves accepting the natural resistance (strength and compressibility) of the existing soft foundation soil as it exists and employing strategies to sufficiently reduce the loads acting on the soft soils to achieve the goals stated in Equations (3.1)

and (3.2). This is accomplished by using *lightweight fill* materials such as EPS-block geofoam. The most significant aspect of lightweight fill materials is that lightweight fill materials have densities less than that of soil and rock so that the resulting gravity or seismic forces from the fill material are less than those from normal earth materials (*5*). The use of this concept in designing embankments over soft soils may yield a more technically effective and cost efficient embankment.

MAJOR COMPONENTS OF AN EPS – BLOCK GEOFOAM EMBANKMENT

As indicated in Figure 3.2, an EPS – block geofoam embankment consists of three major components:

- The existing foundation soil which may have undergone ground improvement prior to placement of the fill mass.
- The proposed fill mass, which primarily consists of EPS-block geofoam although some amount of soil fill is often used between the foundation soil and bottom of the EPS blocks for overall economy. In addition, depending on whether the embankment has sloped (trapezoidal embankment) or vertical (vertical embankment) sides, there is either soil or structural cover over the sides of the EPS blocks.
- The proposed pavement system, which is defined as including all material layers, bound and unbound, placed above the EPS blocks. The uppermost pavement layer, which serves as the finished road surface, is usually either asphaltic concrete (AC) or portland-cement concrete (PCC) to provide a smooth traveling surface for motor vehicles. AC appears to be the most predominant road surface type because AC pavements tend to tolerate postconstruction settlements better than PCC pavements as well as for economic reasons. However, in certain

applications (e.g., vehicle escape ramps in mountainous regions, logging roads) an unbound gravel or crushed-rock surface layer may be utilized.

Figure 3.2. Major components of an EPS-block geofoam embankment.

DESIGN PHASES

To design against failure, the overall design process is divided into three phases:

- Design for external (global) stability of the overall embankment. This considers how the combined fill mass and overlying pavement system interact with the existing foundation soil. It includes consideration of serviceability issues (SLS), such as global total and differential settlement, and collapse failure issues (ULS), such as bearing capacity and slope stability under various load cases, e.g., applied gravity, seismic, water and wind loading. These failure considerations together with other project-specific design inputs, such as right-of-way constraints, limiting impact on underlying and/or adjacent structures, and construction time, usually govern the overall cross-sectional geometry of the fill. Because EPS-block geofoam is typically a more expensive material than soil on a cost-per-unit-volume basis for the material alone, it is desirable to optimize the design to minimize the volume of EPS used yet still satisfy design criteria concerning settlement and stability. Therefore, it is not necessary for the EPS blocks to extend the full height vertically from the top of the foundation soil to the bottom of the pavement system.
- Design for internal stability within the embankment mass. The primary consideration is the proper selection and specification of EPS properties so that the geofoam mass can support the overlying pavement system without excessive immediate and time-dependent (creep) compression that can lead to excessive settlement of the pavement surface (an SLS consideration).

- Design of an appropriate pavement system for the subgrade provided by the underlying EPS blocks. This design criterion is to prevent premature failure of the pavement system, as defined by rutting, cracking, or similar criterion, which is an SLS type of failure. Also, when designing the pavement cross-section overall consideration should be given to providing sufficient support, either by direct embedment or structural anchorage, for any road hardware (guardrails, barriers, median dividers, lighting, signage and utilities).

A summary of the three-phased design procedure is shown in Table 3.1. Each of the three primary design phases shown in Table 3.1 has been divided into various failure mechanisms that need to be considered for each design phase. Each failure mechanism has also been categorized into either an ULS or SLS failure. These three design phases are conceptually similar to those used in the design process for other types of geosynthetic structures used in road construction, e.g. mechanically stabilized earth walls (MSEWs).

Table 3.1. Summary of Proposed Design Procedure for EPS-block geofoam roadway embankments.

DESIGN PROCEDURE

The design of an EPS-block geofoam roadway embankment over soft soil requires consideration of the interaction between the three major components of the embankment, i.e., foundation soil, fill mass, and pavement system. Because of this interaction, the three-phased design procedure involves interconnected analyses between the three components. For example, some issues of pavement system design act opposite to some of the design issues involving internal and external stability of a geofoam embankment, i.e., the thickness of the pavement system will affect both external and internal stability of the embankment. Additionally, the dead load imposed by the pavement system and fill mass may decrease the factor of safety of some failure mechanisms, e.g., slope stability, while increasing it in others e.g., uplift. Therefore, some compromise is required during design.

It is possible in concept to optimize the final design of both the pavement system and the overall embankment considering both performance and cost so that a technically effective and cost efficient embankment is obtained. However, because of the inherent interaction between components, overall design optimization of a roadway embankment incorporating EPS-block geofoam requires an iterative analysis to achieve a technically acceptable design at the lowest overall cost. In order to minimize the iterative analysis, the solution algorithm shown in Figure 3.3 was developed to obtain an optimal design. The design procedure considers a pavement system with the minimum required thickness, a fill mass with the minimum thickness of EPS-block geofoam, and the use of an EPS block with the lowest possible density. Therefore, the design procedure will produce a cost efficient design.

The design procedure is similar for both trapezoidal and vertical embankments except that overturning of the entire embankment at the interface between the bottom of the assemblage of EPS blocks and the underlying foundation soil as a result of horizontal forces should be considered for vertical embankments as part of seismic stability, translation due to water, and translation due to wind analysis during the external stability design phase.

The purpose of the first step in the design process, background investigation, is to obtain the subsoil conditions at the project site, to obtain estimates of the loads that the embankment system will be subjected to, and to obtain the geometrical parameters of the embankment. Background investigations will be discussed in detail later in this chapter.

The second step of the design procedure is to select a preliminary type of EPS-block geofoam and to design a preliminary pavement system. Although the pavement system has not been designed at this point, the pavement system should be equal to or greater than 610 mm (24 in.) in thickness to minimize the effects of differential icing and solar heating as will be discussed in Chapter 4. The design procedure depicted in Figure 3.3 is based on obtaining a pavement system that provides the least amount of stress on top of the EPS-block geofoam embankment to satisfy internal and external stability requirements. Therefore, it is recommended that the

preliminary pavement system be assumed to be 610 mm (24 in.) thick and the various component layers of the pavement system be assumed to have a total (moist) unit weight of 20 kN/m^3 (130 lbf/ft^3) for initial design purposes.

Figure 3.3. Flow chart of design procedure for an EPS-block geofoam roadway embankment.

Figure 3.3. (continued).

Figure 3.3. (continued).

The third step of the design procedure is to determine a preliminary embankment arrangement. Because EPS-block geofoam is typically more expensive than soil on a cost-per-unit-volume basis for the material alone, it is desirable to optimize the volume of EPS used yet still satisfy design criteria concerning settlement and stability. Therefore, to achieve the most cost-effective design, a design goal is to use the minimum amount of EPS blocks possible that will meet the external and internal stability requirements. The design failure mechanisms that will dictate the maximum stress that can be imposed on the soft foundation soil, which dictates the minimum thickness of EPS blocks needed, include settlement, bearing capacity, slope stability, and seismic stability (external).

A minimum of two layers of blocks should be used for lightweight fills beneath roads because a single layer of blocks can shift under traffic loads and lead to premature failure (*6*). Block thicknesses typically range between 610 mm (24 in.) to 1000 mm (39 in.). Therefore, it is recommended that a minimum of two EPS blocks with a thickness of 610 mm (24 in.) each or a total initial height of 1.2 m (4 ft) be considered for the EPS block height to determine the preliminary embankment arrangement during the design process. The preliminary height of conventional soil fill is the total embankment height required based on the background investigation less the preliminary pavement system thickness of 600 mm (24 in.) and the thickness of two EPS blocks of 1.2 m (4 ft).

After the design loads, subsurface conditions, embankment geometry, preliminary type of EPS, preliminary pavement design, and preliminary fill mass arrangement have been obtained, the design continues with external (global) stability evaluation (Steps 4 through 10), internal stability evaluation (Steps 11 through 14), and final pavement system design (Step 15). Because pavement system design aspects must be considered to obtain a preliminary pavement system design, it is presented first (see Chapter 4). External (global) stability evaluation and internal stability evaluations are presented in Chapters 5 and 6, respectively.

As with any design in geotechnical engineering practice, the design procedure of embankments over soft foundations must incorporate tolerable criteria such as minimum factor of safety and maximum allowable settlement. Minimum factor of safety values typically utilized in geotechnical design are based on precedence and can be found in local codes, design manuals, and geotechnical literature. The recommended factors of safety for each failure mechanism calculation that can be considered in preliminary design is summarized in Figure 3.3. However, tolerable settlements for highway embankments are not well established in practice nor is information concerning tolerable settlements available in the geotechnical literature. Postconstruction settlements as much as 0.3 to 0.6 m (1 to 2 ft) during the economic life of a roadway are generally considered tolerable provided that the settlements are uniform, occur slowly over a period of time, and do not occur next to a pile-supported structure (*7*). If postconstruction settlement occurs over a long period of time, any pavement distress caused by settlement can be repaired when the pavement is resurfaced. Although rigid pavements have undergone 0.3 to 0.6 m (1 to 2 ft) of uniform settlement without distress or objectionable riding roughness, flexible pavements are usually selected where doubt exists about the uniformity of postconstruction settlements and some states utilize a flexible pavement when predicted settlements exceed 150 mm (6 in.) (*7*). Tolerable settlements of bridge approach embankments depend on the type of structure, location, foundation conditions, operational criteria, etc (*1*). The

following references are recommended for information on abutment movements: (*8-11*). Settlement considerations are further discussed in Chapter 5.

Design charts were developed as part of this research to aid in obtaining a technically optimal design. Therefore, these design aids can be used with the proposed design algorithm to assist in developing a cost efficient design. As indicated previously, the design algorithm will assist the designer in developing a cost efficient design.

LIMITATIONS TO THE PROPOSED DESIGN METHODOLOGY AND DESIGN GUIDELINES

The design methodology in Chapters 4, 5, and 6 and the design guideline in Appendix B are intended to provide guidance to civil engineers experienced in geotechnical engineering and pavement engineering when designing lightweight fills that incorporate EPS-block geofoam. The proposed design guideline is limited to embankments that have a transverse (cross-sectional) geometry such that the two sides are more or less of equal height as shown conceptually in Figure 3.4 and are underlain by soft soil defined as relatively compressible and weak. Applications where the fill sides are markedly different and closer to those shown in Figure 3.5 (sometimes referred to as side-hill fills) are excluded from this study because they are the subject of a separate study (*12*). It should be noted from Figure 3.4 (b) that unlike other types of lightweight fill embankments, a vertical embankment can be utilized with EPS- block geofoam. The use of a vertical-face fill embankment, sometimes referred to as a geofoam wall (see Figure 3.4 (b)), will minimize the amount of right-of-way needed and will also minimize the impact of the embankment loads on nearby structures.

The design charts developed as part of this research are based on embankment models with various geometric parameters. Embankment side slopes of 0 (horizontal):1 (vertical), 2 (horizontal):1 (vertical), 3 (horizontal):1 (vertical), and 4 (horizontal):1 (vertical) were predominantly evaluated. Widths at the top of the embankment of 11 m (36 ft), 23 m (76 ft), and 34 m (112 ft) were evaluated. These widths are based on a 2-lane roadway with 1.8 m (6 ft)

shoulders, 4-lane roadway with two 3 m (10 ft) exterior shoulders and two 1.2 m (4 ft) interior shoulders, and a 6-lane roadway with four 3 m (10 ft) shoulders. Each lane was assumed to be 3.66 m (12 ft) wide. Embankment heights ranging between 1.5 m (4.9 ft) to 16 m (52 ft) were evaluated. For simplicity, the fill mass was assumed to consist entirely of EPS blocks.

Figure 3.4. Typical EPS-block geofoam applications involving embankments (*13*).

Figure 3.5. Typical EPS-block geofoam applications involving side-hill fills (*13*).

The design guideline included in Appendix B is expected to be suitable for the preliminary design for most typical projects (projects with either critical or noncritical conditions) and for final design for projects with predominantly noncritical conditions. Examples of critical and noncritical design conditions are provided in Table 3.2. Engineering judgment is required to determine if critical or noncritical design procedures exist for a specific project situation. The concept of critical and noncritical design and construction conditions was adapted by (*1*) from (*14*) which applies this concept to filtration and drainage applications using geotextiles. More detailed design is required for embankments with critical conditions than with noncritical conditions.

Table 3.2. Examples of critical and noncritical embankment design and construction conditions (*1*).

BACKGROUND INVESTIGATIONS

Introduction

Prior to beginning design of a proposed embankment on soft soil, certain background investigations need to be conducted and the relevant results communicated to the embankment designer. Background studies required for typical projects can be categorized into studies related to transportation, hydraulic, structural, and geotechnical engineering. An overview of issues that should be evaluated during the background investigation phase are presented subsequently. Special projects may require modification of these studies and/or additional studies. In addition,

various design jurisdictions may find it useful to reallocate responsibilities from those given here to better match jurisdictional practice or historical precedent.

Transportation Engineering

Transportation engineering issues that the designer needs to assess include issues related to general planning, traffic, and site specific. General transportation items include whether the project involves the rehabilitation or widening of an existing road or an entirely new or relocated road, general vertical and horizontal road geometry, unusual or non-standard vehicle loading, design life of the embankment if not permanent, restrictions on the posted speed limit, and restrictions on the number of traffic lanes. Known restraints and considerations for the general area where construction will occur should also be assessed. Examples of project restrictions and constraints include:

- Any restrictions on maximum duration of construction time, season of construction, days of construction (e.g., no weekends or holidays), times of day for construction and access roads prohibited for construction traffic.
- Any restrictions on physical limits on the right-of-way to be occupied by the permanent structure as well as land available for temporary construction purposes (areas for temporary storage, etc.).
- Identification of known surface and subsurface structures (buildings, utility lines, etc.), especially those that might be particularly sensitive to settlement (e.g., natural gas transmission lines) and thus impact design.
- Identification of overhead obstructions that could impact design or construction, both "hard" (e.g., electrical transmission wires) and "soft" (e.g., glide paths to airports).

Traffic issues that will impact design of the embankment include: vertical, horizontal and cross-sectional geometry of the road surface; posted speed limit; maximum vehicle loading;

estimated annual traffic mix and volume; and ancillary road hardware requirements (shoulder guardrails or barriers, median barriers, overhead lighting, signage).

Civil Engineering

Site specific items that will impact design include existing topography; minimum desired pavement life based on policy of the owning agency; criterion for defining pavement failure (e.g., rutting of a certain depth) for pavement-life calculations; owner preferences, if any, for pavement type; pavement drainage requirements; and below-ground utility requirements for pavement drainage, electrical conduits for overhead lighting and signage, and any others that may cross the proposed right-of-way. The use of an EPS-block geofoam embankment may alleviate the need to relocate underground utilities that may cross the proposed embankment alignment. The Interstate 15 project in Utah presented in Chapter 11 is an example of the use of EPS-block geofoam to alleviate the need for removing underground utilities that crossed the embankment. The use of an EPS-block geofoam with vertical sides will minimize the impact to nearby structures including underground utilities.

Hydraulic Engineering

Evaluation of hydraulic engineering issues is important if the project site is located adjacent or nearby surface-water bodies, particularly rivers and tidal water bodies, that may be subject to significant increases in elevation of their water surface at some time during the design life of the structure due to extreme events such as floods or storms. The hydraulic specialist should estimate the design water elevation for extreme events based on a probability of occurrence that is consistent with the design life of the embankment.

Structural Engineering

If the project involves use of the EPS-block geofoam as backfill behind the abutment of a bridge, the structural engineering specialist designing the bridge should be contacted about overall details such as the type of bridge superstructure, nature of the approach slab (if any), any special geotechnical requirements regarding settlement of the bridge or approach slab, and the

velocity of extreme wind events for which the bridge is being designed. Even if the proposed embankment does not involve a bridge, the structural specialist should still be consulted for input concerning design wind velocity for the project area.

Geotechnical Engineering

Geotechnical engineering issues that the designer needs to assess include issues related to site characterization, design criteria and considerations, and assessment of alternatives. The geotechnical site characterization program should focus on the following four areas: defining the nature and geometry of the relevant soil and rock strata; defining variations with depth of stress history, compressibility, and shear strength of the soft-soil strata in the proposed area of construction; determining the piezometric profile through all relevant soil strata, including potential seasonal and other variations in the ground water table; and assessing relevant seismic design issues based on owning-agency policy and/or the methodologies given in (*15*). The geoenvironmental site characterization program should focus on identifying any potential sources of ground and ground water contamination within the area of proposed construction. If any excavation into or placement of EPS blocks below ground water (including an allowance for future rises in ground water) is anticipated, particular attention must be placed on the nature and concentration of contaminants in the ground water that may affect disposal during construction dewatering or durability of the EPS.

Geotechnical design criteria and considerations that should be evaluated include relevant aspects related to the proposed fill, adjacent structures, and the existing soil conditions. Relevant geotechnical design criteria for the proposed embankment must be established with regard to maximum allowable total settlement of the completed structure and minimum Allowable Stress Design (ASD) safety factor for slope stability of the completed structure. An assessment should be made of any adjacent structures, utilities and transportation facilities (roads, railroads), both existing or proposed, that may be affected by the loads imposed on the ground by the proposed embankment. An assessment should be made of any foundation soil issues over which the use of

EPS-block geofoam in the embankment would have little or no benefit. This includes but is not limited to issues such as creep of existing soft soils, seismic liquefaction of any coarse-grain strata above or below the soft soils, and long-term decomposition and concomitant vertical compression of any underlying non-soil waste materials. The need for pre-construction ground improvement to correct any potential problems should be identified (*15,16*). A summary of ground improvement methods was presented in Chapter 1.

Because the use of EPS-block geofoam is a category of ground improvement, i.e., lightweight fill, the geotechnical engineer should perform an assessment of alternatives. As discussed in Chapter 1, typical alternatives include:

- an embankment consisting of traditional soil fill plus the use of ground improvement (*16*). The possibility that an all-soil embankment would require a different cross-sectional geometry (e.g., flatter side slopes) and thus a larger volume of material as well as right-of-way acquisition should be considered. Note that the direct and indirect costs of time for ground improvement strategies such as preloading and staged construction as well as the cost of necessary geotechnical instrumentation to monitor and quantify ground improvement should be included in this assessment. A discussion of the necessary instrumentation can be found in (*17,18*);
- other lightweight fill materials (*16*). The unique issues associated with alternative fill materials (e.g., compressibility, environmental impact, weather restrictions on construction) should also be considered; and

  a structure (bridge or viaduct) supported on deep foundations.

Design alternatives to the use of EPS-block geofoam should be identified, a preliminary design for each alternative performed, and a cost estimate for each alternative prepared to provide baseline information against which the geofoam alternative will be assessed.

DESIGN LOADS

Introduction

Loads that need to be considered when designing an EPS-block geofoam embankment on soft ground include gravity, traffic, water, seismic, and wind loads. For ultimate limit state calculations, the worst expected loadings are typically used while for serviceability limit state calculations, the typical or average expected loadings are used. It should be noted that the load chosen to represent the worst expected loading in ultimate limit state calculations may differ depending on the failure mechanism being analyzed. For example, for design against hydrostatic uplift (flotation), translation due to water (hydrostatic sliding), and seismic stability the worst expected dead load from the EPS-block geofoam is the dry unit weight. However, for design against bearing capacity failure, slope stability, and load bearing of the EPS, the worst expected dead load from the EPS-block geofoam is the greatest dead load expected, which may be a higher unit weight that considers the potential increase in unit weight of the EPS due to water absorption especially if the EPS blocks are permanently submerged.

Gravity

Components of the embankment system, which are depicted in Figure 3.6, that contribute to gravity loading and need to be considered in external and internal stability analysis include

- The weight of the overlying pavement system (Item A in Figure 3.6), which includes any reinforced PCC slab that might be used at the pavement system and geofoam interface. The issue of utilizing a PCC slab at the bottom of the pavement system is discussed in Chapters 4 and 6.
- The weight of soil cover placed on the sides of a sloped-side embankment (Item B in Figure 3.6) or the weight of the wall elements of a vertical-side embankment (geofoam wall, Figure 3.4(b)).
- The net effective weight of any earth material placed between the existing ground surface and the bottom of the EPS blocks (Item C in Figure 3.6).

Figure 3.6. Components contributing to gravity loads.

Gravity loads can be calculated based on a preliminary assumed cross-section of the embankment, including the pavement system, and any cover material over the sides of the embankment. Although the pavement system has not been designed at this point, it will typically be equal to or greater than 610 mm (24 in.) in thickness to minimize the effects of differential icing and solar heating. The design procedure depicted in Figure 3.3 is based on obtaining a pavement system that provides the least amount of stress on top of the EPS-block geofoam embankment to satisfy internal and external stability requirements. Therefore, it is recommended that the preliminary pavement system be assumed to be 610 mm (24 in.) thick and the various component layers of the pavement system be assumed to have a total (moist) unit weight of 20 kN/m^3 (130 lbf/ft^3) for initial design purposes.

EPS-block geofoam used for lightweight fill applications has a density of the order of 20 kg/m^3 (1.25 lbf/ft^3), which is approximately 1 percent of the density of earth materials. Consequently, the effect of gravity on the assemblage of EPS blocks is negligible and can be omitted in internal stability calculations although this quantity is easily included in calculations if desired. The dry unit weight of the EPS can be taken to be 200 N/m^3 (1.25 lbf/ft^3). Any portion of the EPS blocks that is permanently submerged under normal ground water conditions is assumed to have a total unit weight of 1,000 N/m^3 (6.37 lbf/ft^3) not the dry value of 200 N/m^3 (1.25 lbf/ft^3) for general gravity stress calculations, to conservatively allow for long-term water absorption. Supplemental water considerations such as the potential for flotation from unanticipated rises in water level and horizontal sliding due to any unbalanced water head across the embankment are discussed as part of water loads.

If any permanent excavation of any existing material is performed such that the embankment subgrade level on which the EPS blocks are to be placed is below the existing ground surface, the reduction in load should be considered.

Traffic

The effect of vehicle loads on the road surface is generally negligible compared to the dead load of the pavement system and thus can be ignored in global settlement and stability calculations. However, vehicle loads can be included if desired by dividing the total assumed weight of a vehicle by its footprint area to arrive at an equivalent uniform vertical stress that can be included in calculations. The magnitude of the vehicle weight and footprint area of the design vehicle can be based on either design policy of the owning agency or information in textbooks such as (*19*). Alternatively, 0.67 m (2 ft) of a 18.9 kN/m^3 (120 lbf/ft^3) surcharge material can be used to model traffic stresses at the top of the embankment. Traffic loading should be considered when assessing the internal stability of an embankment containing EPS-block geofoam and for design of the pavement system. A more detailed discussion on estimating traffic loads is included in Chapter 6.

Water

Sites that have soft soil conditions where EPS-block geofoam is usually used will often have ground water at or close to the ground surface. In addition, such sites are often close to surface water bodies such as rivers that are subject to periodic significant changes in water level due to storms and floods (extreme events). Therefore, both normal as well as extreme-event water levels must be considered in design. The 100-year flood water level is typically utilized to represent the extreme-event water level. However, a suitable extreme-event water level should be based on local codes and/or recommendations by a civil engineer.

Three design issues related to water that need to be addressed include increase in total unit weight of the EPS due to long-term water absorption, potential for flotation from unanticipated rises in the normal water level, and horizontal sliding due to an unbalanced water head across the embankment.

Any portion of the EPS blocks that is permanently submerged under normal ground water conditions is assumed to have a total unit weight of 1,000 N/m^3 (6.37 lbf/ft^3), not the dry value of

200 N/m^3 (1.25 lbf/ft^3) suggested for general gravity stress calculations, to conservatively allow for long-term water absorption.

EPS is a closed-cell foam that contains approximately 98 percent air per unit volume. EPS is different than soil in that its void spaces are essentially sealed against any significant water intrusion. Thus, a block of EPS will tend to float if subjected to immersion in water. Consequently, ground and surface water intrusion is a particularly important consideration in problems involving embankments containing EPS-block geofoam and the effect of buoyancy of the EPS must be considered in the net vertical stress calculations. Increases in ground water levels due to extreme events such as floods and a hurricane storm surge should be considered. There have been a few projects (*6*) where embankments containing EPS-block geofoam have suffered an ULS failure due to flotation from unanticipated rises in ground water. As reported in (*20*) and (*6*), the first EPS embankment built in Norway in 1972 failed due to hydrostatic uplift (flotation) in 1987. Although the embankment was designed against the potential for uplift, the design water level used was 0.85 m (2.8 ft) lower than the flood level that occurred in 1987. Thus, the biggest uncertainty in design against uplift is the selection of an appropriate flood elevation to utilize in the design. It is also important that proper temporary dewatering be maintained during construction to prevent hydrostatic uplift due to groundwater rise or surface water intrusion that may collect along the embankment during heavy rainfall. A project in Orland Park, Illinois partially failed during construction due to hydrostatic uplift during a heavy rainfall (*21*). Consequently, each project where EPS-block geofoam is being considered for embankment construction requires a careful assessment of not only the normal seasonal range of ground water levels but also the potential for extreme events due to severe storms that could lead to a temporary rise in ground water.

As an approximate rule of thumb, each meter (3.28 ft) of submergence of a block of EPS below water requires approximately 500 mm (20 in.) of normal-weight surcharge fill material

(soil, pavement, etc.) on top of the EPS blocks to counteract the effects of buoyancy or for every 100 millimeters (4 in.) of submergence of an EPS block there must be 50 millimeters (2 in.) of soil or pavement on top of the EPS blocks to counteract buoyancy effects. Chapters 5 and 6 provide procedures for estimating the overburden required on top of the EPS-block to counteract the effects of hydrostatic uplift. Therefore, the use of EPS-block geofoam alone may not be feasible in areas where there can be significant rises in ground water elevations during the design life of the structure because the overburden required to prevent flotation of the EPS blocks during an extreme flood event may cause excessive settlement and/or instability. In such cases, other design alternatives, including the use of other types of lightweight fill materials that do not have the buoyancy potential of EPS blocks, such as a lightweight fill material with an open texture to better accommodate inundation, should be considered at least for the lower portion of the embankment that may be inundated (*22*). One possible type of lightweight fill that can be considered is *ultra light cellular structures* (ULCS) now called *geocomb* because of their honeycomb appearance in cross section (*22,23*). Geocomb blocks have an open-cell structure that can flood and drain, and thus will not float. Alternatively, the assemblage of EPS blocks can be tied down using passive (initially unstressed) vertical ground anchors. The use of vertical ground anchors has been successfully used in Japan (*24*). The vertical ground anchors can penetrate the EPS blocks and be founded in the underlying foundation soil. The heads of the anchors could be secured by a reinforced-concrete slab cast over the surface of the EPS blocks.

The potential for the embankment to act as a de facto levee for surface water intrusion during extreme-event water levels also needs to be considered especially in cases where the road embankment is adjacent to an open body of water such as a stream, river or lake. An unbalanced head of water acting on the embankment would produce an unbalanced lateral force that may result in translation (horizontal sliding) of the embankment in addition to uplift (Figure 3.7).

Chapters 5 and 6 provide procedures for estimating the overburden required on top of the EPS-blocks to counteract the effects of translation due to water (hydrostatic sliding).

Figure 3.7. Unbalanced water force acting on the side of an EPS-block geofoam embankment.

Seismic

Seismic loading is a short-term event that must be considered in geotechnical problems including road embankments. Seismic loading can affect both external and internal stability of an embankment containing EPS-block geofoam. Most of the considerations for static and seismic external stability analyses are the same for embankments constructed of EPS-block geofoam or earth materials. These considerations include various SLS and ULS mechanisms such as seismic settlement and liquefaction that are primarily independent of the nature of the embankment material because they depend on the seismic risk at a particular site and the nature and thickness of the natural soil overlying the bedrock. A discussion of these topics can be found in (*15*). Mitigation of seismic induced subgrade problems by ground improvement techniques prior to embankment construction is beyond the scope of this study. However, a discussion on ground improvement to reduce potential seismic-induced subgrade problems can be found in (*1,15,25,26*).

The state of practice for evaluating the external seismic stability of geofoam embankments involves using pseudo-static slope-stability analyses (*15*) involving the critical failure surface obtained from the static stability analyses, e.g., Figure 3.8(a). Several road embankments (*27,28*) incorporating EPS-block geofoam have survived relatively severe earthquakes in Japan without any observable damage, which also suggests that this is a conservative analysis and is the basis for the design charts presented in Chapters 5 and 6. Terzaghi (*29*) developed the pseudo-static stability analysis to simulate earthquake loads on slopes and the analysis involves modeling the earthquake shaking with a horizontal force that acts permanently, not temporarily, and in one direction on the slope. Thus, the primary difference between a pseudo-static and static external

stability analyses is that a horizontal force is permanently applied to the center of gravity of the critical slide mass and in the direction of the exposed slope. If a stability method is used that involves dividing the slide mass into vertical slices, the horizontal force is applied to the center of gravity of each vertical slice that simulates the inertial forces generated by horizontal shaking. This horizontal force (F) equals the slide mass or the mass of the vertical slide (m) multiplied by the seismic acceleration (a), i.e., F=m*a. The seismic acceleration is usually derived by multiplying a seismic coefficient, k, by gravity.

In addition to gravity loads of the overlying pavement and soil cover on the sides of the embankment (if a sloped-sided embankment design is used) and transient traffic loads, seismic forces must be considered in the internal stability analyses. Extensive research in Japan during the late 1980s to early 1990s period demonstrated two key aspects with respect to internal seismic response of geofoam embankments:

- The internal seismic response is more complex than the overall external response. This is caused by the EPS-block geofoam acting as a flexible, not rigid, structure and slippage possibly occurring between the blocks. This slippage may result in the mobilization of a post-peak interface strength, which did not have to be considered in the external stability analyses because the shear resistance of the geofoam was assumed to be negligible.
- The inherent inter-block friction between EPS blocks is insufficient to prevent lateral shifting between blocks during a "significant" seismic event. Therefore, the friction must be supplemented by using some mechanical connectors between blocks. From a solid-mechanics perspective, these connectors provide a component of an apparent pseudo cohesion at the interface that is additive to the inherent frictional component provided by the EPS-EPS interface. These connectors are typically some type of barbed metal plate. Unfortunately, no criteria are currently available to quantify "significant" in terms of any of the

magnitude scales (moment, local (Richter), etc.) traditionally used for rating earthquakes on an energy basis. Therefore, the present state of knowledge suggests that a conservative approach is warranted so any embankment designed for seismic loading should incorporate mechanical connectors on all horizontal surfaces between blocks and the geofoam interface shear resistance be measured using laboratory tests that do not utilize mechanical connectors.

The main difference between internal and external seismic stability analysis is that sliding is assumed to occur only within the geofoam embankment in internal seismic stability analysis. Therefore, the interface shear strength data presented in Chapter 2 is used in the internal stability analyses to represent the shear resistance mobilized along geofoam interfaces.

(a) Failure considering the shear strength of embankment materials.

(b) Failure ignoring the shear strength of embankment materials.

Figure 3-8. Typical slope modes of failure involving EPS-block geofoam.

Wind

EPS-block geofoam used as lightweight fill usually has a density of 20 kg/m^3 (1.25 lbf/ft^3), which is approximately 1 percent of the density of earth materials. Because of this extraordinarily low density, the potential for translation (horizontal sliding) of the entire embankment at the interface between the bottom of the assemblage of EPS blocks and the underlying soil foundation due to wind is a potential failure mechanism. This ULS failure mechanism, which is an external stability issue, is unique to embankments containing EPS-block geofoam. The short-term tendency of the entire embankment, such as during construction or immediately after construction, to slide under wind loading is resisted primarily by the undrained shear strength, Su, of the foundation soil if it is a soft clay. However, the long-term tendency of the entire embankment to slide under wind loading is resisted primarily by the EPS-foundation interface friction angle at the base of the embankment. Although the friction angle, δ, for this interface is relatively high (it approaches the Mohr-Coulomb angle of internal friction, ϕ, of the

foundation soil), the resisting force (which equals the dead weight times the tangent of δ) is small because the dead weight of the overall embankment is small. Additionally, geosynthetics such as geotextiles are sometimes used as a separation layer between the fill mass and the natural foundation soil. Consequently, the potential for the entire embankment to slide in a direction perpendicular to the proposed road alignment due to wind is a possible failure mechanism, however there is no documented sliding failure of a geofoam embankment due to wind. At the present time there is no case history data available that provides data on the behavior of an EPS-block geofoam embankment subjected to extreme wind events such as hurricanes, typhoons, and tornados, which might produce a sliding failure.

To date only the French national design guide for EPS-block geofoam road embankments explicitly recognizes the potential for translation of the entire embankment due to wind loading (*30*). The wind driving forces come from applied stresses on both the windward and leeward sides of the embankment as shown in Figure 3.9. Note that the downwind (leeward side) stress is due to suction. The magnitudes of these horizontal stresses can be derived from fluid mechanics theory and are given in (*30*) as:

$$p_U = 0.75V^2 \sin\theta_U \quad \textbf{(3.4)}$$

$$p_D = 0.75V^2 \sin\theta_D \quad \textbf{(3.5)}$$

with V = the wind speed in meters per second, p_U and p_D have units of kilopascals and the other variables are defined in Figure 3.9.

Figure 3.9. Definition of parameters for wind-loading analysis (*13*).

As will be shown in Chapter 5, results from analyses performed during this study on typical EPS-block geofoam embankment geometries indicate that the wind pressures obtained from Equations (3.4) and (3.5) may be too conservative. It is recommended that a more realistic procedure for evaluating the potential for basal translation (sliding) due to wind loading especially under Atlantic hurricane conditions be developed.

REFERENCES

1. Holtz, R. D., "Treatment of Problem Foundations for Highway Embankments." *NCHRP Synthesis 147,* Transportation Research Board, Washington, D.C. (1989) 72 pp.
2. Harr, M. E., *Reliability-Based Design in Civil Engineering*, McGraw-Hill, New York (1987) 291 pp.
3. Hunt, R. E., *Geotechnical Engineering Analysis and Evaluation*, McGraw-Hill, Inc., New York (1986) 729 pp.
4. Goble, G., "Geotechnical Related Development and Implementation of Load and Resistance Factor (LRFD) Methods." *NCHRP Synthesis of Highway Practice 276,* Transportation Research Board, Washington, D.C. (1999) 69 pp.
5. Horvath, J. S., "Geofoam and Geocomb: Lessons from the Second Millennium A.D. as Insight for the Future." *Research Report No. CE/GE-99-2,* Manhattan College, Bronx, NY (1999) 24 pp.
6. Horvath, J. S., "Lessons Learned from Failures Involving Geofoam in Roads and Embankments." *Research Report No. CE/GE-99-1,* Manhattan College, Bronx, NY (1999) 18 pp.
7. "Treatment of Soft Foundations for Highway Embankments." *NCHRP Synthesis 29,* Transportation Research Board, Washington, D.C. (1975) 25 pp.
8. "Bridge Approach Design and Construction Practices." *NCHRP Synthesis of Highway Practice 2,* Transportation Research Board, Washington, D.C. (1969) 30 pp.
9. Wahls, H. E., "Shallow Foundations for Highway Structures." *NCHRP Synthesis of Highway Practice 107,* Transportation Research Board, Washington, D.C. (1983) 38 pp.
10. Moulton, L. K., GangaRao, H. V. S., and Halvorsen, G. T., "Tolerable Movement Criteria for Highway Bridges." *FHWA/RS-85/107,* Federal Highway Administration, Washington D.C. (1985) .
11. Moulton, L. K., "Tolerable Movement Criteria for Highway Bridges." *FHWA-TS-85-228,* Federal Highway Administration, Washington, D.C. (1986) 93 pp.
12. "Slope Stabilization with Geofoam (in prep.)." Syracuse University and The Society of Plastics Industries .
13. Horvath, J. S., *Geofoam Geosynthetic*, , Horvath Engineering, P.C., Scarsdale, NY (1995) 229 pp.
14. Carroll, R. G., Jr., "Geotextile Filter Criteria." *Transportation Reserach Record 916: Engineering Fabrics in Transportation Construction,* Transportation Research Board, National Reserach Council, Washington, D.C. (1983) pp. 46-53.
15. Kavazanjian, E., Jr., Matasovic, N., Hadj-Hamou, T., and Sabatini, P. J., "Geotechnical Engineering Circular No. 3; Design Guidance: Geotechnical Earthquake Engineering for Highways; Volume I - Design Principles." *FHWA-SA-97-076,* U.S. Department of Transportation, Federal Highway Administration, Washington, D.C. (1997) 186 pp.
16. Elias, V., Welsh, J., Warren, J., and Lukas, R., "Ground Improvement Technical Summaries." *Publication No. FHWA-SA-98-086,* 2 Vols, U.S. Department of Tranportation, Federal Highway Administration, Washington, D.C. (1999) .
17. Dunnicliff, J., "Geotechnical Instrumentation for Monitoring Field Performance." *NCHRP Synthesis of Highway Practice 89,* Transportation Research Board, Washington, D.C. (1982) 46 pp.
18. Dunnicliff, J., *Geotechnical Instrumentation for Monitoring Field Performance*, , Wiley-Interscience, New York (1988) 577 pp.
19. Huang, Y. H., "Pavement Analysis and Design." , Prentice-Hall, Inc., Englewood Cliffs, NJ (1993) 805 pp.

20. Frydenlund, T. E., and Aaboe, R., "Expanded Polystyrene - A Light Solution." *International Symposium on EPS Construction Method (EPS Tokyo '96),* Tokyo, Japan (1996) pp. 31-46.
21. Taccola, L. J., Telephone conversation with Arellano, D. 16 November 1999.
22. "Matériaux Légers pour Remblais/Lightweight Filling Materials." *Document No. 12.02.B,* PIARC-World Road Association, La Defense, France (1997) 287 pp.
23. Perrier, H., "Ultra Light Cellular Structure - French Approach." *Geotextiles and Geomembranes*, Vol. 15, No. 1-3 (1997) pp. 59-76.
24. Ninomiya, K., and Ikeda, M., "Design & construction of EPS method which surfacing and uses anchor for prevention." *International Symposium on EPS Construction Method (EPS Tokyo '96),* Tokyo (1996) pp. 162-167.
25. Elias, V., Welsh, J., Warren, J., and Lukas, R., "Ground Improvement Technical Summaries." *FHWA-SA-98-086,* U.S. Department of Transportation, Federal Highway Adminstration, Washington, D.C. (1999) .
26. Elias, V., Welsh, J., Warren, J., and Lukas, R., "Ground Improvement Technical Summaries." *FHWA-SA-98-086,* Vol. 2, 2 Vols, U.S. Department of Transportation, Federal Highway Adminstration, Washington, D.C. (1999) .
27. Hotta, H., Nishi, T., and Kuroda, S., "Report of Results of Assessments of Damage to EPS Embankments Caused by Earthquakes." *Proceedings of the International Symposium on EPS Construction Method (EPS Tokyo '96),* Tokyo, Japan (1996) pp. 307-318.
28. Miki, G., and Tsukamoto, H., "Behaviour of EPS Embankment in a Scale of Actual Banking by Using EPS Construction Method." *Technical Reports of Construction Method Using Expanded Polystyrol,* Expanded Polystyrol Construction Method Development Method, Tokyo, Japan (undated) .
29. Terzaghi, K., "Mechanisms of Landslides." *Application of Geology to Engineering Practice, Berkey Vol.,* Geological Society of America (1950) pp. 83-123.
30. "Utilisation de Polystyrene Expanse en Remblai Routier; Guide Technique." Laboratoire Central Ponts et Chaussées/SETRA, France (1990) 18 pp.

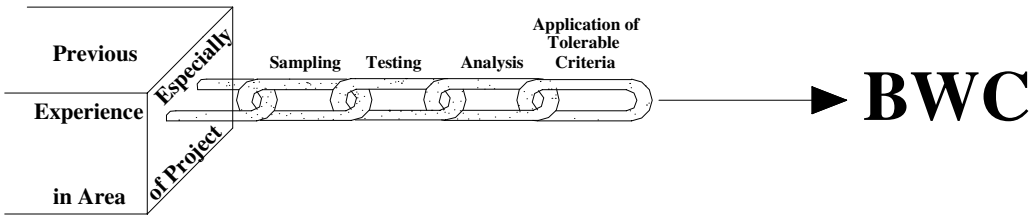

FIGURE 3.1 PROJ 24-11.doc

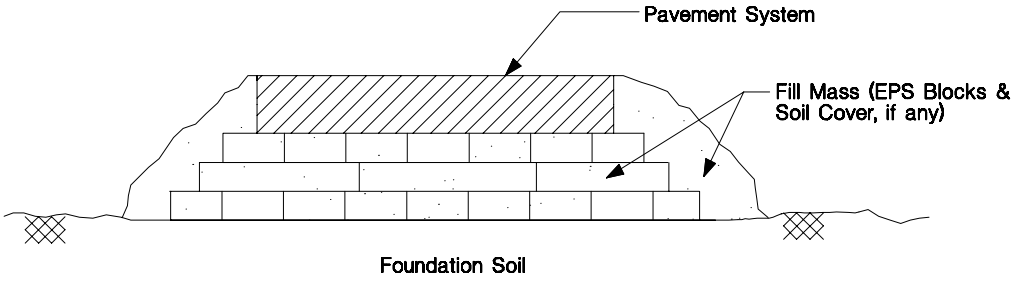

FIGURE 3.2 PROJ 24-11.doc

Main Procedure

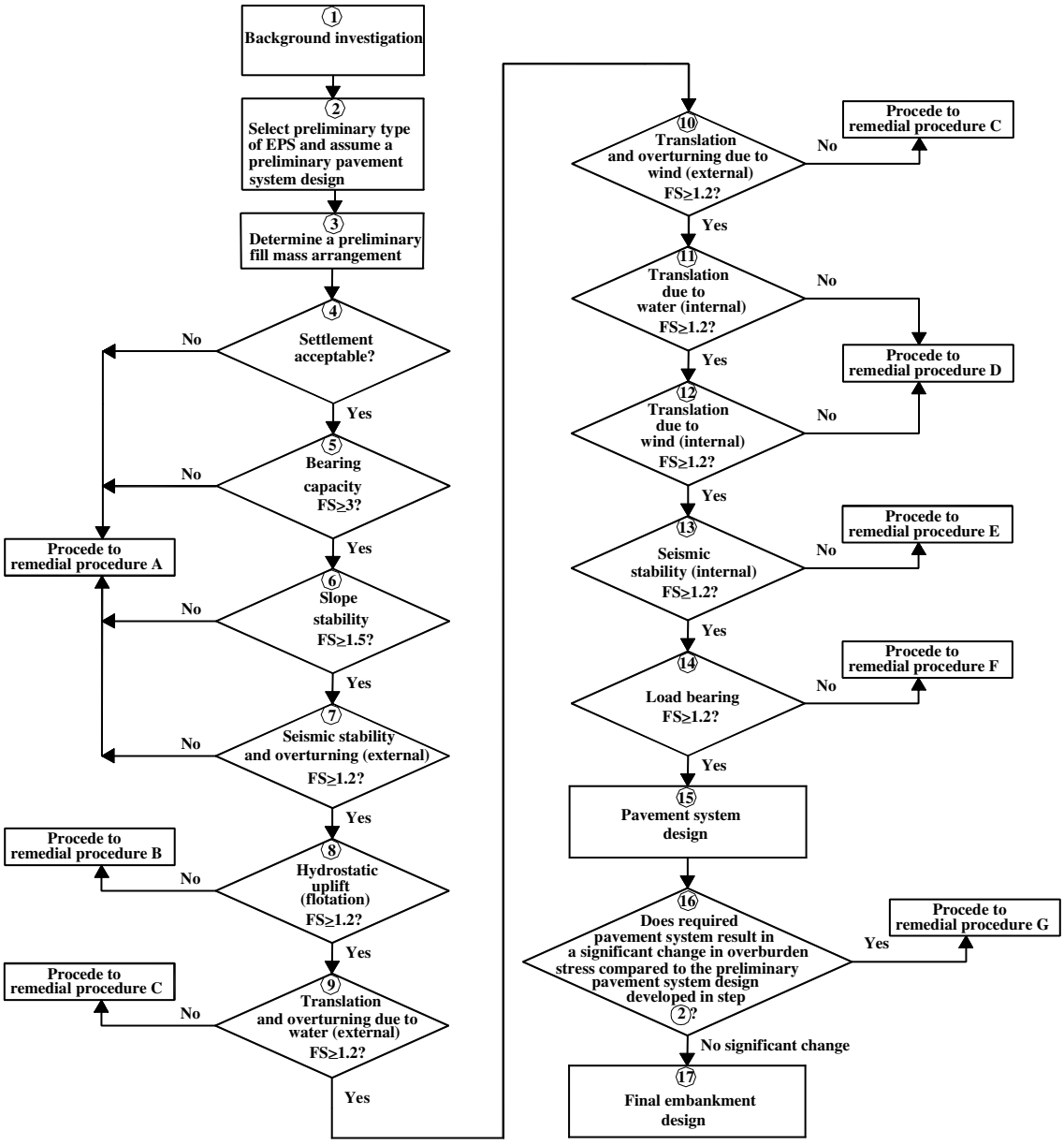

FIGURE 3.3 PROJ 24-11.doc

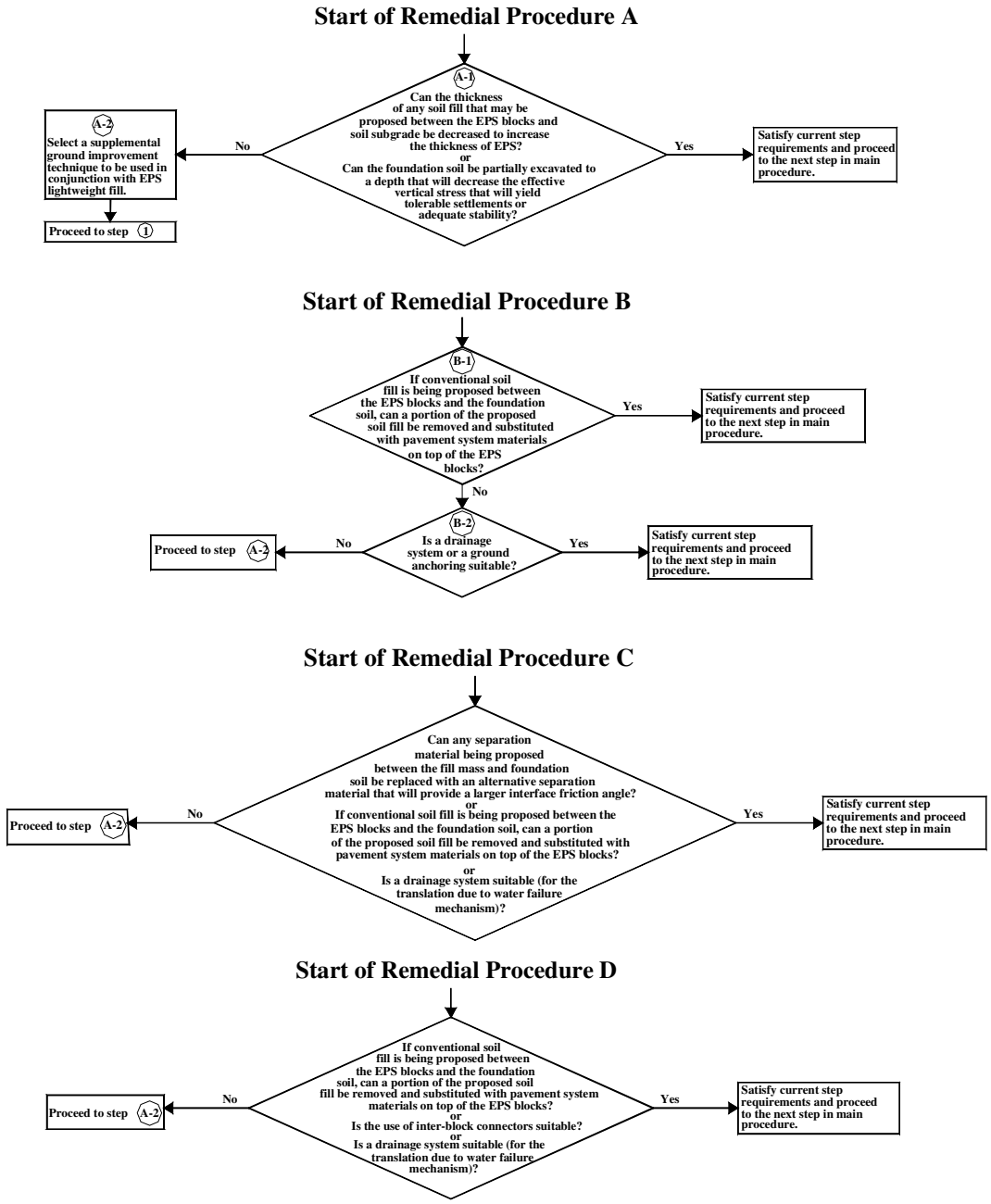

Note: These remedial procedures are not applicable to overturning of a vertical embankment about the toe of the embankment at the embankment and foundation soil interface. If the factor of safety against overturning of a vertical embankment is less than 1.2, consideration can be given to adjusting the width or height of the vertical embankment.

FIGURE 3.3 PROJ 24-11.doc

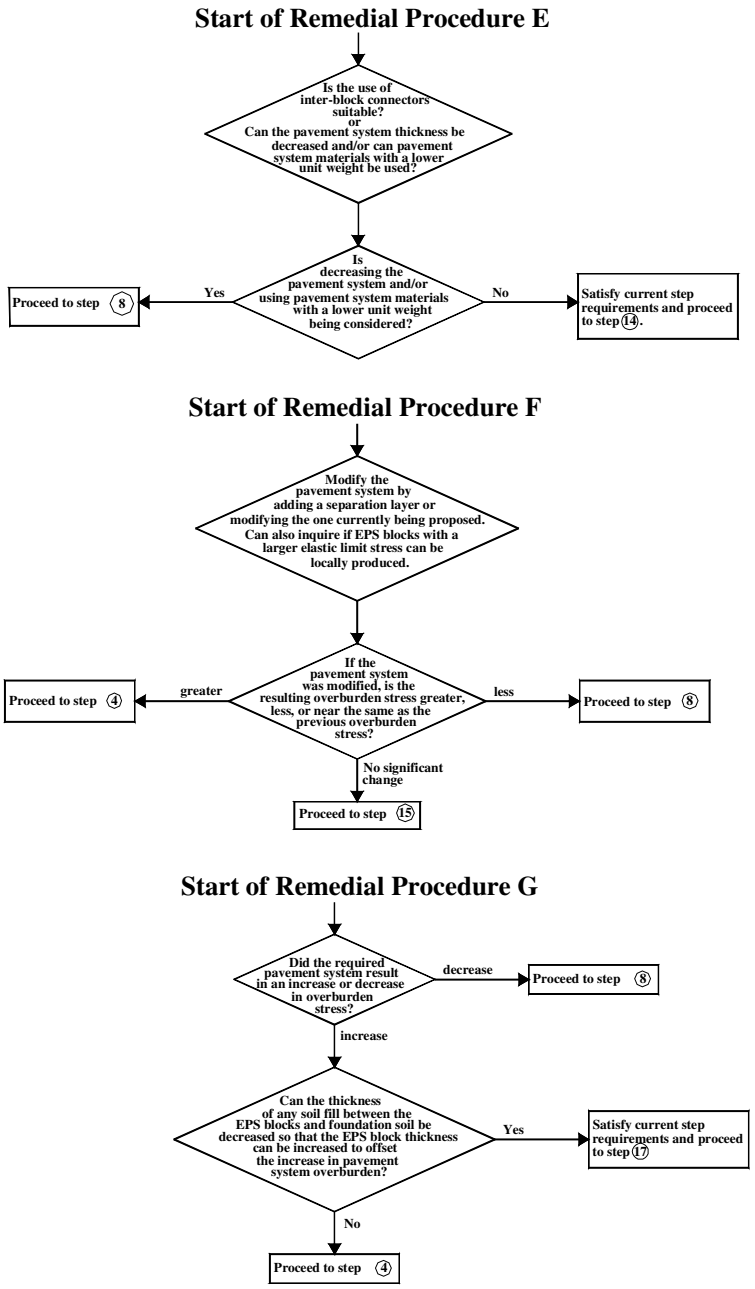

Note: These remedial procedures are not applicable to overturning of a vertical embankment about the toe of the embankment at the embankment and foundation soil interface. If the factor of safety against overturning of a vertical embankment is less than 1.2, consideration can be given to adjusting the width or height of the vertical embankment.

FIGURE 3.3 PROJ 24-11.doc

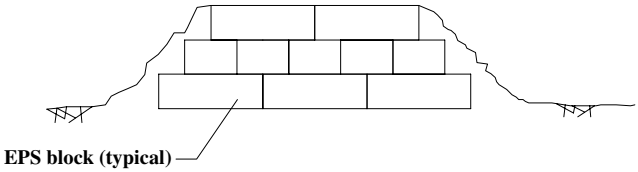

(a) Sloped-side fill.

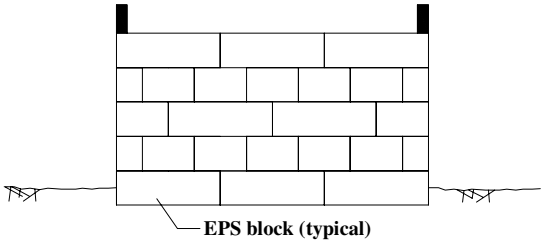

(b) Vertical-face fill.

FIGURE 3.4 PROJ 24-11.doc

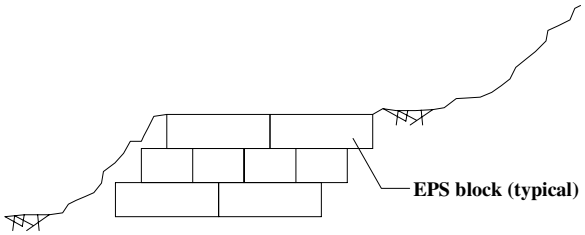

(a) Sloped-side fill.

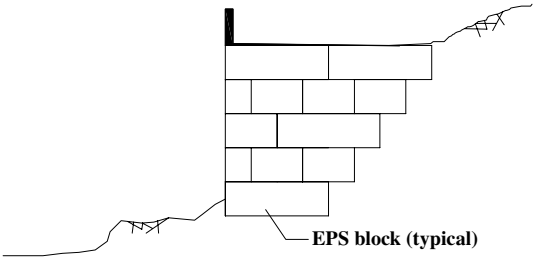

(b) Vertical-face fill.

FIGURE 3.5 PROJ 24-11.doc

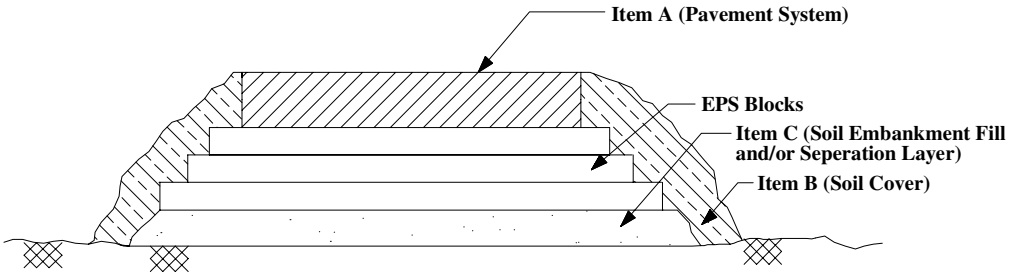

FIGURE 3.6 PROJ 24-11.doc

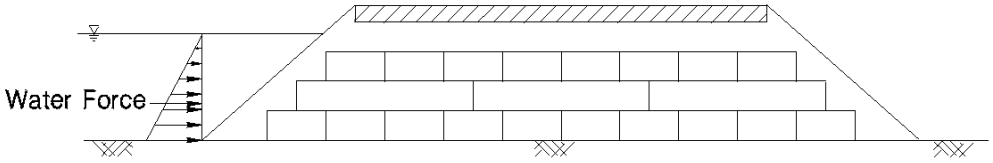

FIGURE 3.7 PROJ 24-11.doc

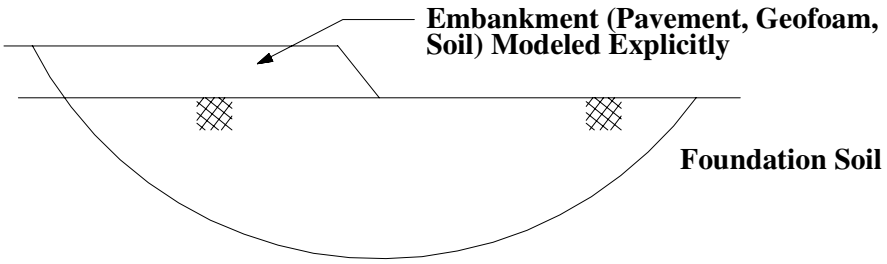

FIGURE 3.8A PROJ 24-11.doc

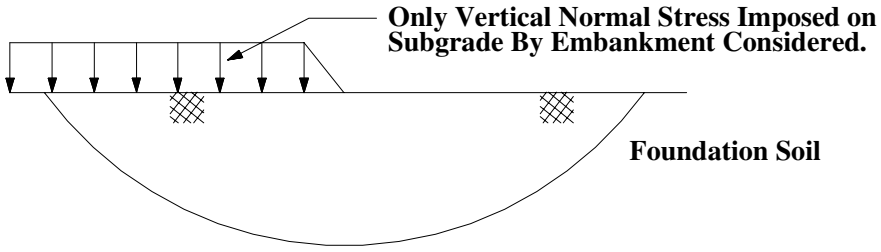

FIGURE 3.8B PROJ 24-11.doc

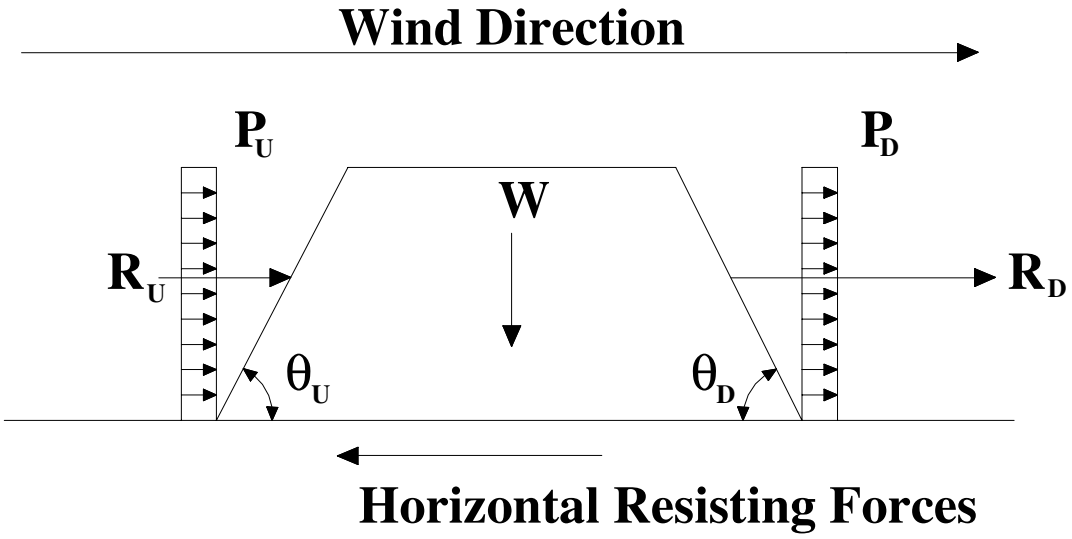

FIGURE 3.9 PROJ 24-11.doc

DESIGN PHASE	Limit State*	Failure Mechanism	Determines	Accounts for
External (global) Stability	SLS	Settlement*	Need for additional ground improvement (See Table 1.1)	Excessive and/or differential settlement from vertical and lateral deformations of the underlying foundation soil.
	ULS	Bearing capacity*	Need for additional ground improvement (See Table 1.1)	Downward vertical movement of the entire embankment into the foundation soil due to bearing capacity failure of the entire embankment
	ULS	Slope stability*	Need for additional ground improvement (See Table 1.1)	Downward vertical movement of the entire embankment into the foundation soil due to deep-seated rotational type slope instability
	ULS	Seismic stability*	Need for additional horizontal shear resistance between the embankment and foundation soil	Horizontal sliding of entire embankment due to seismic loading.
			Need for adjusting the width or height of an embankment with vertical walls.	Overturning of a vertical embankment about the toe of the embankment at the embankment and foundation soil interface
	ULS	Hydrostatic Uplift (flotation)	Need for ground anchors	Upward vertical movement of the entire embankment due to a rise in ground water table
	ULS	Translation due to water (hydrostatic sliding)	Need for additional horizontal shear resistance between the embankment and foundation soil	Horizontal sliding of entire embankment due to an unbalanced water head across the embankment.
			Need for adjusting the width or height of an embankment with vertical walls.	Overturning of a vertical embankment about the toe of the embankment at the embankment and foundation soil interface
	ULS	Translation due to wind	Need for additional horizontal shear resistance between the embankment and foundation soil	Horizontal sliding of entire embankment due to an extreme wind event.
			Need for adjusting the width or height of an embankment with vertical walls.	Overturning of a vertical embankment about the toe of the embankment at the embankment and foundation soil interface
Internal Stability	ULS	Seismic stability*	Need for additional horizontal shear resistance between blocks and	Adequate horizontal shear resistance between blocks and adequate shear resistance between the pavement system

			between the pavement system and the upper layer of blocks	and the EPS mass to include the separation material, if any used.
	ULS	Translation due to water (hydrostatic sliding)	Need for additional horizontal shear resistance between blocks	Adequate horizontal shear resistance between blocks due to an unbalanced water head across the embankment.
	ULS	Translation due to wind	Need for additional horizontal shear resistance between blocks	Adequate horizontal shear resistance between blocks
	SLS	Load bearing*	EPS properties	Excessive vertical deformation
Pavement System	SLS	Flexible or rigid pavement design procedure	Most economical arrangement and thickness of pavement system materials, density of upper EPS block, and need for a separation layer between the pavement system and EPS mass	Subgrade support provided by the EPS blocks and loads from traffic and environment to protect the pavement and EPS mass from distress and to minimize the potential for differential icing and solar heating effects

Notes: SLS = serviceability limit state

ULS = ultimate limit state

*An increase in overburden defined as the dead load stress imposed by the pavement system and/or fill mass may decrease the factor of safety of the failure mechanism.

	Critical	Noncritical
Stability	Large, unexpected, catastrophic movements	Slow, creep movements
	Structures involved	No structures involved
	No evidence of impending instability failure	
Settlements	Large total and differential	Small total and differential
	Occur over relatively short distances	Occur over large distances
	Rapid direction of traffic	Slow transverse to direction of traffic
Repairs	Repair cost much greater than original construction cost	Repair cost less than original construction cost

CHAPTER **4**

PAVEMENT SYSTEM DESIGN

Contents

INTRODUCTION

The objective of pavement system design is to select the most economical arrangement and thickness of pavement materials for the subgrade provided by the underlying expanded

polystyrene (EPS) blocks. The design criteria are to prevent premature failure of the pavement system, as defined by rutting, cracking, or similar criterion, which is a SLS type of failure, as well as to minimize the potential for differential icing (a potential safety hazard) in those areas where climatic conditions make this a potential problem. Also, when designing the pavement cross-section overall, consideration must be given to providing sufficient support, either by direct embedment or structural anchorage, for any road hardware (guardrails, barriers, median dividers, lighting, signage and utilities). However, a unique aspect of pavement design over lightweight fill is that the design must also consider the external and internal stability of the embankment. The pavement system is defined as including all materials, bound and unbound, placed above the EPS blocks.

Table 4.1 provides a summary of EPS-block geofoam engineering parameters typically used in pavement design. Resilient modulus values for typical EPS densities range from 5 to 10 MPa (725 to 1,450 lbs/in²) and the corresponding California Bearing Ratio (CBR) values range between 2 and 4 percent. Therefore, depending on the design traffic loads and desired pavement life a relatively thick pavement system, minimum 610 mm (24 in.), will be required for embankments containing EPS-block geofoam. The benefits of using a thicker pavement system include increased pavement life, increased internal stability of the embankment (see Table 3.1), reduced potential for differential icing, reduced potential for solar heating, and better accommodation of shallow utilities and road hardware. The drawbacks of a thicker pavement system include increased weight which will decrease external stability of the embankment (see Table 3.1). Thus, some compromise is required to optimize the final design of both the pavement system and overall fill. The benefits and drawbacks of utilizing a thicker pavement system are further discussed in the subsequent sections. Procedures for design of pavement systems over EPS-block geofoam embankments are also summarized and recommendations regarding

preliminary pavement system thickness and material unit weights to utilize for preliminary external and internal stability analysis are provided.

Table 4.1. Equivalent Soil Subgrade Values of EPS-Block Geofoam for Pavement Design.

This chapter presents detailed information on the pavement design aspect of the EPS-block geofoam design methodology. An abbreviated form of the pavement design procedure can be found in the provisional design guideline included in Appendix B.

BENEFITS OF A THICKER PAVEMENT SYSTEM

Increase in the Life of the Pavement

The objective of "flexible" pavement design using asphaltic-cement concrete (AC) is to determine the type, thickness, and arrangement of the various pavement layers to minimize critical pavement responses and provide a serviceable pavement for the intended design life (*1*). Pavement responses are the stresses, strains, and deflections that occur in AC pavements from traffic loading, daily or seasonal temperature variations, moisture changes, and changes in the pavement support conditions. Critical pavement responses are those material responses which, through a single or repeated occurrence, will result in structural deterioration of the pavement (*1*). Critical AC pavement responses include the tensile strain at the bottom of the AC or stabilized base layer, the vertical stress on the top of any unbound granular layer, and the vertical stress at the top of the subgrade (*1*). Each layer of the pavement system must be designed to prevent overstressing of the underlying layers. The load that a pavement layer can carry is related to the stiffness of the layer. Stiffness of a material is its ability to resist deformation within the linear elastic range of the stress-strain relationship (*2*). It is the magnitude of force that must be applied at some point to produce a unit displacement at that point (*3*). Stiffness of a pavement layer is often measured by $E*D^3$ where E is the modulus of elasticity of the layer and D is the thickness of the layer (*1*). This relationship indicates that the thickness has more influence than the material modulus in the performance of the layer. Thus, the best method of preventing overstressing of the

underlying layers is primarily accomplished by increasing the thickness of selected upper layer(s). A thicker layer will also reduce the tensile stresses and strains at the bottom of a stiff layer that is placed on a less stiff layer as is typically the case in pavement sections. Additionally, the most cost effective method of reducing the compressive stresses in the subgrade is to increase the thickness of the subbase or the layer that provides the most stiffness for the least cost (*1*).

The objective of "rigid" pavement design using portland-cement concrete (PCC) is to determine the slab thickness, base type, joint spacing, load transfer, and drainage that will limit stresses in the PCC pavement and that will result in the lowest annual cost, as shown by both initial construction costs and future maintenance costs. Stresses in PCC slabs result from traffic loads and from environmental sources. Environmental sources of stress include thermal gradients, moisture gradients, drying shrinkage, thermal expansion and contraction, and foundation movements. Critical PCC pavement responses include the maximum bending stress due to load and curl along the longitudinal shoulder joint, midway between transverse joints; the combined load and curl stress along the transverse joints; the maximum corner deflection; and the maximum bending stress between the concrete and dowels (*1*). Since PCC is stronger in compression than tension, tensile stresses that develop from these responses are of primary concern. Stresses in the slab can be reduced by increasing the thickness of the PCC slab and/or subbase. Additionally, shorter joint spacing and drainage improvements can also reduce stresses in the slab.

Increase in Internal Stability

The thickness of the pavement system affects the internal stability of the embankment by two mechanisms. As the thickness of the pavement system increases, the dead-load stress on the EPS increases. However, as the thickness of the pavement increases and the corresponding distance between the pavement surface and the top of the EPS mass increases, the live-load stress on the EPS from vehicle tires decreases. Theoretically, there is an optimum pavement thickness for which the combined dead- and live-load stresses are minimized. This optimum pavement

thickness depends on the unit weights of the pavement materials and the pressure magnitude and footprint area of the vehicle tire.

Differential Icing

Lightweight fill materials, especially non-earth type of materials, have thermal properties that differ from earth materials. The difference in thermal properties will result in the pavement surface overlying lightweight fills to have a temperature different than the pavement surface overlying a soil subgrade. The non-earth pavement section will generally be cooler in winter and warmer in summer (*4*). Two consequences of the variance in thermal properties include the development of differential icing conditions during cold temperatures and increased solar heating of the pavement surface during warm temperatures. The potential safety and maintenance costs associated with the thermal properties of non-earth materials is rarely considered in practice at the present time (*4*).

Differential icing is caused by the formation of ice on the pavement surface that is underlain by non-earth material adjacent to pavement underlain by soil that is ice free (*4*). Differential icing is similar to the "bridge deck" problem whereby the bridge deck freezes before the adjacent road sections in that they both are considered safety hazards (*5*). Thus, differential icing must be considered in the design of the pavement system. A detailed discussion on differential icing, which is included in (*5*), indicates that based on the detailed studies in Norway (*6*) and Sweden (*7*), differential icing can be minimized by providing a sufficient thickness of soil between the top of the EPS mass and the top of the pavement surface. Differential icing can also be minimized by utilizing base and/or subbase materials with sufficient "fines" to hold water, which has a relatively high heat capacity, to provide sufficient retained heat to keep the pavement surface as close to the temperature of the adjacent pavement sections. Fine materials are materials with particle size less than the No. 200 sieve. However, specific recommendations for material particle distributions to include the minimum amount of fines is currently unavailable.

Because using base and/or subbase materials with fines affects the structural quality of the base and/or subbase and due to the lack of standardized tests to determine thermal properties of non-earth materials as well as the lack of a thermal design procedure that considers pavement material thickness and composition, it is recommended that a sufficient thickness of soil between the top of the EPS mass and the top of the pavement surface be used. Based on the minimum recommended pavement system thickness from the Norwegian design guidelines (*5,8*) of 400 mm (16 in.) to 800 mm (32 in.) and the Swedish guidelines of 400 mm (16 in.) to 500 mm (20 in.) (*5,7*), it is recommended that a minimum pavement system thickness of 610 mm (24 in.) be used with EPS blocks. It should be noted that the type of separation layer if any, used between the EPS and pavement system might affect the potential for differential icing. In particular, the use of a PCC slab as a separation layer may actually increase the potential for differential icing.

Solar Heating

The pavement surface overlying lightweight fills will generally be warmer in the summer than a pavement surface overlying a soil subgrade (*4*). Solar heating occurs due to solar heat becoming trapped within the pavement section due to the thermal-insulative characteristics of non-earth lightweight materials (*4*). It is anticipated that solar heating of AC pavements will be greater than that of PCC pavements. This solar heating may accelerate deterioration of the AC pavement layer(s) due to the decrease in the Young's modulus of the AC layer with an increase in temperature. As the modulus decreases, the tensile strain that occurs within the AC with each application of a vehicle load increases. Fatigue failure of AC is linked to the magnitude of tensile strain within the AC under each load application, i.e., the more strain per load cycle the fewer load cycles to achieve a given level of permanent pavement distortion (cracking or rutting).

Although there has not been any explicit study of whether or not AC pavements underlain by EPS-block geofoam experience premature failure, based on the differential icing studies, it is

anticipated that the greater the distance between the top of the pavement and top of the EPS mass, the less of an increase in pavement surface temperature.

Accommodation of Utilities and Road Hardware

Shallow utilities and road hardware (barriers and dividers, light poles, signage) can be accommodated by providing a sufficient thickness of the pavement system to allow conventional burial or embedment within soil or, in the case of appurtenant elements, by anchoring to a PCC slab or footing that is constructed within the pavement section.

DRAWBACKS OF A THICKER PAVEMENT SYSTEM

A thicker pavement system will yield a heavier pavement system. This increase in weight will affect the external stability of the embankment through increased settlement and reduced stability. It is possible to reduce the total thickness of the pavement system and still provide a technically efficient pavement system by utilizing an EPS with a higher density for the uppermost layer of blocks within the horizontal limits of the paved area and by providing a separation material between the EPS and pavement system that will provide reinforcement of an unbound pavement layer placed directly above the separation material. The subsequent paragraphs discuss these two alternatives for decreasing the thickness of the pavement system.

UTILIZING GEOFOAM LAYERS WITH VARYING PROPERTIES

Two possible reasons for utilizing geofoam layers with varying properties in embankment construction are provided below.

- allow a minimum pavement section thickness by utilizing an EPS with a higher density, e.g., *EPS100*, for the uppermost layer of blocks within the horizontal limits of the paved area. The resilient modulus of the EPS blocks directly underlying the pavement system influences the thickness of the proposed pavement system. The use of an EPS with a higher density, and thus higher resilient modulus, in the upper most layer of blocks will allow a thinner

pavement system thickness. However, the predominant practice in the U.S.A. is to utilize a single EPS density for the whole embankment. An investigation into the benefits of using a higher density geofoam layer in the uppermost layer of blocks is required so that a cost-benefit analysis of providing a higher density geofoam versus providing a thicker pavement section can be performed. Preliminary indications are that although the use of a higher density EPS for the uppermost layer will yield a thinner pavement system, the thinner pavement section may not offset the higher cost of using a higher density EPS as shown in the cost data in Chapter 12 where the material cost increases at 55 percent for increasing density from *EPS50* (lowest, recommended directly below paved areas) to *EPS100* (highest). The impact of using a higher density EPS directly below the pavement system is further discussed later in this chapter.

- allow a more cost effective embankment by using lower density blocks at greater depths. Because the total calculated vertical stresses will decrease with depth within the EPS mass as well as be less under the side slopes as opposed to beneath the paved area, it is possible to use multiple densities of EPS blocks, e.g. lower density blocks at greater depths and/or under side slopes. This will reduce overall costs of the EPS-block geofoam. However, for constructability it is recommended that no more than two different density EPS blocks be used on the same project. This use of different densities of EPS blocks affects internal stability and is further discussed in Chapter 6.

SEPARATION MATERIALS

A separation layer between the top of the EPS blocks and the overlying pavement system can have two functions.

- To enhance the overall performance and life of the pavement system by providing reinforcement, separation, and/or filtration. A separation layer used for these purposes is, technically, part of the pavement system.
- To enhance the durability of the EPS blocks both during and after construction.

A separation layer provides reinforcement to the unbound pavement layer by providing additional horizontal confinement. This additional confinement increases the strength and stiffness of the unbound layer because the stress-strain behavior of typical unbound layers, which typically consist of coarse-grained soil, is dependent on the effective confining stress. It is concluded in (*9*) that unbound roadbase materials have a lower "effective" stiffness in pavement structures without a cement-bound load-spreading layer above the EPS subbase compared to a pavement structure with a cement-treated capping layer. It is recommended in (*10*) that a modulus of elasticity value for the unbound material of up to 50 percent lower be assumed in linear-elastic design calculations if the unbound material is placed directly over an EPS subbase than typically assumed for unbound roadbase materials. A cement-treated capping layer is recommended for heavy-duty roads because it neutralizes the effects of open joints between the EPS blocks, provides support to overlying unbound base material under high traffic intensity, and eliminates any restriction for use of less-expensive, low density EPS types (*10*).

The use of a 100 to 150 mm (4 to 6 in.) thick reinforced PCC slab is currently the state of practice primarily because it is considered to be a necessity for providing sufficient lateral confinement of unbound pavement layers when using EPS-block geofoam and because of historical usage of PCC slabs dating back to the earliest EPS-block geofoam lightweight fills in Norway in the 1970s. As a rule of thumb, the slab was found equivalent to unbound material on a 1-to-3 basis, i.e., 1 mm (0.04 in.) of slab replaced 3 mm (0.12 in.) of unbound pavement material although this equivalency has been disputed recently in (*9*). The original function of the PCC slab was for pavement reinforcement and the intent was to allow the use of a minimum pavement

system thickness. In later designs, the PCC slab was also used for the function of a barrier against potential petroleum spills. However, the use of a PCC slab for this function is questionable due the long-term development of cracks in PCC slabs. Problems with the use of a PCC slab include

- The potential for sliding of the slab during an earthquake (the Japanese require L-shaped reinforcing bar dowels cast into the slab that penetrate down into the EPS blocks).
- The potential for ponding of water within the pavement system.
- The increased potential for differential icing and solar heating (due to both a thinner pavement system as well as the thermal properties of PCC).

Additionally, PCC slabs generally represent a significant relative cost. It may be the only PCC work on a project (a major consideration in remote areas). The results of a cost analysis, which is included in Chapter 12, reveal that the cost of a reinforced slab is high and can range from 20 to 30 percent of the total project cost. A survey conducted as part of this study (see Appendix A) listed the cost of the PCC slab as one of the major cost concerns of U.S. engineers in current practice. Alternative separation layers for reinforcement that can be considered in pavement design include a geogrid, a reinforced geomembrane that will also resist hydro-carbon spills, geocell with soil or PCC fill, and soil cement.

One application where a PCC slab is typically required is when an embankment with vertical sides, i.e., geofoam wall, is used (*11*). The primary function of the PCC slab is to support the upper part of the exterior facing system. A secondary function is to provide anchorage for various highway hardware such as safety barriers, signage, and lighting. A PCC slab used for these functions will act primarily as a structural member for the benefit of other embankment system components and not the EPS. Therefore, the PCC slab should be designed for the intended function.

The following is an assessment of the various separation layer alternatives that have either been used or proposed for use over the approximately 30 years that EPS-block geofoam has been used as lightweight fill for road embankments. They are listed in an approximate order of increasing complexity of construction (and, therefore, probable increasing cost):

- No separation material. This is acceptable practice in a number of published design manuals in other countries (*12-14*) and therefore is the baseline against which all other alternatives are compared.
- Separation Geotextile. This offers positive protection against soil particles from the pavement system migrating downward into any gaps between the EPS blocks. A geotextile is known to have been used on a least one road project in Germany where the lowest pavement layer was a fine sand. Interface friction angles between geotextiles and EPS block are provided in Chapter 2.
- Geomembrane. This offers positive protection against both petroleum spills (assuming a petroleum-compatible polymer is chosen for the geomembrane) and soil particle migration. Interface friction angles between geomembranes and EPS block are provided in Chapter 2. For seismic considerations, it is proposed that a Newmark (*15*) sliding block analysis be conducted to assess the magnitude of seismically induced permanent deformation that could occur along the EPS/geomembrane interface. This analysis relates the interface friction to the magnitude of permanent deformation. The magnitude of permanent deformation should not exceed about 50 mm (2 in.). If it does, a different type of geomembrane should be used to increase the frictional resistance. Of course, the geomembrane should be installed and welded by a geomembrane installer that has experience with geomembranes, e.g., landfill liner experience, to reduce the

potential for geomembrane holes. However, the geomembrane surface should not be horizontal because liquid (including surface water infiltrating through the pavement system) could become trapped which could lead to strength loss of the pavement system due to pore-pressure buildup. It is of interest to note that the practice in the U.K. (*14*) is to put a 50 mm (2 in.) (minimum) thick sand bed directly on top of the EPS blocks and then put the geomembrane on the sand bed. The sand bed is crowned to allow gravity flow of any liquid to the sides of the fill.

- Geogrid. This would only stiffen the unbound layer(s) of the pavement system. This alternative has not been researched to date (although the benefit for soil subgrades with CBRs similar to that of EPS-block geofoam has been studied) and there has been no known use of this to date. The geogrid would probably be placed not on top of the EPS blocks but within the lower half of the unbound layer(s) as research to date indicates that this is the most effective location.
- Geocell with soil fill. This would have a primary benefit of stiffening the unbound layer(s) of the pavement system as well as providing a reinforced working surface as a constructability aid. This alternative has not been researched to date for EPS-block geofoam and there has been no known use of this to date. The geocell would be placed directly on top of the EPS blocks.
- Soil cement. This technique involves mixing a relatively small percentage of portland cement with a coarse-grain soil to form what is basically a weak concrete. This would have a primary benefit of stiffening the unbound layer(s) of the pavement system as well as providing both a reinforced working surface as a constructability aid and some protection against petroleum spills (although ponding of water within the pavement system would be a concern as it is with a

geomembrane). An additional concern would be the potential for exacerbating differential icing due to the fact that heat is removed easily from concrete due to the minimal water content of the cement. This alternative has received limited research in Germany solely for its efficacy of stiffening the pavement system and enhancing pavement life. It is not known to have been used for actual fills to date.

- Pozzolanic stabilized materials: These materials consist of flyash, an activator (lime, cement, lime-kiln dust, and/or cement-kiln-dust), and aggregate. The pros and cons of this alternative would be similar to those of soil cement. This alternative is not known to have been used for EPS fills to date.
- Geocell with PCC fill. The pros and cons of this alternative would be similar to those of the soil cement. This alternative is not known to have been used for EPS fills to date.
- Reinforced PCC slab. Although the alternative of no separation layer is the baseline case for technical and cost comparisons, use of a 100 to 150 mm (4 to 6 in.) thick reinforced PCC slab (which is at the opposite end of the design spectrum in terms of cost and complexity) is the state of practice even though mistakenly considered to be a necessity when using EPS-block geofoam. This is due to historical usage of PCC slabs dating back to the earliest EPS-block geofoam lightweight fills in Norway in the 1970s. However, contrary to a widely held belief, the reason for using a slab in Norway was originally and primarily for its pavement reinforcement benefit. As a result, it allowed a minimum pavement system thickness but this is now recognized as increasing the potential for differential icing. It was only later that its benefit to act as a barrier against potential petroleum spills was suggested. However, some have questioned this as

the long-term development of cracks in PCC slabs is not uncommon. Additional problems with using a PCC slab include sliding of the slab during an earthquake (the Japanese require L-shaped reinforcing bar dowels cast into the slab and penetrating down into the EPS blocks); ponding of water within the pavement system; and increased potential for differential icing (due to both a thinner pavement system as well as the thermal properties of PCC). The cost and the fact that it often requires the only PCC work on a project (a major consideration in remote areas) are construction concerns. In summary, a PCC slab is not required and if the cost is excessive one of the alternatives listed above should be used. In addition, if the roadway is not heavily loaded, the unbound pavement layer may not need additional confinement and thus only a geomembrane can be used to protect against hydrocarbon spills.

The need for stiffening the unbound pavement layer(s) should be investigated on a project-specific basis to evaluate whether stiffening or a thicker unbound layer(s) is more cost effective. Some of these alternatives such as the use of a geocell will also provide a stiff working platform during construction and provide some protection of the EPS blocks during construction. The use of a soil-filled geocell is particularly promising because

- It can be placed with relative ease and speed
- It makes use of the granular soils that would be used anyway as part of the pavement system to fill within its cells.
- It enhances constructability as it provides a working surface for placement of subsequent pavement layers.

Migration of the finer soil particles from the unbound layer(s) of the pavement system into the gaps between the EPS blocks may occur due to gravity and erosion due to infiltration (rain or melted snow/ice runoff). Both migration and infiltration could lead to void formation and

settlement of the pavement system. A separation layer to prevent migration and filtration of the finer soil particles from the unbound layer(s) of the pavement system into the small gaps between EPS blocks is only required if the unbound pavement layer(s) contain a relatively large proportion of smaller particles (fine sand and smaller). Small gaps between blocks will occur due to manufacturing tolerances of the EPS blocks, human error, and sloppiness in block placement at the project site. Experience indicates that gaps of the order of 25 mm (1 in.) are acceptable in terms of performance of the overall fill.

A geosynthetic separation layer could be used between the top of the EPS blocks and bottom of the unbound pavement layer to provide separation and filtration of the fine soil particles. An appropriate geotextile would be able to serve both of these functions.

The primary durability concern for EPS in road embankments is the fact that liquid petroleum hydrocarbons (gasoline, diesel fuel/heating oil) will dissolve EPS if the EPS is inundated with the liquid. Therefore, the concern about the potential for a motor vehicle accident involving some type of fuel transport truck wherein large volumes of liquid petroleum hydrocarbons are released, seep downward into the fill, and dissolve the EPS blocks has been expressed in projects that have utilized or considered utilizing EPS. It is suggested that the potential for such an accident is relatively small. When such an accident occurs, it is likely that most of the petroleum is consumed in the fire that often ensues. The petroleum that does seep onto the ground would attack the uppermost pavement layer first (if it is AC as is the more common case). Further, any petroleum that seeped into the embankment would generally trigger an environmental concern requiring excavation and removal of any contaminated material. Therefore, concern over protecting EPS-block geofoam from petroleum spills does not appear great nor cost effective. This position is supported by the German national design manual (*12,13*) which is the most recent developed outside the U.S.A. Consideration may be given to performing

a risk analysis by obtaining petroleum spill occurrence data from a transportation agency or the Environmental Protection Agency (EPA).

If protection of the EPS from vehicle fuel spills is desired, a geomembrane of appropriate composition can be used (*14*). For example, the specifications for the I-15 reconstruction specified a minimum 0.7 mm (28 mil) gasoline-resistant geomembrane manufactured from a tripolymer consisting of polyvinyl chloride, ethylene interpolymer alloy, and polyurethane or a comparable polymer combination.

In summary a separation material between the EPS blocks and pavement system should not be used without a project-specific needs assessment due to the costs involved and the technical viability of not using any separation material. This needs assessment should be based primarily on two considerations:

- The need to prevent soil particles from migrating downward between any small gaps between the EPS blocks. This will depend solely on the gradation of the unbound pavement layer directly on top of the EPS blocks and the care taken during construction to minimize the development of gaps along the vertical joints between EPS blocks.
- The desire to stiffen the unbound pavement layer(s). This becomes more important as the overall thickness of the pavement system decreases and the traffic loads increase.

PAVEMENT DESIGN PROCEDURES

Traditional pavement design procedures may be used by considering the EPS to be an equivalent soil subgrade. The resilient modulus or equivalent CBR value of the EPS can be used in the design procedure. A summary of these design parameters is provided in Table 4.1. These CBR values, which range from 2 to 5 percent, were measured as part of the A47 Great Yarmouth Western Bypass project in the United Kingdom (*14*).

Results of field studies of flexible pavement systems over EPS-block geofoam are available in (*9,16-20*). The findings of these studies are incorporated in the current Dutch design manual for lightweight pavements with expanded polystyrene geofoam (*10*). A summary of these findings is provided below.

- The horizontal strain at the bottom of an asphalt layer, is approximately 15 percent higher when an EPS subbase is used below an unbound roadbase compared to a sand subbase. This strain difference results in a two times lower allowable number of standard axle load repetitions or a two times shorter pavement design life (*9*).
- Because of the low modulus of elasticity of EPS, the thickness of the EPS has only a marginal influence on the pavement behavior under loading and on the pavement design life. The stress and strain values in the upper pavement layers are similar in pavement structures with different thicknesses of the EPS layer (*9*).
- The presence of an EPS subbase in a pavement structure has a significant influence on stress and strain development in the pavement. Unbound roadbase materials have a lower 'effective' stiffness in pavement structures without a cement-bound separation layer above the EPS subbase compared to the stiffness of unbound materials placed over a cement-based separation layer. Although not specifically indicated in (*10*), the most likely reason for these differences in stiffness is that better compaction of the unbound material can be achieved over a cement-bound separation layer than directly over EPS blocks. Therefore, in linear-elastic calculations the assumed modulus of elasticity value for the unbound material should be lower when this material is laid directly over an EPS subbase than when the material is placed over a cement-bound layer (*9*). It is

recommended that the modulus of elasticity of unbound materials placed directly over EPS blocks be reduced by up to 50 percent in design. (*10*).

- Implementation of a cement-treated separation layer on top of the EPS subbase substantially increases the design life of the pavement structure with an EPS subbase. The application of such a layer is therefore recommended for pavement structures subjected to heavy traffic loading (*9*). As noted earlier, this does not mean that a reinforced PCC slab is required in all applications.

Results of field studies of rigid pavement systems over EPS-block geofoam could not be found in the current literature probably because EPS-block geofoam is typically utilized over soft soils where flexible pavements are traditionally used. However, the Interstate 15 reconstruction project in Salt Lake City, Utah used a rigid pavement system over EPS blocks. Therefore, long-term rigid pavement performance will be available in the near future.

Two approaches to pavement system design that can be used for the design of pavements over EPS-block geofoam include mechanistic-empirical methods and empirical-regression methods. Mechanistic analyses involve the external calculation of stresses and strains in various critical regions of a pavement cross-section due to external application of a load, i.e., traffic, using appropriate modeling tools such as an elastic layer analysis or finite element analysis (*21*). The calculated stresses and strains are compared with values known from experimental or theoretical studies to be the maximum allowable, based on predictions of pavement performance (physical distress, such as cracking, rutting, or roughness) (*1*). The pavement can then be designed by adjusting the different layer thicknesses so that the calculated responses are less than the allowable maximum values. The Shell pavement design procedure (*22*) is an example of a mechanistic-empirical procedure. The AASHTO 1993 pavement design procedure (*23*) is an example of an empirical-regression method. The AASHTO pavement design procedure is based on data obtained from a series of road tests and equations obtained from regression methods.

However, it is anticipated that the revised AASHTO 1993 design procedure will include mechanistic-empirical procedures.

The Dutch pavement design procedure is based on the Shell Pavement design procedure (*22*), which is a mechanistic procedure that is based on limiting the horizontal tensile strains at the bottom of the asphalt layer in order to prevent asphalt fatigue cracking and limiting vertical compressive strains at the top of the soil subgrade to prevent excessive permanent deformation in the subgrade. However, the Shell Pavement design procedure was modified to include an EPS subbase. The Dutch pavement design procedure is based on limiting elastic deformation in the EPS subbase due to cyclic (traffic) loading to 0.4 percent (*10*). The Dutch design procedure consists of explicitly calculating the horizontal strain at the bottom of the asphalt layer, the vertical compressive strain on top of the soil subgrade, and the vertical compressive strain on top of the EPS block. The Shell Pavement Design Manual (*22*) provides maximum allowable strain values based on the allowable number of load applications. After the strains of the various layers are calculated, the pavement design life can be determined in terms of the allowable number of 100 kN (22.5 kip) axle load repetitions (*10*).

As part of the research reported herein, pavement design catalogs were developed to facilitate pavement system design. A design catalog is a means for designers to obtain pavement structural designs based on a unique set of assumptions relative to design requirements (*23*). The AASHTO 1993 design procedure was used to develop a flexible and rigid pavement design catalog. The AASHTO design procedure was used because most pavement designers in the U.S. are familiar with this design procedure. However, as with any pavement design, the limitations of the design procedure utilized need to be considered. This is especially true when designing a pavement system over EPS because traditional pavement design procedures were developed for pavement design over a soil subgrade. Therefore, the design obtained using one procedure should be checked by using other design methods, modeling tools, and analytical tools. As more

performance data of pavements over geofoam in the U.S. becomes available, the typical design methods used in the U.S. can be refined and adapted to an EPS subgrade. For pavement design procedures that do not require explicit calculations of stresses and strains within the various layers of the pavement system, it is recommended that the vertical stress on top of the EPS blocks be estimated to verify that it does not exceed the elastic limit stress of the EPS blocks. This checking can be performed utilizing a procedure similar to the one suggested for load bearing analysis of the EPS blocks outlined in Chapter 6.

FLEXIBLE PAVEMENT SYSTEM DESIGN CATALOG

A design catalog or design chart was developed herein for flexible pavements. A design catalog is a means for designers to obtain pavement structural designs based on a unique set of assumptions relative to design requirements (*23*). The flexible pavement design catalog, which is shown in Table 4.2 and developed herein, is based on the following assumptions:

1. All designs are based on the structural requirement for one performance period, regardless of the time interval. Performance period is defined as the period of time that an initial (or rehabilitated) structure will last before reaching its terminal serviceability (*23*).
2. The range of traffic levels for the performance period is limited to between 50,000 and 1,000,000 80 kN (18 kip) ESAL (equivalent single axle loads) applications. An ESAL is the summation of equivalent 80 kN (18 kip) single axle loads used to combine mixed traffic to design traffic for the performance period (*23*).
3. The designs are based on either a 50- or-75-percent level of reliability, which AASHTO considers acceptable for low-volume road design.
4. The designs are based on the resilient modulus values indicated in Table 4.1 for the three typical grades of EPS: *EPS50*, *EPS70*, and *EPS100*.
5. The designs are based on an initial serviceability index of 4.2 and a terminal serviceability index of 2. The average initial serviceability at the AASHO (American Association of State

Highway Officials) road test was 4.2 for flexible pavements. AASHTO recommends a terminal serviceability index of 2 for highways with lesser traffic than major highways.

6. The designs are based on a standard deviation of 0.49 to account for variability associated with material properties, traffic, and performance. AASHTO recommends a value of 0.49 for the case where the variance of projected future traffic is not considered.
7. The designs do not consider the effects of drainage levels on predicted pavement performance.

Table 4.2 is similar in format to the design catalogs provided in (*23*). Although the design catalog in Table 4.2 is for low-volume roads, the use of EPS-block geofoam is not limited to low-volume roads and has been used for high-volume traffic roads such as interstate highways. For example, in the U.S.A., EPS-block geofoam has been used for portions of the Interstate 15 project in Salt Lake City, Utah. A design catalog is typically provided for low-volume roads to limit the number of design variables required in developing pavement structural designs.

Table 4.2. Flexible Pavement Design Catalog for Low-Volume Roads.

Once a design structural number (SN) is determined, appropriate flexible pavement layer thicknesses can be identified that will yield the required load-carrying capacity indicated by the structural number in accordance with the following AASHTO flexible pavement design equation:

$$SN = a_1D_1 + a_2D_2 + a_3D_3 \quad \textbf{(4.1)}$$

where a_1, a_2, and a_3 = layer coefficients for surface, base, and subbase course materials, respectively, and

D_1, D_2, and D_3 = thickness (in inches) of surface, base, and subbase course, respectively.

Layer coefficients can be obtained in (*23*) or from state department of transportation design manuals. However, layer coefficient values for PCC slabs are not provided in (*23*). If a reinforced PCC slab is considered as a separation layer between the top of the EPS blocks and the overlying pavement system, it may be possible to incorporate the PCC slab into the AASHTO

1993 flexible pavement design procedure by determining a suitable layer coefficient to represent the PCC slab. In (*24*), it is indicated that based on test results performed in Illinois, a PCC base with a 7-day strength of 17.2 MPa (2,500 lbs/in²) exhibits a layer coefficient of 0.5.

It can be seen that for a given set of layer coefficients, Equation (4.1) does not provide a unique solution of the surface, base, and subbase thicknesses. Cost effectiveness, construction, and maintenance constraints must be considered to produce a practical design (*23*). However, some guidance is available for estimating these thicknesses from AASHTO. For example, AASHTO recommends the minimum thickness values indicated in Table 4.3 for asphalt concrete and aggregate base to overcome placement impracticalities, ensure adequate performance, and for economic reasons. Additionally, these recommended minimum thicknesses consider the minimum layer thickness requirements for stability and cohesion under traffic loadings. This provides guidance in fixing a value of D_1 and D_2 so D_3 can be estimated in Equation (4.1). In addition, it is recommended herein that a minimum pavement system thickness of 610 mm (24 in.) be used over EPS-block geofoam to minimize the potential for differential icing and solar heating. After various layer thickness combinations have been determined and checked against construction and maintenance constraints, a cost-effective layer thickness combination is typically selected.

Table 4.3. Minimum Practical Thicknesses for Asphalt Concrete and Aggregate Base (*23*).

A sensitivity analysis was performed to demonstrate the effects of varying EPS types at the top of the fill mass on the design structural number (SN). The input values for the sensitivity analysis are shown in Table 4.4. The sensitivity analysis was performed by varying the resilient modulus of the EPS while keeping the remainder of the input variables constant. Although the resilient modulus for the highest density EPS type, *EPS100*, is approximately 10 MPa (1,450 lbs/in²), higher resilient modulus values were also considered in the sensitivity analysis to analyze any potential behavioral trend.

Table 4.4. Standard Set of Inputs for Sensitivity Analysis.

Figure 4.1 illustrates the effect of the EPS block resilient modulus on the design SN. The effect on the design SN is greater at lower resilient modulus values within the range of typical EPS types. The effect of varying the resilient modulus decreases at higher modulus values especially at resilient modulus values greater than 13.8 MPa (2,000 lbs/in²). From Figure 4.1, the required SN is 7.5, 6.8, and 6.1 for an *EPS50*, *70*, and *100*, respectively. Thus, the change in SN between EPS types is 0.7. Therefore, a decrease in structural number may be obtained by using an EPS with a higher density. The sensitivity results with respect to changes in resilient modulus is of special interest because these results indicate the effects of geofoam density on the structural number which can then be used to reduce the cost of the pavement system. This can be accomplished by considering the cost impact of using a higher density geofoam as the upper layer of the fill mass or increasing the thickness of the pavement structure which would impact internal and external stability.

Figure 4.1. Sensitivity of AASHTO design procedure to resilient modulus.

In order to further investigate the potential technical and cost benefits of utilizing an EPS with a higher density for the uppermost layer of blocks within the horizontal limits of the paved area, an example pavement system design was performed based on the design inputs shown in Table 4.4. The pavement system was assumed to consist of asphalt concrete and a crushed stone base. Based on an assumed asphalt concrete thickness of 102 mm (4 in.) with a layer coefficient of 0.44 and a crushed stone base with a layer coefficient of 0.14, the thickness of crushed stone base required would be 1,041 mm (41 in.), 914 m (36 in.), and 787 mm (31 in.) if *EPS50*, *70*, and *100*, respectively, was used for the top layer in the embankment directly underlying the pavement system. Thus, as shown in Figure 4.2, each increase in EPS grade translates into about a 127 mm (5 in.) decrease of crushed stone base.

Figure 4.2. Effect of EPS density on the required base thickness for design example

for an asphalt concrete thickness of 102 mm (4 in.).

Table 4.5 provides a summary of a cost comparison for this example. The use of *EPS50* block is the baseline for comparison against the other two EPS types. Using an *EPS70* would decrease the required crushed stone thickness by 127 mm (5 in.) and would cost about $6.71 per m^2 ($5.62 per yd^2) more than the *EPS50* alternative. However, this cost comparison does not include the cost associated with the time savings of placing EPS blocks versus placing and compacting crushed stone. Using an *EPS100* would decrease the required crushed stone thickness by 254 mm (10 in.) and would cost about $19.15 per m^2 ($16.01 per yd^2) more than the *EPS50* alternative. The final decision as to which EPS type to select will be based on the impact the dead load stresses of each alternative will have on external and internal stability. Assuming that all three alternatives satisfy external and internal stability requirements *EPS50* may be the most economical if placement and compaction of the crushed stone base is not considered. This example suggests that the use of a higher density EPS type for the uppermost layer of blocks may not be cost beneficial for low-volume roads but may be cost beneficial for high-volume roads.

Table 4.5 . Example cost comparison between using various EPS grades versus using additional crushed stone base.

RIGID PAVEMENT SYSTEM DESIGN CATALOG

Design catalogs for rigid pavements developed herein and based on the AASHTO 1993 design procedure are presented in Tables 4.6 and 4.7. The rigid pavement design catalogs are similar to the rigid pavement design catalogs provided in (*23*) except that the designs are based on the resilient modulus values representative of an EPS subgrade shown in Table 4.1. Tables 4.6 and 4.7 can be used by design engineers to obtain a concrete thickness with a geofoam embankment. As with the design catalogs provided in (*23*), Tables 4.6 and 4.7 are based on the following assumptions:

- Slab thickness design recommendations apply to all six U.S. climatic regions.

- The procedure is based on the use of dowels at transverse joints.
- The range of traffic loads for the performance period is limited to between 50,000 and 1,000,000 applications of 80 kN (18 kip) ESALs (equivalent single axle loads). An ESAL is the summation of equivalent 80 kN (18 kip) single axle loads used to combine mixed traffic to design traffic for the performance period (*23*).
- The designs are based on either a 50-percent and 75-percent level of reliability, which AASHTO considers acceptable for low-volume road design.
- The designs are based on a minimum thickness of high quality material subbase equivalent to 610 mm (24 in.) less the PCC slab thickness used. This provides a minimum recommended pavement system thickness over the EPS blocks of 610 mm (24 in.) to minimize the potential for differential icing and solar heating.
- The designs are based on the resilient modulus values indicated in Table 4.1 for *EPS70* and *100*. *EPS40* is not recommended directly beneath paved areas. *EPS50* was not considered because the design chart for estimating the composite modulus of subgrade reaction included in (*23*) does not consider a roadbed soil resilient modulus of less than 6.9 MPa (1,000 lbs/in^2).
- The designs are based on a mean PCC modulus of rupture (S'_c) of 4.1 or 4.8 MPa (600 or 700 lbs/in^2).
- The designs are based on a mean PCC elastic modulus (E_c) of 34.5 GPa (5,000,000 lbs/in^2).
- Drainage (moisture) conditions are fair (C_d = 1.0).
- The 80 kN (18-kip) ESAL traffic levels are:
    - High 700,000 to 1,000,000
    - Medium 400,000 to 600,000

- Low 50,000 to 300,000

- A factor termed the "loss of support" factor is included in the AASHTO rigid pavement design procedure to account for the potential loss of support resulting from base and subbase erosion and/or differential vertical soil movements. Loss of support factors for typical base and subbase materials range between 0 and 3. A loss of support factor of 0 indicates that no loss of pavement support is anticipated and is indicated in the design catalog as edge support equal to "yes". A value greater than 0 indicates that some loss of support may occur. In the design catalog, a loss of support is indicated as edge support equal to "no" and the design is based on a loss of support factor of 3.

Tables 4.6 and 4.7 are similar in format to the design catalogs provided in (*23*). As discussed previously, for the flexible pavement design catalog, although the design catalog in Tables 4.6 and 4.7 are for low-volume roads, EPS-block geofoam can be and has been used for high-volume traffic roads such as interstate highways. A design catalog is typically provided for low-volume roads to limit the number of design variables required in developing pavement structural designs.

Table 4.6. Rigid pavement design catalog for low-volume roads for inherent reliability of 50 percent.

Table 4.7. Rigid pavement design catalog for low-volume roads for inherent reliability of 75 percent.

SUMMARY OF PAVEMENT SYSTEM DATA FROM CASE HISTORIES

Table 4.8 provides a summary of various pavement system designs that have been utilized in the U.S.A. over EPS-block geofoam. Both embankment and bridge approach case histories are included in Table 4.8. These case histories are discussed in Chapter 11. Based on the five case

histories for which pavement thickness data is available, the total pavement system thicknesses range from 508 to 864 mm (20 to 34 in.) and average 660 mm (26 in.).

Table 4.8. Summary of EPS-block geofoam pavement system data from case histories.

TYPICAL DEAD LOAD STRESS RANGE IMPOSED BY A PAVEMENT SYSTEM

The proposed EPS-block geofoam embankment design procedure discussed in Chapter 3 requires that a preliminary pavement system design be assumed to estimate the gravity loads for use in the external and internal stability analyses prior to performing the final pavement design. Therefore, it is useful to establish a dead load stress range that a typical pavement system may impose on the EPS-blocks for use in preliminary internal and external stability analysis.

Two approaches were used to investigate the dead load stresses imposed by typical pavement systems on an EPS-block geofoam embankment. The first approach was to analyze pavement system designs based on the AASHTO 1993 flexible and rigid pavement design procedures for low-volume roads. The second approach was to investigate pavement system data from EPS-block geofoam case histories.

Flexible pavement systems were designed herein by assuming the pavement system over the EPS blocks consists of an asphalt concrete surface, a crushed stone base, and a sandy gravel subbase. The AASHTO minimum recommended thicknesses for asphalt concrete and aggregate base, shown in Table 4.3, were used to determine the thickness of subbase required to provide the required SN. Table 4.9 provides the pavement material layer coefficients and compacted unit weight values that were assumed. The unit weight of the asphalt concrete represents a bulk unit weight and not the maximum theoretical unit weight, the later being the unit weight value that would be obtained if the bituminous layer was compacted such that no voids would remain in the aggregate-bitumen mixture. The unit weight values for the crushed stone base and the sandy gravel subbase were estimated from typical values of optimum moisture content and maximum

dry unit weights based on the ASTM D 698 laboratory procedure indicated in (*26*) and a compaction effort of 97 percent of the maximum dry unit weight.

For each traffic range shown in Table 4.3, the subbase thickness required for the SN values of 3 to 9 was determined. The minimum SN value was selected based on the minimum value of 3.1 obtained for the flexible pavement design catalog for low-volume roads with an EPS subgrade (Table 4.2) The maximum value of 9 was selected because this is the maximum value provided in the AASHTO nomograph provided in (*23*) for obtaining the design SN for a flexible pavement.

Table 4.9. Material layer coefficients and density values used in the analyses of flexible pavements.

For SN values ranging from 3 to 9, an asphalt concrete pavement, and the base thicknesses in Table 4.3, the overall pavement system thickness was less than the minimum pavement system thickness of 610 mm (24 in.), which is recommended over EPS-block geofoam embankments to minimize the potential for differential icing and solar heating. In order to obtain the recommended 610 mm (24 in.) pavement system thickness, the thickness of the sandy gravel subbase was increased to a thickness that would provide a pavement section thickness of 610 mm (24 in.).

Table 4.10 presents a summary of the dead load stresses and average unit weight values of the final flexible pavement systems determined. Stresses ranged from 12.6 to 12.9 kPa (263 to 269 lbs/ft^2) and the average unit weight values ranged from 20.8 to 21.2 kN/m^3 (132 to 135 lbf/ft^3) for the case of a flexible pavement system without a PCC separation layer. The additional stress imposed by a PCC slab separation layer was also investigated. However, the PCC slab was not considered in the design of the pavement system, i.e., the strength contribution of the PCC slab was not considered. The additional stress from the PCC slab was determined by replacing a thickness of subbase equivalent to the thickness of the PCC slab. Thus, in all cases the minimum

recommended pavement system thickness of 610 mm (24 in.) was maintained. Table 4.10 also shows the resulting overall stresses and average unit weights for a flexible pavement system with a 102 and 152 mm (4 and 6 in.) PCC separation layer. Based on an assumed unit weight for the PCC slab of 23.6 kN/m^3 (150 lbf/ft^3), additional stresses imposed by the PCC slab of 0.3 and 0.5 kPa (6.7 and 10 lbs/ft^2) for a 102 and 152 mm (4 and 6 in.) slab, respectively, were calculated. These supplemental stresses yielded average unit weight values for the entire pavement system ranging between 21.3 and 22.0 kN/m^3 (135 and 140 lbf/ft^3).

Table 4.10. Typical dead load stress range for a low-volume road flexible pavement system.

Rigid pavement systems were designed by assuming the PCC slab thicknesses to be between 127 and 216 mm (5 and 8.5 in.) because these PCC slab thicknesses were obtained in the rigid pavement design catalogs (Tables 4.6 and 4.7). A total pavement system thickness of 610 mm (24 in.) was used in all cases because this is the minimum recommended pavement system thickness to minimize the potential for differential icing and solar heating. The thickness of the crushed stone base was determined by taking the difference between 610 mm (24 in.) and the PCC slab thickness. A material unit weight value of 23.6 and 21.7 kN/m^3 (150 and 138 lbf/ft^3) was assumed for the PCC slab and the subbase, respectively. Table 4.11 presents a summary of the dead load stresses and average unit weight values of typical rigid pavement systems. As shown in Table 4.11, stresses obtained ranged from 13.5 to 13.6 kPa (282 to 284 lbs/ft^2) and the average unit weight values ranged from 22.1 to 22.3 kN/m^3 (140 to 142 lbf/ft^3).

Table 4.11. Typical dead load stress range for a low-volume road rigid pavement system.

The results of the analysis for flexible pavement design for low-volume roads, revealed that the thickness of the pavement system was controlled by the minimum thickness of 610 mm (24 in.) recommended to minimize the potential for differential icing and solar heating. The analysis of both flexible and rigid pavement systems indicate that overall average pavement system material unit weight values ranging from 20.8 to 22.3 kN/m^3 (132 to 142 lbf/ft^3). These

average unit weights are based on a 610 mm (24 in.) overall pavement system thickness and low-volume traffic, which is defined in (*23*) as less than 1,000,000 applications of 80 kN (18-kip) ESALs. Average dead load stresses calculated ranged from 12.6 to 13.6 kPa (263 to 284 lbs/ft^2).

The case history data shown in Table 4.8 shows total pavement system thicknesses ranging from 508 to 864 mm (20 to 34 in.). This is an overall average of 660 mm (26 in.). Case history data of EPS-block geofoam projects in Norway reported in (*27*) indicate an average pavement system thickness of 660 mm (26 in.).

The proposed design procedure outlined in Figure 3.3 is based on obtaining a pavement system that provides the least amount of stress on top of the EPS-block geofoam embankment to satisfy internal and external stability requirements. Therefore, it is recommended that the various component layers of the pavement system be assumed to have a total (wet) unit weight of 20 kN/m^3 (130 lbs/ft^3) for initial design purposes, which is the approximate unit weight of typical less costly subbase materials. It is also recommended that the pavement system be assumed to have a thickness of 610 mm (24 in.) for preliminary external and internal stability analyses. Alternatively, the design catalogs (Tables 4.2, 4.6, and 4.7) can be used to obtain a pavement system that can be used for the external and internal stability analyses.

SUMMARY

The thickness of the pavement system will affect both external and internal stability of the embankment**.** The benefits of using a thicker pavement system include increased life of the pavement and factor of safety of certain failure mechanisms affecting internal stability of the embankment (see Table 3.1), reduced potential for differential icing and solar heating, and better accommodation of shallow utilities and road hardware. However, a thicker pavement system will yield a heavier pavement system. This increase in weight will decrease the factor of safety of certain external stability failure modes of the embankment (see Table 3.1). Thus, some compromise is required to optimize the final design of both the pavement system and overall fill.

Regardless of the design process used, the goal of the pavement design should be to use the most economical arrangement and thickness of each material to protect the pavement from distress caused by both traffic loads and the environment (*1*). However, a unique aspect of pavement design over lightweight fill is that the design must also consider the external and internal stability of the embankment.

As indicated in Figure 3.3, a preliminary pavement system must be assumed to perform external and internal stability analysis. Gravity loads can be calculated based on a preliminary assumed cross-section of the embankment, including the pavement system, and any cover over the sides of the embankment. Although the pavement system has not been designed at this point, it should be greater than 610 mm (24 in.) in thickness to minimize the effects of differential icing and solar heating. The design procedure depicted in Figure 3.3 is based on obtaining a pavement system that provides the least amount of stress on top of the EPS-block geofoam embankment to satisfy external and internal stability requirements. Therefore, it is recommended that the preliminary pavement system be assumed to be 610 mm (24 in.) thick and the various component layers of the pavement system be assumed to have a total (moist) unit weight of 20 kN/m^3 (130 lbf/ft^3) for initial design purposes. Alternatively, the design catalogs (Tables 4.2, 4.6, and 4.7) can be used to obtain a pavement system that can be used for external and internal stability analysis.

Results from preliminary analysis performed during this study indicate that the use of a higher density EPS for the uppermost layer of blocks may not be cost beneficial for low-volume roads but may be cost beneficial for high-volume roads.

REFERENCES

1. ERES Consultants Inc., "Pavement Design, Principles and Practices, A Training Course Participant Notebook." Federal Highway Administration (1987) .
2. Beer, F. P., and Johnston Jr., R., *Mechanics of Materials*, , McGraw-Hill, Inc., New York (1981) 616 pp.
3. West, H. H., *Analysis of Structures*, , John Wiley & Sons, Inc., New York (1980) 689 pp.
4. Horvath, J. S., "Non-Earth Subgrade Materials and Their Thermal Effects on Pavements: An Overview." *Report No. CGT-2001-2,* Manhattan College, Bronx, NY (2001) .

5. Horvath, J. S., *Geofoam Geosynthetic*, Horvath Engineering, P.C., Scarsdale, NY (1995) 229 pp.
6. Refsdal, G., "Frost Protection of Road Pavements." *Frost Action in Soils - No. 26,* Committee on Permafrost, ed., Oslo, Norway (1987) pp. 3-19.
7. Gandahl, R., "Polystyrene Foam as a Frost Protection Measure on National Roads in Sweden." *Transportation Research Record No. 1146,* Transportation Research Board, Washington, D.C. (1987) pp. 1-9.
8. "Expanded Polystyrene Used in Road Embankments - Design, Construction and Quality Assurance." *Form 482E,* Public Roads Administration, Road Research Laboratory, Oslo, Norway (1992) 4 pp.
9. Duskov, M., "EPS as a Light-Weight Sub-Base Material in Pavement Structures," Doctor of Engineering thesis, Delft University of Technology, Delft, The Netherlands (1998).
10. Duskov, M., "Dutch Design Manual for Lightweight Pavements with Expanded Polystyrene Geofoam." *Transportation Research Record 1736,* Tranportation Research Board, Washington, D.C. (2000) pp. 103-109.
11. Horvath, J. S., "Is a Concrete Slab *Really* Necessary for EPS-Geofoam Lightweight Fills: Myth versus Reality," In Manhattan College-School of Engineering, Center for Geotechnolgy [website]. [updated 9 August 2001; cited 20 September2001]. Available from http://www.engineering.manhattan.edu/civil/CGT/T2olrgeomat3.html; INTERNET.
12. "Merkblatt für die Verwendung von EPS-Hartschaumstoffen beim Bau von Straßendämmen." Forschungsgesellschaft für Straßen- und Verkehrswesen, Arbeitsgruppe Erd- und Grundbau, Köln, Deutschland (1995) 27 pp.
13. "Code of Practice; Using Expanded Polystyrene for the Construction of Road Embankments." BASF AG, Ludwigshafen, Germany (1995) 14 pp.
14. Sanders, R. L., and Seedhouse, R. L., "The Use of Polystyrene for Embankment Construction." *Contractor Report 356,* Transport Research Laboratory, Crowthorne, Berkshire, U.K. (1994) 55 pp.
15. Newmark, N. M., "Effects of Earthquakes on Dams and Embankments." *Geotechnique*, Vol. 15, No. 2 (1965) pp. 139-159.
16. Bull-Wasser, R., "EPS-Hartschaum als Baustoff für Straßen." *Straßenbau Heft S 4,* Berichte der Bundesanstalt für Straßenwesen, Bergisch Gladbach, Germany (1993) 156 pp.
17. Duskov, M., "Falling Weight Deflection Measurements on Asphalt Test Pavements with EPS at the Bundesanstalt für Straßenwesen." *EPS-Hartschaum als Baustoff für Straßen,* R. Bull-Wasser, ed. Berichte der Bundesanstalt für Straßenwesen, Bergisch Gladbach, Germany (1993) pp. 129-156.
18. Duskov, M., and Bull-Wasser, R., "Analysis of Asphalt Test Pavements with a Sub-Base of Expanded Polystyrene Foam." *Proceedings of the 7th International Conference on Asphalt Pavements-Design, Construction and Performance,*1992, Nottingham, Vol. III (1992) pp. 96-109.
19. Duskov, M., "Materials Research on Expanded Polystyrene Foam (EPS)." *Report 7-94-211-2,* Delft University of Technology, Delft, The Netherlands (1993) .
20. Duskov, M., "DIANA Non-linear Analysis of Pavement Structures with an EPS Sub-base under Static Loading." *Report 7-94-211-3,* Delft University of Technology, Delft, The Netherlands (1994) 41 pp.
21. Huang, Y. H., "Pavement Analysis and Design." Prentice-Hall, Inc., Englewood Cliffs, NJ, (1993) 805.
22. "Shell Pavement Design Manual." Shell International Petroleum Company Limited, London (1983) .

23. American Association of State Highway and Transportation Officials, *AASHTO Guide for Design of Pavement Structures, 1993*, , American Association of State Highway and Transportation Officials, Washington, D.C. (1993) .
24. Van Til, C. J., McCullough, B. F., Vallerga, B. A., and Hicks, R. G., "Evaluation of AASHO Interim Guides for Design of Pavement Structures." *NCHRP Report 128,* Transportation Research Board, Washington, D.C. (1972) .
25. RSMeans Company Inc., *RSMeans Site Work & Landscape Cost Data, 20th Annual Edition, 2001*, , RSMeans Company Inc., Kingston, MA (2000) 638 pp.
26. Lindeburg, M. R., *Civil Engineering Reference Manual*, 4th, Professional Publications, Inc., San Carlos, CA (1986) .
27. Aabøe, R., "13 years of experience with EPS as a lightweight fill material in road embankments." *Plastic Foam in Road Embankments, Publication No. 61,* Norwegian Road Research Laboratary, Oslo, Norway (1987) pp. 21-27.

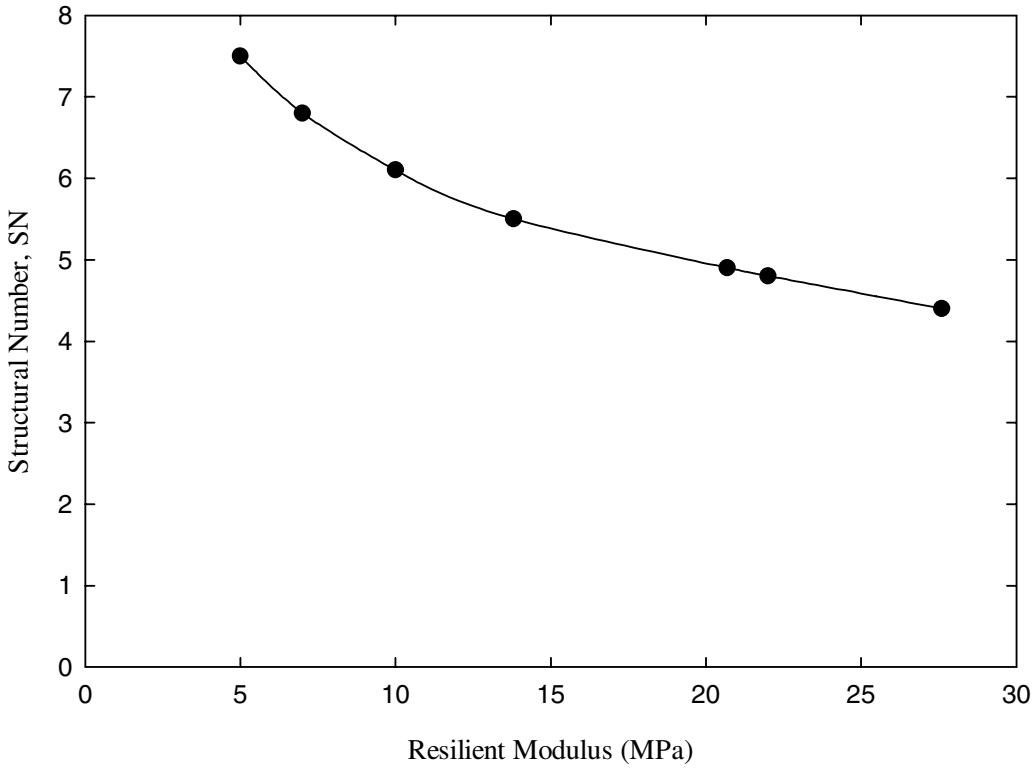

FIGURE 4.1 PROJ 24-11.doc

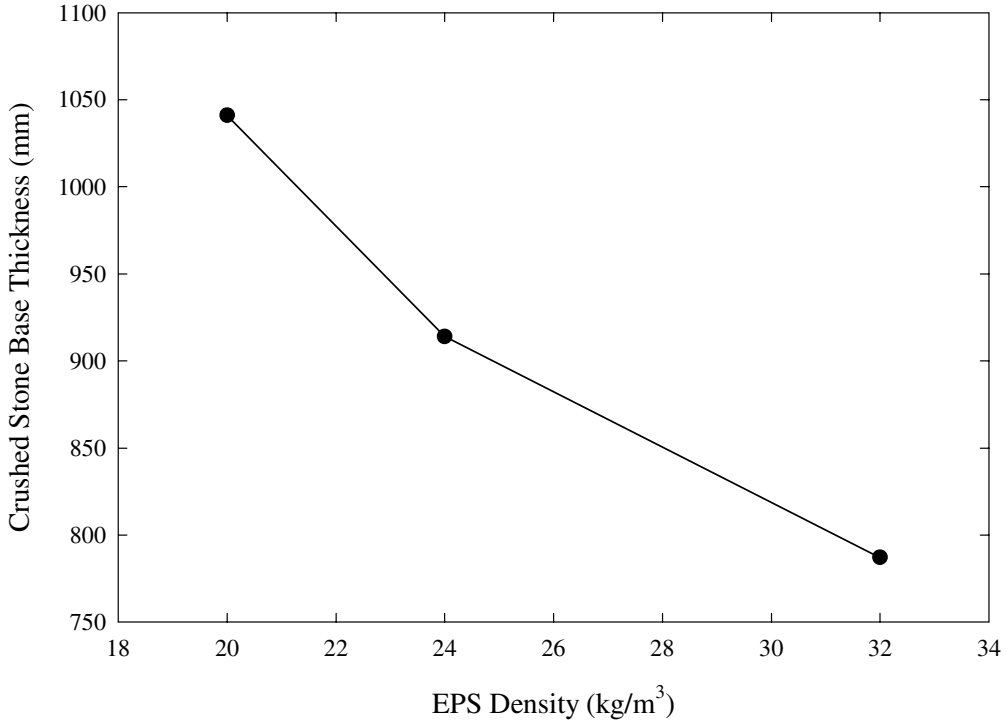

FIGURE 4.2 PROJ 24-11.doc

Proposed AASHTO Material Designation	Design Values of Engineering Parameters			
	Minimum Allowable Full Block Density, kg/m^3(lbf/ft^3)	**CBR (%)**	**Initial Tangent Young's Modulus, E_{ti} MPa(lbs/in^2)**	**Resilient Modulus, M_R MPa(lbs/in^2)**
EPS50	20 (1.25)	2	5 (725)	5 (725)
EPS70	24 (1.5)	3	7 (1015)	7 (1015)
EPS100	32 (2.0)	4	10 (1450)	10 (1450)

Note: The use of *EPS40* directly beneath paved areas is not recommended and thus does not appear in this table because of the potential for settlement problems. The minimum allowable block density is based on density obtained on a block as whole or full-sized block. The proposed AASHTO material type designation system, which is presented in Chapter 9, is based on the minimum elastic limit stress of the block as a whole in kilopascals.

R	**EPS Type**	**Traffic Level**					
(%)		Low		Medium		High	
		50,000	300,000	400,000	600,000	700,000	1,000,000
50	*EPS50*	4*	5.1	5.3	5.5	5.7	5.9
	EPS70	3.5	4.6	4.7	5	5.1	5.3
	EPS100	3.1	4.1	4.2	4.5	4.6	4.8
75	*EPS50*	4.4	5.6	5.8	6.1	6.2	6.5
	EPS70	3.9	5	5.2	5.5	5.6	5.9
	EPS100	3.5	4.5	4.7	5	5.1	5.3

Note: R = Reliability level.

* design structural number, SN.

Traffic, ESALs	Minimum Thickness , mm (in.)	
	Asphalt Concrete	**Aggregate Base**
Less than 50,000	25 (1.0)	100 (4.0)
50,001 – 150,000	50 (2.0)	100 (4.0)
150,001 – 500,000	64 (2.5)	100 (4.0)
500,001 – 2,000,000	76 (3.0)	150 (6.0)
2,000,001 – 7,000,000	90 (3.5)	150 (6.0)
Greater than 7,000,000	100 (4.0)	150 (6.0)

Variable	Initial or Constant Input Value
(18-kip) ESALs Over Initial Performance Period	1,000,000
Initial Serviceability	4.2
Terminal Serviceability	2.5
Reliability Level (%)	90
Overall Standard Deviation	0.44
EPS Block Resilient Modulus	Varied

EPS Type	Total Crushed Stone Thickness mm (in.)	EPS Cost $/m^2 ($/yd^2)	EPS Cost Difference between EPS types $/m^2 ($/yd^2)	Crushed Stone Cost $/m^2 ($/yd^2)	Crushed Stone Cost Difference between EPS types $/m^2 ($/yd^2)	Cost Difference Between Higher EPS Grade and Crushed Stone $/m^2 ($/yd^2)
EPS50	1,041 (41)	26.21 (22.42)	-	27.08 (22.64)	-	-
EPS70	914 (36)	30.48 (25.49)	4.27 (3.07)	23.77 (19.87)	-3.31 (-2.77)	6.71 (5.62)
EPS100	787 (31)	39.62 (33.13)	13.41 (10.71)	20.47 (17.12)	-6.61 (-5.52)	19.15 (16.01)

Note: Cost of EPS is based on a cost of $43.00, $50.00, and $65.00 per cubic meter ($32.88, $38.23 $49.70 per cubic yard) for *EPS50*, *70*, and *100*, respectively, and on a 0.61m (24 in.) block thickness. See Chapter 12 for EPS cost information.

Cost of crushed stone is based on a cost of $26.00 per cubic meter ($19.88 per cubic yard) obtained from (*25*).

			LOAD TRANSFER DEVICES	No				Yes			
			EDGE SUPPORT	No		Yes		No		Yes	
			S'c MPa (lbs/in^2)	4.1 (600)	4.8 (700)	4.1 (600)	4.8 (700)	4.1 (600)	4.8 (700)	4.1 (600)	4.8 (700)
INHERENT RELIABILITY	**EPS TYPE**	**EPS RESILIENT MODULUS**	**Traffic**								
%		MPa (lbs/in^2)	ESALs								
50	*EPS70*	7 (1015)	50,000	5	5	5	5	5	5	5	5
	EPS100	10 (1450)		5	5	5	5	5	5	5	5
	EPS70	7 (1015)	300,000	6.5	6	6	6	6	5.5	5.5	5
	EPS100	10 (1450)		6.5	6	6	6	6	5.5	5.5	5
	EPS70	7 (1015)	400,000	7	6.5	6.5	6	6	5.5	6	5.5
	EPS100	10 (1450)		7	6.5	6.5	6	6	5.5	6	5.5
	EPS70	7 (1015)	600,000	7.5	7	7	6.5	6.5	6	6	5.5
	EPS100	10 (1450)		7.5	7	7	6.5	6.5	6	6	5.5
	EPS70	7 (1015)	700,000	7.5	7	7	6.5	6.5	6	6	6
	EPS100	10 (1450)		7.5	7	7	6.5	6.5	6	6	6
	EPS70	7 (1015)	1,000,000	8	7.5	7.5	7	7	6.5	6.5	6
	EPS100	10 (1450)		8	7.5	7.5	7	7	6.5	6.5	6

			LOAD TRANSFER DEVICES	No				Yes			
			EDGE SUPPORT	No		Yes		No		Yes	
			S'c MPa (lbs/in^2)	4.1 (600)	4.8 (700)	4.1 (600)	4.8 (700)	4.1 (600)	4.8 (700)	4.1 (600)	4.8 (700)
INHERENT RELIABILITY	**EPS TYPE**	**EPS RESILIENT MODULUS**	**Traffic**								
%		MPa (lbs/in^2)	ESALs								
75	*EPS70*	7 (1015)	50,000	5.5	5	5	5	5	5	5	5
	EPS100	10 (1450)		5.5	5	5	5	5	5	5	5
	EPS70	7 (1015)	300,000	7	6.5	6.5	6	6.5	6	6	5.5
	EPS100	10 (1450)		7	6.5	7	6	6.5	6	6	5.5
	EPS70	7 (1015)	400,000	7.5	7	7	6.5	6.5	6	6	6
	EPS100	10 (1450)		7.5	7	7	6.5	6.5	6	6	6
	EPS70	7 (1015)	600,000	8	7.5	7.5	7	7	6.5	6.5	6
	EPS100	10 (1450)		8	7.5	7.5	7	7	6.5	6.5	6
	EPS70	7 (1015)	700,000	8	7.5	7.5	7	7	6.5	7	6
	EPS100	10 (1450)		8	7.5	7.5	7	7	6.5	7	6
	EPS70	7 (1015)	1,000,000	8.5	8	8	7.5	7.5	7	7	6.5
	EPS100	10 (1450)		8.5	8	8	7.5	7.5	7	7	6.5

New York: State Route 23A, Town of Jewett, Greene County: 230 mm (9 in.) asphalt pavement 381 mm (15 in.) graded crushed-stone subbase 100 mm (4 in.) reinforced-concrete cap *Total Pavement System Thickness=711 mm (28 in.)* 2.8 m (9 ft) of 20 kg/m^3 (1.25 lbf/ft^3) EPS	**Utah: I-15 Reconstruction** Pavement layer thicknesses varied. PCCP Open graded base Dense graded base Granular borrow Load distribution slab designed for HS 20 loading *Total Pavement System Thickness=varies* Various thicknesses of 18 kg/m^3 minimum (1.12 lbf/ft^3) EPS
Illinois: 143rd Street, Orland Park: 44 mm (1.75 in.) bituminous concrete surface 38 mm (1.5 in.) bituminous concrete binder 229 mm (9 in.) PCC Base 165 mm (6.5 in.) over crown Aggregate Subgrade but varies to accommodate a crowned roadway. 102 mm (4 in.) PCC Base Special with welded wire fabric *Total Pavement System Thickness=578 mm (22.75 in.)* 0.9 - 1.2 m (3 - 4 ft.) of 24 kg/m^3 (1.5 lbf/ft^3) EPS	**Wyoming: Bridge Rehabilitation, N.F. Shoshone River** 50 mm (2 in.) plant mix bit. 255 mm (10 in.) approach reinforced PCC slab 205 mm (8 in.) min. sand *Total Pavement System Thickness=510 mm (20 in.)* 2.75m (9 ft) of 24kg/m^3 (1.5 lbf/ft^3) EPS
Indiana: State Route 109, Noble County 330 mm (13 in.) bituminous pavement 406 mm (16 in.) #8 Stone 102 - 127 mm (4 in.-5 in.) reinforced concrete slab *Total Pavement System Thickness=863 mm (34 in.)* 0.4 - 1.5 m (1.25 - 5 ft) of 24 kg/m^3 (1.5 lbf/ft^3) EPS	**Wyoming: Moorcraft Bridge, Crook County** 305 mm (12 in.) Asphalt pavement and Concrete approach slab 305 mm (12 in.) Crushed base Impermeable membrane *Total Pavement System Thickness=610 mm (24 in.)* 1.2 m (4 ft) 24 kg/m^3 (1.5 lbf/ft^3) EPS

Note: PCC is Portland Cement Concrete and PCCP is Portland Cement Concrete Pavement.

	Material	**Layer Coefficient (1)**	**Unit Weight kN/m^3 (lbf/ft^3)**
Surface Course or Base	Asphalt Concrete-plant mix	0.44	23.3 (148)
Base	Crushed Stone	0.14	21.7 (138)
Subbase	Sandy gravel	0.11	20.4 (130)

(1) Layer coefficients obtained from (*26*).

Asphalt Concrete mm (in.)	Crushed Stone Base mm (in.)	Sandy Gravel Subbase mm (in.)	No PCC Slab Separation Layer		4-In PCC Slab Separation Layer		6-In PCC Slab Separation Layer	
			Stress kPa (lbs/ft^2)	Avg. Unit Weight Kg/m^3 (lbf/ft^3)	Stress kPa (lbs/ft^2)	Avg. Unit Weight kg/m^3 (lbf/ft^3)	Stress kPa (lbs/ft^2)	Avg. Unit Weight kg/m^3 (lbf/ft^3)
25.4 (1)	101.6 (4)	482.6 (19)	12.6 (263)	20.8 (132)	12.9 (269)	21.3 (135)	13.1 (274)	21.5 (136)
50.8 (2)	101.6 (4)	457.2 (18)	12.7 (265)	20.9 (133)	13 (272)	21.4 (136)	13.2 (276)	21.7 (138)
63.5 (2.5)	152.4 (6)	444.5 (17.5)	12.8 (267)	20.9 (133)	13.1 (274)	21.5 (136)	13.3 (278)	21.7 (138)
76.2 (3)	152.4 (6)	381 (15)	12.9 (269)	21.1 (134)	13.2 (276)	21.6 (137)	13.4 (280)	21.9 (139)
88.9 (3.5)	152.4 (6)	368.3 (14.5)	12.9 (269)	21.1 (134)	13.2 (276)	21.7 (138)	13.4 (280)	21.9 (139)
101.6 (4)	152.4 (6)	355.6 (14)	12.9 (269)	21.2 (135)	13.2 (276)	21.7 (138)	13.4 (280)	22.0 (140)

PCC Slab Thickness mm (in.)	**Crushed Stone Subbase** Mm (in.)	**Stress** kPa (lbs/ft^2)	**Avg. Density** kg/m^3 (lbf/ft^3)
127 (5)	482.6 (19)	13.5 (282)	22.1 (140)
139.7 (5.5)	469.9 (18.5)	13.5 (282)	22.1 (140)
152.4 (6)	457.2 (18)	13.5 (282)	22.2 (141)
165.1 (6.5)	444.5 (17.5)	13.5 (282)	22.2 (141)
177.8 (7)	431.8 (17)	13.6 (284)	22.2 (141)
190.5 (7.5)	419.1 (16.5)	13.6 (284)	22.3 (142)
203.2 (8)	406.4 (16)	13.6 (284)	22.3 (142)
215.9 (8.5)	393.7 (15.5)	13.6 (284)	22.3 (142)

CHAPTER **5**

EXTERNAL (GLOBAL) STABILITY EVALUATION OF GEOFOAM EMBANKMENTS

Contents

INTRODUCTION

Design for external (global) stability of the overall EPS-block geofoam embankment involves consideration of how the combined fill mass and overlying pavement system interact with the foundation soil. External stability consideration in the proposed design procedure includes consideration of Serviceability Limit State (SLS) issues, such as total and differential settlement caused by the soft foundation soil and Ultimate Limit State (ULS) issues, such as bearing capacity, slope stability, seismic stability, hydrostatic uplift (flotation), translation due to water (hydrostatic sliding), and translation due to wind (see Table 3.1). All of these external stability considerations are described in this chapter and illustrated in design examples in Chapter 7. These external stability considerations together with other project-specific design inputs, such as right-of-way constraints, limiting impact on underlying and/or adjacent structures, and construction time, largely govern the overall cross-sectional geometry of the embankment as well as the relative amount of geofoam used within the embankment. Because EPS-block geofoam is typically a more expensive material than soil on a cost-per-unit-volume basis, it is desirable to optimize the design to minimize the volume of EPS used yet still satisfy design criteria concerning settlement and stability. Therefore, it is not necessary for the EPS blocks to extend the full height vertically from the top of the soil subgrade to the bottom of the pavement system.

The overburden stress imposed by the pavement system and fill mass on the soft foundation soil may decrease the stability of some of the external failure mechanisms, e.g., settlement, bearing capacity, slope stability, and seismic stability, while increasing the stability of others, e.g., hydrostatic uplift, translation due to water, and translation due to wind. Therefore, overall design optimization of an embankment incorporating EPS-block geofoam requires iterative analyses to achieve a technically acceptable design at the lowest overall cost. In order to minimize iterative analyses, the design flowchart shown in Figure 3.3 was developed to obtain a technically optimal design using a trial and error process. The design procedure considers a pavement system with the minimum required thickness, a fill mass with a minimum thickness of

EPS-block geofoam, and the use of an EPS block with the lowest possible density. Therefore, the design procedure starts with the least expensive pavement/embankment system in the anticipation that a cost efficient design will be produced.

Design for external stability begins with the selection of a cross-section geometry of the overall embankment in a plane perpendicular to the proposed road alignment. The type of cross-section selected will dictate the type of cover that will be required, such as facing panels for a vertical embankment and usually soil cover for a trapezoidal embankment. The cover system will impose vertical stresses directly on the EPS blocks or on the foundation soil. These vertical stresses due to the weight of the cover system must be included in calculations for the various external stability failure mechanisms. Steps 1 through 3 of the design process involve (1) background investigation, (2) selection of preliminary pavement system, and (3) preliminary arrangement of the fill mass (see Figure 3.3) and are presented in Chapter 3. In this chapter, the external (global) stability failure mechanisms, Steps 4 through 10 of the design process in Figure 3.3, are discussed.

This chapter presents detailed background information on the external stability aspect of the EPS-Block geofoam design methodology. An abbreviated form of the external stability design procedure can be found in the provisional design guideline included in Appendix B.

EMBANKMENT GEOMETRY

The cross-sectional geometry in the direction transverse (perpendicular) to the road alignment is the critical geometry for performing external stability analysis because conventional settlement and two-dimensional limit equilibrium stability analyses utilize the transverse cross-section. However, the longitudinal geometry of the embankment along the road alignment must also be considered for construction and settlement purposes as described subsequently.

Cross-Sectional Geometry

The designer must choose the type of embankment, e.g., trapezoidal (sloped-side fill) or vertical (vertical-face fill), that will be most feasible for the project. These types of embankments

are shown in Figure 3.4. Unlike other types of lightweight and soil fills, EPS is actually a solid material with internal strength. Therefore, each block is self-stable and collectively the blocks are also inherently self-stable to a certain extent even when the blocks are vertically stacked. Consequently, a benefit of EPS-block geofoam compared to other types of lightweight fills and traditional soil embankments is that a vertical embankment, also referred to as a geofoam wall (*1*), can be used.

There are several benefits of using a geofoam wall over a traditional trapezoidal embankment. First, the volume of fill material, especially of EPS blocks, is minimized. This results in reduction of both material cost and construction time. Second, the footprint of the embankment is smaller and consequently the amount of right-of-way required is minimized. This can minimize cost as well as have positive environmental benefits. However, there are also some disadvantages of using a geofoam wall, which may offset the benefits mentioned above. These disadvantages include the need to cover the vertical faces of the exposed EPS blocks with a facing material that typically consists of a structural material. Types of facing materials available for geofoam walls are subsequently discussed in the "Embankment Cover" section of this chapter. The facing panel will place a concentrated vertical stress on the soft foundation soil and must be considered in overall stability and settlement analyses. Additionally, a portland cement concrete (PCC) slab on top of the EPS may be required in a vertical embankment for the function of providing anchorage for the facing panels or road hardware.

If a trapezoidal embankment is used, a maximum overall slope angle of two horizontal to one vertical (2H:1V) should be used to accommodate the maintenance of vegetation typically placed for erosion control on the sloped sides of the embankment. Further discussion on the types of cover materials typically used to cover the EPS blocks in a trapezoidal embankment is provided subsequently in the "Embankment Cover" section of this chapter.

Longitudinal Geometry

Two aspects of the geometry of the embankment in the longitudinal direction (parallel to the roadway) that need to be considered during design include orientation of the EPS blocks and the transition zone between the geofoam and non-geofoam sections of the roadway.

The top surface of the assemblage of EPS blocks should always be parallel with the final pavement surface (*2*) to facilitate construction and performance. Thus, any desired change in elevation (grade) along the road alignment must be accommodated by sloping the foundation soil surface as necessary prior to placement of the first layer of EPS blocks. Additionally, the upper surface of the EPS blocks should always be horizontal when viewed in transverse cross-section so any crown desired in the final pavement surface should be achieved by varying the thickness of the pavement system (*2*).

In the longitudinal cross-section, the transition zone between geofoam and soil should be gradual to minimize differential settlement. The EPS blocks could be stepped as shown in Figure 5.1 to ease the transition. However, the specific pattern should be determined on a project-specific basis based on calculated differential settlements such as the criteria given in (*3*) which suggests that the calculated gradient within the transition zone should not exceed 1:200 (vertical: horizontal).

Figure 5.1. Typical EPS block transition to a soil subgrade (*1*).

EMBANKMENT COVER

The EPS blocks should be permanently covered to protect against ultraviolet (UV) radiation. Although EPS does not suffer UV deterioration to the extent that many other geosynthetics do (the surface of the EPS will just yellow and become chalky after some weeks or months of exposure), it is still recommended that the surface of the EPS be covered as rapidly as possible after block placement. The type of covering system selected will depend on the type of embankment cross-sectional geometry that will be used.

Trapezoidal Embankments

For a trapezoidal fill embankment, the covering system typically consists of a thin layer of soil placed directly over the stepped edges of the EPS blocks. Vegetation is incorporated on the surface of the soil layer for erosion control. The angle of a trapezoidal embankment is governed by the stability of the soil cover as well as by maintenance requirements. Typically, the steepest slope angle used is two horizontal to one vertical (2H:1V), or 26.6 degrees which is similar to the maximum of 25 degrees recommended in the recent PIARC guidelines (*2*). However, steeper slopes may be possible if geosynthetics such as geotextiles, geogrids, geocells, or erosion-control geosynthetics are utilized.

The current Norwegian design standards (*4*) and the recent PIARC guidelines (*2*) require a minimum thickness of soil cover of 250 mm (10 in.). This minimum thickness has been in use for more than 25 years. However, a thicker soil cover of 500 to 1,000 mm (20 to 39 in.) has been incorporated in the current United Kingdom design guidelines (*5*). The recommended thicker soil cover amount may be based on the following three reasons:

- The results from full-scale fire tests in Japan (*6*) show that 500 mm (20 in.) of soil cover is adequate to prevent the EPS blocks from melting even after a one-hour fire consisting of burning kerosene on the sloped surface of the test embankment. However, these tests did not explore if less than 500 mm (20 in.) of soil would have also been satisfactory.
- The desire to provide increased soil depth for surface vegetation roots.
- The desire to provide greater protection to the EPS against unspecified hazards.

Selection of the soil cover thickness is important because costs increase with increasing soil cover and the vertical stress imposed on the soft foundation soil increases. Based on the recommended thickness ranges from existing design standards and guidelines, it is recommended that the minimum thickness of the soil cover should be in the range of 300 to 500 mm (12 to 20 in.). The soil cover on the sides of a trapezoidal embankment can be assumed to be 400 mm (16

in.) thick with a total (moist) unit weight of 18.8 kN/m³ (120 lbf/ft³) for preliminary design purposes.

Vertical Embankments

For vertical geofoam embankment walls, the exposed sides should be covered with a facing. The facing does not have to provide any structural capacity to retain the blocks because the blocks are self-stable so the primary function is to protect the blocks from environmental factors. The selection of the type of facing system to use is based on three general criteria:

- facing must be self-supporting or physically attached to the EPS blocks,
- architectural/aesthetic requirements, and
- cost.

The following materials have been successfully used for facing geofoam walls:

- prefabricated metal (steel or aluminum) panels,
- precast PCC panels, either full height or segmental (such as used in mechanically stabilized earth walls, MSEWs),
- segmental retaining wall (SRW) blocks which are typically precast PCC,
- shotcrete, and
- geosynthetic vegetative mats.

Other materials that might be suitable for facing geofoam walls include:

- wood panels or planks,
- the stucco-like finish used for exterior insulation finish systems (EIFS), and
- EPS-compatible paint for temporary fills

Regardless of the facing used, the resulting vertical stress on the foundation soil must be considered in the calculations for settlement and global stability. The weight of the facing elements needs to be obtained from a supplier or estimated because of the various types of vertical wall systems.

SETTLEMENT OF EMBANKMENT

Introduction

Settlement is the amount of vertical deformation that occurs from immediate or elastic settlement of the fill mass or foundation soil, consolidation and secondary compression of the foundation soil, and long-term creep of the fill mass at the top of a highway embankment. Settlement caused by lateral deformation of the foundation soil at the edges of an embankment is not considered because (*7*) presents inclinometer measurements that show the settlements from lateral deformation are generally small compared with the five previously mentioned settlement mechanisms if the factor of safety against external instability during construction remains greater than about 1.4. If the factor of safety remains greater than 1.4, settlement caused by lateral deformation is likely to be less than 10 percent of the end-of primary settlement (*7*). The proposed design procedure recommends a factor of safety against bearing capacity failure and slope instability greater than 1.5. Therefore, settlement resulting from lateral deformations is not considered herein. However, lateral creep deformations should be considered if the proposed embankment will be placed near structures such as underground utilities. A discussion on lateral creep deformations can be found in (*7,8*).

Total settlement of an EPS-block geofoam embankment considered herein, S_{total}, consists of five components as shown by Equation (5.1):

$$S_{total} = S_{if} + S_i + S_p + S_s + S_{cf} \quad \textbf{(5.1)}$$

where S_{if} = immediate or elastic settlement of the fill mass,

S_i = immediate or elastic settlement of the foundation soil,

S_p = end-of-primary (EOP) consolidation of the foundation soil,

S_s = secondary consolidation of the foundation soil, and

S_{cf} = long-term vertical deformation (creep) of the fill mass.

Immediate or elastic settlement of both the fill mass and foundation soil occur during construction and will not impact the condition of the final pavement system. Therefore,

immediate settlements are not typically included in the total settlement estimate and the settlement analysis presented herein focuses on primary and secondary consolidation of the foundation soil and creep of the fill mass. However, immediate settlement of the foundation soil should be considered if the embankment will be placed over existing utilities. Immediate settlement can be estimated by elastic theory and is discussed in (*9*).

Differential settlements may occur in clays with a desiccated crust even if the clay thickness and induced stresses are the same below the embankment because of random variations in compressibility and preconsolidation pressure within the clay and the desiccated crust. A method for estimating settlement of clay deposits that have a desiccated crust can be found in (*10*).

Settlement Due to End-of-Primary (EOP) Consolidation

The EOP consolidation of the foundation soil is the amount of compression that occurs during the period of time required for the excess porewater pressure to dissipate for an increase in effective stress. Equation (5.2) can be used to estimate the EOP consolidation of the foundation soil which allows for overconsolidated and normally consolidated soil deposits (*7*):

$$S_p = \frac{C_r}{1+e_o} L_o \log \frac{\sigma'_p}{\sigma'_{vo}} + \frac{C_c}{1+e_o} L_o \log \frac{\sigma'_{vf}}{\sigma'_p} \qquad \textbf{(5.2)}$$

where S_p = settlement resulting from one-dimensional EOP consolidation,

C_r = recompression index,

σ'_p = preconsolidation pressure,

σ'_{vo} = in situ effective vertical stress, effective overburden pressure,

e_o = in situ void ratio under effective overburden pressure σ'_{vo},

C_c = compression index,

L_o = preconstruction thickness of the compressible layer with void ratio e_o,

σ'_{vf} = final effective vertical stress = $\sigma'_{vo} + \Delta \sigma'_Z$, and

$\Delta\sigma'_Z$ = change in effective vertical stress.

Soils that have not been subjected to effective vertical stresses higher than the present effective overburden pressure are considered normally consolidated and have a value of σ'_p/σ'_{vo} of unity. For normally consolidated foundation soil, Equation (5.2) can be simplified

$$S_p = \frac{C_c}{1+e_o} L_o \log \frac{\sigma'_{vf}}{\sigma'_p} \quad \textbf{(5.3)}$$

If the estimated settlement of the proposed EPS block embankment exceeds the allowable settlement, one expedient soft ground treatment method that can be utilized is to partially overexcavate the existing soft foundation soil and to place EPS blocks in the overexcavation. This treatment method decreases settlement by decreasing the final effective vertical stress. Note that L_o to be used in Equation (5.3) is the preconstruction thickness. If an overexcavation procedure is performed, L_o will be the thickness of the soft foundation soil prior to the overexcavation procedure. If the foundation soil is overconsolidated, i.e., $\sigma'_p/\sigma'_v > 1$, but the proposed final effective vertical stress will be less than or equal to the preconsolidation pressure, i.e., $\sigma'_{vf} \leq \sigma'_p$, Equation (5.2) can be simplified to

$$S_p = \frac{C_r}{1+e_o} L_o \log \frac{\sigma'_{vf}}{\sigma'_{vo}} \quad \textbf{(5.4)}$$

Values of C_r, C_c, and σ'_p are determined from the results of laboratory consolidation tests as described in (*11*). However, empirical correlations can be used to obtain preliminary estimates of the input parameters for an EOP consolidation settlement analysis. Empirical correlations between C_c and in situ water content are provided in (*7,9,11*). Two widely used equations for estimating C_c are:

$$C_c = 1.15(e_o - 0.35) \quad \textbf{(5.5)}$$

$$C_c = 0.009(\text{LL-10}) \quad \textbf{(5.6)}$$

where LL = liquid limit of the soil.

Equation (5.5) (*12*) is applicable to all clays and Equation (5.6) (*13*) is applicable to clays of low-to-medium sensitivity (sensitivity less than 4) (*11*). Most values of C_r/C_c are in the range of 0.02 to 0.2 with the lower values corresponding to highly structured and bonded soft clay and silt deposits and the higher values corresponding to micaceous silts and fissured stiff clays and shales (*7*). A widely used approximation C_r/C_c is 0.1. Therefore, C_r can be estimated by multiplying the value of C_c by 0.1.

Settlement Due to Secondary Consolidation

Secondary consolidation of the foundation soil is the amount of compression that occurs after the dissipation of the excess porewater pressure induced by an increase in effective stress occurs and thus secondary consolidation occurs under the final effective vertical stress σ'_{vf}. Equation (5.7) can be used to estimate the secondary consolidation of the foundation soil (*7*).

$$S_s = \frac{[C_\alpha / C_c] \times C_c}{1 + e_o} L_o \log \frac{t}{t_p} \qquad \textbf{(5.7)}$$

where S_s = settlement resulting from one-dimensional secondary compression,

C_α = secondary compression index,

e_o = in situ void ratio under effective overburden pressure, σ_{vo},

L_o = preconstruction thickness of the compressible layer with void ratio e_o,

t = time, and

t_p = duration of primary consolidation.

C_α is determined from the results of laboratory consolidation tests. However, for preliminary settlement analyses, empirical values of C_α/C_c, such as those provided in Table 5.1, can be used to estimate C_α. The validity of the C_α/C_c concept has been verified using field case histories (*14,15*).

Table 5.1 Values of C_α/C_c for Soils (*7*).

Field values of t_p for layers of soil that do not contain permeable layers and peats can range from several months to many years. However, for the typical useful life of a structure, the value of the t/t_p rarely exceeds 100 and is often less than 10 (*7*).

The determination of secondary settlement is important in high water content materials, such as peats, for the following three reasons (*16*): (1) peat materials exist at high natural water contents and void ratios; (2) peat materials have high C_α/C_c values; and (3) the duration of EOP consolidation for peat or other highly organic materials is very short because peat materials have a high initial permeability. The application of the C_α/C_c concept for high-water content material with and without surcharging can be found in (*16*). The C_α/C_c concept can also be used to predict the behavior of postsurcharge secondary settlement (*14*).

Settlement Due to Long-Term Vertical Deformation (Creep) of the Fill Mass

The creep behavior of EPS-block geofoam is discussed in Chapter 2 and as indicated, current creep models do not provide reliable estimates of the time-dependent total vertical strains. Further research is required to either refine current creep models or develop a new model. The current state of practice for considering creep strains in the design of EPS block embankments and bridge approaches is to base the design on laboratory creep tests on small specimens trimmed from an EPS block that will be used in construction or to base the design on published observations of the creep behavior of EPS, such as:

- If the applied stress produces an immediate strain of 0.5 percent or less, the creep strains, ε_c, will be negligible even when projected for 50 years or more. The stress level at 0.5 percent strain corresponds to approximately 25 percent of the compressive strength defined at a compressive normal strain of 1 percent or 33 percent of the yield stress.
- If the applied stress produces an immediate strain between 0.5 percent and 1 percent, the geofoam creep strains will be tolerable (less than 1 percent) in

lightweight fill applications even when projected for 50 years or more. The stress level at 1 percent strain corresponds to approximately 50 percent of the compressive strength or 67 percent of the yield stress.

- If the applied stress produces an immediate strain greater than 1 percent, creep strains can rapidly increase and become excessive for lightweight fill geofoam applications. The stress level for significant creep strain corresponds to the yield stress which is approximately 75 percent of the compressive strength.

In summary, the compressive stress at a vertical strain of 1 percent, i.e., the elastic-limit stress, appears to correspond to a threshold stress level for the development of significant creep effects. As a result, the field applied stresses should not exceed the elastic limit stress until more reliable creep models are developed (*1*). Based on these observations, it is concluded that creep strains within the EPS mass under sustained loads are expected to be within acceptable limits (0.5 percent to 1 percent strain over 50 years) if the applied stress is such that it produces an immediate strain between 0.5 percent and 1 percent (*1*). The load bearing design recommended as part of internal stability in Chapter 6 is based on selecting an EPS block that will provide an immediate or elastic vertical strain of less than 1 percent. Therefore, the contribution of settlement due to geofoam creep is neglected in Equation (5.1) and Equation (5.1) reduces to the following for design purposes because S_{if}, S_i, and S_{cf} are likely to be negligible:

$$S_{total} = S_p + S_s \quad \textbf{(5.8)}$$

The initial (immediate) or elastic vertical strain of the EPS-block geofoam can be estimated from Equation (5.9) to determine if the vertical strain is between 0.5 percent and 1 percent which will result in negligible creep effects:

$$\varepsilon_o = \frac{\sigma}{E_{ti}} \quad \textbf{(5.9)}$$

where ε_o = immediate or elastic vertical strain of the geofoam in decimal format,

σ = applied stress over the EPS, and

E_{ti} = initial tangent Young's modulus of the EPS.

Values of E_{ti} can be estimated from Table 4.1 that presents values of E_{ti} for different geofoam densities. This procedure only considers the long-term deformation of the EPS-block geofoam. If conventional soil fill is placed between the foundation soil and the EPS-blocks, both primary and secondary settlement of the soil fill needs to be estimated to obtain the total settlement of the fill mass.

Allowable Settlement

Tolerable settlements for highway embankments are not well established in practice nor is information concerning tolerable settlements readily available in the geotechnical literature. Postconstruction settlements of 0.3 to 0.6 m (1 to 2 ft) during the economic life of a roadway are generally considered tolerable provided the settlements are uniform, occur slowly over a period of time, and do not occur next to a pile-supported structure (*17*). If postconstruction settlement occurs over a long period of time, any pavement distress caused by settlement can be repaired when the pavement is resurfaced. Although rigid pavements have performed well after 0.3 to 0.6 m (1 to 2 ft) of uniform settlement, flexible pavements are usually selected where doubt exists about the uniformity of postconstruction settlements and some states utilize a flexible pavement when predicted settlements exceed 150 mm (6 in.) (*17*).

Tolerable settlements of bridge approach embankments depend on the type of structure, location, foundation conditions, operational criteria, etc. (*8*). The following references are recommended for information on tolerable abutment movements: (*18-21*).

The transition zone between geofoam and embankment soil should be gradual to minimize differential settlement. The EPS blocks should be stepped as shown in Figure 5.1 as the embankment transitions from a soft foundation soil that requires geofoam to a stronger foundation soil that can support the soil embankment. However, a minimum of two layers of blocks is recommended to minimize the potential of the blocks to shift under traffic loads. The

only exception to this is the final step of the geofoam embankment, which can consist of one block as shown in Figure 5.1. The specific layout of the EPS blocks should be determined on a project-specific basis based on calculated differential settlements such as the criteria given in (*3*) which suggests that the calculated settlement gradient within the transition zone should not exceed 1:200 (vertical: horizontal). An allowable differential settlement of less than 10 cm (4 in.) is recommended by (*22*) to minimize the potential for detrimental shifting of the EPS blocks. However, the distance over which this recommended differential settlement value is based on is not provided.

Stress Distribution for Total Settlement Calculations

Based on Equation (5.8), the main contributors to embankment settlement are EOP consolidation and secondary consolidation of the foundation soil. Of these two mechanisms, the largest component of total settlement is EOP consolidation which occurs from an increase in effective vertical stress on the foundation soil. Therefore, reliable estimates of EOP consolidation settlement require knowledge of the stress distribution within the embankment and foundation soil. Although solutions for the determination of vertical stresses under embankments have been developed (*23*), these solutions were developed for conventional earth fill embankments and are based on the assumption that the embankment consists of one type of fill with a single unit weight. However, an EPS-block geofoam embankment typically consists of EPS-block geofoam, soil or a facing over the sides of the EPS blocks, and the pavement system above the EPS blocks (see Figure 3.6). Additionally, some amount of soil fill may also be used between the foundation soil and the bottom of the EPS blocks for overall economy and/or leveling purposes. Thus, an EPS-block geofoam embankment will consist of more than one type of material with varying unit weights.

The soil cover on the sides of a slope-side embankment can be assumed to be 400 mm (16 in.) thick with a total (moist) unit weight of 18.8 kN/m³ (120 lbf/ft³). This is equivalent to a surcharge of 7.7 kPa (160 lbs/ft^2). No guidance on the weight of the facing elements of a vertical-

side embankment (geofoam wall) is provided because of the various types of facing systems so this weight must be estimated or provided by the supplier. The effect of vehicle loads on the road surface is generally negligible compared to the dead load of the pavement system and thus can typically be ignored in global settlement calculations. However, traffic loads are occasionally considered for embankments of low height that will experience a large volume of traffic (*22*).

The critical locations along the embankment cross section for calculating total settlements are at the center and edge. These two locations will typically yield the greatest and least settlement magnitudes, respectively, and consequently yield the greatest differential settlement. Computation of stresses induced by the overall embankment on the foundation soil can be facilitated by dividing the embankment into three zones as shown in Figure 5.2.

To calculate the increase in stress at the center and edge of the embankment, a new stress distribution procedure was developed herein to allow for a non-homogenous embankment. The next section presents the derivation or the stress distribution method for the center of the embankment and the following section describes the stress distribution method for the edge of the embankment. These solutions are based on the assumptions that the embankment is flexible and in full contact with the foundation soil.

Figure 5.2. Zones of EPS embankment for stress distribution analyses.

Stress Distribution at Center of Embankment

To estimate the increase in vertical stress at the centerline of the geofoam embankment the effect of the stresses applied by zones I, II, and III in Figure 5.2 must be evaluated at the embankment centerline. The law of superposition allows the increase in vertical stresses for zone II to be considered and then multiplied by 2 to estimate the increase in vertical stress caused by zones II and III. The increase in vertical stress caused by zone I is added to the vertical stress increases caused by zones II and III to obtain the increase in vertical stress caused by the entire embankment. The increase in vertical stress caused by zone I is estimated by:

$$\Delta\sigma_{Z_I} = \frac{q_I}{\pi}\left(\alpha + \sin\alpha\right) \quad \text{where } \alpha \text{ is in radians,} \tag{5.10}$$

$$\alpha = 2 * \arctan\left(\frac{b}{Z}\right) \quad \text{where } \alpha \text{ is calculated in radians,} \tag{5.11}$$

and the variables are defined in Figure 5.3. The surcharge from the center of embankment, q_I, is estimated by the following expression:

$$q_I = q_{fill} + q_{pavement} \tag{5.12}$$

where $$q_{fill} = \gamma_{EPS} * T_{EPS}, \tag{5.13}$$

$$q_{pavement} = \gamma_{pavement} * T_{pavement}, \tag{5.14}$$

$T_{pavement}$ = thickness of the pavement system in m,

T_{EPS} = maximum thickness of EPS block geofoam in embankment in m (see Figure 5.5),

γ_{EPS} = unit weight of the EPS block geofoam in kN/m^3, and

$\gamma_{pavement}$ = unit weight of the pavement system in kN/m^3.

If other materials are included in the embankment besides EPS, they can be included in the estimate of q_I by multiplying the unit weight by the thickness of the material.

Figure 5.3. Geometry and variables for the surcharge induced by Zone I at the embankment center.

The increase in vertical stress caused by zones II or III, i.e., the triangular loads of the side of the embankment in Figure 5.2, is estimated by:

$$\Delta\sigma_{Z_{II}} = \frac{q_{II}}{2\pi}\left[\frac{x}{0.5*a}\alpha - \sin 2\delta\right] \quad \text{where } \alpha, \delta \text{ are in radians,} \tag{5.15}$$

$$\delta = \arctan\left(\frac{b}{Z}\right) \quad \text{where } \delta \text{ is calculated in radians,} \tag{5.16}$$

$$\alpha = \arctan\left(\frac{a+b}{Z}\right) - \delta \quad \text{where } \delta \text{ and } \alpha \text{ is calculated in radians,} \tag{5.17}$$

and the other variables are defined in Figure 5.4. The surcharge induced at the center of the embankment from the triangular loaded areas, i.e., zones II and III, is estimated below for zone II because the law of superposition and the symmetry of the embankment allows consideration of only one side of the embankment:

$$q_{II} = q_{fill} + q_{cover} \quad \textbf{(5.18)}$$

where

q_{fill} is given by Equation (5.13),

$$q_{cover} = \gamma_{cover} * \frac{T_{cover}}{\cos\theta} \text{ (see Figure 5.5),} \quad \textbf{(5.19)}$$

γ_{cover} = unit weight of cover soil in kN/m^3,

T_{cover} = thickness of soil cover over the geofoam in m, and

θ= angle embankment slope makes with the horizontal in degrees.

Figure 5.4. Geometry and variables for the surcharge induced by Zone II at the embankment center.

Figure 5.5. Components of surcharges that are applied to the foundation soil.

For example, if a 0.6 m (2 ft) thick soil cover with a unit weight of 18.8 kN/m^3 (120 lbf/ft^3) is used on the sides of an embankment with a slope of 4H: 1V (θ = 14 degrees), the vertical thickness of the soil cover is given by $T_{Cover}/\cos\theta$ which is 0.62 m (2 ft) and the value of q_{cover} is 11.7 kPa (244 lbs/ft^3). If other materials are included in zones II and III besides EPS, these materials can be included in the estimates of q_{II} by multiplying the unit weight by the thickness of the material.

Therefore, the total increase in vertical stress at the center of a trapezoidal embankment is estimated as follows:

$$\Delta\sigma_{Z_{@center}} = \Delta\sigma_{Z_I} + \left(2 * \Delta\sigma_{Z_{II}}\right) \quad \textbf{(5.20)}$$

where $\Delta\sigma_{Z_{II}}$ is multiplied by 2 to account for the vertical stress increase caused by zone III. The total increase in vertical stress at the center of a vertical embankment is only due to the vertical stress increase applied by zone I, i.e., no contributions from zones II and III because of the vertical sides of the embankment, and is estimated as follows:

$$\Delta\sigma_{Z_{@center}} = \Delta\sigma_{Z_I} \quad \textbf{(5.21)}$$

The thickness of the soil cover, T_{cover}, is defined herein as the thickness measured from the outer edge of the EPS blocks as shown in Figure 5.5 (b). The weight of the soil wedges between the inner and outer edges of the EPS blocks will add an additional surcharge to the surcharge value determined using Equation (5.19). An effective thickness of the soil cover, T'_{cover}, can be determined and used instead of T_{cover} in Equation (5.19). The surcharge induced by the soil wedge will depend on the block thickness and the slope of the embankment. Additionally, note that the soil wedges only occupy half the cross-sectional area of the embankment between the outer and inner EPS block edges. Therefore, the additional thickness of soil cover that will impose a surcharge is approximately ½ of the thickness formed between the outer and inner EPS block edges. Therefore, $T'_{cover} = T_{cover} + (\frac{1}{2} * T_{block\ edges})$. For embankment slopes ranging from 2H:1V to 4H:1V and for a block thickness of 760 mm (30 in.), the additional thickness to be added to T_{cover} to obtain T'_{cover} will range between 340 mm (13 in.) to 370 mm (15 in.).

Stress Distribution at Edge of Embankment

The increase in vertical stress at the edge of the embankment is complex because the embankment is not symmetric for stress distribution purposes. Therefore, the increase in vertical stress for zones I, II, and III in Figure 5.2 must be considered separately. The vertical stress increase at the edge of the embankment caused by zone II can be estimated by Figure 5.6 and Equations (5.22) and (5.23) provide the solution for determining the increase in vertical stress, $\Delta\sigma_{Z_{II}}$, at the edge of the embankment from a vertical loading increasing linearly.

$$\Delta\sigma_{Z_{II}} = \frac{q_{II}}{2\pi}\left(\sin 2\delta\right) \quad \text{where } \delta \text{ is in radians,} \qquad \textbf{(5.22)}$$

$$\delta = \arctan\left(\frac{a}{Z}\right) \quad \text{where } \delta \text{ is calculated in radians,} \qquad \textbf{(5.23)}$$

and the variables are defined in Figure 5.6. The surcharge, q_{II}, is estimated as shown in Equation (5.18).

Figure 5.6. Geometry and variables for the surcharge induced by Zone II at the edge of the embankment.

Figure 5.7 illustrates the solution for determining the increase in vertical stress, $\Delta\sigma_{Z_{III}}$, at the edge of the embankment by zone III, which is located at the opposite end of the embankment.

$$\Delta\sigma_{Z_{III}} = \frac{q_{III}}{2\pi}\left[\frac{x}{0.5 * a}\alpha - \sin 2\delta\right] \quad \text{where } \alpha, \delta \text{ are in radians,} \qquad \textbf{(5.24)}$$

$$\delta = \arctan\left(\frac{a + 2b}{Z}\right) \quad \text{where } \delta \text{ is calculated in radians,} \qquad \textbf{(5.25)}$$

$$\alpha = \arctan\left(\frac{2a + 2b}{Z}\right) - \delta \quad \text{where } \delta \text{ and } \alpha \text{ is calculated in radians,} \qquad \textbf{(5.26)}$$

and the variables are defined in Figure 5.7. The value of surcharge induced by zone III, q_{III}, is equal to q_{II} and can be estimated as shown in Equation (5.18).

Figure 5.7. Geometry and variables for the surcharge induced by Zone III at the edge of the embankment.

Figure 5.8 illustrates the solution for determining the increase in vertical stress, $\Delta\sigma_{Z_I}$, at the edge of the embankment caused by zone I or the center of the embankment. The value of surcharge induced by zone I, q_I, is estimated as shown in Equation (5.12).

$$\Delta\sigma_{Z_I} = \frac{q_I}{\pi}\left[\alpha + \sin\alpha\cos\left(\alpha + 2\delta\right)\right] \quad \text{where } \alpha, \delta \text{ are in radians,} \qquad \textbf{(5.27)}$$

$$\delta = \arctan\left(\frac{a}{Z}\right) \quad \text{where } \delta \text{ is calculated in radians,} \qquad \textbf{(5.28)}$$

$$\alpha = \arctan\left(\frac{a+2b}{Z}\right) - \delta \qquad \text{where } \delta \text{ and } \alpha \text{ is calculated in radians,} \qquad \textbf{(5.29)}$$

and the variables are defined in Figure 5.8. Therefore, the total increase in stress at the edge of a trapezoidal embankment is estimated as follows:

$$\Delta\sigma_{Z@edge} = \Delta\sigma_{Z_I} + \Delta\sigma_{Z_{II}} + \Delta\sigma_{Z_{III}} \; . \qquad \textbf{(5.30)}$$

The total increase in vertical stress at the edge of a vertical embankment is estimated as follows:

$$\Delta\sigma_{Z@edge} = \Delta\sigma_{Z_I} \qquad \textbf{(5.31)}$$

Note comparing Figures 5.8 and 5.9, the angle δ depicted in Figure 5.8 is set equal to zero in Figure 5.9 because of the vertical sides of the embankment.

Figure 5.8. Geometry and variables for the surcharge induced by Zone I at the edge of a trapezoidal embankment.

Figure 5.9. Geometry and variables for the surcharge induced by Zone I at the edge of a vertical embankment.

If stresses from traffic loads are to be considered, the procedure for stress distribution through the fill mass described in the load bearing section of Chapter 6 can be used.

Steps in EOP Consolidation Settlement Calculation

The steps that can be used to estimate the EOP consolidation settlement are summarized below:

1. Divide soft soil stratum into sublayers using at least two sublayers depending on the thickness of the soft layer. For example, a 3 m (10 ft) thick soft layer could be subdivided into three 1 m (3.3 ft) thick sublayers.
2. Determine geostatic effective vertical stress at the mid-height of each sublayer. For a normally consolidated clay, this effective vertical stress, σ'_{vo} equals the preconsolidation pressure, σ'_p. .

3. Determine the final effective vertical stress, σ'_{vf} , at the mid-height of each sublayer, which includes the change in effective vertical stress, $\Delta \sigma'_Z$. Equations (5.20) and (5.30) provide $\Delta \sigma'_Z$ at the center and edge of the embankment, respectively.

$$\sigma'_{vf} = \sigma'_{vo} + \Delta \sigma'_Z \quad \textbf{(5.32)}$$

4. Calculate the EOP consolidation settlement of each sublayer using Equation (5.2), (5.3), or (5.4).

5. Determine total EOP consolidation settlement of the soft soil stratum by summing the EOP consolidation settlement of each sublayer.

$$S_p = \sum_{i-1}^{n} S_{pi} \quad \textbf{(5.33)}$$

6. Determine total settlement by adding S_s to the value of S_p from Equation (5.33).

Remedial Procedures for Excessive Total Settlements

If the estimated total settlement of the proposed embankment is excessive, the geotechnical engineer can consider reducing the load of the embankment by replacing any soil fill that is being proposed between the EPS blocks and foundation soil or a portion of the foundation soil materials with EPS-block geofoam. The replacement height or excavation depth is based on the required decrease in effective vertical stress or incremental stress that will yield tolerable settlements. If removal of soil fill or foundation soil and replacement with EPS blocks is not suitable, a ground improvement technique can be performed in conjunction with the use of EPS-block geofoam. An overview of ground improvement methods is presented in Chapter 1.

As indicated above, in order to limit the magnitude of postconstruction settlement, it may be beneficial to partially excavate a portion of the soft foundation soil and replace the excavated material with EPS-block geofoam to limit the final effective vertical stress, σ'_{vf}, to a tolerable level. This removal and replacement procedure is actually a combination of the following initial

two categories of soft ground treatment methods indicated in Table 1.1: reducing the load by using EPS-block geofoam and replacing the problem materials by more competent materials.

If the foundation soil is partially excavated, the excavation will typically need to be widened from the toe of the embankment so that the excavation side slopes remain stable during construction. Typically, the overexcavation should be widened a minimum of 1H:1V as measured from the bottom of the excavation to the toe of the embankment (*8*).

Several key issues should be considered with a partial excavation procedure. First, temporary dewatering and/or adequate overburden may be required above the EPS blocks during construction to minimize the potential for hydrostatic uplift of the EPS blocks due to a relatively high groundwater level or accumulation of surface runoff within the excavation. Second, partial excavation of the foundation soil may not be desirable if a dessicated layer of soil is present at the surface of the foundation soil because the dessicated layer may contribute to the bearing capacity of the foundation soil and may decrease the magnitude of settlement of the embankment. (*8*).

EXTERNAL BEARING CAPACITY OF EMBANKMENT

Introduction

This section presents an evaluation of bearing capacity as a potential external failure mode of an EPS-block geofoam embankment. Bearing capacity failure occurs if the applied stress exceeds the bearing capacity of the foundation soil which is related to the shear resistance of the soil. Failure is only considered through the foundation soil in this chapter because Chapter 6 addresses internal stability or load bearing failure through the geofoam embankment. If an external bearing capacity failure occurs, the embankment can undergo excessive vertical settlement and impact adjacent property.

The general expression for the ultimate bearing capacity of soil, q_{ult}, is defined by (*24*) as:

$$q_{ult} = cN_c + \gamma D_f N_q + \gamma B_W N_\gamma \quad \textbf{(5.34)}$$

where:

c = Mohr-Coulomb shear strength parameter termed cohesion, kN/m^2,

N_c, N_γ, N_q = Terzaghi shearing resistance bearing capacity factors,

γ = unit weight of soil, kN/m^3,

B_W = bottom width of embankment, m, and

D_f = depth of embedment, m.

It is anticipated that most, if not all, EPS-block geofoam embankments will be founded on soft, saturated cohesive soils, because traditional fill material cannot be used in this situation without pre-treatment. Narrowing the type of foundation soil to soft, saturated cohesive soils allows Equation (5.34) to be simplified. The Mohr-Coulomb parameter termed undrained angle of internal friction, ϕ, is equal to zero, and the cohesion, c, equals the undrained shear strength, s_u, for a soft, saturated cohesive soil tested under undrained triaxial compression conditions. The undrained shear strength, s_u, of the cohesive soil is defined herein as the average s_u between the bottom of the embankment and a depth below the bottom of the embankment equal to the bottom width of the embankment, B_W. This procedure is valid if s_u is fairly uniform with depth. Because ϕ equals zero, $N_\gamma = 0$, $N_q = 1$, and Equation (5.34) reduces to:

$$q_{ult} = \gamma D_f + s_u N_c \quad \textbf{(5.35)}$$

The EPS embankment is usually placed on the ground surface, which means that D_f (depth of embedment) equals zero and thus Equation (5.35) simplifies to:

$$q_{ult} = s_u N_c \quad \textbf{(5.36)}$$

The following expression for N_c was developed in (*25*):

$$N_c = 5\ (1+0.2\frac{B_W}{L})(1+0.2\frac{D_f}{B_W}) \quad \textbf{(5.37)}$$

where:

L = length of the embankment, m, and

because D_f equals zero, Equation (5.37) simplifies to:

$$N_c = 5\ (1+0.2\frac{B_W}{L}) \quad \textbf{(5.38)}$$

For design purposes, an EPS-block geofoam embankment is assumed to be modeled as a continuous footing; and thus, the length of the embankment can be assumed to be significantly larger than the width such that the term B_W/L in Equation (5.38) approaches zero. Upon including the B_W/L simplification in Equation (5.38), N_c reduces to 5.

Typical shallow foundation design requires a factor of safety, FS, of 3 against external bearing capacity failure (*26*), and the same factor of safety is used herein for EPS-block geofoam embankment design. By applying a FS of 3, the allowable soil pressure, q_a, is:

$$q_a = \frac{s_u * 5}{3} \quad \textbf{(5.39)}$$

where:

$s_u = 0.5 * q_u$

q_u = undrained unconfined compressive strength, kPa.

By transposing Equation (5.39), the following expression is obtained:

$$s_u = \frac{3 * \sigma_{n@0m}}{5} \quad \textbf{(5.40)}$$

where:

$\sigma_{n@0m}$ = normal stress applied by the embankment at the ground surface or at a depth of 0 metres, kPa

$$= \sigma_{n,\ pavement@0m} + \sigma_{n,\ traffic@0m} + \sigma_{n,geofoam@0m}\ , \quad \textbf{(5.41)}$$

$\sigma_{n,\ pavement@0m}$ = normal stress applied by pavement system at the ground surface, kPa,

$\sigma_{n,\ traffic@0m}$ = normal stress applied by traffic surcharge at the ground surface, kPa,

$\sigma_{n,geofoam@0m}$ = normal stress applied by weight of EPS geofoam at the ground surface, kPa

$$= \gamma_{EPS} * T_{EPS}, \quad \textbf{(5.42)}$$

γ_{EPS} = unit weight of the EPS-block geofoam, kN/m³, and

T_{EPS} = thickness or total height of the EPS-block geofoam, m.

Stress Distribution Theory

The following sections detail how the values comprising $\sigma_{n@0m}$ are estimated for the design process. To evaluate the factor of safety against an external bearing capacity failure through the underlying soft, saturated cohesive soil, the normal stress applied by the pavement system, traffic, and embankment must be evaluated at the ground surface and not at the top of the embankment. This requires stress distribution theory to be used to transfer the pavement and traffic stresses from the top of the embankment to the bottom of the embankment. This stress distribution differs from the stress distribution analysis presented for EOP consolidation settlement analyses because this stress distribution analysis is estimating the amount of stress dissipated by the geofoam to determine the increase in vertical stress at the top of the foundation due to the overlying embankment. The stress distribution for the EOP consolidation settlement analyses is used to evaluate the increase in stress in the foundation soil due to the overlying embankment assuming that the embankment loads are placed directly on the surface of the foundation soil and not at the top of the embankment. This is a conservative approach because it results in greater increases in vertical stress in the foundation soil and thus greater EOP consolidation settlements.

The transfer of the pavement and traffic stresses from the top of the embankment to the top of the foundation soil is accomplished using the 2V:1H stress distribution method (*11*) as follows:

$$\sigma_{n,\ pavement@0m} + \sigma_{n,\ traffic@0m} = \frac{(\sigma_{n,\ pavement} + \sigma_{n,\ traffic}) * T_W}{(T_W + T_{EPS})} \quad \textbf{(5.43)}$$

where:

$\sigma_{n,\ pavement}$ = normal stress applied by pavement at top of embankment, kPa,

$\sigma_{n,\ traffic}$ = normal stress applied by traffic surcharge at top of embankment, kPa, and

T_W = top width of embankment, m.

The 2V:1H stress distribution method was used because full-scale instrumented geofoam embankments in Norway (*27,28*), which were analyzed during this study, show that the stresses at the base of the embankment correspond to a stress distribution pattern of approximately 2V:1H. Further discussion on the full-scale tests can be found in Chapter 2.

Boussinesq (*29*) stress distribution theory for an embankment-type loading is used herein to transfer the stress applied by the geofoam to the top of the foundation soil. The Boussinesq analysis reveals that the normal stress at the ground surface (0 m) due to the weight of the geofoam embankment, $\sigma_{n,EPS@0m}$, has a maximum value of ½ (γ_{EPS} * T_{EPS}). This solution for embankment-type loading is presented in (*11*). Incorporating $\sigma_{n,EPS@0m}$ and Equation (5.43) into Equation (5.41) yields the following:

$$\sigma_{n@0m} = \frac{\left(\sigma_{n,pavement} + \sigma_{n,traffic}\right) * T_W}{\left(T_W + T_{EPS}\right)} + \frac{\left(\gamma_{EPS} * T_{EPS}\right)}{2} \qquad \textbf{(5.44)}$$

Incorporating Equation (5.44) into Equation (5.38), the undrained shear strength required to satisfy a factor of safety of 3 for a particular embankment height is as follows:

$$s_u = \frac{3}{5} * \left\{ \left[\frac{(\sigma_{n,pavement} + \sigma_{n,traffic}) * T_W}{(T_W + T_{EPS})} \right] + \frac{(\gamma_{EPS} * T_{EPS})}{2} \right\} \qquad \textbf{(5.45)}$$

Pavement systems range in thickness from 610 – 1,500 mm (24 – 59 in.), with 1,000 mm (39 in.) being a typical thickness. The various component layers of the pavement system can be assumed to have a total unit weight of 20 kN/m³ (130 lbf/ft³). Therefore, the stress induced by the pavement system, $\sigma_{n,\ pavement}$, can range from 12 kPa (250 lbs/ft²) to 30 kPa (626 lbs/ft²), with 20 kPa (418 lbs/ft²) being typical. However, a more conservative estimate of 21.5 kPa (450 lbs/ft²)

was used in the development of the external bearing capacity design chart presented subsequently.

In accordance with (*30*), 0.67 m (2 ft) of a 18.9 kN/m^3 (120 lbf/ft³) surcharge material is used to model the design traffic stress, $\sigma_{n,traffic}$, of 11.5 kPa (240 lbs/ft²) at the top of the embankment. As indicated in Chapter 3, γ_{EPS} can be assumed to be 1 kN/m^3 (6.37 lbf/ft^3) to conservatively allow for potential long-term water absorption.

Substituting the design values of $\sigma_{n,pavement}$, and $\sigma_{n,traffic}$, and γ_{EPS} into Equation (5.45) yields the following expression for the undrained shear stress required to satisfy a factor of safety of 3 for a particular embankment height:

$$s_u = \frac{3}{5} * \left\{ \left[\frac{(21.5\ \text{kPa} + 11.5\ \text{kPa}) * T_W}{(T_W + T_{EPS})} \right] + \frac{(1\ \text{kN/m}^3) T_{EPS}}{2} \right\} \quad \textbf{(5.46)}$$

which simplifies to:

$$s_u = \frac{99\ \ T_W}{5\ \ (T_W + T_{EPS})} + 0.3\ \ T_{EPS} \quad \textbf{(5.47)}$$

Based on Equation (5.47) and various values of T_{EPS}, Figure 5.10 presents the minimum thickness of geofoam required for values of foundation soil undrained shear strength. The results show that if the foundation soil exhibits a value of s_u greater than or equal to 19.9 kPa (415 lbs/ft²), external bearing capacity will not control the external stability of the EPS embankment. However, if the value of s_u is less than 19.9 kPa (415 lbs/ft²), the allowable thickness of the EPS-block geofoam can be estimated from Figure 5.10 to prevent bearing capacity failure.

Figure 5.10 also shows that as the number of lanes supported by the EPS embankment increases, the required height of EPS-block geofoam increases for a given undrained shear strength. The pavement widths used in the parametric study correspond to a 2-lane roadway (11 m or 36 ft) that consists of 2 lanes and with 2-shoulders that are 1.8 m (6 ft) wide, a 4-lane roadway (23 m or 76 ft) consists of 2-exterior shoulders that are 3 m (10 ft) wide and 2-interior

shoulders that are 1.2 m (4 ft) wide, and a 6-lane roadway (34 m or 112 ft) consists of 4-shoulders that are 3 m (10 ft) wide. Each lane is assumed to be 3.66 m (12 ft) wide.

The use of EPS blocks as lightweight fill benefits the external bearing capacity of an EPS-block geofoam embankment underlain by soft clay or other low-strength soils in two ways. First, the EPS-blocks induce a much smaller stress on the weak foundation than a traditional soil fill. Second, the height of the EPS-block embankment decreases the normal stress applied to the top of the foundation soil, because it distributes the pavement and traffic stresses over its height via stress distribution. As a result, the larger the thickness of EPS or higher the embankment, the lower the applied pavement and traffic surcharge stresses at the base of the embankment. Likewise, the larger the stresses at the base of the embankment or the lower the undrained shear strength, the thicker the EPS or higher the embankment must be to maintain a FS of 3. For example, at a s_u value less than 19.9 kPa (415 lbs/ft²) the thickness of EPS or height of the embankment must be greater than zero to distribute the applied stress to maintain a factor of safety of 3. As the value of s_u decreases the minimum thickness of EPS or embankment height required increases to distribute the applied stresses to a low enough level that satisfies a factor of safety of 3.

Figure 5.10 also illustrates that the benefit of using an EPS-block geofoam embankment decreases with increasing road width, T_W. An increased road width results in the pavement system and the traffic stress of 21.5 kPa (450 lbs/ft²) and 11.5 kPa (240 lbs/ft²), respectively, being applied over a larger width or area at the top of the embankment. This larger area reduces the amount of stress that is dissipated via the 2V:1H stress distribution theory because the value of T_W increases relative to T_{EPS} in Equation (5.43). As T_W increases, the impact of T_{EPS} on the normal stress at the base of the embankment is reduced because the T_W term in the numerator and denominator override the value of T_{EPS}. Despite reducing the stress-distribution effect of the EPS embankment with increasing road width, the EPS-block still provides a better alternative to soil

materials that have higher unit weights because the reduction of stress-distribution effects with increasing road width will also occur in these materials.

Figure 5.10 Design chart for obtaining the minimum thickness or height of geofoam, T_{EPS}, for a factor of safety of 3 against external bearing capacity failure of a geofoam embankment.

Interpretation of External Bearing Capacity Design Chart

As can be observed from Figure 5.10, the critical external bearing capacity scenario involves a 6-lane embankment (34 m or 112 ft). For the 6-lane embankment, the lowest value of s_u that can accommodate this embankment is approximately 18.3 kPa (382 lbs/ft²) for a minimum height of EPS foam equal to 12.2 m (40 ft). This means that for a 6-lane embankment and an s_u value of 18.3 kPa (382 lbs/ft²), the required T_{EPS} will be 12.2 m (40 ft). Conversely, if the height of the EPS embankment desired is 4.6 m (15 ft), an s_u of 18.9 kPa (394 lbs/ft²) would be required. If the available s_u of the foundation soil is less than 18.3 kPa (382 lbs/ft²), the height of the geofoam embankment would have to exceed 15.3 m (50 ft) to satisfy a factor of safety greater than 3. A geofoam embankment height of 15.3 m (50 ft) is not common and thus foundation improvement measures would have to be undertaken to increase the value of s_u to 18.9 kPa (394 lbs/ft²). Another example involves estimating the foundation soil s_u value required for a 2-lane highway and an embankment height of 6.1 m (20 ft). From Figure 5.10, the required s_u value is 15 kPa (304 lbs/ft²) which can also be calculated from Equation (5.45) for the 2-lane embankment width of 11 m (36 ft) as shown below:

$$s_u = \frac{3}{5}\left\{\left[\frac{33\ \text{kPa} * 11\ \text{m}}{(11\ \text{m}+6.1\ \text{m})}\right] + \frac{(1.27\ \text{kN/m}^3 * 6.1\ \text{m})}{2}\right\} = 15\ \text{kPa}\ (304\ \text{lbs/ft}^2) \qquad \textbf{(5.48)}$$

Remedial Procedures

Remedial procedures that can be considered to increase the factor of safety against external bearing capacity failure are similar to the remedial procedures for decreasing the magnitude of settlement. In addition, the analyses indicate that increasing the thickness of EPS or

height of the embankment will also increase the external bearing capacity because the pavement and traffic stresses are distributed over a larger height which reduces the increase in vertical stress at the top of the foundation soil resulting in an increase in bearing capacity resistance.

EXTERNAL SLOPE STABILITY OF TRAPEZOIDAL EMBANKMENTS

Introduction

This section presents an evaluation of external slope stability as a potential failure mode of EPS-block geofoam trapezoidal embankments or embankments with sloped sides. A supplemental section of Chapter 5 considers external slope stability of vertical embankments. A slope stability failure occurs if the driving shear stresses equal or exceed the shear resistance of material(s) along the failure surface. If a slope stability failure occurs, the embankment can undergo substantial vertical settlement and impact adjacent property. Serious safety hazards, even death, and economic implications are associated with a slope stability failure. The general expression for the limit equilibrium factor of safety, FS, is given as:

$$FS = \frac{\text{Shear Resistance}}{\text{Driving Shear Stresses}} \qquad \textbf{(5.49)}$$

The driving shear stresses in this case are due to the overlying soil cover, EPS block, and the traffic and pavement surcharges. The shear resistance is primarily attributed to the undrained shear strength of the foundation soil and EPS blocks.

Typical Cross-Section

A typical cross-section through an EPS embankment with side-slopes of 2H:1V is shown in Figure 5.11. It can be seen that a soil cover is placed over the entire embankment including the top to facilitate input of the geometry in the slope stability software and to increase numerical stability. If the soil cover layer was terminated at the top of the embankment, this would cause a discontinuity in this soil layer in the slope stability software which caused some numerical difficulties. As a result, the soil cover is extended across the top of the embankment even though in a typical embankment it is terminated at the top of the embankment and the pavement system

is placed on top of the embankment. The soil cover is 0.46 m (1.5 ft) thick, which is typical for the side slopes, and is assigned a moist unit weight of 18.9 kN/m^3 (120 lbf/ft^3). Because the soil cover is not usually placed on top of the embankment, the traffic and pavement surcharges were simply reduced by the weight of 0.46 m (1.5 ft) of soil cover or 8.7 kPa (181.7 lbs/ft^2). As discussed in the section on external bearing capacity of the embankment in this chapter, the pavement system is modeled using a surcharge of 21.5 kPa (450 lbs/ft^2). This surcharge is based on a typical pavement system thickness of 1,000 mm (39.4 in.) and a total unit weight of 20 kN/m^3 (127.3 lbf/ft^3), which yields a typical stress of 20 kPa (418 lbs/ft^2) so the use of 21.5 kPa (450 lbs/ft^2) is slightly conservative. The traffic surcharge is 11.5 kPa (240 lbs/ft^2) based on the AASHTO recommendations (*30*) of using 0.67 m (2 ft) of a 18.9 kN/m^3 (120 lbf/ft^3) soil to represent the traffic surcharge at the top of the embankment. Therefore, the total surcharge used to represent the pavement and traffic surcharges is 21.5 kPa (450 lbs/ft^2) plus 11.5 kPa (240 lbs/ft^2) or 33.0 kPa (690 lbs/ft^2). Because the soil cover artificially placed on top of the embankment for analysis purposes corresponds to 8.7 kPa (181.7 lbs/ft^2), the surcharge placed on top of the embankment for the static slope stability analyses is 33.0 kPa (690 lbs/ft^2) minus 8.7 kPa (181.7 lbs/ft^2) or 24.3 kPa (508.3 lbs/ft^2) as shown in Figure 5.11.

Figure 5.11. Typical cross-section used in static external slope stability analyses of trapezoidal embankments.

Static Stability Analysis Procedure

Static slope stability analyses were conducted on a range of embankment geometries to investigate the effect of various embankment heights (3.1 m (10 ft) to 15.3 m (50 ft)), slope inclinations (2H:1V, 3H:1V, and 4H:1V), and road widths of 11, 23, and 34 m (36, 76, and 112 ft) on external slope stability. The results of these analyses were used to develop design charts to facilitate design of roadway embankments that utilize geofoam. The static analysis of each geometry or cross-section was conducted in two-steps. This first step involved locating the critical static failure surface and the second step involved calculating the factor of safety for the

critical static failure surface. The Simplified Janbu stability method (*31*) was used to locate the critical static failure surface because a rotational failure mode surface was assumed for the external stability analyses, versus a translational failure mode for the internal stability analyses, and the microcomputer program XSTABL Version 5 (*32*) only allows searches for the critical failure surface using the Simplified Janbu method or Simplified Bishop (*33*) stability method.

After locating the critical static failure surface using the Simplified Janbu stability method, the critical static factor of safety for this failure surface was calculated using Spencer's (*34*) two-dimensional stability method because the method satisfies all conditions of equilibrium and provides the best estimate of the limit equilibrium factor of safety (*35*). Spencer's method could not be used initially to locate the critical static failure surface because XSTABL only allows searches for the critical failure surface using the Simplified Janbu and Simplified Bishop stability methods.

Material Properties

The input parameters, i.e., unit weight and shear strength, used in the external slope stability analyses are presented in Table 5.2. It can be seen that Mohr-Coulomb shear strength parameters were used to represent the shear strength of the embankment and foundation materials. The foundation soil is represented using total stress shear strength parameters because the soft foundation soil material is assumed to behave in an undrained condition. Therefore, the angle of internal friction, ϕ, is assumed to be zero and the cohesion is assumed to equal the undrained shear strength, s_u, because the foundation soil is assumed to consist of soft and saturated cohesive soil. At most EPS-block geofoam sites, the phreatic surface is located at or near the ground surface and the foundation soil is saturated. The shear strength and unit weight values for the cover soil on the side slopes of the embankment are also shown in Table 5.2 and it can be seen that the soil cover is modeled using an effective stress friction angle of 28 degrees because it is anticipated that the soil cover will not be saturated at all times nor loaded rapidly and thus it will not experience an undrained failure.

Selection of the shear strength parameters for the EPS-block geofoam within the embankment revealed some uncertainties in the modeling of geofoam in slope stability analyses. The lack of field case histories that illustrate the actual failure mode of the geofoam during an external slope stability failure resulted in uncertainty in whether during such a failure sliding occurs between the EPS blocks or through the EPS blocks. If sliding occurs between the EPS blocks, the applicable shear strength is the EPS/EPS interface friction angle of 30 degrees reported in Chapter 2. If failure occurs through the EPS bocks, the applicable shear strength is the strength of an individual block. The lack of field guidance as to whether sliding occurs between the EPS blocks or through the EPS blocks prompted an analysis to determine which shear strength produced the desired failure through the foundation soil. Because the external stability analyses focus on the soft, saturated foundation soil versus the internal stability analyses in Chapter 6 that focus on the EPS-block geofoam embankment, it was anticipated that circular failure surfaces through the foundation soil is the appropriate failure mode for the external stability analyses. As a result, the geofoam shear strength parameters that yielded the best approximation of failure through the foundation soil were selected. Considerable stability analyses were conducted to investigate how to represent the geofoam embankment to yield failure through the foundation soil. Some of the scenarios considered involve conservatively modeling the geofoam embankment with a friction angle of one degree and a cohesion of zero so the embankment did not contribute significantly to the factor of safety because of the uncertainties in estimating how much shear resistance the geofoam actually contributes in the field. Although this scenario is commonly used in practice, this scenario resulted in the critical failure surface being located in the embankment and not the foundation soil because of the small shear strength assigned to the geofoam. As a result, this approach was not accepted because it did not result in failure through the foundation soil. Another scenario was to apply a surcharge to the surface of the foundation soil that approximates the weight of the embankment and the pavement and traffic

Table 5.2. Input parameters for external slope stability analysis with XSTABL.

surcharges so the strength of the geofoam did not have to be considered. This approach was not selected because it could not be used for seismic stability analyses because the seismic force is applied at the center of gravity of the slide mass (see following section of this chapter) and if only a surcharge is used a seismic force cannot be applied. The third scenario involved assuming failure occurred between the EPS blocks, and thus sliding occurring along EPS/EPS interfaces, and using an interface friction angle of 30 degrees. This approach also resulted in the critical failure surface occurring through the embankment and not the foundation soil because the shear resistance provided by the geofoam even with a friction angle of 30 degrees is small. The shear resistance is small because the normal stress, σ_n, applied to any failure surface passing through the embankment is low because of the low unit weight of the geofoam and the failure surface is nearly vertical through the geofoam, which results in the normal stress on the failure surface being similar to the horizontal earth pressure of the geofoam. The horizontal earth pressure is low, which is one of the reasons geofoam is used for bridge abutments and vertical embankments, and results in a low normal stress being applied to the failure surface. If the normal stress on the failure surface is low, the shear resistance, τ, is low because of the following expression:

$$\tau = c + \sigma_n \tan \varphi \qquad \textbf{(5.50)}$$

It can be seen that the shear resistance is directly related to the normal stress and thus a low normal stress results in a small shear resistance. The shear resistance is further impacted because the normal stress is multiplied by the tangent of the friction angle. As a result, the impact of a high friction angle is reduced because the tangent of the friction angle is used to estimate the shear resistance. In summary, modeling the geofoam using a friction angle did not result in the critical failure surfaces being located in the foundation soil so a scenario in which the geofoam was modeled using a cohesion value was sought so the strength would be independent of the normal stress and result in failure through the foundation soil. A friction angle of 30 degrees can

be used to model the geofoam in the internal stability analyses in Chapter 6 because failure is assumed to occur between the EPS blocks and thus the EPS/EPS interface strength is applicable.

The scenario used to model the geofoam strength for external slope stability analyses assumes that failure occurs through the EPS blocks and thus a cohesion value that adequately represents the shear strength of a geofoam block was sought. From Figure 2.15 and an EPS density of 20 kg/m^3 (1.25 lbf/ft^3) the internal shear strength of an individual block of geofoam is 145.1 kPa (3,030 lbs/ft²). This shear strength can be represented using a Mohr-Coulomb friction angle of zero and a cohesion value of 145.1 kPa (3,030 lbs/ft²). The geofoam is not continuous and thus the effect of joints or discontinuities between the blocks had to be considered to estimate a global shear strength of the EPS embankment. Based on typical block layouts observed in the case histories studied herein (see Chapter 11), it was estimated that a failure surface passing through the embankment would consist of 25 percent shearing through intact EPS blocks and 75 percent shearing through joints between the blocks. Therefore, the representative cohesion value for the global shear strength of the geofoam is estimated to be one-quarter of the compressive strength of the geofoam, i.e., 145.1 kPa (3,030 lbs/ft²), or 36.3 kPa (758 lbs/ft²) as shown in Table 5.2.

The representative cohesion value needs to be corrected for the strain incompatibility between the soft foundation soil and the EPS-block geofoam and thus the potential for progressive failure of the embankment. Figure 5.12 shows a schematic of the stress-strain relationships for the geofoam and foundation soil and it can be seen that the failure through the geofoam results in a brittle failure and a post-peak strength loss at a small strain while the foundation soil exhibits a plastic failure and a peak shear strength at a large strain. Therefore, if the strains mobilized in the embankment and foundation are equal, failure would occur through the geofoam when only a fraction of the foundation strength had been mobilized. Conversely, after the peak strength of the foundation soil had been mobilized, the strength of the geofoam would correspond to a post-peak value. Thus, the peak strength of the geofoam should not be

used in conjunction with the peak strength of the foundation soil in order to prevent progressive failure of the embankment. Progressive failure can occur when one material fails, e.g., the geofoam, and the stresses that were being resisted by that material are transferred to the another material, e.g., the foundation soil, which can result in overstressing of this material especially if it does not mobilize its peak strength at the same strain as the failed material. Therefore, the main geofoam issue is the determination of the shear strength of the geofoam and foundation soil that can be relied on because the stress-strain behavior for these two materials are not compatible.

Figure 5.12. Typical stress-strain behaviors of geofoam and soft foundation soil (*36*).

Chirapuntu and Duncan (*36*) used nonlinear finite element analyses to develop shear strength reduction factors for a compacted soil embankment overlying a soft clay foundation. The reduction factor for a compacted soil embankment is presented in Chirapuntu and Duncan (*36*) in graphical form but was converted to the following equation herein:

$$R_E = 0.89 - 0.089\left(\frac{S_E}{S_F}\right) \qquad \textbf{(5.51)}$$

where

R_E = embankment strength reduction factor

S_E = average embankment shear strength, kN/m^2

S_F = average foundation soil shear strength, kN/m^2

For a geofoam embankment, the strength of the geofoam is reduced to account for the strain incompatibility with the foundation soil while the peak strength of the foundation soil is used. The value of embankment strength used in this expression is assumed to be as 36.3 kPa (758 lbs/ft²) as discussed earlier and shown in Table 5.2. The ratio of the embankment strength to the foundation strength was calculated for the various values of undrained shear strength used to model the foundation soil. After determining this ratio, the embankment strength reduction factor was estimated from the above expression. Typical values of R_E for values of foundation soil undrained shear strength are shown in Table 5.3 and it can be seen that R_E ranges from 0.62 to 0.82.

Therefore, consideration of strain incompatibility results in a reduction of the cohesion value used to represent the shear strength of the geofoam of approximately 20 to 40 percent. The value of cohesion shown in Table 5.2 was reduced by the appropriate reduction factor and the resulting value was used in the external slope stability analyses to model the geofoam.

Table 5.3. Typical reduction factors for geofoam to account for strain incompatibility.

Location of Critical Static Failure Surface

The first step in the external slope stability analyses was to locate the critical static failure surface in the foundation soil. Because the analysis involves soft, saturated foundation soil, only circular failure surfaces were analyzed in the external stability analysis. Figure 5.13 presents a cross-section through a 12.2 m (40 ft) high EPS embankment with side-slopes of 2H:1V and a road width of 34 m (112 ft). The behavior of the critical static failure surface depicted in this figure is typical of the other geometries considered and is used to illustrate the effect of the foundation soil shear strength on the location of the critical failure surface. It can be seen that as the value of undrained shear strength increases, the depth of the critical failure surface decreases. In other words, as the value of s_u increases, it is more likely that the critical failure will remain in the geofoam embankment because the strength of the foundation soil is approaching the strength of the embankment. If the critical failure surface remained in the foundation soil it was termed an external failure mode while it was termed an internal failure if the critical surface remained in the embankment. It can be seen when the value of s_u reaches 36 kPa (752 lbs/ft^2), the critical failure surface remains in the embankment. The focus of this section is external stability so the subsequent design charts and seismic stability analyses only utilize critical failure surfaces that remained completely in the foundation soil because seismic internal stability of the geofoam embankment is addressed in Chapter 6. It can also be seen that as the critical failure surface changes from the foundation soil to the embankment, the failure surface exits on the embankment slope and the failure surface through the geofoam is no longer near vertical.

The transition from the critical failure surface remaining in the foundation soil versus remaining in the embankment can be used to identify the value of s_u for the foundation soil that corresponds to internal stability being more critical than external stability. For example, if the s_u value for the foundation soil at a particular site is equal to or greater than 36 kPa (752 lbs/ft^2**)** and the embankment geometry corresponds to Figure 5.13, internal stability will control the design of the geofoam embankment. If the s_u value for the foundation soil at a particular site is less than 36 kPa, (752 lbs/ft^2**)** external stability will control the design of the geofoam embankment. Therefore, the subsequent design charts for external slope stability terminate at the value of s_u that corresponds to the transition from the critical failure surface remaining in the foundation soil versus moving into the embankment. This results in a different relationship for each embankment geometry because the transition point is a function of embankment geometry and s_u of the foundation soil. The value of s_u at which each relationship terminates signifies the transition from external slope stability being critical to internal stability being critical.

However, if internal stability is determined to be critical, a static internal slope stability analysis does not have to be performed to locate the critical failure surface because there is little or no static driving force applied to any of the three potential failure modes described in the internal seismic stability section in Chapter 6 and shown in Figure 6.2. The driving force is small because the horizontal portion of the internal failure surfaces is assumed to be completely horizontal. Therefore, if Figures 5.14 through 5.16 indicate that internal static stability controls, i.e., s_u of the foundation soil exceeds the value of s_u at which a relationship shown in the figure terminates, the factor of safety against a slope stability failure is expected to exceed 1.5. The fact that embankments with vertical sides can be constructed demonstrates this conclusion.

Figure 5.13. Behavior of critical static failure surface of a trapezoidal embankment as a function of the undrained shear strength of the foundation soil.

Design Charts

The results of the stability analyses were used to develop the static external slope stability design charts in Figures 5.14 through 5.16 for a 2-lane (road width of 11 m (36 ft)), 4-lane (road width of 23 m (76 ft)), and 6-lane (road width of 34 m (112 ft)) roadway embankment, respectively. Figure 5.14 presents the results for a 2-lane geofoam embankment and the three graphs correspond to the three slope inclinations considered, i.e., 2H:1V, 3H:1V, and 4H:1V, for various values of s_u for the foundation soil. It can be seen that for a 2H:1V embankment the affect of geofoam thickness or height, T_{EPS}, is small where as geofoam height is an important variable for a 4H:1V embankment. The geofoam height corresponds to only the height of the geofoam and thus the total height of the embankment is T_{EPS} plus the thickness of the pavement system. In the graph for the 4H:1V embankment, it can be seen that each relationship terminates at a different s_u value for the foundation soil. The value of s_u at which each relationship terminates signifies the transition from external slope stability being critical to internal stability being critical. For example, for a geofoam height of 12.2 m (40 ft), external slope stability controls for s_u values less than approximately 40 kPa (825 lbs/ft²). Therefore, a design engineer can enter this figure with an average value of s_u for the foundation soil and determine whether external or internal stability controls the design. If internal stability is determined to be critical, a static internal slope stability analysis does not have to be performed as previously discussed because the factor of safety against internal slope stability failure is expected to exceed 1.5. If external stability controls, the designer can use this figure to estimate the critical static factor of safety for the embankment, which must exceed a value of 1.5.

It can be seen from Figures 5.14 through 5.16 that the critical static factor of safety for the embankment for the 2-lane, 4-lane, and 6-lane roadway embankment, respectively, all exceed a value of 1.5 for values of s_u greater than or equal to 12 kPa (250 lbs/ft²). These results indicate that external static slope stability will be satisfied, i.e., factor of safety greater than 1.5, if the foundation undrained shear strength exceeds 12 kPa (250 lbs/ft²). If the undrained shear strength

of the foundation soil exceeds the value that corresponds to the maximum value of the appropriate relationship in Figures 5.14 through 5.16, internal stability is more critical than external stability.

In summary, external slope stability does not appear to be the controlling external failure mechanism, instead it appears that settlement will be the controlling external failure mechanism. However, Figures 5.14 through 5.16 can be used to quickly estimate the critical static factor of safety for 2-lane, 4-lane, and 6-lane roadway embankments, respectively, to facilitate the design process.

Figures 5.14 through 5.16 can also be used to investigate the behavior of geofoam embankments. It can be seen for 4-lane and 6-lane roadway embankments, Figures 5.15 and 5.16, respectively, that the critical static factor of safety decrease as the embankment height increases. In addition, as the embankment height decreases the value of s_u that corresponds to the transition between external and internal stability being critical decreases. Therefore, a higher foundation soil shear strength will be required to support higher 4-lane and 6-lane geofoam embankments. The opposite of the behavior was observed for the 2-lane roadway embankment (Figure 5.14) because with a narrower roadway a smaller length of the failure surface is being subjected to the pavement and traffic surcharges and the greater embankment height results in a greater contribution of the cohesion value that is used to represent the shear strength of the geofoam. As a result, the critical static factor of safety increases as the embankment height increases instead of decreasing as in Figures 5.15 and 5.16. It can be seen from Figure 5.14 that the 12.2 m (40 ft) high embankment has a higher factor of safety than the 6.1 m (20 ft) and 3.1 m (10 ft) high embankments. In the 4-lane and 6-lane geofoam embankments the critical failure surface extends at or near the full width of the roadway (see Figure 5.13) and thus a larger portion of the failure surface is subjected to the pavement and traffic surcharges.

Interpretation of External Slope Stability Design Chart

Comparison of the factors of safety in Figures 5.14 through 5.16 also reveals that the critical case for external slope stability is a 6-lane embankment (34.1 m or 112 ft) with a 2H:1V slope and a height of EPS block equal to 12.2 m (40 ft) because this case yields factors of safety of 1.6 to 3.2 for the entire range of s_u values. This is important because the static stability controls the seismic external stability. The greater the static external stability the greater the seismic external stability. The results of the seismic stability analyses will be presented in the next section.

Figures 5.14 through 5.16 can be used for the design of a geofoam embankment by entering the appropriate graph with a value of s_u, e.g., 15 kPa (315 lbs/ft²), EPS-block geofoam thickness or height, T_{EPS}, of 12.2 m (40 ft), and a required slope inclination of 3H:1V and obtaining a critical static factor of safety of approximately 1.9 for a 6-lane roadway embankment (see Figure 5.16).

Remedial Procedures

The main remedy procedure that can be used to increase the factor of safety against external slope instability is to increase the undrained shear strength of the foundation soil by using a ground improvement method. A discussion on ground improvement is provided in Chapter 1. However, the external slope stability analyses indicate that settlement will control the design of a geofoam embankment and not external slope stability, which is in agreement with the lack of field case histories involving external slope instability.

Figure 5.14. Static external slope stability design chart for trapezoidal embankments with a 2-lane roadway with a total road width of 11 m (36 ft).

Figure 5.15. Static external slope stability design chart for a trapezoidal embankment with a 4-lane roadway with a total road width of 23 m (76 ft).

Figure 5.16. Static external slope stability design chart for a trapezoidal embankment with a 6-lane roadway with a total road width of 34 m (112 ft).

EXTERNAL SEISMIC STABILITY OF TRAPEZOIDAL EMBANKMENTS

Introduction

Seismic loading is a short-term event that must be considered in geotechnical problems including road embankments. Seismic loading can affect both external and internal stability of an embankment containing EPS-block geofoam. This section of Chapter 5 considers external seismic slope stability of EPS-block geofoam trapezoidal embankments or embankments with sloped sides while internal seismic stability is addressed in Chapter 6. A supplemental section of Chapter 5 considers external seismic slope stability of EPS block vertical embankments. Most of the considerations for static and seismic external stability analyses are the same for embankments constructed of geofoam or earth materials. These considerations include various SLS and ULS mechanisms such as seismic settlement and liquefaction that are primarily independent of the nature of the embankment material because they depend on the seismic risk at a particular site and the nature and thickness of the natural soil overlying the bedrock. A discussion of these topics can be found in (*37*). Mitigation of seismic induced subgrade problems by ground improvement techniques prior to embankment construction is beyond the scope of this study. However, a discussion on ground improvement to reduce potential seismic-induced subgrade problems can be found in (*8,37-39*).

This section focuses on the effect of seismic forces on the external slope stability of EPS-block geofoam embankments. This issue is addressed using a pseudo-static slope-stability analysis (*37*) involving circular failure surfaces through the foundation soil. Terzaghi (*40*) developed the pseudo-static stability analysis to simulate earthquake loads on slopes and the analysis involves modeling the earthquake shaking with a horizontal force that acts permanently, not temporarily, and in one direction on the slope. Thus, the primary difference between a pseudo-static and static external stability analyses is that a horizontal force is permanently applied to the center of gravity of the critical slide mass and in the direction of the exposed slope. If a stability method is used that involves dividing the slide mass into vertical slices, the horizontal

force is applied to the center of gravity of each vertical slice that simulates the inertial forces generated by horizontal shaking. This horizontal force (F) equals the slide mass or the mass of the vertical slide (m) multiplied by the seismic acceleration (a), i.e., F=m*a. The seismic acceleration is usually derived by multiplying a seismic coefficient, k, by gravity.

The pseudo-static horizontal force must be applied to the slide mass that is delineated by the critical static failure surface. Therefore, the steps in a pseudo-static analysis are:

1. Locate the critical static failure surface, i.e., the static failure surface with the lowest factor of safety, that passes through the foundation soil, i.e., external failure mechanism, using a slope stability method that satisfies all conditions of equilibrium, e.g., Spencer's (*34*) stability method. This value of factor of safety should satisfy the required value of static factor of safety of 1.5 before initiating the pseudo-static analysis.
2. Modify the static shear strength values for cohesive or liquefiable soils situated along the critical static failure surface to reflect a strength loss due to earthquake shaking, which is discussed subsequently.
3. Determine the appropriate value of horizontal seismic coefficient (discussed subsequently) that will be multiplied by gravity to determine the horizontal seismic acceleration and applied to the center of gravity of the critical static failure surface. A search for a new critical failure surface should not be conducted with a seismic force applied because the search may and usually does not converge. The search may not converge because a failure surface that delineates a larger slide mass will result in a larger seismic force being applied to the slope and usually a lower factor of safety. It is reasonable to simply apply the horizontal seismic force to the critical static failure because if an earthquake occurs, the most vulnerable failure surface is the critical static failure surface.

4. Calculate the pseudo-static factor of safety, FS', for the critical static failure surface and ensure it meets the required value. In (*41*) it is indicated that for transient loads, such as earthquakes, safety factors as low as 1.2 or 1.15 may be tolerated. It is indicated in (*42*) that in southern California, a minimum factor of safety of 1.1 to 1.15 is considered acceptable for a pseudo-static slope stability analysis. A factor of safety between 1.0 and 1.2 is indicated in (*37*). The safety of factor required will most likely vary from state to state. Therefore, local Departments of Transporation factor of safety requirements for seismic stability should be used. The seismic design charts included in this report are based on a factor of safety of 1.2. A factor of safety of 1.2 was used for seismic stability to keep the factor of safety uniform for all temporary loading conditions, which includes design for hydrostatic uplift and translation (sliding).

Seismic Shear Strength Parameters

The static shear strength parameters should not be changed for a pseudo-static stability analysis unless a cohesive soil or liquefiable soil is involved. If a cohesive soil is located along the critical static failure surface, the peak shear strength of this material can be reduced by as much as 20 percent of the static peak undrained shear strength by seismic loading (*43*). As a result, in (*43*), the use of an undrained shear strength for a cohesive soil that is 80 percent or more of the static peak undrained shear strength is recommended. Thus, the value of s_u used to represent the foundation soil under the geofoam embankment should be reduced by not more than 20 percent. If a cohesionless soil is situated along the critical failure surface and is predicted to liquefy due to the earthquake shaking, this material should be assigned a liquefied shear strength as proposed in (*44*). Based on the geofoam interface strength testing described in Chapter 2, the value of static EPS shear strength shown in Table 5.2 can be used for the pseudo-static analyses. This conclusion is also supported by the results of shake table tests on geosynthetic interfaces (*45*) that showed the seismic interface strength of geosynthetic interfaces exceeds the static

interface strength. However, this value of shear strength should be reduced for strain incompatibility with the foundation soil as was described for the external slope stability analyses.

Horizontal Seismic Coefficient

The horizontal seismic coefficient, $k_{h,}$, at the center of gravity of the slide mass is estimated using the seismic acceleration at the base (subgrade level) and top of the embankment and linearly interpolating between these two values to obtain k_h, at the center of gravity. This analysis approach is based on the assumption that the horizontal acceleration within the embankment can be assumed to vary linearly between the base and top of the embankment values. At any level within the embankment, the interpolated value of horizontal acceleration can be divided by gravity to determine the horizontal seismic coefficient which can be inputted into slope stability software to conduct a pseudo-static analysis. If a circular failure surface is used for the static stability analysis, the center of gravity of the sliding mass is usually located near the center or mid-height of the sliding mass. This location can be used in the linear interpolation process to estimate the seismic acceleration, and thus seismic coefficient, at the center of gravity of the critical static slide mass.

One difficulty with this process is that estimating the seismic acceleration at the base and top of the geofoam embankment is difficult because a geofoam embankment is not rigid. The base acceleration must be estimated first and then this acceleration is transferred from the base to the top of the embankment to estimate the acceleration at the embankment crest. Because this project is focused on geofoam embankments, most, if not all, of the embankments will not be founded on bedrock. Therefore, the bedrock horizontal acceleration must be transmitted from the underlying bedrock through the overlying soil deposit at the base of the geofoam embankment. The base acceleration can be estimated from the bedrock acceleration in two primary ways: (1) conducting a one-dimensional site response analysis in which a representative earthquake record is inserted at the bedrock elevation and propagated vertically through the overlying soil to estimate the acceleration at the base of the geofoam embankment or (2) using empirical

relationships that relate the bedrock acceleration to the ground surface acceleration for different soil types.

If a one-dimensional site response analysis is conducted using a program such as SHAKE (*46*), the acceleration at the base and top of the embankment can be calculated and the horizontal seismic coefficient at the center of gravity of the slide mass can be estimated using the following expression presented in (*47*):

$$k_h = \frac{\tau_h * g}{\gamma * z'} \qquad \textbf{(5-52)}$$

where:

z' = depth from the top of the geofoam embankment at which the seismic coefficient is to be estimated

γ = average unit weight of the material above depth z

g = gravity, and

τ_h = horizontal shear stress at depth z calculated by a one-dimensional site response analysis.

The main issues encountered in conducting a site response analysis are determining representative earthquake records to propagate though the soil deposit overlying the bedrock and the seismic properties of the soil layers comprising the soil deposit. An extensive discussion of one-dimensional site response analyses for man-made embankments is presented by (*48*). If a site response analysis is conducted, the values of initial tangent Young's modulus, Poisson's ratio, and shear modulus indicated in Table 5.4 can be assumed for the EPS-block geofoam. Any portion of the EPS blocks that is permanently submerged under normal ground water conditions is assumed to have a total unit weight of 1,000 N/m³ (6.37 lbf/ft³), not the dry unit weight value of 200 N/m³ (1.25 lbf/ft³) suggested for general gravity stress calculations, to conservatively allow for long-term water absorption in the geofoam.

Table 5.4. Seismic Material Properties for EPS-Block Geofoam for Site Response Analyses.

Additional discussion of one-dimensional site response analyses for geofoam embankments is beyond the scope of this project. Thus, the use of existing empirical relationships for estimating the base acceleration from the bedrock acceleration is discussed in detail. Empirical site response relationships, developed using one-dimensional site response analyses and field observations, are typically used to estimate the ground surface acceleration. However, on large projects it may be prudent to conduct a site-specific response analyses to accurately estimate the acceleration at the ground surface and top of the embankment accelerations. Figure 5.17 presents relationships between bedrock acceleration and ground surface acceleration, i.e., acceleration at the base of the embankment, for various soil types. To utilize this chart, the peak horizontal bedrock acceleration needs to be estimated from local information or from seismic hazard maps prepared by the U.S. Geological Survey (USGS) (*49*). The USGS maps presents contours of peak horizontal bedrock acceleration for various probabilities of exceedance and return periods. For example, the maps corresponding to a probability of exceedance of 10 percent in 50 years is frequently used for civil engineering design purposes and can be used to estimate the bedrock peak horizontal acceleration for a particular location in the United States. This bedrock acceleration and Figure 5.17 can be used to estimate the ground surface acceleration, which can be assumed to be equal to the acceleration at the base of the geofoam embankment. This assumption appears valid for geofoam embankments because the normal stress applied to the subsurface soils by a geofoam embankment is small and thus probably has little, if any, effect on the response of the subsurface soils. This may not be a valid assumption for soil embankments because the applied normal stress can be significant.

One important note concerning the relationships in Figure 5.17 is that the figure should not be used for soft soil sites such as soft clays or peats. Field observations of site response since publication of the site response relationships in Figure 5.17 has shown that soft soil sites can amplify the bedrock acceleration, especially at bedrock accelerations less than 0.4g. Thus, if the majority of the subsurface soils with depth at the EPS-block geofoam embankment site are

characterized as a soft clay or peat, the site response relationship in Figure 5.18 should be used to estimate the ground surface acceleration from the bedrock acceleration. It can be seen that the median relationship at bedrock accelerations less than 0.4g predicts ground surface accelerations that are greater than the bedrock accelerations with a maximum amplification factor of approximately two. This amplification of the bedrock acceleration at soft soil sites has been verified by case histories such as the 1985 Mexico City and 1989 Loma Prieta earthquakes (see Figure 5.18). For example, in the 1985 Mexico City earthquake the ground surface acceleration was 1.5 to 2 times greater than the bedrock acceleration (see Figure 5.18). It has been postulated that this amplification contributed to the significant damage caused by the earthquake (*50*). For comparison with geofoam project sites, Mexico City is located on 100 to 200 feet thick soft clay deposits that fill an old lakebed (*50*).

Figure 5.17. Relationship between bedrock and ground surface horizontal acceleration for various soil types (*51*).

Figure 5.18. Relationship between bedrock and ground surface horizontal acceleration for soft soil sites (*52*).

After estimating the base acceleration, the acceleration at the top of the embankment must be estimated so the acceleration at the center of gravity of the slide mass be estimated from linearly interpolating the accelerations at the base and top of the embankment. If the geofoam embankment was rigid the acceleration at the top would equal the acceleration at the base of the embankment. Japanese research (*53*) demonstrates that the seismic response of a geofoam embankment is not rigid but flexible. Therefore, the acceleration at the top generally will not equal the base acceleration. The acceleration at the top of the embankment could be greater or less than the base acceleration depending on the response of the embankment. However, it is anticipated that the top acceleration will be less than the base acceleration because of the potential for shear deformation to occur between geofoam blocks as the seismic shear waves propagate

vertically through the embankment. Amplification has been observed in soil embankments (*37*) but no published accounts of amplification in EPS-block geofoam embankments were located during this study. The acceleration at the top of a geofoam embankment will primarily affect the factor of safety against lateral sliding of the pavement system on the top of the EPS mass.

As with the base acceleration, there are two primary ways for estimating the acceleration at the top of the geofoam embankment: (1) conducting a one-dimensional site response analysis that models the foundation soils as well as the geofoam embankment and thus directly calculating the acceleration at the top of the embankment and at the center of gravity or (2) using empirical relationships to relate the base acceleration to the top acceleration. As mentioned previously, empirical site response relationships are frequently used to estimate the ground surface acceleration and it is proposed herein that they be used to estimate the top acceleration. On large projects it may be prudent to conduct a site-specific response analyses that models the geofoam embankment to accurately estimate acceleration at the center of gravity of the slide mass.

To utilize empirical site response relationships, it must be determined what soil type should be used to approximate the geofoam. It is proposed herein that the geofoam be assumed to behave as the deep cohesionless soil depicted in Figure 5.17. The deep cohesionless soil behavior was chosen because the geofoam embankment will probably not behave as rock or a stiff soil because of the slippage that can occur between blocks. This slippage will result in some dissipation of shear stress as the seismic waves propagate through the embankment. The deep cohesionless soil relationship will yield accelerations at the top of embankment that are less than the base accelerations because the relationship does not indicate amplification (see Figure 5.17). A deep cohesionless soil was also selected because the shear resistance is frictional which is in agreement with the frictional nature of the EPS/EPS interface strengths reported in Chapter 2. It was also decided that modeling the geofoam embankment as a soft soil, and thus assuming amplification, probably would be too conservative. Finally, the stiff clay and sand relationship

was disregarded because of the potential for slippage between the blocks and the deep cohesionless soil relationship provides a more conservative design.

In summary, Figure 5.17 can be used with the base acceleration to estimate the acceleration at the top of the embankment and linear interpolation can be used to estimate the acceleration, and thus horizontal seismic coefficient, at the center of gravity of the critical static slide mass. The base acceleration should be used on the horizontal axis in Figure 5.17 and the acceleration at the top of the embankment should be estimated from the vertical axis using the deep cohesionless soil relationship.

Seismic Stability Analysis Procedure

Pseudo-static slope stability analyses were conducted on the range of embankment geometries used in the external static stability analyses to investigate the effect of various embankment heights (3.1 m (10 ft) to 12.2 m (40 ft)), slope inclinations (2H:1V, 3H:1V, and 4H:1V), and road widths of 11, 23, and 34 m (36, 76, and 112 ft) on external seismic slope stability. The results of these analyses were used to develop design charts to facilitate seismic design of roadway embankments that utilize geofoam. The seismic analyses utilized the critical static failure surfaces identified for each geometry in the external static stability analyses. A pseudo-static analysis was conducted on only the critical failure surfaces that passed through the foundation soil because external stability is being evaluated. As a result, the design charts for seismic stability terminate at the s_u value for the foundation soil that corresponds to the transition from a critical failure surface in the foundation soil to the geofoam embankment determined during external static stability analysis. This resulted in the seismic stability design charts terminating at the same value of s_u as the static stability charts in Figures 5.14 through 5.16.

A typical cross-section through an EPS embankment with side-slopes of 2H:1V used in the pseudo-static stability analyses is shown in Figure 5.19. This cross-section differs from the cross-section used for the static analyses in Figure 5.11 because the surcharge used to represent the pavement and traffic surcharges is replaced by assigning the soil cover layer on top of the

embankment a unit weight of 71.8 kN/m^3 (460 lbf/ft^3). The soil cover is 0.46 m (1.5 ft) thick so the stress applied by this soil cover equals 0.46 m times the increased unit weight or 33.0 kPa (690 lbs/ft^2). A stress of 33.0 kPa (690 lbs/ft^2) corresponds to the sum of the design values of pavement surcharge (21.5 kPa (450 lbs/ft^2)) and traffic surcharge (11.5 kPa (240 lbs/ft^2)) used previously for external bearing capacity and slope stability. The surcharge in Figure 5.11 had to be replaced because a seismic coefficient is not applied to a surcharge in limit equilibrium stability analyses only material layers because the horizontal force that represents the seismic loading must be applied at the center of gravity of the material layer.

Figure 5.20 illustrates the location and magnitude of the pseudo-static forces used to represent earthquake loading for a particular value of horizontal seismic coefficient. The length of the horizontal arrows corresponds to the relative magnitude of the horizontal force for a given horizontal seismic coefficient. It can be seen that the pavement and traffic surcharges yields the largest horizontal force because the weight of the soil layer used to model the surcharge results in the largest weight. The soil cover and EPS exhibit a small weight and thus the horizontal seismic force is small for both materials. The weight is small for these materials because the thickness of the soil cover is small and the unit weight of the EPS is small, respectively. The foundation soil also contributes a significant horizontal seismic force because of the unit weight of the material.

Figure 5.19. Typical cross-section used in seismic external slope stability analyses of trapezoidal embankments.

Figure 5.20. Typical cross-section showing location and relative magnitude of pseudo-static forces used to represent an earthquake loading in a trapezoidal embankment.

Design Charts

The results of the stability analyses were used to develop the seismic external slope stability design charts for a 2-lane (road width of 11 m (36 ft)), 4-lane (road width of 23 m (76 ft)), and 6-lane (road width of 34 m (112 ft)) roadway embankment. Three seismic coefficients, low (0.05), medium (0.10), and high (0.20), were used for each roadway embankment. Values of

seismic coefficient greater 0.20 indicate a severe seismic environment and a site-specific seismic analysis, including a site response analysis, should be conducted instead of using simplified design charts.

The pseudo-static factor of safety for the critical static failure surfaces previously identified using the Simplified Janbu stability method was calculated for each geometry considered for the development of the design charts. The factor of safety was calculated using Spencer's slope stability method (*34*) as coded in the microcomputer program XSTABL Version 5 (*32*) because it satisfies all conditions of equilibrium. The analyses were conducted without reducing the shear strength of the foundation soil 80 percent as discussed above because the design charts present the pseudo-static factor of safety for the critical versus undrained shear strength (see Figure 5.21) and a design engineer can utilize these charts with an s_u value that reflects any strength loss that might occur during earthquake shaking.

Figures 5.21 through 5.23 present the seismic external stability results for a 2-lane geofoam roadway embankment with a total road width of 11 m (36 ft) and the three values of horizontal seismic coefficient, i.e., 0.05, 0.10, and 0.20, respectively. Comparison of these figures results in the following conclusions about the seismic performance of a 2-lane geofoam embankment:

(1) Seismic stability is not a concern for a horizontal seismic coefficient less than or equal to 0.05 because all of the computed values of factor of safety exceed the required value of 1.2 (see Figure 5.21).

(2) A horizontal seismic coefficient of 0.10 results in values of FS' that do not satisfy the required value of 1.2 for embankment inclinations of 3H:1V and 4H:1V (see Figure 5.22). The flatter embankments are more critical than the 2H:1V embankment because the weight of the materials above the critical static failure surface is greater which results in a greater seismic force being applied in the 3H:1V and 4H:1V embankments versus the 2H:1V embankment.

(3) A horizontal seismic coefficient of 0.20 results in values of FS' that do not satisfy the required value of 1.2 for all embankment inclinations (see Figure 5.23). Again the flatter embankments are more critical and thus a higher undrained shear strength will be required to satisfy the required factor of safety of 1.2 especially for the 4H:1V embankment.

Figure 5.21. Seismic external slope stability design chart for trapezoidal embankments with a 2-lane roadway with a total road width of 11 m (36 ft) and a k_h of 0.05.

Figure 5.22. Seismic external slope stability design chart for trapezoidal embankments with a 2-lane roadway with a total road width of 11 m (36 ft) and a k_h of 0.10.

Figure 5.23. Seismic external slope stability design chart for trapezoidal embankments with a 2-lane roadway with a total road width of 11 m (36 ft) and a k_h of 0.20.

Figures 5.24 through 5.26 present the seismic external stability results for a 4-lane geofoam roadway embankment with a total road width of 23 m (76 ft) and the three values of horizontal seismic coefficient, i.e., 0.05, 0.10, and 0.20, respectively. Comparison of these figures results in the following conclusions about the seismic performance of a 4-lane geofoam embankment:

(1) Seismic stability is a concern even for a horizontal seismic coefficient less than or equal to 0.05 because some of the computed values of factor of safety do not satisfy the required value of 1.2 (see Figure 5.24) at the lowest value of undrained shear strength (12.0 kPa or 250 lbs/ft²). The reason for the decreased seismic stability from the 2-lane geofoam embankment is the wider roadway results in a larger critical slide mass and thus a larger weight above the critical failure surface. The larger the weight of the slide mass above the critical static failure surface the greater seismic force being applied in the analysis.

(2) The increased roadway width results in large values of undrained shear strength being required for the foundation soil to achieve the required value of pseudo-static

factor of safety of 1.2. It can been seen in Figure 5.26 that an s_u of at least 36 kPa (750 lbs/ft²) will be required for a 4H:1V embankment and a horizontal seismic coefficient of 0.20.

Figure 5.24. Seismic external slope stability design chart for trapezoidal embankments with a 4-lane roadway with a total road width of 23 m (76 ft) and a k_h of 0.05.

Figure 5.25. Seismic external slope stability design chart for trapezoidal embankments with a 4-lane roadway with a total road width of 23 m (76 ft) and a k_h of 0.10.

Figure 5.26. Seismic external slope stability design chart for trapezoidal embankments with a 4-lane roadway with a total road width of 23 m (76 ft) and a k_h of 0.20.

Figures 5.27 through 5.29 present the seismic external stability results for a 6-lane geofoam roadway embankment with a total road width of 34 m (112 ft) and the three values of horizontal seismic coefficient, i.e., 0.05, 0.10, and 0.20, respectively. The 6-lane roadway results in the most critical seismic stability condition because the widest roadway results in the largest critical slide mass and thus the largest horizontal seismic force. This results in seismic stability concerns for the smallest horizontal seismic coefficient (see Figure 5.27), the shortest embankment height of 3.1 m (10 feet) (see Figure 5.28), and the flattest slope inclination of 4H:1V (see Figure 5.29).

Figure 5.27. Seismic external slope stability design chart for trapezoidal embankments with a 6-lane roadway with a total road width of 34 m (112 ft) and a k_h of 0.05.

Figure 5.28. Seismic external slope stability design chart for trapezoidal embankments with a 6-lane roadway with a total road width of 34 m (112 ft) and a k_h of 0.10.

Figure 5.29. Seismic external slope stability design chart for trapezoidal embankments with a 6-lane roadway with a total road width of 34 m (112 ft) and a k_h of 0.20.

Interpretation of Seismic Slope Stability Design Chart

Figures 5.21 through 5.29 can be used for the design of a geofoam embankment by entering the appropriate graph, which is determined by the horizontal seismic coefficient and

slope inclination, using a value of s_u that reflects seismic loading and the thickness or height of EPS used in the embankment to obtain the pseudo-static factor of safety. For example, a 6-lane geofoam roadway embankment is proposed for a soft foundation soil that exhibits an undrained shear strength of 20 kPa (418 lbs/ft²). The height of EPS geofoam height is 6.1 m (20 ft) and the required slope inclination is 4H:1V. The critical pseudo-static factor of safety for this scenario with a horizontal seismic coefficient of 0.20 can be obtained from Figure 5.29 and is approximately 0.75 for a 6-lane roadway embankment. If the undrained shear strength of 20 kPa (418 lbs/ft²) is reduced by 80 percent to reflect strength loss during seismic loading as proposed in (*43*), the critical pseudo-static factor of safety Figure 5.29 is approximately 0.58.

In summary, seismic external slope stability can control the design of a geofoam roadway embankment depending on the width, or number of roadway lanes, on the embankment and the magnitude of the horizontal seismic coefficient. Most of the geometries considered herein are safe for a horizontal seismic coefficient of less than or equal to 0.10. If the particular embankment is expected to experience a horizontal seismic coefficient greater than or equal to 0.20, seismic external slope stability could control the design of the embankment. Observations of EPS-block geofoam embankments after various earthquakes has revealed little or no series damage to the EPS embankments (*6,54*), which is in agreement with these findings. These observations include damage assessments after the 1993 Kushiro-Oki earthquake (Japan Meteorological Agency Intensity Scale (JMA)=5), 1993 Noto-Hanto-Oki earthquake (JMA=5), and 1995 Hyogo-Ken Nanbu earthquake (JMA= 7). Damage assessments made on nine EPS embankments after the 1995 Hyogo-Ken Nanbu earthquake, also known as the Kobe earthquake, revealed little or no damage except for one embankment which settled about 10 cm (3.9 in.) due to liquefaction of the embankment foundation soils.

Remedial Procedures

The main remedial procedure that can be used to increase the factor of safety against external seismic instability is to increase the undrained shear strength of the foundation soil by

using a ground improvement method. A discussion on ground improvement is provided in Chapter 1.

EXTERNAL SLOPE STABILITY OF VERTICAL EMBANKMENTS

Introduction

As shown by Figure 3.4 (b), an embankment with vertical side walls, sometimes referred to as a geofoam wall, can be constructed with EPS-block geofoam. The use of a vertical embankment minimizes the amount of right-of-way needed and the impact of embankment loads on nearby structures, which is an important advantage over other lightweight fills. This section presents an evaluation of external slope stability as a potential failure mode of EPS-block geofoam fill embankments with vertical walls. The general expression for the limit equilibrium factor of safety, FS, against a slope stability failure is given by Equation 5.49. As indicated by this equation, a slope stability failure occurs if the driving shear stresses equal or exceed the shear resistance of the material(s) along the failure surface. The driving shear stresses of an EPS-block geofoam vertical embankment are due to the weight of the EPS blocks and the overlying pavement and the traffic loads. The shear resistance is primarily attributed to the undrained shear strength of the foundation soil and/or EPS blocks.

Typical Cross-Section

The typical cross-section through an EPS vertical embankment with vertical walls used in the external static stability analyses is shown in Figure 5.30. This cross-section differs from the cross-section used for the static analyses of trapezoidal embankments in Figure 5.11 because the surcharge used to represent the pavement and traffic surcharges is replaced by placing a 0.61 m (2 ft) soil layer on top of the embankment with a unit weight of 54.1 kN/m^3 (345 lbf/ft^3). The soil layer is 0.61 m (2 ft) thick to represent the minimum recommended pavement section thickness discussed in Chapter 4. Therefore, the vertical stress applied by this soil layer equals 0.61 m (2 ft) times the increased unit weight of 54.1 kN/m^3 (345 lbf/ft^3) or 33.0 kPa (690 lbs/ft^2). A vertical stress of 33.0 kPa (690 lbs/ft^2) corresponds to the sum of the design values of pavement surcharge

(21.5 kPa (450 lbs/ft²)) and traffic surcharge (11.5 kPa (240 lbs/ft²)) used previously for external bearing capacity and slope stability of trapezoidal embankments.

Figure 5.30. Typical cross-section used in static and seismic external slope stability analyses of vertical embankments.

The pavement and traffic surcharge in Figure 5.11 was replaced by an equivalent soil layer because a seismic slope stability analysis can only be performed with material layers and not surcharge loads as discussed in the next section. In a pseudo-static analysis a seismic coefficient cannot be applied to a surcharge in limit equilibrium stability analyses only material layers because the horizontal force that represents the seismic loading must be applied at the center of gravity of the material layer. The equivalent soil layer, which is equivalent to the pavement and traffic surcharge, was also used for the static stability analyses of embankments with vertical walls instead of a surcharge to minimize the number of stability analyses that would be required if two models were utilized, i.e., an embankment modeled with a surcharge and one modeled with a soil layer. A slight difference in the critical factor of safety value and the location of the critical failure surface may result between the two different models because surcharge forces exert an additional force at the top of each slice in the computer program XSTABL (*32*) while the force exerted by the weight of the soil layer is located at the center of each slice. In summary, the surcharge of the pavement system and traffic loads were modeled as a soil layer for both static and seismic slope stability analysis of embankments with vertical walls.

Static Stability Analysis Procedure

Static slope stability analyses were conducted on a range of embankment geometries to investigate the effect of various embankment heights (3.1 m (10 ft) to 12.2 m (40 ft)) and road widths of 11, 23, and 34 m (36, 76, and 112 feet) on external slope stability. The results of these analyses were used to develop design charts to facilitate design of roadway embankments that utilize geofoam. The static stability analysis of each geometry or cross-section was conducted in two-steps. This first step involved locating the critical static failure surface and the second step

involved calculating the factor of safety for the critical static failure surface. The Simplified Janbu stability method (*31*) was used to locate the critical static failure surface because a rotational failure mode surface was assumed for the external stability analyses, versus a translational failure mode for the internal stability analyses. In addition, the microcomputer program XSTABL Version 5 (*32*) only allows searches for the critical failure surface using the Simplified Janbu method or Simplified Bishop (*33*) stability method.

After locating the critical static failure surface using the Simplified Janbu stability method, the critical static factor of safety for this failure surface was calculated using Spencer's (*34*) two-dimensional stability method because the method satisfies all conditions of equilibrium and provides the best estimate of the limit equilibrium factor of safety (*35*). Spencer's method could not be used initially to locate the critical static failure surface because XSTABL only allows searches for the critical failure surface using the Simplified Janbu and Simplified Bishop stability methods. However, for the narrow and tall embankment with a width of 11 m (36 ft) and height of 12.2 m (40 ft), Spencer's method yielded an unreasonable location of interslice forces. For these embankment geometries, the factor of safety value was determined using Bishop's simplified method because Bishop's simplified method provides similar values of factor of safety as Spencer's method (*35*) for circular failure surfaces.

Material Properties

The same material input parameters, i.e., unit weight and shear strength, used in the external slope stability analyses of embankments with sloped sides, which are presented in Table 5.2, were used for external stability analysis of vertical embankments. However, since embankments with vertical walls do not have a soil cover on the side walls, the soil cover material parameters shown in Table 5.2 were not used. A friction angle of 0 degrees was used for the soil layer on top of the EPS-block geofoam that was used to model the pavement and traffic surcharges. The value of undrained shear strength for the EPS-block geofoam shown in Table 5.2 was reduced by the appropriate reduction factor shown in Table 5.3 to account for strain

incompatibility as discussed previously in the sub-section entitled "Material Properties" and in the section entitled "External Slope Stability of Trapezoidal Embankments." The phreatic surface was located at or near the ground surface and the foundation soil was assumed to be saturated as is typically the case at most EPS-block geofoam sites.

Location of Critical Static Failure Surface

The first step in the external slope stability analyses was to locate the critical static failure surface in the foundation soil. The critical failure surface is the failure surface that yields the lowest factor of safety for each foundation soil undrained shear strength investigated. Because the analysis involves soft, saturated foundation soil, only circular failure surfaces were analyzed in the external stability analysis. During the search for the critical circular failure surface, it was observed that the critical failure surface was located within the EPS-block geofoam for all foundation shear strengths analyzed. However, a critical failure surface within the EPS blocks is not representative of actual field conditions because stress distribution through the EPS blocks from the pavement and traffic loads is not considered. Additionally, analysis of a failure surface within only the EPS blocks should not be performed with the reduced shear strength values because strain incompatibility between the EPS blocks and the foundation soil is not an issue. Additionally, if internal stability is determined to be critical, a static internal slope stability analysis does not have to be performed to locate the critical failure surface because there is little or no static driving force applied to any of the three potential internal stability failure modes shown in Figure 6.7. The driving force is small because the horizontal portion of the internal failure surfaces is assumed to be completely horizontal along the surface of a row of blocks. The fact that embankments with vertical sides can be constructed demonstrates this conclusion. The focus of this section is external stability so the subsequent design charts and seismic stability analyses only utilize critical failure surfaces that remain completely in the foundation soil because seismic internal stability of the geofoam embankment is addressed in Chapter 6. Therefore, the

search for the critical failure surface was limited to critical failure surfaces that extend into the foundation soil.

Figure 5.31(a) and 5.31(b) presents a cross-section through a 12.2 m (40 ft) high EPS embankment with a road width of 11 m (36 ft) and 34 m (112 ft), respectively. For the 11 m (36 ft) wide embankment, as the undrained shear strength (s_u) of the foundation soil decreases, the critical failure surface extends further out from the toe of the embankment and terminates near the top outer edge of the embankment as shown in Figure 5.31(a). For the 34 m (112 ft) wide embankment, the s_u of the foundation soil does not have a significant impact on the location of the failure surface except at an s_u of 48 kPa (1,000 lbs/ft^3) where the failure surface extends further out from the toe of the embankment.

The behavior of the critical static failure surface depicted in Figure 5.31 is typical of the other geometries considered and is used to illustrate the effect of the foundation soil shear strength on the location of the critical failure surface within the foundation soil. It can be seen by comparing Figures 5.31(a) and 5.31(b) that no general conclusions can be made about the influence of foundation soil undrained shear strength on the location of the critical failure surface. As noted previously, the critical failure surface was located within the EPS-block geofoam for all foundation shear strengths analyzed. Thus, unlike the behavior of the critical static failure surface for trapezoidal embankments depicted in Figure 5.13, the transition from the critical failure surface remaining in the foundation soil versus remaining in the embankment cannot be used to identify the value of foundation s_u that corresponds to internal stability being more critical than external stability in embankments with vertical walls. Thus, a value of s_u cannot be identified at which the transition from external slope stability being critical to internal stability being critical occurs.

Figure 5.32 presents cross-sections through a 12.2 m (40 ft) high EPS embankment with vertical walls for the three road widths investigated at an s_u of the foundation soil of 48 kPa (1,000 lbs/ft^3). At embankment widths of 23 m (76 ft) and 34 m (112 ft), the factors of safety are

similar and the failure surface originates near the toe of the embankment and terminates near the center of the embankment. At the smaller embankment width of 11 m (36 ft), the failure surface extends further out from the toe of the embankment and terminates near the top outer edge of the embankment. The narrower embankment width of 11 m (36 ft) also produces a higher factor of safety because the heavier foundation soil below the toe of the embankment provides more of the resisting load to the failure surface than the wider embankments for a given height. The failure surface extends further out because if the shape of the failure surface is assumed to be circular, the failure surface must extend further out for narrow and tall embankments to accommodate the circular failure surface. Additionally, a narrower embankment yields a smaller length of the failure surface that is subjected to the pavement and traffic driving stresses.

(a) Road width = 11 m (36 ft)

(b) Road width = 34 m (112 ft)

Figure 5.31. Behavior of critical static failure surface of a vertical embankment as a function of the undrained shear strength of the foundation soil.

Figure 5.32. Behavior of critical static failure surface of a vertical embankment as a function of the width of the embankment.

Figure 5.33 presents a cross-section through an 11 m (36 ft) wide embankment with vertical walls for the three heights investigated at a foundation s_u of 48 kPa (1,000 lbs/ft^3). Note that the factor of safety decreases when the embankment height is increased from 3.1m (10 ft) to 6.1 m (20 ft) but then increases when the embankment height is increased from 6.1 m (20 ft) to 12.2 m (40 ft). At embankment heights of 3.1 m (10 ft) and 6.1 m (20 ft), the failure surface originates near the toe of the embankment and terminates near the center of the embankment while for the taller embankment with a height of 12.2 m (40 ft), the failure surface extends further out from the toe of the embankment and terminates near the top outer edge of the embankment. Although a taller embankment results in a greater contribution of EPS undrained shear strength to the shear resistance along the failure surface, the factor of safety is less for an embankment height

of 6.1 m (20 ft) than 3.1 m (10 ft) because the length of the failure surface within the embankment is larger for the higher embankment and thus a larger percentage of the failure surface is subjected to the pavement and traffic loads. However, the taller embankment height of 12.2 m (40 ft) produces a higher factor of safety because the failure surface extends further out from the toe of the embankment and, consequently, the heavier foundation soil below the toe of the embankment provides more resisting force to the failure surface than the shorter embankments for a given width. The failure surface extends further out because if the failure surface is assumed to be circular, the failure surface must extend out for narrow and tall embankments to accommodate the circular failure surface.

In summary, no general conclusions can be made about the influence of foundation undrained shear strength on the location of the critical static failure surface because there is little affect of s_u on failure surface location. Unlike the behavior of the critical static failure surface for trapezoidal embankments, a value of s_u cannot be identified for vertical embankments at which the transition from external stability being critical to internal stability being critical occurs. However, narrow and tall embankments with vertical walls will yield larger factors of safety because the failure surface will extend further out from the toe of the embankment and, consequently, the heavier foundation soil below the toe of the embankment provides more of the resisting load to the failure surface. The failure surface extends further out because if the failure surface is assumed to be circular, the failure surface must extend further out for narrow and tall embankments to accommodate the circular failure surface.

Figure 5.33. Behavior of critical static failure surface of a vertical embankment as a function of the height of the embankment.

Design Charts

The results of the stability analyses were used to develop the static external slope stability design charts in Figures 5.34 and 5.35. Figure 5.34 presents the results for a 2-lane (road width of 11 m (36 ft)), 4-lane (road width of 23 m (76 ft)), and 6-lane (road width of 34 m (112 ft))

roadway embankment, respectively, and the three graphs correspond to the three embankment heights considered, i.e., 3.1 m (10 ft), 6.1 m (20 ft), and 12.2 m (40 ft), for various values of foundation soil s_u. As shown in Figure 5.34 as the foundation s_u increases, the overall embankment slope stability factor of safety increases. It can be seen that for a 23 m (76 ft) and 34 m (112 ft) wide embankment, as the geofoam thickness or height, T_{EPS}, increases for a given foundation s_u , the critical factor of safety decreases. The geofoam height corresponds to only the height of the geofoam and thus the total height of the embankment is T_{EPS} plus the thickness of the pavement system. However, for the narrower embankment of 11 m (36 ft), the geofoam height of 12.2 m (40 ft) yielded a larger factor of safety than the shorter embankments of 3.1 m (10 ft) and 6.1 m (20 ft). As discussed in the previous section, narrow and tall embankments yield larger factors of safety because the failure surface will extend further out from the toe of the embankment and, consequently, the heavier foundation soil below the toe of the embankment provides more resisting force to the failure surface. The failure surface extends further out because if the failure is assumed to be circular, the failure surface must extend further out for narrow and tall embankments to accommodate the circular failure surface.

Figure 5.34. Effect of embankment height on static external slope stability for vertical embankments and a road width of 11 m (36 ft), 23 m (76 ft), and 34 m (112 ft).

Figure 5.35 presents the static external slope stability results for the three embankment widths considered, i.e., a 2-lane (road width of 11 m (36 ft)), 4-lane (road width of 23 m (76 ft)), and 6-lane (road width of 34 m (112 ft)), and various values of foundation s_u, for a given embankment height. Figure 5.35 shows that roadway width has little influence on the critical factor of safety for short embankments, e.g., at a height of 3.1 m (10 ft), but the influence of embankment width increases with increasing embankment height. This conclusion is supported by the observation made previously on the behavior of the critical static failure surface that narrow and tall embankments with vertical walls will yield larger factors of safety because the failure surface will extend further out from the toe of the embankment and, consequently, the

heavier foundation soil below the toe of the embankment provides more of the resisting load to the failure surface.

Figure 5.35. Effect of embankment width on static external slope stability for vertical embankments at heights of 3.1 m (10 ft), 6.1 m (20 ft), and 12.2 m (40 ft).

The results of static external slope stability analyses performed for trapezoidal embankments, which are shown in Figures 5.14 through 5.16, show that as the slope inclination increases, the critical factor of safety decreases for each of the three embankment widths considered. A comparison between Figure 5.34 and Figures 5.14 through 5.16 also supports this observation because for a given embankment width, an embankment with vertical walls yields lower factors of safety values than an embankment with a 2H:1V side slope.

It can be seen from Figures 5.34 and 5.35 that the critical static factors of safety for an embankment with vertical walls and with a width of 11 m (36 ft), 23 m (76 ft), and 34 m (112 ft) all exceed a value of 1.5 for s_u greater than or equal to 12 kPa (250 lbs/ft²). These results indicate that external static slope stability will be satisfied, i.e., factor of safety greater than 1.5, if the foundation undrained shear strength exceeds 12 kPa (250 lbs/ft²). In summary, external slope stability does not appear to be the controlling external failure mechanism of geofoam embankments with vertical walls, instead it appears that settlement will be the controlling external failure mechanism. However, Figures 5.34 or 5.35 can be used to quickly estimate the critical static factor of safety to facilitate the design process.

Interpretation of External Slope Stability Design Charts

Comparison of the factors of safety in Figures 5.34 and 5.35 also reveals that the critical case for external slope stability for vertical embankments and with widths of 23 m (76 ft) and 34 m (112 ft) is an embankment with a height of 12.2 m (40 ft) over a foundation soil with an s_u of less than 12 kPa (250 lbs/ft²). This case may yield factors of safety that are less than 1.5. For a vertical embankment with a narrow width of 11m (36 ft), the critical case for external slope stability is an embankment height of 6.1 m (20 ft) and a foundation s_u of less than 12 kPa (250

lbs/ft²) because this case may yield factors of safety of less than 1.5. Knowledge of these critical cases is important because the static stability controls the seismic external stability. The greater the static external stability, the greater the seismic external stability. The results of the seismic stability analyses will be presented in the next section.

Figure 5.34 can be used for the design of a geofoam embankment by entering the appropriate graph with a value of s_u, e.g., 36 kPa (750 lbs/ft²), geofoam height of 6.1 m (20 ft), and obtaining a critical static factor of safety of approximately 2.7 for a roadway embankment width of 34 m (112 ft) (see Figure 5.34).

Remedial Procedures

As with trapezoidal embankments, the main remedy procedure that can be used to increase the factor of safety against external slope instability of embankments with vertical walls is to increase the undrained shear strength of the foundation soil by using a ground improvement method. A discussion on ground improvement is provided in Chapter 1. However, the external slope stability analyses indicate that settlement will control the design of a vertical geofoam embankment and not external slope stability, which is in agreement with the lack of field case histories involving external slope instability.

EXTERNAL SEISMIC STABILITY OF VERTICAL EMBANKMENTS

Introduction

This section focuses on the effect of seismic forces on the external slope stability of vertical EPS-block geofoam embankments. This analysis uses the same pseudo-static slope stability analysis used for external seismic stability of trapezoidal embankments and circular failure surfaces through the foundation soil. The pseudo-static stability analysis is used to simulate earthquake loads on slopes and involves modeling the earthquake shaking with a horizontal force that acts permanently, not temporarily, and in one direction on the slope. The pseudo-static horizontal force is applied to the slide mass that is delineated by the critical static failure surface.

The same steps outlined in this chapter in the sub-sections entitled "Introduction," "Seismic Shear Strength," and "Horizontal Seismic Coefficient" of the section entitled "External Seismic Stability of Trapezoidal Embankments" are used in an external pseudo-static stability analysis of EPS-block geofoam vertical embankments.

In seismic design of vertical embankments the following two analyses should be performed: 1) psuedo-static slope-stability analysis involving circular failure surfaces through the foundation soil, and 2) overturning of the entire embankment about one of the bottom corners of the embankment at the interface between the bottom of the assemblage of EPS blocks and the underlying foundation soil due to pseudo-static horizontal forces acting on the embankment especially for tall and narrow vertical embankments.

Seismic Stability Analysis Procedure

Pseudo-static slope stability analyses were conducted on the range of vertical embankment geometries used for the external static stability analyses to investigate the effect of various embankment heights (3.1 m (10 ft) to 12.2 m (40 ft)) and road widths of 11, 23, and 34 m (36, 76, and 112 ft) on external seismic slope stability. The results of these analyses were used to develop design charts to facilitate seismic design of vertical roadway embankments that utilize geofoam. The seismic analyses utilize the critical static failure surfaces identified for each geometry in the external static stability analyses. A pseudo-static analysis was conducted on only the critical failure surfaces that passed through the foundation soil because external stability is being evaluated.

The same typical cross-section through an EPS embankment used in the static slope stability analysis of embankments with vertical walls was also used for the pseudo-static stability analyses and is shown in Figure 5.30.

Figure 5.36 illustrates the location and magnitude of the pseudo-static forces used to represent earthquake loading for a particular value of horizontal seismic coefficient. The length of the horizontal arrows corresponds to the relative magnitude of the horizontal force for a given

horizontal seismic coefficient. It can be seen that the pavement and traffic surcharges yield the largest horizontal force because the weight of the soil layer used to model the surcharge results in the largest weight. The EPS exhibits a small weight and thus the horizontal seismic force is small for the EPS blocks. The foundation soil also contributes a significant horizontal seismic force because of the unit weight of the material.

Figure 5.36. Typical cross-section showing location and relative magnitude of pseudo-static forces used to represent an earthquake loading in a vertical embankment.

Design Charts

The results of the seismic stability analyses were used to develop the seismic external slope stability design charts for a 2-lane (road width of 11 m (36 ft)), 4-lane (road width of 23 m (76 ft)), and 6-lane (road width of 34 m (112 ft)) roadway embankment in Figures 5.37 to 5.39. Three seismic coefficients, low (0.05), medium (0.10), and high (0.20), were used for each roadway embankment. Values of seismic coefficient greater 0.20 indicate a severe seismic environment and a site-specific seismic analysis, including a site response analysis, should be conducted instead of using the enclosed simplified design charts.

The pseudo-static factor of safety for the critical static failure surfaces previously identified using the Simplified Janbu stability method was calculated for each geometry considered to develop the design charts. The factor of safety was calculated using Spencer's slope stability method (*34*) as coded in the microcomputer program XSTABL Version 5 (*32*) because it satisfies all conditions of equilibrium. However, for some of the narrow embankment widths with large heights such as at an embankment width of 11 m (36 ft) and height of 12.2 m (40 ft), Spencer's method yielded an unreasonable location of interslice forces. For these narrow embankments, the factor of safety value was calculated using Bishop's simplified method because for circular failure surfaces it provides similar factors of safety as Spencer's method (*35*). Additionally, at a seismic coefficient of 0.2, Spencer's (*34*) slope stability method did not

converge for the vertical wall embankment geometries investigated and Bishop's simplified method was also used for these cases.

The seismic analyses were conducted without reducing the shear strength of the foundation soil to account for strain incompatibility or seismic loading as discussed in this chapter in the sub-section entitled "Material Properties" of the section entitled "External Slope Stability of Trapezoidal Embankments" because the design charts present the pseudo-static factor of safety for the critical versus undrained shear strength (see Figure 5.37) and a design engineer can utilize these charts with an s_u value that reflects any strength loss that might occur during earthquake shaking.

Figures 5.37 through 5.39 present the seismic external stability results for an 11 m (36 ft), 23 m (76 ft), and 34 m (112 ft) geofoam roadway embankment with vertical walls, respectively. Each figure shows the critical factor of safety versus foundation s_u for the three values of horizontal seismic coefficient, i.e., 0.05, 0.10, and 0.20. Comparison of these figures results in the following conclusions:

(1) Seismic stability is not a concern for vertical embankments with the geometries considered and horizontal seismic coefficients of 0.05, 0.10, and 0.20 because all of the computed values of factor of safety exceed the required value of 1.2. The factor of safety values obtained for embankments with vertical walls is greater than the embankment with 2H:1V side slopes. This conclusion is in agreement with the conclusion made for trapezoidal embankments that flatter embankments are more critical than the 2H:1V embankment because the weight of the soil cover materials above the critical static failure surface increases as the side slope becomes flatter which results in a greater seismic force being applied in the 3H:1V and 4H:1V embankments versus the 2H:1V embankment. The flatter embankments are more critical and thus a higher foundation undrained shear strength will be

required to satisfy a factor of safety of 1.2 especially for the 4H:1V embankment.

(2) Unlike the observations made for trapezoidal embankments, a wider roadway does not necessarily result in a decrease in seismic stability. Based on the static external stability results shown in Figure 5.32, the factors of safety are similar and the failure surface originates near the toe of the embankment and terminates near the center of the embankment for embankment widths of 23 m (76 ft) and 34 m (112 ft). At the smaller embankment width of 11 m (36 ft), the failure surface extends further out from the toe of the embankment and terminates near the top outer edge of the embankment.

(3) The narrower embankment width of 11 m (36 ft) produces a higher factor of safety because the heavier foundation soil below the toe of the embankment provides more resisting force to the failure surface than the wider embankments for a given height. The failure surface extends further out because if the shape of the failure surface is assumed to be circular, the failure surface must extend further out for narrow and tall embankments to accommodate the circular failure surface. Additionally, a narrower embankment yields a smaller length of the failure surface that is subjected to the pavement and traffic driving stresses. This same behavior is exhibited in the external seismic stability analysis shown in Figures 5.37 through 5.39. At embankment widths of 23 m (76 ft) and 34 m (112 ft), the seismic factors of safety are similar. However, the narrower embankment with a width of 11 m (36 ft) yields a higher factor of safety.

Figure 5.37. Seismic external stability design chart for a 2-lane roadway vertical embankment and a total width of 11 m (36 ft).

Figure 5.38. Seismic external stability design chart for a 4-lane roadway vertical

embankment and a total width of 23 m (76 ft).

Figure 5.39. Seismic external stability design chart for a 6-lane roadway vertical embankment and a total width of 34 m (112 ft).

Remedial Procedures

As with trapezoidal embankments, the main remedy to increase the external seismic factor of safety for vertical embankments is to increase the undrained shear strength of the foundation soil by using a ground improvement method. A discussion on ground improvement is provided in Chapter 1.

Overturning

For tall and narrow vertical embankments the overturning of the entire embankment at the interface between the bottom of the assemblage of EPS blocks and the underlying foundation soil as a result of pseudo-static horizontal forces should be considered. These horizontal forces create an overturning moment about the toe at point O as shown in Figure 5.40.

Figure 5.40. Variables for determining the factor of safety against overturning of a vertical embankment due to pseudo-static horizontal forces used to represent an earthquake loading.

Vertical loads such as the weight of the EPS blocks and the pavement system and traffic surcharges will provide a stabilizing moment. A factor of safety against overturning of 1.2 is recommended for design purposes because overturning due to earthquake loading is a temporary loading condition. The factor of safety against overturning is expressed as follows:

$$FS = \frac{\sum \text{stabilizing moments}}{\sum \text{overturning moments}} = \frac{\left(\frac{1}{2} * T_W\right) * \left(W_{EPS} + W_{\text{pavement \& traffic surcharges}}\right)}{\left[\left(\frac{1}{2} * H\right) * \left(k_h * W_{EPS}\right)\right] + \left[\left(T_{EPS} + \left(\frac{1}{2} * T_{\text{pavement}}\right)\right) * \left(k_h * W_{\text{pavement \& traffic surcharges}}\right)\right]} \quad \textbf{(5.54)}$$

The soil pressure under a vertical embankment is a function of the location of the vertical and horizontal forces. It is generally desirable that the resultant of the vertical and horizontal forces be located within the middle third of the base of the embankment, i.e., eccentricity, $e \leq (T_W/6)$, to minimize the potential for overturning. If $e = 0$, the pressure distribution is rectangular. If $e < (T_W/6)$, the pressure distribution is trapezoidal, and if $e = (T_W/6)$, the pressure distribution is triangular. Therefore, as e increases, the potential for overturning of the embankment increases. Note that if $e > (T_W/6)$, the minimum soil pressure will be negative, i.e., the foundation soil will be in tension. Therefore, separation between the vertical embankment and foundation soil may occur, which may result in overturning of the embankment, because soil cannot resist tension. This is the primary reason for ensuring that $e \leq (T_W/6)$. Equation (5.55) can be used to determine the location of the resultant a distance x from the toe of the embankment and Equation (5.56) can be used to determine e. Equation (5.57) can be used to estimate the maximum and minimum pressures under the embankment.

$$x = \frac{\sum \text{stabilizing moments} - \sum \text{overturning moments}}{\sum N} \quad \textbf{(5.55)}$$

where x = location of the resultant of the forces from the toe of the embankment

ΣN = summation of normal stresses

$$e = \frac{T_W}{2} - x \quad \textbf{(5.56)}$$

where e = eccentricity of the resultant of the forces with respect to the centerline of the embankment

T_W = top width of the embankment

$$q = \frac{\sum N}{T_w}\left(1 \pm \frac{6e}{T_w}\right) \leq q_a \quad \textbf{(5.57)}$$

where q = soil pressure under the embankment

q_a = allowable soil pressure

The soil pressures should not exceed the allowable soil pressure, q_a, which is given by Equation (5.39).

HYDROSTATIC UPLIFT (FLOTATION)

Introduction

EPS-block geofoam used as lightweight fill usually has a density that is approximately 1 percent of the density of earth materials. Because of this extraordinarily low density, the potential for hydrostatic uplift (flotation) of the entire embankment at the interface between the bottom of the assemblage of EPS blocks and the foundation soil must be considered in external stability evaluations.

The factor of safety against upward vertical movement of the entire embankment due to a rise in the ground water table is the ratio of the total vertical stress from the embankment applied to the foundation soil (the unit weight of EPS is conservatively taken as the dry value, i.e., 0.2 kN/m³ (1.25 lbs/ft³)) divided by the uplift water pressure under some extreme event as shown in Equation (5.58). Figures 5.41 and 5.47 show the two cases of uplift of the embankment, equal water and non-equal water on both sides of the embankment, respectively, that were analyzed herein. In both cases, it is assumed that the EPS blocks extend down to the foundation soil and uplift will occur at the EPS block/foundation soil interface.

$$FS = \frac{\sum N}{\sum U} \qquad \textbf{(5.58)}$$

where $\sum N$ = summation of normal forces = $W_{EPS} + W_W + W'_W$

$\sum U$ = summation of uplift forces, U, at base of embankment

W_{EPS} = weight of EPS-block geofoam embankment

W_W = vertical component of weight of water on the embankment face above the base of the embankment on the accumulated water side.

W'_W = vertical component of weight of water on the face of the embankment on

the tailwater side.

With postconstruction settlements of 0.3 to 0.6 m (1 to 2 ft) generally considered tolerable for highway embankments during the economic life of a roadway as discussed in "Settlement of Embankments" in this chapter, the long-term total settlement might have a significant effect on the factor of safety against flotation. Therefore, the estimated total settlement as defined by Equation (5.1) should be included in the calculation of uplift force, U. The height of the embankment will remain the same after settlement occurs. However, the total depth of the design water level will increase. Thus, U should be based on the vertical height of accumulated water or tailwater, h or h', respectively, to the bottom of the embankment at the start of construction, plus the estimated total settlement, S_{total}, as indicated by Equations (5.59) and (5.60). The water pressures, P and P', are derived from the vertical height of accumulated water at the start of construction plus the estimated total settlement, $h+S_{total}$, and the vertical height of tailwater at the start of construction plus the estimated total settlement, $h'+S_{total}$, and result in triangular pressure distributions acting on the sides of the embankment with a magnitude of $\gamma_W * (h+S_{total})$ or $\gamma_W * (h'+S_{total})$.

For the case of the vertical height of accumulated water to the bottom of the embankment at the start of construction, h, equal to the vertical height of tailwater to the bottom of the embankment at the start of construction, h', (see Figure 5.41), Equation (5.58) becomes:

$$FS = \frac{W_{EPS} + W_W + W'_W + O_{REQ}}{\gamma_W * (h + S_{total}) * B_W} \qquad \textbf{(5.59)}$$

where γ_W = unit weight of water,

S_{total} = total settlement as defined by Equation (5.1),

B_W = bottom embankment width, and

O_{REQ} = additional overburden force required above the EPS blocks to obtain the desired factor of safety.

Figure 5.41. Variables for determining hydrostatic uplift for the case of water equal on both sides of the embankment.

Figure 5.41 defines the forces and pressures acting on a generic trapezoidal embankment with a side-slope inclination of θ, height of H, and top-width of T_W. It can be seen that the water is at the same level on each side of the embankment, which represents the worst case scenario because the water on each side of the embankment creates a uniform uplift pressure at the base of the embankment. These water pressures create an uplift force, U, on the bottom of the embankment that equals:

$$U = \gamma_W * B_W * (h+S_{total}) = \gamma_W * B_W * (h'+S_{total}) \quad \textbf{(5.60)}$$

The water pressures represent static water level pressures. Seepage pressures are not considered herein.

The value of O_{REQ} is the additional overburden force required above the EPS blocks to obtain the desired factor of safety in Equation (5.59). The components usually contributing to O_{REQ} are the weight of the pavement system and the cover soil on the embankment side slopes. The weight of pavement system can be taken to be equal to the pavement surcharge of 21.5 kPa (450 lbs/ft²) used previously for external bearing capacity and slope stability or it can be calculated by multiplying the unit weight of the pavement system, $\gamma_{pavement}$, by the pavement thickness, $T_{pavement}$, and width, T_W. The traffic surcharge of 11.5 kN/m^2 (240 lbs/ft²) used previously is not included in O_{REQ} because it is a live or transient load and may not be present at the time of the design hydrostatic uplift condition. The weight of the cover soil imposes overburden weight on the EPS blocks on both side slopes of the embankment and can be calculated using the variables in Figure 5.42 and the following expressions:

$$W_{cover} = 2 * \left(\gamma_{cover} * L_{cover} * H_{cover}\right) \quad \textbf{(5.61)}$$

where $L_{cover} = \dfrac{T_{EPS}}{\sin\theta}$ and **(5.62)**

$$H_{cover} = \frac{T_{cover}}{\cos\theta}. \quad \textbf{(5.63)}$$

Substituting Equations (5.62) and (5.63), Equation (5.61) becomes

$$W_{cover} = \gamma_{cover}\ 2 * \left(\frac{T_{EPS}}{\sin\theta} * \frac{T_{cover}}{\cos\theta} \right) \quad \textbf{(5.64)}$$

Equation (5.64) utilizes the slope length of the cover soil, $T_{EPS}/\sin\theta$, times the vertical thickness of the cover soil, $T_{cover}/\cos\theta$, and the unit weight of the cover soil to estimate the weight of the cover soil per length of the geofoam embankment. Therefore, to ensure the desired factor of safety used in Equation (5.59) is satisfied for hydrostatic uplift, the calculated value of O_{REQ} should be less than the sum of the pavement and cover soil weights as shown below:

$$O_{REQ} < (\gamma_{pavement} * T_{pavement} * T_W) + W_{cover} \quad \textbf{(5.65)}$$

Note that the pavement weight is $\gamma_{pavement} * T_{pavement} * T_W$. If other weights, W_{other}, are applied to the embankment besides the pavement system and the soil cover, these weights can be included in Equation (5.65) and used to increase the applied vertical stress to meet the required value of O_{REQ} as shown below:

$$O_{REQ} < (\gamma_{pavement} * T_{pavement} * T_W) + W_{cover} + W_{other} \quad \textbf{(5.66)}$$

The design charts, which will be presented subsequently, are based on the assumption that the EPS blocks extend for the full height of the embankment, i.e., $H = T_{EPS}$. Therefore, the weight of the EPS equivalent to the height of the pavement system times the unit weight of the EPS must be subtracted in the result of O_{REQ} in Equation (5.65) as shown below:

$$O_{REQ} < \left(\gamma_{pavement} * T_{pavement} * T_W\right) - \left(\gamma_{EPS} * T_{pavement} * T_W\right) + W_{cover} \quad \textbf{(5.67)}$$

Figure 5.42. Variables for the weight induced by the soil cover.

If other weights, W_{other}, are applied to the embankment besides the pavement system and soil cover, Equation (5.67) becomes

$$O_{REQ} < \left(\gamma_{pavement} * T_{pavement} * T_W\right) - \left(\gamma_{EPS} * T_{pavement} * T_W\right) + W_{cover} + W_{other} \quad \textbf{(5.68)}$$

Equation (5.59) also can be rearranged and used to obtain the value of O_{REQ} required to obtain the desired factor of safety of 1.2. A factor of safety against hydrostatic uplift of 1.2 is recommended for design purposes because hydrostatic uplift is a temporary loading condition and a factor of safety of 1.2 is being used for other temporary loading conditions in the design procedure, such as seismic loading. Therefore, the value of O_{REQ} corresponding to a factor of safety of 1.2 and the various embankment geometries considered during this study was calculated to develop design charts for hydrostatic uplift. This rearrangement results in the following expression:

$$O_{REQ} = \left[1.2 * (\gamma_W * (h + S_{total}) * B_W)\right] - \left[(W_{EPS} + W_W + W'_W)\right] \quad \textbf{(5.69)}$$

Design charts were prepared for each embankment geometry because calculation of W_{EPS}, W_W, and W'_W is cumbersome. The design charts simplify the process because a design engineer can enter a design chart and obtain the value of O_{REQ} corresponding to a factor of safety of 1.2. The values of O_{REQ} provided by the design charts are based on the assumption that the EPS blocks extend for the full height of the embankment and that the accumulated water level is the sum of the vertical accumulated water level to the bottom of the embankment at the start of construction and the estimated total settlement, $h+S_{total}$. The design engineer then compares this value of O_{REQ} with the weight of the pavement system and cover soil as shown in Equation (5.67). For example, Figure 5.43 presents the hydrostatic uplift design charts for a 4H:1V (14 degrees) embankment and the tailwater level equal to the upstream water level. If the proposed geofoam embankment has a 4-lane roadway (middle chart), a height of 12 m (40 feet), and a ratio of accumulated water level to embankment height of 0.2, which means the total water depth to include the estimated total settlement is 20 percent of the embankment height, the required value of O_{REQ} is approximately 936 kN/m (64,150 lbs/ft) length of embankment. If the typical pavement system with a $T_{pavement}$ of 1,000 mm (39 in.) used in previous external stability calculations is used the pavement weight, $W_{pavement}$, equals the surcharge times the pavement width:

$$W_{pavement} = 21.5 \text{ kN/m}^2 * 23.2 \text{ m} = 498.8 \text{ kN/m of roadway} \quad \textbf{(5.70)}$$

Note that $W_{pavement}$ is the initial part of Equation (5.67), i.e., $\gamma_{pavement} * T_{pavement.} * T_W$. If the typical cover soil thickness of 0.46 m (1.5 feet) and moist unit weight of 18.9 kN/m^3 (120 lbf/ft^3) (see Table 5.2) used in previous external stability calculations is used, the cover soil weight equals:

$$W_{cover} = 2 * \left(\gamma_{cover} * \frac{T_{EPS}}{\sin\theta} * \frac{T_{cover}}{\cos\theta} \right) = 2 * \left(18.9 \text{ kN/m}^3 * \frac{12 \text{ m}}{\sin 14^\circ} * \frac{0.46 \text{ m}}{\cos 14^\circ} \right) = 889 \text{ kN/m} \quad \textbf{(5.71)}$$

From Equation (5.67) and assuming an *EPS40*,

$$936 \text{ kN/m} = O_{REQ} = < 498.8 \text{ kN/m} - (0.16 \text{ kN/m}^3 * 1 \text{ m} * 23 \text{ m}) + 889 \text{ kN/m} \quad \textbf{(5.72)}$$

$$936 \text{ kN/m} = O_{REQ} < 1{,}384.1 \text{ kN/m of roadway}$$

Thus, the pavement and cover soil will provide sufficient overburden for a factor of safety of 1.2.

Equal water level on both sides of the embankment is the worst-case scenario and construction measures should be taken to try avoid the situation of equal water level being created on both sides of the embankment. It will be shown in the following paragraphs that limiting the accumulation of water to one side of the embankment greatly reduces the value of O_{REQ} for a factor of safety of 1.2. Figures 5.43 through 5.46 present the design charts for all of the embankment geometries considered during this study for equal upstream and tailwater levels and uplift at the EPS block/foundation soil interface. The values of O_{REQ} shown in Figures 5.43 through 5.46 is the required weight of material over the EPS blocks in kN per linear meter of embankment length. Embankment top widths of 11m (36 ft), 23 m (76 ft), and 34 m (112 ft), side slope inclinations of 0H:1V, 2H:1V, 3H:1V, 4H:1V, and six heights between 1.5 m (4.92 ft) and 16 m (52.49 ft) were used in developing the charts. The accumulated water level is the total water depth to include the estimated total settlement, i.e., $h+S_{total}$. The design charts only extend to a maximum ratio of accumulated water level to embankment height of 0.5, which means the total water depths to include the estimated total settlement is limited to 50 percent of the embankment height, because an embankment with a high accumulated water level is essentially a

dam structure that may require unreasonable overburden forces on top of the EPS blocks to obtain the desired factor of safety.

The design charts were only created for *EPS40* and not *EPS50*, *70*, or *100* because the results of a sensitivity analysis revealed that the value of O_{REQ} required on top of an EPS-block geofoam embankment for a factor of safety of 1.2 is not sensitive to the density of the EPS geofoam. Therefore, the lighter *EPS40* (density = 16 kg/m³ (1 lbf/ft³)) was used in determining the values of O_{REQ} for the design charts. Because some embankments may utilize various types of EPS-blocks, the use of *EPS40* for design against hydrostatic uplift will yield a worst-case scenario, which is desirable for ULS calculations. Even if a higher density is used, the value of O_{REQ} did not change significantly because the density does not change significantly. For example, the density for *EPS50* is 20 kg/m³ (1.25 lbf/ft³) versus 16 kg/m³ (1 lbf/ft³) for *EPS40*.

Figure 5.43. Hydrostatic uplift (flotation) design for a factor of safety of 1.2 with tailwater level equal to upstream water level, 4H:1V embankment slope, and three road widths.

Figure 5.44. Hydrostatic uplift (flotation) design for a factor of safety of 1.2 with tailwater level equal to upstream water level, 3H:1V embankment slope, and three road widths.

Figure 5.45. Hydrostatic uplift (flotation) design for a factor of safety of 1.2 with tailwater level equal to upstream water level, 2H:1V embankment slope, and three road widths.

Figure 5.46. Hydrostatic uplift (flotation) design for a factor of safety of 1.2 with tailwater level equal to upstream water level, vertical embankment (0H:1V), and three road widths.

Figure 5.47. Variable for determining hydrostatic uplift analysis for the case of water on one side of the embankment only.

For the case of the total vertical height of tailwater, h'+S_{total}, equals zero (see Figure 5.47), Equation (5.59) becomes:

$$FS = \frac{W_{EPS} + W_W + O_{REQ}}{\frac{1}{2} * \gamma_W * (h + S_{total}) * B_W} \quad \textbf{(5.73)}$$

It can be seen that the weight of the tailwater is removed from the numerator and the uplift force corresponds to the resultant force of the water pressure diagram on the upstream side of the embankment. Equation (5.73) also can be rearranged and used to obtain the value of O_{REQ} required to obtain the desired factor of safety of 1.2 against hydrostatic uplift. Therefore, the value of O_{REQ} corresponding to a factor of safety of 1.2 and the various embankment geometries considered during this study was calculated to develop design charts for hydrostatic uplift with zero tailwater as shown below:

$$O_{REQ} = \left[1.2 * (\frac{1}{2} * \gamma_W * (h + S_{total}) * B_W) \right] - \left[(W_{EPS} + W_W) \right] \quad \textbf{(5.74)}$$

Figures 5.48 through 5.51 present the design charts for all of the embankment geometries considered during this study for a total tailwater depth of zero. These charts can be used to estimate the value of O_{REQ} required to obtain the desired factor of safety of 1.2 against hydrostatic uplift at the EPS block/foundation soil interface. The same conditions used to generate the design charts for the equal upstream and tailwater levels were used to develop the design charts for zero tailwater

Figure 5.48. Hydrostatic uplift (flotation) design for a factor of safety of 1.2 with no tailwater, 4H:1V embankment slope, and three road widths.

Figure 5.49. Hydrostatic uplift (flotation) design for a factor of safety of 1.2 with no tailwater, 3H:1V embankment slope, and three road widths.

Figure 5.50. Hydrostatic uplift (flotation) design for a factor of safety of 1.2 with no tailwater, 2H:1V embankment slope, and three road widths.

Figure 5.51. Hydrostatic uplift (flotation) design for a factor of safety of 1.2 with no tailwater, vertical embankment (0H:1V), and three road widths.

The design charts, i.e., Figures 5.43-5.46 and 5.48-5.51, are based on a factor of safety against hydrostatic uplift of 1.2. The Japanese design manual also recommends a minimum factor of safety of 1.2 (*22*) but the Norwegian design manual (*4*) recommends a minimum factor of safety of 1.3 for estimating the values of O_{REQ}. The values of O_{REQ} can be adjusted to other values of factor of safety by multiplying O_{REQ} by the ratio of the factors of safety. For example, if the desired of factor of safety is 1.3, the value of O_{REQ} obtained from one of the design charts should be multiplied by 1.3/1.2 or 1.08. However, a better estimate of O_{REQ} can be obtained by using Equations (5.59) and (5.73). Because the design guidelines developed herein utilize a factor of safety of 1.2 for temporary loading conditions, the design charts utilize a safety factor of 1.2.

As reported in (*55*) and (*56*), in 1987 the first EPS embankment built in Norway in 1972 failed due to hydrostatic uplift (flotation). Although the embankment was designed against the potential for uplift, the design water level used was 0.85 m (2.8 ft) lower than the flood level that occurred in 1987. Thus, the largest uncertainty in design against hydrostatic uplift is the selection of an appropriate flood elevation to utilize in the calculation and the water level on each side of the embankment. In addition to designing the completed embankment against uplift, it is important that proper temporary dewatering be maintained during construction to prevent hydrostatic uplift due to groundwater rise or surface water intrusion that may collect along the embankment during a heavy rainfall. A project in Orland Park, Illinois partially failed during construction due to hydrostatic uplift during a heavy rainfall (*57*).

Remedial Procedures

Remedial procedures that can be considered to increase the factor of safety against hydrostatic uplift of the entire embankment include:

- If conventional soil fill is being proposed between the EPS blocks and the natural subgrade, a portion of this proposed soil fill can be removed and substituted with

pavement system materials on top of the EPS thereby increasing the overburden over the EPS blocks.

- A drainage system can be incorporated to minimize the potential for water to accumulate along the embankment.
- An anchoring system that anchors the EPS blocks to the underlying foundation soil can be utilized. Details of a typical anchoring system that has used to resist hydrostatic uplift of an EPS-block geofoam embankment is included in Chapter 10.

TRANSLATION AND OVERTURNING DUE TO WATER (HYDROSTATIC SLIDING AND OVERTURNING)

Introduction

Because of the extraordinarily low density of EPS-block geofoam, the potential for translation (horizontal sliding) of the entire embankment at the interface between the bottom of the assemblage of EPS blocks and the underlying foundation soil due to an unbalanced water pressure must be considered. This scenario is similar to the hydrostatic uplift case with zero tailwater but the failure mode is sliding and not uplift. Additionally, for vertical geofoam embankments, the potential for overturning of the entire embankment about one of the bottom corners of the embankment at the interface between the bottom of the assemblage of EPS blocks and the underlying foundation soil due to an unbalanced water pressure must be considered.

Translation

The short-term tendency of the entire embankment, such as during construction or immediately after construction, to slide under an unbalanced water pressure is resisted primarily by the undrained shear strength, s_u, of the foundation soil if it is a soft clay. However, the long-term tendency of the entire embankment to slide under an unbalanced water pressure is resisted primarily by EPS/foundation soil interface friction. Although the friction angle, δ, for this interface is relatively high (it approaches the Mohr-Coulomb angle of internal friction, ϕ, of the

foundation soil), the resisting force (which equals the dead weight times the tangent of δ) is small because the dead weight of the overall embankment is small. Consequently, the potential for the entire embankment to slide under an unbalanced water pressure loading is a possible failure mechanism and the potential for translation (horizontal sliding) of the entire embankment in a direction perpendicular to the proposed road alignment should be considered.

The factor of safety against horizontal sliding of the entire embankment is the ratio of shearing resistance along the EPS/foundation soil interface to the total horizontal driving force as shown in Equation (5.75). The total horizontal driving force is the net unbalanced water pressure, shown in Figure 5.47, which equals the resultant force of the triangular water pressure diagram or $\frac{1}{2}(\gamma_W)h^2$ where h equals the vertical height of accumulated water to bottom of embankment.

$$FS=\frac{\sum \text{horizontal resisting forces}}{\sum \text{horizontal driving forces}} = \frac{c*A+\left(\sum N-\sum U\right)\tan\delta}{\sum HF} \qquad \textbf{(5.75)}$$

where c = interface cohesion along the horizontal sliding surface

A = area of the horizontal sliding surface being considered

ΣN = summation of normal forces = $W_{EPS} + W_W + O_{REQ}$

ΣU = summation of uplift forces = $\frac{1}{2} * (\gamma_W * h + S_{total}) * (B_W)$

δ = interface friction angle along the sliding surface

ΣHF = summation of horizontal forces

R_p=horizontal component of accumulated water on side slope above base of embankment on accumulated water side. The horizontal force, $R_p=\frac{1}{2}*(\gamma_W * h^2)$, is located ⅓ * h above the base of the embankment

γ_W = unit weight of water

h = vertical height of accumulated water to bottom of embankment at the start of construction

S_{total}=total settlement as defined by Equation (5.1)

B_W = bottom of embankment width

As described for the analysis of hydrostatic uplift, O_{REQ} is the additional overburden force required above the EPS blocks to obtain the desired factor of safety. In this case the desired factor of safety pertains to horizontal sliding because the resistance to horizontal sliding is controlled by the vertical normal force acting on the sliding interface just as uplift is controlled by the vertical normal force acting on the base of the embankment.

For the case of no interface cohesion along the sliding surface, which is typical for geosynthetic interfaces (see Chapter 2), the expression for factor of safety against hydrostatic sliding simplifies to the following:

$$FS=\frac{\left[\left(W_{EPS}+W_W+O_{REQ}\right)-\left(\frac{1}{2}\left(\left(h+S_{total}\right)*\gamma_W\right)*\left(B_W\right)\right)\right]*\tan\delta}{\frac{1}{2}\left(\gamma_W*\left(h+S_{total}\right)^2\right)} \quad \textbf{(5.76)}$$

A factor of safety against hydrostatic sliding of 1.2 is recommended for design purposes because hydrostatic sliding is also a temporary loading condition and a factor of safety of 1.2 is being used for other temporary loading conditions in the design guidelines, such as seismic loading and hydrostatic uplift. For a factor of safety of 1.2 and solving for O_{REQ}, Equation (5.76) becomes:

$$O_{REQ}=\frac{1.2(\frac{1}{2})\left(\gamma_W*\left(h+S_{total}\right)^2\right)}{\tan\delta}+\left(\frac{1}{2}\left(\left(h+S_{total}\right)*\gamma_W\right)*\left(B_W\right)\right)-W_{EPS}-W_W \quad \textbf{(5.77)}$$

Equation (5.77) can be used to obtain the required value of O_{REQ} for a factor of safety of 1.2 against hydrostatic sliding. Figures 5.53 through 5.56 present the design charts for all of the embankment geometries considered during this study for horizontal sliding caused by accumulation of water on one-side of the embankment. These charts can be used to estimate the value of O_{REQ} per linear meter of embankment length required to obtain the desired factor of

safety of 1.2 against hydrostatic sliding at the EPS block/foundation soil interface as was demonstrated for the hydrostatic uplift design charts. Embankment top widths of 11m (36 ft), 23 m (76 ft), and 34 m (112 ft), side slope inclinations of 0H:1V, 2H:1V, 3H:1V, 4H:1V, and six heights between 1.5 m (4.9 ft) and 16 m (52.5 ft) were used in developing the charts. For example, the design charts in each figure signify a different slope inclination where Figures 5.53 through 5.56 correspond to slope inclinations of 4H:1V, 3H:1V, 2H:1V, and 0H:1V, respectively.

As described in the section on hydrostatic uplift, the value of O_{REQ} is the additional overburden force required above the EPS blocks to obtain the desired factor of safety of 1.2. The components usually contributing to O_{REQ} are the weight of the pavement system and the cover soil on the embankment side slopes. Therefore, to ensure the desired factor of safety, the calculated value of O_{REQ} should be less than the sum of the pavement and cover soil weight as shown in Equation (5.65). If other weights, W_{other}, are applied to the embankment besides the pavement system and the soil cover, Equation (5.66) can be used to ensure that the desired factor of safety is obtained. The design charts, which will be presented subsequently, are based on the assumption that the EPS blocks extend for the full height of the embankment. Therefore, Equations (5.67) or (5.68) should be used to estimate the weight provided by the pavement system and soil cover.

The design charts were only created for *EPS40* and not *EPS50*, *70*, or *100* because the results of a sensitivity analysis revealed that the value of O_{REQ} required on top of an EPS-block geofoam embankment for a factor of safety of 1.2 is not sensitive to the density of the EPS geofoam. Therefore, the lighter *EPS40* (density = 16 kg/m³ (1 lbf/ft³)) was used in determining the values of O_{REQ} for the design charts. Because some embankments may utilize various types of EPS-blocks, the use of *EPS40* for design against hydrostatic uplift will yield a worst-case scenario. However, even if a higher density is used, the value of O_{REQ} did not change significantly because the density does not change significantly. The accumulated water level used in the design charts is the sum of the vertical accumulated water level to the bottom of the embankment at the

start of construction and the estimated total settlement, i.e., $h+S_{total}$. The design charts only extend to a maximum ratio of accumulated water level to embankment height of 0.5, which means the total water depth plus the estimated total settlement is limited to 50 percent of the embankment height. The maximum ratio is limited to 50 percent of the embankment height because a greater percentage may require an unreasonable overburden force on top of the EPS blocks to obtain the desired factor of safety.

A factor of safety against hydrostatic sliding of 1.2 is recommended for design purposes because hydrostatic sliding is a temporary loading condition. However, other values of minimum factor of safety have been used for horizontal sliding such as 1.5 for mechanically stabilized earth (MSE) walls for design against sliding (*58*). A minimum factor of safety of 1.5 is also recommended for retaining walls for design against sliding in (*7,59*). However, since the potential for translation due to an unbalanced water head is an extreme event, a temporary loading condition, and the value of O_{REQ} is sensitive to the design factor of safety, it was decided to use a minimum factor of safety of 1.2 for design of geofoam embankments against hydrostatic sliding. However, the values of O_{REQ} can be adjusted to other values of factor of safety by multiplying O_{REQ} by the ratio of the factors of safety. For example, if the desired of factor of safety is 1.3, the value of O_{REQ} obtained from one of the design charts should be multiplied by 1.3/1.2 or 1.08. However, a better estimate of O_{REQ} can be obtained by using Equation (5.76).

Various sliding interfaces may need to be evaluated during design depending on the types of materials that are placed, if any, between the EPS blocks and the foundation soil. Chapter 2 discussed interface friction values between EPS and dissimilar materials as well as between EPS and EPS. A representative value of interface friction angle should be measured using laboratory direct shear testing, e.g., ASTM D 5321, and used in Figures 5.53 through 5.56 to obtain the required value of O_{REQ} to resist horizontal sliding. The design charts are based on an EPS/other material interface friction angle between 20 degrees and 40 degrees, which covers the typical range of interface friction angle for geofoam embankments.

Overturning

For vertical embankments, the tendency of the entire embankment to overturn at the interface between the bottom of the assemblage of EPS blocks and the underlying foundation soil is a result of an unbalanced water pressure acting on the embankment. Overturning may be critical for tall and narrow vertical embankments. These horizontal forces create an overturning moment about the toe at point O as shown in Figure 5.52. The worst case scenario is for water accumulating on only one side of the embankment as shown in Figure 5.52. Vertical loads, such as the weight of the EPS blocks, the pavement system, and traffic surcharges, will provide a stabilizing moment. As described for the analysis of hydrostatic uplift, O_{REQ} is the additional overburden force required above the EPS blocks to obtain the desired factor of safety.

Figure 5.52. Variables for determining the factor of safety against overturning due to hydrostatic horizontal forces for the case of water on one side of the embankment.

The factor of safety against overturning due to horizontal hydrostatic forces is expressed as

$$FS = \frac{\sum \text{stabilizing moments}}{\sum \text{overturning moments}} = \frac{(\frac{1}{2} * T_W) * (W_{EPS}+O_{REQ})}{\frac{1}{3}(h+S_{total}) * R_p} \quad \textbf{(5.78)}$$

A factor of safety against hydrostatic overturning of 1.2 is recommended for design purposes because hydrostatic overturning is a temporary loading condition and a factor of safety of 1.2 is being used for other temporary loading conditions, such as hydrostatic uplift and sliding and seismic loading. For a factor of safety of 1.2 and solving for O_{REQ}, Equation (5.78) becomes

$$O_{REQ} = \frac{1.2 * \left(\frac{1}{3}\right) * (h+S_{total}) * (R_p)}{\left(\frac{1}{2} * T_W\right)} - W_{EPS} \quad \textbf{(5.79)}$$

Equation (5.79) can be used to obtain the required value of O_{REQ} for a factor of safety of 1.2 to resist hydrostatic overturning.

The resultant of the vertical and horizontal forces should be checked to verify that the resultant is located within the middle third of the base, i.e., eccentricity, $e \leq (B_w/6)$, to minimize the potential for the wall to overturn. Equations (5.55) and (5.56) can be used to determine e. Additionally, the maximum and minimum soil pressures under the embankment should not exceed the allowable soil pressure, q_a, which is given by Equation (5.39). Equation (5.57) can be used to determine the maximum and minimum pressures under the embankment.

Remedial Procedures

Remedial procedures that can be considered to increase the factor of safety against hydrostatic sliding and overturning include:

- Removing any separation material that is being proposed between the EPS blocks and the foundation soil and replacing with an alternative separation material that will provide a larger interface friction angle. This remedial procedure will reduce the potential for sliding.
- If conventional soil fill is being proposed between the EPS blocks and the foundation soil, a portion of this proposed soil fill can be removed and substituted with heavier pavement system materials on top of the EPS thereby increasing the overburden over the EPS blocks. This remedial procedure will reduce the potential for both horizontal sliding and overturning.
- A drainage system can be incorporated to minimize the potential for water to accumulate along a side of the embankment. This will reduce the potential for horizontal sliding and overturning, as well as hydrostatic uplift.
- If an anchoring system is used to resist hydrostatic uplift, this system will also provide resistance against horizontal sliding and overturning.

Figure 5.53. Hydrostatic sliding (translation due to water) design for a factor of safety of 1.2 with no tailwater, 4H:1V embankment slope, and three road widths for various interface friction angles.

Figure 5.54. Hydrostatic sliding (translation due to water) design for a factor of safety of 1.2 with no tailwater, 3H:1V embankment slope, and three road widths for various interface friction angles.

Figure 5.55. Hydrostatic sliding (translation due to water) design for a factor of safety of 1.2 with no tailwater, 2H:1V embankment slope, and three road widths for various interface friction angles.

Figure 5.56. Hydrostatic sliding (translation due to water) design for a factor of safety of 1.2 with no tailwater, vertical embankment (0H:1V), and three road widths for various interface friction angles.

TRANSLATION AND OVERTURNING DUE TO WIND

Introduction

As discussed in Chapter 3, translation due to wind is an external stability ULS failure mechanism that is unique to embankments containing EPS-block geofoam because of the extremely low density of EPS blocks compared to other types of lightweight fill. Additionally, for vertical geofoam embankments, the potential for overturning of the entire embankment about one of the bottom corners of the embankment at the interface between the bottom of the assemblage of EPS blocks and the underlying foundation soil due to horizontal wind forces must be considered.

Translation

The factor of safety against translation of the entire embankment due to wind is the ratio of the shearing resistance along the EPS/foundation soil interface to the total horizontal driving force as shown in Equation (5.75). Equation (5.75) was presented in the previous section of this chapter during the discussion of "Translation Due to Water." Equation (5.75) is restated below

with the variable definitions re-defined for calculating wind forces instead of hydrostatic forces. Figure 5.57 defines the forces and pressures acting on a generic trapezoidal embankment with a side-slope inclination of θ, height of H, and top-width of T_W.

$$FS=\frac{\sum \text{horizontal resisting forces}}{\sum \text{horizontal driving forces}} = \frac{c*A+\left(\sum N-\sum U\right)\tan\delta}{\sum HF} \quad \textbf{(5.75)}$$

where c = interface cohesion along the horizontal sliding surface

A = area of the horizontal sliding surface being considered

ΣN = summation of normal stresses = $W_{EPS} + O_{REQ}$

ΣU = summation of uplift forces

δ = interface friction angle along the sliding surface

ΣHF = summation of horizontal forces = $R_U + R_D$

R_U = upwind force = $p_U * H$

R_D = downwind force = $p_D * H$

H = height of embankment = $T_{EPS} + T_{Pavement}$

Figure 5.57. Variables for determining wind analysis.

It can be seen that the wind is acting on the left side of the embankment tending to push the embankment to the right and the horizontal resisting force acting along the base of the embankment is acting in the opposite direction and counteracting the wind. The worst-case scenario involves the wind acting on only one-side of the embankment as shown in Figure 5.57 and is considered herein. The resultant wind forces, R_U and R_D, are obtained from wind pressure diagrams. It can be seen from Figure 5.57 that the wind is modeled with a uniform pressure distribution with a magnitude of p_U or p_D. The expressions used to calculate p_U or p_D were obtained from the French national design guide (*60*) for EPS-block geofoam road embankments, are discussed in Chapter 3, and are re-stated below:

$$p_U = 0.75V^2 \sin\theta_U \quad \textbf{(3.4)}$$

$$p_D = 0.75V^2 \sin\theta_D \quad \textbf{(3.5)}$$

with V = the wind speed in meters per second, p_U and p_D have units of kilopascals and the other variables are defined in Figure 5.57. Both of these equations treat a side-sloped embankment as a vertical wall. Therefore, the wind pressures are conservative in that the wind pressures are assumed to be horizontal instead of perpendicular to the side-slope. The wind driving forces come from applied stresses on both the windward and leeward sides of the embankment as shown in Figure 5.57. The downwind (leeward side) pressure diagram is due to suction while the windward pressure diagram is due to the wind.

For the case of no interface cohesion along the basal sliding surface, c = 0, which is typical for geosynthetic interfaces (see Chapter 2), and no uplift wind forces, U = 0, the expression for factor of safety against translation due to wind in Equation (5.75) simplifies to the following:

$$FS = \frac{\left(W_{EPS} + O_{REQ}\right) * \tan\delta}{R_U + R_D} \quad \textbf{(5.80)}$$

Equation (5.80) can be used to obtain the required value of O_{REQ} for a factor of safety of 1.2 against translation due to wind. A factor of safety against sliding of 1.2 is recommended for design purposes because sliding due to wind is another temporary loading condition and a factor of safety of 1.2 is being used for other temporary loading conditions in the design guidelines, such as seismic loading and hydrostatic uplift. In addition, low safety factors (1.0 to 1.2) are considered acceptable for this load case because of the low probability of occurrence of the event. For a factor of safety of 1.2 and solving for O_{REQ}, Equation (5.80) becomes:

$$O_{REQ} = \frac{1.2*(R_U + R_D)}{\tan\delta} - W_{EPS} \quad \textbf{(5.81)}$$

The components usually contributing to O_{REQ} are the weight of the pavement system and the cover soil on the embankment side slopes. Therefore, to ensure the desired factor of safety, the calculated value of O_{REQ} should be less than the sum of the pavement and cover soil weights as shown in Equation (5.65). If other weights, W_{other}, are applied to the embankment besides the pavement system and the soil cover, Equation (5.66) can be used to ensure that the desired factor of safety is obtained.

Figure 5.58 presents the design charts for the embankment geometries considered during this study for translation due to wind. These charts can be used to estimate the value of O_{REQ} per linear meter of embankment length required to obtain the desired factor of safety of 1.2 against translation due to wind. Figure 5.58 is based on the assumption that the EPS blocks extend down to the EPS/foundation soil interface and thus occurs at the EPS block/foundation soil interface. The charts differ from the hydrostatic uplift and sliding charts because the charts only correspond to a 2-lane road width (11m (36 ft)) but are applicable to 4-lane (23 m (76 ft)) and 6-lane embankments (34 m (112 ft)). This applicability is caused by the interface cohesion being assumed equal to zero, embankment width has a small influence on W_{EPS} because of the small density of EPS, and the assumption that the wind acts on a vertical wall. The application of the design charts in Figure 5.58 to 4-lane and 6-lane roadways was verified with a comparison of the three top embankment widths for the 2H:1V case that showed little difference in the value of O_{REQ}. Therefore, the slightly more conservative results for the 2-lane (11 m (36 ft)) roadway width are presented in Figure 5.58. The charts are a function of embankment heights between 1.5 m (4.92 ft) and 16 m (52.5 ft), side-slope inclinations of 0H:1V, 2H:1V, 3H:1V, 4H:1V, and two wind velocities (40 and 60 m/s (90 and 135 miles/hr)). It can also be seen that the design charts in Figure 5.58 utilize an interface friction angle, δ, of 20 degrees to 40 degrees for the EPS/foundation soil interface. The design charts correspond to *EPS40*, which has a density of 16 kg/m³ (1 lbf/ft³). Other densities were not considered because the value of O_{REQ} for a factor of

safety of 1.2 against translation to wind is not sensitive to other values of EPS density as noted previously in the hydrostatic uplift and hydrostatic sliding sections of this chapter.

Figure 5.58. Design against translation due to wind for factor of safety of 1.2 and a road width of 11 m (36 ft) and four embankment slopes.

The value of O_{REQ} obtained from Figure 5.58 is the additional overburden force in kN per linear meter of embankment length required above the weight of the EPS blocks to obtain the desired factor of safety of 1.2. Figure 5.58 is based on the assumption that the EPS blocks extend for the full height of the embankment. Therefore, Equations (5.67) or (5.68) should be used to estimate the weight provided by the pavement system and soil cover.

Various sliding interfaces may need to be evaluated during design depending on the types of materials that are placed, if any, between the EPS blocks and the foundation soil. Chapter 2 discussed interface friction values between EPS and dissimilar materials as well as between EPS and EPS. A representative value of interface friction angle should be measured using laboratory direct shear testing, e.g., ASTM D 5321, and used in Figure 5.58 to obtain the required value of O_{REQ} to resist translation due to wind.

The design wind speed can be obtained from local building codes or from references such as (*61*). Based on the wind speed contour map included in (*61*), wind speeds of 40 and 60 m/s (90 and 135 miles/hour) were used in developing Figure 5.58 because this is the range of wind speeds that predominate in the continental U.S. except for some coastal regions. However, as indicated in Chapter 3, no guidance is provided in (*60*) on the proper selection of wind speed.

The wind pressures obtained from Equations (3.4) and (3.5) may be too conservative because there is no documented sliding failure of an embankment containing EPS-block geofoam due to wind loading. As shown in Table 5.5, for a relatively low embankment height of 2 m (6.6 ft), an overburden on top of the EPS-block geofoam equivalent to a pavement system thickness of 7.2 m (24 ft) would be required for an embankment with side slopes of 4H:1V, an EPS/foundation interface friction angle of 40 degrees, and a cover soil thickness of 0.46 m (1.5 ft)

to provide sufficient stability against a 40 m/s (90 mph) wind speed. This pavement system thickness is greater than the typical pavement system thickness range of 0.6 to 1.5 m (2 to 4.9 ft). Table 5.5 also shows that the required value of O_{REQ} increases dramatically for a vertical embankment and a decrease in the interface friction angle from 40 to 20 degrees.

Table 5.5. Required overburden force and equivalent pavement system thickness for wind loading example problems.

A comparison of Equations (3.4) and (3.5) with the ANSI/ASCE 7-95 wind load provisions for buildings revealed the following three potential problems with the use of Equations (3.4) and (3.5) for the design of geofoam embankments:

- A draft version (*60*) of (*61*) used the coefficient 0.5, not 0.75 in Equation (3.5). A review of the ANSI/ASCE 7-95 (*62*) wind design parameters for the case of a building with a flat roof, which would be comparable to an embankment with vertical walls, revealed that the French design guideline pressure coefficients of 0.75 and 0.5 for the windward and leeward cases, respectively, are the same as the ANSI/ASCE 7-95 pressure coefficients for buildings with a length to width ratio ranging from 0 to 1 where the width of the building is perpendicular to the wind direction. This ratio would be applicable to most roadway embankments. However, unlike the ANSI/ASCE 7-95 design procedure, the French design guideline does not consider suction pressures on top of the structure. Suction pressures will decrease with the horizontal distance from the windward edge and will tend to decrease the translational stability of a vertical embankment. Therefore, the larger 0.75 downwind pressure coefficient that appeared in the later French guideline may compensate for the suction pressures on top of the structure.
- Equations (3.4) and (3.5) treat a side-sloped embankment as a vertical wall. Therefore, the wind pressures are conservative in that the wind pressures are

assumed to be horizontal instead of perpendicular to the side-sloped surface, which would yield both a horizontal and a vertical component to the wind pressure.

- No guidance is provided in (*60*) or (*61*) on the selection of wind speed. The ANSI/ASCE 7-95 design procedure includes a wind speed contour map of the United States that does not include tornado winds because of their rare occurrence. However, the ANSI/ASCE building design equations include an exposure velocity pressure coefficient which reflects change in wind speed with height and terrain roughness, a topographic factor which accounts for wind speed up and over hills and escarpments, a gust effect factor, and an importance factor which adjusts wind speed to a 50-year mean recurrence interval.

Based on the results in Table 5.5, the design charts in Figure 5.58, the potential problems presented herein with the use of Equations (3.4) and (3.5), and the absence of documented sliding failure due to wind loading, it is recommended that the translation due to wind failure mechanism not be considered until further research is performed on the applicability of Equations (3.4) and (3.5) to EPS-block geofoam embankments. However, the analysis procedure was presented herein for completeness and because future research may develop lower coefficients for Equations (3.4) and (3.5) that are in better agreement with field observations and the analysis presented above can be utilized with the lower coefficients. It is recommended that a more realistic procedure be developed for evaluating the potential for basal translation (sliding) due to wind loading especially under Atlantic hurricane conditions. An evaluation of the applicability of roof design shapes and procedures to side-sloped EPS-block geofoam embankments is recommended. Development of new wind pressure coefficients was outside the scope of this project but is listed as a topic for future research.

Overturning

For vertical embankments, the entire embankment can overturn at the interface between the bottom of the assemblage of EPS blocks and the underlying foundation soil due to horizontal wind forces acting on the embankment. These wind forces can create an overturning moment about the toe at point O as shown in Figure 5.59. Vertical loads such as the weight of the EPS blocks and any overburden material placed on top of the blocks such as the pavement system and traffic surcharges will provide a stabilizing moment. As described for the analysis of hydrostatic uplift, O_{REQ} is the additional overburden force required above the EPS blocks to obtain the desired factor of safety.

Figure 5.59. Variables for determining the factor of safety against overturning due to horizontal wind forces.

The factor of safety against overturning due to wind is expressed as

$$FS = \frac{\sum \text{stabilizing moments}}{\sum \text{overturning moments}} = \frac{(\frac{1}{2} * T_W) * (W_{EPS}+O_{REQ})}{\left(\frac{1}{2} * H\right) * \left(R_U+R_D\right)} \quad \textbf{(5.82)}$$

A factor of safety against hydrostatic overturning of 1.2 is recommended for design purposes because overturning due to wind is a temporary loading condition and a factor of safety of 1.2 is being used for other temporary loading conditions, such as hydrostatic uplift and sliding and seismic loading. For a factor of safety of 1.2 and solving for O_{REQ}, Equation (5.82) becomes

$$O_{REQ} = \frac{\left[1.2 * \frac{1}{2} * H * \left(R_U+R_D\right)\right] - \left[\frac{1}{2} * T_W * W_{EPS}\right]}{\left(\frac{1}{2} * T_W\right)} \quad \textbf{(5.83)}$$

Equation (5.83) can be used to obtain the required value of O_{REQ} for a factor of safety of 1.2 to resist overturning by wind forces.

The resultant of the vertical and horizontal forces should be checked to verify that the resultant is located within the middle third of the base, i.e., eccentricity, $e \leq (B_w/6)$, to minimize

the potential for the wall to overturn. Equations (5.55) and (5.56) can be used to determine e. Additionally, the maximum and minimum soil pressures under the embankment should not exceed the allowable soil pressure, q_a, which is given by Equation (5.39). Equation (5.57) can be used to determine the maximum and minimum pressures under the embankment.

Remedial Procedures

Remedial procedures that can be considered to increase the factor of safety against translation due to wind are similar to those for increasing the factor of safety against hydrostatic sliding discussed in the previous section except that the use of a drainage system would not apply to wind loading.

REFERENCES

1. Horvath, J. S., *Geofoam Geosynthetic*, Horvath Engineering, P.C., Scarsdale, NY (1995) 229 pp.
2. "Matériaux Légers pour Remblais/Lightweight Filling Materials." *Document No. 12.02.B,* PIARC-World Road Association, La Defense, France (1997) 287 pp.
3. Briaud, J.-L., James, R. W., and Hoffman, S. B., "Settlement of Bridge Approaches (The Bump at the End of the Bridge)." *NCHRP Synthesis 234,* Transportation Research Board, Washington, D.C. (1997) 75 pp.
4. "Expanded Polystyrene Used in Road Embankments - Design, Construction and Quality Assurance." *Form 482E,* Public Roads Administration, Road Research Laboratory, Oslo, Norway (1992) 4 pp.
5. Sanders, R. L., and Seedhouse, R. L., "The Use of Polystyrene for Embankment Construction." *Contractor Report 356,* Transport Research Laboratory, Crowthorne, Berkshire, U.K. (1994) 55 pp.
6. Miki, G., "Ten Year History of EPS Method in Japan and its Future Challenges." *Proceedings of the International Symposium on EPS Construction Method (EPS Tokyo '96),* Tokyo, Japan, (1996) pp. 394-410.
7. Terzaghi, K., Peck, R. B., and Mesri, G., *Soil Mechanics in Engineering Practice*, 3rd, John Wiley & Sons, Inc., New York (1996).
8. Holtz, R. D., "Treatment of Problem Foundations for Highway Embankments." *NCHRP Synthesis 147,* Transportation Research Board, Washington, D.C. (1989) 72 pp.
9. "Settlement Analysis." *Technical Engineering and Design Guides as Adapted From the U.S. Army Corps of Engineers, No. 9,* ASCE, New York (1994) 144 pp.
10. Duncan, J. M., Javete, D. F., and Stark, T. D., "The Importance of a Desiccated Crust on Clay Settlements." *Soils and Foundations*, Vol. 31, No. 3 (1991) pp. 77-90.
11. Holtz, R. D., and Kovacs, W. D., *An Introduction to Geotechnical Engineering*, Prentice Hall, Englewood Cliffs,NJ (1981) 733 pp.

12. Nishida, Y., "A brief note on compression index of soil." *Journal of the Soil Mechanics and Foundations Division, ASCE*, Vol. 82, No. SM3 (1956) pp. 1027-1 - 1027-14.
13. Terzaghi, K., and Peck, R. B., *Soil Mechanics in Engineering Practice*, 2nd, John Wiley and Sons, New York (1967) 729 pp.
14. Mesri, G., "Discussion: Postconstruction Settlement of An Expressway Built on Peat by Precompression by Samson, L." *Canadian Geotechnical Journal*, Vol. 23, No. 3 (1986) pp. 403-407.
15. Mesri, G., and Choi, Y. K., "Settlement Analysis of Embankments on Soft Clays." *Journal of Geotechnical Engineering*, Vol. 111, No. 4 (1985) pp. 441-464.
16. Mesri, G., Stark, T. D., Ajlouni, M. A., and Chen, C. S., "Secondary Compression of Peat With or Without Surcharging." *Journal of Geotechnical and Geoenvironmental Engineering*, Vol. 123, No. 5, May 1997 (1997) pp. 411-421.
17. "Treatment of Soft Foundations for Highway Embankments." *NCHRP Synthesis 29,* Transportation Research Board, Washington, D.C. (1975) 25 pp.
18. "Bridge Approach Design and Construction Practices." *NCHRP Synthesis of Highway Practice 2,* Transportation Research Board, Washington, D.C. (1969) 30 pp.
19. Wahls, H. E., "Shallow Foundations for Highway Structures." *NCHRP Synthesis of Highway Practice 107,* Transportation Research Board, Washington, D.C. (1983) 38 pp.
20. Moulton, L. K., GangaRao, H. V. S., and Halvorsen, G. T., "Tolerable Movement Criteria for Highway Bridges." *FHWA/RS-85/107,* Federal Highway Administration, Washington D.C. (1985).
21. Moulton, L. K., "Tolerable Movement Criteria for Highway Bridges." *FHWA-TS-85-228,* Federal Highway Administration, Washington, D.C. (1986) 93 pp.
22. "Design and Construction Manual for Lightweight Fill with EPS." The Public Works Research Institute of Ministry of Construction and Construction Project Consultants, Inc., Japan (1992) Ch. 3 and 5.
23. Osterberg, J. O., "Influence Values for Vertical Stresses in a Semi-Infinite Mass Due to an Embankment Loading." *Proc. 4th Int. Conf. Soil Mech.,* London, Vol. 1 (1957) pp. 393-394.
24. Prandtl, L., "Über die Eindringungsfestigkeit (Härte) plastischer Bauttoffe und die Festigkeit von Schneiden (On the penetrating strengths (hardness) of plastic construction materials and the strength of cutting edges)." *Zeit. angew. Math. Mech.*, Vol. 1, No. 1 (1921) pp. 15-20.
25. Skempton, A. W., "The bearing capacity of clays." *Proc. British Bldg. Research Congress*, Vol. 1 (1951) pp. 180-189.
26. Peck, R. B., Hanson, W. E., and Thornburn, T. H., *Foundation Engineering*, 2nd, John Wiley & Sons, NY (1974).
27. Aabøe, R., "Deformasjonsegenskaper og spenningsforhold i fyllinger av EPS (Deformation and stress conditions in fills of EPS)." *Intern Rapport Nr. 1645,* Public Roads Administration (1993) 22 pp. Norwegian.
28. Aabøe, R., "Long-term performance and durability of EPS as a lightweight fill." *Nordic Road & Transport Research*, Vol. 12, No. 1 (2000) pp. 4-7.

29. Boussinesq, J., *Application des Potentiels à l' Étude de l' Équilibre et du Mouvement des Solides Élastiques*, Gauthier-Villard, Paris (1885).
30. American Association of State Highway and Transportation Officials, *Standard Specifications for Highway Bridges*, 16th, American Association of State Highway and Transportation Officials, Washington, D.C. (1996).
31. Janbu, N., "Slope Stability Computations." *Embankment Dam Engineering,* Hirschfield and Poulos, eds., John Wiley & Sons, New York (1973) pp. 47-86.
32. Sharma, S., *XSTABL: An Integrated Slope Stability Analysis Program for Personal Computers*, Interactive Software Designs, Inc., Moscow, Idaho (1996) 150 pp.
33. Bishop, A. W., "The Use of the Slip Circle in the Stability Analysis of Slopes." *Geotechnique*, Vol. V. No. 1, pp. 7-17.
34. Spencer, E., "A Method of Analysis of the Stability of Embankments Assuming Parallel Inter-slice Forces." *Geotechnique*, Vol. 17, No. 1 (1967) pp. 11-26.
35. Duncan, J. M., and Wright, S. G., "The Accuracy of Equilibrium Methods of Slope Stability Analysis." *International Symposium on Landslides,* New Delhi, India, (1980) pp. 247-254.
36. Chirapuntu, S., and Duncan, J. M., "The Role of Fill Strength in the Stability of Embankments on Soft Clay Foundations." *TE 75-3,* Department of Civil Engineering, Institute of Transportation and Traffic Engineering, University of California, Berkeley (1975) 231 pp.
37. Kavazanjian, E., Jr., Matasovic, N., Hadj-Hamou, T., and Sabatini, P. J., "Geotechnical Engineering Circular No. 3; Design Guidance: Geotechnical Earthquake Engineering for Highways; Volume I - Design Principles." *FHWA-SA-97-076,* U.S. Department of Transportation, Federal Highway Administration, Washington, D.C. (1997) 186 pp.
38. Elias, V., Welsh, J., Warren, J., and Lukas, R., "Ground Improvement Technical Summaries." *FHWA-SA-98-086,* U.S. Department of Transportation, Federal Highway Adminstration, Washington, D.C. (1999).
39. Elias, V., Welsh, J., Warren, J., and Lukas, R., "Ground Improvement Technical Summaries." *FHWA-SA-98-086,* Vol. 2, 2 Vols, U.S. Department of Transportation, Federal Highway Adminstration, Washington, D.C. (1999).
40. Terzaghi, K., "Mechanisms of Landslides." *Application of Geology to Engineering Practice, Berkey Vol.,* Geological Society of America (1950) pp. 83-123.
41. "Soil Mechanics, *Design Manual 7.01 Revalidated by Change 1 September 1986*." Naval Facilities Engineering Command, Alexandria, VA (1986) 364 pp.
42. Day, R. W., *Geotechnical Earthquake Engineering Handbook*, McGraw-Hill, New York (2002).
43. Makdisi, F., and Seed, H. B., "Simplified Procedure for Estimating Dam and Embankment Earthquake-Induced Deformations." *Journal of Geotechnical Engineering Division ASCE*, Vol. 104, No. 7 (1978) pp. 849-867.
44. Stark, T. D., and Mesri, G., "Undrained Shear Strength of Liquefied Sands for Stability Analysis." *Journal of Geotechnical Engineering Division ASCE*, Vol. 118, No. 11 (1992) pp. 1727-1747.

45. Yegian, M. K., and Lahlaf, A. M., "Dynamic Interface Shear Strength Properties of Geomembranes and Geotextiles." *ASCE Journal of Geotechnical Engineering*, Vol. 118, No. 5 (1992) pp. 760-779.
46. Schnabel, P., Lysmer, J., and Seed, H. B., "SHAKE: A Computer Program for Earthquake Response Analysis of Horizontally Layered Sites.", Earthquake Engineering Research Center, University of California at Berkeley, Richmond, CA, (1972).
47. Chopra, A. K., "Earthquake Effects on Dams," Doctor of Philosophy thesis, University of California at Berkeley, Berkeley, CA (1966).
48. Hashash, M. A. Y., Stark, T. D., and Abdulamit, A., "Equivalent Linear Dynamic Response Analysis of Geosynthetic Lined Landfills." *Industrial Fabrics Association International,* St. Paul, MN, Vol. February, 2001 (2001).
49. Algermissen, S. T., Perkins, D. M., Thenhaus, P. C., Hanson, S. L., and Bender, B. L., "Probabilistic Earthquake Acceleration and Velocity Maps for the United States and Puerto Rica." *Open-File Report 97-131,* U.S. Geological Survey, Open-File Services Section, Denver, CO (1997).
50. Seed, H. B., Romo, M. P., Sun, J., Jaime, A., and Lysmer, J., "Relationships Between Soil Conditions and Earthquake Ground Motions in Mexico City in the Earthquake of Sept. 19, 1985." *UCB/EERC-87/15,* University of California at Berkeley, Earthquake Engineering Research Center, Berkeley, CA (1987) 112 pp.
51. Seed, H. B., and Idriss, I. M., "Ground Motions and Soil Liquefaction During Earthquakes.", Earthquake Engineering Research Center, University of California at Berkeley, Berkeley, CA, (1982).
52. Idriss, I. M., "Response of Soft Soil Sites During Earthquakes." *Proceedings of the H. Bolton Seed Memorial Symposium,* Richmond, British Columbia, Vol. tel. 604-277-4250, fax 604-277-8125 (1990).
53. EDO, "(untitled)." *Proceedings of International Geotechnical Symposium on Polystyrene Foam in Below Grade Applications, March 30, 1994,* Honolulu, HI, Vol. May 1994, Research Report No. CE/GE-94-1 (1994) pp. 168.
54. Hotta, H., Nishi, T., and Kuroda, S., "Report of Results of Assessments of Damage to EPS Embankments Caused by Earthquakes." *Proceedings of the International Symposium on EPS Construction Method (EPS Tokyo '96),* Tokyo, Japan, (1996) pp. 307-318.
55. Frydenlund, T. E., and Aaboe, R., "Expanded Polystyrene - A Light Solution." *International Symposium on EPS Construction Method (EPS Tokyo '96),* Tokyo, Japan, (1996) pp. 31-46.
56. Horvath, J. S., "Lessons Learned from Failures Involving Geofoam in Roads and Embankments." *Research Report No. CE/GE-99-1,* Manhattan College, Bronx, NY (1999) 18 pp.
57. Taccola, L. J., Telephone conversation with Arellano, D. 16 November 1999.
58. Elias, V., and Christopher, B. R., "Mechanically Stabilized Earth Walls and Reinforced Soil Slopes, Design and Construction Guidelines." *FHWA-SA-96-071,* Federal Highway Administration, Washington, D.C. (1997) 371 pp.
59. "Foundations & Earth Structures, *Design Manual 7.02 Revalidated by Change 1 September 1986*." Naval Facilities Command, Alexandria, VA (1986) 253 pp.

60. Magnan, J.-P., "Recommandations pour L'Utilisation de Polystyrene Expanse en Remblai Routier." Laboratoire Central Ponts et Chaussées, France (1989) 20 pp.
61. "Utilisation de Polystyrene Expanse en Remblai Routier; Guide Technique." Laboratoire Central Ponts et Chaussées/SETRA, France (1990) 18 pp.
62. *Minimum Design Loads for Buildings and Other Structures, ANSI/ASCE 7-95, Approved June 6, 1996*, American Society of Civil Engineers, New York (1996).

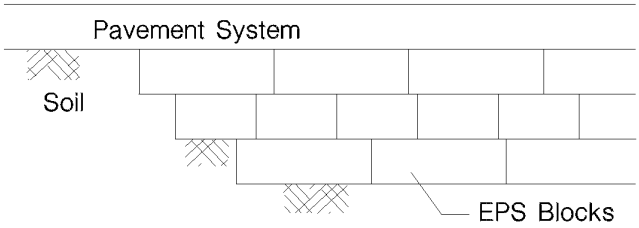

FIGURE 5.1 PROJ 24-11.doc

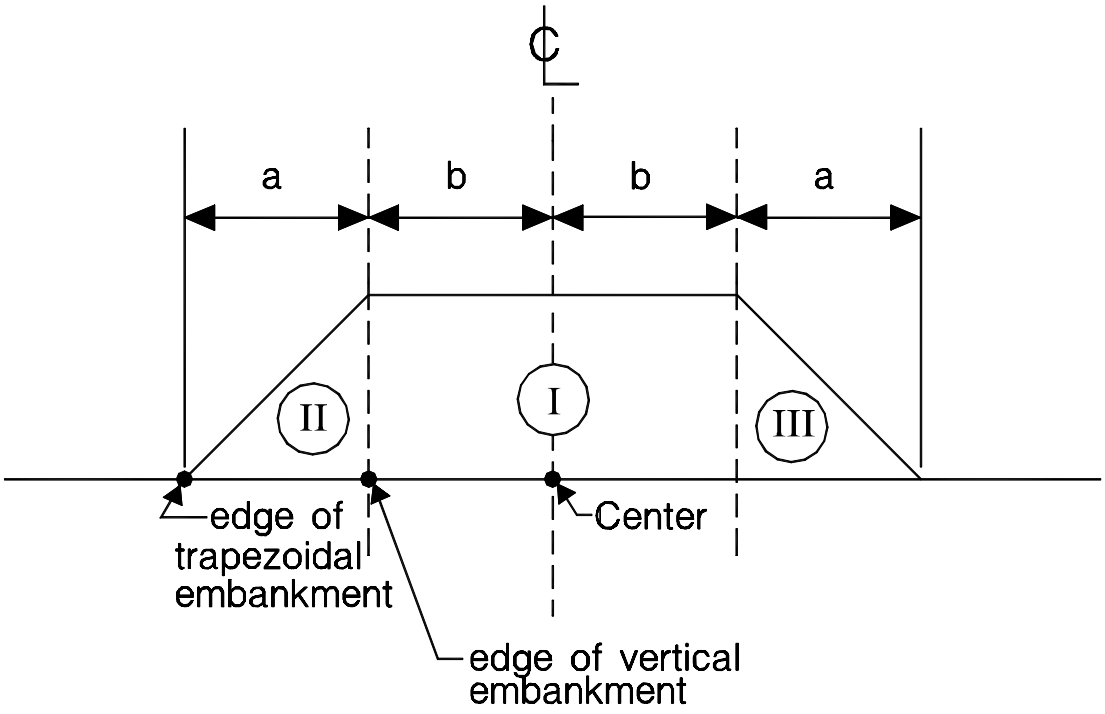

FIGURE 5.2 PROJ 24-11.doc

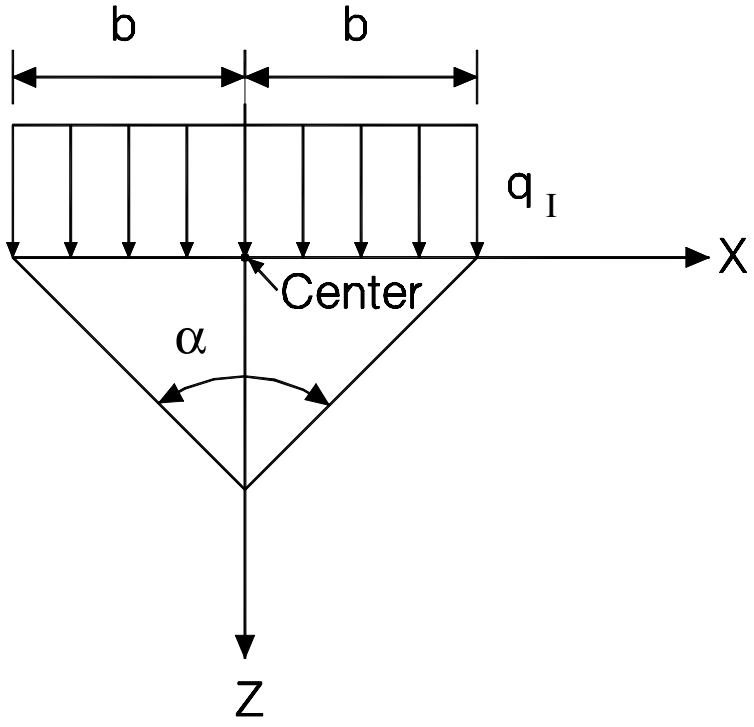

FIGURE 5.3 PROJ 24-11.doc

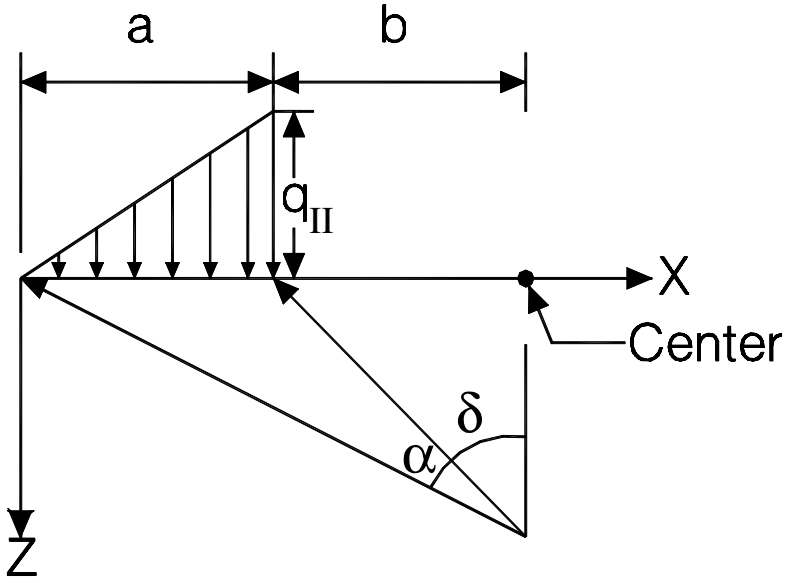

FIGURE 5.4 PROJ 24-11.doc

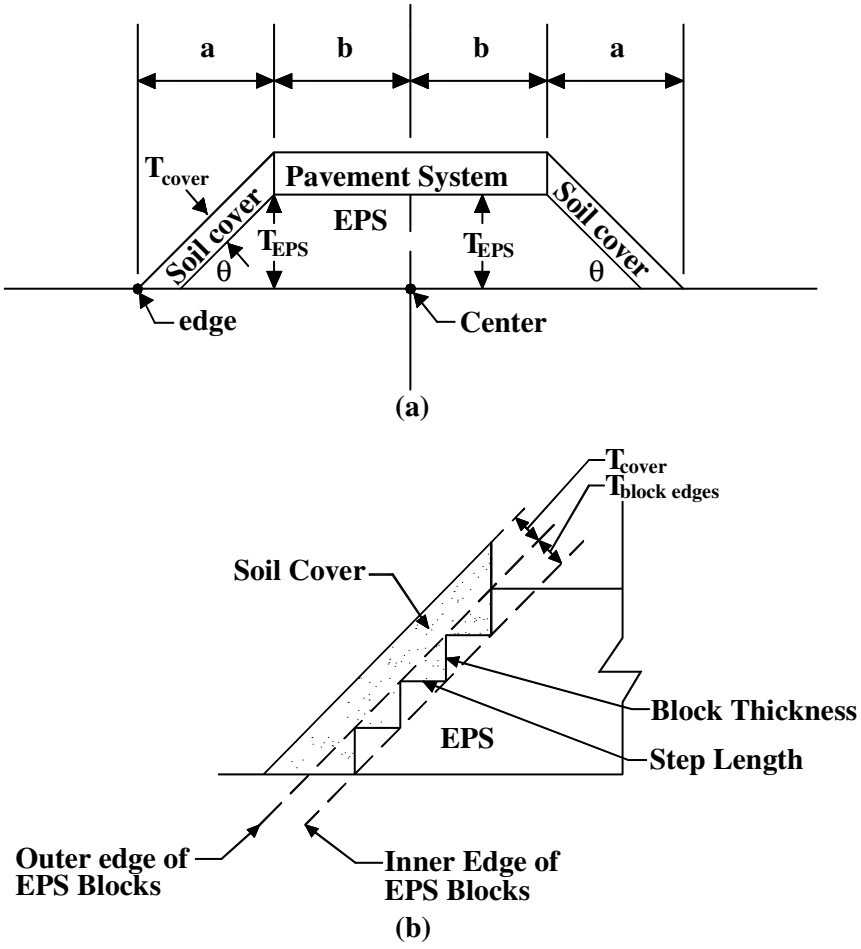

FIGURE 5.5 PROJ 24-11.doc

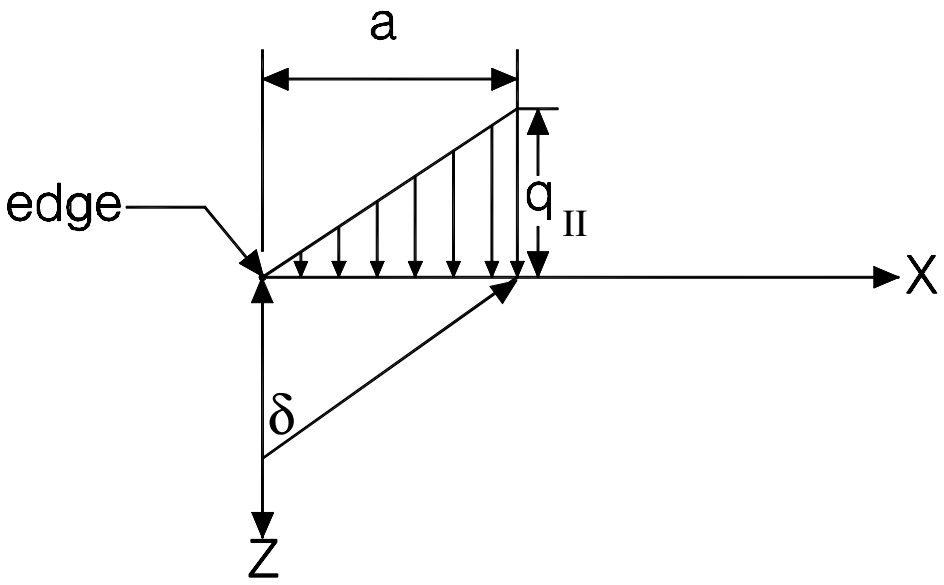

FIGURE 5.6 PROJ 24-11.doc

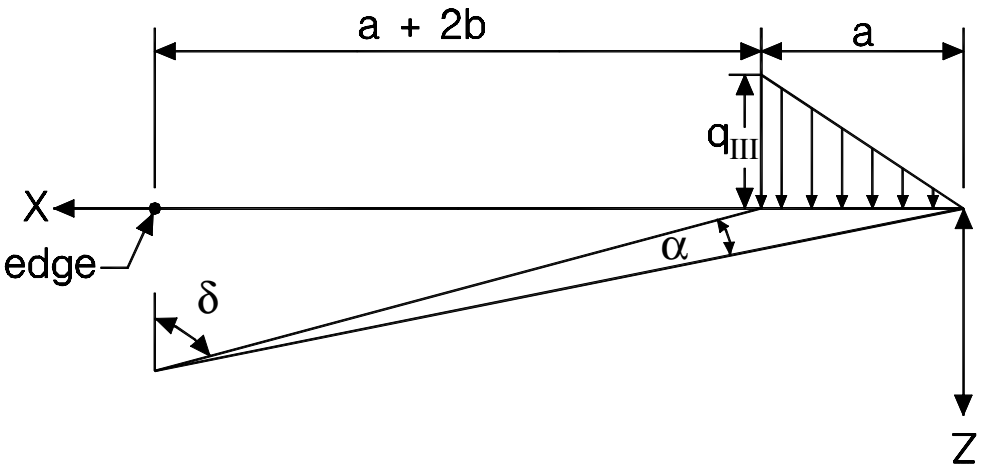

FIGURE 5.7 PROJ 24-11.doc

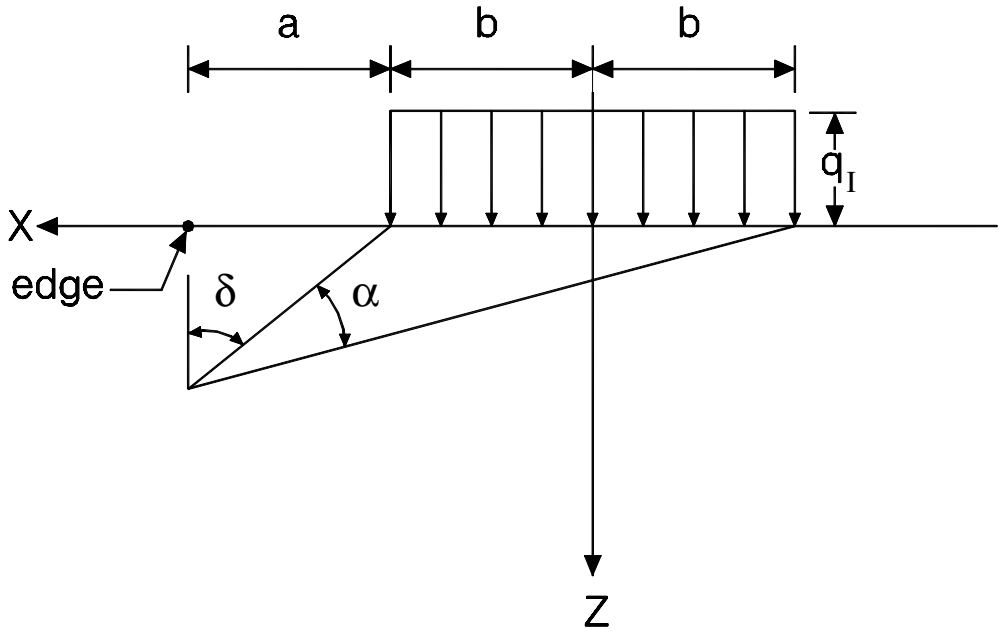

FIGURE 5.8 PROJ 24-11.doc

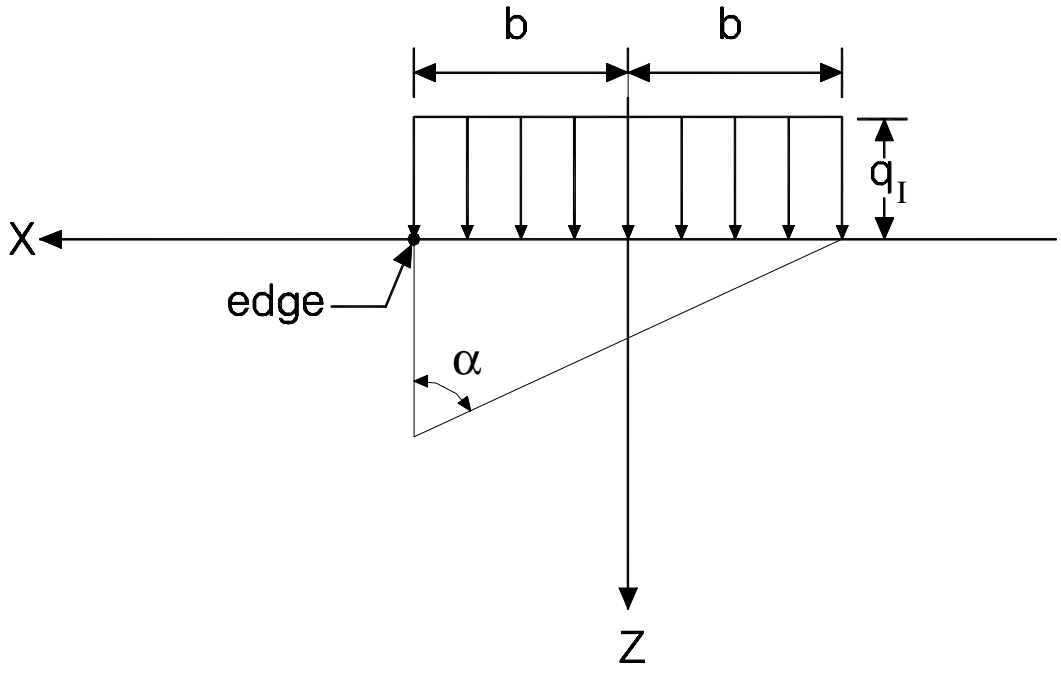

FIGURE 5.9 PROJ 24-11.doc

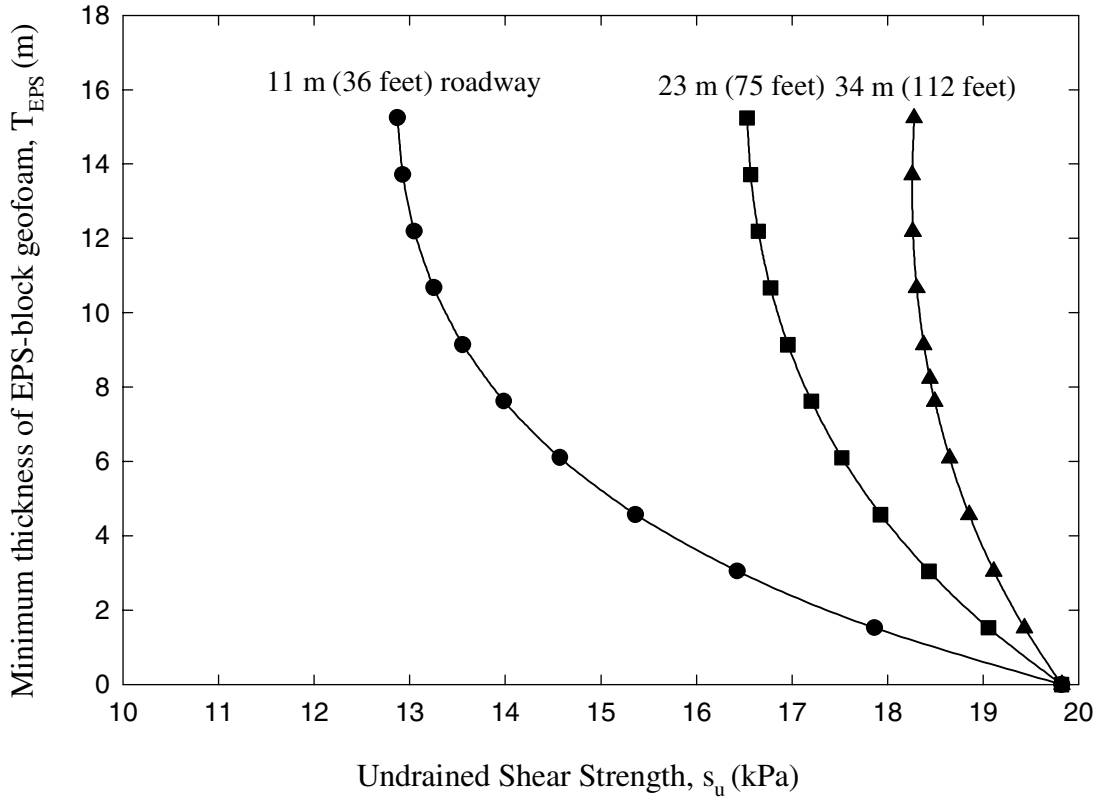

FIGURE 5.10 PROJ 24-11.doc

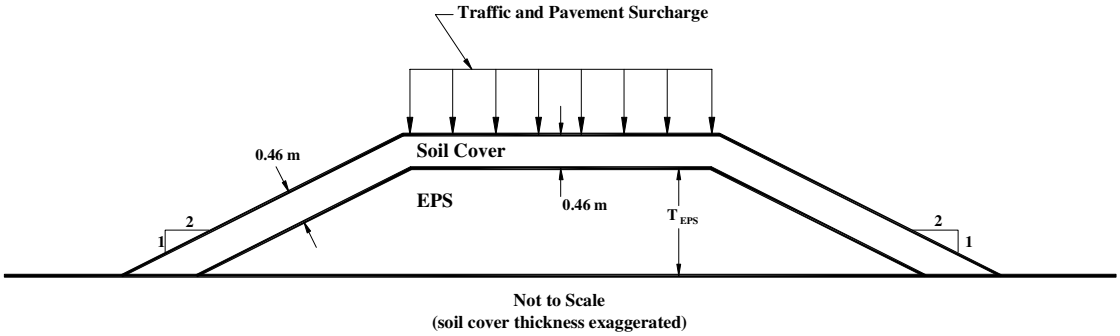

FIGURE 5.11 PROJ 24-11.doc

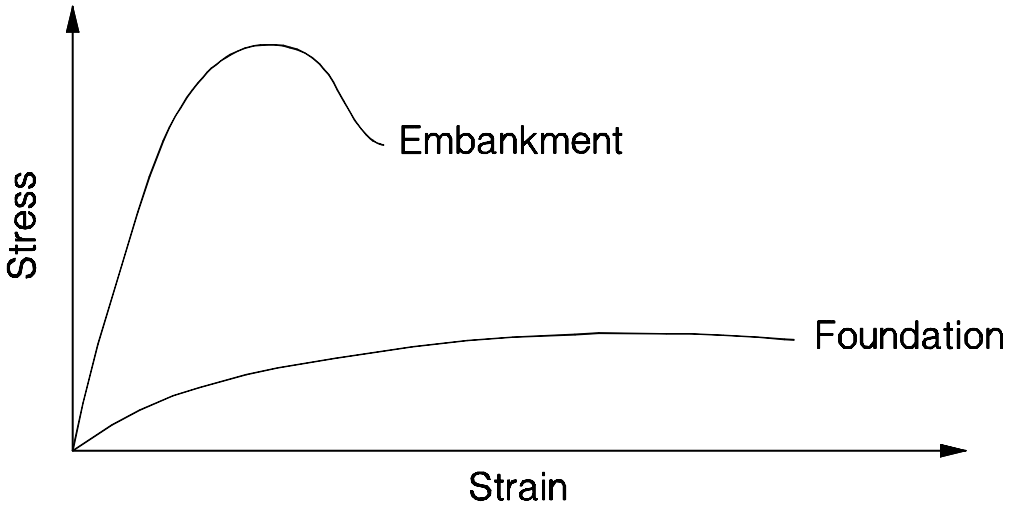

FIGURE 5.12 PROJ 24-11.doc

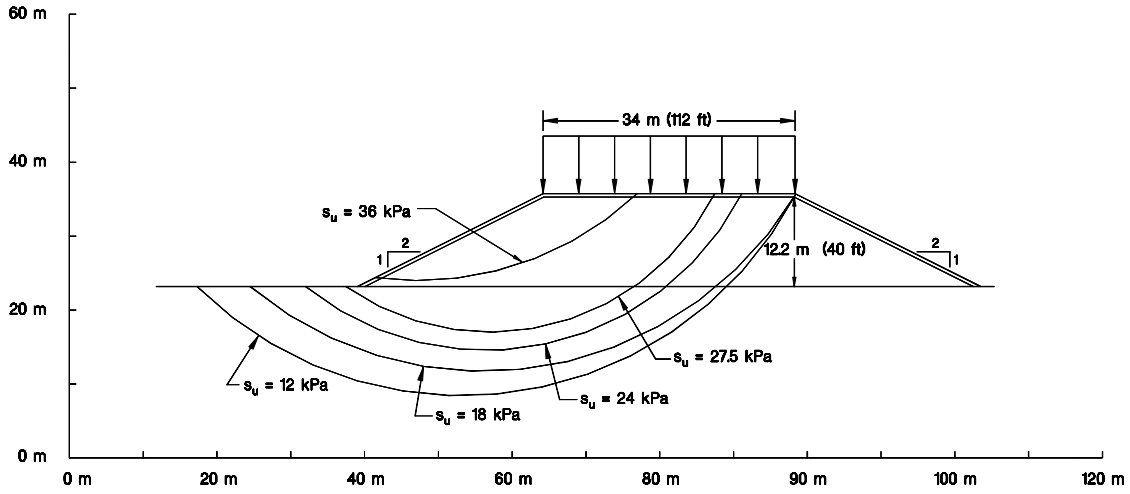

FIGURE 5.13 PROJ 24-11.doc

11 m pavement, static

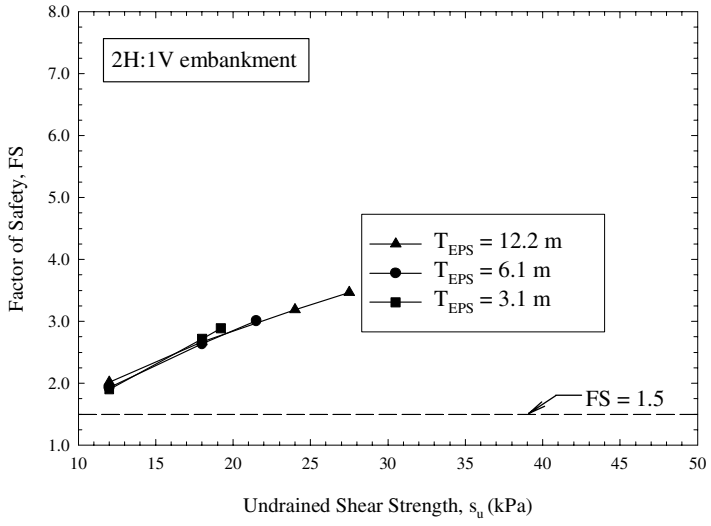

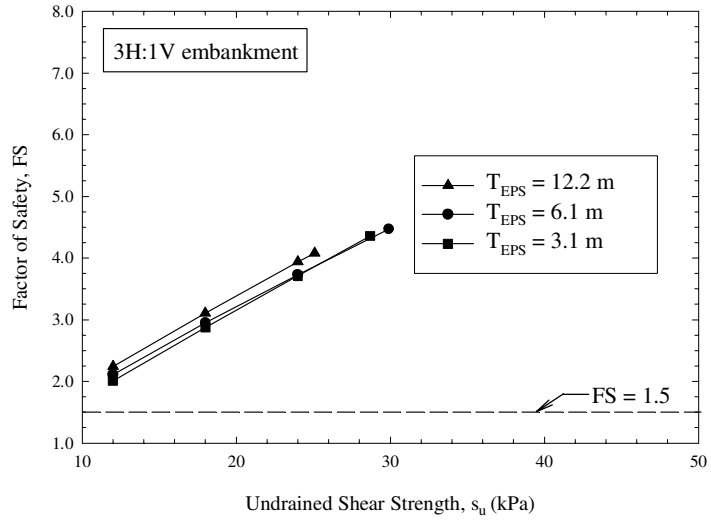

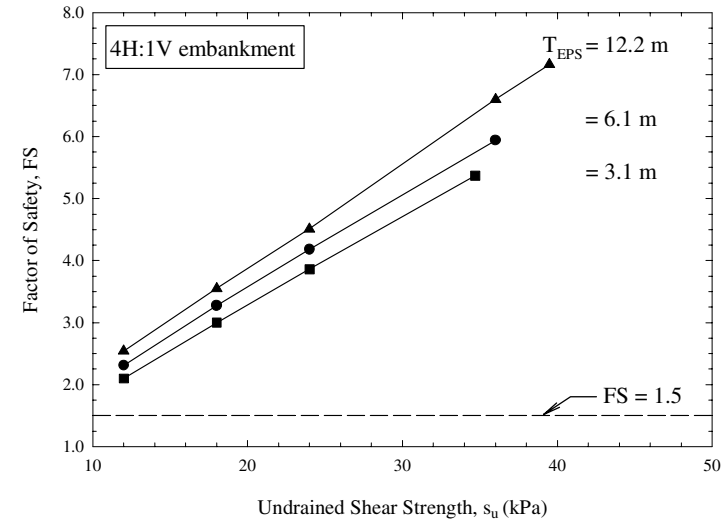

FIGURE 5.14 PROJ 24-11.doc

23 m pavement, static

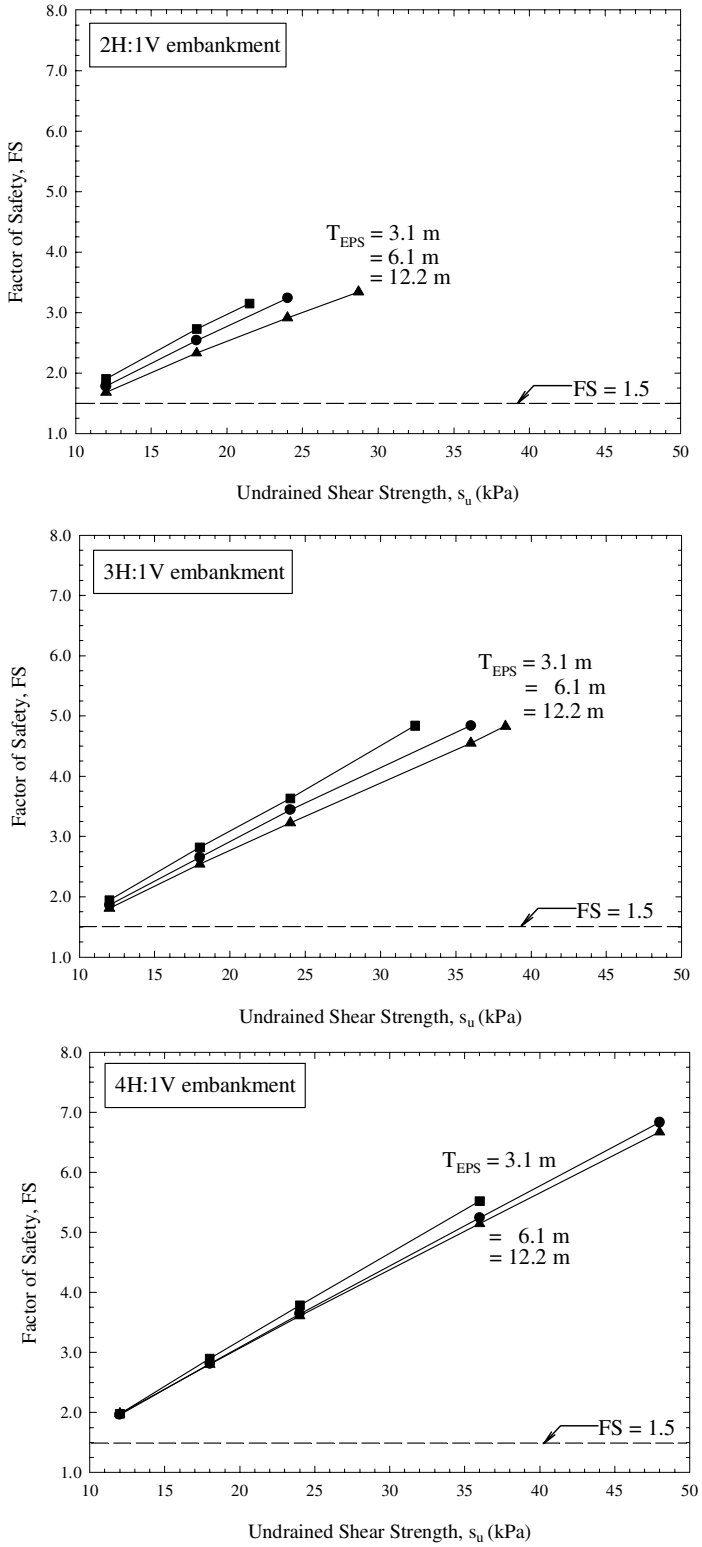

FIGURE 5.15 PROJ 24-11.doc

34 m pavement, static

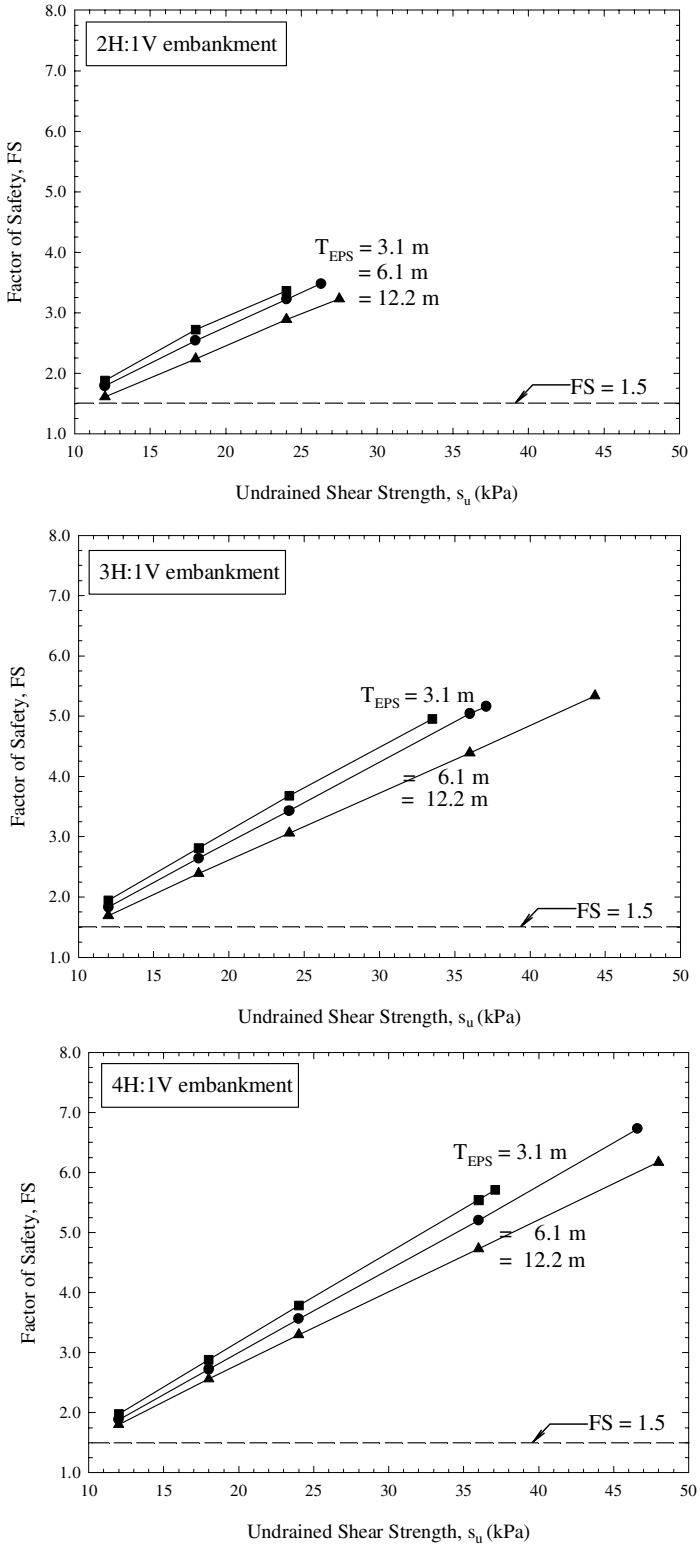

FIGURE 5.16 PROJ 24-11.doc

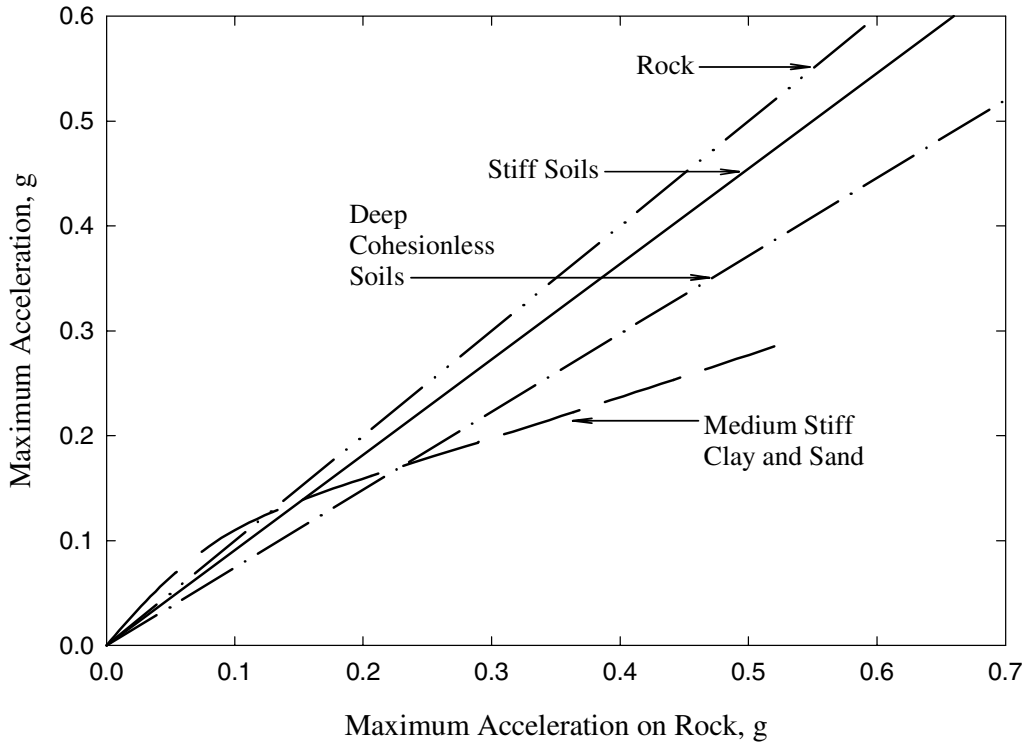

FIGURE 5.17 PROJ 24-11.doc

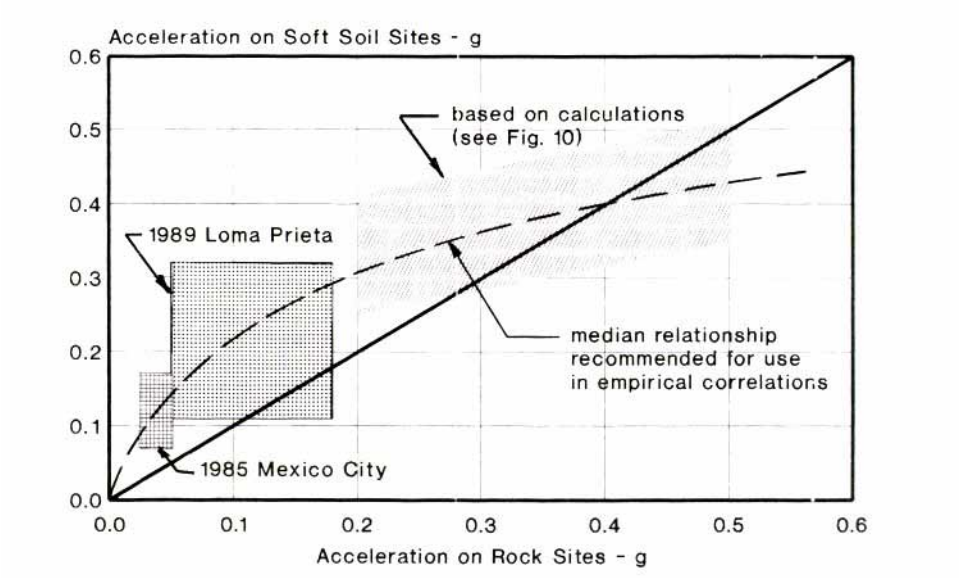

FIGURE 5.18 PROJ 24-11.doc

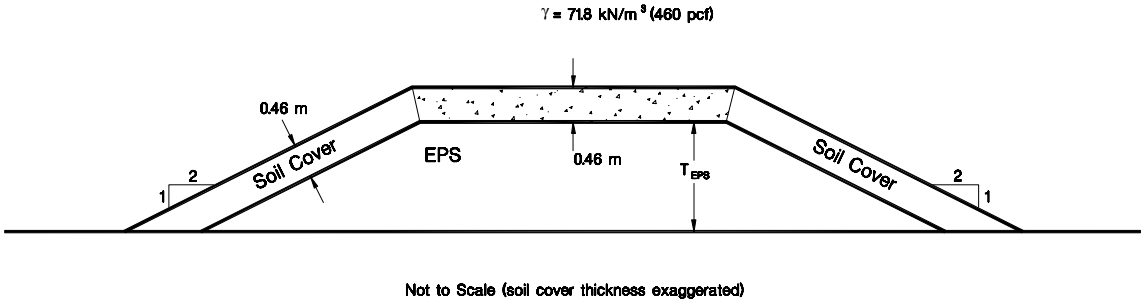

FIGURE 5.19 PROJ 24-11.doc

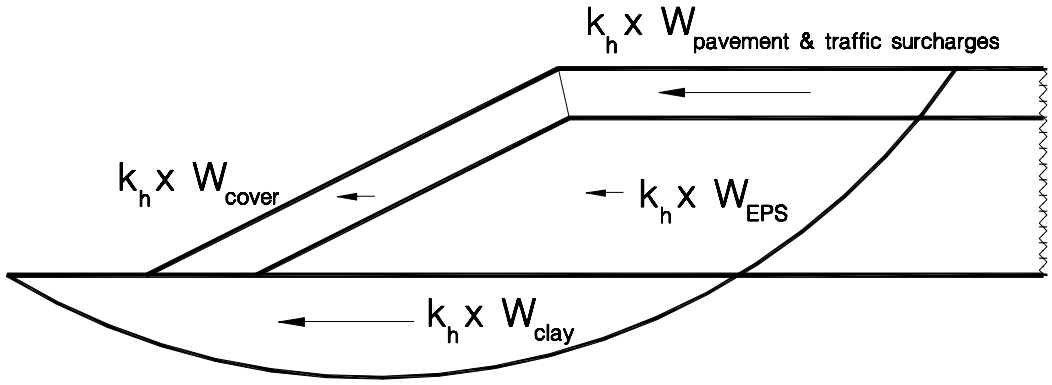

FIGURE 5.20 PROJ 24-11.doc

11 m pavement, k_h=0.05

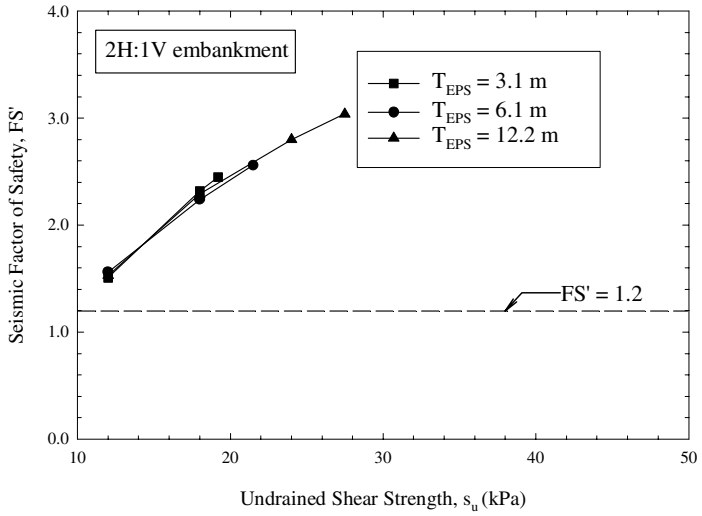

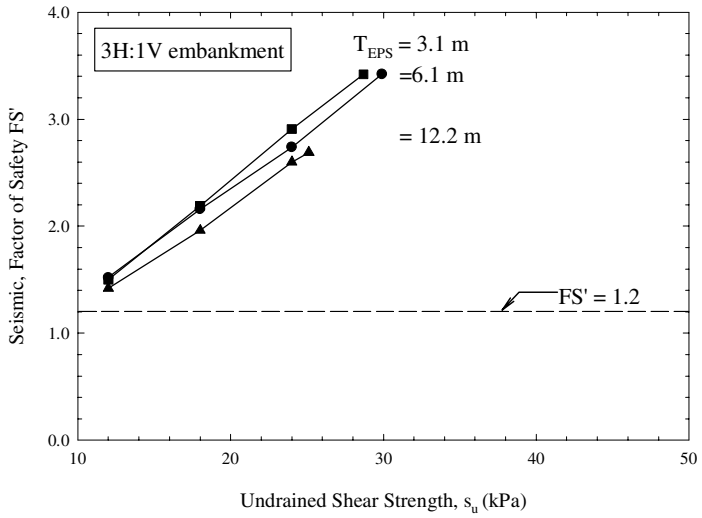

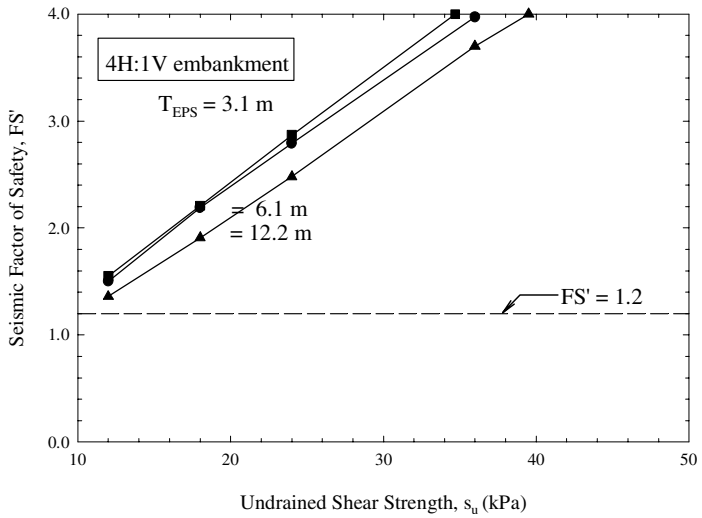

FIGURE 5.21 PROJ 24-11.doc

11 m pavement, k_h=0.10

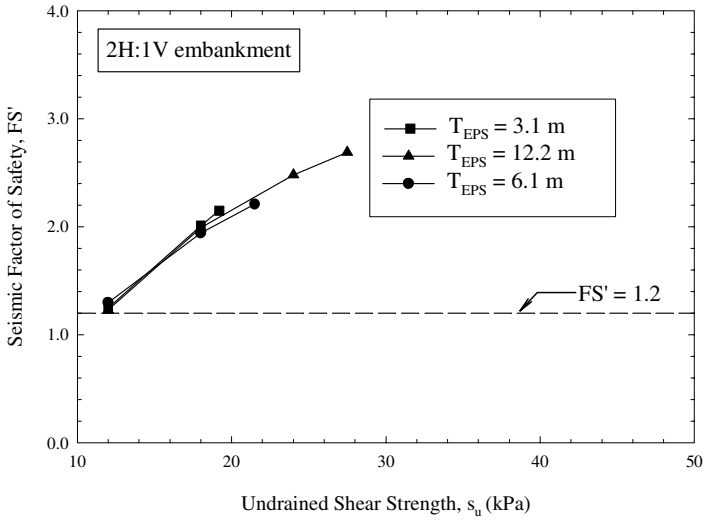

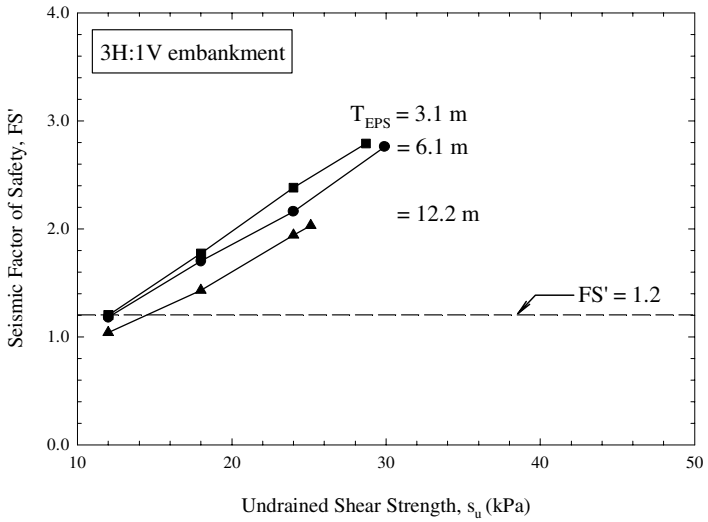

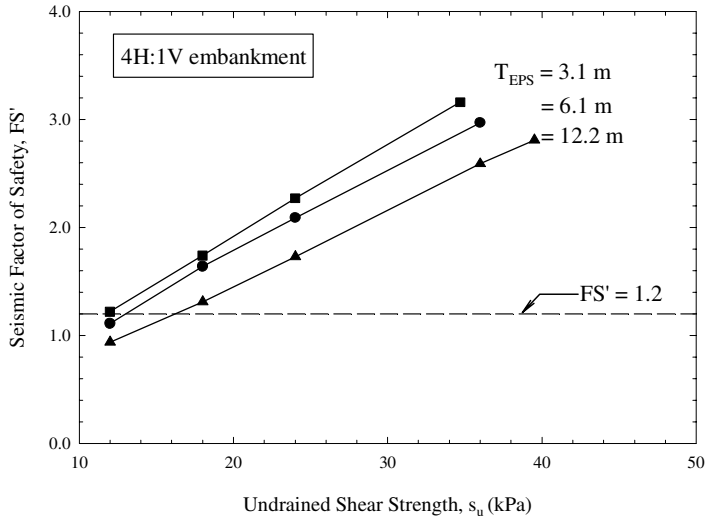

FIGURE 5.22 PROJ 24-11.doc

11 m pavement, k_h=0.20

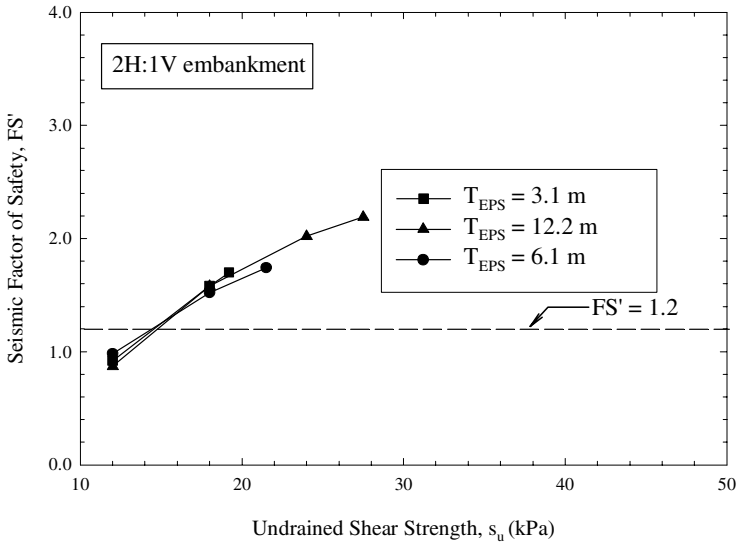

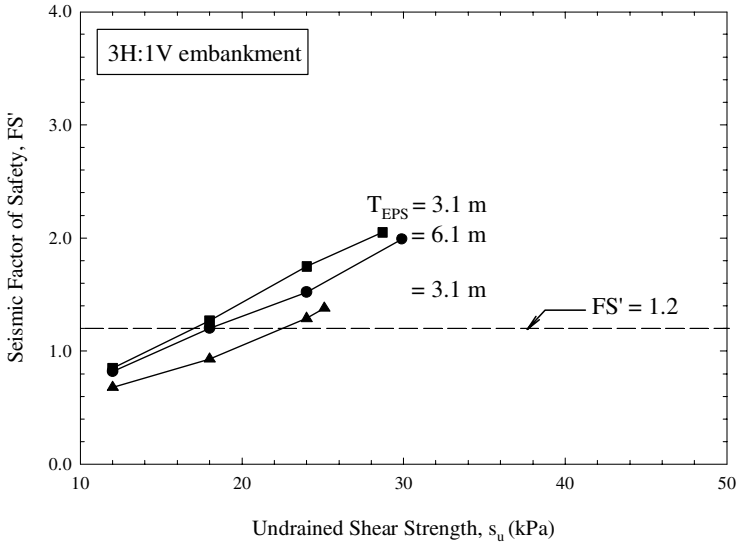

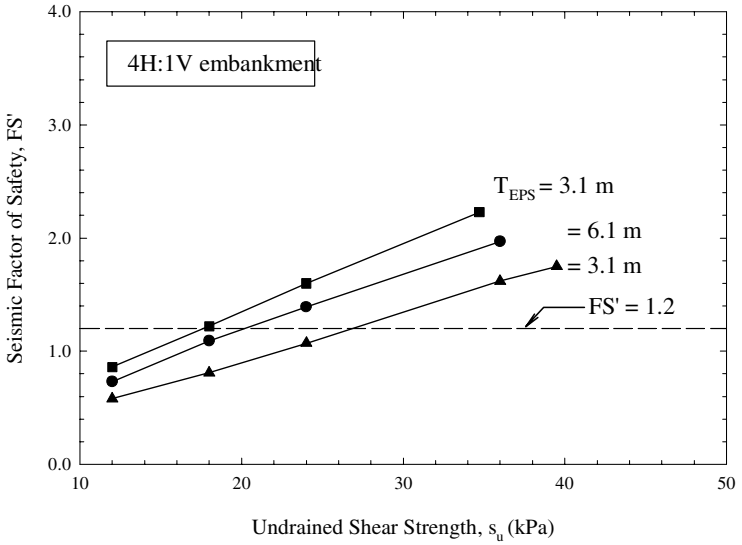

FIGURE 5.23 PROJ 24-11.doc

23 m pavement, k_h=0.05

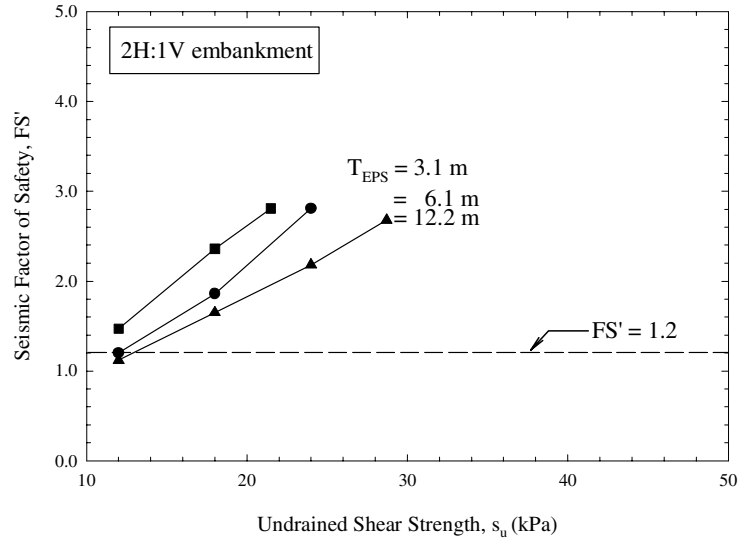

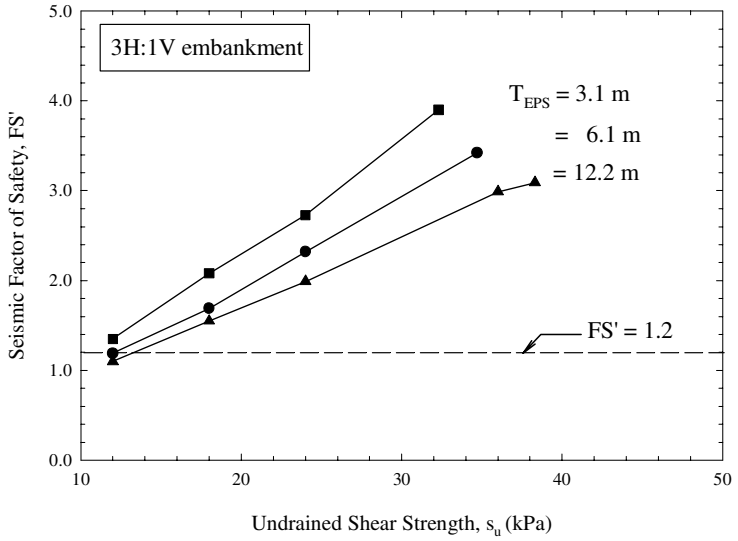

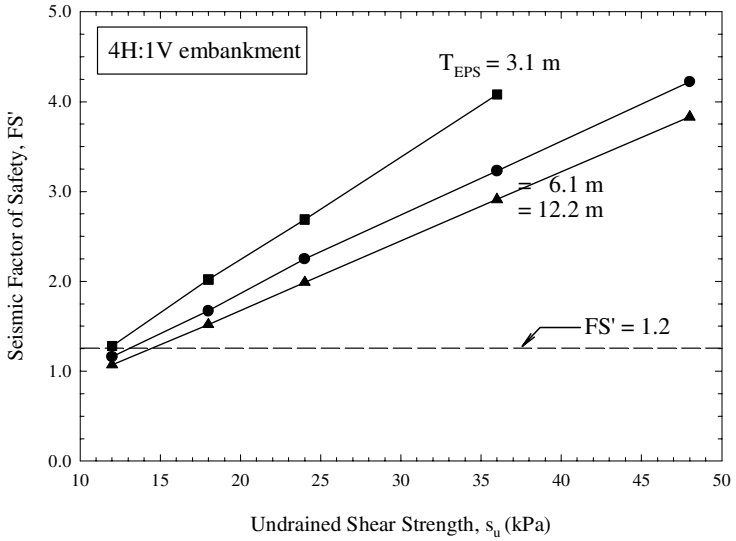

FIGURE 5.24 PROJ 24-11.doc

23 m pavement, k_h=0.10

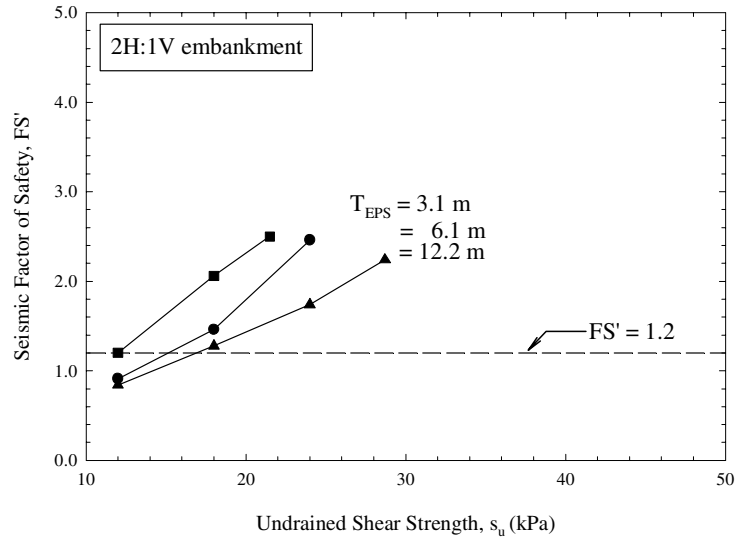

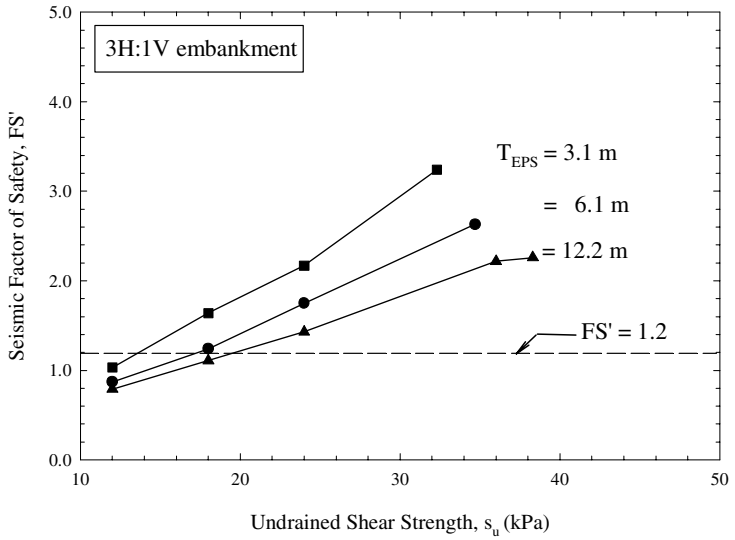

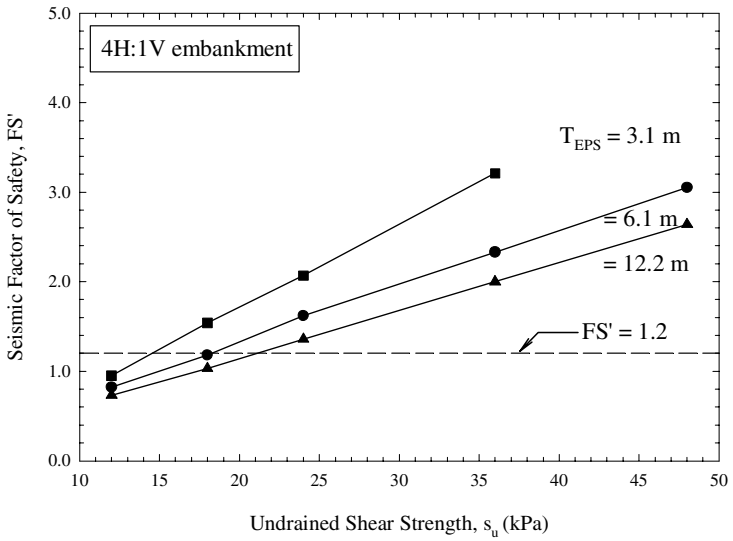

FIGURE 5.25 PROJ 24-11.doc

23 m pavement, k_h=0.20

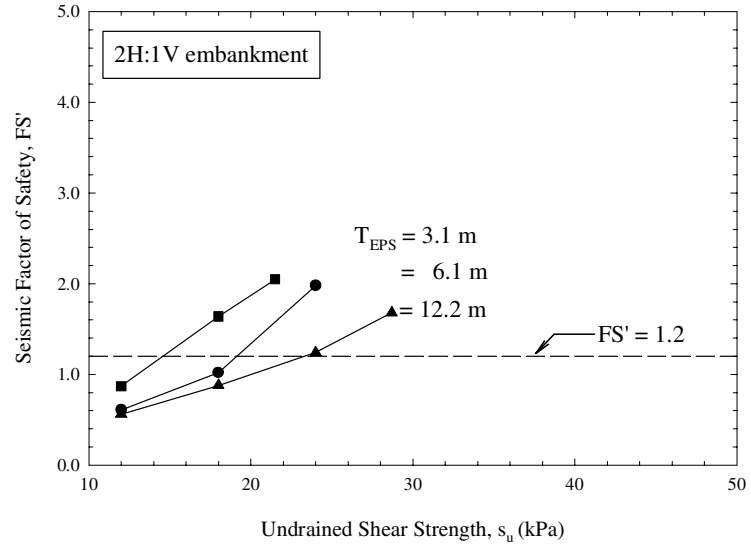

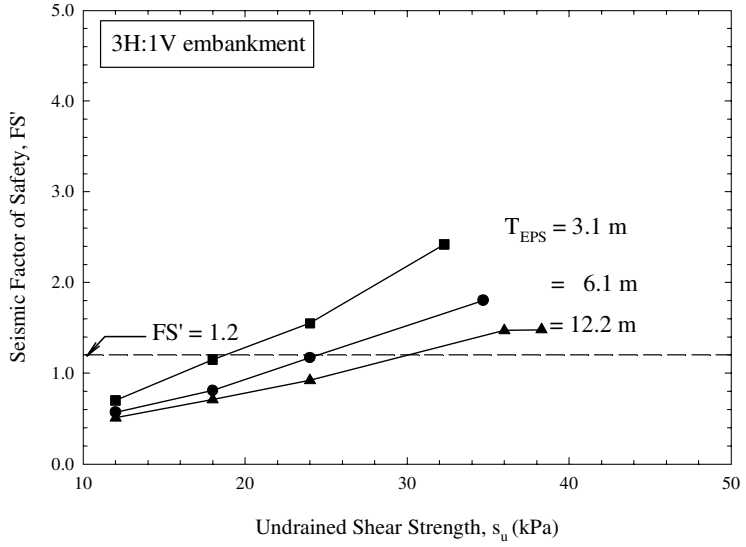

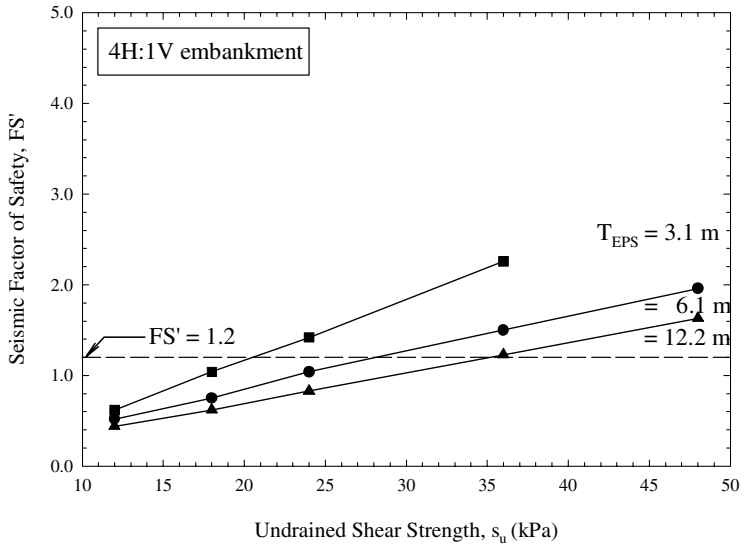

FIGURE 5.26 PROJ 24-11.doc

34 m pavement, k_h=0.05

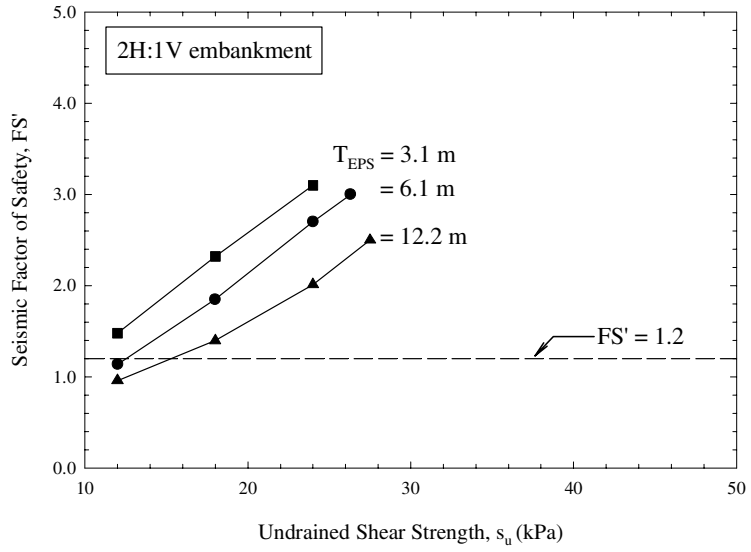

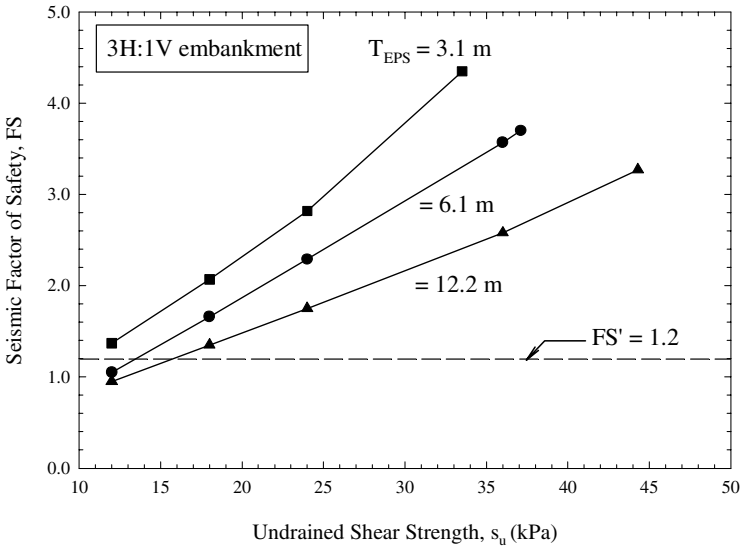

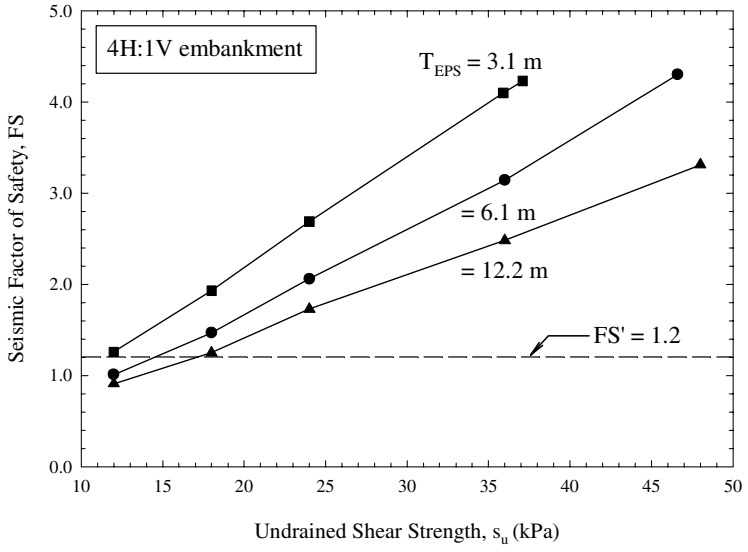

FIGURE 5.27 PROJ 24-11.doc

34 m pavement, k_h=0.10

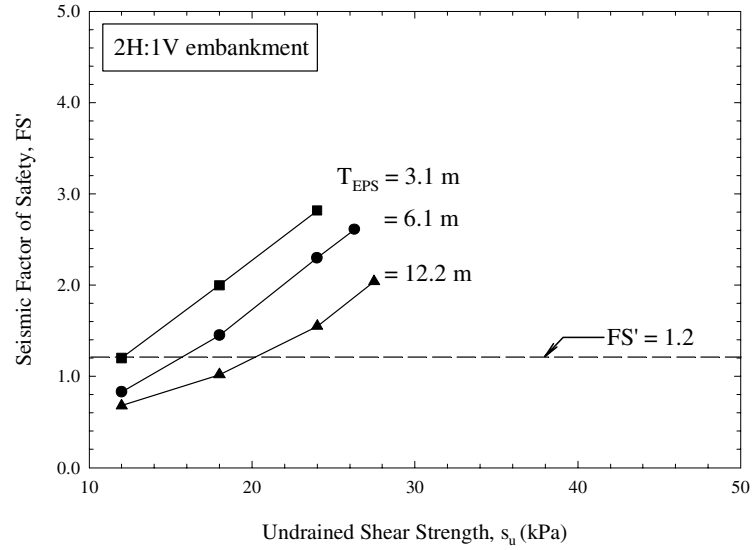

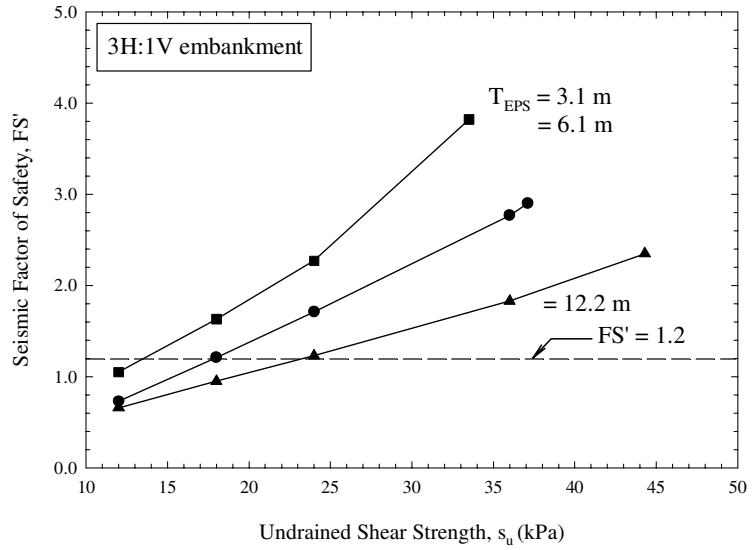

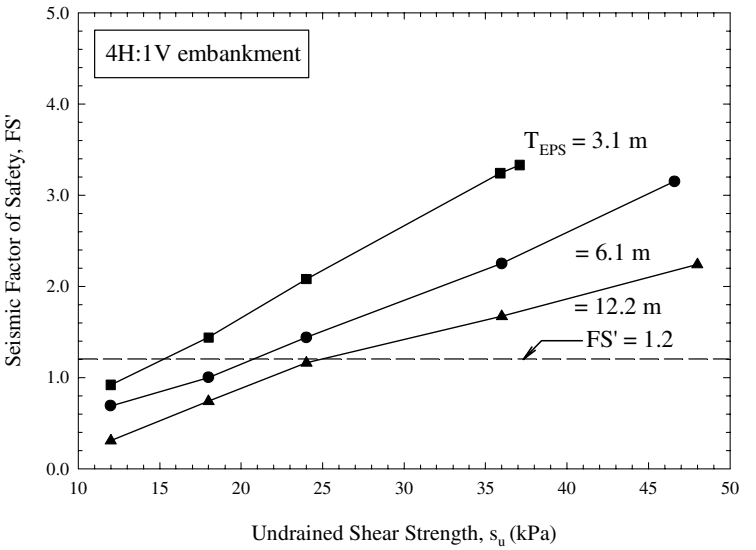

FIGURE 5.28 PROJ 24-11.doc

34 m pavement, k_h=0.20

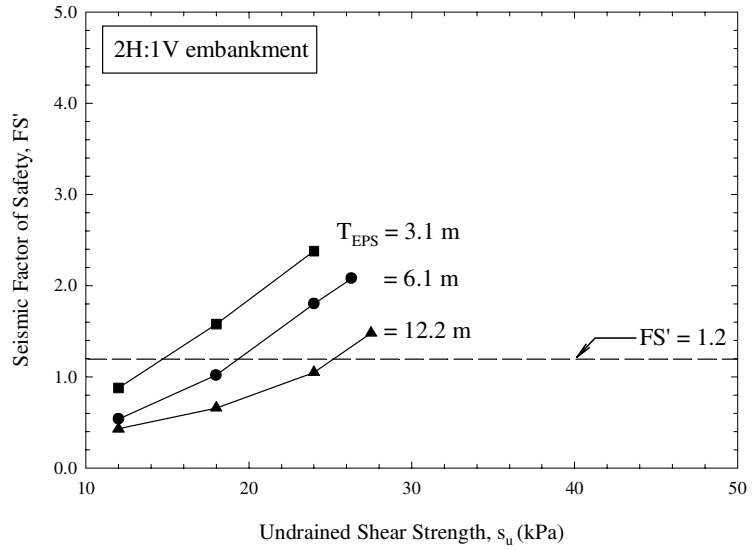

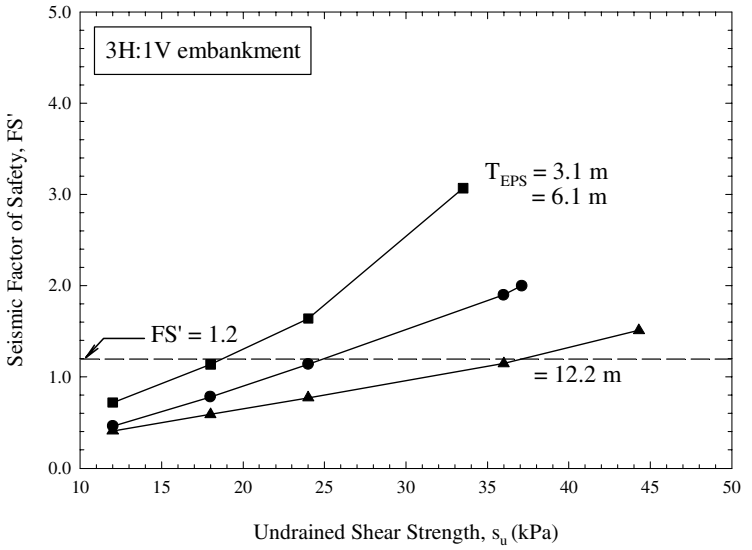

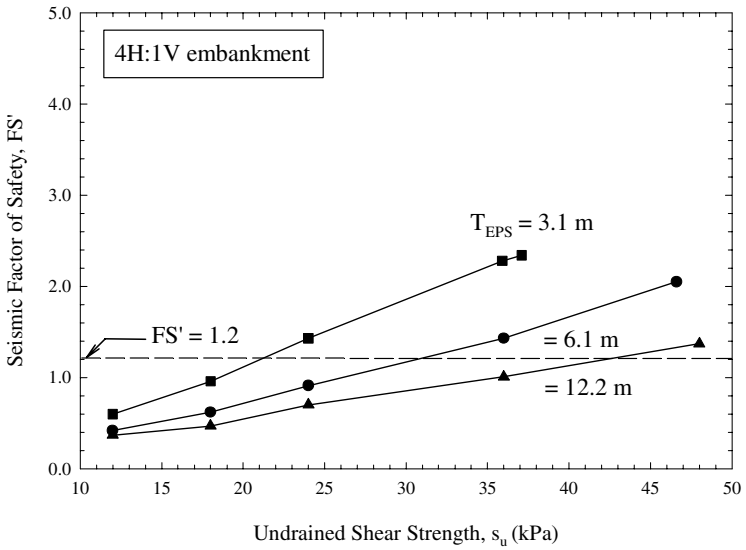

FIGURE 5.29 PROJ 24-11.doc

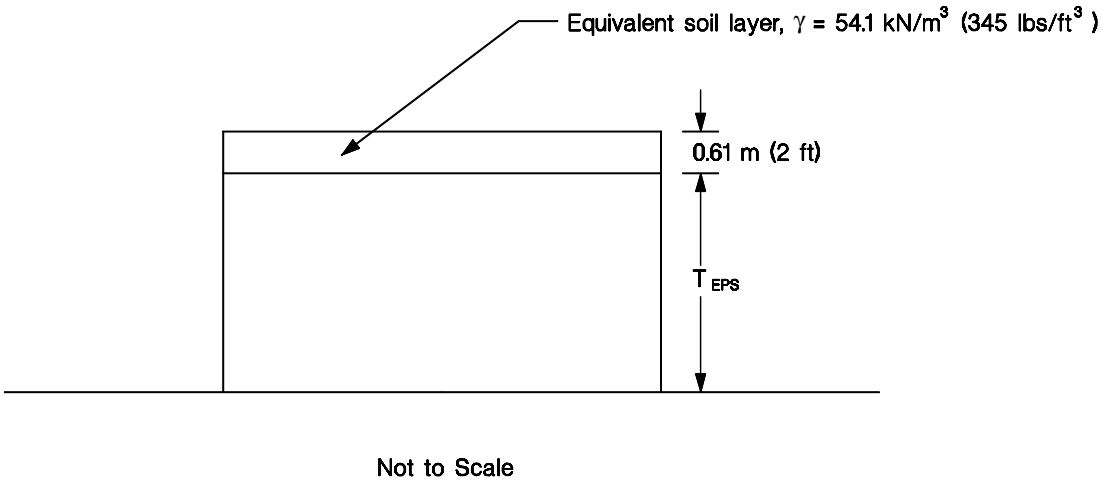

FIGURE 5.30 PROJ 24-11.doc

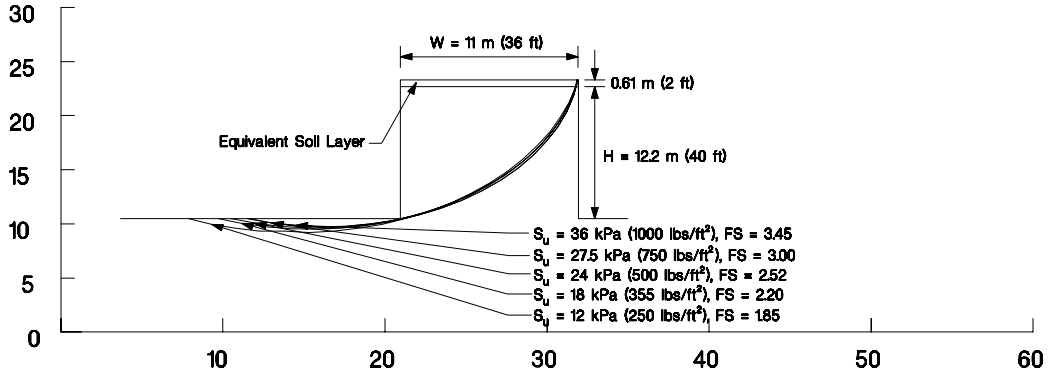

FIGURE 5.31A PROJ 24-11.doc

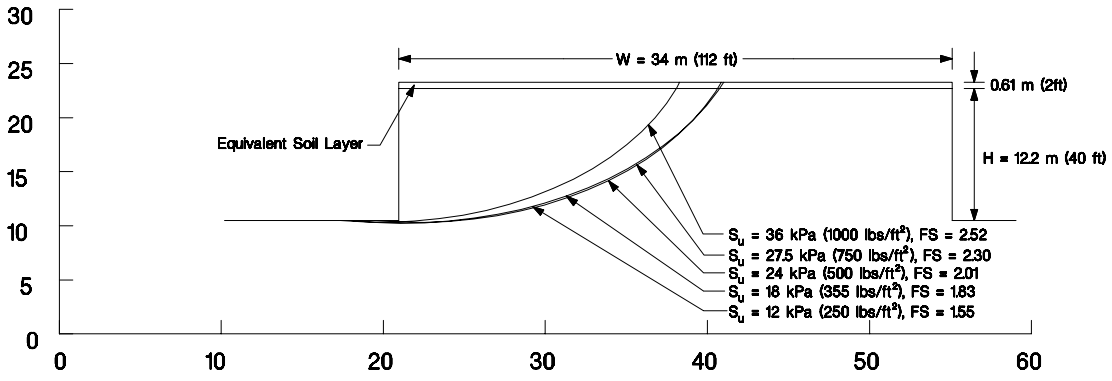

FIGURE 5.31B PROJ 24-11.doc

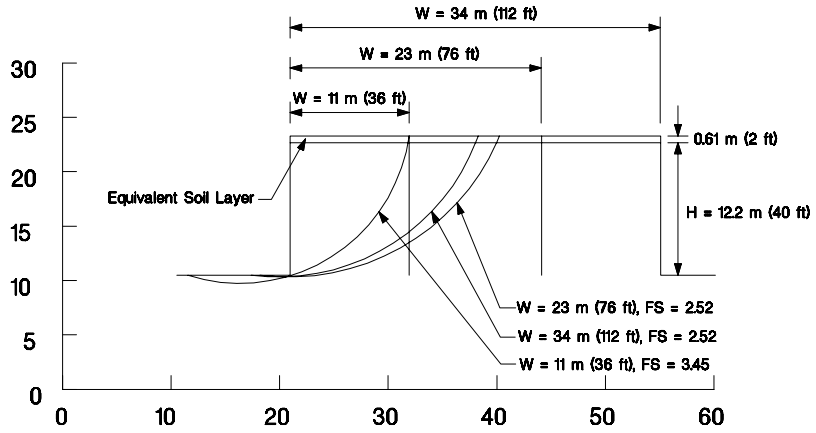

FIGURE 5.32 PROJ 24-11.doc

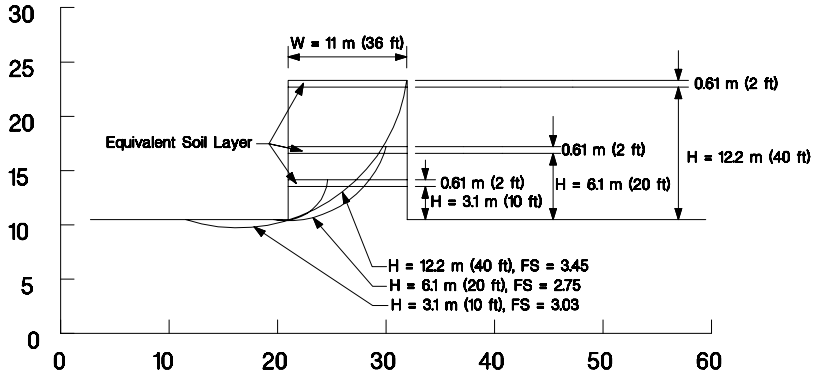

FIGURE 5.33 PROJ 24-11.doc

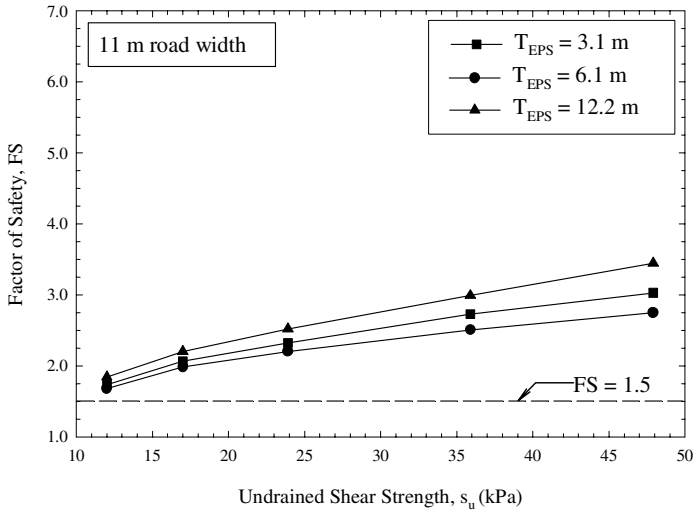

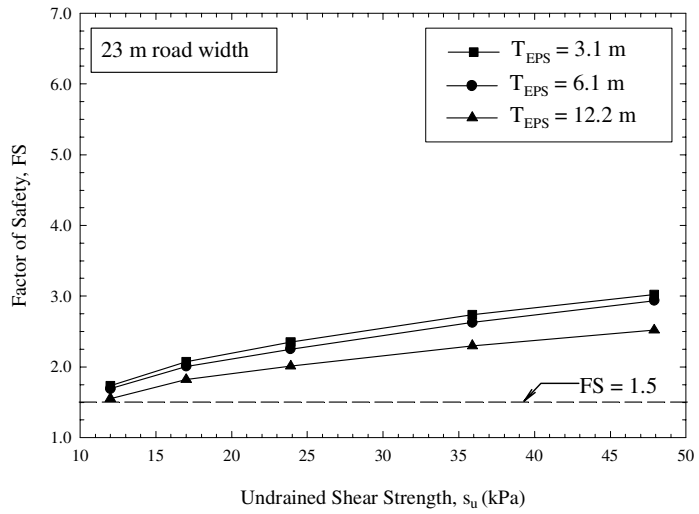

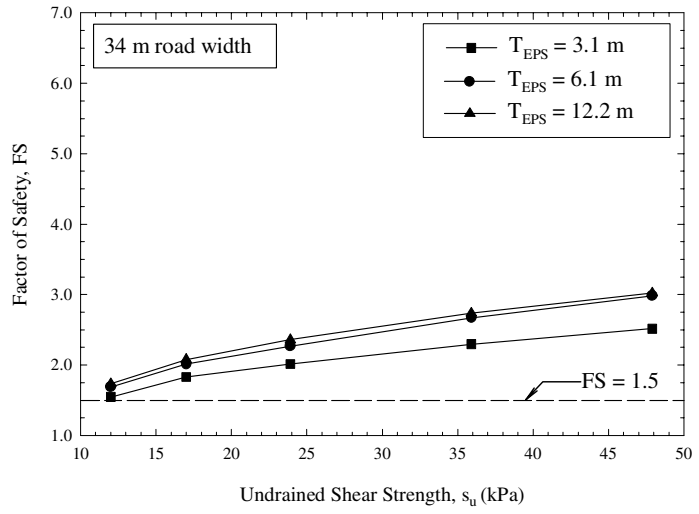

FIGURE 5.34 PROJ 24-11.doc

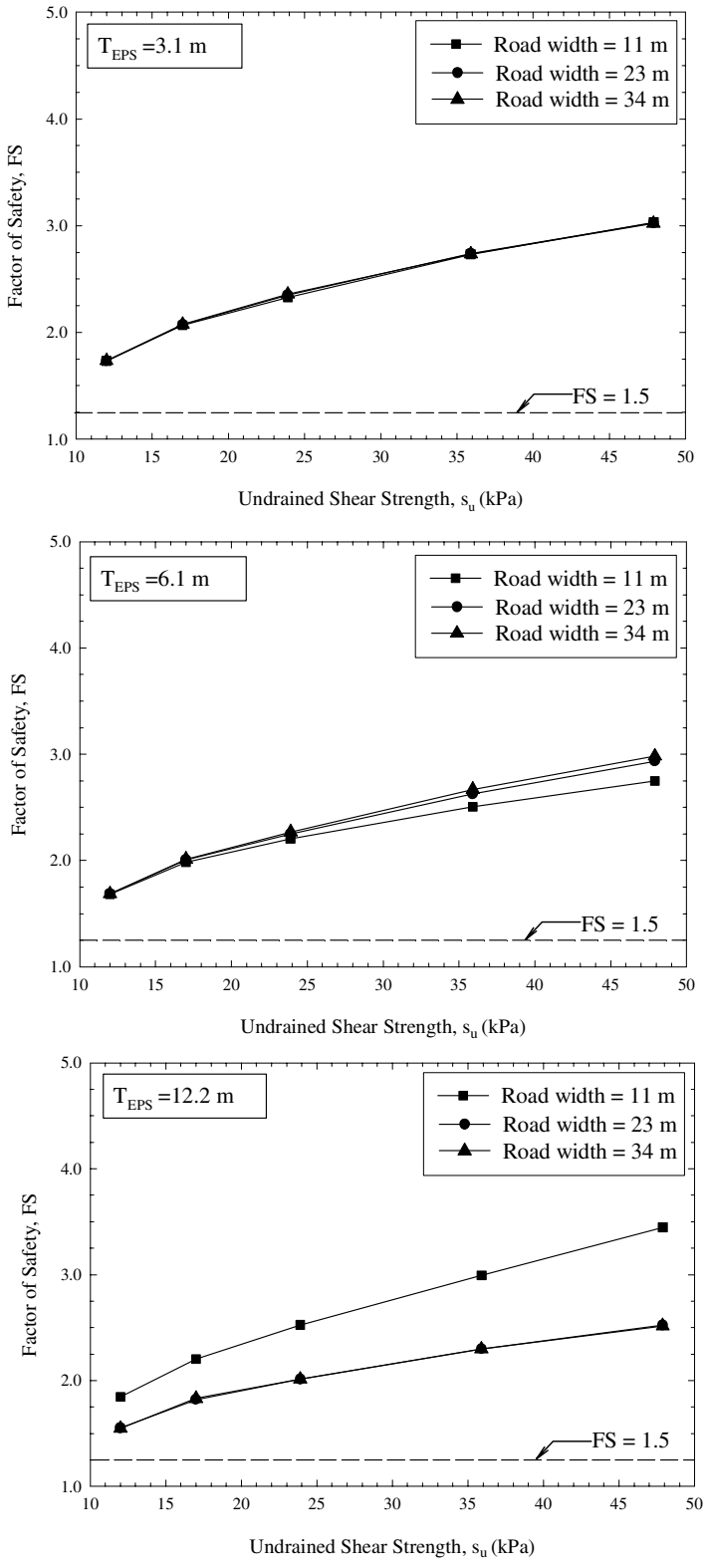

FIGURE 5.35 PROJ 24-11.doc

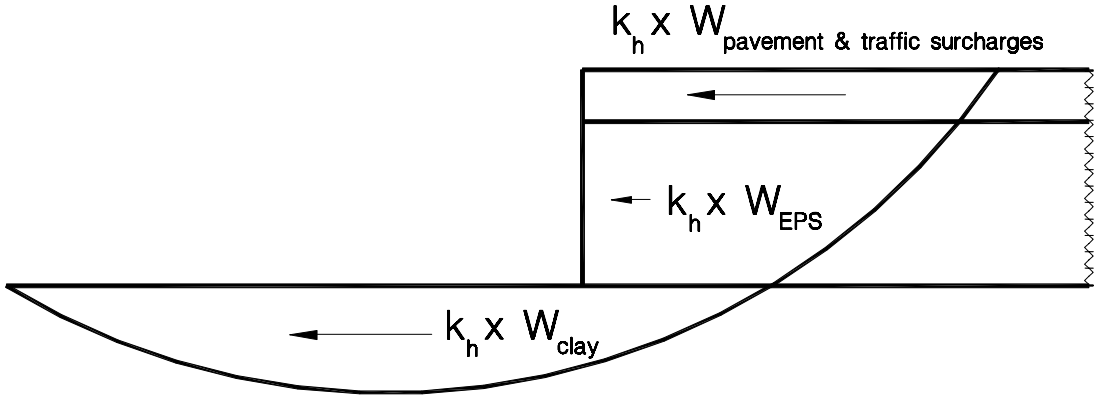

FIGURE 5.36 PROJ 24-11.doc

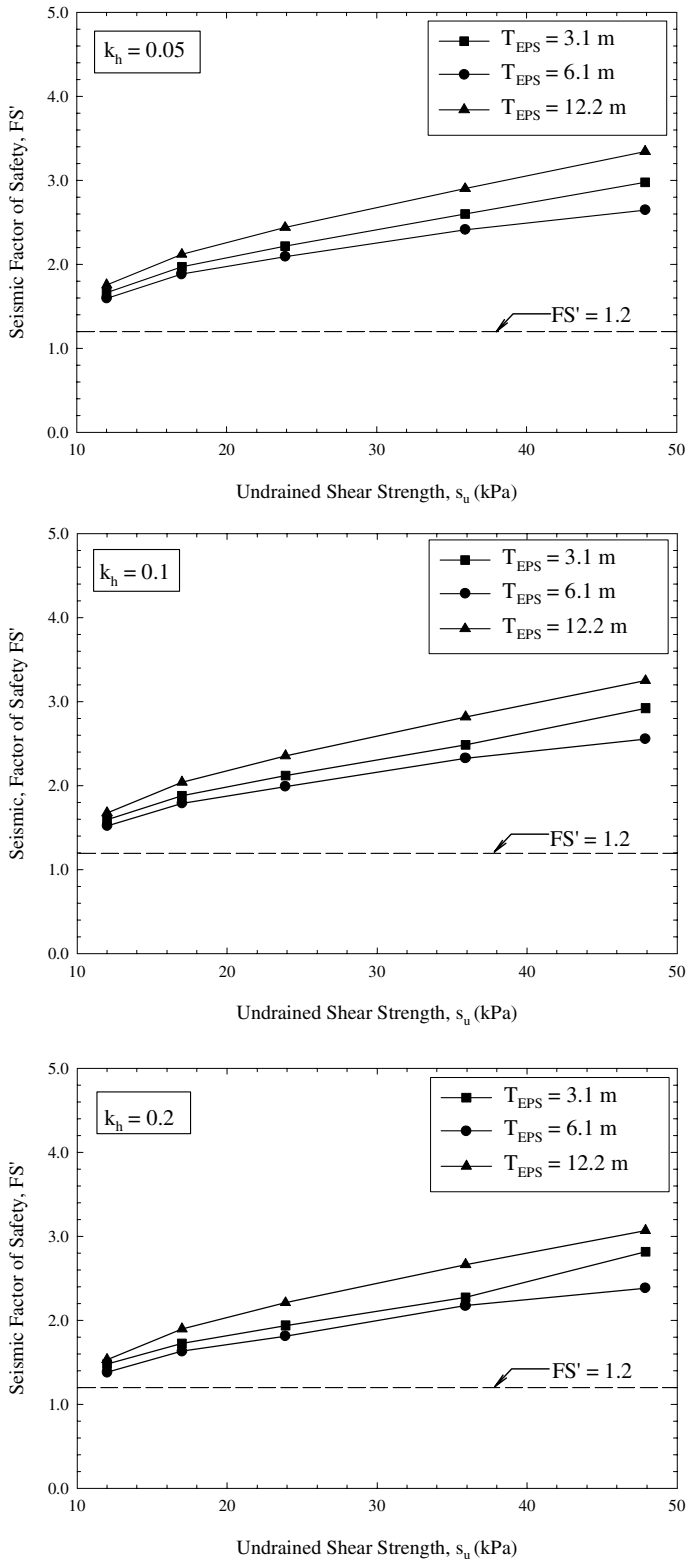

FIGURE 5.37 PROJ 24-11.doc

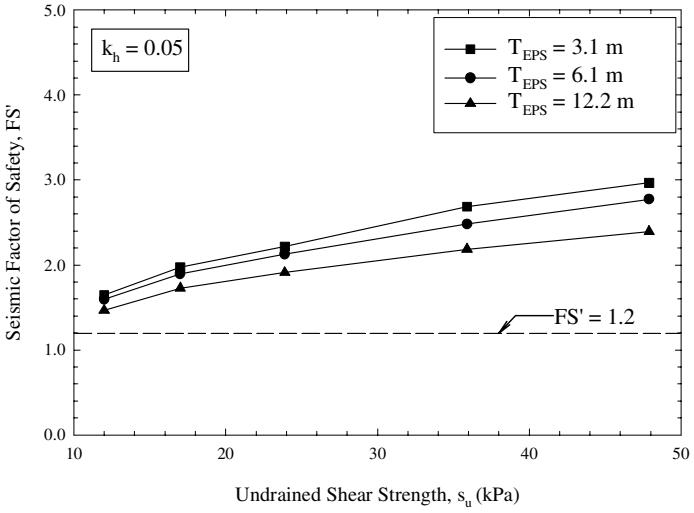

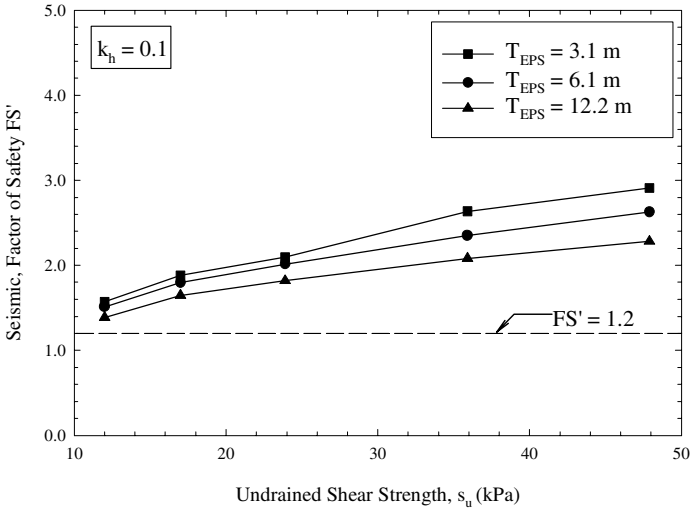

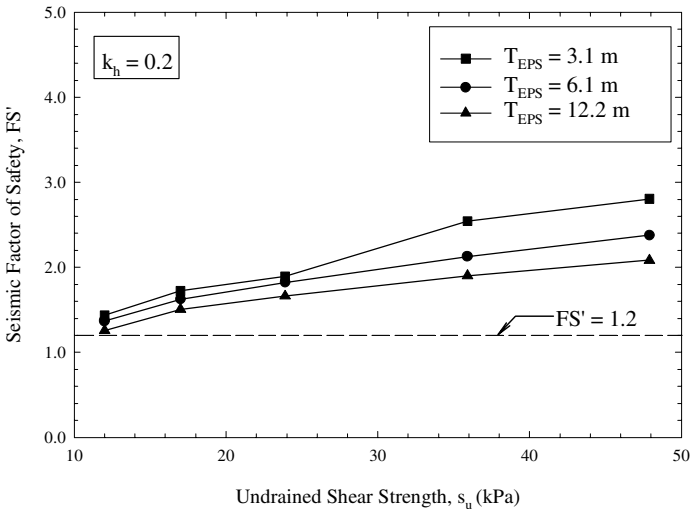

FIGURE 5.38 PROJ 24-11.doc

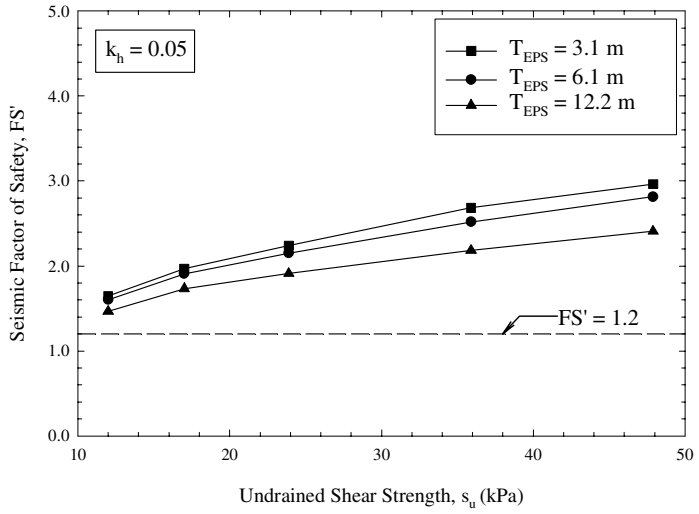

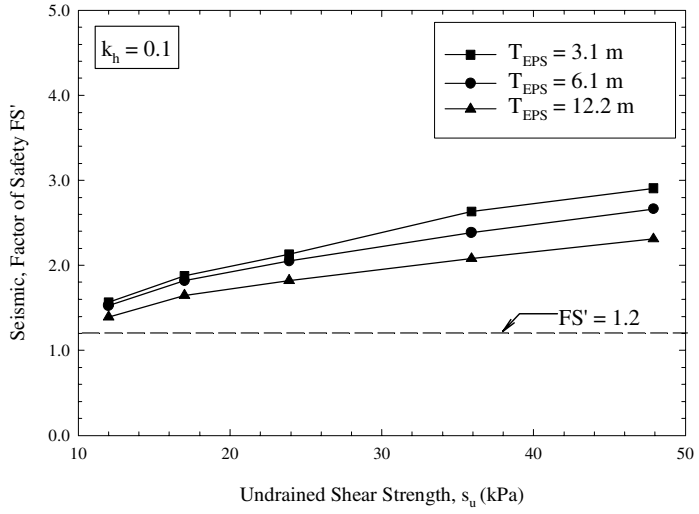

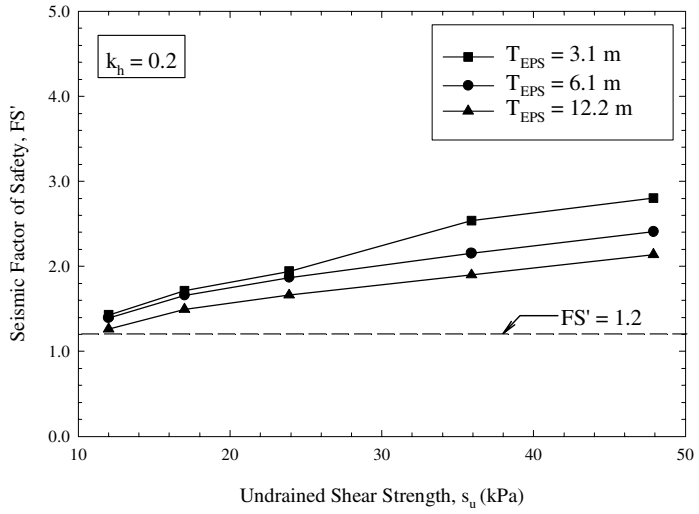

FIGURE 5.39 PROJ 24-11.doc

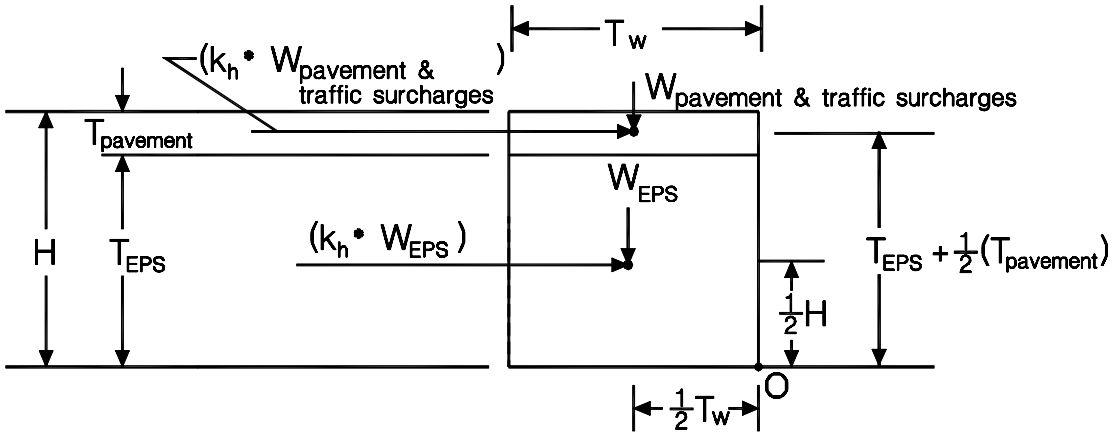

FIGURE 5.40 PROJ 24-11.doc

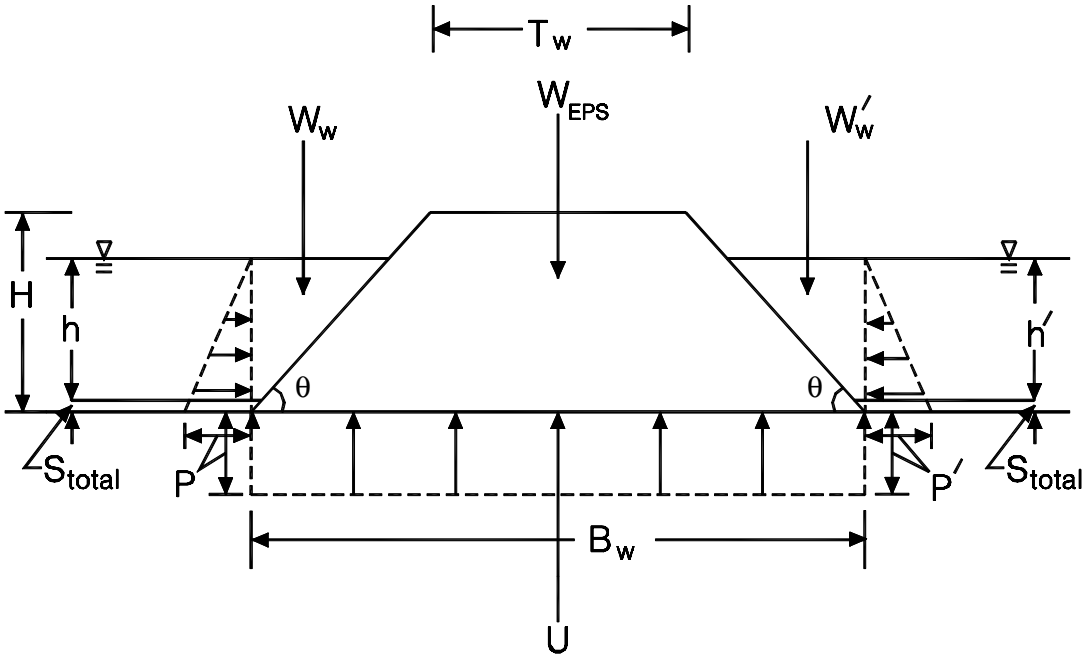

FIGURE 5.41 PROJ 24-11.doc

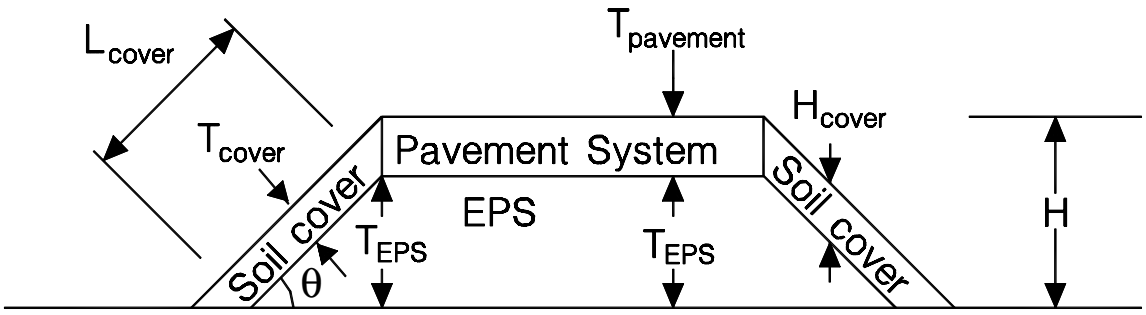

FIGURE 5.42 PROJ 24-11.doc

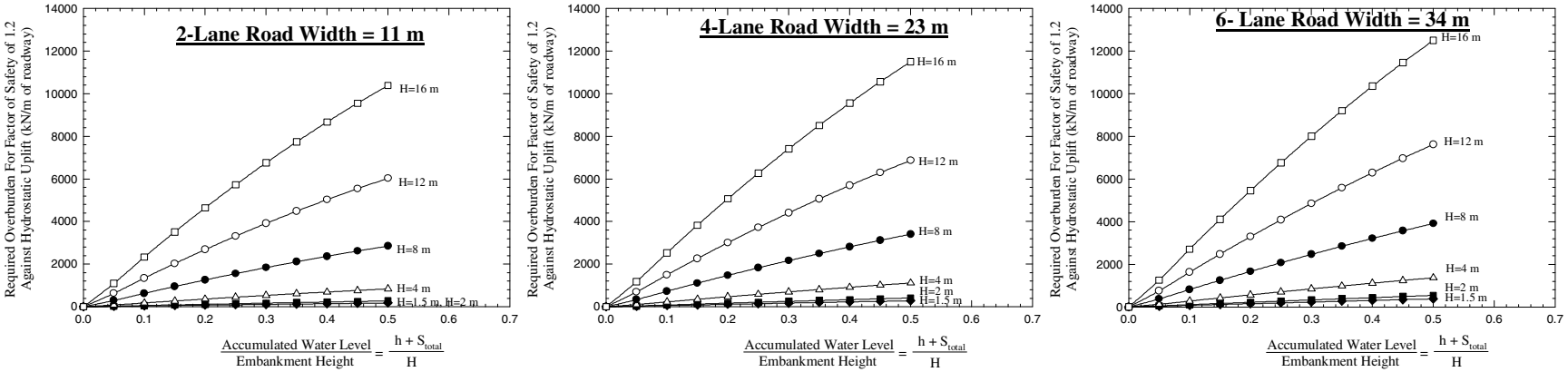

FIGURE 5.43 PROJ 24-11.doc

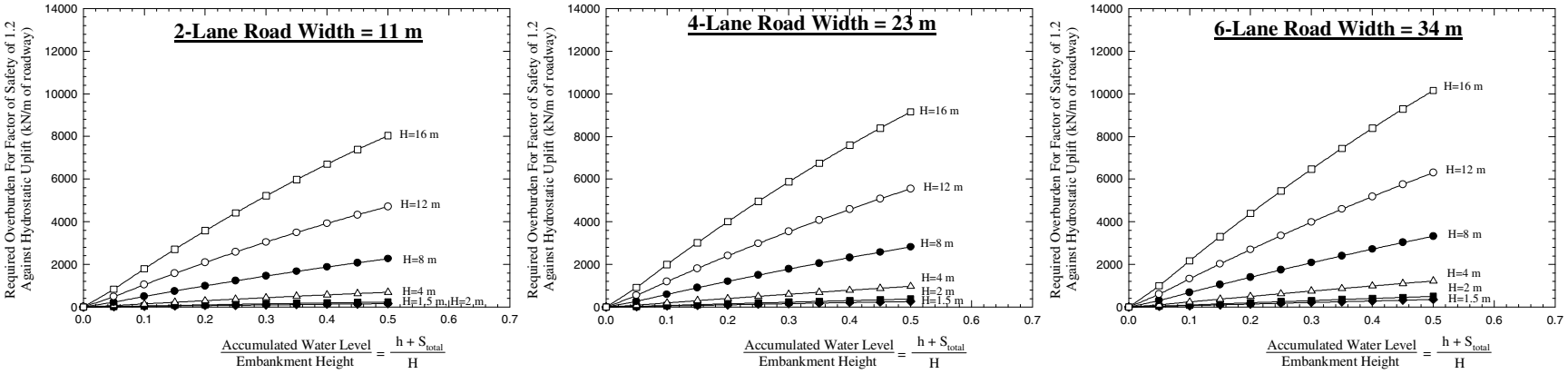

FIGURE 5.44 PROJ 24-11.doc

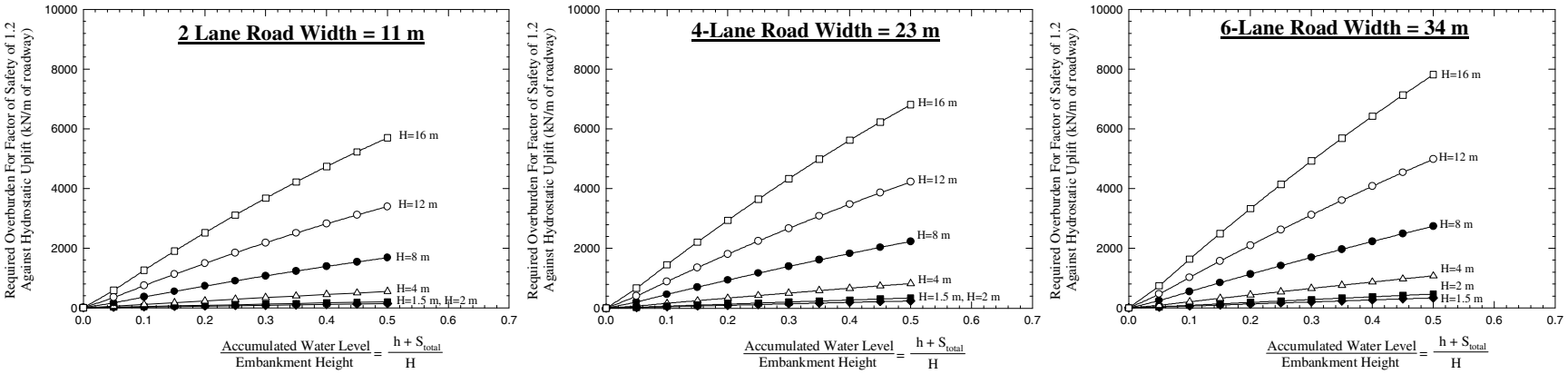

FIGURE 5.45 PROJ 24-11.doc

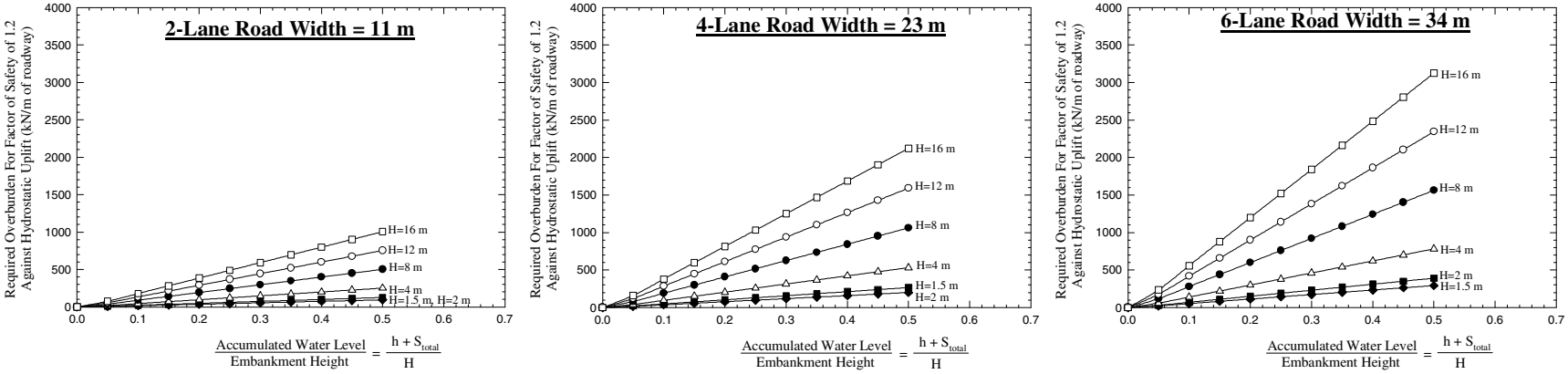

FIGURE 5.46 PROJ 24-11.doc

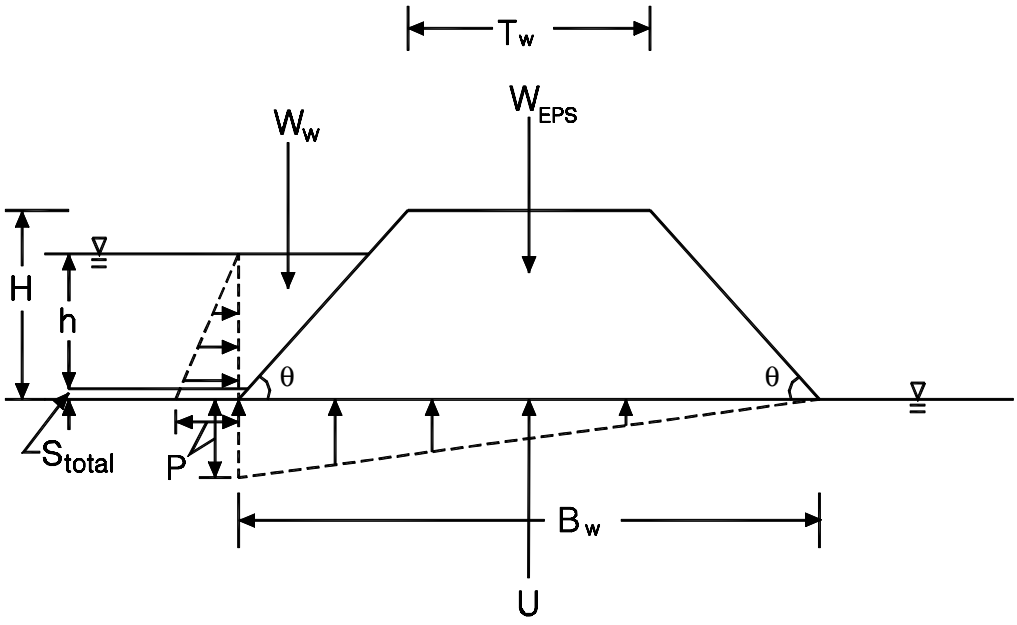

FIGURE 5.47 PROJ 24-11.doc

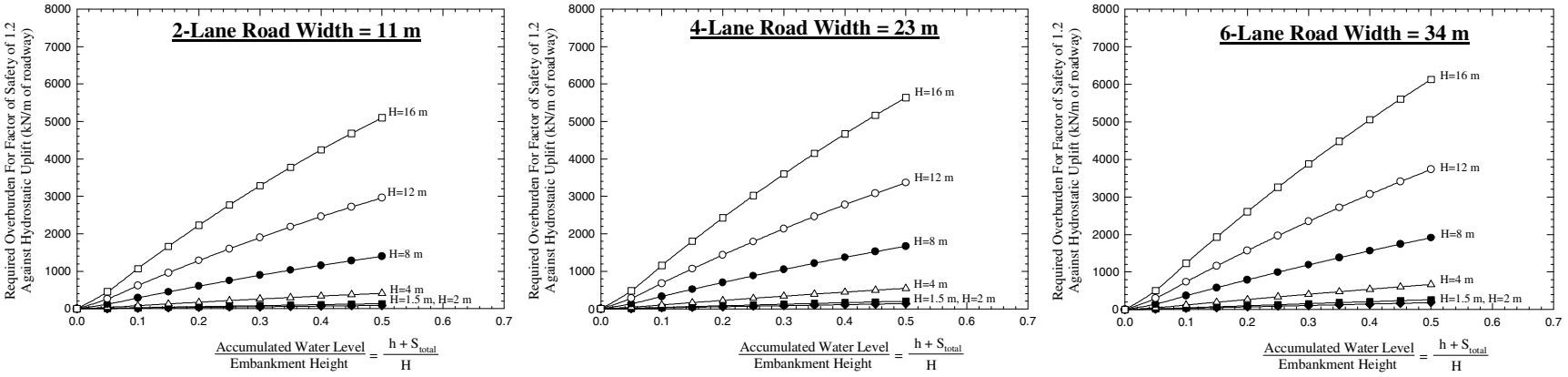

FIGURE 5.48 PROJ 24-11.doc

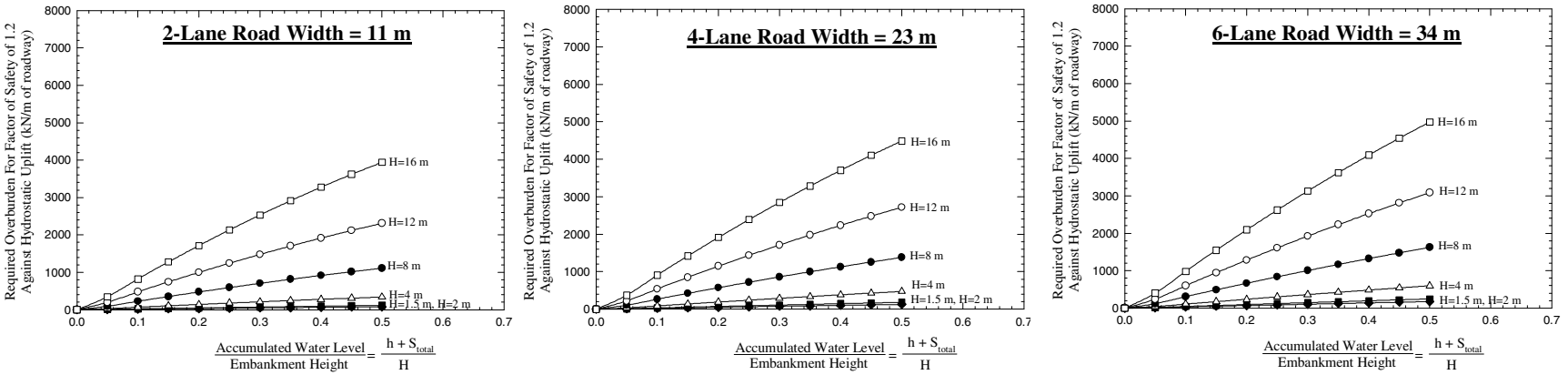

FIGURE 5.49 PROJ 24-11.doc

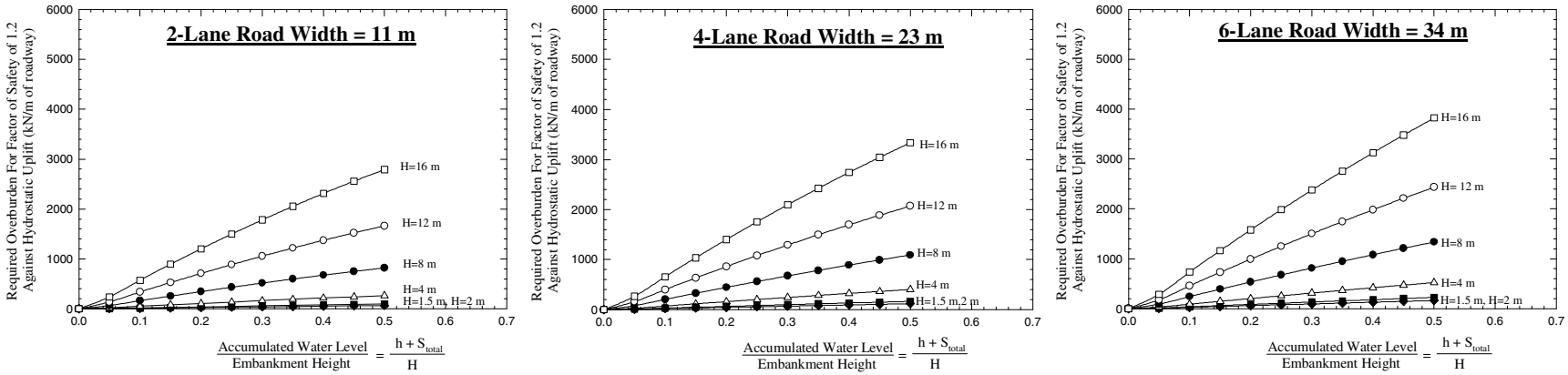

FIGURE 5.50 PROJ 24-11.doc

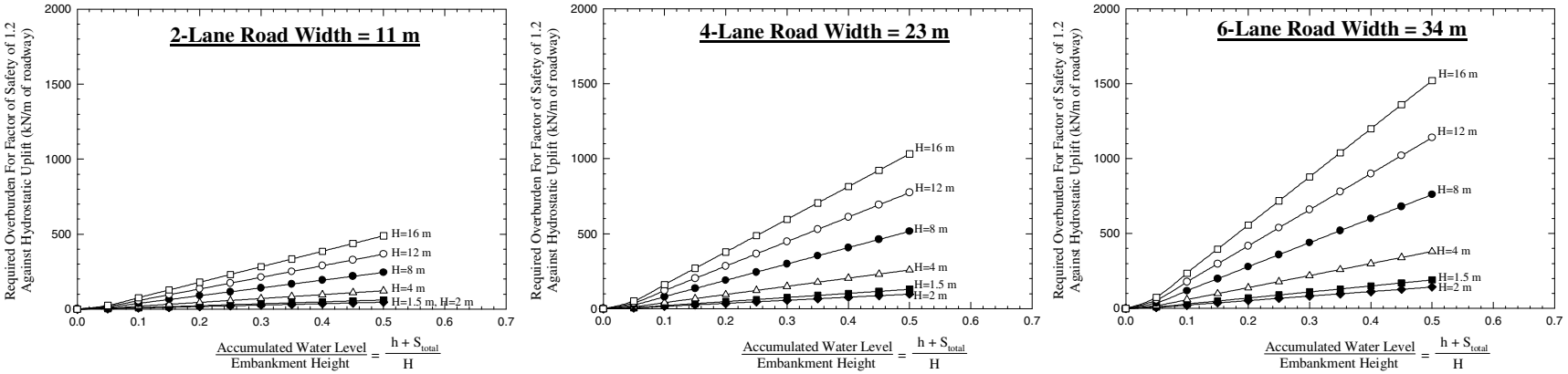

FIGURE 5.51 PROJ 24-11.doc

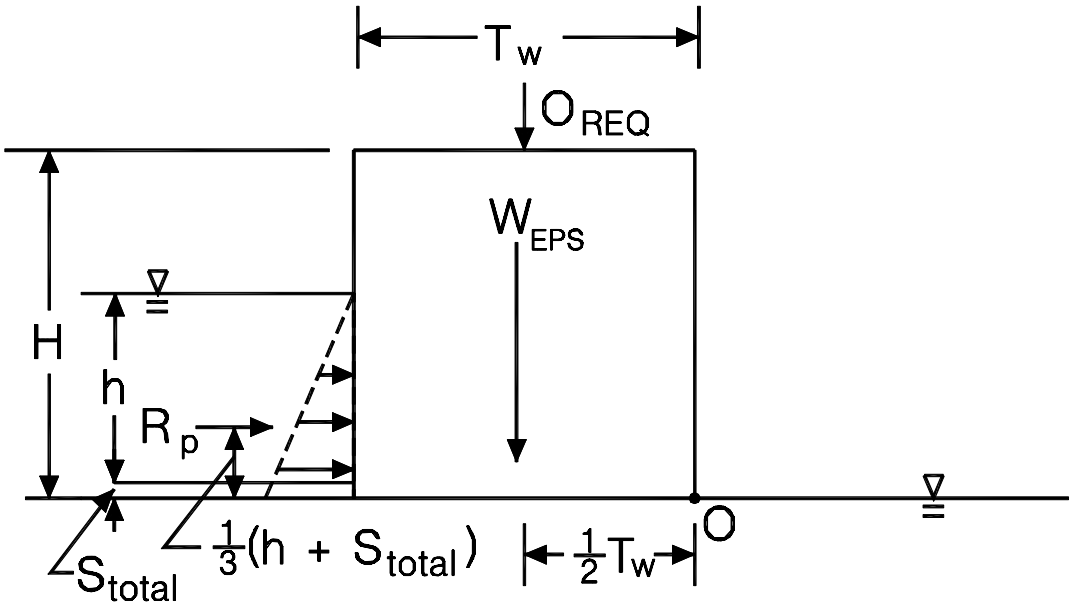

FIGURE 5.52 PROJ 24-11.doc

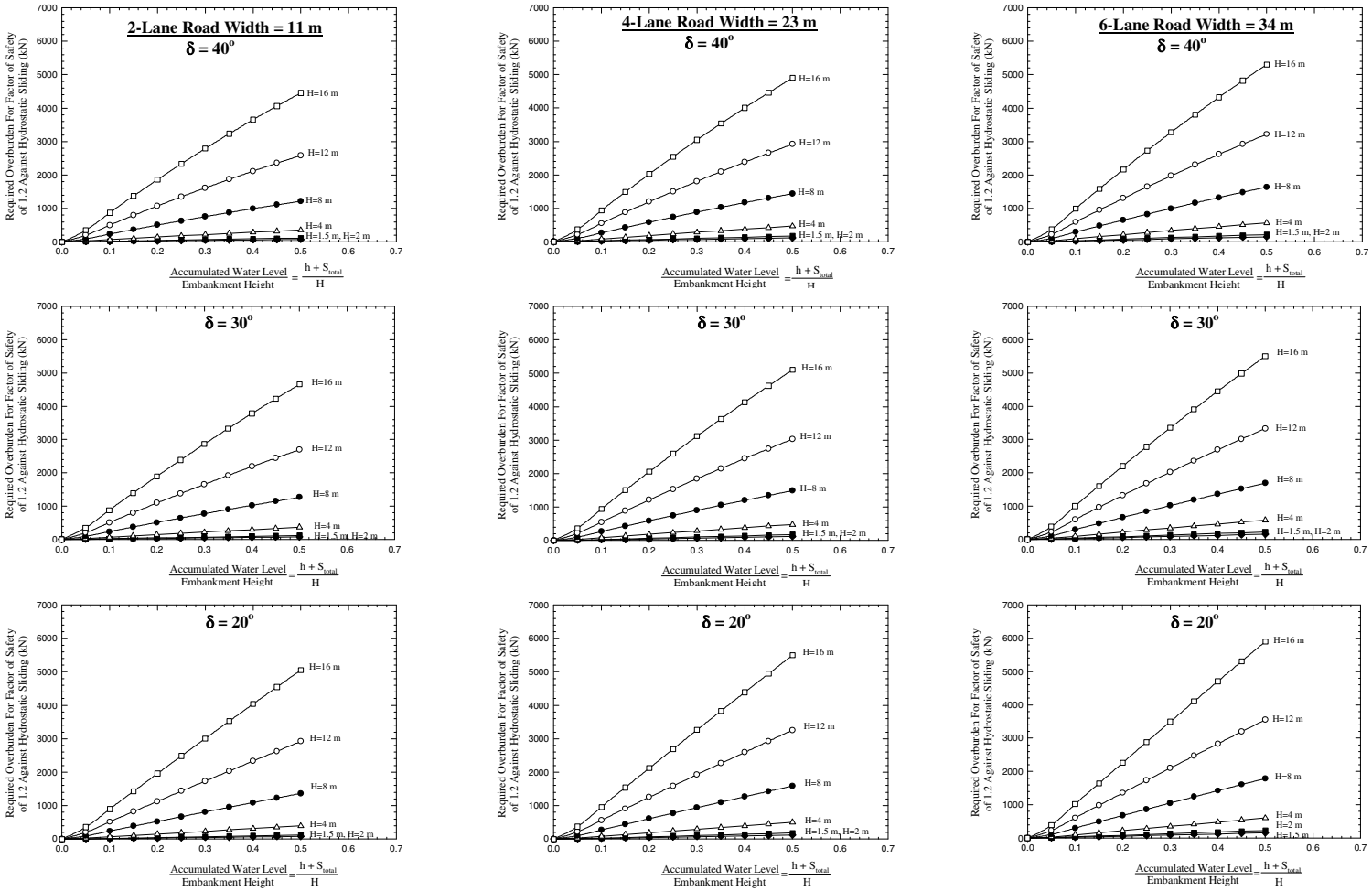

FIGURE 5.53 PROJ 24-11.doc

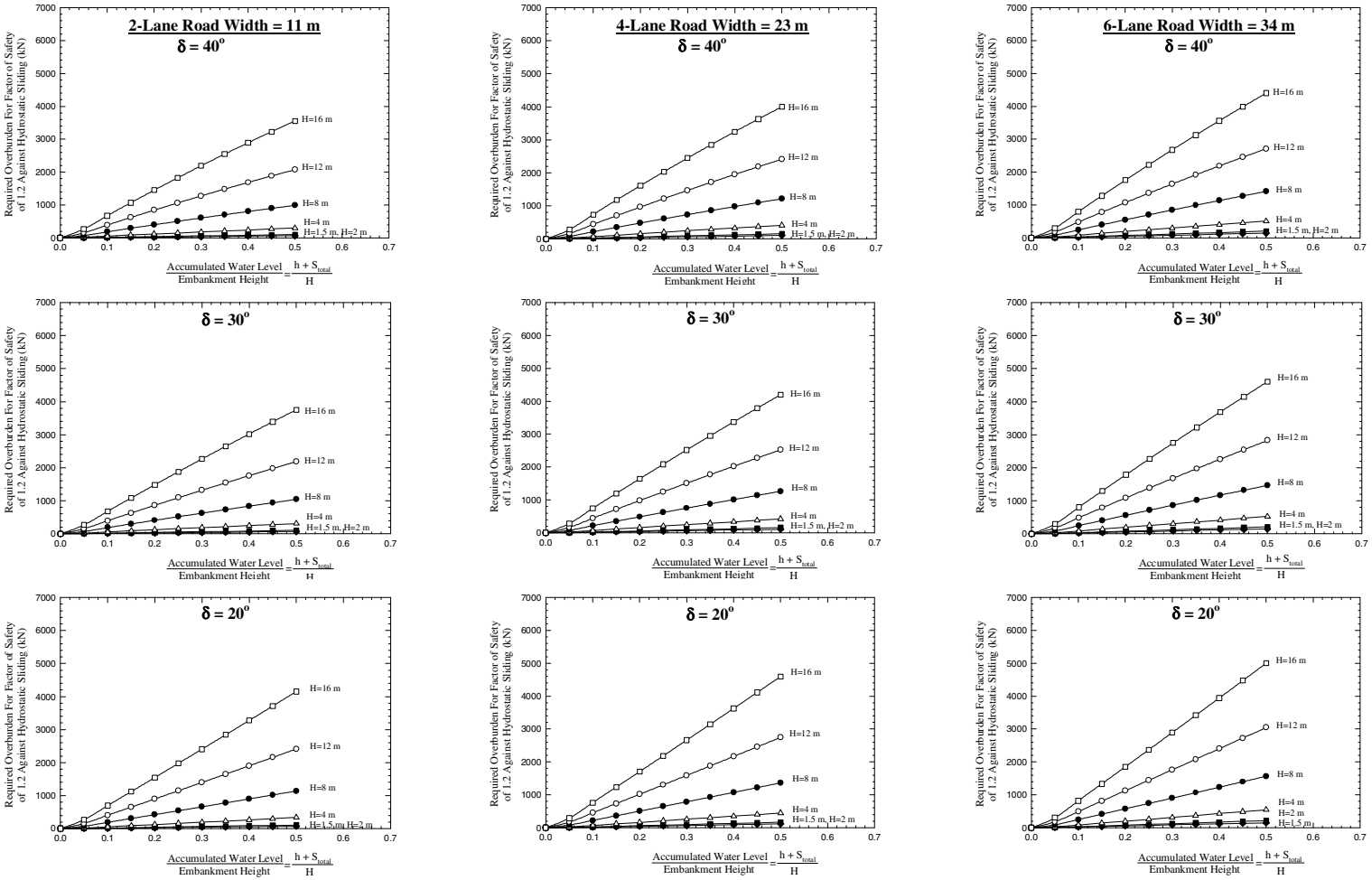

FIGURE 5.54 PROJ 24-11.doc

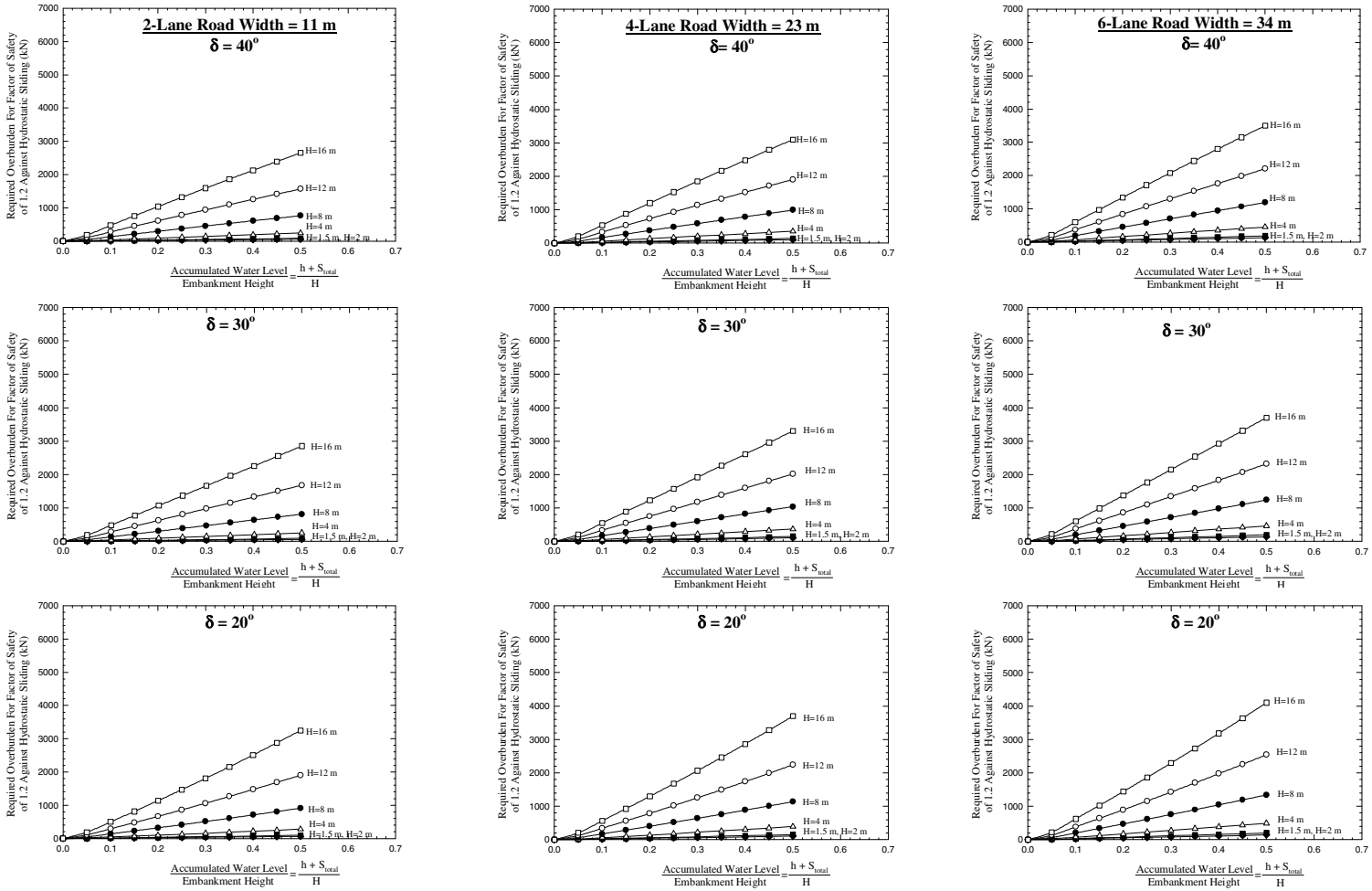

FIGURE 5.55 PROJ 24-11.doc

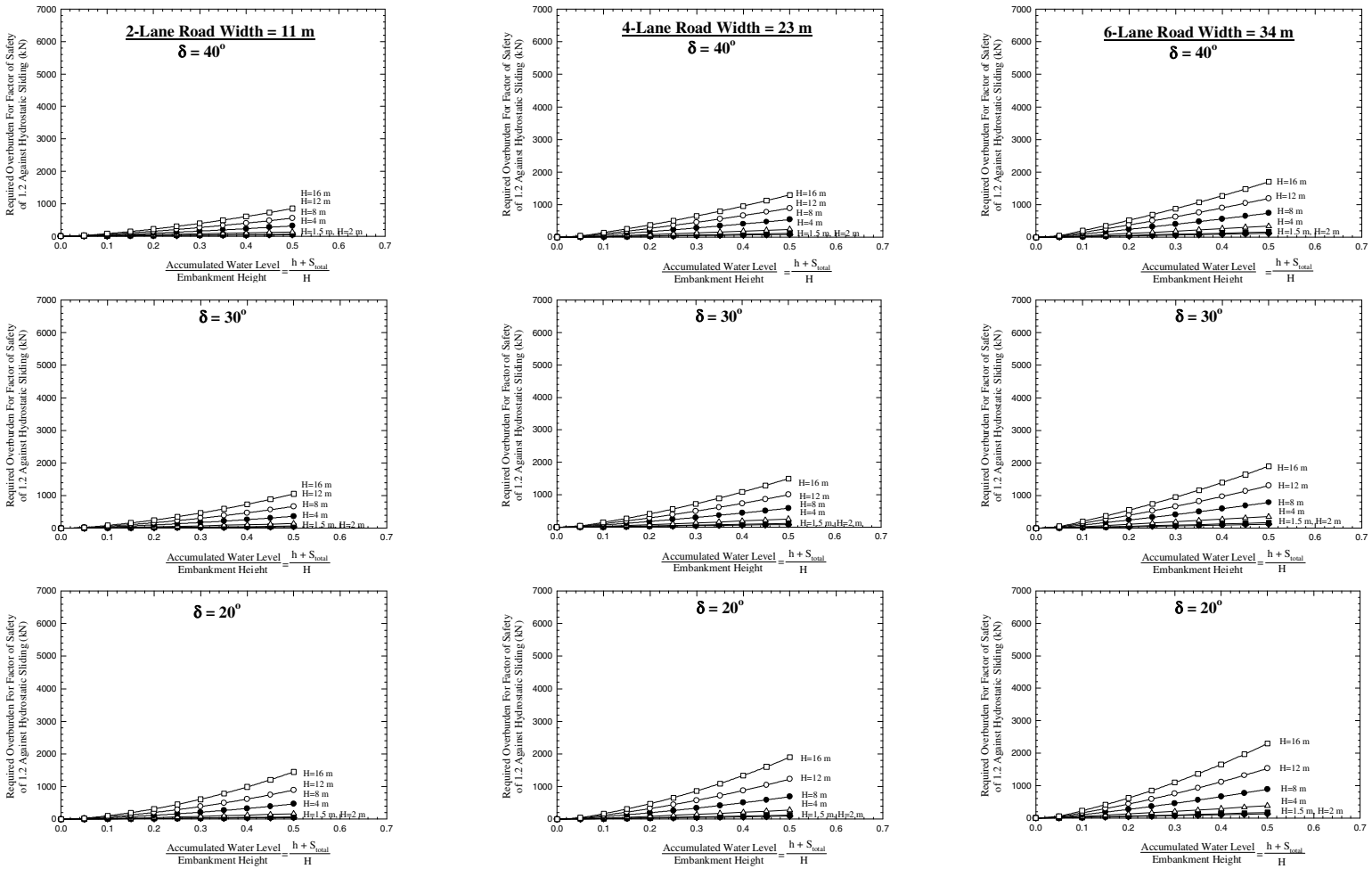

FIGURE 5.56 PROJ 24-11.doc

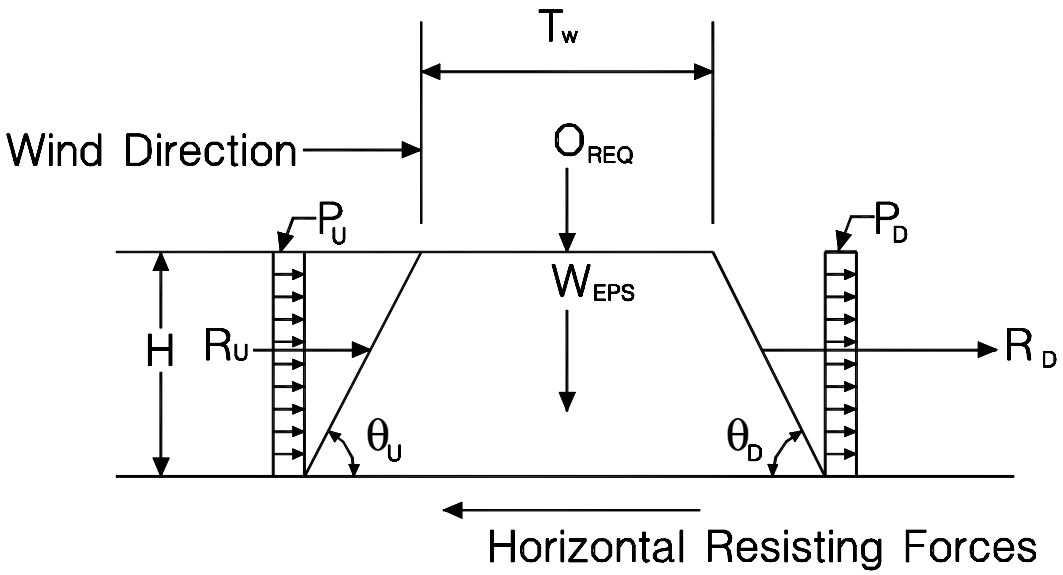

FIGURE 5.57 PROJ 24-11.doc

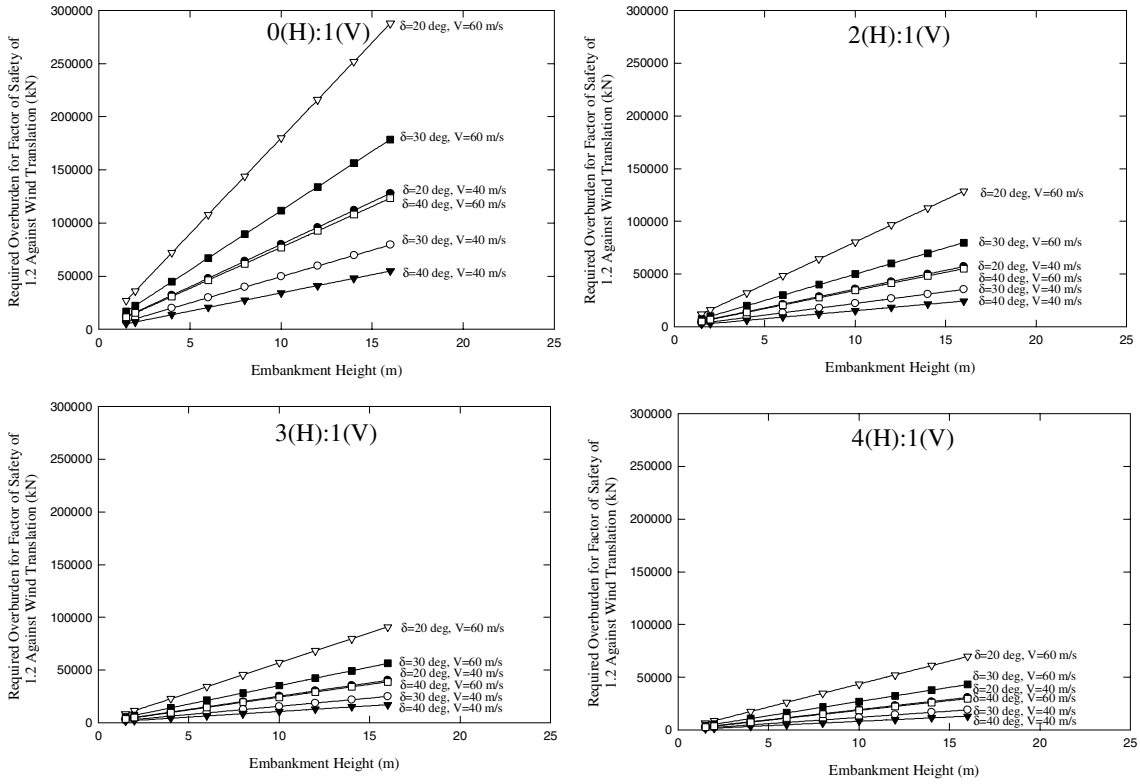

FIGURE 5.58 PROJ 24-11.doc

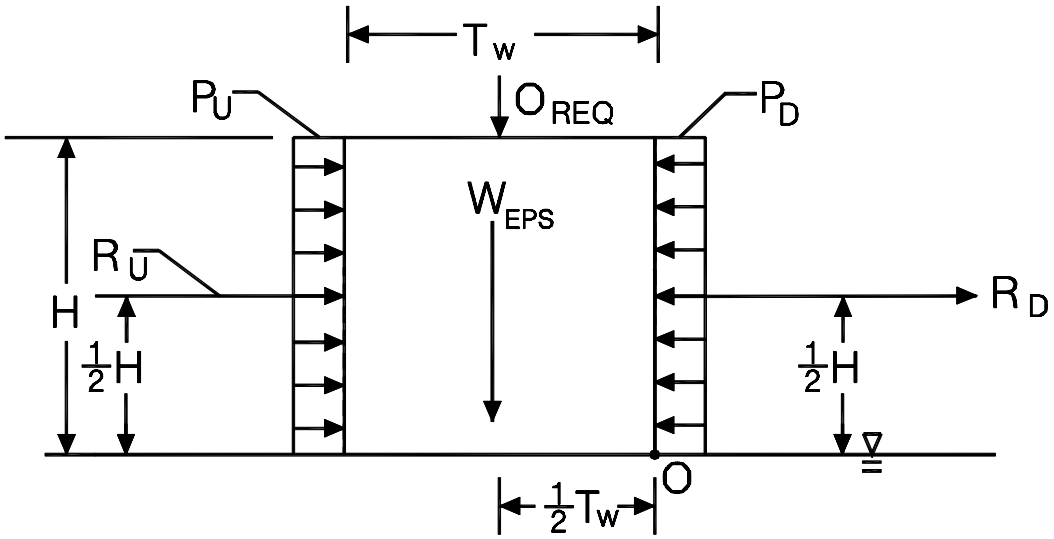

FIGURE 5.59 PROJ 24-11.doc

Material	**C_α/C_c**
Inorganic clays and silts	0.04 ± 0.01
Organic clays and silts	0.05 ± 0.01
Peat and Muskeg	0.06 ± 0.01

			Total Stress Shear Strength Parameters		Effective Stress Shear Strength Parameters	
Material	**Moist Unit Weight, γ_{moist} kN/m^3 (lbf/ft^3)**	**Saturated Unit Weight, γ_{sat} kN/m^3 (lbf/ft^3)**	**Friction Angle, ϕ, (^{o})**	**Undrained Shear Strength, s_u kPa (lbs/ft^2)**	**Friction Angle, ϕ' (^{o})**	**Cohesion, c' kPa (lbs/ft^2)**
Soil cover	18.9 (120)	19.6 (125)	N/A	N/A	28	0
EPS-block Geofoam	1 (6.4)	1 (6.4)	N/A	36.3 (758)	N/A	N/A
Soft underlying clay	15.7 (100)	15.7 (100)	0	12.0, 23.9, 35.9, 47.9 (250, 500, 750, 1,000)	N/A	N/A

Note: N/A = not applicable

Undrained Shear Strength, s_u kPa (lbs/ft^2)	**S_E / S_F**	**R_E**
12.0 (250)	3.0	0.62
17.0 (375)	2.0	0.71
23.9 (500)	1.5	0.75
35.9 (750)	1.0	0.80
47.9 (1,000)	0.75	0.82

Material Designation	Dry Density/Unit Weight for Block as a Whole, kg/m^3 (lbf/ft^3)	Initial Tangent Young's Modulus, MPa (lbs/in^2)	Poisson's Ratio	Shear Modulus G MPa(lbs/in^2)
EPS40	16 (1.0)	4 (580)	0.09	1.8 (266)
EPS50	20 (1.25)	5 (725)	0.11	2.3 (327)
EPS70	24 (1.5)	7 (1015)	0.14	3.1 (445)
EPS100	32 (2.0)	10 (1450)	0.18	4.2 (614)

Note: Shear modulus is based on the following equation:

$$G = \frac{E_{ti}}{2(1+\nu)}. \qquad \textbf{(5.53)}$$

δ	Slope (H:V)	T_W m (ft)	H m (ft)	V m/s (mi/hr)	O_{REQ}* kN/m (kip/ft)	Equivalent Pavement System thickness ** m (ft)
20˚	4:1	11 (36)	2 (6.6)	40 (90)	3,870 (265)	17.2 (56)
20˚	0:1	11 (36)	2 (6.6)	40 (90)	15,990 (1,096)	72.3 (237)
40˚	4:1	11 (36)	2 (6.6)	40 (90)	1,656 (114)	7.2 (24)
40˚	0:1	11 (36)	2 (6.6)	40 (90)	6,852 (470)	30.8 (101)

Note: *O_{REQ} at FS = 1.2

** Based on an equivalent overall pavement system unit weight of 20 kN/m³ (125 lbf/ft^3).

CHAPTER **6**

INTERNAL STABILITY EVALUATION OF GEOFOAM EMBANKMENTS

Contents

INTRODUCTION

Design for internal stability of an EPS-block geofoam embankment involves consideration of EPS block behavior under various loadings, which are discussed in this chapter and illustrated via the design examples in Chapter 7. Internal stability in the proposed design procedure includes consideration of Serviceability Limit State (SLS) issues such as the proper selection and specification of EPS properties so the geofoam mass can provide adequate load bearing capacity to the overlying pavement system without excessive settlement and Ultimate Limit State (ULS) issues such as translation due to water (hydrostatic sliding), translation due to wind, and seismic stability (See Table 3.1). The evaluation of these three internal ULS failure mechanisms involves determining whether the geofoam embankment will behave as a single, coherent mass when subjected to external loads. This is determined by the shear resistance between the pavement system and the upper surface of the EPS mass and the interface friction between adjacent EPS blocks. Therefore, a discussion of methods that can be used to insure adequate block interlock is presented prior to describing the various internal stability analyses for translation due to water and wind and seismic shaking.

Another internal stability issue involves the long-term durability of EPS blocks. To the extent that durability affects the in-situ and long-term mechanical properties of the EPS blocks, it must be considered as part of the internal stability assessment of an embankment and is discussed in this chapter. Other issues that impact internal stability include site preparation, type of cover material placed on the sides of the embankment, and utility placement.

This Chapter presents detailed background information on the internal stability aspect of the EPS-block geofoam design methodology. An abbreviated form of the internal stability design procedure can be found in the provisional design guideline included in Appendix B.

BLOCK INTERLOCK

Although a lightweight fill embankment constructed using EPS-block geofoam will consist of a large number of individual blocks, current design procedures assume that the geofoam acts as a single, coherent mass when subjected to external loads (*1,2*). An EPS-block geofoam embankment will behave as a coherent mass if the individual EPS blocks exhibit vertical and horizontal interlock. Sufficient interlock between blocks involves consideration of the overall block layout (which primarily controls interlocking in a vertical direction) and inter-block shear (which primarily controls interlocking in the horizontal direction), both of which are discussed subsequently.

Block Layout

Guidelines for an appropriate layout of EPS blocks to obtain adequate interlocking in the vertical direction are summarized in Chapter 8. These guidelines include recommended block placement patterns for roadway embankments and inter-block resistance as described below.

Inter-Block Shear Resistance

EPS/EPS interface shear resistance and any interlocking along the horizontal interfaces between layers of EPS blocks are the primary mechanisms for resisting horizontal loads. Although the Mohr-Coulomb interface friction angle, δ, for EPS/EPS interface sliding is comparable to that of sand ($\delta \sim 30$ degrees) as shown in Chapter 2, the shear resistance, $\sigma'_n * \tan \delta$, is generally small in magnitude because the effective vertical normal stress, σ'_n , is relatively small. This resistance may be insufficient to resist significant driving forces that result from horizontal loads such as unbalanced water head, wind, or seismic shaking. Recommended analysis procedures to evaluate the potential for horizontal sliding under these loads are described later in this chapter.

If the calculated resistance forces along the horizontal planes between EPS blocks are insufficient to resist the horizontal driving forces, additional resistance between EPS blocks is

generally provided by adding mechanical inter-block connectors (typically prefabricated barbed metal plates) along the horizontal interfaces between the EPS blocks. The use of mechanical connectors between layers of EPS blocks can be modeled by considering the horizontal interface between blocks follows the classical Mohr-Coulomb failure criterion:

$$\tau = c_a + \sigma'_n \tan\delta \qquad \textbf{(6.1)}$$

where: c_a = pseudo cohesion produced by connectors expressed as an average value per unit area,

δ = EPS/EPS interface friction angle which testing conducted herein suggests is 30 degrees,

σ'_n = effective vertical normal stress at the interface, and

τ = total shear resistance at the interface expressed as an average value per unit area.

Equation (6.1) is illustrated conceptually in Figure 6.1 where it can be seen that mechanical connectors provide a pseudo cohesion to the otherwise frictional interface resistance. Experience in the U.K. (*2*) and elsewhere suggests that mechanical connectors are not required for typical gravity and vehicle-braking loads. However, mechanical connectors may be required where seismic or other lateral loads are deemed to be significant (*3*). The design chart for internal seismic stability discussed subsequently in this chapter shows that the critical interface for horizontal sliding is usually the pavement system/EPS interface and mechanical connectors are not required for a horizontal seismic coefficient less than or equal to 0.2.

At the present time, all mechanical connectors available in the U.S. are of proprietary designs. Therefore, the resistance provided by such connectors and placement location must be obtained from the supplier or via independent testing. The designer should determine if the mechanical connector shear strength data provided is based on a rapid loading rate or long-term loading rate. Test data from short-term loading is appropriate for evaluating the shear resistance under transient or short-term loading such as earthquakes and is not suitable for sustained loads.

Long-term shear resistance data should be obtained to evaluate connector shear resistance under sustained loads.

Because the connector plates are propriety the cost of installing the plates may be significant. Therefore, unless the internal stability analyses indicate their necessity, the plates do not have to be installed. To overcome the proprietary nature of the common metal connector plates, new mechanical connectors such as barbed timber fasteners, special barbed geofoam connector plates, and sections of steel reinforcing bars are being developed and is a topic for future research.

In addition to their role in resisting design loads, mechanical connectors have proven useful in keeping EPS blocks in place when subjected to wet, icy, or windy working conditions during construction (*4*) and to prevent shifting under traffic loads when only a few layers of blocks are used (*5*). At present, there is no consensus on where mechanical connectors should be used. One recommended practice is to place the connectors across every horizontal joint between blocks (*3,6*). Connectors are also used across horizontal joints on the outside face of the EPS block. A minimum of two timber fasteners per block was specified by the Washington Department of Transportation for the SR 516 project. In (*7*), it is recommended that a minimum of two plates for each 1.2 m (4 ft) by 2.4 m (8 ft) area of EPS be used.

The resistance provided by mechanical connectors will depend on the type of connector used. In (*7*), it is indicated that each 102 mm by 102 mm (4 in by 4 in) plate exhibits a design pseudo cohesion of 267 N (60 lbs). This resistance is based on tests performed on EPS block with a density of 16 kg/m³ (1 lbf/ft³) in accordance with ASTM C 578 and includes a factor of safety of two. However, the effectiveness of mechanical connectors, especially under reverse loading conditions has been disputed in (*2,8*).

Figure 6.1. Interface shear strength of EPS blocks with mechanical connectors.

TRANSLATION DUE TO WATER (HYDROSTATIC SLIDING)

Internal stability for translation due to water consists of verifying that adequate shear resistance is available between EPS block layers and between the pavement system and the EPS blocks to withstand the forces of an unbalanced water head. Equation (5.76) can be used to determine the factor of safety against hydrostatic sliding at various heights of the EPS embankment. Alternatively, Equation (5.77) can be used to determine the required overburden force, O_{REQ}, to achieve a factor of safety of 1.2 against horizontal sliding. As discussed in Chapter 5, a minimum factor of safety of 1.2 is recommended for design of geofoam embankments against hydrostatic sliding. The vertical height of accumulated water to the bottom of the embankment at the start of construction, h, should be taken as the height of the accumulated water level to the interface that will be analyzed for hydrostatic sliding. As described in the section on hydrostatic sliding as part of external stability in Chapter 5, the value of O_{REQ} is the additional overburden force required above the EPS blocks to obtain the desired factor of safety of 1.2. The components usually contributing to O_{REQ} are the weight of the pavement system and the cover soil on the embankment side slopes. Therefore, to ensure the desired factor of safety, the calculated value of O_{REQ} should be less than the sum of the pavement and cover soil weights as shown in Equation (5.65). If other weights, W_{other}, are applied to the embankment besides the pavement system and the soil cover, Equation (5.66) can be used to ensure that the desired factor of safety is obtained. Figures 5.53 through 5.56 can be used to determine the required overburden force, O_{REQ}, to achieve a factor of safety of 1.2 against horizontal sliding. The accumulated water level used in the design charts is the sum of the height from the top of the accumulated water level to the interface that will be analyzed and the estimated total settlement, i.e., $h+S_{total}$. Figures 5.53 through 5.56 are based on the assumption that the EPS blocks extend the full height of the embankment, i.e., $H = T_{EPS}$. Therefore, the weight of the EPS equivalent to the height of the pavement system times the unit weight of the EPS must be subtracted in the result of O_{REQ} as shown by Equations (5.67) and (5.68).

The thickness of EPS blocks typically range between 610 mm (24 in.) to 1,000 mm (39 in.). Therefore, if the water level to be analyzed is less than about 610 mm (24 in.), an internal stability analysis for hydrostatic sliding is not required.

Remedial Procedures

Remedial procedures that can be used to increase the factor of safety against hydrostatic sliding include:

- including a drainage system to minimize the potential for water to accumulate along the embankment.
- install mechanical connectors between blocks.
- if conventional soil fill is being proposed between the EPS blocks and the natural subgrade, a portion of this proposed soil fill can be removed and substituted with pavement system materials on top of the EPS thereby increasing the overburden acting on the EPS blocks.

TRANSLATION DUE TO WIND

Internal stability for translation due to wind consists of verifying that adequate shear resistance is available between EPS block layers and between the pavement system and EPS blocks to withstand the design wind forces. Equation (5.80) can be used to determine the factor of safety against translation due to wind. Alternatively, Equation (5.81) can be used to determine the required overburden for a factor of safety of 1.2. The bottom of the embankment should be taken as the same level as the interface that will be analyzed for translation due to wind. As described in the section on translation due to wind as part of external stability in Chapter 5, the value of O_{REQ} is the additional overburden force required above the EPS blocks to obtain the desired factor of safety of 1.2. The components usually contributing to O_{REQ} are the weight of the pavement system and the cover soil on the embankment sideslopes. Therefore, to ensure the desired factor of safety, the calculated value of O_{REQ} should be less than the sum of the pavement and cover soil

weights as shown in Equation (5.65). If other weights, W_{other}, are applied to the embankment besides the pavement system and the soil cover, Equation (5.66) can be used to ensure that the desired factor of safety is obtained. Figure 5.58 can be used to determine the required overburden for a factor of safety of 1.2. The bottom of the embankment should be taken as the same level as the interface that will be analyzed for translation due to wind. Figure 5.58 is based on the assumption that the EPS blocks extend to the full height of the embankment, i.e., $H = T_{EPS}$. Therefore, the weight of the EPS equivalent to the height of the pavement system times the unit weight of the EPS must be subtracted in the result of O_{REQ} as shown by Equations (5.67) and (5.68).

Remedial Procedures

Remedial procedures that can be used to increase the factor of safety against translation due to wind are similar to those for increasing the factor of safety against hydrostatic sliding presented in the previous section except the use of a drainage system.

INTERNAL SEISMIC STABILITY OF TRAPEZOIDAL EMBANKMENTS

Introduction

This section focuses on the effect of seismic forces on the internal stability of EPS-block geofoam trapezoidal embankments or embankments with sloped sides. The internal seismic response of an EPS-block geofoam embankment is discussed in the design loads section of Chapter 3. The main difference in this analysis and the external seismic stability analysis in Chapter 5 is that sliding is assumed to occur only within the geofoam embankment or along an EPS interface. This analysis uses a pseudo-static slope stability analysis, discussed in Chapter 5, and non-circular failure surfaces through the EPS or the EPS interface at the top or bottom of the embankment. The pseudo-static stability analysis is used to simulate earthquake loads on slopes and involves modeling the earthquake shaking with a horizontal force that acts permanently, not temporarily, and in one direction on the slope. The pseudo-static horizontal force is applied to the

slide mass that is delineated by the critical static failure surface. Therefore, the steps in an internal pseudo-static stability analysis are:

1. Identify the potential critical static failure surfaces, i.e., the static failure surface with the lowest factor of safety, that passes through the EPS embankment or an EPS interface at the top or bottom of the EPS. This is accomplished by measuring the interface strength between EPS blocks and the interfaces at the top and bottom of the EPS blocks and determining which of the interfaces yield the lowest factor of safety. In the analyses presented subsequently, it was found that the critical interface varies as the interface friction angle varies. Therefore, the factor of safety for all three interfaces should be calculated unless one of the interfaces exhibits a significantly lower interface friction angle than the other two interfaces and can be assumed to control the internal stability.

2. Determine the appropriate value of horizontal seismic coefficient (discussed in Chapter 5) that will be multiplied by gravity to determine the horizontal seismic acceleration and applied to the center of gravity of the slide mass delineated by the critical static failure surface. The horizontal seismic force is obtained by multiplying the horizontal seismic acceleration by the slide mass. As discussed in Chapter 5, estimation of the horizontal seismic coefficient can utilize empirical site response relationships and the horizontal acceleration within the embankment can be assumed to vary linearly between the base and crest values. At any level within the embankment, the interpolated value of horizontal acceleration can be multiplied by the mass of material (pavement system, EPS, etc.) above that level to determine the horizontal driving force due to seismic loading.

3. Calculate the internal seismic factor of safety, FS', for the critical internal static failure surface and ensure that it meets the required value of 1.2. A minimum factor of safety of 1.2 is recommended for internal seismic stability of EPS geofoam embankments because earthquake shaking is a temporary loading. The seismic factor of safety for the EPS/pavement system interface is calculated using a sliding block analysis and a pseudo-static stability analysis is used for the EPS/EPS and EPS/foundation soil interfaces. The pseudo-static factor of safety should be calculated using a slope stability method that satisfies all conditions of equilibrium, e.g., Spencer's (*9*) stability method.

Typical Cross-Section

A typical cross-section through a 12.2 m (40 ft) high EPS trapezoidal embankment with side-slopes of 2H:1V that was used in the pseudo-static internal stability analyses is shown in Figure 6.2. It can be seen that a soil cover material is placed over the entire embankment. The material layer at the top of the embankment is used to model the pavement and traffic surcharges as discussed in Chapter 5. The pavement and traffic surcharges are modeled with a material layer on top of the embankment that has a unit weight of 71.8 kN/m^3 (460 lbf/ft^3). The soil cover is 0.46 m (1.5 ft) thick so the stress applied by this soil cover equals 0.46 m times the unit weight of 71.8 kN/m^3 (460 lbf/ft^3) or 33.0 kPa (690 lbs/ft^2). A stress of 33.0 kPa (690 lbs/ft^2) corresponds to the sum of the design values of pavement surcharge (21.5 kPa (450 lbs/ft^2)) and traffic surcharge (11.5 kPa (240 lbs/ft^2)) used previously in the external seismic slope stability analyses in Chapter 5. The pavement and traffic surcharges had to be modeled with a high unit weight soil layer instead of a surcharge. A surcharge could not be used because a seismic coefficient cannot be applied to a surcharge in limit equilibrium stability analyses because the horizontal seismic force must be applied at the center of gravity of a material layer. In summary, a pseudo-static force cannot be applied at the center of gravity of a surcharge because the surcharge does not have a center of gravity. The soil cover on the side-slopes of the embankment is also 0.46 m (1.5

ft) thick, which is typical for the side slopes, and is assigned a typical moist unit weight of 18.9 kN/m^3 (120 lbf/ft^3).

Figure 6.2 also presents the three failure surfaces or modes considered in the internal seismic stability analyses. It can be seen that the first failure mode, i.e., Mode I, corresponds to translational sliding at the pavement system/EPS interface at the top of the EPS blocks. This interface could involve a separation material such as a geomembrane placed over the EPS to protect the EPS against hydrocarbon spills or a geotextile to provide separation between the pavement system and the EPS. If a geosynthetic is not used on the top of the EPS blocks, the interface would consist of a pavement system material overlying the EPS blocks or a separation layer material that is not a geosynthetic placed between the pavement system and EPS blocks. The second failure mode, i.e., Mode II, corresponds to translational sliding between adjacent layers of EPS blocks, e.g., at the top of the last layer of EPS blocks, and thus consists of sliding along an EPS/EPS interface. The third failure mode, i.e., Mode III, corresponds to translational sliding at the EPS/foundation soil surface at the base of the EPS blocks. If a geosynthetic is not used at the base of the EPS blocks, the interface would consist of EPS overlying either a leveling soil or the in situ foundation soil. All three of these failure modes were assumed to initiate at or near the embankment centerline because it is anticipated that a pavement joint or median will exist near the embankment centerline in the field and provide a discontinuity that allows part of the embankment to displace. In addition, the embankment is symmetric.

Figure 6.2. Typical trapezoidal cross-section used in seismic internal slope stability analyses with the three applicable failure modes.

Stability Analysis Procedure

Slope stability analyses were conducted on a range of trapezoidal embankment geometries to investigate the effect of embankment height (3.1 m (10 ft) to 12.2 m (40 ft)), slope inclination (2H:1V, 3H:1V, and 4H:1V), and roadway width (11 m (36 ft), 23 m (76 ft), and 34 m (112 ft)) on internal seismic slope stability. The results of these analyses were used to develop

design charts to facilitate internal design of trapezoidal roadway embankments that utilize geofoam.

Failure mode I in Figure 6.2 was modeled using a sliding block analysis in which a block slides on a surface with a frictional resistance equal to tan(ϕ). A similar analysis is used for retaining wall design to investigate the potential for sliding at the wall/soil interface. The weight of the block cancels out of the numerator and denominator leaving the seismic sliding factor of safety equal to:

$$FS' = \frac{\tan(\varphi)}{k_h} \qquad \textbf{(6.2)}$$

where k_h = horizontal seismic coefficient.

The seismic factor of safety for Mode I depends only on the shear resistance of the pavement system/EPS interface and the magnitude of the horizontal seismic coefficient, i.e., size of the earthquake. The small amount of resistance that will be contributed in the field by the passive resistance of the soil cover at the edge of the pavement system was assumed to be negligible. This passive resistance could be mobilized if the pavement system slides toward the face of the side slope. This resistance was neglected in the calculations because it corresponds to approximately 165 kg (364 lbs) of passive resistance from a soil wedge weighing 102 kg (225 lbs) compared to 2,625 kg (5,790 lbs) of shear resistance developed along the pavement system interface with an interface friction angle of 25 degrees from a pavement weighing 5,634 kg (12,420 lbs). In summary, the passive resistance of the soil cover appears to be negligible and was not included in the analysis of pavement sliding along the top of the EPS and thus the seismic factor of safety is given by Equation (6.2).

Failure modes II and III involve a failure surface that initiates at or near the centerline of the pavement, extends into the EPS embankment to a certain depth, and then travels horizontally until it terminates either on the embankment slope face or near the toe of the embankment, respectively. This is caused by the high intact shear strength of the EPS blocks (cohesion of 145

kPa (3,030 lbs/ft²) from Chapter 2) and low unit weight of the EPS, which results in failure developing between the EPS blocks instead of through the EPS blocks. Therefore, the failure surface in Figure 6.2 for failure modes II and III follow pre-existing discontinuities between EPS blocks because the internal strength of the blocks is greater than the EPS/EPS interface strength. The shear resistance along these discontinuities corresponds to the EPS/EPS interface shear strength parameters of ϕ=30 degrees and c = 0 as shown in Table 6.1 and described in Chapter 2.

These two failure modes result in a steep failure surface through the EPS blocks (see Figure 6.2) and the failure modes model a failure surface descending between adjacent blocks and not through EPS blocks. This results in a stair-stepped failure surface through the EPS that was modeled in the slope stability program XSTABL (*10*) by identifying the exact geometry of the failure surface through the EPS. A typical EPS block size of 760 mm (30 in.) high and 4,900 mm (193 in.) long was used to model the failure surfaces extending through the EPS blocks because this size was recently used on the Interstate-15 geofoam projects near Salt Lake City, Utah (*8*). It was assumed that the EPS blocks are offset laterally in the field so a continuous failure surface cannot develop through the blocks without generating any horizontal resistance through the EPS. The overall stair-stepped angle was assumed to be inclined at 45 degrees + $\phi_{EPS/EPS}/2$ from the horizontal to simulate an active earth pressure condition where $\phi_{EPS/EPS}$ is the interface friction angle between two blocks of EPS. Thus, for a $\phi_{EPS/EPS}$=30 degrees, the stair-stepped inclination was assumed to be 60 degrees. This inclination results in a minimum lateral earth pressure condition and a minimum shear resistance along the horizontal segments of the EPS blocks during failure. For a 0.76 m (2.5 ft) high EPS block and a 60 degrees overall stair-stepped inclination, the lateral offset of the failure surface is 0.76 * $\tan^{-1}(60^{\circ})$ or 0.44 m (1.4 ft).

Thus, it can be seen in Figure 6.2 that as the failure surface extends through the EPS, it creates a stair-stepped pattern to reflect the blocks being laterally offset. On the vertical portions of the stair-stepped pattern no shear resistance was applied in the stability analyses, however an

interface friction angle of 30 degrees was assigned to the horizontal segments to reflect sliding between EPS blocks. The stair-stepped failure surface could travel horizontally along a horizontal joint between adjacent rows of EPS blocks (mode II) or continue to the base of the EPS and travel along the EPS/foundation interface (mode III).

The factor of safety for failure mode II is a function of the depth at which the failure surface travels along a horizontal joint between adjacent rows of EPS blocks. The analyses conducted herein show that the seismic factor of safety decreases as the failure mode II extends further into the EPS and the critical failure surface was found to be located at the top of the bottom row of EPS blocks. As a result, failure mode II is similar to mode III with the only difference being that failure mode III extends to the EPS/foundation soil interface and the applicable interface friction angle along the horizontal portion of the failure surface is controlled by the EPS/foundation soil interface strength or by the type of geosynthetic or soil used between the EPS and the foundation soil instead of simply the EPS/EPS interface strength.

Material Properties

The input parameters, i.e., unit weight and shear strength, used in the internal slope stability analyses are presented in Table 6.1. It can be seen that Mohr-Coulomb shear strength parameters were used to represent the shear strength of the cover soil and the EPS interfaces. The soil cover is modeled using an effective stress friction angle of 28 degrees because it is anticipated that the soil cover will not be saturated at all times nor loaded rapidly and thus it will not experience an undrained failure. Based on the geofoam shear strength testing described in Chapter 2, the value of EPS/EPS interface shear strength of 30 degrees can be used for the internal seismic analyses and does not have to be adjusted for seismic loading. This conclusion is also supported by the results of shake table tests on geosynthetic interfaces (*11*) that show the seismic strength of geosynthetic interfaces is at least as great as the static interface strength. It can be seen from Chapter 2 that the geofoam interface friction angle ranges from 24 degrees (geofoam/geotextile interface) to 52 degrees (geofoam/geomembrane interface) for

EPS/geosynthetic interfaces and thus the design charts presented subsequently were developed for an interface friction angle ranging from 10 to 40 degrees (see Table 6.1). The design charts do not extend to an interface friction of 52 degrees because the analyses show that stability is not an issue with an interface friction angle greater than 40 degrees because the design chart relationships (discussed subsequently) are independent of interface friction angle at angles greater than 40 degrees. Sometimes a sand layer is placed between the geotextile and the geofoam at the bottom of an embankment and thus the geofoam/geotextile interface may not be present. In this case, an EPS/sand interface strength should be used and can be measured using direct shear tests (ASTM D 5321) to obtain a representative interface friction angle for use in the design charts.

In summary, for the internal stability analysis performed for this study, an effective stress friction angle of 28 degrees was used for the soil cover and an interface friction angle of 30 degrees was used for the EPS/EPS interface in all of the analyses. Only the pavement system/EPS and EPS/foundation soil interface was varied between 10 and 40 degrees.

Table 6.1. Input Parameters for Internal Slope Stability Analyses.

Location of Critical Failure Mode

Location of the critical failure mode, e.g., I, II, or III, for a particular embankment geometry was found to be a function of the three interface friction angles used to model these three failure modes. Failure modes I, II, and III depend on the interface friction angle between the pavement system and EPS, EPS and EPS, and EPS and the foundation geosynthetic or soil, respectively. The effect of the interface friction angle on the location of the critical failure surface is illustrated in Figure 6.3, which presents the seismic factor of safety for a 6-lane roadway on a 12.2 m (40 ft) high embankment for the three values of horizontal seismic coefficient (0.05, 0.10, and 0.20) used in Chapter 5. It can be seen for a horizontal seismic coefficient of 0.05, failure mode I, i.e., failure at the EPS/pavement system interface, is critical for an interface friction angle equal to or less than 15 to 20 degrees. For interface friction angles between 15 and about 30 degrees, failure mode III, i.e., failure at the EPS/foundation interface, is critical. For interface

friction angles greater than about 30 degrees, failure mode II, i.e., failure within the embankment along an EPS/EPS interface, is critical. Therefore, the critical internal failure mode will vary depending on the design value of internal friction angle. A similar change in critical failure surface with changes in interface friction angle has been observed by (*12*) for the design of geosynthetic composite liner systems for landfills. As a result, the seismic factor of safety relationships presented subsequently in the design chart for failure modes II and III are combined because it can be seen that failure mode III is critical until an interface friction angle of approximately 30 degrees is reached. At interface friction angles greater than approximately 30 degrees, failure mode II controls because the friction angle for an EPS/EPS interface is 30 degrees.

The effect of the interface friction angle on the seismic factor of safety is important because if the interface friction angle is increased on one interface, a different interface may become critical and might have to be strengthened to achieve the required factor of safety. For example, if the interface friction angle for failure mode I is increased from 10 to 15 degrees for a horizontal seismic coefficient of 0.2, the seismic factor of safety increases from approximately unity to greater than the required value of 1.2 (see Figure 6.3). However, if the interface friction angle for either failure mode II or III is 10 degrees, these interfaces will exhibit a seismic factor of safety at or below 1.2 and be critical. This may require the interface friction angle to be increased for failure mode III but probably not for failure mode II because the EPS/EPS interface friction angle usually exceeds 10 degrees as described in Chapter 2.

Figure 6.3. Effect of interface friction angle and slope inclination on seismic factor of safety, for 12.2 m high EPS-block geofoam trapezoidal embankment with a 6-lane roadway with a total road width of 34 m (112 ft).

Design Charts

Figure 6.3 also illustrates the sensitivity of the seismic internal factor of safety to the inclination of the side slopes of the embankment. For all slope inclinations considered (2H:1V,

3H:1V, and 4H:1V), the internal seismic factor of safety for failure mode I is not a function of the side slope inclination because the analysis simply involves a sliding block along a horizontal plane at the pavement system/EPS interface. For failure modes II and III, the slope inclination does not significantly influence the seismic internal factor of safety especially at horizontal seismic coefficients of 0.1 and 0.2. In addition, the largest variation of seismic factor of safety occurs at large values of factor of safety, i.e., $k_h = 0.05$, with factors of safety of approximately 8 which is well above the required value of 1.2. As a result, the subsequent design chart is based on the most critical slope inclination of 2H:1V and thus the design chart is independent of inclination of the embankment side slopes. It can be seen that the sensitivity studies were conducted for a 6-lane roadway with a total road width of 34 m (112 ft) on top of a 12.2 m (40 ft) high EPS embankment in Figure 6.3.

Figure 6.4 illustrates the sensitivity of the seismic internal factor of safety to the width of the embankment for a 12.2 m (40 ft) high EPS embankment with side-slope inclinations of 2H:1V. It can be seen that the critical failure mode is again a function of the interface friction angle with failure mode I controlling at low interface friction angles and mode II controlling at high values of interface friction angle. It can also be seen that roadway width does not significantly influence the seismic internal factor of safety especially at horizontal seismic coefficients of 0.1 and 0.2. At a horizontal seismic coefficient of 0.05, it can be seen that the seismic internal factor of safety is influenced by the difference in embankment width for a 2-lane (11 m (36 ft) wide) and a 6-lane (34 m (112 ft) wide) roadway with the 2-lane roadway being slightly more critical than the 6-lane roadway. However, the seismic factor of safety varies from approximately 7 to 8, which is well above the required value of 1.2 and thus will not control the embankment design. As a result, the subsequent design chart is based on the most critical slope inclination and roadway width of 2H:1V and 11 m (36 ft), 2-lane roadway.

Figure 6.4. Effect of roadway width on seismic factor of safety for 12.2 m high trapezoidal embankment with a side-slope inclination of 2H:1V.

Figure 6.5 illustrates the final sensitivity study used to develop the design chart, which involves the effect of embankment height on the seismic internal factor of safety. Based on the sensitivity studies in Figures 6.3 and 6.4, a 12.2 m (40 ft) high EPS embankment with a side-slope inclination of 2H:1V and a 2-lane roadway were used for this sensitivity study. It can be seen that embankment height does not significantly influence the seismic internal factor of safety especially at horizontal seismic coefficients of 0.1 and 0.2. At a horizontal seismic coefficient of 0.05, it can be seen that the seismic internal factor of safety is influenced by the difference in embankment height from 3.1 m (10 ft) to 12.2 m (40 ft). However, the seismic factor of safety varies from approximately 7 to about 9.5, which is well above the required value of 1.2 and thus will not control the embankment design. As a result, the subsequent design chart is based on the most critical slope inclination (2H:1V) and roadway width (11 m (36 ft) or 2-lane roadway). In addition, the relationship for failure modes II and III in the design chart depict the critical embankment height which varies from 3.1 m (10 ft) at an interface friction angles less than about 20 degrees to 12.2 m (40 ft) at an interface friction angles greater than or equal 20 degrees. The difference in the seismic factor of safety for heights of 3.1 m (10 ft) and 12.2 m (40 ft) is small, thus the design chart can be used for any embankment height between 3.1 m (10 ft) and 12.2 m (40 ft).

Figure 6.5. Effect of EPS embankment height on seismic factor of safety for a trapezoidal embankment with a side-slope inclination of 2H:1V and a 2-lane roadway.

The internal seismic stability design chart in Figure 6.6 presents the seismic factor of safety for each seismic coefficient as a function of interface friction angle. Based on the previously described parametric study, this chart can be used for any of the geometries considered during this study, i.e., embankment heights of 3.1 m (10 ft) to 12.2 m (40 ft), slope inclinations of 2H:1V, 3H:1V, and 4H:1V, and roadway widths of 11 m, 23 m, and 34 m (36, 76, and 112 feet), even though it is based on a side-slope inclination of 2H:1V, a 2-lane roadway, and an embankment height from 3.1 m (10 ft) to 12.2 m (40 ft). It can be seen that an EPS embankment

will exhibit a suitable seismic factor of safety if the minimum interface friction angle exceeds approximately 15 degrees. However, an important aspect of Figure 6.6 is to develop the most cost-effective internal stability design by selecting the lowest interface friction angle for each interface that results in a seismic factor of safety of greater than 1.2. For example, a lightweight geotextile can be selected for the EPS/foundation interface because the interface only needs to exhibit a friction angle greater than 10 degrees. More importantly, the EPS/EPS interface within the EPS also only needs to exhibit a friction angle greater than 10 degrees, which suggests that mechanical connectors are not required between EPS blocks for internal seismic stability because the interface friction angle for an EPS/EPS interface is approximately 30 degrees (see Chapter 2). In summary, it appears that internal seismic stability will be controlled by the shear resistance of the pavement system/EPS interface.

Figure 6.6. Design chart for internal seismic stability of EPS trapezoidal embankments.

Remedial Procedures

Remedial procedures that can be used to increase the factor of safety against internal seismic instability are decreasing the pavement system thickness, using pavement system materials with a lower unit weight, increasing the interface resistance at the pavement system/EPS interface and EPS/geosynthetic or soil interface at the bottom of the EPS blocks, and possibly using inter-block mechanical connectors to increase the interface strength between the EPS blocks.

INTERNAL SEISMIC STABILITY OF VERTICAL EMBANKMENTS

Introduction

As shown by Figure 3.4 (b), an embankment with vertical sides, sometimes referred to as a geofoam wall, can be utilized with EPS- block geofoam. The use of an embankment with vertical walls minimizes the amount of right-of-way needed and the impact of embankment loads on nearby structures, which is an important advantage over other lightweight fills. This section focuses on the effect of seismic forces on the internal stability of EPS-block geofoam

embankments with vertical walls. The main difference in this analysis and the analysis for external seismic stability of embankments with vertical walls in Chapter 5 is that sliding is assumed to occur only within the geofoam embankment or along an EPS interface. This analysis uses the same pseudo-static slope stability analysis used for internal seismic stability of trapezoidal embankments and non-circular failure surfaces through the EPS or the EPS interface at the top or bottom of the embankment. The pseudo-static stability analysis is used to simulate earthquake loads on slopes and involves modeling the earthquake shaking with a horizontal force that acts permanently, not temporarily, and in one direction on the slope. The pseudo-static horizontal force is applied to the center of gravity of the slide mass that is delineated by the critical static failure surface. The same steps outlined in the "Introduction" sub-section of the "Internal Seismic Stability of Trapezoidal Embankments" section of this chapter can be used to conduct an internal pseudo-static stability analysis of vertical geofoam embankments.

Typical Cross-Section

A typical cross-section through a vertical EPS embankment used in the internal static stability analyses is shown in Figure 6.7. This cross-section is similar to the cross-section used for static analyses of vertical embankments in Figure 5.29 but differs from the cross-section used for the static analyses of trapezoidal embankments in Figure 5.10 because the surcharge used to represent the pavement and traffic surcharges is replaced by placing a 0.61 m (2 ft) thick soil layer on top of the embankment with a unit weight of 54.1 kN/m^3 (345 lbs/ft^3). The soil layer is 0.61 m (2 ft) thick to represent the minimum recommended pavement section thickness discussed in Chapter 4. Therefore, the vertical stress applied by this soil layer equals 0.61 m times the increased unit weight or 33.0 kN/m^2 (690 lbs/ft^2). A vertical stress of 33.0 kN/m^2 (690 lbs/ft^2) corresponds to the sum of the design values of pavement surcharge (21.5 kN/m^2 (450 lbs/ft^2)) and traffic surcharge (11.5 kN/m^2 (240 lbs/ft^2)) used previously for external bearing capacity and static slope stability of trapezoidal embankments in Chapter 5.

The surcharge in Figure 5.10 had to be replaced by an equivalent soil layer for the seismic slope stability analysis because a seismic coefficient cannot be applied to a surcharge in limit equilibrium stability analyses. The horizontal force that represents the seismic loading must be applied at the center of gravity of a material layer and not on a surcharge because a surcharge does not have a center of gravity. As noted in Chapter 5, this soil layer, which is equivalent to the pavement and traffic surcharge, was also used for the static stability analyses of vertical embankments instead of a surcharge to minimize the number of stability analyses that would be required to determine the critical static factor of safety and critical static failure surface for each model, i.e., an embankment modeled with a surcharge and one modeled with a soil layer. A slight difference in the critical factor of safety value and the location of the critical failure surface may result between the two different models because surcharge forces exert an additional force at the top of each vertical slice in the limit equilibrium analysis while the force exerted by the weight of the soil layer is located at the center of each vertical slice. In summary, a pseudo-static seismic force cannot be applied at the center of gravity of a surcharge so the pavement system and traffic loads were modeled as an equivalent soil layer and not a surcharge.

Figure 6.7. Typical cross-section used in seismic internal slope stability analyses for vertical embankments with the three applicable failure modes.

Figure 6.7 also presents the three failure modes considered in the internal seismic stability analyses for vertical geofoam embankments. These failure modes are similar to the three failure modes analyzed in seismic internal slope stability analysis of trapezoidal embankments and a description of each is included in the "Typical Cross-Section" and "Stability Analysis Procedure" sub-sections of the "Internal Seismic Stability of Trapezoidal Embankments" section of this chapter.

Stability Analysis Procedure

Slope stability analyses were conducted on a range of vertical embankment geometries to investigate the effect of embankment height (3.1 m (10 ft) to 12.2 m (40 ft)) and roadway width

(11 m (36 ft), 23 m (76 ft), and 34 m (112 ft)) on internal seismic slope stability. The results of these analyses were used to develop design charts to facilitate internal design of roadway embankments with vertical walls that utilize geofoam. The three failure modes shown in Figure 6.7 are similar to the three failure modes used in the analysis of trapezoidal embankments shown in Figure 6.2. Therefore, the analysis procedures used to model the three failure modes are similar to the procedures used in seismic internal slope stability analyses of trapezoidal embankments and are described in the "Stability Analysis Procedure" sub-section of the "Internal Seismic Stability of Trapezoidal Embankments" section of this chapter. However, Spencer's (*9*) slope stability method did not converge for the vertical wall embankment geometries investigated. Therefore, Simplified Janbu's method (*13*) was used to perform the internal slope stability analyses shown in Figures 6.8 through 6.12. The factor of safety obtained using the Simplified Janbu's method is based on horizontal and vertical force equilibrium. Moment equilibrium is not satisfied, which is undesirable, but more importantly horizontal force equilibrium is satisfied which allows the seismic force to be directly incorporated into the analysis. Spencer's (*9*) stability method, which satisfies all conditions of equilibrium, was used to obtain the seismic factor of safety, FS', values for trapezoidal embankments shown in Figures 6.3 through 6.6. Therefore, a quantitative comparison cannot be made between the trapezoidal embankment design charts shown in Figures 6.3 through 6.6 and the vertical embankment design charts shown in Figures 6.8 through 6.12 but qualitative comparisons are suitable.

Material Properties

The same input parameters, i.e., unit weight and shear strength, used in the internal seismic stability analyses of trapezoidal embankments, which are presented in Table 6.1, were used for the internal seismic stability analysis of embankments with vertical walls. The basis for these input material parameters is presented in the "Material Properties" sub-section of the "Internal Seismic Stability of Trapezoidal Embankments" section of this chapter. However, since vertical embankments do not have a soil cover on the side walls, the soil cover material

parameters shown in Table 6.1 were not used. A friction angle of 0 degrees was used for the soil layer on top of the EPS-block geofoam that was used to model the pavement and traffic surcharges. The phreatic surface is located at or near the ground surface and the foundation soil is saturated as is typically the case at most EPS-block geofoam sites.

Location of Critical Failure Mode

Location of the critical failure mode, e.g., either I, II, or III, for a particular embankment geometry was found to be a function of the three interface friction angles used to model these three failure modes. This behavior is similar to the behavior observed for trapezoidal embankments. Failure modes I, II, and III depend on the interface friction angle between the pavement system and EPS, EPS and EPS, and EPS and the foundation geosynthetic or soil, respectively. The effect of the interface friction angle on the location of the critical failure surface is illustrated in Figure 6.8, which presents the seismic factor of safety for a 6-lane roadway with a width of 34 m (112 ft) on a 12.2 m (40 ft) high embankment for the three values of horizontal seismic coefficient (0.05, 0.1, and 0.2). It can be seen for a horizontal seismic coefficient of 0.05, failure mode I or failure at the EPS/pavement system interface, is critical for an interface friction angle less than or equal to 11 degrees (see Figure 6.8). For interface friction angles between 10 and about 30 degrees, failure mode III, i.e., failure at the EPS/foundation interface, is critical. For interface friction angles greater than 30 degrees, failure mode II, i.e., failure within the embankment along an EPS/EPS interface, is critical. Therefore, the critical internal failure mode depends on the design value of internal friction angle. A similar change in critical failure surface with changes in interface friction angle has been observed by (*12*) for the design of geosynthetic composite liner systems for landfills and for trapezoidal embankments as shown in Figure 6.3. As a result, the seismic factor of safety relationships presented subsequently in the design chart for failure modes II and III are combined because it can be seen that failure mode III is critical until an interface friction angle of approximately 30 degrees is reached. At interface friction

angles greater than approximately 30 degrees, failure mode II controls because the friction angle for an EPS/EPS interface is 30 degrees. A similar behavior was observed for seismic coefficients of 0.10 and 0.20 with only the transition from failure mode I and failure modes II and III occurring at a higher interface friction angle (see Figure 6.8).

The effect of the interface friction angle on the seismic factor of safety is important because an increase in interface friction angle on one interface may result in a different interface being critical. The resulting critical interface may have to be strengthened to achieve the required factor of safety. For example, if the interface friction angle for failure mode I is increased from 10 to 15 degrees for a horizontal seismic coefficient of 0.2, the seismic factor of safety increases from approximately unity to greater than the required value of 1.2 (see Figure 6.8).

Design Charts

Failure mode I in Figure 6.7 was modeled using a sliding block analysis with the same procedure utilized for internal seismic stability of trapezoidal embankments. The seismic factor of safety, which is given by Equation 6.2, depends only on the shear resistance of the pavement system/EPS interface and the magnitude of the horizontal seismic coefficient, i.e. size of the earthquake. As was shown by Figure 6.3, the internal seismic factor of safety for failure mode I is not a function of the side slope inclination for the case of trapezoidal embankments. Therefore, the factor of safety for failure mode I for the case of vertical embankments in Figure 6.8 is similar to the factor of safety for the case of trapezoidal embankments in Figure 6.3 because the analysis for failure mode I simply involves a sliding block along a horizontal plane at the pavement system/EPS interface.

For failure modes II and III within a trapezoidal embankment, the slope inclination influences the seismic internal factor of safety at a horizontal seismic coefficient of 0.05 but this influence decreases with increasing value of horizontal seismic coefficient (see Figure 6.3). Slope inclination does not significantly influence the seismic internal factor of safety at horizontal seismic coefficients of 0.1 and 0.2. Figure 6.3 also shows that for a given horizontal seismic

coefficient, the seismic factor of safety decreases as the side slope becomes steeper. Although a quantitative comparison cannot be made between the internal seismic stability results of vertical embankments and trapezoidal embankments, e.g., between Figures 6.8 and 6.3, respectively, the seismic factor of safety values shown by modes III/II for vertical embankments in Figure 6.8 are less than the factor of safety values for trapezoidal embankments in Figure 6.3, with the difference becoming smaller with increasing horizontal seismic coefficient. The qualitative comparison of design charts also shows the difference in seismic factor of safety between a vertical wall and a 2H:1V sloped embankment is greater than between a 2H:1V and a 3H:1V sloped embankment. This difference is attributed to the difference in the slope stability method and the small passive resistance that the soil cover may contribute in a trapezoidal embankment. In addition, the traffic and pavement surcharges were modeled using a 0.61 m (2 ft) soil layer for the embankment with vertical walls case while the trapezoidal case was modeled using a 0.46 m (1.5 ft) soil layer, which is equivalent to the thickness of soil cover. This difference in soil layer thickness between the two models would have an impact on the location of the center of gravity of the soil layer where the horizontal force that represents the seismic loading is located. Also, for the vertical wall model, the soil layer had a shear strength of 0 degrees while for the sloped embankment model, the soil layer had a shear strength of 28 degrees, which is the same as the soil cover.

Figure 6.8. Effect of interface friction angle on seismic factor of safety for 12.2 m high vertical embankment and with a 6-lane roadway with a total road width of 34 m (112 ft).

Figures 6.9 and 6.10 illustrate the sensitivity of the seismic internal factor of safety to the width of the vertical embankment for a 3.1 m (10 ft) and 12.2 m (40 ft) high EPS embankment, respectively. It can be seen that the critical failure mode is a function of the interface friction angle. For a 3.1 m (10 ft) high embankment (Figure 6.9), failure mode III controls at low interface friction angles except at a horizontal seismic coefficient of 0.2 where failure mode I is

slightly more critical. However, for a 12.2 m (40 ft) high embankment (Figure 6.10), failure mode I controls at low interface friction angles. A similar observation was made for trapezoidal embankments as shown by Figure 6.4. Mode II controls at high values of interface friction angles for both a 3.1 m (10 ft) and 12.2 m (40 ft) high embankment.

For the 3.1 m (10 ft) high embankment (Figure 6.9), it can be seen that the seismic internal factor of safety is influenced by the difference in embankment width for an 11 m (36 ft) and 34 m (112 ft) wide roadway with the 11 m (36 ft) wide roadway being more critical than the 34 m (112 ft) roadway for failure modes II and III. For the 12.2 m (40 ft) high embankment (Figure 6.10), an embankment width of 11 m yields similar or lower seismic factors of safety than the 11 m (36 ft) wide embankment for failure mode II. Because a 11 m (36 ft) roadway is more critical for both embankment heights investigated, the subsequent design chart (Figure 6.12) is based on an 11 m (36 ft) wide, 2-lane roadway.

Figure 6.11 illustrates the final sensitivity study used to develop the design chart, which involves the effect of embankment height on the seismic internal factor of safety. An embankment width of 11.1 m (36 ft) or a 2-lane roadway was used for this sensitivity study because the sensitivity studies in Figures 6.9 and 6.10 indicate that a 2-lane roadway is critical. It can be seen that the seismic internal factor of safety is influenced by the difference in embankment height from 3.1 m (10 ft) to 12.2 m (40 ft) for the three horizontal seismic coefficients investigated with the difference becoming less with an increase in horizontal seismic coefficient. Although the seismic factor of safety at interface friction angles of less than 30 degrees could not be determined for failure mode III for an embankment height of 12.2 m, it is anticipated that for a given width, an embankment height 12.2 m (40 ft) will provide larger seismic factors of safety than the shorter embankment of 3.1m (10 ft). Therefore, the subsequent design chart is based on the most critical embankment height of 3.1 m (10 ft).

As indicated by Figure 6.10, no data is shown for failure mode III for the 12.2 m (40 ft) high and 11 m (36 ft) wide embankment because the critical failure mode could not be modeled.

Based on the assumed stair-stepped internal failure surface used in the analyses with an overall inclination of 60 degrees to the horizontal, the internal failure surface will terminate within the EPS for tall and narrow embankments and will not extend to the EPS/foundation soil interface. Although slope stability analyses could not be performed for failure mode III for the 12.2 m (40 ft) high and 11 m (36 ft) wide embankment, based on the results shown in Figure 6.9 for the 3.1 m (10 ft) high embankments, it is anticipated that an embankment width of 11 m (36 ft) will provide less shear resistance within the blocks than the 34 m (112 ft) wide embankment and, consequently, the 11 m (36 ft) wide embankment will yield lower seismic factor of safety values for failure mode III than the 34 m wide (112 ft) embankment. This conclusion is in accordance with the previous conclusion made above that the critical embankment width is 11 m (36 ft) for both the 3.1 m (10 ft) and 12.2 m (40 ft) high embankments. Additionally, Figure 6.11 indicates that the critical embankment height is 3.1 m (10 ft). Therefore, failure mode III for the 12.2 m (40 ft) high embankment is not critical.

Figure 6.9. Effect of roadway width on seismic factor of safety for 3.1 m high vertical embankment.

Figure 6.10. Effect of roadway width on seismic factor of safety for 12.2 m high vertical embankment.

Figure 6.11. Effect of EPS embankment height on seismic factor of safety for a vertical embankment with a 2-lane roadway with a width of 11 m (36 ft).

The internal seismic stability design chart for vertical embankments in Figure 6.12 presents the seismic factor of safety for each seismic coefficient as a function of interface friction angle. Based on the previously described parametric study, this chart provides estimates of seismic internal factor of safety for vertical embankments with any of the geometries considered during this study, i.e., embankment heights of 3.1 m (10 ft) to 12.2 m (40 ft) and roadway widths

of 11 m, 23 m, and 34 m (36, 76, and 112 feet), even though it is based on a roadway width of 11 m (36 ft) and an embankment height from 3.1 m (10 ft).

It can be seen that an EPS embankment will exhibit a suitable seismic factor of safety if the minimum interface friction angle exceeds approximately 15 degrees, which is similar for trapezoidal embankments (see Figure 6.6). However, an important aspect of Figure 6.12 is that it can be used to develop the most cost-effective internal stability design by selecting the lowest interface friction angle for each interface that results in a seismic factor of safety of greater than 1.2. For example, a lightweight geotextile can be selected for the EPS/foundation interface because the interface only needs to exhibit a friction angle greater than 15 degrees. More importantly, the EPS/EPS interface within the EPS also only needs to exhibit a friction angle greater than 15 degrees, which suggests that mechanical connectors are not required between EPS blocks for internal seismic stability because the interface friction angle for an EPS/EPS interface is approximately 30 degrees (see Chapter 2). In summary, as with trapezoidal embankments, it appears that internal seismic stability will be controlled by the shear resistance of the pavement system/EPS interface.

Remedial Procedures

Remedial procedures that can be used to increase the factor of safety against internal seismic instability are decreasing the pavement system thickness, using pavement system materials with a lower unit weight, increasing the interface resistance at the pavement system/EPS interface and EPS/geosynthetic or soil interface at the bottom of the EPS blocks, and possibly using inter-block mechanical connectors to increase the interface strength between the EPS blocks.

Figure 6.12. Design chart for internal seismic stability of EPS vertical embankments.

LOAD BEARING

Introduction

The primary internal stability issue for EPS-block geofoam embankments is the load bearing of the EPS geofoam mass. A load bearing capacity analysis consists of selecting an EPS type with adequate properties to support the overlying pavement system and traffic loads without excessive EPS compression that could lead to excessive settlement of the pavement surface. Therefore, a knowledge of the mechanical (stress-strain-time-temperature) properties of block-molded EPS is required to understand the basis for past and current load bearing analysis procedures. The mechanical properties at small strains are the most relevant otherwise the settlements may become excessive if the large strain properties of the EPS block are mobilized.

The three design goals for a load bearing analysis to ensure adequate performance of the EPS-block geofoam are:

- The initial (immediate) deformations under dead or gravity loads from the overlying pavement system must be within acceptable limits.
- Long-term (for the design life of the fill) creep deformations under the same gravity loads must be within acceptable limits.
- Non-elastic or irreversible deformations under repetitive traffic loads must be within acceptable limits.

Two load bearing analysis procedures have been used with EPS-block geofoam embankments to achieve these design goals. The first approach used in the early use of EPS-block geofoam as lightweight fill in the 1970s and 1980s consists of limiting the maximum applied vertical stress under any combination of loads to some fraction or percentage of the "compressive strength" of the EPS without regard to the level of deformation. This empirical approach is based solely on the ULS (collapse failure) design concept with no consideration of SLS design (deformations). Although this approach has resulted in EPS-block geofoam fills that have performed satisfactorily, it is not the most desired or theoretically sound because it can result in smaller deformations than can be tolerated.

The current design approach, which is recommended herein, is an explicit deformation-based design methodology. It is based on the recognition that the compressive strength of EPS does not quantify the deformation characteristics of the geofoam. Consequently, the parameter of compressive strength is not used for a load bearing analysis but is still used for MQC/MQA purposes. The small-strain analysis utilizes the elastic limit stress, σ_e , and the initial tangent Young's modulus, E_{ti} , both of which are fully defined in Chapter 2, to evaluate the three settlement issues presented above.

As shown in Chapter 2, current creep models for EPS-block geofoam do not provide reliable estimates of long-term vertical strain. However, creep strains within the EPS mass under sustained loads (primarily due to the overlying pavement system) are within acceptable limits (0.5 percent to 1 percent strain over 50 years) if the applied vertical stress produces an immediate strain between 0.5 percent and 1 percent. Consequently, if the applied vertical stress produces an immediate strain greater than 1 percent in laboratory testing, the EPS creep strains will rapidly increase and be considered excessive for lightweight fill applications. The initial (immediate) settlement can be estimated by dividing the applied vertical stress by the initial Young's modulus (see Equation (5.9) in Chapter 5).

Results of uniaxial compression tests (rapid loading, repetitive traffic loading, and creep) on specimens of EPS block test specimens indicate that if the maximum applied vertical stress under repetitive traffic loading has a magnitude not exceeding the elastic limit stress, the non-elastic or irreversible deformations will be tolerable and there will be no degradation of the initial Young's modulus of the EPS.

Table 6.2 provides the minimum recommended values of elastic limit stress for various EPS densities. The use of the elastic limit stress values indicated in Table 6.2 is slightly conservative because the elastic limit stress of the block as a whole is somewhat greater than these minimums, but this conservatism is not unreasonable and would ensure that no part of a block (where the density might be somewhat lower than the overall average) would become

overstressed. Table 6.2 also contains recommended values of initial tangent Young's modulus for determination of the initial (immediate) deformations.

Table 6.2. Minimum allowable values of elastic limit stress and initial tangent Young's Modulus for the proposed AASHTO EPS material designations.

One advantage of a deformation-based design procedure is that the calculation of stresses and strains within the EPS mass allows the density of the EPS blocks to be optimized and thus specified for various portions of the embankment. In the 1970s and 1980s, there was a tendency to use EPS blocks of a single density for every project. The most commonly used density was 20 kg/m^3 (1.25 lbf/ft^3) (sometimes referred to as "EPS20" in European literature). EPS of this density was found to produce acceptable results so there was a tendency to simply replicate this on every project which resulted in an empirical approach. As a result, there was no rational basis for varying from a density that produced acceptable results. However, with a deformation-based design it is possible to select an EPS density that provides adequate load-bearing capacity within tolerable settlements without requiring an inefficient density. Because the applied vertical stress decreases with depth under the pavement and side slopes, it is possible to use multiple densities of EPS blocks in an embankment. For example, lower density blocks can be used at greater depths and/or under side slopes than higher density blocks that have to be used under the pavement system. The reason for not wanting to use an excessively high density of EPS is that the manufacturing cost of EPS block is significantly linked to the relative amount of raw material (expandable polystyrene) used. For example, an EPS block with an overall average density of 32 kg/m^3 (2.0 lbf/ft^3) would use twice as much raw material as an EPS block with an overall average density of 16 kg/m^3 (1.0 lbf/ft^3). In the U.S., raw material cost accounts for one half or more of the manufacturing cost of an EPS block so the impact of EPS density on project costs can be significant. Thus, there is an incentive to rationally select one or more EPS densities to use on a given project, with blocks of different density placed according to the applied vertical stresses. It is now routine in the U.K. to use three or four EPS densities within a given road embankment

cross section. However, for constructability it is recommended that no more than two different density EPS blocks be used on the same project. As indicated in Chapter 4, the use of *EPS40* directly below the pavement system is not recommended because the elastic limit stress of 40 kPa (5.8 lbs/in^2) has been found to result in excessive settlements directly under a pavement system.

Design Procedures

The procedure for evaluating the load bearing capacity of EPS as part of internal stability is outlined in the following thirteen steps:

1. Estimate traffic loads.
2. Add impact allowance to traffic loads.
3. Estimate traffic stresses at top of EPS blocks.
4. Estimate gravity stresses at top of EPS blocks.
5. Calculate total stresses at top of EPS blocks.
6. Determine minimum required elastic limit stress for EPS under pavement system.
7. Select appropriate EPS block to satisfy the required EPS elastic limit stress for underneath the pavement system, e.g., *EPS50*, *EPS70*, or *EPS100*.
8. Select preliminary pavement system type and determine if a separation layer is required.
9. Estimate traffic stresses at various depths within the EPS blocks.
10. Estimate gravity stresses at various depths within the EPS blocks.
11. Calculate total stresses at various depths within the EPS blocks.
12. Determine minimum required elastic limit stress at various depths.
13. Select appropriate EPS block to satisfy the required EPS elastic limit stress at various depths in the embankment.

The load bearing design procedure can be divided into two parts. Part 1 consists of Steps 1 through 8 and focuses on the determination of the traffic and gravity load stresses applied by

the pavement system to the top of the EPS blocks and selection of the type of EPS that should be used directly beneath the pavement system (see steps above). Part 2 consists of Steps 9 through 13 and focuses on the determination of the traffic and gravity load stresses applied at various depths within the EPS blocks and selection of the appropriate EPS for use at these various depths within the embankment. Each of the design steps are subsequently described in detail. Additionally, in Chapter 7, Tables 7.6 through 7.8 are provided that summarize the load bearing design procedure for an example problem.

In summary, the basic procedure for designing against load bearing failure is to calculate the maximum vertical stresses at various levels within the EPS mass (typically the pavement system/EPS interface is most critical) and select the EPS that exhibits an elastic limit stress that is greater than the calculated or required elastic limit stress at the depth being considered.

Step 1: Estimate Traffic Loads

Traffic loads are a major consideration in the load bearing capacity calculations. There are three procedures for considering the effects of traffic loading, traffic frequency (number of repetitions), and traffic configuration in the load bearing analysis: (1) fixed traffic, (2) fixed vehicle, and (3) variable traffic and vehicle (*14*). In the fixed traffic procedure, the thickness of the pavement is based on the heaviest single-wheel load anticipated and the number of load repetitions is not considered. Loads from axles with multiple wheels such as dual tires are converted to an equivalent single-wheel load (ESWL) (*14*) in this procedure.

In the fixed vehicle procedure the pavement design is based on the number of repetitions of a standard vehicle or axle load such as the 80-kN (18-kip) single-axle load used in the AASHTO design procedure. In the variable traffic and vehicle procedure, loading magnitude, configuration, and number of load repetitions are considered by dividing the loads into a number of groups and determining the stresses, strains, and deflections under each load group.

The recommended procedure for use in the geofoam load bearing design procedure presented below is the fixed traffic procedure because the design procedure limits static and

dynamic loads to less than the elastic limit stress, which should result in tolerable deformations and the number of load repetitions do not have to be considered..

Figure 6.13 shows the wheel configuration of a typical semitrailer truck with a tandem axle with dual tires at the rear. Trucks with a tridem axle, each spaced at 122 to 137 cm (48 to 54 in.) apart, with dual tires also exists. The largest live or traffic load expected on the roadway above the embankment should be used for design. The magnitude and vehicle tire configuration that will provide the largest live load is typically not known during the preliminary design phase. Therefore, the AASHTO standard classes of highway loading (*15*) can be used for preliminary load bearing analyses.

Figure 6.13. Wheel configuration of a typical semitrailer truck (*14*).

Step 2: Add impact allowance to traffic loads

Allowance for impact forces from dynamic, vibratory, and impact effects of traffic are generally only considered where they act across the width of the embankment or adjacent to a bridge abutment. In (*1*) an impact coefficient of 0.3 is recommended for design of EPS-block geofoam. Equation (6.3) can be used to include the impact allowance to the live loads estimated in Step 1 if impact loading is deemed necessary for design:

$$Q=LL*(1+I) = 1.3\ (LL) \qquad \textbf{(6.3)}$$

where Q = traffic load with an allowance for impact,

LL = live load for traffic from AASHTO standard classes of highway loading (*15*) obtained in Step 1, and

I = impact coefficient = 0.3.

Step 3: Estimate traffic load stresses at top of EPS blocks

The objective of this step is to estimate the dissipation of vertical stress through the pavement system so that an estimate of the traffic stresses at the top of the EPS blocks can be obtained. The vertical stress at the top of the EPS is used to evaluate the load bearing capacity of the blocks directly under the pavement system. Various pavement systems, with and without a

separation layer between the pavement system and the EPS blocks, should be evaluated to determine which alternative is the most cost effective.

The three main procedures to determine the vertical stress at the top of the EPS are the Boussinesq solution (*16*), 1 (horizontal): 2 (vertical) stress distribution solution, and Burmister's elastic layered solution (*17*). In each method the pavement system is assumed to behave as a linearly elastic material.

The Boussinesq stress distribution solution does not accommodate layers with different elastic stress-strain properties and thus the stiffer pavement system over the softer EPS-blocks cannot be simulated. As a result, the Boussinesq solution is not recommended for estimating dissipation of vertical stress through the pavement system.

The 1(horizontal): 2(vertical) stress distribution solution assumes that the applied vertical stress on the pavement surface is distributed over an area of the same shape as the loaded area on the surface, but with dimensions that increase by an amount equal to the depth below the surface as shown in Figure 6.14 (*18*). For example, for a rectangular shaped loaded area with dimensions of B x L at the surface, the vertical stress at a depth z is assumed to be distributed over an area (B + z) by (L + z). The vertical stress is assumed to be uniform over the stressed area and is determined by dividing the total applied loads at the surface by the stressed area. The load distribution through typical pavement system materials (asphalt concrete, Portland Cement Concrete, granular materials) will generally exceed the distribution of 1(horizontal): 2(vertical) or 26.6 degrees. Hunt (*19*) indicates that (*20*) suggests an angle of 30 degrees within relatively weak soil and 45 degrees for relatively strong soil. Greater load-spreading in the range of 35 to 45 degrees may be obtained through stiffer materials such as well-compacted granular fill over soft clay (*21*). Therefore, a 1(horizontal): 1(vertical) or 45 degree load distribution can be assumed through pavement materials except for concrete. Concrete can be substituted for granular material using a 1 concrete to 3 gravel ratio (*22,23*).

The third and recommended procedure for estimating the stress at the top of the EPS is Burmister's elastic layered solution (*24*). Burmister's elastic layered solution is based on a uniform pressure applied to the surface over a circular area on top of an elastic half-space mass. Each layer has a finite thickness except for the lowest layer which is assumed to be infinite in thickness and each layer is assumed to be homogeneous, isotropic, and linearly elastic. The primary advantage of Burmister's theory is that it considers the influence of layers with different elastic properties within the system being considered. The primary disadvantage is that vertical stress calculations are time consuming if not performed by computer. However, design charts are presented below that alleviate the use of computer software to utilize Burmister's elastic layered solutions.

Figure 6.14. Approximate stress distribution by the 1(horizontal): 2 (vertical) method.

In summary, Burmister's elastic layered solution (*24*) is recommended to estimate the stress distribution through the pavement system to obtain the applied vertical stress at the top of the EPS-block fill due to a load applied to the pavement surface. To facilitate estimation of stresses on top of the EPS blocks from traffic and impact loads, stress design charts (see Figures 6.15 through 6.17) were developed during this study for various vehicle tire loads and pavement systems. The computer program KENLAYER (*14*), which is based on Burmister's solution, was used to calculate vertical stresses through various thicknesses of the following types of pavement systems: asphalt concrete, portland cement concrete (PCC), and a composite pavement system. A composite pavement system is defined here as an asphalt concrete pavement system with a PCC slab separation layer placed between the asphalt concrete pavement system and the EPS-block geofoam. The main assumption in the KENLAYER analysis is that the interface of the various pavement system layers and the interface between the pavement system and the EPS blocks are frictionless. This assumption yields more conservative values of applied vertical stress on top of the EPS. The vertical stress charts in Figures 6.15 through 6.17 can be used to estimate the applied vertical stress on top of the EPS due to a tire load on top of an asphalt concrete, PCC, and

composite pavement system, respectively. For example, the vertical stress applied to the top of the EPS blocks under a 178 mm (7 in.) thick asphalt pavement with a total wheel load of 100 kN (22,481 lbs) is approximately 55 kPa (8 lbs/in^2) (see Figure 6.15). This value of 55 kPa (8 lbs/in^2) is then used in the load bearing analysis described subsequently.

Loads Used in Developing Design Vertical Stress Charts

Axle loads ranging between 89 to 445 kN (20,000 and 100,000 lbs) were analyzed because this is the range of axle loads provided in the tables of axle load equivalency factors for calculating equivalent single-axle loads (ESALs) for single and tandem axles in the AASHTO 1993 pavement design guide (*25*). Based on these axle loads and on a tire pressure of 689 kPa (100 lbs/in²), a range of circular contact areas were obtained for both an axle system with two single tires and an axle system with two sets of dual tires using the equations shown below. These circular areas were used in KENLAYER. Both a single tire and a set of dual tires was modeled as a single contact area. Therefore, both a single tire and a set of dual tires can be represented by the total load of a single tire or on the dual tires and a contact area.

The contact pressure is typically assumed to be equal to the tire pressure (*14*) and the tire and pavement surface interface is assumed to be free of shear stress. Typical tire pressures for legal highway trucks with single and dual tires range from of 414 to 621 kPa (60 to 90 lbs/in²) (*26*). A tire pressure of 689 kPa (100 lbs/in²) appears to be representative and is recommended for preliminary design purposes. This tire pressure is near the high end of typical tire pressures but is used for analysis purposes by transportation software such as ILLI-PAVE (*27*).

The contact pressure is converted to a traffic load by multiplying by the contact area of the tire. For the case of a single axle with a single tire, the contact area is given by Equation (6.4) and the radius of the contact area is given by Equation (6.5):

$$A_C = \frac{Q_t}{q} \qquad \textbf{(6.4)}$$

$$r = \left(\frac{A_C}{\pi} \right)^{\frac{1}{2}} \quad \textbf{(6.5)}$$

where A_C = contact area of one tire,

Q_t = live load on one tire,

q = contact pressure = tire pressure, and

r = radius of contact area

For the case of a single axle with dual tires, the contact area can be estimated by converting the set of duals into a singular circular area by assuming that the circle has an area equal to the contact area of the duals as indicated by Equation (6.6). The radius of contact is given by Equation (6.7). Equation (6.6) yields a conservative value, i.e., smaller area, for the contact area because the area between the duals is not included.

$$A_{CD} = \frac{Q_D}{q} \quad \textbf{(6.6)}$$

$$r = \left(\frac{A_{CD}}{\pi} \right)^{\frac{1}{2}} \quad \textbf{(6.7)}$$

where A_{CD} = contact area of dual tires

Q_D = live load on dual tires

q = contact pressure on each tire = tire pressure

Pavement Systems Used in Developing Design Vertical Stress Charts

Asphalt Concrete Pavement System. Based on the design catalog for flexible pavements, see Table 4.2, an asphalt thickness ranging from 76 to 178 mm (3 to 7 in.) was utilized with a corresponding crushed stone base thickness equal to 610 mm (24 in.) less the thickness of the asphalt. This provides the minimum recommended pavement system thickness of 610 mm (24 in.) to minimize the potential for differential icing and solar heating. For the asphalt concrete, a typical unit weight of 23 kN/m³ (148 lbf/ft³), Poisson's ratio of 0.46, and modulus of elasticity of 689 MPa (100 x 10^3 lbs/in²) were utilized (*14*). For the crushed stone base, a unit weight of 22

kN/m³ (138 lbf/ft³), Poisson's ratio of 0.35, and modulus of elasticity of 21 MPa (3,000 lbs/in²) was utilized in KENLAYER. The unit weight and Poisson's ratio was obtained from average values reported in (*14*). The modulus of elasticity was conservatively based on average values reported in (*19*) for a loose sand and gravel.

The resulting vertical stress at the top of the EPS, σ_{LL}, obtained from Figure 6.15 increases with the modulus of elasticity of the EPS. To maximize design values of σ_{LL} the properties of *EPS100* geofoam, which is the stiffest EPS considered herein, were used in the analysis. The properties of *EPS100* include a unit weight of 0.31 kN/m³ (2.0 lbf/ft³), Poisson's ratio of 0.18, and modulus of elasticity of 9,997 kPa (1,450 lbs/in²). Figure 6.15 presents values of σ_{LL} obtained from the analysis due to a single or dual wheel loads on an asphalt concrete pavement system.

Figure 6.15. Vertical stress on top of the EPS blocks, σ_{LL}, due to traffic loads on top of a 610 mm (24 in.) asphalt concrete pavement system.

Portland Cement Concrete. Based on the design catalog for rigid pavements, see Tables 4.6 and 4.7, a PCC thickness ranging from 127 to 229 mm (5 to 9 in.) was utilized with a crushed stone base thickness equal to 610 mm (24 in.) less the thickness of the PCC. This provides a minimum recommended pavement system thickness of 610 mm (24 in.) to minimize the potential for differential icing and solar heating. For the PCC, an average unit weight of 23.5 kN/m³ (150 lbf/ft³), Poisson's ratio of 0.15, and modulus of elasticity of 20,684 MPa (3×10^6 lbs/in²) were utilized from (*14*). The same properties for the crushed stone base and EPS fill used in the analysis of an asphalt concrete pavement system were utilized to develop the vertical stress applied by a PCC pavement system. Figure 6.16 presents the design vertical stress chart of a single or dual wheel acting on a PCC pavement system which can be used to estimate the vertical stress due to traffic loads, σ_{LL}, at the top of the EPS.

Figure 6.16. Vertical stress on top of the EPS blocks, σ_{LL}, due to traffic loads on top of a

610 mm (24 in.) portland cement concrete pavement system.

Composite Pavement System. The asphalt concrete pavement system used to create the design chart in Figure 6.15 was utilized for this scenario except that a 102 mm (4 in.) concrete separation layer was added between the crushed stone base and the EPS blocks. A crushed stone base thickness equal to 610 mm (24 in.) less the thickness of the asphalt concrete and the separation slab was used to complete the remainder of the composite pavement system. This also provides a minimum recommended pavement system thickness of 610 mm (24 in.) to minimize the potential for differential icing and solar heating. The material properties utilized for the analysis of the composite pavement system are the same as those used for the asphalt concrete and PCC pavement systems in Figures 6.15 and 6.16, respectively. Figure 6.17 presents the design charts for vertical stress, σ_{LL}, on top of the EPS block due to a single or dual wheel acting on this composite pavement system.

Figure 6.17. Vertical stress on top of the EPS blocks, σ_{LL}, due to traffic loads on top of a 610 mm (24 in.) asphalt concrete pavement system with a 102 mm (4 in.) concrete separation layer between the pavement system and EPS blocks.

Conversion of Circular Loaded Areas to Rectangular Loaded Area

It is more convenient to use a rectangular loaded area at the top of the EPS to calculate the vertical stresses acting on the EPS block in Step 9 of the load bearing analysis. This is similar to converting single and dual tire loadings to a single loaded circular area to estimate the stress through the pavement system. To perform the conversion the tire contact pressure on top of the pavement system is distributed over a circular area. The Portland Cement Association 1984 method as described in (*14*) can be used to convert the circular loaded area to an equivalent rectangular loaded area, as shown in Figure 6.18. The rectangular area shown is equivalent to a circular contact area that corresponds to a single axle with a single tire, A_C , or a single axle with

dual tires, A_{CD}. The values of A_C and A_{CD} can be obtained from Equations (6.4) and (6.6), respectively, using the following procedure:

1) Estimate σ_{LL} from Figure 6.15, 6.16, or 6.17 depending on the pavement system being considered.

2) Use σ_{LL} in Equation (6.4) or (6.6) as the contact pressure, q, and the recommended traffic loads from Step 1 to estimate the live load in Equation (6.4) or (6.6) for a single axle with a single tire or a single axle with dual tires, respectively, to calculate A_C or A_{CD} .

3) Use the values of A_C or A_{CD} to calculate the value of L′ in Figure 6.18 by equating A_C or A_{CD} to $0.5227L'^2$ and solving for L′. After solving for L′, the dimensions of the rectangular loaded area in Figure 6.18, i.e., 0.8712L′ and 0.6L′, can be calculated.

Figure 6.18. Method for converting a circular contact area into an equivalent rectangular contact area (*14*).

Step 4: Estimate gravity stresses at top of EPS blocks

Stresses resulting from the gravity load of the pavement system and any road hardware placed on top of the roadway must be added to the traffic stresses obtained in Step 3 to conduct a load bearing analysis of the EPS. The gravity stress from the weight of the pavement system is given by:

$$\sigma_{DL} = T_{pavement} * \gamma_{pavement} \quad \textbf{(6.8)}$$

where σ_{DL} = gravity stress due to dead loads

$T_{pavement}$ = pavement system thickness, and

$\gamma_{pavement}$ = average unit weight of the pavement system.

As discussed in Chapter 4, the various components of the pavement system can be assumed to have an average unit weight of 20 kN/m^3 (130 lbf/ft^3). Because the traffic stresses in

Figures 6.15 through 6.17 are based on a pavement system with a total thickness of 610 mm (24 in.), a value of $T_{pavement}$ equal to 610 mm (24 in.) should be used to estimate σ_{DL} to ensure consistency.

Step 5: Calculate total stresses at top of EPS blocks

The total vertical stress at the top of EPS blocks underlying the pavement system from traffic and gravity loads, σ_{total}, is given by:

$$\sigma_{total} = \sigma_{LL} + \sigma_{DL} \quad \textbf{(6.9)}$$

Step 6: Determine minimum required elastic limit stress for EPS under pavement system

The minimum required elastic limit stress of the EPS block under the pavement system can be calculated by multiplying the total vertical stress from Step 5 by a factor of safety as shown by Equation (6.10).

$$\sigma_e \geq \sigma_{total} * FS \quad \textbf{(6.10)}$$

where σ_e = minimum elastic limit stress of EPS

FS = factor of safety = 1.2

The main component of σ_{total} is the traffic stress and not the gravity stress from the pavement. Because traffic is a main component of σ_{total} and traffic is a transient load like wind loading, a factor of 1.2 is recommended for the load bearing analysis. This is the same value of factor of safety recommended for other transient or temporary loadings such as wind, hydrostatic uplift, and sliding, and seismic used for external stability analyses.

Step 7: Select appropriate EPS block to satisfy the required EPS elastic limit stress for underneath the pavement system, e.g., *EPS50*, *EPS70*, or *EPS100*

Select an EPS type from Table 6.2 that exhibits an elastic limit stress greater than or equal to the required σ_e determined in Step 6. The EPS designation system in Table 6.2 defines the minimum elastic limit stress of the block as a whole in kilopascals. For example, *EPS50* will have a minimum elastic limit stress of 50 kPa (7.2 lbs/in^2). The EPS selected will be the EPS

block type that will be used directly beneath the pavement system for a minimum depth of 610 mm (24 in.) in the EPS fill. This minimum depth is recommended because it is typically the critical depth assumed in pavement design for selection of an average resilient modulus for design of the pavement system (*14*). Thus, the 610 mm (24 in.) depth is only an analysis depth and is not based on the thickness of the EPS blocks. Of course, if the proposed block thickness is greater than 610 mm (24 in.), the block selected in this step will conservatively extend below the 610 mm (24 in.) zone. The use of *EPS40* is not recommended directly beneath paved areas because an elastic limit stress of 40 kPa (5.8 lbs/in^2) has resulted in pavement settlement problems.

Step 8: Select preliminary pavement system type and determine if a separation layer is required

A cost analysis should be performed in Step 8 to preliminarily select the optimal pavement system that will be used over the type of EPS blocks determined in Step 7. The cost analysis can focus on one or all three of the pavement systems evaluated in Step 3, i.e., asphalt concrete, portland cement concrete, and a composite pavement system. The EPS selected for a depth of 610 m (24 in.) below the pavement system is a function of the pavement system selected because the vertical stress induced at the top of the EPS varies with the pavement system as shown in Figures 6.15 through 6.17. Therefore, several cost scenarios can be analyzed, e.g., a PCC versus asphalt concrete pavement system and the accompanying EPS for each pavement system, to determine the optimal combination of pavement system and EPS. The cost analysis will also determine if a concrete separation layer between the pavement and EPS is cost effective by performing a cost analysis on the composite system. The resulting pavement system will be used in Steps 9 through 13.

If a concrete separation slab will be used, the thickness of the concrete slab can be estimated by assuming the slab to be a granular material and will dissipate the traffic stresses to a desirable level at 1(horizontal): 1(vertical) stress distribution. Concrete can then be substituted for granular material using the 1 concrete to 3 gravel ratio previously discussed in Step 3 to estimate

the required thickness of granular material. For example, a 102 mm (4 in.) thick concrete separation layer can be used to replace 306 mm (12 in.) of granular material. Therefore, a 927 mm (36.5 in.) thick asphalt concrete pavement system that consists of 127 mm (5 in.) of asphalt and 800 mm (31.5 in.) of crushed stone base will be 927 mm (36.5 in.) thick less 306 mm (12 in.) of crushed stone base which is replaced by 102 mm (4 in.) thick concrete separation layer. However, as discussed in Chapter 4, it is recommended that a minimum pavement system thickness of 610 mm (24 in.) be used to minimize the potential for differential icing and solar heating.

Step 9: Estimate traffic stresses at various depths within the EPS blocks

This step estimates the dissipation of the traffic induced stresses through the EPS blocks within the embankment. Utilizing the pavement system and separation layer, if included, from Step 8, the vertical stress from the traffic loads at depths greater than 610 mm (24 in.) in the EPS is calculated. The vertical stress is usually calculated at every 1 m (3.3 ft) of depth below a depth of 610 mm (24 in.). Block thickness is typically not used as a reference depth because the block thickness that will be used on a given project will typically not be known during the design stage of the project. The first depth at which the vertical stress will be estimated is 610 mm (24 in.) because in Step 7 the EPS selected to support the pavement system will extend to a depth of 610 mm (24 in.). The traffic vertical stresses should also be determined at any depth within the EPS blocks where the theoretical 1(horizontal): 2(vertical) stress zone overlaps as shown in Figure 6.19. These vertical stress estimates will be used in Step 12 to determine if the EPS type selected in Step 8 for directly beneath the pavement system is adequate for a depth of greater than 610 mm (24 in.) into the EPS and to determine if an EPS block with a lower elastic limit stress, i.e., lower density and lower cost, can be used at a greater depth.

Based on an analysis performed during this study and the results of a full-scale model creep test that was performed at the Norwegian Road Research Laboratory (*28,29*) to investigate the time-dependent performance of EPS-block geofoam, a 1 (horizontal) to 2 (vertical)

distribution of vertical stresses through EPS blocks was found to be in agreement with the measured vertical stresses, which showed a stress distribution of 1 (horizontal) to 1.8 (vertical). The test fill had a height of 2 m (6.6 ft) and measured 4 m (13.1 ft) by 4 m (13.1 ft) in plan at the bottom of the fill decreasing in area with height approximately at a ratio of 2 (horizontal) to 1 (vertical) to about 2 m (6.6 ft) by 2 m (6.6 ft) at the top of the fill. A load of 105 kN (23.6 kips) was applied through a 2 m (6.6 ft) by 1 m (3.3 ft) plate at the top of the fill resulting in an applied stress of 52.5 kPa (1,096 lbs/ft^2). The fill consisted of four layers of full-size EPS blocks with dimensions 1.5 m (4.9 ft) by 1 m (3.3 ft) by 0.5 m (1.6 ft) and densities of 20 kg/m^3 (1.25 lbf/ft^3). The stress at the bottom of the fill was measured using four pressure cells. An average pressure of 7.8 kPa (163 lbs/ft^2) was measured in the pressure cells during the 1,270 day test. Based on this average pressure measured at the bottom of the test fill and the stress of 52.5 kPa (1,096 lbs/ft^2) applied at the top of the fill, the stress distribution within the EPS fill was approximately 1 (horizontal) to 1.8 (vertical). The measured stress distribution is slightly wider but still in agreement with a 1 (horizontal) to 2 (vertical) stress distribution. Thus, the measured stress with depth is slightly less than the typically assumed stress distribution, which results in a slightly conservative design.

In summary, Burmister's layered solution is only applicable to stress distribution through the pavement and thus the 1 (horizontal): 2 (vertical) stress distribution theory is used to estimate the vertical stress within the EPS. In order to use the 1 (horizontal): 2 (vertical) stress distribution method to calculate the vertical stresses applied through the depth of EPS block using hand calculations, it is easier to assume a rectangular loaded area at the top of the EPS and to assume that the total applied load at the surface of the EPS is distributed over an area of the same shape as the loaded area on top of the EPS, but with dimensions that increase by an amount equal to 1(horizontal): 2(vertical) (see Figure 6.14). As shown in Figure 6.14, at a depth z below the EPS, the total load Q applied at the surface of the EPS is assumed to be uniformly distributed over an area (B+z) by (L+z). The increase in vertical pressure, σ_Z, at depth z due to an applied live load

such as traffic is given by Equation (6.11). Figure 6.19 demonstrates the use of the 1 (horizontal): 2(vertical) to estimate overlapping stresses from closely spaced loaded areas such as from adjacent sets of single or dual tires.

Figure 6.19. Approximate stress distribution of closely spaced loaded areas by the 1 (horizontal): 2(vertical) method.

$$\sigma_{Z,LL} = \frac{Q}{(B+z)(L+z)} \quad \textbf{(6.11)}$$

where $\sigma_{Z,LL}$ = increase in vertical stress at depth z caused by traffic loading,

Q = applied traffic load,

B = width of the loaded area,

L = length of the loaded area.

To use the 1(horizontal): 2(vertical) stress distribution method to calculate the vertical stresses through the depth of the EPS block, the assumed circular loaded area below a tire used to determine σ_{LL} in Figures 6.15, 6.16, or 6.17 should be converted to an equivalent rectangular area as discussed previously in Step 3. Alternatively, Equation (6.11) can be modified to determine $\sigma_{Z,LL}$ directly from the σ_{LL}, which is determined from Figures 6.15, 6.16, or 6.17 as shown below:

$$Q = \sigma_{LL} * A_{rect} \quad \textbf{(6.12)}$$

where σ_{LL} is obtained from Figures 6.15, 6.16 or 6.17.

From Figure 6.18,

$$L' = \left(\frac{A_{rect}}{0.5227} \right)^{\frac{1}{2}} \quad \textbf{(6.13)}$$

$$B = 0.6 * L' \quad \textbf{(6.14)}$$

$$L = 0.8712 * L' \quad \textbf{(6.15)}$$

Substituting Equations (6.12) through (6.15) into (6.11),

$$\sigma_{Z,LL} = \frac{\sigma_{LL} * A_{rect}}{(0.6L' + z)(0.8712L' + z)} \quad \textbf{(6.16)}$$

where A_{rect} is either A_C or A_{CD} determined from Equations (6.4) or (6.6), respectively.

Step 10: Estimate gravity stresses at various depths within the EPS blocks

Stresses resulting from the gravity load of the pavement system, any road hardware placed on top of the roadway, and the EPS blocks must be added to the traffic stresses to evaluate the load bearing capacity of the EPS within the embankment. The procedure described in the Stress Distribution at Center of Embankment section of Chapter 5 can be used to obtain an estimate of the increase in vertical stress at the centerline of the geofoam embankment at various depths due to the increase in gravity stress of the pavement system. For example, Equations (5.10), (5.11), and (5.12) can be modified as shown below to determine the increase in vertical stress caused by the gravity load of the pavement system:

$$\Delta\sigma_{Z,DL} = \frac{q_t}{\pi}(\alpha + \sin\alpha) \text{ where } \alpha \text{ is in radians} \quad \textbf{(6.17)}$$

$$\alpha = 2 * \arctan\left(\frac{b}{z}\right) \text{ where } \alpha \text{ is calculated in radians} \quad \textbf{(6.18)}$$

$$q_t = q_{pavement} = \gamma_{pavement} * T_{pavement} \quad \textbf{(6.19)}$$

where $\Delta\sigma_{Z,DL}$ = increase in vertical stress at depth z due to pavement system dead load in m,

$\gamma_{pavement}$ = unit weight of the pavement system in kN/m³,

$T_{pavement}$ = thickness of the pavement system in m, and

the other variables are defined in Figure 5.3. The total gravity stress from the pavement system and the EPS blocks is given by:

$$\sigma_{Z,DL} = (\Delta\sigma_{Z,DL}) + (z * \gamma_{EPS}) \quad \textbf{(6.20)}$$

where $\sigma_{Z,DL}$ = total vertical stress at depth z due to dead loads in kN/m²,

z = depth from the top of the EPS in m,

γ_{EPS} = unit weight of the EPS blocks in kN/m³.

As discussed in Step 5, the various components of the pavement system can be assumed to have an average unit weight of 20 kN/m^3 (130 lbf/ft^3). Because the traffic stresses in Figures 6.15 through 6.17 are based on a pavement system with a total thickness of 610 mm (24 in.), a value of $T_{pavement}$ equal to 610 mm (24 in.) should be used to estimate q_t to ensure consistency. It is recommended that the unit weight of the EPS be assumed to be 1,000 N/m^3 (6.37 lbf/ft^3), to conservatively allow for long-term water absorption in the calculation of $\sigma_{Z,DL}$.

Step 11: Calculate total stresses at various depths within the EPS blocks

The total vertical stress induced by traffic and gravity loads at a particular depth within the EPS is given by:

$$\sigma_{total} = \sigma_{Z,LL} + \sigma_{Z,DL} \quad \textbf{(6.21)}$$

Step 12: Determine minimum required elastic limit stress for EPS at various depths

Determine the minimum required elastic limit stress of the EPS block at each depth that is being considered using the same equations from Step 6 which is shown below:

$$\sigma_e \geq \sigma_{total} * 1.2 \quad \textbf{(6.22)}$$

Step 13: Select appropriate EPS block to satisfy the required EPS elastic limit stress at various depths in the embankment

Select an EPS type from Table 6.2 that exhibits an elastic limit stress greater than or equal to the required σ_e determined in Step 12. *EPS40* is not recommended for directly beneath the pavement system (see Step 7) but can be used at depths below 610 mm (24 in.) in the embankment if the required elastic limit stress is less than 40 kPa (5.8 lbs/in^2). However, for constructability reasons, it is recommended that no more than two different EPS block types be used

Remedial Procedures

Remedial procedures that can be used to increase the factor of safety against load bearing failure includes adding a separation layer, such as a concrete slab, between the pavement system and the EPS blocks. If an EPS with an elastic limit stress greater than 100 kPa or 14.5 lbs/in^2 (*EPS100*) is required, consideration can be given to contacting local molders to determine if EPS-block geofoam with an elastic limit stress greater than 100 kPa (14.5 lbs/in^2) can be molded for the project.

ABUTMENT DESIGN

Introduction

In applications where the EPS-block geofoam is used as part of a bridge approach, the EPS blocks should be continued up to the drainage layer that is placed along the back of the abutment. A geosynthetic sheet drain, not natural aggregate, should be used for this drainage layer to minimize the vertical and lateral earth pressure on the subgrade and abutment, respectively, as well as facilitate construction. The design requirements for abutments as well as design examples can be found in (*30*). The procedure for design of retaining walls and abutments consists of the following steps (*30*):

1. Select preliminary proportions of the wall.
2. Determine loads and earth pressures.
3. Calculate magnitude of reaction force on base.
4. Check stability and safety criteria:
    (a) location of normal component of reactions,
    (b) adequacy of bearing pressure, and
    (c) safety against sliding.
5. Revise proportions of wall and repeat Steps 2 through 4 until stability criteria are satisfied; then check:
    (a) settlement within tolerable limits and
    (b) safety against deep-seated foundation failure.

6. If proportions become unreasonable, consider a foundation supported on driven piles or drilled shafts.

7. Compare economics of completed design with other wall systems.

For a bridge approach consisting of EPS-block geofoam backfill, earth pressures, which are required for Step 2 of the abutment design process, generated by the following two sources should be considered:

- the gravity load of the pavement system, W_P, and EPS blocks W_{EPS} (usually small) pressing directly on the back of the abutment (see Figure 6.20) and
- the active earth pressure from the soil behind the geofoam fill (see Figure 6.20) that can be transferred through the geofoam fill to the back of the abutment.

Figure 6.20. Loads on an EPS-block geofoam bridge approach system.

The magnitude of these loads vary depending on whether gravity and/or seismic loading is evaluated. The procedure for estimating the gravity and seismic loads are discussed in the following sections.

Gravity Loads

The assumed components of the gravity loads acting on a vertical wall or abutment are (see Figure 6.21):

- the uniform horizontal pressure acting over the entire depth of the geofoam caused by the vertical stress applied by the pavement system to the top of the EPS, which can be estimated from Figures 6.15 through 6.17,
- the horizontal pressure generated by the vertical stress imposed by the pavement system, which can be assumed to be equal to 1/10 times the vertical stress,
- the horizontal stress from the EPS blocks is neglected because it is negligible, and

- the lateral earth pressure, P_A, generated by the soil behind the EPS/soil interface, which is conservatively assumed to be transmitted without dissipation through the geofoam to the back of the abutment. The active earth pressure acting along this interface is calculated using a coefficient of active earth pressure, K_A because it is assumed that enough lateral deformation will occur to mobilize an active earth pressure condition in the soil behind the geofoam. The active earth pressure coefficient can be determined from the following equation, which is based on Coulomb's classical earth-pressure theory (*31*).

Figure 6.21. Gravity load components on a vertical wall.

$$K_A = \left[\frac{\sin(\theta-\varphi)\left(\frac{1}{\sin\theta}\right)}{\sqrt{\sin(\theta+\delta)} + \sqrt{\frac{\sin(\varphi+\delta)\sin(\varphi)}{\sin(\theta)}}} \right]^2 \quad \textbf{(6.23)}$$

where δ is the friction angle of the EPS/soil interface, which is analogous to the soil/wall interface in typical retaining wall design. The value of δ can be assumed to be equal to the friction angle of the soil, ϕ. Equation (6.23) is applicable only to horizontally level backfills. The active earth pressure force is expressed in Equation (6.24) as:

$$P_A = \frac{1}{2}\gamma_{Soil} H^2 K_A \quad \textbf{(6.24)}$$

where γ_{Soil} = unit weight of the soil backfill.

Seismic Loads

The following seismic loads acting on the back of an abutment must be added to the gravity loads in Figure 6.22 to safely design a bridge abutment in a seismic area:

- inertia forces from seismic excitation of the pavement system and the EPS blocks (usually negligible). These inertial forces should be reduced by the horizontal

sliding resistance, tan (ϕ) developed along the pavement system/EPS interface; and

- seismic component of the active earth pressure generated by the soil behind the EPS/soil interface, which can be calculated using the solution presented by Mononobe-Okabe (*32*).

Figure 6.22. Seismic load components on a wall.

DURABILITY

Consideration of durability can be divided into construction damage and long-term changes that may occur once the EPS blocks are buried in the ground. Both can affect product performance and therefore need to be considered during design. A recent (1999) state-of-art assessment of failures of all types of geosynthetics concluded that construction damage is the more important of these two durability categories by a significant margin (*33*). A more-specific assessment of geofoam failures came to the same broad conclusion (*34*). Both of these durability factors are discussed in the following paragraphs.

Construction Damage

Construction damage is considered to be physical damage to the geofoam product during its shipment to the project site; its placement on site; or during subsequent placement of other materials above the geofoam. A summary of recommended procedures to minimize construction damage to the EPS blocks is presented in the block shipment, handling, and storage; block placement; and pavement construction sections of Chapter 8.

Long-Term Changes

Long-term in-situ durability relates to chemical changes to or within the polymer that comprises the geofoam. Experience with actual in-ground use of EPS geofoam since the 1960s indicates that there is little or no chemical change or deterioration of EPS due to contact with the ground or ground water because EPS is relatively inert. Although EPS will absorb water to a limited extent once placed in the ground, the absorbed water causes no change in the physical

dimensions of the EPS block or changes in any physical properties that are relevant to lightweight fill applications. However, there are three issues regarding EPS durability that can affect the long-term durability of geofoam in roadway embankments and should be considered in design:

- The surface of EPS must be covered for protection against ultraviolet (UV) radiation. Although EPS does not suffer UV deterioration to the extent that many other geosynthetics do (the surface of the EPS will just yellow and become chalky after some weeks or months of exposure), it is still recommended that the surface of the EPS be covered as rapidly as possible after block placement in the ground.
- Liquid petroleum hydrocarbons (gasoline, diesel fuel/heating oil) will dissolve EPS if the EPS is inundated with the liquid. This consideration in the design process is discussed in the pavement system design section of Chapter 4.
- Although EPS is not a food source for any known living organism, in below-grade residential insulation applications, EPS (and other polymeric foams such as XPS as well) has been found to be damaged by certain types of insects (termites and carpenter ants) tunneling through or nesting in the EPS. There are no known occurrences of this with EPS in any lightweight fill applications. However, an inorganic, natural mineral additive has been approved by the U.S. Environmental Protection Agency for use in EPS that renders the EPS resistant to such insect attack. This additive does not affect the engineering properties of the EPS although it can affect the cost as well as limit those who can supply the material because not all EPS block molders in the U.S. have a license to use this material. A license is required because this additive is covered by at least two U.S. patents (*35*). Experience indicates that some U.S. designers of EPS-block geofoam fills have opted to specify treated EPS block to be cautious and conservative. However, it is recommended that the insect additive be used only after careful

evaluation because there is no documented need for the additive and it is proprietary which affects cost.

OTHER INTERNAL DESIGN CONSIDERATIONS

Site Preparation

Proper site preparation prior to placing the EPS blocks is important for both internal stability as well as overall constructability. This is important because each layer of blocks should be placed as level as possible to avoid high spots that will cause stress concentrations and rocking of the blocks. If the first block layer is not sufficiently level, block-alignment problems will tend to be compounded with each succeeding layer. Recommended site preparation details are provided in the site preparation section of Chapter 8.

Slope Cover

An assessment of the stability of the slope cover, e.g., a soil or a structural material, must be made. For a soil cover, this assessment generally requires a sufficiently flat side slope (typically two horizontal to one vertical or flatter) to be used so the soil is inherently stable and not easily eroded. For a structural material cover, the material must either be self stable or physically attached to the assemblage of EPS blocks.

Utilities

Where possible, utilities that are either part of the road structure (e.g. storm drains, electrical conduit) or crossed by the road should be buried either within the pavement system or below the EPS blocks. If this is not possible, utilities may be buried within the EPS mass by creating trenches (either by judicious block placement or cutting out of a trench with a chain saw after placement) and placing the utility line within the trench using a conventional soil bed. The volume of soil placed under and around the utility line should be minimized to minimize the localized stress concentration on the underlying EPS and foundation soil. Normal EPS block placement can be continued above the utility line.

Whether a utility line is buried beneath or within the EPS mass, a concern is sometimes expressed as to how such a utility line will be accessed should service, maintenance, or upgrading be required. This cannot be answered definitively because there is no documented knowledge on this problem. In the interim, it would seem reasonable to saw-cut (using a chain saw) a vertical trench through the overlying EPS blocks as necessary to access the utility line. After the required utility work has been performed, the cut pieces of EPS (and not soil or other standard-weight material) should be placed within the trench, taking care not to leave voids between the replaced pieces. Consideration should be given to using an EPS-compatible glue to physically attach the cut pieces to the in-place EPS as well as each other. Alternatively, it might be possible to fill the trench with a geofoam material such as polyurethane that is compatible chemically and mechanically with the EPS and can be formed in place.

REFERENCES

1. "Design and Construction Manual for Lightweight Fill with EPS." The Public Works Research Institute of Ministry of Construction and Construction Project Consultants, Inc., Japan (1992) Ch. 3 and 5.
2. Sanders, R. L., and Seedhouse, R. L., "The Use of Polystyrene for Embankment Construction." *Contractor Report 356,* Transport Research Laboratory, Crowthorne, Berkshire, U.K. (1994) 55 pp.
3. "EPS." Expanded Polystyrol Construction Method Development Organization, Tokyo, Japan (1993) 310 pp.
4. Horvath, J. S., "A Concept for an Improved Inter-Block Mechanical Connector for EPS-Block Geofoam Lightweight Fill Applications: 'The Ring's the Thing'," In Manhattan College-School of Engineering, Center for Geotechnolgy [web site]. [updated 8 September 2001; cited 20 September2001]. Available from http://www.engineering.manhattan.edu/civil/CGT/T2olrgeomat2.html; INTERNET.
5. Duskov, M., "EPS as a Light Weight Sub-base Material in Pavement Structures; Final Report." *Report Number 7-94-211-6,* Delft University of Technology, Delft, The Netherlands (1994).
6. Horvath, J. S., *Geofoam Geosynthetic*, Horvath Engineering, P.C., Scarsdale, NY (1995) 229 pp.
7. "AFM ® Gripper $_{TM}$ Plate." AFM ® Corporation, Excelsior, MN (1994).
8. Bartlett, S., Negussey, D., Kimble, M., and Sheeley, M., "Use of Geofoam as Super-Lightweight Fill for I-15 Reconstruction (Paper Pre-Print)." *Transportation Research Record 1736,* Transportation Research Board, Washington, D.C. (2000).

9. Spencer, E., "A Method of Analysis of the Stability of Embankments Assuming Parallel Inter-slice Forces." *Geotechnique*, Vol. 17, No. 1 (1967) pp. 11-26.
10. Sharma, S., *XSTABL: An Integrated Slope Stability Analysis Program for Personal Computers*, Interactive Software Designs, Inc., Moscow, Idaho (1996) 150 pp.
11. Yegian, M. K., and Lahlaf, A. M., "Dynamic Interface Shear Strength Properties of Geomembranes and Geotextiles." *ASCE Journal of Geotechnical Engineering*, Vol. 118, No. 5 (1992) pp. 760-779.
12. Stark, T. D., and Poeppel, A. R., "Landfill Liner Interface Strengths From Torsional-Ring-Shear Tests." *ASCE Journal of Geotechnical Engineering*, Vol. 120, No. 3 (1994) pp. 597-615.
13. Janbu, N., "Slope Stability Computations." *Embankment Dam Engineering,* Hirschfield and Poulos, eds., John Wiley & Sons, New York (1973) pp. 47-86.
14. Huang, Y. H., "Pavement Analysis and Design.", Prentice-Hall, Inc., Englewood Cliffs, NJ, (1993) 805.
15. American Association of State Highway and Transportation Officials, *Standard Specifications for Highway Bridges*, 16th, American Association of State Highway and Transportation Officials, Washington, D.C. (1996).
16. Boussinesq, J., *Application des Potentiels à l' Étude de l' Équilibre et du Mouvement des Solides Élastiques*, Gauthier-Villard, Paris (1885).
17. Burmister, D. M., "The Theory of Stresses and Displacements in Layered Systems and Applications to the Design of Airport Runways." *Proceedings, Highway Research Board,*1958, Vol. 23 pp. 126-144.
18. "Settlement Analysis." *Technical Engineering and Design Guides as Adapted From the U.S. Army Corps of Engineers, No. 9,* ASCE, New York (1994) 144 pp.
19. Hunt, R. E., *Geotechnical Engineering Analysis and Evaluation*, McGraw-Hill, Inc., New York (1986) 729 pp.
20. Sowers, G. F., *Introductory Soil Mechanics and Foundations: Geotechnical Engineering*, 4th, Macmillan Publishing, NY (1979).
21. Jewell, R. A., *Soil Reinforcement with Geotextiles*, Construction Industry Research and Information Association, London (1996).
22. Refsdal, G., "Frost Protection of Road Pavements." *Frost Action in Soils - No. 26,* Committee on Permafrost, ed., Oslo, Norway (1987) pp. 3-19.
23. "Matériaux Légers pour Remblais/Lightweight Filling Materials." *Document No. 12.02.B,* PIARC-World Road Association, La Defense, France (1997) 287 pp.
24. Burmister, D. M., "The Theory of Stresses and Displacements in Layered Systems and Applications to the Design of Airport Runways." *Proceedings, Highway Research Board,* Vol. 23, (1943) pp. 126-144.
25. American Association of State Highway and Transportation Officials, *AASHTO Guide for Design of Pavement Structures, 1993*, American Association of State Highway and Transportation Officials, Washington, D.C. (1993).
26. Schroeder, W. L., *Soils In Construction*, 3rd, Wiley, NY (1984) 330 pp.
27. Raad, L., and Figueroa, J. L., "Load Response of Transportation Support Systems." *Transportation Engineering Journal, ASCE*, Vol. 106, No. TE1 (1980) pp. 111-128.

28. Aabøe, R., "Deformasjonsegenskaper og spenningsforhold i fyllinger av EPS (Deformation and stress conditions in fills of EPS)." *Intern Rapport Nr. 1645,* Public Roads Administration (1993) 22 pp. Norwegian.
29. Aabøe, R., "Long-term performance and durability of EPS as a lightweight fill." *Nordic Road & Transport Research*, Vol. 12, No. 1 (2000) pp. 4-7.
30. Barker, R. M., Duncan, J. M., Rojiani, K. B., Ooi, P. S. K., Tan, C. K., and Kim, S. G., "Manuals for the Design of Bridge Foundations, NCHRP Report 343." Transportation Research Board, National Research Council, Washington, D.C. (1991) 308 pp.
31. Coulomb, C. A., "Essai sur une Application des Règles des Maximis et Minimis à quelques Problèmes de Statique Relatifs à l' Architecture (An attempt to apply the rules of maxima and minima to several problems of stability related to architecture)." Mém. Acad. Roy. des Sciences, Paris (1776) 343-382 pp.
32. Kavazanjian, E., Jr., Matasovic, N., Hadj-Hamou, T., and Sabatini, P. J., "Geotechnical Engineering Circular No. 3; Design Guidance: Geotechnical Earthquake Engineering for Highways; Volume I - Design Principles." *FHWA-SA-97-076,* U.S. Department of Transportation, Federal Highway Administration, Washington, D.C. (1997) 186 pp.
33. Giroud, J.-P., "Lessons Learned from Failures Associated with Geosynthetics." *Proceedings of Geosythetics '99,*1999, Vol. I pp. 1-66.
34. Horvath, J. S., "Lessons Learned from Failures Involving Geofoam in Roads and Embankments." *Research Report No. CE/GE-99-1,* Manhattan College, Bronx, NY (1999) 18 pp.
35. Savoy, T., "Building Material, with Protection from Insects, Molds, and Fungi." *U.S. Patent No. 5,194,323* (1993).

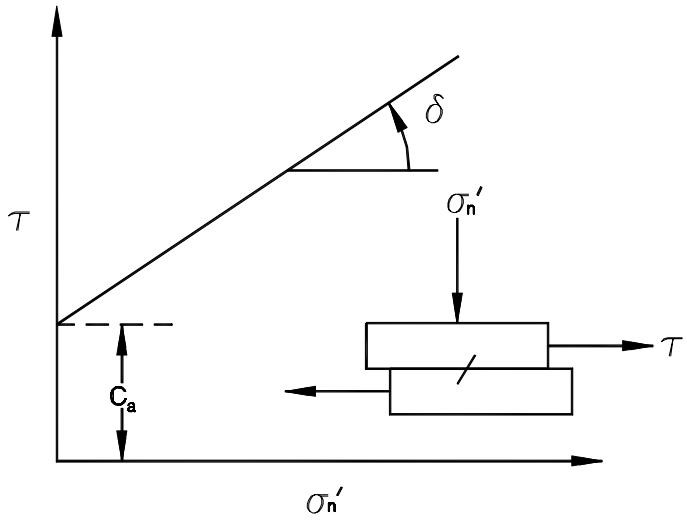

FIGURE 6.1 PROJ 24-11.doc

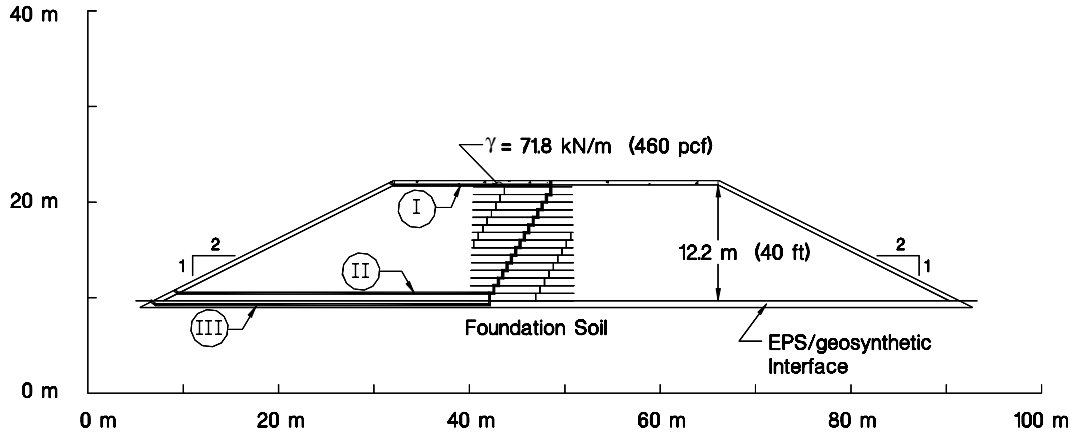

FIGURE 6.2 PROJ 24-11.doc

34 m road width, 12.2 m high embankment

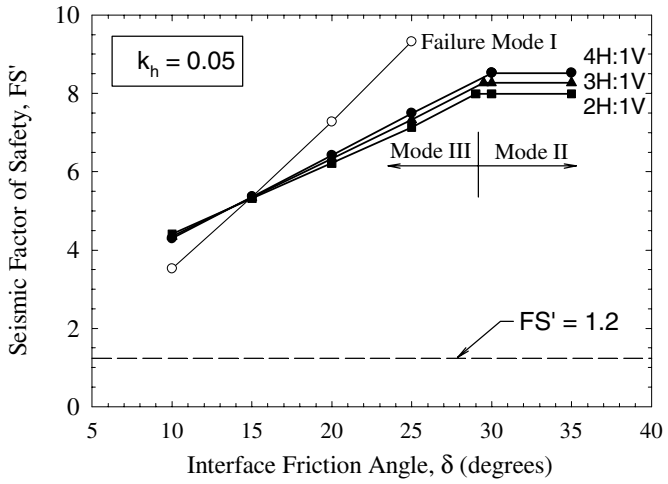

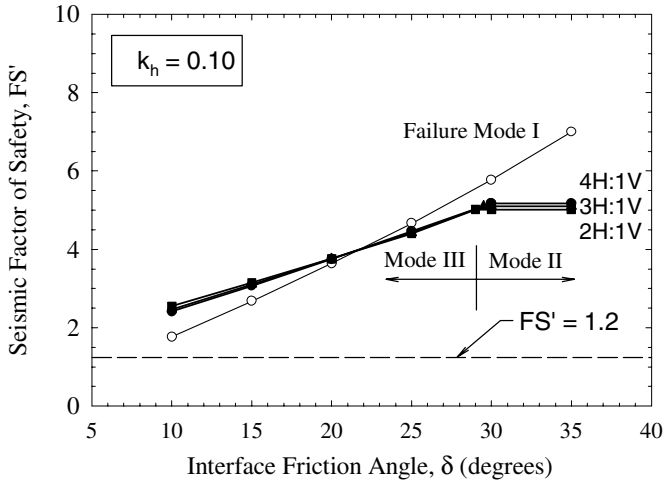

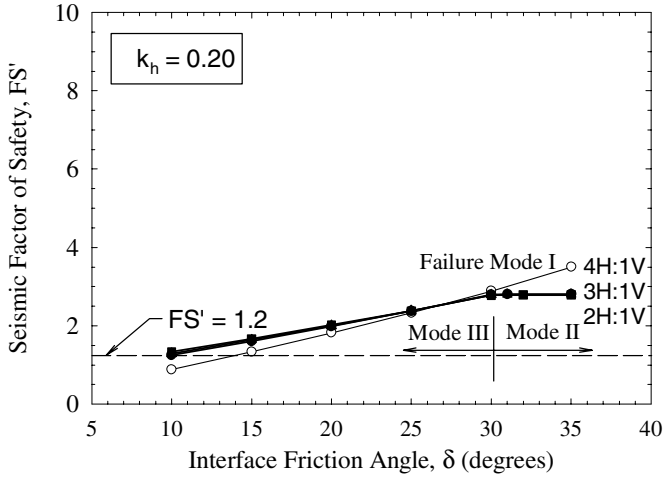

FIGURE 6.3 PROJ 24-11.doc

2H:1V slope, 12.2 m high embankment

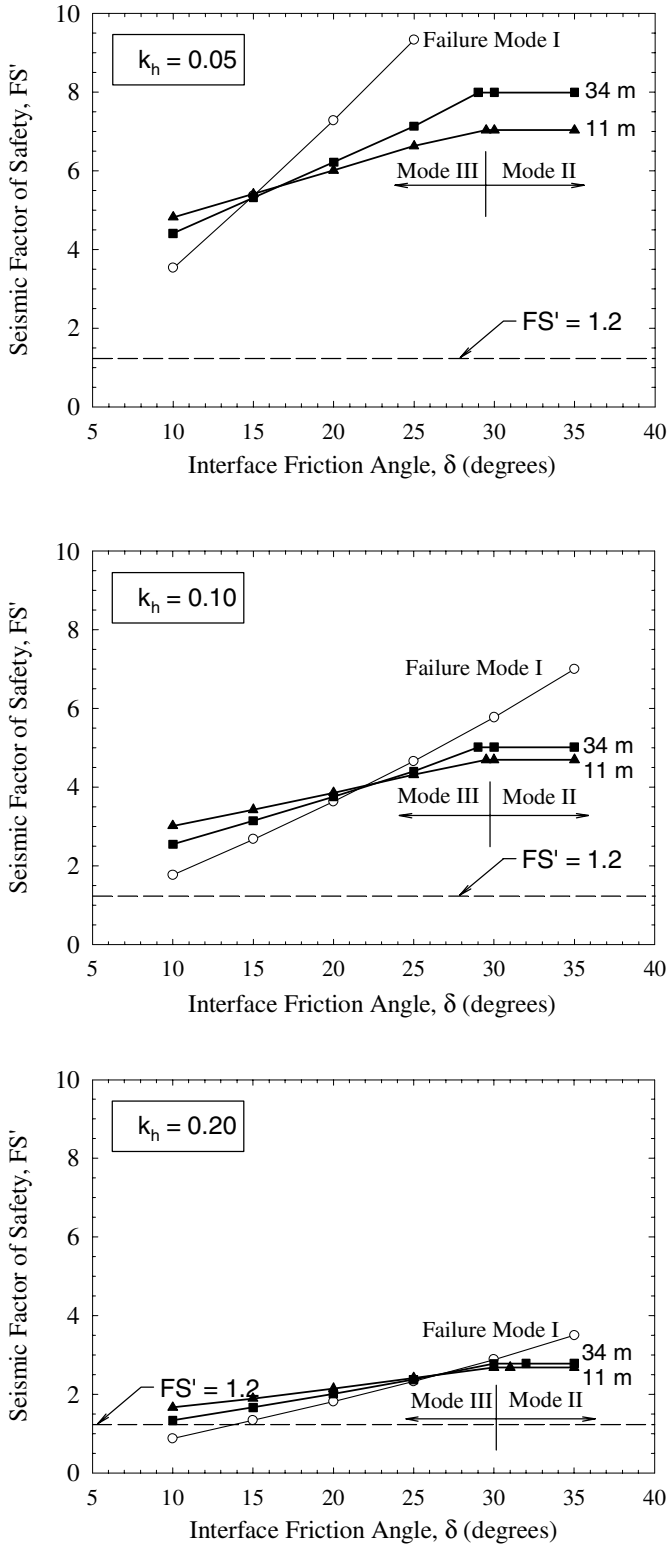

FIGURE 6.4 PROJ 24-11.doc

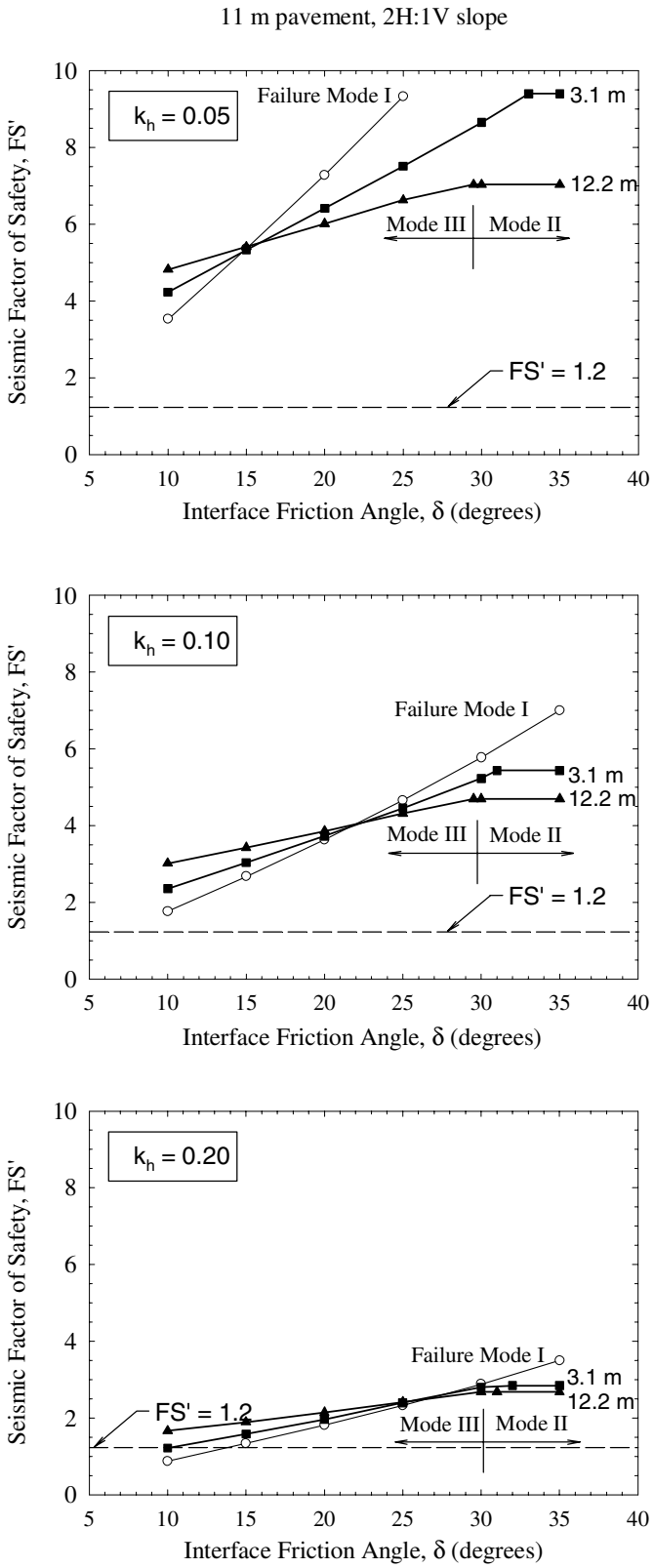

FIGURE 6.5 PROJ 24-11.doc

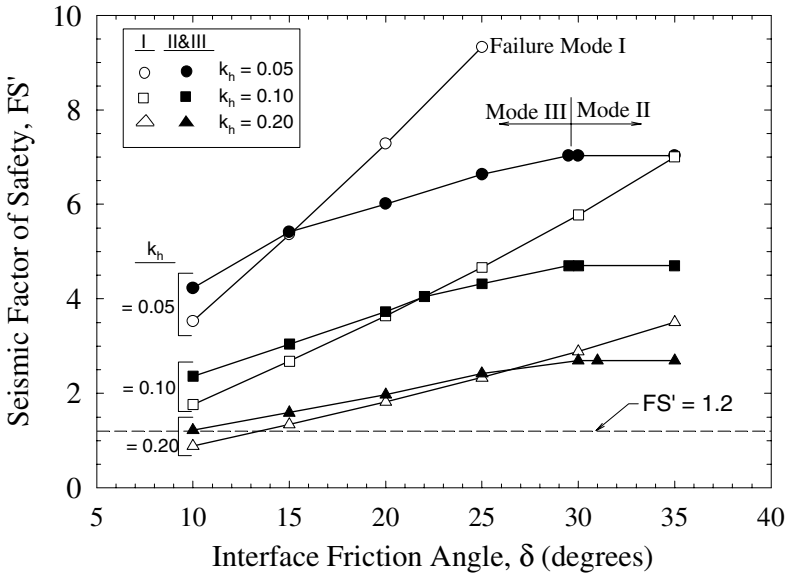

FIGURE 6.6 PROJ 24-11.doc

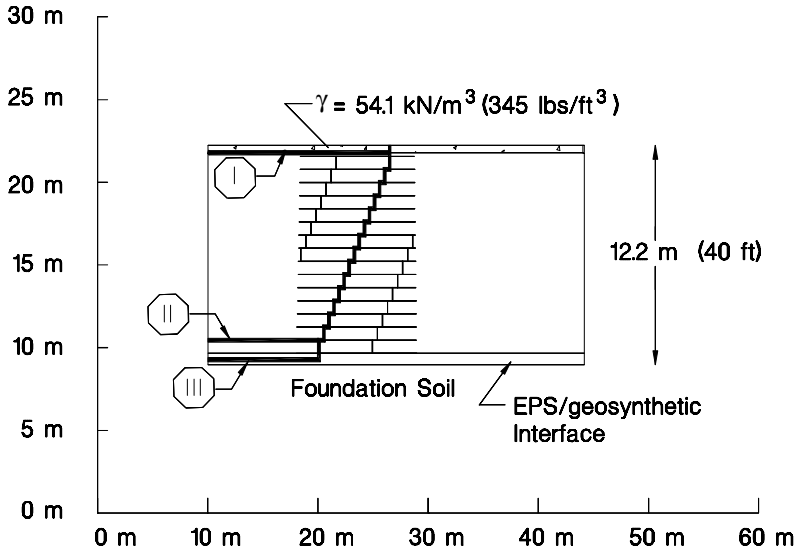

FIGURE 6.7 PROJ 24-11.doc

34 m road width, 12.2 m high embankment

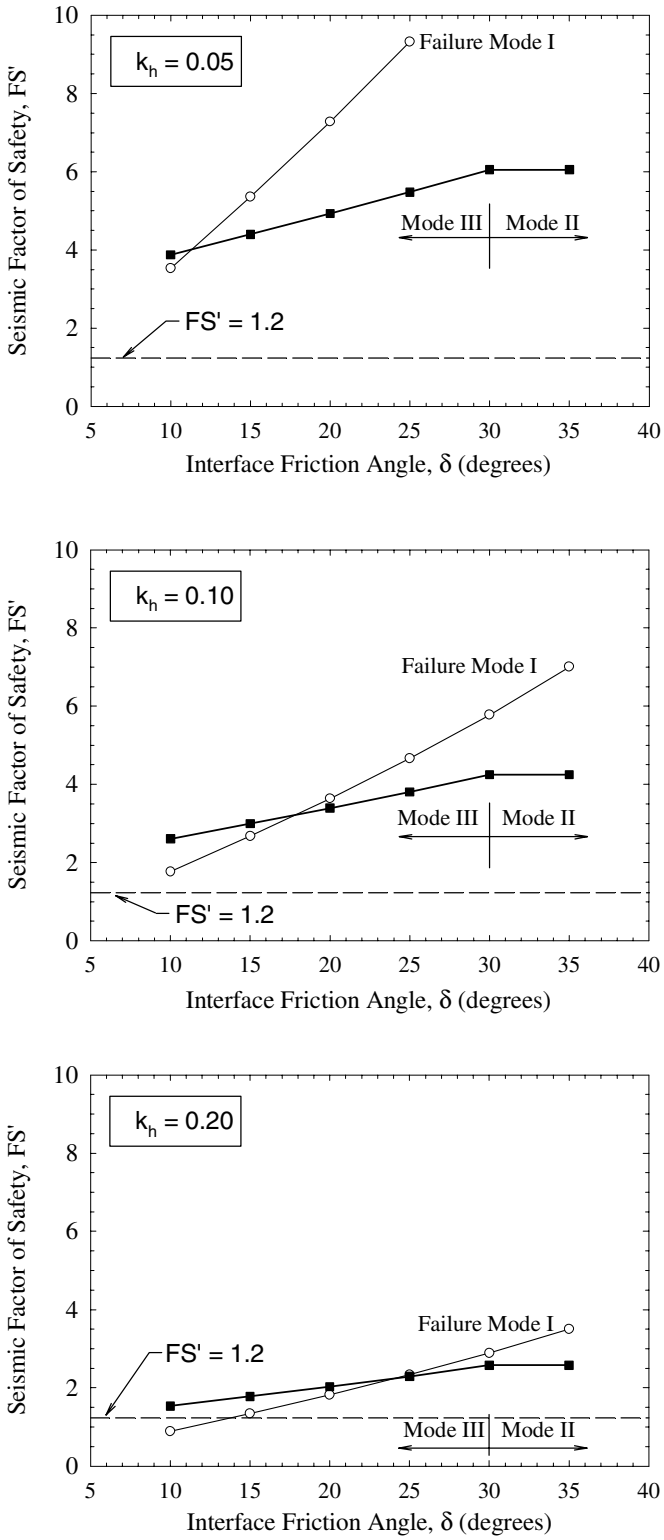

FIGURE 6.8 PROJ 24-11.doc

3.1 m high embankment

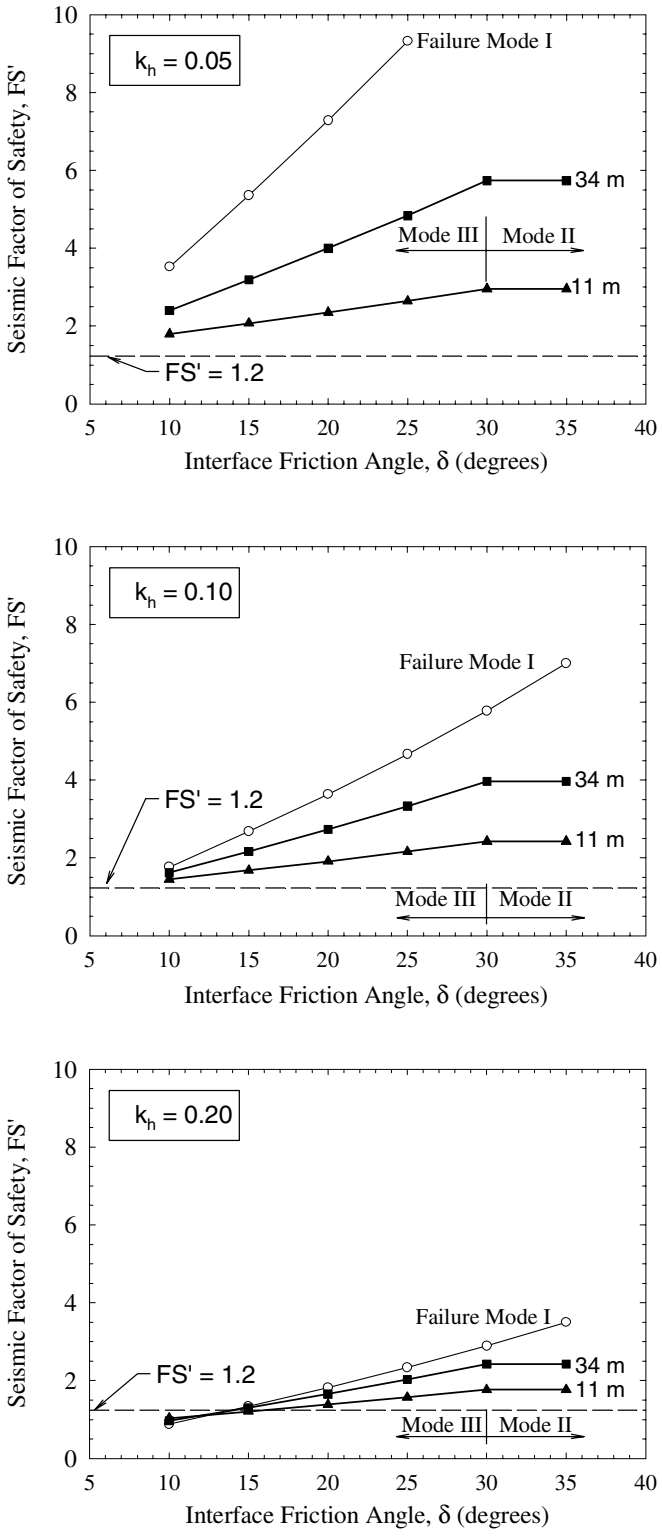

FIGURE 6.9 PROJ 24-11.doc

12.2 m high embankment

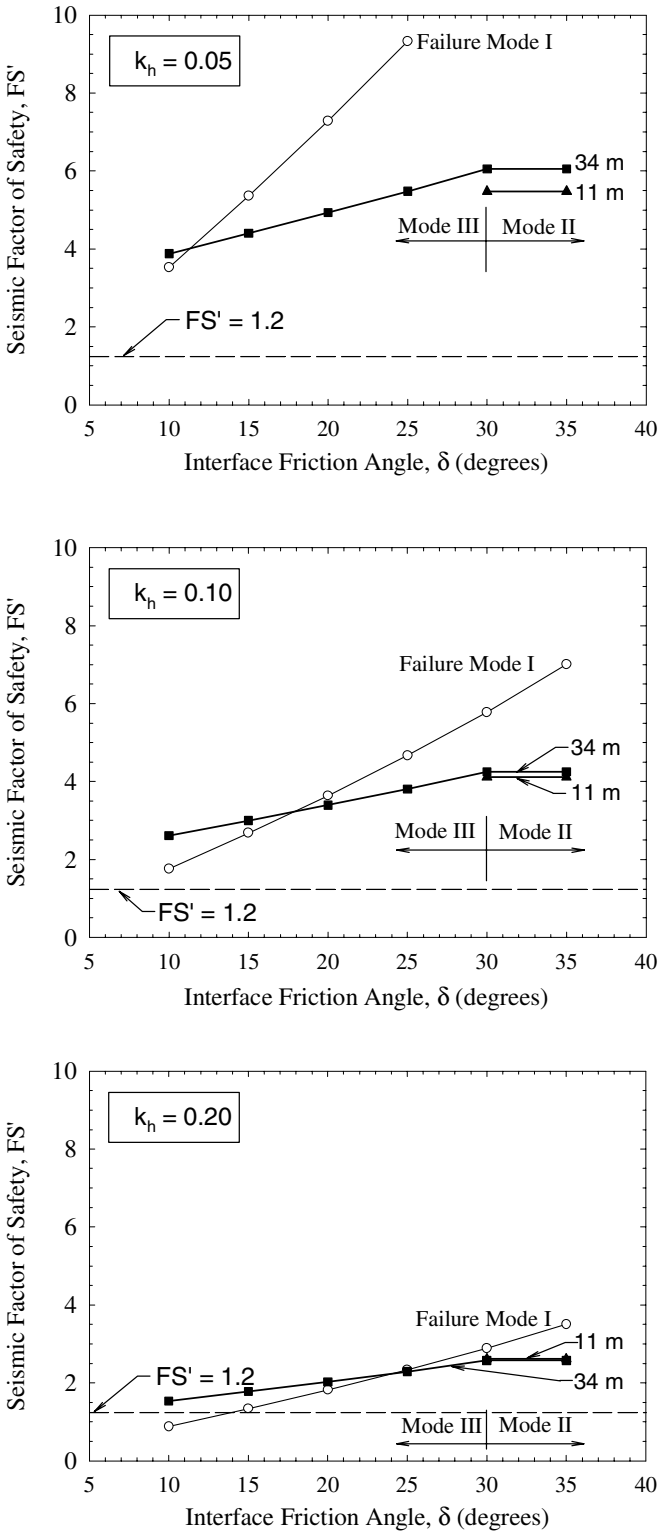

FIGURE 6.10 PROJ 24-11.doc

11 m wide pavement

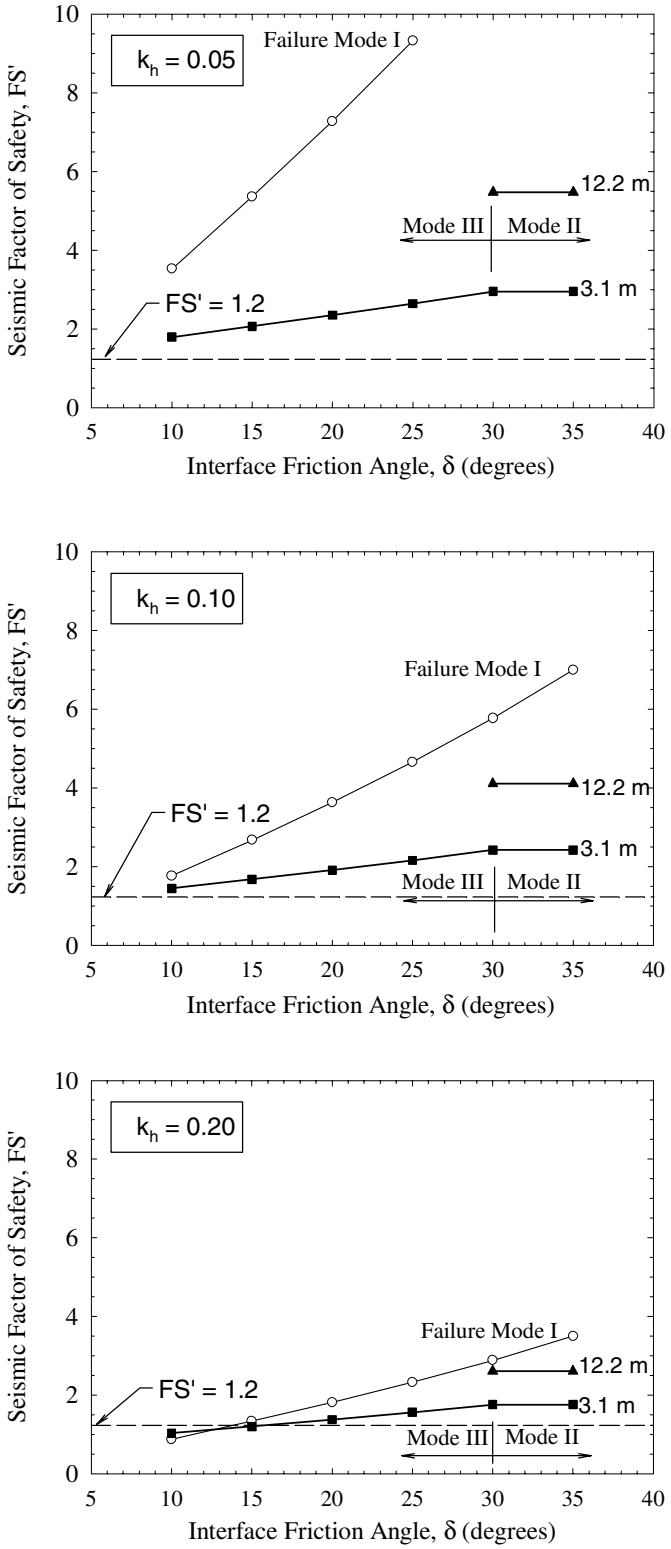

FIGURE 6.11 PROJ 24-11.doc

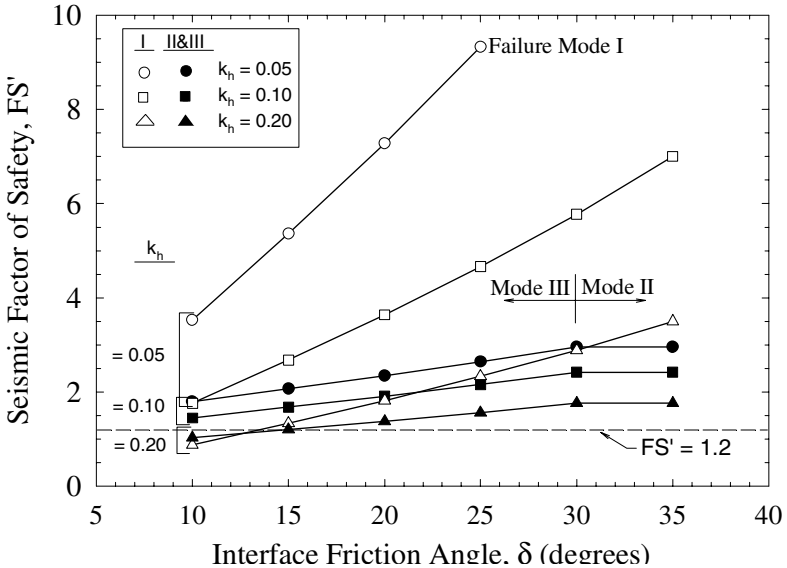

FIGURE 6.12 PROJ 24-11.doc

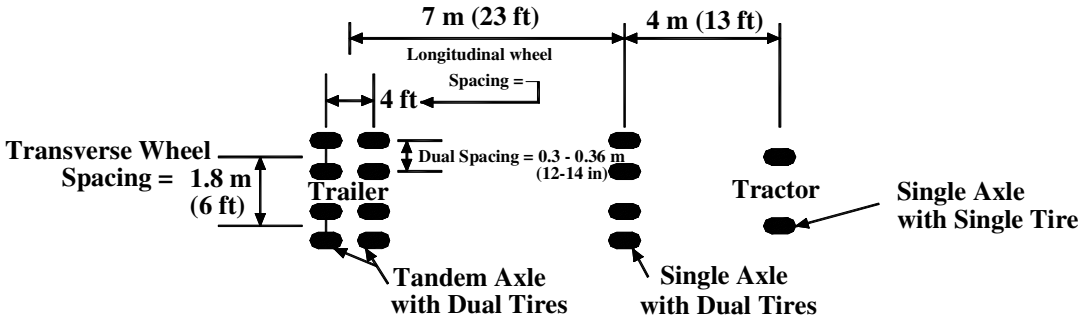

FIGURE 6.13 PROJ 24-11.doc

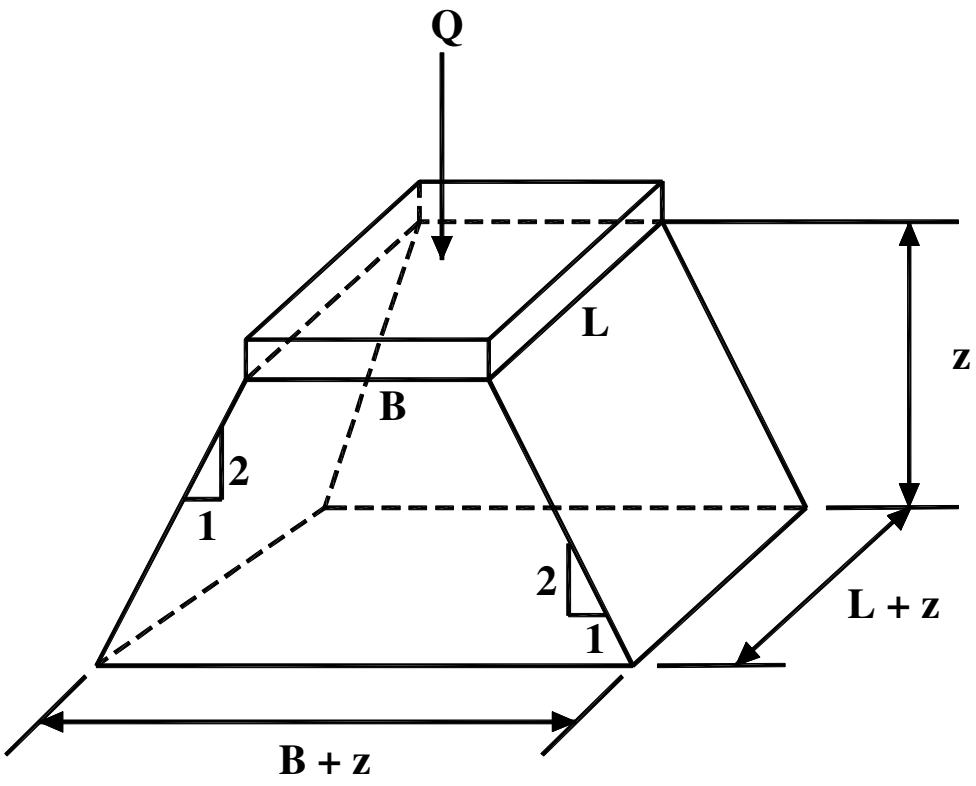

FIGURE 6.14 PROJ 24-11.doc

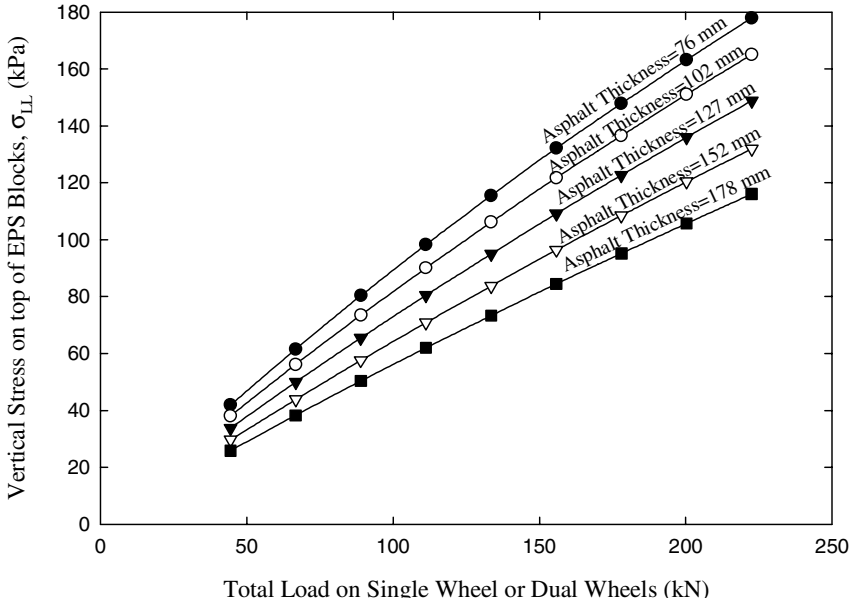

FIGURE 6.15 PROJ 24-11.doc

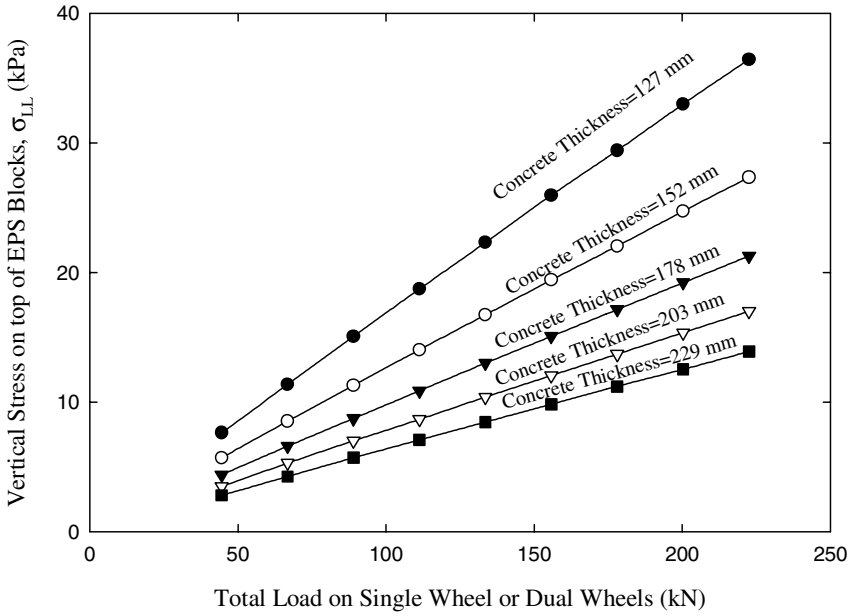

FIGURE 6.16 PROJ 24-11.doc

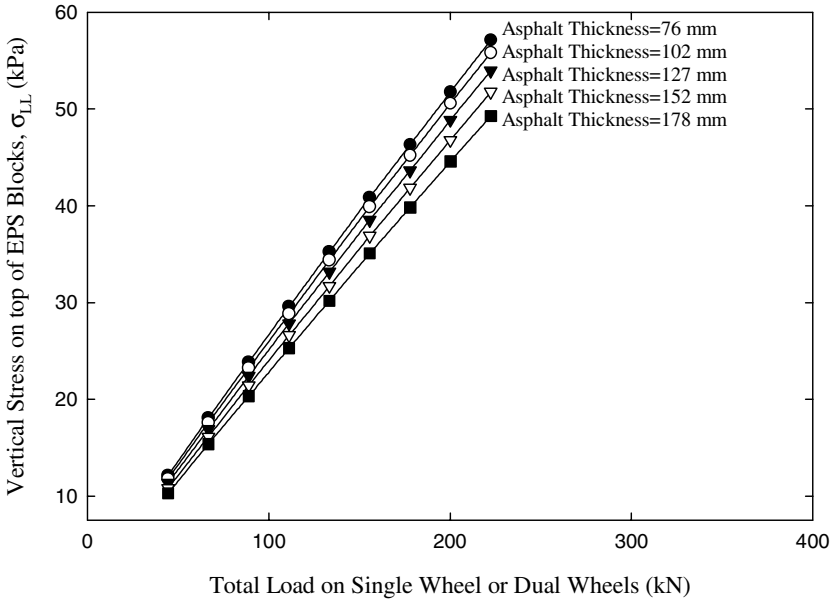

FIGURE 6.17 PROJ 24-11.doc

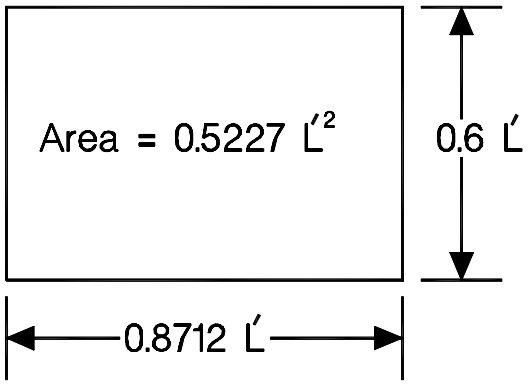

FIGURE 6.18 PROJ 24-11.doc

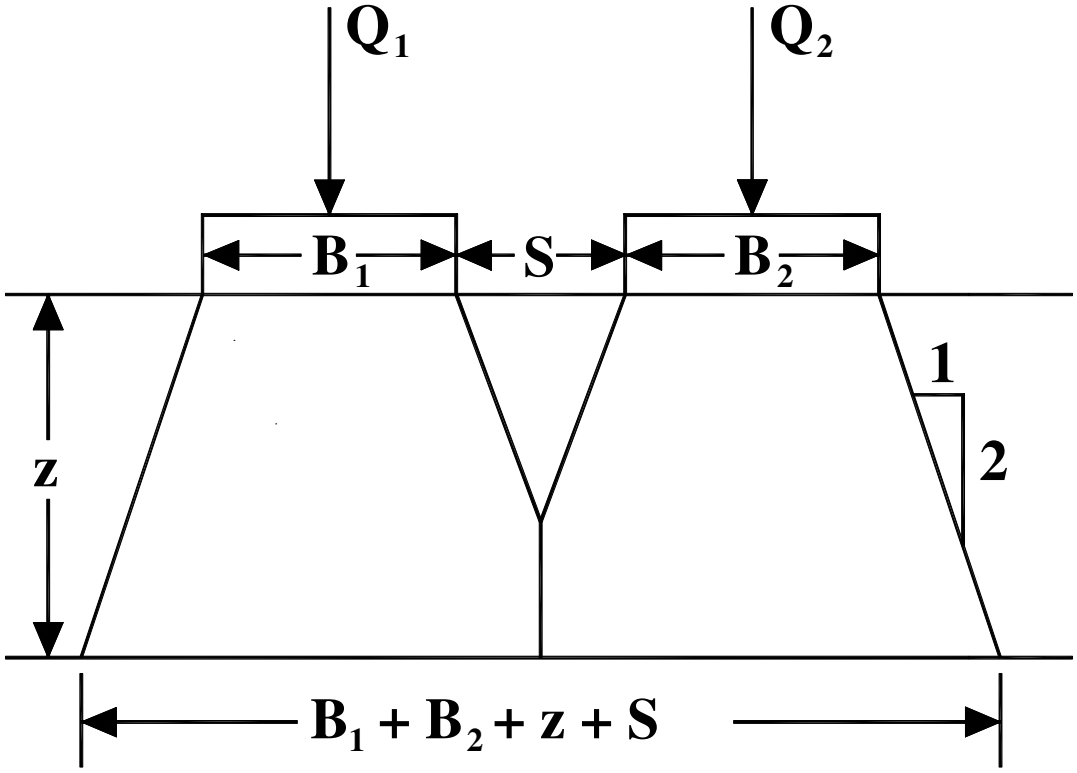

FIGURE 6.19 PROJ 24-11.doc

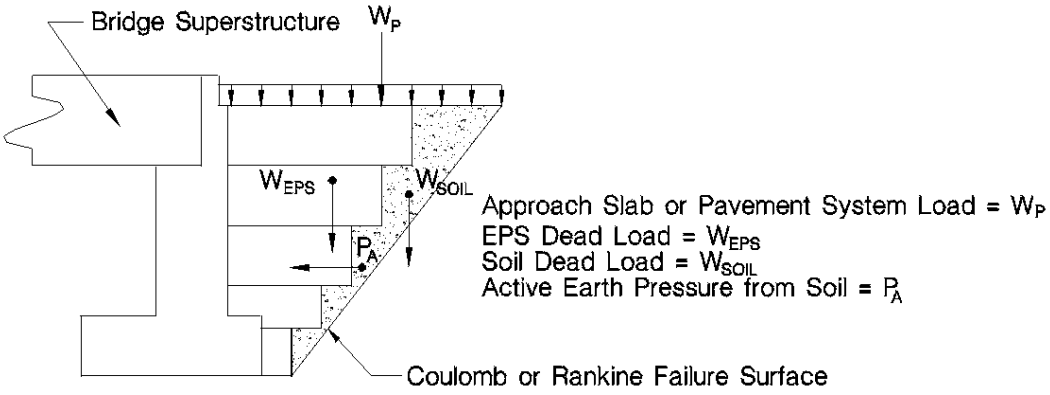

FIGURE 6.20 PROJ 24-11.doc

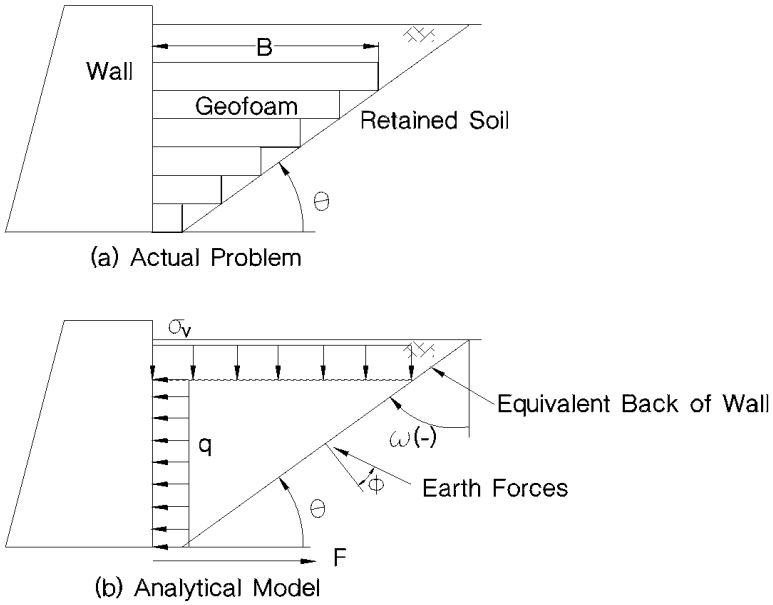

FIGURE 6.21 PROJ 24-11.doc

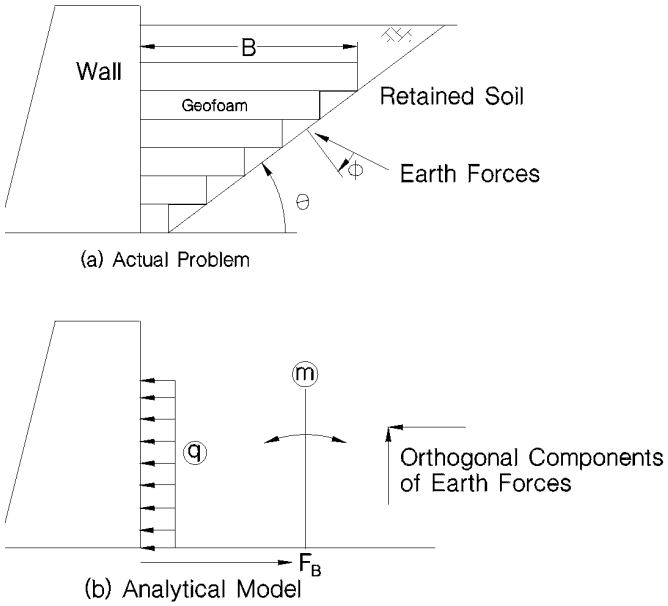

FIGURE 6.22 PROJ 24-11.doc

			Effective Stress Shear Strength Parameters	
Material	**Moist Unit Weight, γ_{moist} kN/m^3 (lbf/ft^3)**	**Saturated Unit Weight, γ_{sat} kN/m^3 (lbf/ft^3)**	**Friction Angle, ϕ' or δ (degrees)**	**Cohesion, c' kPa (lbs/ft^2)**
Soil cover	18.9 (120)	19.6 (125)	28	0
EPS/EPS interface	1 (6.4)	1 (6.4)	30	0
Pavement System/EPS and/or EPS/Foundation Soil Interface	1 (6.4)	1 (6.4)	10 – 40	0

Note: ϕ' = friction angle of a natural soil.
δ = interface friction angle of a geosynthetic interface to include EPS blocks with another geosynthetic or natural soil.

Material Designation	Dry Density of Each Block as a Whole, kg/m^3 (lbf/ft^3)	Dry Density of a Test Specimen, kg/m^3 (lbf/ft^3)	Elastic Limit Stress, kPa (lbs/in^2)	Initial Tangent Young's Modulus, MPa (lbs/in^2)
EPS40	16 (1.0)	15 (0.90)	40 (5.8)	4 (580)
EPS50	20 (1.25)	18 (1.15)	50 (7.2)	5 (725)
EPS70	24 (1.5)	22 (1.35)	70 (10.1)	7 (1015)
EPS100	32 (2.0)	29 (1.80)	100 (14.5)	10 (1450)

CHAPTER **7**

DESIGN EXAMPLES

Contents

INTRODUCTION

This chapter presents two design examples that illustrate the design of an EPS-block geofoam embankment. The design principles and methods are discussed in detail in Chapters 3 through 6 and summarized in the flow chart illustrated in Figure 3.3. Example 1 presents the complete design for a trapezoidal geofoam embankment. Example 2 shows how to calculate earth pressures generated by an EPS-block geofoam bridge approach fill on an abutment. In each example, detailed calculations are shown with the appropriate equation and design chart numbers that appear in Chapters 3 through 6. Additionally, tables have been extensively used to summarize design calculation input values and results. These tables can serve as the basis for developing computer design spreadsheets. Only SI units have been used in the design examples. Appendix F includes conversion factors that can be used to convert between SI units and I-P units.

DESIGN EXAMPLE 1 – TRAPEZOIDAL GEOFOAM EMBANKMENT

STEP 1 – BACKGROUND INVESTIGATION

- Geometric Requirements:
  - Two lane roadway with each lane 3.7 m wide and two 1.8 m wide shoulders. Therefore, the required total width at the top of the embankment is 11 m (T_W=11 m).
  - Side slope of 3 (H) : 1 (V).
  - Height of embankment, H, of 5 m.
- Site Conditions:

- Site is in Urbana, Illinois.
- Subsurface conditions shown in Figure 7.1.
- The 100-year flood water level is expected to be 1.12 m. It is anticipated that water will only accumulate on one side of the embankment.

- Design Requirements
  - Maximum allowable settlement is 400 mm during 20 years service life.
  - Use peak horizontal bedrock acceleration for 10 percent probability of exceedance in 50 years to evaluate seismic stability.
  - Use AASHTO H 20-44 standard loading to estimate live loads from traffic for geofoam load bearing calculations.
  - Local transportation agency prefers a flexible pavement system design based on a 75 percent level of reliability.
  - The proposed roadway embankment will be located along a low-volume road with an estimated traffic level of 300,000 equivalent single axle loads (ESAL).

STEP 2 – SELECT PRELIMINARY EPS TYPE AND ASSUME A PRELIMINARY PAVEMENT SYSTEM DESIGN

- Preliminary EPS Type:
  - Start with an *EPS50*. From Table 6.2, *EPS50* has a dry density of 20 kg/m^3, which is equivalent to a dry unit weight of $\gamma_{\text{EPS Dry}} = 0.2 \text{ kN/m}^3$.
  - From the Design Loads section of Chapter 3, assume a saturated unit weight of $\gamma_{\text{EPS Abs}} = 1 \text{ kN/m}^3$ to account for potential water absorption.

- Preliminary Pavement System Design:
  - From the Design Loads section of Chapter 3, assume a thickness of pavement of $T_{\text{pavement}} = 610 \text{ mm}$.

— From the Design Loads section of Chapter 3, assume an overall unit weight for the pavement system of $\gamma_{pavement} = 20\ kN/m^3$.

STEP 3 – DETERMINE A PRELIMINARY FILL MASS ARRANGEMENT

- Start the design process with fill mass (see Figure 3.2) consisting of only EPS blocks and soil cover on the sides of the embankment. This will provide an indication of the suitability of using an EPS-block geofoam embankment.
- Thickness of EPS, T_{EPS}, equals $H - T_{pavement} = 5\ m - 0.6\ m = 4.4\ m$.
- From the Embankment Cover section of Chapter 5, assume a total (moist) unit weight for the soil cover, γ_{cover}, of 18.8 kN/m³ and a thickness, T_{cover}, of 400 mm.
- Figure 7.1 shows the preliminary fill mass arrangement.

Figure 7.1 Embankment geometry, subsurface conditions, and preliminary pavement system and fill mass arrangement.

STEP 4 – FOUNDATION SOIL SETTLEMENT ANALYSIS

- From Figure 5.2, the proposed embankment will have the following geometric dimensions:

  — $a = H * \dfrac{\text{slope change in the horizontal direction}}{\text{slope change in the vertical direction}} = 5\ m * \dfrac{3}{1} = 15\ m$

  — $b = \dfrac{11\ m}{2} = 5.5\ m$

- Divide the soft clay into 10 sublayers.

  — Each layer will be $\dfrac{15\ m}{10\ layers} = 1.5\ m$ thick

- Determine the magnitude of settlement at the center and edge of the embankment as shown in Figure 5.2. Therefore, determine the change in effective vertical stress, $\Delta\sigma'_z$, of each soil layer at the center and edge of the embankment as shown in Figure 7.2. To

demonstrate the use of the procedure to estimate $\Delta\sigma'_z$ and the overall settlement described in Chapter 5, a detailed calculation will be performed for Layer 5.

Figure 7.2 Subdivision of soft clay layer for settlement analysis.

- Determine the total increase in vertical stress at the center of the embankment, $\Delta\sigma_{Z@center}$, at mid-height of Layer 5.
  - — Determine $\Delta\sigma_Z$ caused by zone I as shown in Figure 5.2.
    - — From Equation (5.13),

      $$q_{fill} = \gamma_{EPS} * T_{EPS} = 1 \text{ kN/m}^3 * 4.4 \text{ m} = 4.4 \text{ kPa}$$

      Note that $\gamma_{EPS\ Abs}$ is used for γ_{EPS} in settlement calculations.
    - — From Equation (5.14),

      $$q_{pavement} = \gamma_{pavement} * T_{pavement} = 20 \text{ kN/m}^3 * 0.61 \text{ m} = 12.2 \text{ kPa}$$
    - — From Equation (5.12),

      $$q_I = q_{fill} + q_{pavement} = 4.4 \text{ kPa} + 12.2 \text{ kPa} = 16.6 \text{ kPa}$$
    - — From Fig. 5.3 and Equation (5.11),

      $$\alpha = 2 * \arctan\left(\frac{b}{z}\right) = 2 * \arctan\left(\frac{5.5 \text{ m}}{6.75 \text{ m}}\right) = 1.3674 \text{ radians}$$
    - — From Equation (5.10),

      $$\Delta\sigma_{Z_I} = \frac{q_I}{\pi}(\alpha + \sin\alpha)$$
      $$= \frac{16.6 \text{ kPa}}{\pi}(1.3674 \text{ radians} + \sin(1.3674 \text{ radians}))$$
      $$= 12.40 \text{ kPa}$$
  - — Determine $\Delta\sigma_Z$ caused by zone II as shown in Figure 5.2.
    - — From Equation (5.19),

$$q_{cover} = \gamma_{cover} * \frac{T_{cover}}{\cos\theta} = 18.8 \text{ kN/m}^3 * \frac{0.4 \text{ m}}{\cos 18.43^\circ} = 7.9 \text{ kPa}$$

$q_{fill} = 4.4$ kPa as previously determined

— From Equation (5.18),

$$q_{II} = q_{fill} + q_{cover} = 4.4 \text{ kPa} + 7.9 \text{ kPa} = 12.3 \text{ kPa}$$

— From Fig. 5.4 and Equation (5.16),

$$\delta = \arctan\left(\frac{5.5 \text{ m}}{6.75 \text{ m}}\right) = 0.6836 \text{ radians}$$

— From Equation (5.17),

$$\alpha = \arctan\left(\frac{a+b}{z}\right) - \delta = \arctan\left(\frac{15 \text{ m} + 5.5 \text{ m}}{6.75 \text{ m}}\right) - 0.6836 = 0.5691 \text{ radians}$$

— From Equation (5.15),

$$\sigma_{Z_{II}} = \frac{q_{II}}{2\pi}\left[\frac{x}{0.5 * a}\alpha - \sin 2\delta\right]$$
$$= \frac{12.3}{2\pi}\left[\frac{20.5 \text{ m}}{0.5 * 15 \text{ m}} 0.5691 \text{ radians} - \sin\left(2 * 0.6836 \text{ radians}\right)\right]$$
$$= 1.13 \text{ kPa}$$

— Determine the total increase in vertical stress at the center of the embankment, $\Delta\sigma_{Z@center}$.

— From Equation (5.20),

$$\Delta\sigma_{Z@center} = \Delta\sigma_{Z_I} + \left(2 * \Delta\sigma_{Z_{II}}\right)$$
$$= 12.40 \text{ kPa} + \left(2 * 1.13 \text{ kPa}\right)$$
$$= 14.66 \text{ kPa}$$

- Determine the total increase in vertical stress at the edge of the embankment, $\Delta\sigma_{Z@edge}$, at the mid-height of Layer 5.

— Determine $\Delta\sigma_Z$ caused by zone II as shown in Figure 5.2

— From Equation (5.23) and Fig. 5.6,

$$\delta = \arctan\left(\frac{a}{z}\right) = \arctan\left(\frac{15\text{ m}}{6.75\text{ m}}\right) = 1.1479\text{ radians}$$

— From Equation (5.22),

$$\Delta\sigma_{Z_{II}} = \frac{q_{II}}{2\pi}(\sin 2\delta) = \frac{12.3\text{ kPa}}{2\pi}\left(\sin\left(2 * 1.1479\text{ radians}\right)\right)$$
$$= 1.47\text{ kPa}$$

— Determine $\Delta\sigma_Z$ caused by zone III as shown in Figure 5.2.

— From Equation (5.25) and Fig. 5.7,

$$\delta = \arctan\left(\frac{a + 2b}{z}\right) = \arctan\left(\frac{15\text{ m} + \left(2 * 5.5\text{ m}\right)}{6.75\text{ m}}\right) = 1.3168\text{ radians}$$

— From Equation (5.26),

$$\alpha = \arctan\left(\frac{2a+2b}{z}\right) - \delta = \arctan\left(\frac{\left(2 * 15\text{ m}\right) + \left(2 * 5.5\text{ m}\right)}{6.75\text{ m}}\right) - 75.45^\circ = 0.0908\text{ radians}$$

— From Equation (5.24),

$$\Delta\sigma_{Z_{III}} = \frac{q_{III}}{2\pi}\left[\frac{x}{0.5 * a}\alpha - \sin 2\delta\right]$$
$$= \frac{12.3}{2\pi}\left[\frac{41\text{ m}}{0.5 * 15\text{ m}}0.0908\text{ radians} - \sin\left(2 * 1.3168\text{ radians}\right)\right]$$
$$= 0.02\text{ kPa}$$

Note that $q_{III} = q_{II}$

— Determine $\Delta\sigma_Z$ caused by zone I as shown in Figure 5.2.

— From Equation (5.28) and Fig. 5.8,

$$\delta = \arctan\left(\frac{a}{z}\right) = \arctan\left(\frac{15\text{ m}}{6.75\text{ m}}\right) = 1.1479\text{ radians}$$

— From Equation (5.29),

$$\alpha = \arctan\left(\frac{a+2b}{z}\right) - \delta = \arctan\left(\frac{15\text{ m} + (2 * 5.5\text{ m})}{6.75\text{ m}}\right) - 65.77^\circ = 0.1689\text{ radians}$$

— From Equation (5.27),

$$\Delta\sigma_{Z_I} = \frac{q_I}{\pi}\left[\alpha + \sin\alpha\ \cos(\alpha + 2\delta)\right]$$
$$= \frac{16.6}{\pi}[0.1689 \text{ radians} + \sin 0.1689 \text{ radians}$$
$$\cos(0.1689 \text{ radians} + (2*1.1479 \text{ radians}))]$$
$$= 0.20 \text{ kPa}$$

— Determine the total increase in vertical stress at the edge of the embankment, $\Delta\sigma_{Z@edge}$.

— From Equation (5.30),

$$\Delta\sigma_{Z@edge} = \Delta\sigma_{Z_I} + \Delta\sigma_{Z_{II}} + \Delta\sigma_{Z_{III}}$$
$$= 0.20 \text{ kPa} + 1.47 \text{ kPa} + 0.02 \text{ kPa} = 1.69 \text{ kPa}$$

- Determine geostatic or insitu effective vertical stress at mid-height of each sublayer. This is the preconstruction effective vertical stress, σ'_{vo} . For Layer 5,

$$\sigma'_{vo} = (\gamma_{sat} - \gamma_w) * z = \left(16 \text{ kN/m}^3 - 9.81 \text{ kN/m}^3\right) * 6.75 \text{ m} = 41.78 \text{ kPa}$$

- Determine the postconstruction effective vertical stress, at mid-height of each sublayer, σ'_{vf} . For Layer 5,

— At the center of the embankment, from Equation (5.32),

$$\sigma'_{vf} = \sigma'_{vo} + \Delta\sigma'_z = \Delta\sigma'_{vo} + \Delta\sigma_{Z@center} = 41.78 \text{ kPa} + 14.66 \text{ kPa}$$
$$= 56.44 \text{ kPa}$$

— At edge of embankment, from Equation (5.32),

$$\sigma'_{vf} = \sigma'_{vo} + \sigma'_Z = \sigma'_{vo} + \Delta\sigma_{Z@edge} = 41.78 \text{ kPa} + 1.69 \text{ kPa}$$
$$= 43.47 \text{ kPa}$$

Note the use of geofoam results in a small increase in effective vertical stress after construction.

- Determine settlement due to the consolidation of the soft clay, S_p. For Layer 5,

— From Figure 7.1, OCR = $\frac{\sigma'_p}{\sigma'_{vo}} = 1$. Therefore,

$$\sigma'_p = 1 * \sigma'_{vo} = 1 * 41.78 \text{ kPa} = 41.78 \text{ kPa}$$

— At the center of the embankment OCR = 1, therefore, use Equation (5.3) to determine S_p. For Layer 5,

$$Sp_5 = \frac{C_c}{1+e_o} L_o \log \frac{\sigma'_{vf}}{\sigma'_p}$$
$$= \frac{0.35}{1+1.7} * 1.5 \text{ m} * \log \frac{56.44 \text{ kPa}}{41.78 \text{ kPa}} = 0.0254 \text{ m}$$
$$= 25.4 \text{ mm}$$

— At the edge of the embankment, OCR = 1, therefore, use Equation (5.3) to determine S_p. For Layer 5,

$$Sp_5 = \frac{0.35}{1+1.7} * 1.5 \text{ m} * \log \frac{43.47 \text{ kPa}}{41.78 \text{ kPa}} = 0.0033 \text{ m}$$
$$= 3.3 \text{ mm}$$

- Tables 7.1 and 7.2 provide a summary of S_p values for each layer and total S_p at the center and edge of the embankment, respectively.
- Determine settlement due to secondary compression.

  From Figure 7.1,

  $\frac{C_\alpha}{C_c} = 0.04$ $C_c = 0.35$ $e_o = 1.7$ t_p=15 years $L_o = 15$ m

  — For roadway embankments, the critical time for obtaining settlement estimates is typically the life of the pavement system. A maximum settlement of 400 mm during a 20 year duration is allowed as part of the design requirements for this embankment. Therefore, use t = 20 years.

  — From Equation (5.7),

$$S_s = \frac{(C_\alpha / C_c) * C_c}{1 + e_o} L_o \log \frac{t}{t_p} = \frac{(0.04) * 0.35}{1 + 1.7} * 15 \text{ m} * \log\left(\frac{20 \text{ yrs}}{15 \text{ yrs}}\right)$$

$$= 0.0097 \text{ m}$$

$$= 9.7 \text{ mm}$$

Since secondary compression is a function of time and not on effective stress, the magnitude of secondary consolidation will be the same at both the center and edge of the embankment.

Table 7.1 Summary of settlement due to consolidation of the soft clay at the center of the trapezoidal embankment.

Table 7.2 Summary of settlement due to consolidation of the soft clay at the edge of the trapezoidal embankment.

- Determine the total settlement due to consolidation and secondary compression of the soft clay foundation using Equation (5.8),
  - At the center of the embankment,

    $S_{Total} = S_p + S_s = 369.4 \text{ mm} + 9.7 \text{ mm} = 379.1 \text{ mm}$
  - At the edge of the embankment,

    $S_{Total} = S_p + S_s = 32.5 \text{ mm} + 9.7 \text{ mm} = 42.2 \text{ mm}$

    For an embankment consisting of soil fill instead of EPS blocks with a total (moist) unit weight of 19 kN/m^3, the total settlement is expected to be 1,113 and 214 mm at the center and edge of the embankment, respectively. Therefore, in order to meet the maximum allowed settlement requirement for this embankment of 400 mm, the fill mass can either consist entirely of EPS blocks or a combination of EPS blocks and soil fill. For this example, the fill mass is assumed to only consist of EPS blocks.
- Settlement due to long-term vertical deformation (creep) of the fill mass will be negligible if the applied vertical stress is such that it produces an immediate geofoam

strain of less than 1 percent. The immediate or elastic vertical strain can be estimated from Equation (5.9). However, load bearing design, which is performed as part of internal stability, is based on selecting an EPS block that will provide an immediate vertical strain of less than 1 percent. Therefore, it can be assumed that long-term vertical deformation of the EPS blocks will be negligible.

STEP 5 – BEARING CAPACITY

- Determine the normal stress applied by the pavement system at the top of the embankment, $\sigma_{n,pavement}$.

  $\sigma_{n,pavement} = q_{pavement}$ determined in Step 4

  = 12.2 kPa

- Determine the normal stress applied by the traffic surcharge at the top of the embankment.

  $\sigma_{n,traffic} = \gamma_{soil\ fill} * 0.61$ m per (*1*)

  If $\gamma_{soil\ fill}$ =18.9 kN/m^3 as an estimate,

  $\sigma_{n,traffic}$ = 18.9 kN/m^3 *0.61 m = 11.5 kN/m^2

- From Equation (5.44), T_w =11 m, and γ_{EPS} = 1 kN/m^3, the minimum required undrained shear strength to satisfy a factor of safety of 3 is:

$$s_u = \frac{3}{5} * \left\{ \left[\frac{\left(\sigma_{n,\,pavement} + \sigma_{n,\,traffic}\right) * T_W}{T_W + T_{EPS}} \right] + \frac{\left(\gamma_{EPS} * T_{EPS}\right)}{2} \right\}$$

$$= \frac{3}{5} * \left\{ \left[\frac{(12.2\ \text{kPa} + 11.5\ \text{kPa}) * 11\ \text{m}}{11\ \text{m} + 4.4\ \text{m}} \right] + \frac{\left(1\ \text{kN/m}^3 * 4.4\ \text{m}\right)}{2} \right\}$$

$$= 11.48\ \text{kPa}$$

From Figure 7.1, $s_{u\ foundation\ soil}$ = 15 kPa

$s_{u\ foundation\ soil} > s_{u\ REQ}$ so the factor of safety against bearing capacity failure of 3 is exceeded.

Alternatively, Figure 5.10 can be used.

For T_{EPS} = 4.4 m and an 11 m roadway width, Figure 5.10 indicates that $s_{u\ REQ}$ = 15.3 kPa. Thus, Figure 5.10 indicates that the $s_{u\ foundation\ soil}$ of 15 kPa does not meet the factor of safety against bearing capacity failure of 3. However, Figure 5.10 is based on a $T_{pavement}$ of 1,000 mm and $\gamma_{pavement}$ of 20 kN/m^3 or $\sigma_{n,pavement}$ of 21.5 kPa. In this example problem, the preliminary pavement system also has a $\gamma_{pavement}$ of 20 kN/m^3 but $T_{pavement}$ is 610 mm or $\sigma_{n,pavement}$ of 12.2 kPa. Therefore, Figure 5.10 yields a more conservative $s_{u\ REQ}$ and Equation 5.44 provides a better estimate $s_{u\ REQ}$.

STEP 6 – EXTERNAL SLOPE STABILITY

- Determine the static external slope stability factor of safety. For the roadway width of 11 m, Fig. 5.14 can be used.

  For s_u = 15 kPa, Fig. 5.14 indicates that the factor of safety exceeds 1.5 for both T_{EPS} = 3.1 m and T_{EPS} = 6.1 m. Therefore for T_{EPS} = 4.4 m, the factor of safety will exceed the required 1.5.

STEP 7 – EXTERNAL SEISMIC STABILITY

- As shown in the Design Requirements of Step 1, a 10 percent probability of exceedance in 50 years is required for this example.
- Select a peak horizontal bedrock acceleration, a_{rock}, with a 10 percent probability of exceedance in 50 years. From the USGS zip code earthquake ground motion hazard on the USGS website (www.USGS.gov),
  - a_{rock} = 0.04 g for Urbana, Illinois.
- Estimate the ground surface acceleration. This is the acceleration at the base of the embankment, a_{base}. Because the foundation soil consists of soft clay, Figure 5.18 can be used.
  - a_{base} = 0.13 g

- Estimate the acceleration at the top of the embankment, a_{emb}. As presented in the External Seismic Stability of Trapezoidal Embankments section of Chapter 5, the EPS-block geofoam can be assumed to behave as a deep cohesionless soil. Fig. 5.17 can be used to estimate a_{emb} from a_{base}.

  — $a_{emb} = 0.09$ g

- Estimate the acceleration at the center of gravity of the slide mass as determined from the critical static failure surface. As noted in Chapter 5, if a circular failure surface is used for the external static stability analysis, the center of gravity of the sliding mass is usually located near the center or mid-height of the slide mass. For preliminary analysis, the acceleration at the base of the embankment can be used for external seismic stability analysis if the site has soft soil and the bedrock acceleration has been corrected for amplification through the soft soil.
- Estimate the horizontal seismic coefficient, k_h, at the center of gravity of the slide mass. As indicated previously, the acceleration at the base of the embankment can be used to provide a conservative estimate of the horizontal seismic coefficient, k_h, for preliminary design.

  — $k_h = \frac{a_{base}}{g} = \frac{0.13\ g}{g} = 0.13$

- Determine the pseudo-static factor of safety, FS′, for the critical static failure surface and ensure that it exceeds 1.2. For an embankment with a top width of 11m and a k_h = 0.13, Figures 5.22 and 5.23 can be used to obtain an estimate of FS′. For a 3H:1V embankment at s_u = 15 kPa and T_{EPS} = 4.4 m, Figure 5.22 provides a FS′ = 1.5 for a k_h = 0.1 and Figure 5.23 provides a FS′ = 1.1 for a k_h=0.2. Therefore, by linear interpolation, at k_h = 0.13, the FS′ will be approximately 1.2, which meets the required FS′.

STEP 8 – HYDROSTATIC UPLIFT (FLOTATION)

- Determine the weight of the EPS-block geofoam, W_{EPS}. For simplicity, assume the EPS blocks extend for the full height of the embankment, i.e., $T_{EPS} = H$. The 100-year flood water level is expected to be 1.12 m. It is anticipated that water will only accumulate on one side of the embankment,

—
$$W_{EPS} = \frac{H(T_w + B_w)}{2} * \gamma_{EPS\ Dry} = \frac{5\ m(11\ m + 41\ m)}{2} * 0.2\ kN/m^3$$
$$= 26\ kN/m\ of\ roadway$$

- Determine the vertical weight component of water on the embankment face above the base of the embankment on the accumulated water side, W_w.

$$W_w = \frac{1}{2} * (h+S_{total}) * \left(\frac{sh}{sv} * (h+S_{total})\right) * \gamma_w$$

where sh:sv is the horizontal to vertical slope change of the embankment.

$$W_w = \frac{1}{2} * (1.12\ m + 0.38\ m) * \left(\frac{3}{1} * (1.12\ m + 0.38\ m)\right) * 9.81\ kN/m^3 = 33.1\ kN/m\ of\ roadway.$$

- Determine the additional overburden force required above the EPS blocks to obtain a factor of safety of 1.2, O_{REQ}. From Equation (5.74),

$$O_{REQ} = \left[1.2 * \left(\frac{1}{2} * \gamma_w * (h+S_{total}) * B_w\right)\right] - \left[(W_{EPS} + W_w)\right]$$
$$= \left[1.2 * \left(\frac{1}{2} * 9.81\ kN/m^3 * (1.12\ m+0.38\ m) * 41\ m\right)\right] - \left[(26\ kN/m + 33.1\ kN/m)\right]$$
$$= 302.9\ kN/m\ of\ roadway$$

Alternatively, for a 3H:1V embankment slope with no tailwater, Figure 5.49 can be used to estimate O_{REQ}.

For a road width = 11 m, H = 5 m,

$$\frac{Accumulated\ water\ level}{Embankment\ height} = \frac{h+S_{total}}{H} = \frac{1.12\ m + 0.38\ m}{5\ m} = \frac{1.5}{5} = 0.3$$

Figure 5.49 indicates O_{REQ} = 310 kN/m of roadway

- Determine if the pavement system and soil cover provide an adequate overburden force to resist hydrostatic uplift.

  — Determine the weight of the soil cover, W_{cover}. From Equation (5.64),

$$W_{cover} = 2 * \left(\gamma_{cover} * \frac{T_{EPS}}{\sin\theta} * \frac{T_{cover}}{\cos\theta} \right)$$
$$= 2 * \left(18.8 \text{ kN/m}^3 * \frac{4.4 \text{ m}}{\sin 18.4^\circ} * \frac{0.4 \text{ m}}{\cos 18.4^\circ} \right)$$
$$= 220.1 \text{ kN/m of roadway}$$

  — Because the calculation of W_{EPS} is based on the assumption that the EPS blocks extends the full height of the embankment, the weight of the EPS equivalent to the height of the pavement system must be subtracted from the total overburden weight. Therefore, use Equation (5.67).

$$O_{REQ} < \left(\gamma_{pavement} * T_{pavement} * T_w \right) - \left(\gamma_{EPS} * T_{pavement} * T_w \right) + W_{cover}$$
$$302.9 \text{ kN/m} < \left(20 \text{ kN/m}^3 * 0.6 \text{ m} * 11 \text{ m} \right) - \left(0.2 \text{ kN/m}^3 * 0.6 \text{ m} * 11 \text{ m} \right) + 220.1 \text{ kN/m}$$

  302.9 kN/m < 350.8 kN/m of roadway. Therefore, the pavement system and soil cover provide sufficient overburden force to resist hydrostatic uplift.

STEP 9 – TRANSLATION DUE TO WATER (EXTERNAL)

- Determine the lowest interface friction angle, δ, between the EPS/foundation soil or, if a separation material is placed between the EPS fill and foundation soil, the lowest interface friction between the EPS/separation material and separation material/foundation soil. The exact type of separation material, if one is required, will typically not be known until construction begins. Four possible interface cases between the EPS blocks and the foundation soil, which are summarized in Table 7.3, will be considered herein. As shown in Table 7.3, the lowest and most critical interface δ is 20 degrees. Therefore, δ = 20 degrees will be used in the analysis of translation due to water and translation due to wind in Steps 9 and 10, respectively.

Table 7.3 Summary of interface friction angles, δ, considered between the EPS blocks and the foundation soil.

- Determine the additional overburden force required above the EPS blocks to obtain a factor of safety against translation due to water of 1.2, O_{REQ}. From Equation (5.77) and the values of W_{EPS} = 26 kN/m of roadway and W_W = 33.11 kN/m of roadway determined in Step 8,

$$O_{REQ} = \frac{1.2\left(\frac{1}{2}\right)\left(\gamma_w * (h+S_{total})^2\right)}{\tan\delta} + \left(\frac{1}{2}(h+S_{total}) * \gamma_w * \left(B_w\right)\right) - W_{EPS} - W_w$$

$$= \frac{1.2\left(\frac{1}{2}\right)\left(9.81\ \text{kN/m} * (1.12\ \text{m}+0.38\ \text{m})^2\right)}{\tan 20^\circ} + \left(\frac{1}{2}\left((1.12\ \text{m}+0.38\ \text{m}) * 9.81\ \text{kN/m}^3\right) * \left(41\ \text{m}\right)\right)$$
$$- 26\ \text{kN/m} - 33.11\ \text{kN/m}$$

$$= 278.9\ \text{kN/m of roadway}$$

Alternatively, for a 3H:1V embankment slope with no tailwater, Fig. 5.54 can be used to estimate O_{REQ}.

For a road width = 11 m, H = 5 m,

$$\frac{\text{Accumulated water level}}{\text{Embankment height}} = \frac{h + S_{total}}{H} = \frac{1.12\ \text{m} + 0.38\ \text{m}}{5\ \text{m}} = \frac{1.5}{5} = 0.3,\ \delta = 20^\circ$$

O_{REQ} = 300 kN/m of roadway.

- Determine if the pavement system and soil cover will provide an adequate overburden force to resist translation due to water.
  - — Determine the weight of the soil cover, W_{cover}. W_{cover} was determined to be 220.14 kN/m of roadway in Step 8.
  - — Because the calculation of W_{EPS} is based on the assumption that the EPS blocks extend the full height of the embankment, the weight of the EPS equivalent to the height of the pavement system must be subtracted from the total overburden

weight. Therefore, use Equation (5.67). Note that the right side of the equation was determined in Step 8 to be 350.82 kN/m of roadway. Therefore,

$$O_{REQ} < \left(\gamma_{pavement} * T_{pavement} * T_w\right) - \left(\gamma_{EPS} * T_{pavement} * T_w\right) + W_{cover}$$

$$278.9 \text{ kN/m} < \left(20 \text{ kN/m}^3 * 0.6 \text{ m} * 11 \text{ m}\right) - \left(0.2 \text{ kN/m}^3 * 0.6 \text{ m} * 11 \text{ m}\right) + 220.1 \text{ kN/m}$$

278.9 kN/m < 350.8 kN/m of roadway. Therefore, the pavement system and soil cover will provide sufficient overburden force.

STEP 10 – TRANSLATION DUE TO WIND (EXTERNAL)

- As presented in Chapter 5, it is recommended that the translation due to wind failure mechanism not be considered until further research is performed on the applicability of Equations (3.4) and (3.5) to EPS-block geofoam embankments. However, the wind loading failure mechanism will be evaluated herein to demonstrate the use of the applicable equations and Figure 5.58.
- Determine the upwind and downwind pressures, p_u and p_D, respectively, on the sides of the embankment.
  - Obtain the design wind speed, V.

    From ANSI/ASCE 7-95 (*8*), V = 40 m/s
  - From Equation (3.4),

    $p_U = 0.75\ V^2 \sin \theta_u = 0.75\ (40 \text{ m/s})^2 \sin 18.4^\circ = 378.8 \text{ kPa}$
  - From Equation (3.5),

    $p_D = 0.75\ V^2 \sin\theta_D = 0.75\ (40 \text{ m/s})^2 \sin 18.4^\circ = 378.8 \text{ kPa}$
- Determine the upwind and downwind force, R_U and R_D, respectively, on the sides of the embankment.
  - $R_U = p_U * H = 378.8 \text{ kPa} * 5 \text{ m} = 1{,}894.0 \text{ kN/m of roadway}$
  - $R_D = p_D * H = 378.8 \text{ kPa} * 5 \text{ m} = 1{,}894.0 \text{ kN/m of roadway}$

- Determine the additional overburden force required above the EPS blocks to obtain a factor of safety against translation due to wind of 1.2, O_{REQ}. From Equation (5.81) and the value of W_{EPS} = 26 kN/m of roadway determined in Step 8,

$$O_{REQ} = \frac{1.2 * (R_U + R_D)}{\tan \delta} - W_{EPS} = \frac{1.2 * (1{,}894.0 \text{ kN/m} + 1{,}894.0 \text{ kN/m})}{\tan 20^\circ} - 26 \text{ kN/m}$$

$$= 12{,}462.9 \text{ kN/m of roadway}$$

Alternatively, Fig. 5.58 can be used to estimate O_{REQ}. For a 3H:1V, 5 m high embankment with V=40 m/s and δ = 20 degrees,

O_{REQ} = 12,500 kN/m of roadway.

- Determine if the pavement system and soil cover provide adequate overburden force.
  - — Determine the weight of the soil cover, W_{cover}. W_{cover} was determined to be 220.1 kN/m of roadway in Step 8.
  - — Because the calculation of W_{EPS} is based on the assumption that the EPS blocks extend the full height of the embankment, the weight of the EPS equivalent to the height of the pavement system must be subtracted from the total overburden weight. Therefore, use Equation (5.67). Note that the right side of the equation was determined in Step 8 to be 350.8 kN/m of roadway. Therefore,

$$O_{REQ} < (\gamma_{pavement} * T_{pavement} * T_w) - (\gamma_{EPS} * T_{pavement} * T_w) + W_{cover}$$

$$12{,}462.9 \text{ kN/m} < (20 \text{ kN/m}^3 * 0.6 \text{ m} * 11 \text{ m}) - (0.2 \text{ kN/m}^3 * 0.6 \text{ m} * 11 \text{ m}) + 220.1 \text{ kN/m}$$

12,462.9 kN/m is not < 350.8 kN/m of roadway.

Therefore, the pavement system and soil cover will not provide sufficient force. However, as indicated previously, it is recommended that the translation due to wind failure mechanism not be considered until further research is performed on the applicability of Equations (3.4) and (3.5). The wind failure mechanism was

evaluated herein to demonstrate the use of these equations. Thus, the wind failure mechanism will not be considered in the design of this embankment.

STEP 11 – TRANSLATION DUE TO WATER (INTERNAL)

- Determine the levels within the embankment that will be used to analyze the potential for translation due to water. The 100-year flood water level is 1.12 m. The thickness of EPS blocks typically range between 610 mm to 1,000 mm. Because the 100-year flood water level is greater than the typical thickness range of EPS blocks, the translation due to water failure mechanism should be evaluated. Check the potential for sliding at h=0.37 m above the embankment and foundation soil interface.

  — Accumulated water level = h + S_{total} = 0.37 m + 0.38 m = 0.75 m

  — From Fig. 5.47, determine the new geometric parameters.

  T_w = 11m remains the same

  H = 5 m – 0.75 m = 4.25 m

$$B_w = T_w + \left[2 * \left(\frac{sh}{sv} * H\right)\right] = 11\text{ m} + \left[2 * \left(\frac{3}{1} * 4.25\text{ m}\right)\right]$$

  = 36.5 m

- Determine the weight of EPS-block geofoam, W_{EPS}, for the new embankment height to be analyzed. For simplicity, assume the EPS blocks extend the full height of the new embankment height, i.e., T_{EPS} = H.

$$W_{EPS} = \frac{H\left(T_w + B_w\right)}{2} * \gamma_{EPS\,Dry} = \frac{4.25\text{ m}\left(11\text{ m} + 36.5\text{ m}\right)}{2} * 0.2\text{ kN/m}^3$$

  = 20.2 kN/m of roadway.

- Determine the vertical component of water weight on the embankment face above the base of the embankment on the accumulated water side, W_w.

$$W_w = \frac{1}{2} * h * \left(\frac{sh}{sv} * (h + S_{total})\right) * \gamma_w = \frac{1}{2} * 0.75\text{ m} * \left(\frac{3}{1} * 0.75\text{ m}\right) * 9.81\text{ kN/m}^3$$

  = 8.3 kN/m of roadway.

- Assume the interface friction angle, δ, between the EPS blocks is 30 degrees (from Chapter 2).
- Determine the additional overburden force required above the EPS blocks to obtain a factor of safety against translation due to water of 1.2, O_{REQ}. From Equation (5.77),

$$O_{REQ} = \frac{1.2\left(\frac{1}{2}\right)\left(\gamma_w * (h+S_{total})^2\right)}{\tan\delta} + \left(\frac{1}{2}\left((h+S_{total}) * \gamma_w\right) * \left(B_w\right)\right) - W_{EPS} - W_w$$

$$= \frac{1.2\left(\frac{1}{2}\right)\left(9.81\ \text{kN/m}^3 * (0.75\ \text{m})^2\right)}{\tan 30^\circ} + \left(\frac{1}{2}\left(0.75\ \text{m} * 9.81\ \text{kN/m}^3\right) * \left(36.5\ \text{m}\right)\right) - 20.2\ \text{kN/m} - 8.3\ \text{kN/m}$$

= 111.5 kN/m of roadway.

Alternatively, for a 3H:1V embankment slope with no tailwater, Fig. 5.54 can be used to estimate O_{REQ}.

For a road width = 11m, H = 4.25,

$$\frac{\text{Accumulated water level}}{\text{Embankment height}} = \frac{h+S_{total}}{H} = \frac{0.75}{4.25} = 0.18,\ \delta = 30^\circ$$

O_{REQ} = 120 kN/m of roadway.

- Determine if the pavement system and soil cover provide adequate overburden force.
  - — Determine the weight of the soil cover, W_{cover}.

    Thickness of EPS, $T_{EPS} = H - T_{pavement}$ = 4.25 m – 0.6 m = 3.65 m.
  - — From Equation (5.64),

$$W_{cover} = 2 * \left(\gamma_{cover} * \frac{T_{EPS}}{\sin\theta} * \frac{T_{cover}}{\cos\theta}\right) = 2 * \left(18.8\ \text{kN/m}^3 * \frac{3.65\ \text{m}}{\sin 18.4^\circ} * \frac{0.4\ \text{m}}{\cos 18.4^\circ}\right)$$

= 182.6 kN/m of roadway.

  - — Because the calculation of W_{EPS} is based on the assumption that the EPS blocks extend the full height of the embankment, the weight of the EPS equivalent to the

height of the pavement system must be subtracted from the total overburden weight. Therefore, use Equation (5.67).

$$O_{REQ} = \left(\gamma_{pavement} * T_{pavement} * T_w\right) - \left(\gamma_{EPS} * T_{pavement} * T_w\right) + W_{cover}$$

111.5 kN/m < (20 kN/m³ * 0.6 m * 11 m) – (0.2 kN/m³ * 0.6 m *11 m) + 182.6 kN/m

111.5 kN/m < 313.2 kN/m of roadway. Therefore, the pavement system and soil cover will provide sufficient overburden force.

STEP 12 – TRANSLATION DUE TO WIND (INTERNAL)

- As presented in Chapter 5, it is recommended that the translation due to wind failure mechanism not be considered until further research is performed on the applicability of Equations (3.4) and (3.5) to EPS-block geofoam embankments. However, the wind loading failure mechanism will be evaluated herein to demonstrate the use of the applicable equations and Figure 5.58.
- Determine the levels within the embankment that will be used to analyze the potential for translation due to wind. Determine the potential for sliding at mid-height of the embankment.
  - From Figure 5.57, determine new geometric parameters.

$$H = \frac{1}{2} * 5\text{ m} = 2.5\text{ m}$$

$$T_w = 11\text{ m (remains the same)}$$

$$B_w = T_w + \left[2 * \left(\frac{sh}{sv} * H\right)\right] = 11\text{ m} + \left[2 * \left(\frac{3}{1} * 2.5\text{ m}\right)\right]$$

$$= 26\text{ m}$$

- Determine the upwind and downwind pressures, p_U and p_D, respectively, on the sides of the embankment.
  - Obtain a design wind speed, V.

    From Step 10, V = 40 m/s

— From Equation (3.4),

$p_U = 0.75\ V^2 \sin \theta_u = 0.75\ (40\ m/s)^2 \sin 18.4^\circ = 378.8\ kPa$

— From Equation (3.5),

$p_D = 0.75\ V^2 \sin \theta_D = 0.75\ (40\ m/s)^2 \sin 18.4^\circ = 378.8\ kPa$

- Determine the upwind and downwind force, R_U and R_D, respectively, on the sides of the embankment.

— $R_U = p_U * H = 378.8\ kPa * 2.5\ m = 947.0\ kN/m$

— $R_D = p_D * H = 378.8\ kPa * 2.5\ m = 947.0\ kN/m$

- Determine weight of EPS-block geofoam, W_{EPS}, for the new embankment height to be analyzed. For simplicity, assume the EPS blocks extend the full height of the new embankment height, i.e., $T_{EPS} = H$.

$$W_{EPS} = \frac{H\left(T_w + B_w\right)}{2} * \gamma_{EPS\ Dry} = \frac{2.5\ m\left(11\ m + 26\ m\right)}{2} * 0.2\ kN/m^3$$

= 9.2 kN/m of roadway.

- From Chapter 2, assume the interface friction angle, δ, between the EPS blocks is 30 degrees.
- Determine the additional overburden force required above the EPS blocks to obtain a factor of safety of 1.2, O_{REQ}. From Equation (5.81),

$$O_{REQ} = \frac{1.2 * \left(R_U + R_D\right)}{\tan \delta} - W_{EPS} = \frac{1.2 * \left(947.0\ kN/m + 947.0\ kN/m\right)}{\tan 30^\circ} - 9.2\ kN/m$$

= 3,927.4 kN/m of roadway.

Alternatively, Fig. 5.58 can be used to estimate O_{REQ}. For a 3H:1V, 2.5 m high embankment with V = 40 m/s and δ = 30 degrees,

O_{REQ} = 3,900 kN/m of roadway.

- Determine if the pavement system and soil cover provide an adequate overburden force.

— Determine the weight of the soil cover, W_{cover}.

Thickness of EPS, $T_{EPS} = H - T_{pavement} = 2.5\text{ m} - 0.6\text{ m} = 1.9\text{ m}$

— From Equation (5.64),

$$W_{cover} = 2 * \left(\gamma_{cover} * \frac{T_{EPS}}{\sin\theta} * \frac{T_{cover}}{\cos\theta} \right) = 2 * \left(18.8\text{ kN/m}^3 * \frac{1.9\text{ m}}{\sin 18.4^\circ} * \frac{0.4\text{ m}}{\cos 18.4^\circ} \right)$$

= 94.7 kN/m of roadway.

- Because the calculation of W_{EPS} is based on the assumption that the EPS blocks extend the full height of the embankment, the weight of the EPS equivalent to the height of the pavement system must be subtracted from the total overburden weight. Therefore, use Equation (5.67).

$$O_{REQ} = \left(\gamma_{pavement} * T_{pavement} * T_w \right) - \left(\gamma_{EPS} * T_{pavement} * T_w \right) + W_{cover}$$

3,927.4 kN/m < (20 kN/m^3 * 0.6 m * 11 m) – (0.2 kN/m^3 * 0.6 m * 11 m) + 94.7 kN/m

3,927.4 kN/m is not < 225.4 kN/m.

Therefore, the pavement system and soil cover will not provide sufficient force. However, as presented in Chapter 5, it is recommended that the translation due to wind failure mechanism not be considered until further research is performed on the applicability of Equations (3.4) and (3.5). The wind failure mechanism was evaluated herein to demonstrate the use of these equations. Thus, the wind failure mechanism will not be considered in the design of this embankment.

STEP 13 – SEISMIC STABILITY (INTERNAL)

- Identify the critical interface friction angle, δ, for each of the three failure modes shown in Fig. 6.2 and briefly described below.

— Mode I: Determine the lowest interface friction angle between the pavement system/EPS or, if a separation material is placed between the pavement system and EPS blocks, the lowest interface friction between the pavement

system/separation material and separation material/EPS. The type of separation material, if one is required, will typically not be initially known. Four possible interface cases between the pavement system and EPS blocks, which are summarized in Table 7.4 will be considered herein. As shown in Table 7.4, the critical δ is 25 degrees.

— Mode II: From testing described in Chapter 2, δ = 30 degrees for sliding along an EPS/EPS interface.

— Mode III: A δ = 20 degrees was determined to be the critical interface friction angle between the EPS blocks and the foundation soil in Step 9.

Table 7.4 Summary of geosynthetic interface friction angles, δ, considered between the pavement system and the EPS blocks.

- Estimate the horizontal seismic coefficient, k_h, at the center of gravity of the slide mass of each failure mode.

— Mode I: The center of gravity along the height of the slide mass corresponds to approximately the mid-height of the pavement system,

Z_{center} = ½ * $T_{pavement}$ = ½ * (0.61 m) = 0.305 m

By linear interpolation, the acceleration at the center of gravity of the pavement system is close to the acceleration at the top of the embankment, a_{emb}, of 0.09 g, which was determined in Step 7. Therefore, the horizontal seismic coefficient for Mode I is

$$k_h = \frac{a_{emb}}{g} = \frac{0.09\ g}{g} = 0.09$$

— Mode II: Based on the assumption that the bottom of the failure surface is located near the base of the embankment, the center of gravity along the height of the slide mass, Z_{center}, is approximately,

$$Z_{center} = \frac{\left(\bar{Z}_{pavement} * \gamma_{pavement}\right) + \left(\bar{Z}_{EPS} * \gamma_{EPS}\right)}{\gamma_{pavement} + \gamma_{EPS}}$$

where $\bar{Z}_{pavement}$ and $\bar{Z}_{EPS}$ is the vertical distance from the top of the embankment to the center of gravity of the pavement system and EPS fill, respectively.

$$Z_{center} = \frac{\left(0.305 \text{ m} * 20 \text{ kN/m}^3\right) + \left(2.81 \text{ m} * 1 \text{ kN/m}^3\right)}{20 \text{ kN/m}^3 + 1 \text{ kN/m}^3} = 0.424 \text{ m}$$

By linear interpolation, the acceleration at the center of gravity is close to the acceleration at the top of the embankment, a_{emb}, of 0.09 g, which was determined in Step 7. Therefore, the horizontal seismic coefficient for Mode II is approximately the same as for Mode I, i.e., $k_h = 0.09$.

— Mode III: The horizontal seismic coefficient at the center of gravity will be similar to that of Mode II, i.e., $k_h = 0.09$, because the failure surface for Mode III is near the base of the embankment as in Mode II.

— A summary of the critical interface friction angles and horizontal seismic coefficients for the three failure modes is presented in Table 7.5.

Table 7.5 Summary of critical interface friction angles and horizontal seismic coefficients for the three internal seismic stability failure modes.

- Determine the pseudo-static factor of safety against internal seismic stability, FS′, and ensure that it exceeds 1.2. An estimate of FS′ for preliminary design can be obtained from Fig. 6.6.

  The FS′ relationship for $k_h = 0.10$ can be used to obtain an estimate of FS′ at $k_h = 0.09$. A summary of FS′ values is shown in Table 7.5. Note from Fig. 6.6 that it is only necessary to determine FS′ for Mode I and the mode with the critical δ between Mode II and III. As shown in Table 7.5, FS′ exceeds 1.2 for all three potential failure modes.

STEP 14 – LOAD BEARING

- **Sub-Step 1: Estimate traffic loads.**

  For this section of roadway, use AASHTO H 20-44 standard loading.

  Rear axle load = 106.8 kN

  Load per dual set, $LL_D = \frac{106.8 \text{ kN}}{2} = 53.4 \text{ kN}$

- **Sub-Step 2: Add impact allowance to traffic loads.**

  Use impact coefficient, I, of 0.3 and Equation (6.3),

  $Q_D = LL_D * (1 + I) = 53.4 \text{ kN} * (1+0.3) = 69.4 \text{ kN}$

- **Sub-Step 3: Estimate traffic load stresses on top of the EPS blocks.**

  — Consider an asphalt concrete pavement with and without a concrete separation layer. Also consider an asphalt thickness of 76 and 178 mm for preliminary design. The vertical stress due to traffic loads, σ_{LL}, at the top of the EPS blocks can be obtained from Fig. 6.15 for an asphalt concrete pavement system and from Fig. 6.17 for an asphalt concrete pavement system with a 102 mm concrete separation layer. A summary of σ_{LL} values per dual tire set, is presented in Table 7.6.

  — Determine if the applied vertical stresses overlap between the two interior dual tire sets shown as No. 2 and 3 in Figure 7.3. These two dual tire sets are the closest and thus the stresses exerted by these two dual tires will overlap first. The composite pavement system with the 76 mm asphalt layer will be used to demonstrate the procedure.

  $Q_D = 69.4$ kN from Sub-step 2 and $\sigma_{LL} = 19$ kPa as determined in Sub-step 3 and shown in Table 7.6.

  Determine circular contact area from Equation (6.6),

$$A_{CD} = \frac{Q_D}{q} = \frac{Q_D}{\sigma_{LL}} = \frac{69.4 \text{ kN}}{19 \text{ kPa}} = 3.65 \text{ m}^2$$

Figure 7.3 Cross-section of rear axle of two standard H 20-44 trucks on the proposed 11 m wide roadway embankment.

Determine an equivalent rectangular loaded area using Fig. 6.18,

$$L' = \sqrt{\frac{\text{Area}}{0.5227}} = \sqrt{\frac{A_{CD}}{0.5227}} = \sqrt{\frac{3.65 \text{ m}^2}{0.5227}} = 2.64 \text{ m}$$

$L = 0.8712 * L'$

$= 0.8712 * 2.64 \text{ m} = 2.3 \text{ m}$

$B = 0.6 * L'$

$= 0.6 * 2.64 = 1.58 \text{ m}$

From Fig. 7.4, stress overlap occurs if center-to-center wheel spacing ≤ B where B is 0.6*L′ or 1.58 m for this example.

The actual center-to-center spacing between the two dual tire sets (Set No. 2 and 3) is 0.61 m * 2 = 1.22 m. Because the actual center-to-center spacing of the two dual tire sets is less than B, i.e., 1.22 < 1.58 m, the stresses overlap (see Fig. 7.4). Overlap = 1.58 m – 1.22 m = 0.36 m.

The combined rectangular width = (2 * B) – 0.36 m = (2 * 1.58 m) – 0.36 m = 2.80 m

The combined rectangular area = 2.8 m * 2.3 m = 6.44 m²

The combined load of the two dual tire sets = 2 * 69.4 kN = 138.8 kN

The combined vertical stress = $\frac{138.8 \text{ kN}}{6.44 \text{ m}^2} = 21.55 \text{ kPa}$

Figure 7.4. Determination of stress overlap between two sets of dual tires.

— Determine if stresses overlap between an interior dual tire set and an exterior dual tire set, e.g., Set No. 1 and 2 (see Figure 7.3), or, if stresses overlap between the two interior dual tires, and an exterior dual tire set, e.g., Set No. 1 and

Combined set No. 2 and 3. The composite pavement system with the 76 mm asphalt layer and the flexible pavement system with the 178 mm asphalt layer will be used to demonstrate the procedure.

For the composite pavement system with the 76 mm asphalt layer, the center-to-center spacing between the combined interior dual tires (Combined Set No. 2 and 3) and the exterior dual tire set (Set No. 1) is 2.44 m. The spacing between the two loaded area is

$$2.44 \text{ m} - \left[(0.5 * 2.8 \text{ m}) + (0.5 * 1.58 \text{ m}) \right] = 0.25 \text{ m}.$$

Because there is spacing between the two loaded areas, no overlap occurs.

For the flexible pavement system with the 178 mm asphalt layer, the stresses from the two interior dual tires (Set No. 2 and 3) do not overlap. Therefore, since the actual center-to-center spacing between one interior dual tire set and an exterior dual tire set (between Set No. 1 and 2) is greater than B, i.e., 1.83 m > 1.58 m, stress overlap does not occur.

— A summary of combined stresses, if applicable, is presented in Table 7.6.

- **Sub-Step 4: Estimate gravity stresses at top of EPS blocks.**

— $T_{pavement} = 0.61$ m, $\gamma_{pavement} = 20$ kN/m³

— From Equation (6.8),

$\sigma_{DL} = T_{pavement} * \gamma_{pavement} = 0.61 \text{ m} * 20 \text{ kN/m}^3 = 12.2$ kPa

- **Sub-Step 5: Calculate the total vertical stresses at top of EPS blocks.**

— From Equation (6.9),

$\sigma_{total} = \sigma_{LL} + \sigma_{DL}$

A summary of σ_{total} for the various pavement systems is presented in Table 7.6. If applied stresses were found to overlap between adjacent tire sets in Sub-step 3, the largest σ_{LL} is used.

- **Sub-Step 6: Determine minimum required elastic limit stress for EPS under pavement system.**
  - Use factor of safety, FS = 1.2.
  - From Equation (6.10),

    $\sigma_e \geq \sigma_{total} * FS = \sigma_{total} * 1.2$.

    A summary of the required σ_e for the various pavement systems is presented in Table 7.6.
- **Sub-Step 7: Select appropriate EPS block to satisfy the required EPS elastic limit stress for placement underneath the pavement system.**
  - Use Table 6.2 to select an EPS block that exhibits an elastic limit stress greater than or equal to the required σ_e determined in Sub-step 6. A summary of the required EPS block types is presented in Table 7.6.
- **Sub-Step 8: Select preliminary pavement system type and determine if a separation layer is required.**
  - A summary of a cost analysis for the four pavement systems analyzed is presented in Table 7.7. The unit costs for asphalt and granular base were obtained from (*10*). The unit cost for the concrete separation layer was obtained from the Indiana State Route 109 and the Utah Interstate-15 case histories presented in Chapter 11. The cost of the EPS-block geofoam was obtained from Chapter 12.

    The cost analysis shows the following results: (1) an asphalt concrete pavement system without a concrete separation layer is more cost effective than a composite pavement system that includes a concrete separation layer, (2) a

flexible pavement system consisting of 178 mm thick asphalt concrete and 432 mm granular base is the most cost effective of the four pavement systems considered, and (3) *EPS70* is required for the most cost effective flexible pavement system.

- **Sub-Step 9: Estimate traffic stresses at various depths within the EPS blocks.**

  This sub-step starts the second phase of the load bearing analysis because it focuses on the load bearing capacity of the EPS below a depth of 610 mm in the EPS whereas the first phase focused on the load bearing capacity of the EPS within the upper 610 mm of the EPS mass.

  — Summarize the equivalent rectangular loaded areas on top of the EPS blocks from each dual tire set or from combined dual tire sets if the applied stresses were found to overlap in Sub-step 3. Because the pavement system with an asphalt thickness of 178 mm and a 432 mm thick granular base was determined to be the most economical, only this pavement system is analyzed. From Sub-step 3 and from Table 7.6, no stress overlap occurs within the pavement system for this pavement system. The equivalent rectangular loaded areas on top of the EPS blocks are shown in Figure 7.5.

Figure 7.5 Plan view of equivalent rectangular loaded area from live load stresses on top of the EPS blocks.

Table 7.6. Summary of applied vertical stresses on top of the EPS blocks, minimum required elastic limit stress, and required EPS type for the pavement systems analyzed.

Table 7.7. Cost comparison between the pavement systems analyzed.

— Determine the depths within the EPS where stress overlap occurs. Using the 1H:2V assumed stress distribution method, stress overlap between two adjacent loaded areas occurs at a depth Z equal to the spacing, S, between the two loaded areas. Therefore, stress overlap between the adjacent dual tire sets shown in Fig. 7.5 will occur at $S = Z_0 = 0.12$ m and 0.73 m. However, stresses will overlap first at the smaller Z_0 value. At $Z_0 = 0.12$ m stresses between the two sets of interior tires (Set No. 2 and 3) overlap.

— Estimate traffic stresses at any depth where stress overlap occurs.

If stress overlap occurs at $Z_0 < 0.61$ m, the EPS selected in Sub-step 7 for the preliminary pavement system selected in Sub-step 8 must be checked to verify that the EPS can support the combined stresses.

— From Figures 7.5 and 6.19, the combined rectangular loaded area dimensions at $Z_0 = 0.12$ m are

$$\begin{aligned} B_{combined} &= B_2 + B_3 + S_2 + Z_0 \\ &= 1.1 \text{ m} + 1.1 \text{ m} + 0.12 \text{ m} + 0.12 \text{ m} \\ &= 2.44 \text{ m} \end{aligned}$$

$$\begin{aligned} L_{combined} &= L_2 + Z_0 \quad \text{(Note that } L_1 = L_2 = L_3 = L_4 = 1.61 \text{ m)} \\ &= 1.61 \text{ m} + 0.12 \text{ m} \\ &= 1.73 \text{ m} \end{aligned}$$

$$Q_{combined} = Q_2 + Q_3 = 69.4 \text{ kN} + 69.4 \text{ kN} = 138.8 \text{ kN}$$

From Equation (6.11), the vertical stress induced by traffic loading is

$$\begin{aligned} \sigma_{Z,LL} &= \frac{Q_{combined}}{(B_{combined})(L_{combined})} = \frac{138.8 \text{ kN}}{(2.44 \text{ m})(1.73 \text{ m})} \\ &= 32.9 \text{ kPa} \end{aligned}$$

— From Equation (6.11), the vertical stress caused by traffic loading by the exterior dual tire sets (Set No. 1 and 4) is

$$\sigma_{Z,LL} = \frac{Q}{(B+z)(L+Z)} = \frac{69.4 \text{ kN}}{(1.1 \text{ m} + 0.12 \text{ m})(1.61 \text{ m} + 0.12 \text{ m})}$$
$$= 32.9 \text{ kPa}$$

— Check to ensure stress overlap does not occur between the new combined rectangular loaded area and the adjacent exterior dual tire sets. At $Z_0 = 0.12$ m the width of the loaded area from the two exterior dual tire sets is

$B_1 = B_4 = 1.1 \text{ m} + Z_0 = 1.1 \text{ m} + 0.12 \text{ m} = 1.22 \text{ m}$

Therefore, the spacing between the center combined loaded area and the adjacent exterior dual tire sets is 0.61 m as shown in Fig. 7.6. Therefore, stress overlap will occur at 0.12 m + 0.61 m = 0.73 m below the top of the EPS blocks.

Figure 7.6. Equivalent rectangular loaded areas from live load stresses at 0.12 m below the top of the EPS blocks.

— Estimate traffic stresses at Z = 0.61 m. From Equation (6.11), the vertical stress caused by the interior combined loaded area from dual tire sets 2 and 3 is

$$\sigma_{Z,LL} = \frac{Q_{2,3}}{(B_{2,3} + (0.61 \text{ m} - 0.12 \text{ m}))(L_{2,3} + (0.61 \text{ m} - 0.12 \text{ m}))}$$

$$= \frac{138.8 \text{ kN}}{(2.44 \text{ m} + 0.49 \text{ m})(1.73 + 0.49 \text{ m})}$$

$$= 21.3 \text{ kPa}$$

From Equation (6.11), the vertical stress caused by the exterior dual tires, Set 1 and 4, is

$$\sigma_{Z,LL} = \frac{Q}{(B+z)(L+Z)} = \frac{69.4 \text{ kN}}{(1.1 \text{ m} + 0.61 \text{ m})(1.61 \text{ m} + 0.61 \text{ m})} = 18.28 \text{ kPa}$$

— Estimate traffic stresses at $Z_0 = 0.73$ m. At this depth, the vertical stresses imposed by the exterior dual tires, Set No. 1 and 4, will overlap with the combined interior loaded area of dual tire sets No. 2 and 3.

$$B_{combined} = B_1 + B_{2,3} + B_4 + S_1 + S_3 + (0.73\text{ m} - 0.12\text{ m})$$

$$= 1.22\text{ m} + 2.44\text{ m} + 1.22\text{ m} + 0.61\text{ m} + 0.61\text{ m} + (0.61\text{ m})$$
$$= 6.71\text{ m}$$

$$L_{combined} = L_1 + Z_0 = 1.61\text{ m} + 0.73\text{ m} = 2.34\text{ m}$$

$$Q_{combined} = Q_1 + Q_{2,3} + Q_4 = 69.4\text{ kN} + 138.8\text{ kN} + 69.4\text{ kN} = 277.6\text{ kN}$$

$$\sigma_{Z,LL} = \frac{Q_{combined}}{(B_{combined})(L_{combined})} = \frac{277.6\text{ kN}}{(6.71\text{ m})(2.34\text{ m})} = 17.68\text{ kPa}$$

— Estimate traffic stresses at 1 m intervals after 0.73 m. Table 7.8 provides a summary of traffic stresses, σ_{LL}, within the EPS.

Table 7.8. Summary of applied vertical stresses, minimum required elastic limit stress, and required EPS types at various depths within the EPS blocks.

- **Sub-Step 10: Estimate the gravity stresses at various depths within the EPS blocks.**

  The procedure for estimating the gravity stresses will be illustrated for $Z_0 = 0.73$ m.

  — Determine the surcharge at the center of the embankment from the pavement system and any road hardware placed on top of the roadway, q_t. In this example, no excessive surcharge loads from road hardware are anticipated. Therefore, use Equation (6.19),

  $$q_t = q_{pavement} = \gamma_{pavement} * T_{pavement} = 20\text{ kN/m}^3 * 0.61\text{ m} = 12.2\text{ kPa}$$

  — From Fig. 5.3 and Equation (6.18) determine α,

  $$\alpha = 2 * \arctan\left(\frac{b}{Z}\right) = 2 * \arctan\left(\frac{5.5\text{ m}}{0.73\text{ m}}\right) = 2.8777\text{ radians}$$

  — From Equation (6.17), determine the increase in vertical stress due to the pavement system gravity load, $\sigma_{Z,DL}$.

$$\Delta\sigma_{Z,DL} = \frac{q_t}{\pi}(\alpha + \sin\alpha) = \frac{12.2 \text{ kPa}}{\pi}(2.8777 \text{ radians} + \sin(2.8777 \text{ radians}))$$

$$= 12.2 \text{ kPa}$$

— From Equation (6.20), determine the total gravity stress from the pavement system and the EPS blocks,

$$\sigma_{Z,DL} = (\Delta\sigma_{Z,DL}) + (Z * \gamma_{EPS}) = (12.2 \text{ kPa}) + (0.73 \text{ m} * 1 \text{ kN/m}^3)$$

$$= 12.93 \text{ kPa}$$

— Table 7.8 provides a summary of the total gravity stresses within the EPS.

- **Sub-Step 11: Calculate total stresses at various depths within the EPS blocks.**

The procedure for determining the total stresses will be shown for $Z_0 = 0.73$ m.

— From Equation (6.21),

$$\sigma_{total} = \sigma_{Z,LL} + \sigma_{Z,DL} = 17.68 \text{ kPa} + 12.93 \text{ kPa}$$
$$= 30.61 \text{ kPa}$$

Table 7.8 provides a summary of the total stresses, σ_{total}, within the EPS.

- **Sub-Step 12: Determine the minimum required elastic limit stress for EPS at various depths within the EPS blocks.**

— The procedure for determining the required elastic limit stress will be shown for $Z_0 = 0.73$ m. From Equation (6.22),

$$\sigma_e \geq \sigma_{total} * 1.2 = 30.61 \text{ kPa} * 1.2 = 36.73 \text{ kPa}$$

- **Sub-Step 13: Select appropriate EPS block to satisfy the required EPS elastic limit stress at various depths within the EPS blocks.**

Table 7.8 provides a summary of EPS block types obtained from Table 6.2 that meet or exceed the minimum required elastic limit stress. Since stress overlap occur at $Z_0 = 0.12$ m, which is less than 0.61 m, the EPS selected in Sub-step 7 for the preliminary pavement system selected in Sub-step 8 must be checked to verify that the EPS can

support the combined stresses. As shown in Table 7.8, both an *EPS70* and *EPS50* was selected at Z = 0.61 m for the two dual tire load combinations analyzed. Therefore, the EPS with the larger elastic limit stress, *EPS70*, is selected to ensure adequate load bearing. This is the same EPS type selected in Sub-step 7 for the preliminary pavement system of 178 mm of asphalt concrete and 432 mm of granular base selected in Sub-step 8. Therefore, an *EPS70* can be used directly below the pavement system for a depth of 0.61 m.

As shown in Table 7.8, an *EPS40* can be used below the *EPS70* for depths greater than 0.61 m.

STEP 15 – PAVEMENT SYSTEM DESIGN

- The local transportation agency prefers a flexible pavement system. The proposed roadway will be located along a low-volume road with an estimated traffic level of 300,000 equivalent single axle loads, i.e., ESAL = 300,000. The local transportation agency would like the pavement designed based on a 75 percent level of reliability. The pavement design is to be based on the AASHTO 1993 design procedure.

  — Determine the design structural number, SN. From Table 4.2 and based on an *EPS70*, which will be used for the initial 0.61 m of the embankment below the pavement system, $SN_{REQ} = 5$.

  — Verify that the preliminary pavement system will meet the required structural number. It is assumed that the following material layer coefficients have been obtained from the local transportation agency's design manual.

  Asphalt concrete $a_1 = 0.44$

  Crushed stone aggregate base $a_2 = 0.14$

  The preliminary pavement system consists of 178 mm (7 in.) of asphalt concrete and 432 mm (17 in.) of crushed stone base for a total thickness of 610 mm. From Equation (4.1),

$$SN = a_1D_1 + a_2D_2 = (0.44 * 7 \text{ in.}) + (0.14 * 17 \text{ in.})$$
$$= 5.46$$

$$SN \geq SN_{REQ}$$

$$5.46 \geq 5$$

Therefore, the pavement system consisting of 178 mm of asphalt concrete and 432 mm of granular base meets the required SN and can be used for the roadway.

STEP 16 – DETERMINE IF THE FINAL PAVEMENT SYSTEM DESIGN RESULTS IN A SIGNIFICANT CHANGE IN OVERBURDEN COMPARED TO THE PRELIMINARY PAVEMENT SYSTEM DESIGN DEVELOPED IN STEP 2.

— The final pavement system determined in Step 15 has the same thickness as the preliminary pavement system of 0.61 m. However, as will be shown in Figure 7.7, if a crown of 2 percent is used for the top of the pavement, the pavement system thickness at the center of the roadway will need to be increased by 110 mm. Therefore, the total pavement system thickness at the center of the roadway will be 720 mm. Consideration should be given to re-checking the design procedure because of this increase in pavement thickness at the centerline of the roadway. However, this re-checking will not be shown here. For this example, the increase in stress due to the crown may not be significant because of stress distribution with depth.

STEP 17 –FINAL EMBANKMENT DESIGN.

Figure 7.7 provides a cross-section of the proposed design.

Figure 7.7 Cross-section of the proposed EPS-block geofoam roadway embankment.

DESIGN EXAMPLE 2 – LATERAL PRESSURES ON AN ABUTMENT

The design requirements for abutments as well as design examples can be found in (*11*). The steps of the abutment design procedure are summarized in Chapter 6. The purpose of this design example is to demonstrate how to calculate earth pressures generated by an EPS-block

geofoam bridge approach fill on an abutment. Determination of earth pressures is required in Step 2 of the abutment design procedure.

- Estimate the lateral earth pressures generated by an EPS-block geofoam bridge approach fill on the abutment shown in Figure 7.8. The bridge approach detail is the one used as part of the bridge approach rehabilitation project for the bridge over the N.F. Shoshone river in Wyoming, which was presented in Chapter 11.

Figure 7.8 Bridge approach configuration.

The passive pressure of the soil in front of the abutment is ignored because of the large displacement required to mobilize the passive resistance. A live load surcharge equal to 0.61 m of earth acts on the surface of the backfill. The weight of the approach slab and sand base is considered as a dead load surcharge. Figure 7.9 provides a summary of loadings applied to the abutment.

Figure 7.9 Summary of loadings applied to the abutment.

- Determine the horizontal forces generated by the live and dead load surcharges.
  - — Horizontal pressure and force due to live load surcharge.

    $\omega_L = 0.61 \text{ m} * \gamma_t = 0.61 \text{ m} * 18.8 \text{ kN/m}^3 = 11.47 \text{ kN/m}^2$

    $$H_L = \frac{1}{10} * \omega_L * H' = \frac{1}{10} * 11.47 \text{ kN/m}^2 * 2.795 \text{ m} = 3.21 \text{ kN/m of wall}$$

    Note that it is assumed that the lateral pressure imposed by the live load surcharge is equal to 1/10 times the vertical stress (*12*).
  - — Horizontal pressure and force due to the concrete approach slab surcharge.

    $\omega_{D,Conc} = 0.305 \text{ m} * \gamma_{Conc} = 0.305 \text{ m} * 23.6 \text{ kN/m}^3 = 7.2 \text{ kN/m}^2$

    $$H_{D,Conc} = \frac{1}{10} * \omega_{D,Conc} * H' = \frac{1}{10} * 7.2 \text{ kN/m}^2 * 2.795 \text{ m} = 2.01 \text{ kN/m of wall}$$
  - — Horizontal pressure and force due to sand base surcharge.

    $\omega_{D,Sand} = 0.205 \text{ m} * \gamma_t = 0.205 \text{ m} * 18.8 \text{ kN/m}^3 = 3.85 \text{ kN/m}^2$

$$H_{D,Sand} = \frac{1}{10} * \omega_{D,Sand} * H' = \frac{1}{10} * 3.85 \text{ kN/m}^2 * 2.795 \text{ m} = 1.08 \text{ kN/m of wall}$$

- Determine the horizontal force generated by the EPS-block geofoam fill. As indicated in Chapter 6, the horizontal force from the EPS blocks is neglected because it is negligible.
- Determine the horizontal force generated by the soil backfill behind the EPS/soil interface.
  - — As indicated in Chapter 6, the lateral earth pressure force, P_A, generated by the soil behind the EPS/soil interface is conservatively assumed to be transmitted without dissipation through the geofoam to the back of the abutment.
  - — Determine the coefficient of active earth pressure, K_A. From Equation (6.23) and based on the friction angle of the EPS/soil interface, δ, equal to the friction angle of the soil ϕ, the following is obtained:

$$K_A = \left[\frac{\sin(\theta-\varphi)\left(\frac{1}{\sin\theta}\right)}{\sqrt{\sin(\theta+\delta)} + \sqrt{\frac{\sin(\varphi+\delta)\sin(\varphi)}{\sin(\theta)}}} \right]^2$$

$$= \left[\frac{\sin(45^\circ - 35^\circ)\left(\frac{1}{\sin 45^\circ}\right)}{\sqrt{\sin(45^\circ + 35^\circ)} + \sqrt{\frac{\sin(35^\circ + 35^\circ)\sin(35^\circ)}{\sin(45^\circ)}}} \right]^2 = 0.0173 \approx 0.02$$

  - — Determine the lateral earth pressure force, P_A, from Equation (6.24)

$$P_A = \frac{1}{2} * \gamma_t * H'^2 * K_a = \frac{1}{2} * 18.8 \text{ kN/m}^3 * (2.795 \text{ m})^2 * 0.02$$

= 1.47 kN/m of wall

— It can be seen from Figure 7.9 that the largest horizontal force is applied by the live load surcharge.

REFERENCES

1. American Association of State Highway and Transportation Officials, *Standard Specifications for Highway Bridges*, 16th, American Association of State Highway and Transportation Officials, Washington, D.C. (1996).
2. Refsdal, G., "Frost Protection of Road Pavements." *Frost Action in Soils - No. 26,* Committee on Permafrost, ed., Oslo, Norway (1987) pp. 3-19.
3. Jutkofsky, W. S., Sung, J. T., and Negussey, D., "Stabilization of an Embankment Slope with Geofoam." *Transportation Research Record 1736,* Transportation Research Board, Washington, D.C. (2000) pp. 94-102.
4. Bartlett, S., Negussey, D., Kimble, M., and Sheeley, M., "Use of Geofoam as Super-Lightweight Fill for I-15 Reconstruction (Paper Pre-Print)." *Transportation Research Record 1736,* Transportation Research Board, Washington, D.C. (2000).
5. Terzaghi, K., Peck, R. B., and Mesri, G., *Soil Mechanics in Engineering Practice*, 3rd, John Wiley & Sons, Inc., New York (1996).
6. Koerner, R. M., *Designing with Geosynthetics*, 4th, Prentice Hall, Upper Saddle River, N.J. (1998).
7. Scarborough, J. A., Filz, G. M., Mitchell, J. K., Brandon, T. L., Hoppe, E. J., and Hite, S. L., "Design of High Reinforced Embankments Constructed with Poor Quality Soil and Degradable Shale." *Geosynthetics '99 (1999:Boston, MA) Specifying Geosynthetics and Developing Design Details,*1999, Vol. 1 pp. 491-504.
8. *Minimum Design Loads for Buildings and Other Structures, ANSI/ASCE 7-95, Approved June 6, 1996*, American Society of Civil Engineers, New York (1996).
9. "Foundations & Earth Structures, *Design Manual 7.02 Revalidated by Change 1 September 1986*." Naval Facilities Command, Alexandria, VA (1986) 253 pp.
10. RSMeans Company Inc., *RSMeans Site Work & Landscape Cost Data, 20th Annual Edition, 2001*, RSMeans Company Inc., Kingston, MA (2000) 638 pp.
11. Barker, R. M., Duncan, J. M., Rojiani, K. B., Ooi, P. S. K., Tan, C. K., and Kim, S. G., "Manuals for the Design of Bridge Foundations, NCHRP Report 343." Transportation Research Board, National Research Council, Washington, D.C. (1991) 308 pp.
12. Horvath, J. S., "Designing with Geofoam Geosynthetic, Seminar Notes." (1999).

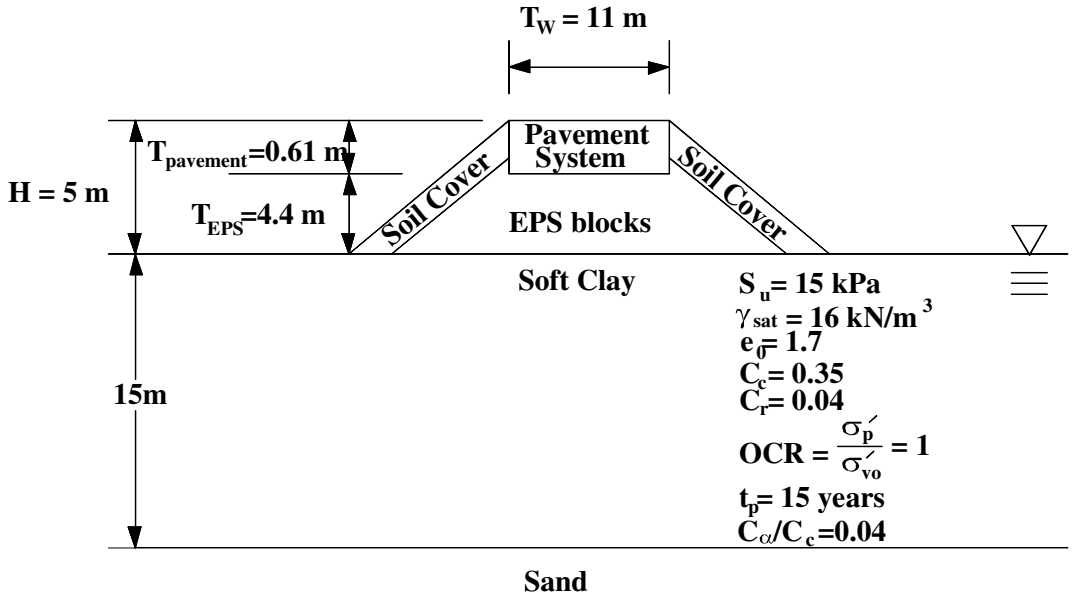

FIGURE 7.1 Proj 24-11.doc

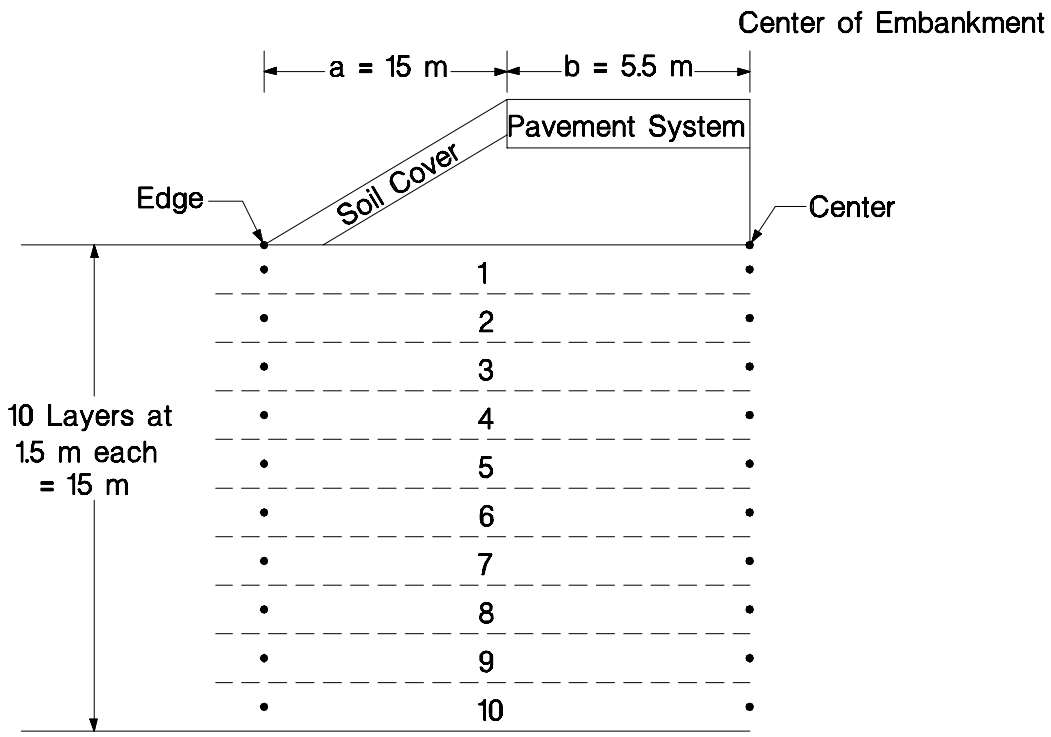

FIGURE 7.2 PROJ 24-11.doc

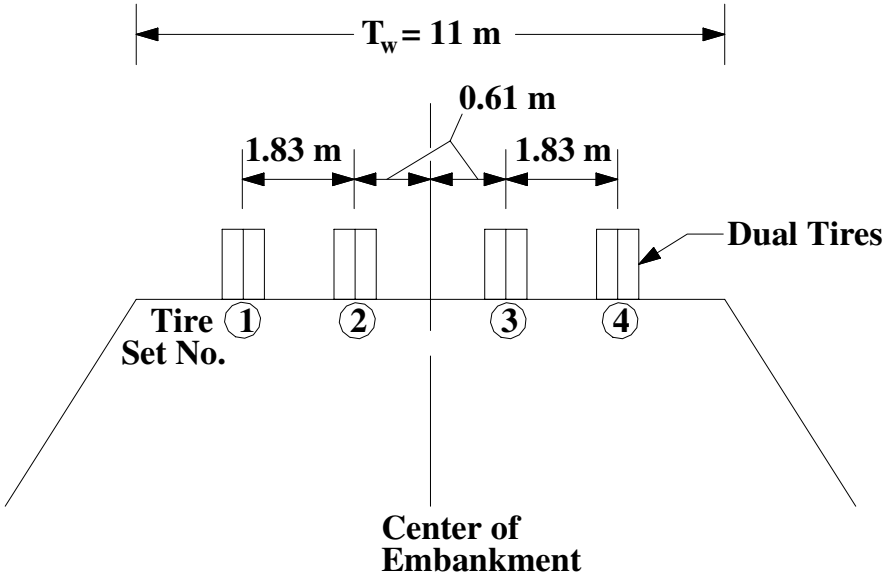

FIGURE 7.3 PROJ 24-11.doc

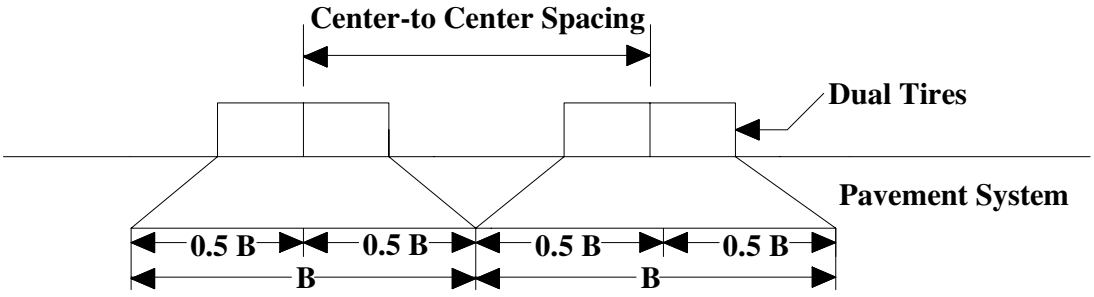

B = Width of equivalent rectangular loaded area for one set of dual tires.

Note: If center-to-center spacing < B, stresses imposed by the two dual tire sets overlap.

FIGURE 7.4 PROJ 24-11.doc

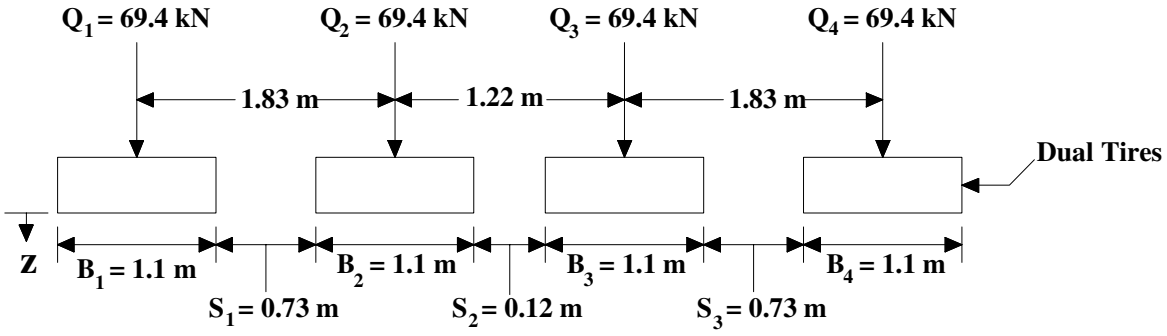

Note: $L_1 = L_2 = L_3 = L_4 = 1.61$ m. These loaded area lengths are not shown in this figure.

FIGURE 7.5 PROJ 24-11.doc

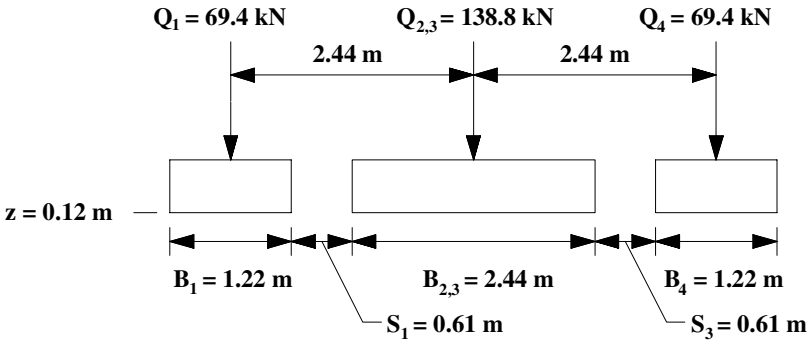

FIGURE 7.6 PROJ 24-11.doc

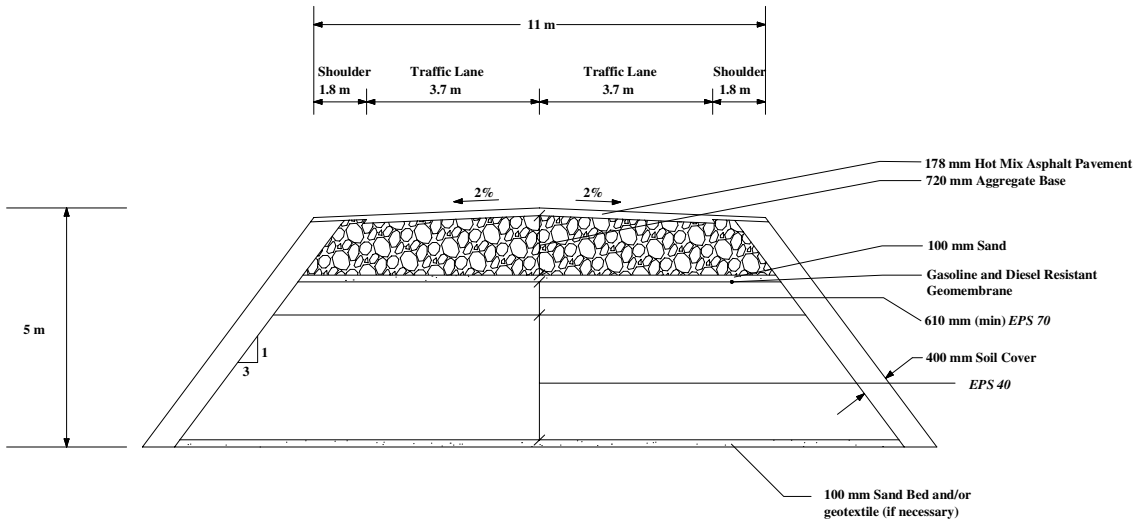

FIGURE 7.7 PROJ 24-11.doc

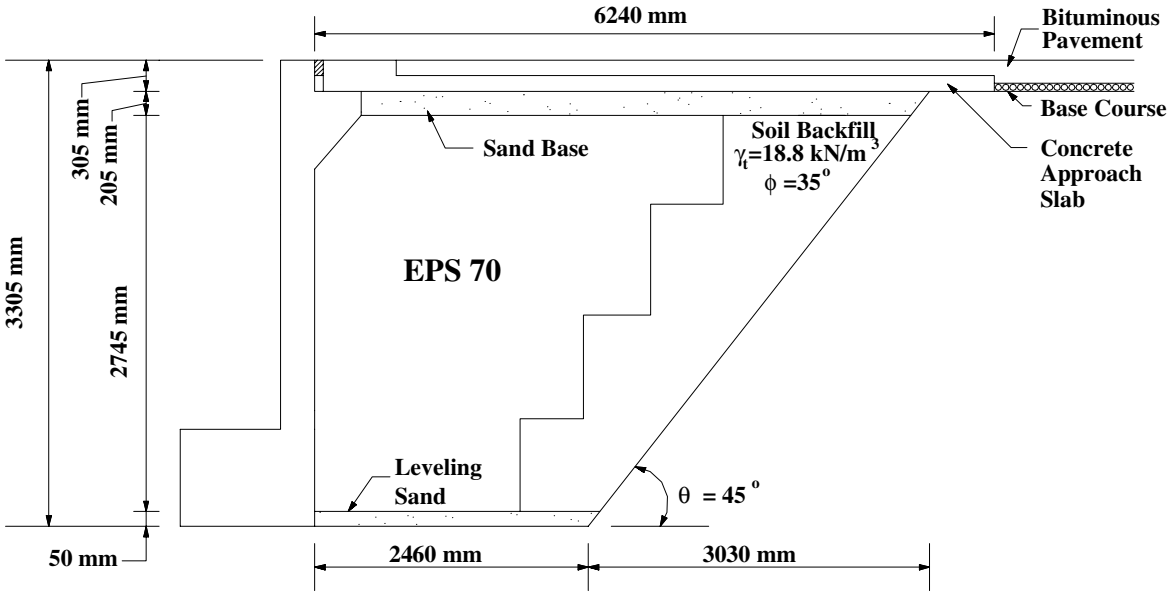

FIGURE 7.8 Proj 24-11.doc

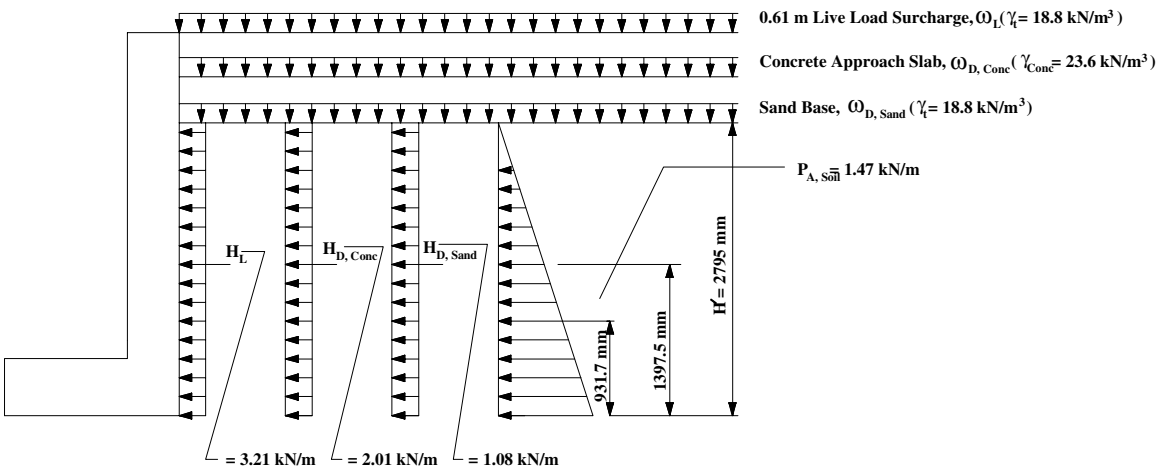

FIGURE 7.9 Proj 24-11.doc

Layer No.	Layer Thickness (m)	z (m)	$\Delta\sigma_{z_I}$ (kPa)	$\Delta\sigma_{z_{II}}$ (kPa)	$\Delta\sigma_{z_{III}}$ (kPa)	$\Delta\sigma_{z@center}$ (kPa)	σ'_{vo} (kPa)	σ'_{vf} (kPa)	σ'_{p} (kPa)	S_p (m)
1	1.5	0.75	16.58	0.01	0.01	16.59	4.64	21.24	4.64	0.1284
2	1.5	2.25	16.20	0.12	0.12	16.44	13.93	30.37	13.93	0.0658
3	1.5	3.75	15.19	0.41	0.41	16.02	23.21	39.23	23.21	0.0443
4	1.5	5.25	13.82	0.78	0.78	15.39	32.50	47.88	32.50	0.0327
5	1.5	6.75	12.40	1.13	1.13	14.66	41.78	56.44	41.78	0.0254
6	1.5	8.25	11.09	1.40	1.40	13.90	51.07	64.97	51.07	0.0203
7	1.5	9.75	9.95	1.61	1.61	13.16	60.35	73.51	60.35	0.0167
8	1.5	11.25	8.98	1.74	1.74	12.46	69.64	82.10	69.64	0.0139
9	1.5	12.75	8.15	1.82	1.82	11.8	78.92	90.72	78.92	0.0118
10	1.5	14.25	7.44	1.87	1.87	11.18	88.21	99.39	88.21	0.0101
									Total Sp =	0.3694

Layer No.	Layer Thickness (m)	z (m)	$\Delta\sigma_{Z_I}$ (kPa)	$\Delta\sigma_{Z_{II}}$ (kPa)	$\Delta\sigma_{Z_{III}}$ (kPa)	$\Delta\sigma_{Z@edge}$ (kPa)	σ'_{vo} (kPa)	σ'_{vf} (kPa)	σ'_{p} (kPa)	S_p (m)
1	1.5	0.75	0	0.20	0	0.20	4.64	4.84	4.64	0.0035
2	1.5	2.25	0.01	0.57	0	0.58	13.93	14.51	13.93	0.0035
3	1.5	3.75	0.04	0.92	0	0.97	23.21	24.18	23.21	0.0034
4	1.5	5.25	0.10	1.22	0.01	1.33	32.50	33.83	32.50	0.0034
5	1.5	6.75	0.20	1.47	0.02	1.69	41.78	43.47	41.78	0.0033
6	1.5	8.25	0.33	1.65	0.03	2.01	51.07	53.08	51.07	0.0033
7	1.5	9.75	0.47	1.79	0.05	2.32	60.35	62.67	60.35	0.0032
8	1.5	11.25	0.63	1.88	0.08	2.59	69.64	72.23	69.64	0.0031
9	1.5	12.75	0.79	1.93	0.10	2.83	78.92	81.75	78.92	0.0030
10	1.5	14.25	0.95	1.96	0.14	3.04	88.21	91.25	88.21	0.0029
									Total Sp =	0.0325

Case Number	Description of Interface	Potential Type of Interface Materials	Estimated δ (degrees)	Source of δ	Notes
1	EPS-block geofoam placed directly on the soil foundation.	EPS/clay	27	(*2*)	(1)
2	Sand placed between the EPS blocks and soil foundation to serve as both a stable construction platform and a leveling material.	EPS/sand	30	(*3*) (*4*)	
		sand/clay	20	(*5*)	
3	Sand over a geotextile placed between the EPS blocks and soil foundation to serve as both a stable construction platform and leveling material.	EPS/sand	30	(*3*) (*4*)	
		sand/ geotextile	26	(*6*)	(2)
		geotextile/clay	26	(*7*)	(3)
4	Geotextile placed between the EPS blocks and soil foundation.	EPS/geotextile	25	Ch. 2 of this study	
		geotextile/clay	26	(*7*)	(3)

Notes: (1) A $\delta = 27^{\circ}$ was provided for EPS and general soil interfaces. The type of soil was not provided.

(2) A $\delta = 26^{\circ}$ was provided for a concrete sand with $\phi = 30^{\circ}$ and a nonwoven, heat bonded geotextile.

(3) δ based on test results between a Trevira 1155 nonwoven geotextile and a red, sandy silt with 50 to 60 percent passing the U.S. No. 200 sieve and a liquid limit and plasticity index of 50 and 10, respectively.

Case Number	Description of Interface	Potential Type of Interface Materials	Estimated δ (degrees)	Source of δ	Notes
1	Pavement system placed directly on the EPS blocks	Crushed stone or sand/EPS	30	(*3*) (*4*)	(1)
2	Geotextile placed between the pavement system and the EPS blocks	crushed stone or sand/geotextile	26	(*6*)	(2)
		geotextile/EPS	25	Ch. 2 of this study	
3	Concrete separation layer placed between the pavement system and the EPS blocks	crushed stone or sand/concrete	29	(*9*)	(3)
		concrete/EPS	66	(*4*)	
4	Geomembrane placed between the pavement system and EPS blocks	crushed stone or sand/geomembrane	25	(*6*)	(4)
		geomembrane/EPS	52	Ch. 2 of this study	

Notes:

(1) δ based on sand/EPS interface. See Chapter 2.

(2) A $\delta = 26^{\circ}$ was provided for a concrete sand with $\phi = 30^{\circ}$ and a nonwoven, heat bonded geotextile.

(3) A range of $\delta = 29^{\circ}$ to 31° was provided for mass concrete on clean gravel, gravel-sand mixtures, and coarse sand.

(4) δ based on a concrete sand with $\phi = 30^{\circ}$ and a smooth PVC geomembrane.

Failure Mode	δ (degrees)	k_h	FS′
I	25	0.09	4.7
II	30	0.09	Not critical
III	20	0.09	3.6

Pavement System and Thickness of Asphalt Concrete	**σ_{LL} (kPa)**	**σ_{LL} if stress overlap occurs between interior dual tire sets (kPa)**	**σ_{LL} if stress overlap occurs between interior and exterior dual tire sets (kPa)**	**Largest σ_{LL} (kPa)**	**σ_{DL}* (kPa)**	**σ_{total} (kPa)**	**Required Elastic Limit Stress, σ_e (kPa)**	**EPS TYPE Needed****
Flexible, 76 mm	64	No Overlap	No Overlap	64	12.2	76.2	91.44	*EPS100*
Flexible, 178 mm	39	No Overlap	No Overlap	39	12.2	51.2	61.44	*EPS70*
Composite, 76 mm	19	21.55	No Overlap	21.55	12.2	33.75	40.5	*EPS50*
Composite, 178 mm	16	18.76	No Overlap	18.76	12.2	30.96	37.15	*EPS50*

*Based on a 0.610 m pavement system at 20 kN/m^3

***EPS40* not recommended directly beneath paved areas.

EPS Type Needed	Cost $/m^2 per 610 mm Thickness	Pavement System and Thickness of Asphalt Concrete	Asphalt Thickness (mm)	Cost $/m^2 per mm Thickness	Cost $/m^2	Concrete Separation Layer Thickness (mm)	Cost $/m^2 per mm Thickness	Cost $/m^2	Granular Base Thickness (mm)***	Cost $/m^3	Cost $/m^2	Total Cost $/m^2
EPS100	$39.65	Flexible, 76 mm	76	$0.10	$7.60	0	$0.36	$0.00	534	$26.00	$13.88	$61.13
EPS70	$30.50	Flexible, 178 mm	178	$0.10	$17.80	0	$0.36	$0.00	432	$26.00	$11.23	$59.53
EPS50	$26.23	Composite, 76 mm	76	$0.10	$7.60	102	$0.36	$36.72	432	$26.00	$11.23	$81.78
EPS50	$26.23	Composite, 178 mm	178	$0.10	$17.80	102	$0.36	$36.72	330	$26.00	$8.58	$89.33

***based on 610 mm pavement system

Dual Tire Load Combination	Q (kN)	σ_{LL} (kPa)	q_t (kPa)*	$\Delta\sigma_{Z,DL}$ Pavement (kPa)	Z(m) (kPa)	$\sigma_{Z,DL}$ Total (kPa)	σ_{total} (kPa)	Required Elastic Limit Stress, σ_e (kPa).	EPS Type Needed
2 and 3 combined	138.8	32.88	12.20	12.20	0.12	12.32	45.20	54.24	*EPS70*
1 or 4 single	69.4	32.88	12.20	12.20	0.12	12.32	45.20	54.24	*EPS70*
2 and 3 combined	138.8	21.34	12.20	12.19	0.61	12.80	34.14	40.97	*EPS50***
1 or 4 single	69.4	18.28	12.20	12.19	0.61	12.80	31.08	37.30	*EPS40*
All combined	277.6	17.68	12.20	12.20	0.73	12.93	30.61	36.73	*EPS40*
All combined	277.6	10.78	12.20	12.06	1.73	13.79	24.57	29.48	*EPS40*
All combined	277.6	7.34	12.20	11.71	3.73	14.44	21.79	26.15	*EPS40*

*Based on a 0.610 m pavement system at 20 kN/m^3

**Indicates that this is the critical EPS type for this depth.

CHAPTER **8**

GEOFOAM CONSTRUCTION PRACTICES

Contents

INTRODUCTION

The focus of this chapter is construction related issues for EPS-block geofoam embankments. However, numerous aspects of both design and manufacturing of EPS-block geofoam for lightweight fill applications, including manufacturing quality control (MQC) and manufacturing quality assurance (MQA), are considered because they interact with and impact construction. Therefore, a discussion of certain design and manufacturing aspects is included in this chapter. Thus, there is some overlap with other chapters in this report, such as Chapter 3 (Design Methodology) and Chapter 9 (Geofoam MQC/MQA) but this overlap allows presentation of a comprehensive chapter on geofoam construction practices. In addition, post-construction activities, including monitoring, are also discussed in this chapter.

DESIGN

Two construction issues that directly interact and impact the design of an EPS-block geofoam embankment are placement of the blocks and the use of mechanical inter-block connectors. Although a lightweight fill embankment constructed using EPS-block geofoam will consist of a large number of individual blocks, experience indicates that the fill can be analyzed as a single, coherent mass provided the individual EPS blocks are sufficiently interlocked both vertically and horizontally so that they collectively respond as a single, coherent mass when subjected to external loads. This involves consideration of both the overall block layout (which primarily controls interlocking in a vertical direction) and inter-block shear resistance (which primarily controls interlocking in the horizontal direction). Both of these considerations are discussed subsequently.

Block Layout

Based on a review of the literature, overall guidelines for an appropriate layout of EPS blocks to obtain adequate interlocking in the vertical direction include:

- Blocks should be placed with their smallest (thickness) dimension oriented vertically.
- All blocks should butt tightly against adjacent blocks on all sides.
- A minimum of two layers of blocks must always be used for lightweight fills beneath roads. Experience has indicated that a single layer of blocks can shift under traffic loads and lead to premature pavement failure (*1*).
- The blocks must be placed in a pattern such that continuity of the vertical joints between blocks is minimized. The overall objective is to create a layout of blocks that is geometrically interlocked to the greatest extent possible (see Figure 8.1). This is typically accomplished by:
  - aligning all the blocks within a given layer with their longitudinal axes parallel but offsetting the ends of adjacent lines of blocks,
  - orienting the longitudinal axes of all blocks in a given layer perpendicular to the longitudinal axes of the blocks within layers placed above and/or below, and
  - aligning the blocks within the uppermost layer transverse to the longitudinal axis of the road.

Figure 8.1. Isometric view of typical EPS block layout for a road embankment.

Longitudinal Geometry

Two aspects of the geometry of the embankment in the longitudinal direction that need to be considered during design and construction include orientation of the EPS blocks and the transition zone of the geofoam and the non-geofoam sections of the roadway.

The top surface of the assemblage of EPS blocks should always be parallel with the final pavement surface (*2*). Thus, any desired change in elevation (grade) along the road alignment must be accommodated by sloping the foundation soil surface as necessary prior to placement of

the first layer of EPS blocks. Additionally, the upper surface of the EPS blocks should be horizontal when viewed in cross-section so any crown desired in the cross-section of the final pavement surface should be achieved by varying the thickness of the pavement system (*2*).

The transition zone between geofoam and embankment soil should be gradual to minimize differential settlement. The EPS blocks should be stepped as shown in Figure 8.2 as the embankment transitions from a soft foundation soil that requires geofoam to a stronger foundation soil that can support a soil embankment. However, a minimum of two layers of blocks is recommended to minimize the potential of the blocks to shift under traffic loads. The only exception to this is the final step, which can consist of one block as shown in Figure 8.2. The specific pattern should be determined on a project-specific basis based on calculated differential settlements such as the criteria given in (*3*) which suggests that the calculated settlement gradient within the transition zone should not exceed 1:200 (vertical: horizontal).

Figure 8.2. Typical EPS block transition to a soil foundation (*4*).

Block Layout Design

The block layout design can be performed by either the project design engineer or the EPS block molder. Traditionally the block layout design was performed by the design engineer for the project. However, this is appropriate only if the designer knows the exact block dimensions beforehand. In current U.S. practice, there will generally be more than one EPS block molder who could potentially supply a given project. In most cases, block sizes will vary somewhat between molders due to different mold sizes. Therefore, the trend in U.S. practice is to leave the exact block layout design to the molder. The design engineer simply:

- shows the desired limits of the EPS mass on the contract drawings, specifying zones of different EPS densities as desired;
- includes the above conceptual guidelines in the contract specifications for use by the molder in developing shop drawings; and
- reviews the submitted shop drawings during construction.

Mechanical Connectors

If the calculated resistance forces along the nominally horizontal planes between EPS blocks are insufficient to resist the horizontal driving or imposed forces, additional resistance between EPS blocks is required to supplement the inherent inter-block friction. This is generally accomplished by adding mechanical inter-block connectors (typically prefabricated barbed metal plates) along the horizontal interfaces between the EPS blocks. Such connectors provide a pseudo cohesion when viewed from a Mohr-Coulomb strength perspective. At the present time, all such plates available in the U.S.A. are of proprietary designs. Therefore, the resistance provided by such plates and placement location must be obtained from the supplier or via independent testing.

Because of the relative costs of these plates, they should only be used where calculations indicate their need. In addition, research and experience indicates that their use is mandatory whenever seismic loads are to be resisted. However, the indiscriminate routine use of mechanical connectors should be avoided because, while not detrimental, they tend to add a significant cost to a project.

In addition to their role in resisting horizontal design loads, mechanical connectors have proven useful as a constructability tool to keep EPS blocks in place when subjected to wet, icy, or windy working conditions (*5*) and to prevent shifting under traffic where relatively few layers of blocks are used (*6*). Additional information on the use of mechanical connectors can be found in the "Block Interlock" section of Chapter 6.

MANUFACTURING

Introduction

There are three distinct manufacturing issues that impact construction and constructability of EPS-block geofoam embankments:

- flammability of the EPS blocks,
- dimensional tolerances of the EPS blocks, and
- the broad aspect of MQC and MQA.

Flammability

The primary manufacturing issue that impacts construction is flammability. Like most polymeric materials, polystyrene is inherently flammable as is the blowing agent, pentane (butane also has been used but not in the U.S.A.), used in manufacturing EPS. Any residual blowing agent left over from molding EPS blocks outgasses within a few days and is replaced by air. In addition, experience indicates that this inherent flammability of polystyrene ceases to be an issue once EPS is buried in the ground because there is no ignition source and, at least in the long term, there is no oxygen to support combustion, even within the vadose zone. Flammability has been a problem, albeit very rare, during construction when the EPS blocks are exposed to both ample atmospheric oxygen as well as potential ignition sources. As discussed in (*1*), problems have been encountered from two separate and distinct mechanisms:

- Direct ignition of the EPS blocks due to construction activities such as flame cutting or welding that are unrelated to geofoam usage but performed in close proximity of the EPS blocks.
- Ignition of residual blowing agent that outgasses after block placement and collects in the joints between blocks (all known EPS blowing agents are heavier than air as thus will not readily disperse into the atmosphere absent positive ventilation). The ignition source is usually some construction activity unrelated to the geofoam.

These issues are easily addressed to eliminate the potential for their occurrence in practice.

With regard to the direct combustibility of the EPS blocks, specifications, either directly or indirectly, can mandate the use of *modified expandable polystyrene* as the raw material (a.k.a. bead or resin) for the EPS. The modified resin incorporates an inorganic, bromine-based flame retardant that has proven effective and has no effect on the visual or physical properties of the resulting EPS block. Although the practice in some countries (most notably Norway, the pioneer of EPS-block geofoam as lightweight fill) is to use normal or regular (non-flame-retardant)

expandable polystyrene raw material for cost reasons (it can be slightly cheaper), the recommended practice incorporated in the provisional standard in Appendix C of this report is to require the use of flame retardant EPS. As this is already the de facto standard practice in the U.S.A., this should present little, if any adjustment issues for the industry. Specification of flame retardancy is accomplished using the indirect method incorporated in ASTM Standard C 578 (*7*) by requiring a minimum Oxygen Index (OI) of 24 percent which is above the OI of normal atmospheric air (21 percent).

The second issue dealing with outgassing of post-molding residual blowing agent is addressed by requiring an adequate seasoning period prior to delivery of the EPS blocks to the project site. This issue has not been formally studied to date for EPS blocks produced in the U.S.A. because seasoning time is affected by the exact formulation (pentane content) of the expandable polystyrene and block dimensions among other factors. Based on available published information (*8*) as well as anecdotal information obtained by personal communication with both resin suppliers and block molders in the U.S.A., an interim recommendation of three days (72 hours) of seasoning at normal ambient room temperature is proposed and incorporated into the provisional standard in Appendix C of this report. The recommended seasoning time can be accelerated by temporary storage within a heated room.

It is worth noting that the minimum seasoning requirement may create problems on projects that are relatively large in size and/or have tight delivery schedules. For example, there were cases in which lightweight fill projects in the U.S.A. used EPS blocks that were less than one day old. Therefore, project-specific decisions might be required that relaxes this seasoning requirement. Experience indicates that this may be permissible to expedite construction work. However, waiver of this seasoning time should be done only with increased vigilance for fire safety as well as worker safety. This may include a prohibition on personal tobacco smoking near EPS blocks as well as “round-the-clock” security for any unseasoned EPS blocks exposed at the end of a day's construction. Furthermore, unseasoned blocks should never be stored and/or

shipped in any type of enclosed vehicle as any accumulated outgassed blowing agent will pose a potential explosion hazard when the vehicle is opened.

Dimensional Tolerances

The dimensional tolerances of EPS blocks for geofoam applications affects construction through the ability of the blocks to fit together with minimal gaps and maintain a planar or horizontal surface as subsequent layers of blocks are placed. Thus, the dimensional tolerances of block-molded EPS involves the following aspects:

- the permissible variation, relative to some average value, in dimension in each of the three orthogonal linear dimensions (thickness, width and length) of a block,
- the orthogonality (squareness) of all corners of a block and
- permissible warp or curvature in any one face of a block.

To a significant extent, the physical shape and dimensions of EPS blocks are controlled by various factors during manufacturing, especially with regard to the age and quality of the mold used. Because of the wide range in molding equipment currently in use in the U.S.A., blocks of appropriate quality with regard to shape and dimension can neither be assumed nor taken for granted. Therefore, these items must be included in specifications. The provisional standard included in Appendix C to this report incorporates physical and dimensional tolerances used in Norway which are based on decades of experience.

It is worth noting that requirements for physical and dimensional tolerances are known to have been relaxed on a project-specific basis in the U.S.A. for cost reasons. This is caused by molders using older molds and performing some post-molding trimming for EPS blocks to meet the physical and dimensional tolerances normally required for geofoam applications. This trimming adds a cost that can be eliminated by the owner or their representative accepting blocks that do not meet normal specifications. There has been no systematic study of how much deviation from normally accepted practice is acceptable. Thus, owners who, either directly or through their representatives, accept blocks with tolerances that exceed those normally used must

accept a greater, but incalculable, uncertainty with regard to overall final performance of the EPS embankment.

Manufacturing Quality

MQC/MQA is discussed fully in Chapter 9. However, an overview of the MQC/MQA procedure incorporated in the provisional standard in Appendix C is presented herein. The procedures to be followed once the blocks arrive at the construction site are considered to be part of construction quality assurance (CQA) and thus are considered in the following section. Construction is also when Phase II of MQA is executed by the owner's CQA agent. The primary components of the provisional standard include the product MQC requirements, product MQA requirements, product shipment, and construction quality requirements to include construction quality control (CQC) and CQA requirements. The provisional standard includes the proposed EPS material designation system shown in Table 9.1 and the minimum allowable values of MQC/MQA parameters shown in Table 9.2. A new sampling protocol shown in Figure 9.4 and a two-phased MQA procedure were developed in this study. Phase I of the MQA procedure is to be performed prior to shipment of EPS blocks to the project site and Phase II is to be performed as the EPS blocks are delivered to the project site. Another key aspect of the proposed MQA procedure is the implementation of a two-tier MQA system, one for molders with third-party certification and the other for those without. Table 9.3 provides a summary of the MQA procedure.

Pre-Construction Meeting

Once project construction begins, a meeting should be held at the project site prior to the delivery and installation of the EPS blocks. This meeting should, as a minimum, involve the construction contractor and owner's agent who will perform the quality assurance for both the EPS manufacturing (MQA) as well as construction (CQA). Ideally, the design engineer, EPS molder, and EPS supplier (if different from the molder) should also be present. The purpose of this meeting is to review all details relative to the manufacturing and placement of the EPS-block

geofoam. This is important as the use of EPS-block geofoam in road embankments is still a relatively new technology in many parts of the U.S.A. and thus it is important that all project participants be aware of the key issues for a successful application of this technology.

CONSTRUCTION

CQC/CQA

CQC is a series of internal actions taken by the construction contractor to meet the specifications that comprise part of the contract documents. These specifications are prepared by the design engineer and frequently establish criteria for acceptance based on reference to standards. For traditional earthwork projects, CQC is almost always limited to following a set of procedures for compaction that have been established on past projects of a similar nature. It is important to recognize that many contractors in the U.S.A. are unfamiliar with EPS-block geofoam. Not only must they handle and place it properly, but on most projects they will be the purchaser of the geofoam. Thus the construction contractor must be aware of the pre-delivery aspects of MQA that are discussed in Chapter 9. This means that specifications must be particularly clear and detailed. In addition, a pre-construction conference to review the unique issues and aspects of working with EPS-block geofoam (at which a representative of the EPS molder should also be present) is highly recommended.

The contractor shall be directly responsible for all CQC tasks. Items covered by CQC include all earthwork and related activities other than manufacturing and shipment of the EPS-block geofoam. Items of particular relevance include site preparation, block handling and storage, block placement, and pavement construction.

In addition to CQC tasks, CQA tasks must be continuous and particularly vigilant and performed by an organization other than the contractor. The CQA agent is either a part of the owner's organization (as is the case with many state DOTs) or an independent materials testing laboratory or consulting engineer (who may or may not be the original designer) retained by the owner. In either case, it is likely for the near future that the CQA agent will also be unfamiliar

working with EPS-block geofoam. Therefore, both the designer as well as the CQA agent should also be present at the pre-construction conference to review necessary tasks.

Site Preparation

Experience indicates that proper site preparation prior to placing the EPS blocks is an important factor in both internal stability of the embankment as well as overall constructability. The need to adhere closely to the criteria itemized and discussed below tends to increase with thickness of the geofoam portion of the fill because site preparation has a greater effect as more layers of EPS blocks are placed. If sufficient attention has not been given to site preparation, it becomes increasingly difficult to keep subsequent layers of EPS blocks level or horizontal.

Site preparation details to be included in construction specifications are as follows:

- Ideally, there should be no standing water or accumulated ice or snow within the area where EPS blocks are to be placed. The presence of water inhibits assuring that the soil subgrade is sufficiently level and free of material that could damage the blocks. However, from a practical perspective EPS-block geofoam is often used at sites where the soil conditions are poor and ground water is inherently at the surface. Experience indicates that some amount of standing water can be accommodated and still have an EPS fill that performs acceptably. It appears desirable to develop a specification that calls for no standing water then relax this requirement on a project-specific basis based on field decisions. However, the potential for hydrostatic uplift of the blocks during construction must be considered if the no standing water requirement is relaxed. Adequate drainage should be maintained of the site during construction to minimize water accumulation along the EPS embankment from heavy rainfall, which can result in hydrostatic uplift of the EPS blocks.
- EPS blocks should not be placed on frozen soil subgrade except in the case of intentional construction over continuous or discontinuous permafrost terrain

where the consequences of eventual ground thawing beneath the fill have been explicitly considered by the designer.

- There should be no debris on or large pieces of vegetation protruding from the subgrade on which the EPS blocks are to be placed. Furthermore, the soil particles exposed at the subgrade level should be no larger than coarse sand to fine gravel (2 to 19 mm (0.08 to 0.8 in.)). The objective of these requirements is to prevent physical damage such as puncturing, gouging, broken corners, etc. to the EPS blocks as the first layer is placed on the foundation soil. It is difficult to quantify the effects of this damage so it is considered prudent to take all reasonable steps to make sure the damage does not occur. In some cases, it may be necessary to specify that a bed of sand 12 to 25 millimeters thick (approximately 0.5 to 1 in.) be placed over the existing foundation soil surface. This serves both to cover the coarser in-situ material as well as allow for the necessary leveling of the first layer of blocks (this issue is discussed next). When a sand bed is placed it may be desirable if not necessary to first place a geotextile over the existing ground surface to function as a separator to prevent intermixing of the sand bedding and natural soil (which will be wet and soft in many cases).
- Regardless of the foundation soil material (natural soils or sand bed), the surface must be reasonably planar ("smooth") prior to the placement of the first block layer. The required smoothness is a vertical deviation of no more than ±10 mm (0.4 in.) over any 3 meters (9.8 ft) distance. This criterion was developed in Norway over decades of experience (*9*). Typically, this cannot be achieved by mechanical equipment alone so some manual labor will be required. Note that on many projects the required finished subgrade may not necessarily be horizontal in the direction parallel to the road alignment. This is because the top of the

assemblage of EPS blocks (and, therefore, the bottom as well) should always be parallel with the grade of the finished road surface in the longitudinal direction (as noted previously, any crown of the road in the transverse direction is, however, achieved by varying material thickness within the pavement system). Therefore, if the road grade is non-horizontal the subgrade on which the EPS blocks will be placed must be non-horizontal along the road alignment as well. This is noted here as it will not always be possible to use a large carpenter's level to check for subgrade smoothness.

After the site subgrade has been properly prepared, installation of the EPS blocks can commence.

Block Shipment, Handling, and Storage

There is one additional issue that straddles the boundary between manufacturing and construction quality. It is primarily the responsibility of the molder (hence discussed in Chapter 9 as an MQC issue) but is enforced by the construction inspection agent (so is also included here as part of CQA). This is the issue of damage of EPS blocks during shipping. Construction damage is generally considered to be physical damage to a geosynthetic product during its shipment to the project site; its placement on site; or during subsequent placement of other materials above it. Typically, the selection of trucks used to ship EPS blocks (almost always a tractor-pulled trailer, but the trailer may either be flat bed or a closed box), the loading of these trucks and the manner in which the load is secured (important when flat-bed trailers are utilized) are all under the control of the EPS molder. Thus, responsibility for the as-delivered condition of the EPS blocks is largely controlled by the molder. This is an important issue to address and incorporate into manufacturing specifications as recent, anecdotal evidence provided by unpublished, confidential sources indicates that block damage on EPS-block geofoam projects within the U.S.A. is not uncommon and is the source of on-site problems over block acceptance. The reason for the damage appears to be the preferred use of flat-bed trucks to transport EPS blocks because the

blocks have gotten longer with newer molding equipment placed on line during the 1990s. Because the lightweight EPS blocks must be securely strapped to prevent their movement during shipment, it is not uncommon for EPS blocks to arrive at the job site with numerous indentations of the edges along the sides of the blocks from the strapping as well with breakage at the end corners of the blocks. One shipping method that may be considered to minimize damage to the blocks is to use structural angles along the top edge of the exterior blocks that would accommodate the strapping.

At all stages of construction the EPS blocks should be handled in a manner so as to minimize physical damage to the blocks. Lifting or transporting the blocks in any way that creates dents or holes in the block surfaces is strongly discouraged. Careful handling is recommended because it is impossible to quantify when block damage starts to impair performance of the final EPS mass. Therefore, it is recommended that damage to the blocks be discouraged and avoided. Experience indicates that damage during shipping, on-site handling, and temporary on-site storage of EPS blocks can be easily avoidable and thus is unnecessary. However, project specifications must contain appropriate language to the effect that EPS blocks with indentations and pieces broken off will be rejected by the owner's agent on site to encourage careful handling.

If blocks are to be stockpiled until placement, a secure storage area should be designated for this purpose. The blocks should not be trafficked upon, especially by any vehicle or equipment. The storage area should be away from any heat source or construction activity that produces heat or flame because of block flammability. Tobacco smoking should also be prohibited in the storage area. Blocks should be secured with sandbags and similar "soft" weights as necessary to prevent their being dislodged by wind. Protection against ultraviolet (UV) damage in the relatively short term exposure of temporary storage is generally not required. Overall, it is generally unnecessary and, in fact, even undesirable to cover the EPS blocks in any way. There is anecdotal project experience from unpublished, confidential sources that EPS that was covered

temporarily with a dark-colored geomembrane built up sufficient heat to locally melt and distort some of the EPS.

EPS is not an inherently dangerous or toxic material (other than the flammability issues discussed previously) so there are no additional explicit safety issues to be observed other than normal construction safety. However, extra caution is required during wet or cold weather. The surfaces of the EPS blocks tend to be more slippery wet than dry. When air temperatures approach or go below freezing, a thin layer of ice can readily develop on the exposed surfaces of EPS blocks if the dewpoint is sufficiently high. Thus, the surfaces of the EPS blocks can pose handling difficulties and slip hazards in this condition. The air temperature does not have to go below freezing for this phenomenon to occur (it is basically the same phenomenon that can cause differential icing of the final pavement surface). In addition to the safety issue, EPS blocks should not be placed above blocks in which ice has developed on the surface because of the potential for the blocks to slide due to water, wind, or other horizontal loads while the ice is still present between the blocks.

Block Placement

Blocks should be placed according to the pattern specified in the design drawings or approved contractor-submitted shop drawings. Particular care is required if EPS blocks of different density are to be used on the project. Blocks should be placed tight against adjacent blocks on all sides. Every effort should be made to eliminate gaps at the vertical joints between the blocks.

If the blocks meet the specified dimensional tolerances and are placed carefully starting with a planar subgrade as discussed previously, the surface of a given layer of blocks should provide a reasonably planar surface for the next layer of blocks. However, in cases where the block surface may become irregular, the most common solution is to place a thin layer of unreinforced portland cement concrete (PCC) as a "mud slab" or working surface that is leveled for placing subsequent block layers. However, such a slab must not be placed without prior

review by the project designer because the mud slab will induce an additional permanent vertical stress on the foundation soil which needs to be evaluated.

If necessary to field cut blocks, the most precise cutting can be done with a portable hot-wire device that the EPS molder can provide or at least provide assistance with assembling. A wire saw or chain saw can also be used. In particular, a chain saw appears to be the most commonly used cutting tool in U.S. practice when a smooth, precise final surface is not required. Hot-wire cutting devices made for cutting EPS typically do not cause the EPS to ignite. However, consideration should be given to having a fire extinguisher available during any hot-wire cutting of EPS blocks. At all times when the EPS blocks are exposed, extreme care must be exercised to keep all sources of heat or open flame away from the blocks. Even tobacco smoking should be discouraged for safety reasons.

The surfaces of the EPS blocks shall not be directly traversed by any vehicle or construction equipment during or after placement of the blocks. The final surface of the EPS blocks shall be covered as shown on the contract drawings. Care shall be exercised during placement of the cover material so as not to cause any damage to the EPS blocks.

Accommodation of Utilities and Road Hardware

The alternatives for accommodating shallow utilities and road hardware (barriers and dividers, light poles, signage) is to provide a sufficient thickness of the pavement system to allow conventional burial or embedment within soil or, in the case of appurtenant elements, provide for anchorage to a PCC slab or footing that is constructed within the pavement section.

Pavement Construction

The pavement system is defined for the purposes of the standard in Appendix C as all material placed above the EPS blocks within the limits of the roadway, including any shoulders. Care must be exercised when constructing the pavement system so the separation layer (if one is used) and/or EPS blocks are not damaged. If a separation layer is to be placed on the top surface of the final layer of EPS blocks, this surface must be reasonably clean and dry prior to placement.

In addition, care must be exercised during placement of the separation material so that the EPS blocks are not damaged, unleveled, or moved so that gaps occur between the blocks.

In general, the pavement system can be constructed in the normal manner with only a few cautions related to the presence of the EPS blocks. The most critical phase is the placement and compaction of the initial lift or layer of soil on the separation layer or EPS blocks. Vehicles and construction equipment such as earthmoving equipment must not directly traffic on the EPS blocks or separation layer (even if a PCC slab is used as it is still possible to overstress the underlying EPS). The only construction guideline that provides maximum construction equipment loads is in the United Kingdom guidelines where it is recommended that the maximum weight of compaction equipment be limited to 58.8 kN/m width (4 kips/ft) of roll and that construction equipment be limited to a maximum applied pressure of 20 kPa (400 lb/ft^2) (*10*). However, the type and size of construction equipment should be limited to wheel, track, or roller loads that produce maximum applied stresses that do not exceed the elastic limit stress of the EPS, i.e., in no case should vehicle loads exceed the elastic limit stress of the EPS.

One construction procedure that can be used to minimize damage to the EPS blocks is to use relatively lightweight equipment to push approximately 300 mm (12 in.) (minimum) of soil or aggregate onto the EPS blocks or separation layer before compacting the material. Typically placement of the first lift of unbound material is accomplished by pushing the material ahead using a relatively small bulldozer or front-end loader. Placement of additional unbound and bound layers of the pavement system can then be placed in the normal manner although trafficking of the surface by trucks or heavy equipment of all types should be minimized or avoided altogether until the pavement is completed. If necessary, temporary mats should be provided to distribute vehicle loads. Stockpiling of construction materials on the geofoam must be conducted with care to minimize overstressing of the EPS blocks. After completion of the pavement system, vehicle loads should not exceed the design vehicle load.

The most effective type of compaction equipment to utilize to meet the desired compaction requirements will depend on the characteristics of the material to be compacted. For example, in (*11*) it was observed that a plate vibrator was the most suitable equipment for compaction of unbound material in a pavement structure over EPS blocks. The static roller was found to be less efficient than the plate vibrator and the compaction requirements could not be achieved with a vibratory roller. Therefore, consideration can be given to observing and testing a test area or strip with the actual materials that will be placed and compacted to determine the most suitable type of compaction equipment needed to achieve the required compaction requirements.

When verifying compaction of the unbound pavement material, nuclear moisture-density gauges have sometimes yielded incorrect results. This is caused by the water content of the soil being inferred from a count of radioactive scattering caused by hydrogen atoms. In normal soil, hydrogen atoms only occur in water. However, EPS contains hydrogen and thus spurious water content results can be produced from nuclear density gauges. It is suggested that this issue be discussed with the manufacturer of the nuclear moisture-density gauges to determine if this is a potential problem. It is often desirable to check the initial readings obtained with such gauges using a traditional mechanical procedure such as a sand cone apparatus to obtain the total (damp) unit weight or density of the unbound material followed by oven or other traditional methods for drying of a soil specimen to determine its water content.

POST CONSTRUCTION

On routine projects, no instrumentation and post-construction monitoring or testing of EPS-block geofoam is required. However, because EPS-block geofoam is still considered a novel construction material in some states the owner and designer may elect to instrument and monitor various parameters. There is no "standard practice" for this so any instrumentation and observation program would have to be developed on a case-by-case basis. Discussions of instrumentation for post-construction monitoring can be found in (*12,13*).

SUMMARY

Various aspects of both design and manufacturing of EPS-block geofoam for lightweight fill applications interact with and impact construction. Two construction issues that directly impact the design of an EPS-block geofoam embankment is placement of blocks and mechanical connectors. Three manufacturing issues that impact construction and constructability include the flammability of the EPS blocks, dimensional tolerances of the EPS blocks, and the broad aspect of MQC and MQA. Items covered by CQC/CQA include all earthwork and related activities other than manufacturing and shipment of the EPS-block geofoam. Items of particular relevance include site preparation, block handling and storage, block placement, and pavement construction all of which are discussed in this chapter.

REFERENCES

1. Horvath, J. S., "Lessons Learned from Failures Involving Geofoam in Roads and Embankments." *Research Report No. CE/GE-99-1,* Manhattan College, Bronx, NY (1999) 18 pp.
2. "Matériaux Légers pour Remblais/Lightweight Filling Materials." *Document No. 12.02.B,* PIARC-World Road Association, La Defense, France (1997) 287 pp.
3. Briaud, J.-L., James, R. W., and Hoffman, S. B., "Settlement of Bridge Approaches (The Bump at the End of the Bridge)." *NCHRP Synthesis 234,* Transportation Research Board, Washington, D.C. (1997) 75 pp.
4. Horvath, J. S., *Geofoam Geosynthetic*, , Horvath Engineering, P.C., Scarsdale, NY (1995) 229 pp.
5. Horvath, J. S., "A Concept for an Improved Inter-Block Mechanical Connector for EPS-Block Geofoam Lightweight Fill Applications: 'The Ring's the Thing'," In Manhattan College-School of Engineering, Center for Geotechnolgy [web site]. [updated 8 September 2001; cited 20 September2001]. Available from http://www.engineering.manhattan.edu/civil/CGT/T2olrgeomat2.html; INTERNET.
6. Duskov, M., "EPS as a Light Weight Sub-base Material in Pavement Structures; Final Report." *Report Number 7-94-211-6,* Delft University of Technology, Delft, The Netherlands (1994) .
7. ASTM D 578-95, "Standard Specification for Rigid, Cellular Polystyrene Thermal Insulation." Vol. 04.06, American Society for Testing and Materials, West Conshohocken, PA (1999) .
8. Coughanour, R. B., "Pentane Issue." *Presentation at the 16th Annual SPI Expanded Polystyrene Division Conference,* San Diego, CA, (1988).
9. "Guidelines on the Use of Plastic Foam in Road Embankment." Public Roads Administration, Road Research Laboratory, Oslo, Norway (1980) 2 pp.
10. Sanders, R. L., and Seedhouse, R. L., "The Use of Polystyrene for Embankment Construction." *Contractor Report 356,* Transport Research Laboratory, Crowthorne, Berkshire, U.K. (1994) 55 pp.

11. Duskov, M., "EPS as a Light-Weight Sub-Base Material in Pavement Structures," Doctor of Engineering thesis, Delft University of Technology, Delft, The Netherlands (1998).
12. Dunnicliff, J., "Geotechnical Instrumentation for Monitoring Field Performance." *NCHRP Synthesis of Highway Practice 89,* Transportation Research Board, Washington, D.C. (1982) 46 pp.
13. Dunnicliff, J., *Geotechnical Instrumentation for Monitoring Field Performance*, , Wiley-Interscience, New York (1988) 577 pp.

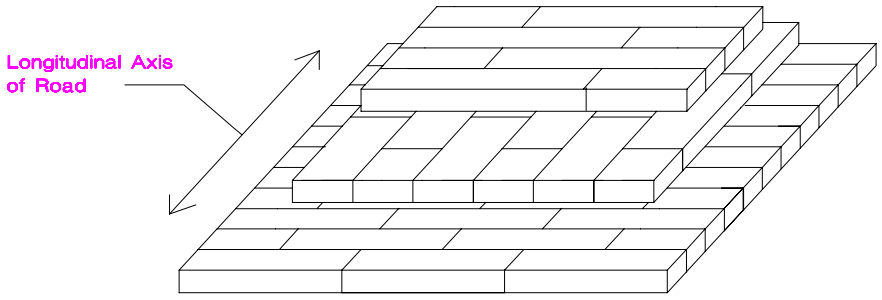

FIGURE 8.1 PROJ 24-11.doc

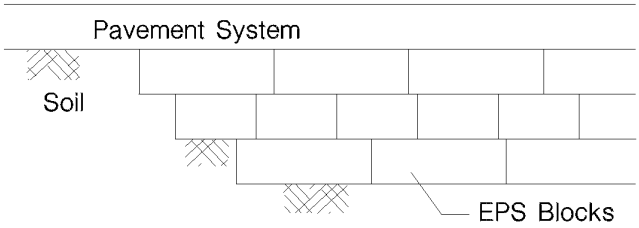

FIGURE 8.2 PROJ 24-11.doc

CHAPTER **9**

GEOFOAM MQC/MQA

Contents

INTRODUCTION

One of the overall objectives of NCHRP Project 24-11 was to develop a standard in the American Association of State Highway and Transportation Officials (AASHTO) format to optimize usage and performance for expanded polystyrene (EPS) - block geofoam as lightweight fill in road embankments. The proposed design methodology incorporated in the design guideline is based on the assumption that the EPS-block geofoam meets a set of minimum material and construction criteria. Therefore, a complementary provisional standard was developed. The provisional standard, which is included in Appendix C, is a combined material, product, and construction standard covering block-molded EPS for use as lightweight fill in road embankments and related bridge approach fills on soft ground. The standard is intended to be used to create a project-specific specification in conjunction with the recommended design guideline included in Appendix B.

The basis for the provisional standard is initially presented followed by a discussion of its key features, which include the proposed EPS material designation system, the minimum allowable values of manufacturing quality control (MQC) and manufacturing quality assurance (MQA) parameters, and the MQC/MQA test requirements. The primary components of the provisional standard include the product MQC, MQA, shipment, and the construction quality requirements. The product MQC, MQA, and shipment requirements are presented herein. The construction quality requirements, e.g. construction quality control (CQC) and construction quality assurance (CQA) requirements, are presented in Chapter 8 (Geofoam Construction Practices).

DEFINITIONS

Quality in both manufactured products and services is an important issue throughout society and thus is an issue raised in this report. It is useful to state the definitions of two quality concepts and two quality aspects related to engineered construction used in this report.

There are two general concepts related to manufactured products and services:

- *Quality control* (QC) refers to those actions taken by a product manufacturer or service provider to ensure that the final product or service meets certain minimum criteria. For engineered construction, these criteria are established by specifications produced by the design engineer for a particular project. These specifications may incorporate via reference standards established by some recognized organization such as AASHTO, the American Society for Testing and Materials (ASTM), or the Geosynthetic Institute (GSI).
- *Quality assurance* (QA) refers to actions taken by some agency other than the manufacturer or service provider to independently verify the product or service quality. The QA agency may be the owner (e.g. a state DOT), the owner's representative (typically a consulting engineering firm), or any one of several companies that provide this service for manufactured products. QA may be provided on either a project-specific or ongoing basis.

There are typically two aspects of both QC and QA in engineered construction:

- *Manufacturing quality control* (MQC) and *manufacturing quality assurance* (MQA) which apply to manufactured products used on a given project that are delivered to the site more or less in a condition for direct use. Therefore, this would apply to the EPS blocks as used for geofoam because they are manufactured in a dedicated offsite plant, not at the project site.
- *Construction quality control* (CQC) and *construction quality assurance* (CQA) which apply to the manner in which various materials and products are handled, stored, and placed at a project site by a construction contractor. Thus, this covers the manner in which the EPS-block geofoam is stored, handled, and placed at the project site.

The distinctions between manufacturing and construction are important not only for the obvious division of responsibility but also because MQA and CQA can be handled in different ways. CQA must be performed on site at the time of construction. However, with any manufactured product there is always the alternative to pre-qualify product quality prior to

delivery to a project site as opposed to performing MQA once the material is delivered on site. As a simple yet common example to illustrate this, structural steel is generally accepted on site based on mill certificates or similar paperwork. Rarely would samples be cut on site from the steel and sent to a laboratory where specimens prepared from these samples would be tested for yield strength, etc. The importance of MQA for manufactured material is emphasized here because it is a significant issue with regard to MQA of EPS-block geofoam.

BASIS OF THE PROVISIONAL STANDARD

Overview

In developing the recommended standards for future practice, problems related to the current use of existing standards were evaluated and reviewed herein. Because standards should complement the design methodology, the main technical attributes for the use of EPS-block geofoam as lightweight fill in road construction are considered so the requirements of the recommended standards are understood.

Problems With Current Standards

Currently, ASTM Standard C 578 (*1*) is the primary standard utilized in practice when developing a material specification for EPS-block geofoam. The standard was written primarily for the use of cellular polystyrene (both EPS and extruded polystyrene (XPS)) in above-ground, non-load-bearing thermal insulation applications and not lightweight fill applications. Therefore, the overall basis of the ASTM C 578 standard may not be applicable nor sufficient for load-bearing geofoam applications. The overall quality of block-molded EPS is more critical in lightweight fill applications than other applications because no other application has such significant load-bearing requirements. Two problems related to the use of ASTM Standard C 578 have emerged.

The first problem is the tendency by EPS block molders to use as much regrind (recycled) material and to reduce the amount of virgin expandable polystyrene raw material to make the EPS-block geofoam blocks less costly and more cost competitive with other soft ground

treatment alternatives. The percentage of in-plant regrind and post-consumer recycled material and how it is fused into blocks may have varying affects on the mechanical properties (*2,3*) and on the time-dependent (creep) behavior of block-molded EPS. For example, tests have revealed that EPS with an average density of the order of 16 kg/m^3 (1 lbf/ft^3) had virtually the same compressive strength with up to 50 percent regrind content yet the initial tangent Young's modulus was reduced by a factor of approximately two between samples with no regrind and 50 percent regrind (*4*). Therefore, it is recommended that MQC/MQA compression tests also include reporting of the elastic limit stress and initial tangent Young's modulus to more accurately measure the impact of regrind content on the stress-strain behavior. The elastic limit stress is defined as the compressive stress at 1 percent strain as measured in a standard rapid-loading test (*5*). The slope of the initial (approximately) linear portion of the stress-strain relation is defined as the initial tangent Young's modulus. Additionally, the flexural strength test is a useful MQC/MQA test in conjunction with compressive strength tests to evaluate pre-puff and fusion quality, especially when regrind material is used (*2,3*).

The second problem is the tendency of the EPS industry to misinterpret the ASTM Standard C 578 density requirements. The standard only states minimum acceptable material properties (including density) of specimens cut from a block for the five standard grades of block-molded EPS covered by that standard. However, the standard is sometimes misinterpreted by the EPS industry to apply to a whole block instead of a specimen cut from a block. For example, if a customer specifies EPS with an average density of 20 kg/m^3 (1.25 lbf/ft^3), ASTM C 578 allows any particular specimen cut from a block tested for MQC/MQA purposes to have a density as low as 18 kg/m^3 (1.15 lbf/ft^3) which is approximately 10 percent less. It appears that the logic for this is related to the inherent density gradients (variations) that occur within block-molded EPS. It is entirely possible for a block of EPS that has an overall density of 20 kg/m^3 (1.25 lbf/ft^3) to have portions within that block of somewhat lower and higher density. Therefore, it appears that ASTM Standard C 578 was written to accommodate the inherent material variations that occur

within an EPS block. Molders in the U.S. have sometimes misinterpreted ASTM Standard C 578 so that the lower bound density provided in the ASTM standard is applied to a whole block instead of a specimen. Thus, a block with an overall density as low as 18 kg/m^3 (1.15 lbf/ft^3) is sometimes incorrectly considered as complying with ASTM C 578 and thus acceptable. Note that a block with an overall density of 18 kg/m^3 (1.15 lbf/ft^3) would have portions with an even lower density. The lesson learned from this emerging problem is that the applicability of lower-bound property values for either a given test specimen versus a block as a whole needs to be explicitly specified because it has important ramifications in load bearing capacity applications. In summary, it is recommended herein that the standard be applied to a specimen cut from a block and not the entire block.

These two emerging problems related to the current use of ASTM Standard C 578 appear to originate from a perception or attitude of EPS block molders that EPS blocks placed in the ground can be of relatively low quality compared to EPS used in above-ground construction. "It's only going be buried in the ground" is a paraphrased sentiment often heard in practice. Of course, the exact opposite is true. If the underlying foundation of any structure is substandard the probability of failure of the entire structure is increased. Therefore, in many ways the overall quality of block-molded EPS is more critical in lightweight fill applications than any other because no other application has such significant load-bearing requirements. A contributing factor to industry perceptions concerning quality is the fact that EPS block is simply more expensive than soil on a volume basis. Thus a frequent sentiment heard in the industry is that "I'm competing with dirt." As a result of these attitudes and contributing factors, there is an overall tendency to reduce the amount of virgin expandable polystyrene raw material used to make EPS-block geofoam. Thus, tactics such as trying to use as much regrind (recycled) material and mold to as low a density as possible are believed to be pervasive in U.S. industry at the present time.

Key Technical Attributes of EPS-Block Geofoam Affecting Design

Standards must complement the design methodology so the necessary engineering properties are present in the geofoam. Therefore, in developing standards for future practice, two primary technical attributes included in the design methodology for EPS-block geofoam used as lightweight fill in road construction were considered. First, lightweight fills are composed of entire blocks of EPS. Thus the overall properties and behavior of an entire block are of primary importance. For an engineer to design with confidence, every block of EPS delivered to a project site must, as a whole have an average block density that equals or exceeds some value that was assumed in design and specified in the design documents. Second, the proposed design methodology incorporates in the provisional design guideline the need to stay within the elastic range of the EPS (which is governed by the elastic limit stress) to limit both creep and plastic deformations and the explicit calculation of initial deformations (which is influenced by the initial tangent Young's modulus). Compressive strength and flexural strength are useful MQC/MQA tests for evaluating pre-puff and fusion quality. Therefore, for an engineer to design with confidence, every block of EPS delivered to a project site must, as a whole, have some minimum values of elastic limit stress, initial tangent Young's modulus, compressive strength, and flexural strength to ensure overall block quality with regard to material stiffness and prepuff fusion. Although the elastic limit stress and initial tangent Young's modulus show approximately linear correlation with EPS density, assuming the material is of appropriate quality, experience indicates that density alone does not sufficiently define EPS quality especially if regrind is used.

Philosophy Incorporated in the Provisional Standard

The basic philosophy adopted in the development of the provisional standard is to utilize the standard densities in ASTM Standard C 578 and add provisions related to the properties and behavior of EPS block that are necessary for a load bearing capacity application. First, the overall properties and behavior of an entire block are of primary importance. Second, EPS-block geofoam density can be used as an index property to estimate some mechanical and thermal properties provided the EPS meets a set of minimum criteria. Third, the proposed design

methodology is based on maintaining the long-term compressive stresses below the elastic-limit stress (within the elastic range) to keep long-term compressive strains within acceptable levels to limit both creep and plastic deformations. Fourth, because ASTM Standard C 578 does not currently contain any requirements for material stiffness (initial tangent Young's modulus) and elastic limit stress, recommended values are given in the proposed standard for these parameters as well.

The proposed standard specifies lower-bound properties, i.e., density, compressive strength, flexural strength, elastic limit stress, and initial tangent Young's Modulus, for a given MQC/MQA test specimen, not a block as a whole. For example, the average density of an entire block must equal or exceed a density that is slightly (approximately 10 percent) greater than the minimum allowed for an individual test specimen. These minimum values of initial tangent Young's modulus and elastic limit stress are the ones used in analysis and design. Although utilizing minimum values of initial tangent Young's modulus and elastic limit stress based on test specimens is slightly conservative because the average stiffness and elastic limit stress of the block as a whole would be somewhat greater than these minimums, this conservatism is not unreasonable because it would ensure that no part of a block (where the density might be somewhat lower than the overall average) would become overstressed.

PROPOSED EPS MATERIAL DESIGNATION AND MINIMUM ALLOWABLE VALUES OF MQC/MQA PARAMETERS

To facilitate and unify future design and specification, a material designation system for EPS-block geofoam was developed. The system selected is being used in western Europe wherein EPS-block geofoam is called "EPSx" where "x" is either two or three integers defining the minimum elastic limit stress of the block as a whole in kilopascals. Thus construction documents (plans and specifications) would indicate, for example, "EPS50 geofoam". Note that this compact notation identifies both the geofoam material (EPS) as well as the minimum elastic limit stress (50 kPa, (1,000 lb/ft^2)) which is the design value. Furthermore, a designer would know that initial

tangent Young's modulus for use in compression calculations is approximately 100 times this value, i.e. 5,000 kPa (100,000 lbs/ft^2)).

Table 9.1 shows the correlation between the proposed EPS-block geofoam designations and ASTM Standard C 578 material types. Also shown are the corresponding minimum allowable densities for every block as a whole and for any MQC/MQA test specimen trimmed from a block. The density values for each block as a whole are 10 percent greater than the minimum allowed for an individual test specimen. For a given material type, the dry density of each EPS block (as measured for the overall block as a whole) after a period of seasoning shall equal or exceed that shown in Table 9.1. The dry density shall be determined by measuring the mass of the entire block by weighing the block on a scale and dividing by the volume of the block. The volume is determined by obtaining dimensional measurements of the block in accordance with ASTM test method C 303 (*6*). The length and width should be measured in at least two locations approximately along lines A-B and C-D lines in Figure 9.1 for the width and lines A-D and B-C for the length. For blocks larger than 1 m^2 (10.8 ft^2) in area, an additional length or width measurement should be made for each additional meter (3.3 ft) increase in length or width over 1 m (3.3 ft) long. These measurements can be spaced approximately equally within the original measurement area defined by A, B, C, D. For blocks larger than 1 m^2 (10.8 ft^2) in area, there should also be an additional two thickness measurements for each additional square meter (10.8 ft^2) in size. These thickness measurements would be spaced approximately equally within the original measurement area defined by A, B, C, D such as locations E and F.

Figure 9.1 Procedure for obtaining dimensional measurements on full-size EPS blocks (*6*).

Table 9.1. Correlation between Current ASTM and Proposed AASHTO EPS Material Designations.

The minimum allowable values of the other design and quality control parameters are given in Table 9.2. Note that these are for individual test specimens and not the block as a whole. The compressive and flexural strength values were adopted from ASTM Standard C 578. The

elastic limit stress and initial tangent Young's modulus were developed from observed correlations with the minimum density values from individual test specimens also shown in Table 9.2. These values of elastic limit stress and initial tangent Young's modulus in Table 9.2 would be the values used in analysis and design. The minimum allowable values of the various material parameters corresponding to each AASHTO material type shown in Table 9.2 are to be obtained by testing specimens prepared from samples taken from actual blocks produced for the project for either MQC by the molder or MQA by the owner's agent.

Table 9.2. Minimum Allowable Values of MQC/MQA Parameters for Individual Test Specimens.

There are four main benefits to the proposed designation system. First, it decreases the importance of compressive strength and focuses on the most important aspect of block-molded EPS for load bearing capacity applications: the initial tangent Young's modulus or small-strain load-carrying capability. The parameter of compressive strength for EPS-block geofoam materials is not the key design parameter in practice because the compressive strength of EPS is defined arbitrarily, EPS does not fail in the traditional sense of material rupture, and compressive strength does not provide any insight into the creep behavior. Second, the proposed standard parallels the proposed design methodology that maintains the long-term compressive stress below the elastic-limit stress. Third, the proposed designation system also decreases the relevance of density which can be a misleading indicator especially if regrind is used. Fourth, this designation system will allow manufacturers maximum flexibility because it does not proscribe how much regrind material they can use but simply holds them accountable to the small-strain load-carrying characteristics of the final material. However, the influence of regrind content on creep behavior is not yet well understood because of the lack of test data on EPS with varying quantities of regrind and thus the topic is a subject for future study.

MQC/MQA TEST REQUIREMENTS

Overview

The requirements of MQC/MQA testing are somewhat different from those for testing for analysis and design parameters that were discussed in Chapter 2 because explicit testing for certain geotechnically relevant parameters, such as creep, are rarely performed for routine projects. The basis for this is almost 30 years of experience with EPS-block geofoam as lightweight fill for road earthworks has demonstrated that acceptable and cost-effective designs can be developed by correlating EPS density with these engineering parameters. However, these correlations with density can only be used with confidence if certain minimum qualities, e.g., a limited amount of regrind, of the EPS are assured by MQC/MQA. An appropriate analogy is that knowledge of only the density or unit weight of a soil conveys limited information as to its geotechnically relevant properties. Additional information is required to be able to use even the simplest empirical correlations for site characterization.

Relevant Aspects of EPS-Block Geofoam for MQC/MQA Testing

Introduction

MQC/MQA of block molded EPS for lightweight-fill geofoam applications should address the following issues:

- Flammability.
- Density.
- Pre-puff quality and fusion during molding.
- Seasoning.

The reasons for each of these is discussed in detail in the following sections.

Flammability

As discussed in Chapter 2, it is generally considered good practice in the U.S.A. to specify flame-retardant EPS for all geofoam applications.

Density

This is probably the single most useful index property of block-molded EPS. Thus, its determination is part of all physical testing performed on EPS.

Pre-Puff Quality and Fusion During Molding

The overall quality of EPS-block geofoam as a load-bearing material (reflected in its elastic limit stress and initial tangent Young's modulus) is strongly dependent on the quality of the pre-puff (overall chemistry and age of the original expandable polystyrene raw material); age of the pre puff; and percentage (if any) of in-plant regrind and post-consumer recycled material and how it is fused into blocks. Although the classical parameters of compressive and flexural strength are of no direct use in design, together they are useful MQC/MQA tests for evaluating pre-puff and fusion quality, especially when regrind material is used (*2,3*). MQC/MQA compression tests should also include reporting of the elastic limit stress and initial tangent Young's modulus in compression which together are the most important mechanical properties for design of EPS-block geofoam as lightweight fill. Experience (*4*) indicates that these design parameters can be significantly affected by the overall quality and molding fusion of pre-puff, and that the traditional MQC/MQA parameter of compressive strength does not adequately reflect these effects.

Seasoning

EPS should not be delivered to a project site until the residual blowing agent (which is likely to be pentane in the U.S.A.) has outgassed sufficiently so there is no possibility that it can collect in joints between blocks and pose a fire or explosion hazard. However, there has been no known research on how long is required to sufficiently outgas or season the EPS for raw material formulations and block sizes in current U.S. practice. This is also a topic for future study. However, based on available published information (*7*) as well as anecdotal information obtained

by personal communication with both resin suppliers and block molders in the U.S.A., the tentative recommendation for the seasoning time is a minimum of three days at normal ambient room temperature although this time might be shortened by storage at elevated temperatures (not all block molders are equipped for this). This three-day minimum is also based on the assumption that the EPS blocks will be stored with air space between blocks as well as positive air circulation (using fans) and ventilation (using roof vents) within the storage space. This is because EPS blowing agents such as pentane are heavier than air and will tend to pool at the ground surface unless actively mixed with air and vented.

Test Protocols

Record Keeping

Every block of EPS delivered to a project site should contain markings sufficient for the supplier to be able to trace the manufacturing history of the block in addition to other markings that may be deemed useful for constructability (density, location for placement relative to some job-specific shop drawing, etc.). The use of a self-adhesive label and/or barcode label would seem efficient for this purpose. The original molder should maintain and be able to produce detailed manufacturing records for every EPS block.

The recommended record keeping procedure incorporated in the standard is that each EPS block shall be labeled to indicate the name of the molder (if there is more than one supplying a given project), the date the block was molded, the mass of the entire block (in kilograms or pounds) as measured after a satisfactory period of seasoning as previously discussed, the dimensions of the block in millimetres or inches and the actual dry density/unit weight in kilograms per cubic metre or pounds per cubic foot. Additional markings using alphanumeric characters, colors and/or symbols shall be applied as necessary by the supplier to indicate the location of placement of each block relative to the shop drawing as well as the density of the block if multiple block densities are to be supplied for a given project. If multiple block densities

are to be supplied, the use of no marking shall be considered an acceptable marking for one of the densities as long as it is used for the lower (lowest) density EPS blocks supplied to the project.

Sampling

In-plant sampling of EPS blocks for MQC/MQA testing purposes should be similar to that suggested for post-delivery MQA sampling performed during Phase IIc MQA (See "Product MQA Requirements" section of this chapter and Table 9.3). Sampling of EPS block is typically performed by cutting samples from various locations of an EPS block perpendicular to the longitudinal axis of the block. Specimens for testing are then trimmed from these samples. The test specimens shall be seasoned and dry density, compressive strength, and flexural strength shall be measured as specified in ASTM C 578. The specimens used for compressive testing shall be cubic in shape with a 50 mm (2 in.) face width. The specimens used for flexural strength are typically rectangular with dimensions varying depending on the length of the support span of the loading system. Chapter 2 provides further testing information.

Basic MQA sampling and testing of production blocks of EPS has traditionally been the primary, even only, MQA tool from the earliest use of EPS-block geofoam as lightweight fill for roadways. Therefore, most national and international design manuals contain explicit recommendations for MQA sampling and testing. However, it appears that all such recommendations published to date have evolved from one single source: the Norwegian Road Research Laboratory of the Directorate of Public Roads. Figures 9.2 (a) and 9.2 (b) illustrate the recommended locations and dimensions of samples and test specimens. Each specimen shown is tested for density and compressive strength (keep in mind that in Norway the atypical definition of compressive strength is the compressive stress at 5 percent strain, not 10 percent as most everywhere else, is used). It appears that the logic for this sampling and testing is based on the traditional assumptions that:

- Compressive strength is the key EPS property for both design and quality, which is now known to be incorrect and potentially misleading.

- Compressive strength is linked primarily to EPS density, which is correct.
- Density of block-molded EPS is always the least at the corners, edges, and sides of a block, which is now known not to be always correct.

Therefore, the basic thrust of the Norwegian MQA plan is to sample and test only the presumed weakest portions of an EPS block.

The only notable deviation from Norwegian practice is reflected in the relatively recent German national design manual (*8,9*). Figure 9.3 shows the location of samples and test specimens recommended in the German design manual. The significant variation from Norwegian practice is the addition of sampling at the center of a block. Specimens prepared from center samples are tested for density and flexural strength only. It appears that the overall logic for the sampling and testing is based on the same assumptions as outlined above for the Norwegian MQA plan plus the following additional assumptions:

- Prepuff fusion is also an important product-quality parameter, which is correct.
- Fusion quality is most easily tested by inducing flexural stress in a specimen as tensile normal stresses are the best check for fusion and flexure induces such stresses in one side of a test specimen, which is correct.
- Fusion is always poorest at the center of an EPS block as it is the most difficult portion of the block for the steam introduced during block molding to reach, which is now known to be not always correct.

(a) Sampling.

(b) Compression test specimens.

Figure 9.2. EPS block sampling and compression test specimens per NRRL guidelines (all dimensions in millimetres) (*5*).

Figure 9.3. EPS block sampling and test specimens per German national design manual (*8,9*).

An assessment of the test protocols used to date indicates that current sampling and testing protocols are not keeping pace with the current state of knowledge. The specific reasons are:

- The stiffness parameters of elastic limit stress and initial tangent Young's modulus must be tested. Compressive strength provides no reliable correlation with these design parameters.
- With modern block molding equipment, the lowest density may not always occur at or near the exterior of the block as appears to be presumed in the Norwegian (*5*) and German (*8,9*) sampling guidelines. Neither will the poorest fusion (and flexural strength) always occur near the center as appears to be presumed in the German (*8,9*) sampling guidelines.
- For the higher EPS densities (up to approximately 32 kg/m^3 (2 lbf/ft^3)) sometimes used in geofoam applications, the lowest density may not always occur at or near the exterior of the block. Neither will the poorest fusion (and flexural strength) always occur near the center.

Consequently, an entirely new sampling and testing protocol is recommended herein for use in practice. The recommended block sampling procedures are shown in Figure 9.4 and are based on the following assumptions:

- The gradients (variation) in both density and fusion within an EPS block tend to be predominantly within planes oriented perpendicular to the longitudinal axis of a block. Therefore, sampling and testing should focus on material variations in this plane. However, the qualitative distribution of these gradients (as done historically and reflected in the Norwegian and German design manuals) cannot be reliably assumed in advance. Therefore, test specimens must be prepared and

all necessary parameters (listed below) tested at each of the three locations (A. B and C) shown in Figure 9.4 to allow for any gradients in both density and fusion.

- At each of the three locations (A, B and C) shown in Figure 9.4, the following parameters should be measured: (1) density, (2) elastic limit stress in compression, (3) initial tangent Young's modulus in compression, (4) compressive strength, and (5) flexural strength. The elastic limit stress in compression and the initial tangent Young's modulus in compression can be obtained during compressive strength testing. Thus, at each sampling location, it is recommended that one compressive strength test and one flexural strength test be performed.

  Note that second through fourth items are all measured in a single test. The actual number of specimens that can be cut at each sample location (A, B, and C) will depend on the thickness of the EPS block.
- All test parameters at all locations must equal or exceed the minimum allowable values given previously in Table 9.2.

Testing

The testing protocols specified in ASTM Standard C 578 should be used with the additional requirements that the elastic-limit stress in compression and initial tangent Young's modulus in compression be measured, reported, and meet the minimum criteria given in Table 9.2. An axial strain rate of 10 percent per minute shall be used for the compressive strength tests. Both the elastic limit stress and initial tangent Young's modulus shall be determined in the same test used to measure compressive strength.

Figure 9.4. Recommended block sampling and test specimens.

BASIS OF THE PROPOSED MANUFACTURING QUALITY CONTROL (MQC) AND MANUFACTURING QUALITY ASSURANCE (MQA) PROCEDURE

Overview

Manufacturing quality control (MQC) is internal actions taken by the manufacturer of a product (EPS block molder in this case). MQC can have two distinct components:

- As a minimum, MQC consists of a series of policies and procedures that a manufacturer must establish beforehand so that the final material or product will meet or exceed some definable, measurable criteria. These criteria must, of course, be defined in advance by the organization who is ultimately responsible for accepting the material (which, for EPS-block geofoam, is generally the civil engineer acting on behalf of the project owner). For the sake of efficiency, it is generally desirable to use some established standards (AASHTO, ASTM, etc.) as the criteria.
- MQC may also include the manufacturer's performing one or more tests on specimens prepared from samples taken from the final product. The purpose of these tests is to verify that the expected results have, in fact, been achieved. Generally these tests are the same as those used for MQA.

Manufacturing quality assurance (MQA) must, by definition, be performed by an organization other than the manufacturer. This can take several contractual forms:

- The MQA agent may be an independent organization retained by the manufacturer, usually on an ongoing as opposed to a project-specific basis. There are a number of business organizations such as Factory Mutual, RADCO, and Underwriters Laboratory (this alphabetical listing is intended to be illustrative and not necessarily complete) and others whose sole or primary business is providing what is generally called *third-party certification* of a myriad of manufactured products. It is important to note that, although these organizations are paid by the manufacturer for whom they are providing oversight, the presumption is that these organizations must protect their business reputation and, therefore, can be expected to remain objective.

- The MQA agent may be a company (typically a materials testing laboratory or geotechnical consulting firm in the case of EPS-block geofoam) hired by the purchaser of the product (generally a construction contractor in the case of EPS-block geofoam). The owner's engineer (who may or may not be the original designer) will generally review the MQA results in this case.
- The MQA agent may be the owner's engineer (who may or may not be the original designer).

The preferred contractual relationship of the MQA agent is a subject often debated in many areas of civil engineering not just geofoam. In any event, the function of the MQA agent is to review certain records maintained by the manufacturer and perform various tests on specimens prepared from samples taken from the manufactured product. Again, whether this is the product manufactured for the specific project in question or simply product judged to be representative is subject to debate.

In summary, there are several aspects regarding manufacturing quality, MQA in particular, that are subject to debate. However, with regard to EPS-block geofoam it should be kept in mind that it is a product that is always manufactured in a controlled environment in a fixed plant dedicated to that purpose. Therefore, the MQC and MQA requirements specified should be consistent with those for similar manufactured products which include most other geosynthetics.

Philosophy Incorporated in the MQC/MQA Procedure

To begin the process of developing a meaningful MQC/MQA procedure, the properties of EPS-block geofoam that are critical to its use as lightweight fill in road applications were identified. These properties include: (1) The EPS should be flame-retardant; (2) Each block must be appropriately seasoned with respect to outgassing of the blowing agent (which will typically be pentane in the U.S.); (3) All blocks must meet the criteria for geometric tolerances with regard to both dimensional variation, orthogonality, and face warp; (4) The average density of each

block delivered for a given project must equal or exceed the specified minimum allowable given in Table 9.1; (5) The density of any test specimen prepared from a sample cut from a production block for a given project must equal or exceed the specified minimum allowable given in Table 9.2 (which will generally be approximately 10 percent less than the overall allowable minimum for an entire block); (6) The small-strain stiffness parameters used for design (elastic limit stress and initial tangent Young's modulus) must equal or exceed the specified minimum allowable given in Table 9.2; (7) The traditional quality control parameters of compressive and flexural strength must equal or exceed the specified minimum allowable given in Table 9.2.

It appears that the optimal way to achieve these goals is to utilize a combination of quality control mechanisms implemented in two phases, one prior to shipment from the block molding plant and the other after delivery of blocks to the project site. In addition, there should be a two-tier system of MQA, one for molders with third-party certification and the other for those without third-party certification. Although third-party certification is not perfect, it clearly offers some level of quality assurance. Therefore, it is reasonable to treat EPS molders who subscribe to a recognized third-party certification agent and program differently than those who do not. Table 9.3 presents an overview of the two-phased system.

Table 9.3. Proposed Manufacturing Quality Assurance (MQA) Procedure for EPS-Block Geofoam Used for the Function of Lightweight Fill in Road Embankments.

The primary components of the provisional specification are the product manufacturing quality control (MQC) requirements, product manufacturing quality assurance (MQA) requirements, product shipment, and construction quality requirements to include construction quality control (CQC) and construction quality assurance (CQA) requirements. An overview of the manufacturing components is presented below with the construction quality requirements being presented in Chapter 8.

PRODUCT MANUFACTURING QUALITY CONTROL (MQC) REQUIREMENTS

Overview

There are numerous factors that affect the final quality of block-molded EPS, beginning with the source and age of the expandable polystyrene raw material used and ending with numerous aspects of the molding process. Because EPS has been manufactured for approximately 50 years, these various factors appear to be sufficiently documented and known in the industry. Therefore, as long as the desired quality of the final product is known (this would be specified by the project design engineer) a molder is able to select the required combination of manufacturing variables to produce the desired final product. Therefore, a molder's primary MQC plan is really a large set of manufacturing variables based on technical guidelines and experience known in the industry.

In general, EPS block molders in the U.S.A. perform relatively little in-plant laboratory type testing of small specimens cut from samples taken from production blocks. About the only physical testing performed on the finished blocks on a routine basis is to weigh the entire block relatively soon after it is molded (some newer molds do this automatically). This allows a determination of the overall average density or unit weight of the block as the dimensions of the block are consistent and known beforehand. However, this immediate post-molding weight and density determination must be viewed with some caution because there will be condensed water vapor trapped within the block from the steam used in the molding process. There will also be some residual blowing agent gas (which is always denser than air) within the block. Taken together, it is not uncommon for the immediate post-molding density to be 10 percent to 20 percent greater than the true dry density of the EPS but decrease with seasoning time. However, the density of blocks made with vacuum cooling molds may increase with seasoning time. Therefore, three days of seasoning at normal ambient room temperatures may be required for the block density to stabilize (i.e. dry and outgas the residual blowing agent) and even that is

dependent on there being adequate air circulation between stored blocks and adequate positive exhaust ventilation within the area used to store blocks during post-molding seasoning.

There is one issue that straddles the boundary between manufacturing and construction quality. It is primarily the responsibility of the molder (hence discussed in this section as an MQC issue) but is enforced by the construction inspection agent (so is also included under the discussion of CQA in Chapter 8). This is the issue of damage to EPS blocks during shipping. Typically, the selection of trucks used to ship EPS blocks (almost always a tractor-pulled trailer, but the trailer may either be flat bed or a closed box), the loading of these trucks and the manner in which the load is secured (important when flat-bed trailers are utilized) are all under the control of the EPS molder. Thus, responsibility for the as-delivered condition of the EPS blocks is largely controlled by the molder. This is an important issue to address and incorporate into manufacturing specifications as recent, anecdotal evidence indicates that block damage on EPS-block geofoam projects within the U.S.A. is not uncommon and is the source of on-site problems with block acceptance. The reason for the damage appears to be the preferred use of flat-bed trucks as EPS blocks used for lightweight fill have gotten longer with newer molding equipment placed on line during the 1990s. Because the very light EPS blocks must be securely and tightly strapped to prevent their movement during shipping, it is not uncommon for EPS blocks to arrive at the job site with numerous indentations of the edges along the sides of the blocks from the strapping as well with breakage at the end corners of the blocks. One shipping method that may be considered to minimize damage to the blocks is to use structural angles along the top edge of the exterior blocks that would accommodate the strapping.

MQC is the primary responsibility of the molder. The MQC parameters are the same parameters that will be measured as part of manufacturing quality assurance (MQA) to be conducted by the owner's agent. In addition to the parameters to be measured during MQC, allowable raw material, flame retardant requirements, seasoning requirements, and EPS block dimensional tolerances are also subsequently addressed.

MQC Parameters To Be Measured

Table 9.2 indicates the proposed material designations and the minimum allowable values of MQC/MQA parameters for individual test specimens.

Allowable Raw Material

The EPS-block geofoam shall consist entirely of expanded polystyrene. At the discretion of the molder, the EPS-block geofoam may consist of some mixture of virgin raw material (expandable polystyrene a.k.a. bead or resin) and recycled EPS (regrind). If regrind is to be used, this shall be identified by the molder as part of the Phase I MQA pre-certification process subsequently discussed. The source of the regrind (block-versus shape-molded EPS, in-plant versus post-consumer) should also be identified.

Flame-Retardant Requirements

Although the practice in some countries is to use normal or regular (non-flame-retardant) expandable polystyrene raw material for cost reasons, the recommended practice in the provisional specifications is to require the use of flame retardant EPS, which is currently the standard practice in the U.S. Thus, all EPS-block geofoam shall satisfy the product flammability requirements specified in ASTM C 578.

Seasoning Requirements

A flammability concern is the potential of ignition of residual blowing agent that outgasses after block placement and collects in the joints between blocks. Outgassing of post-molding residual blowing agent is addressed by requiring an adequate seasoning period prior to delivery of the EPS blocks to the project site. This issue has not been formally studied to date for blocks produced in the U.S.A. (seasoning time is affected by the exact formulation (pentane content) of the expandable polystyrene and block dimensions, among several other factors). Based on available published information (*7*) as well as anecdotal information obtained by personal communication with both resin suppliers and block molders in the U.S.A., an interim recommendation of three days (72 hours) at ambient room temperature (seasoning can be

accelerated by temporary storage within a heated room) is proposed prior to shipment and incorporated into the provisional standards. Seasoning is defined as storage in an area suitable for the intended purpose for a minimum of 72 hours after an EPS block is released from the mold. The molder may request a shortened seasoning period if the EPS blocks are seasoned within an appropriate heated storage space and the molder demonstrates to the satisfaction of the owner's agent that the alternative seasoning treatment produces block that equal or exceed the quality of the blocks subjected to the normal 72-hour seasoning period.

Dimensional Tolerances

Because of the various types of molding equipment currently in use in the U.S., different dimensional variations may occur between blocks produced by different molders. The dimensional tolerances of EPS blocks used for the function of lightweight fill affects construction through the ability of the blocks to fit together with minimal gaps and maintain a planar surface as subsequent layers of blocks are placed. The provisional standard incorporates physical and dimensional tolerances used in Norway which are based on decades of experience. Dimensional tolerances are defined by three geometric variables. (1) Variations in linear dimensions: The thickness, width and length dimensions of an EPS block are defined herein as the minimum, intermediate and maximum overall dimensions of the block, respectively, as measured along a block face. These dimensions of each block shall not deviate from the theoretical dimensions by more than ±0.5 percent. (2) Deviation from perpendicularity of block faces: The corner or edge formed by any two faces of an EPS block shall be perpendicular, i.e. form an angle of 90 degrees. The deviation of any face of the block from a theoretical perpendicular plane shall not exceed 3 mm (0.12 in.) over a distance of 500 mm (20 in.). (3) Overall warp of block faces: Any one face of a block shall not deviate from planarity by more than 5 mm (0.2 in.) when measured using a straightedge with a length of 3 m (9.8 ft).

PRODUCT MANUFACTURING QUALITY ASSURANCE (MQA) REQUIREMENTS

Overview

The traditional approach taken for MQA of EPS-block geofoam in lightweight fill applications is to rely solely on post-delivery block sampling and testing by the owner's testing laboratory or engineer. It is believed that one significant reason for this is the historical evolution of EPS-block geofoam in places where, at the time, pre-delivery MQA alternatives such as third-party certification were unavailable. Thus, MQA handled in the traditional manner also straddles the boundary between manufacturing and construction as the sampling and testing for manufactured quality is handled as a construction activity.

At the present time, MQA for geofoam (pre-delivery, post-delivery or some combination of the two) is still evolving in U.S. practice. This is due to several reasons, each of which has positive and negative aspects:

- Many EPS block molders in the U.S.A. now subscribe to third-party certification by an inspection organization dedicated to providing that service. However, as it exists normally, such certification does not appear to include specific testing of products destined for a specific project. Rather, certification is based on an assessment of management of the overall manufacturing operation, presumably with occasional, random spot checks by physical testing. Thus, civil engineers have been reluctant in some cases to accept third-party certification as the sole MQA because it is not project specific.
- Third-party certification is typically set up for compliance with existing standards, most notably ASTM Standard C 578. However, as discussed previously, geofoam-grade block-molded EPS has requirements for material stiffness that are not in ASTM Standard C 578 or any other known standard at the present time. Therefore, third-party certification as it typically exists currently

for block-molded EPS may not be sufficiently stringent for lightweight fill applications.

- There is recent project experience in the U.S.A. to indicate that third-party certification is not foolproof. Specifically, independent post-delivery testing by at least two state DOTs suggests that EPS-block geofoam of overall quality not meeting specifications has been delivered to projects. While such anecdotal information may not constitute conclusive scientific proof, informal sharing and transmission of such information among civil engineers has added to the wariness of relying solely on third-party certification as it exists now.
- EPS-block geofoam is still a novel construction material to most civil engineers in the U.S.A. Therefore, there is a reluctance to accept this material without at least some post-delivery testing, especially in view of the fact that this is the historical method for performing MQA for EPS-block geofoam.
- EPS-block geofoam is still a novel construction material to most state DOTs in the U.S.A. In addition, such government agencies, as custodians of the public trust and safety, are historically more cautious than the private sector when it comes to accepting and using new technology. Therefore, there is a reluctance to accept this material without at least some post-delivery testing, especially in view of the fact that this is the historical method for performing MQA for EPS-block geofoam.
- Post-delivery testing can be time consuming and delay geofoam placement on site. This is an important issue because the EPS blocks are usually placed directly from the delivery truck. Thus, it would be time consuming and costly to exhume a group of blocks placed days or even weeks earlier if the test results were unacceptable. However, this would have to be done if necessary.

Resolution of the above issues and problems with both pre- and post-delivery MQA practice as they currently exist to develop an MQA strategy that balances both the technical need to verify product quality and the associated cost will require an evolutionary process that includes input from and dialog between both EPS molders, their customers (usually a construction contractor), the design engineer, and the ultimate owner. A goal of this report is to assist in initiating such a dialog by clarifying the relevant issues to be addressed by MQA and incorporating these into the design guidelines and specification that are part of this report. It is expected that the design documents included with this report will see further evolutionary modification in the future.

The purpose of MQA of the EPS-block geofoam product is to verify the molder's MQC procedures. The owner's agent will have primary responsibility for all MQA unless the owner notifies the contractor otherwise. The proposed MQA program consists of two phases. Phase I MQA consists of pre-certification of the molder and shall be conducted prior to shipment of any EPS blocks to the project site. Phase II MQA shall be conducted as the EPS blocks are delivered to the project site. Phase I and all four subphases of Phase II MQA are performed regardless of whether or not the EPS molder has third-party certification. However, there is a difference in terms of the extent to which MQA is conducted. It should be noted that procedures to be followed once the blocks arrive at the construction site are also considered part of CQA. Thus, the owner’s CQA agent will also be performing MQA.

A truckload of EPS blocks is intended to mean either a full length box- or flat-bed trailer of typical dimensions, i.e., approximately 12 metres (40 ft) or more in length, fully loaded with EPS blocks. The volume of EPS in such a truckload would typically be on the order of 50 to 100 m^3 (65 to 130 yd^3). Each MQA phase is discussed below and as is shown in Table 9.3 a two-tier MQA system, one for molders with third-party certification and one for those without, is recommended. The following sections provide more detail on the entries in Table 9.3.

Phase I

Phase I consists of pre-certification of the molder and is performed prior to shipment of EPS blocks to the project site. The purpose of the pre-certification procedure is to verify that the molder has the ability to provide EPS-block geofoam of the desired quality. The proposed Phase I MQA steps that are required prior to shipment to the project site are as follows.

For All Molders

- If the designer has made the block layout the responsibility of the molder, the required shop drawings showing the proposed block layout must be prepared and submitted to the designated representative of the owner for approval prior to shipping any blocks. The required minimum time for shop drawing submittal and acceptance must be specified in the project design documents and be in accordance with owner requirements.
- If the designer has assumed responsibility for the block layout, shop drawings are not required unless changes to the block layout shown in the contract documents are desired by the block molder and/or construction contractor. This should be handled as any other change order request initiated by a contractor.
- Each block delivered to the project site should be labeled with the following minimum information:
  - if multiple plants and/or molders are supplying a given project, the name of the molder and plant location;
  - date block was molded;
  - block dimensions;
  - actual block mass/weight (in kilograms or pounds) and density/unit weight (in kilograms per cubic metre or pounds per cubic foot), as determined by weighing after the required period of seasoning; and

- when multiple densities are to be used on the same project, an easily visible color marking system should be used to distinguish between blocks of different density (no marking can be used as one of the requisite "markings" but it must always be for the lower/lowest density).

It is suggested that molders develop and print a simple self-adhesive label that contains blank spaces in which this information can efficiently be entered at the molding plant.

Molders With Third-Party Certification

- A molder with third-party certification should, prior to shipping any blocks for a project, be required to:
  - identify the organization providing this service,
  - provide detailed information as to the procedures and tests used by this organization, and
  - provide written certification that all EPS blocks supplied to the project will meet the requirements specified in the project specifications.

Molders Without Third-Party Certification

- A molder without third-party certification should, prior to shipping any blocks for a project, be required to submit a letter stating that all EPS blocks supplied for the project are warranteed to meet specifications requirements. They should also be requested to describe what MQC measures they employ, e.g. in-plant testing, etc. In addition, at the owner's discretion the molder should be required to submit a pre-production block to demonstrate that they have the ability to provide product of the desired quality.

Phase II

The procedures to be followed once the blocks arrive at the construction site are considered part of CQA and thus are considered in Chapter 8. However, construction is also when Phase II of MQA is executed by the owner's CQA agent. Phase II MQA has four subphases:

- The first subphase (Phase IIa) consists of verification of the physical condition of the EPS blocks and index properties (age and density) of the EPS. The CQA agent should inventory and inspect each and every block as it arrives on site to check for physical damage during shipment and to verify age and density requirements based on the required factory applied labeling. Any block with significant physical damage or density not meeting the minimum specified in Table 9.1 should be rejected.
- The second subphase (Phase IIb) consists of confirming key physical and index properties of the overall block and EPS respectively. Suggested guidelines for how many blocks to check are given subsequently. At the CQA agent's discretion, additional blocks should be checked, especially at the beginning of a project and/or if the EPS molder does not have third-party certification. Additionally, at the CQA agent’s discretion, representative blocks from each manufacturing day can be checked. The dimensions and warp of blocks should be checked on site by the CQA agent and compared to specified requirements. The weight indicated on the label should be checked using a commercial scale, recently certified with regard to its calibration, provided by the construction contractor for this purpose. It should be possible to make these measurements in a relatively short period of time so as not to delay on-site handling and use of the blocks.
- The third subphase (Phase IIc) consists of confirming the EPS engineering design parameters related to stiffness as well as the quality control strength parameters. Specifically, the CQA agent should sample and test the EPS for compliance with

specified requirements with respect to the elastic limit stress, initial tangent Young's modulus, compressive strength, and flexural strength. Figure 9.4 provides a basic plan for sampling location. At the present time the only reliable testing is conventional laboratory testing in accordance with ASTM Standard C 578 which, at best, will take a few days to accomplish. However, ASTM Standard C 578 should be augmented to include measurement of the elastic-limit stress and initial tangent Young's modulus in compression using an axial strain rate of 10 percent per minute. The elastic limit stress in compression and the initial tangent Young's modulus in compression can be obtained during compressive strength testing. Thus, at each sampling location, it is recommended that one compressive strength test and one flexural strength test be performed. As shown in Figure 9.4, three sampling locations are recommended. Therefore, for each block to be tested, a minimum of three compressive strength tests and three flexural strength tests are recommended. A high priority for the future should be research and development of some type of device for testing the stiffness of EPS blocks at the project site (this is discussed further in Chapter 13 of this report).

- The fourth and final subphase (Phase IId) consists of recording where blocks are placed to the greatest extent possible by marking copies of the drawings that show the block layout (either shop drawings or design drawings as appropriate). The purpose of this is to assist in locating blocks that may need to be exhumed at a later date if some question as to manufacturing quality should arise.

All four subphases of Phase II MQA are conducted regardless of whether or not the EPS molder has third-party certification. However, there is a difference in terms of the extent to which Phase II MQA is conducted.

Molders With Third-Party Certification

For molders with previously approved third-party certification, the following process is recommended for the subphases of Phase II MQA:

- Phase IIa should be applied to each truckload.
- Phase IIb should be applied to each truckload. Initially, only one block per load should be selected and checked by the CQA agent. If the selected block meets specification with respect to its size and shape, and the mass agrees with that marked on the block, no further checking of the load for these parameters is required and the shipment is approved conditionally until the Phase IIc test results verify that the blocks meet specifications. If the block does not meet specification, with respect to its size, shape, and mass, then other blocks in the truckload should be checked and none used until the additional checking has determined what blocks are unsatisfactory. The number of additional blocks to be tested is to be determined by the CQA agent. At the completion of this subphase, the construction contractor should be conditionally allowed to proceed with installing blocks. However, this should be done with the understanding that EPS blocks may have to be exhumed and removed at a later date if Phase IIc testing indicates problems.
- Phase IIc sampling and testing should be done on an ongoing basis during the course of the project. However, the owner and the owner's CQA agent can exercise considerable judgement here. For example, they may choose to do testing only at the beginning of a project to verify that the EPS molder's MQC and third-party certification is achieving the desired goals or even omit testing entirely on a small project.
- Phase IId as-built record keeping should always be performed.

Molders Without Third-Party Certification

For EPS molders without third-party certification, the on-site (Phase II) MQA is more critical than for those molders with third-party certification:

- Phase IIa should be applied to each truckload.
- Phase IIb should be applied to each truckload. For the first load delivered to a project, each block on that load should be checked by the CQA agent. For subsequent loads, at least one block per load should be selected and checked.
- Phase IIc sampling and testing should be applied to all projects, regardless of size, and throughout the entire duration of the project. It is suggested that no blocks be placed until the first truckload for the project has been sampled and tested. For each density of EPS used on a project, at least one block will be selected for sampling from the first truckload of EPS blocks of that density delivered to the job site. Additional blocks may be selected for sampling during the course of the project at the discretion of the owner's agent at a rate of sampling not to exceed one sample for every 250 m^3 (325 yd^3) of EPS delivered. Portions of sampled blocks that are otherwise acceptable can be used as desired by the contractor. For subsequent truckloads, the construction contractor should be allowed to place blocks while sampling and testing is going on with the understanding that it may be necessary to exhume and remove blocks not meeting specifications. The owner's agent will make every reasonable effort to conduct the laboratory testing expeditiously. If unsatisfactory test results are obtained, the contractor may be directed to remove potentially defective EPS blocks and replace them with blocks of acceptable quality at no additional expense to the owner.
- Phase IId as-built record keeping should always be done.

PRODUCT SHIPMENT

Prior to delivery of any EPS-block geofoam to the project site, a meeting shall be held between, as a minimum, the owner's agent and contractor. The supplier and/or molder of the EPS-block geofoam may also attend at the contractor's discretion to facilitate answering any questions. The purpose of this meeting shall be to review the Phase I MQA results and discuss Phase II MQA as well as other aspects of construction to ensure that all parties are familiar with the requirements of the specification. After this meeting, the contractor can begin on-site receipt, storage (if desired), and placement of the EPS-block geofoam.

The molder should label each block delivered to the project site with the following minimum information: if multiple plants and/or molders are supplying a given project, the name of the molder and plant location; the date that the block was molded; the mass/weight of the entire block (in kilograms or pounds) as measured after a satisfactory period of seasoning; the actual dry density/unit weight (in kilograms per cubic metre or pounds per cubic foot); the dimensions of the blocks (in millimetres or inches); and when multiple densities are to be used on the same project, an adequate marking system should be used to identify blocks of different density. If the EPS blocks are to be stockpiled at the project site until placement, a secure storage area shall be designated for this purpose. Additional block handling and storage requirements are provided as part of CQC/CQA in Chapter 8.

SUMMARY

The provisional standard, which is included in Appendix C, is a combined material, product, and construction standard covering block-molded expanded polystyrene (EPS) for use as lightweight fill in road embankments and related bridge approach fills on soft ground. The provisional standard is intended to be used in conjunction with the design guideline included in Appendix B.

The primary components of the provisional standard include the product manufacturing quality control (MQC) requirements, product manufacturing quality assurance (MQA)

requirements, product shipment, and construction quality requirements to include construction quality control (CQC) and construction quality assurance (CQA) requirements. The key features of the provisional standard include the proposed EPS material designation system shown in Table 9.1 and the minimum allowable values of MQC/MQA parameters for individual specimens and not the entire block shown in Table 9.2. The parameters are to be measured using ASTM Standard C 578 and an axial strain rate of 10 percent. A new sampling protocol is shown in Figure 9.4 and a new two-phased MQA procedure is presented in Table 9.3. Phase I of the MQA procedure is to be performed prior to shipment of EPS blocks to the project site and Phase II is to be performed as the EPS blocks are delivered to the project site. Another key aspect of the proposed MQA procedure is the implementation of a two-tier MQA system, one for molders with third-party certification and the other for those without.

Standards always require review and possible modification when developing project-specific specifications. For example, the recommended minimum seasoning requirement of 72 hours may create problems on projects that are relatively large in size and/or have tight delivery schedules. Therefore, project-specific decisions might be necessary to relax this seasoning requirement. Experience indicates that this may be permissible to expedite construction work provided that appropriate safety precautions for fire safety and worker safety are implemented. The requirements for physical and dimensional tolerances are known to have been relaxed on a project-specific basis in the U.S. for cost reasons. There has been no systematic study of how much deviation from normally accepted practice is acceptable. Thus owners who, either directly or through their representatives, accept blocks with tolerances that exceed those normally used must accept a greater, but incalculable, uncertainty with regard to overall final performance of the fill.

The standard presented in this chapter and included in Appendix C should facilitate the use of EPS-block geofoam in civil engineering projects by providing engineers with a combined material, product, and construction standard for use in developing a project-specific specification.

However, there are issues and problems, both real and perceived, with both pre- and post-delivery MQA practice as they currently exist. Resolution of these issues and problems will require an evolutionary process that includes input from and dialog between both EPS molders, their customers (usually a construction contractor), the design engineer, and the ultimate owner. A goal of this report is to assist in initiating such a dialog by presenting relevant issues to be addressed by MQA and incorporating these into the provisional design guideline and standard that are part of the report. It is expected that the provisional standard will see further evolutionary modification in the future.

REFERENCES

1. ASTM D 578-95, "Standard Specification for Rigid, Cellular Polystyrene Thermal Insulation." Vol. 04.06, American Society for Testing and Materials, West Conshohocken, PA (1999) .
2. Bartlett, P. A., "Expanded Polystyrene Scrap Recovery & Recycling." ARCO Chemical Company (undated) .
3. Bartlett, P. A., "Letter report to unnamed customer 11 September." ARCO Chemical Company, Newtown Square, PA (1986) .
4. Horvath, J. S., Personal Communication.
5. Horvath, J. S., *Geofoam Geosynthetic*, , Horvath Engineering, P.C., Scarsdale, NY (1995) 229 pp.
6. ASTM C 303-98, "Standard Test Method for Dimensions and Density of Preformed Block and Board-Type Thermal Insulation." Vol. 04.06, American Society for Testing and Materials, West Conshohocken, PA (2001) .
7. Coughanour, R. B., "Pentane Issue." *Presentation at the 16th Annual SPI Expanded Polystyrene Division Conference,* San Diego, CA, (1988) .
8. "Merkblatt für die Verwendung von EPS-Hartschaumstoffen beim Bau von Straßendämmen." Forschungsgesellschaft für Straßen- und Verkehrswesen, Arbeitsgruppe Erd- und Grundbau, Köln, Deutschland (1995) 27 pp.
9. "Code of Practice; Using Expanded Polystyrene for the Construction of Road Embankments." BASF AG, Ludwigshafen, Germany (1995) 14 pp.

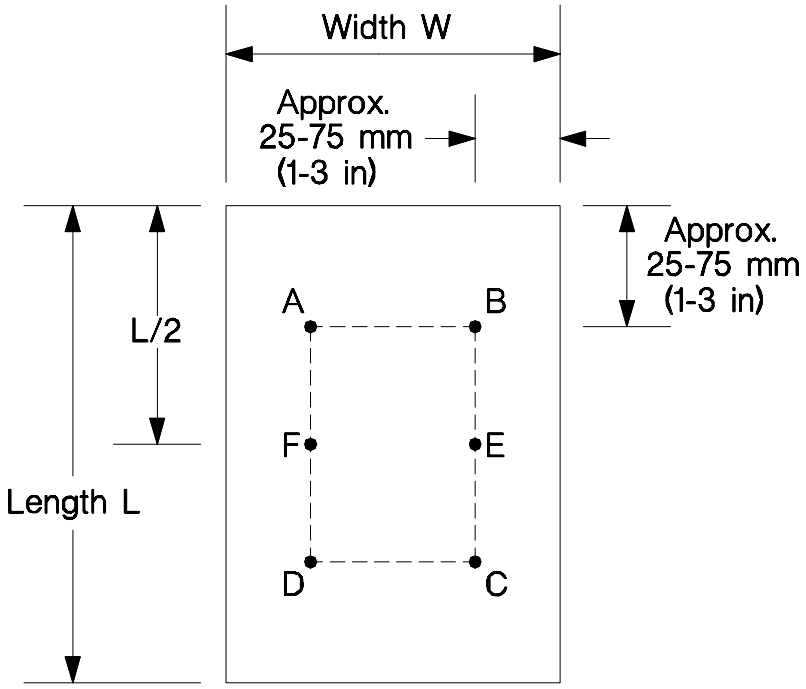

FIGURE 9.1 PROJ 24-11.doc

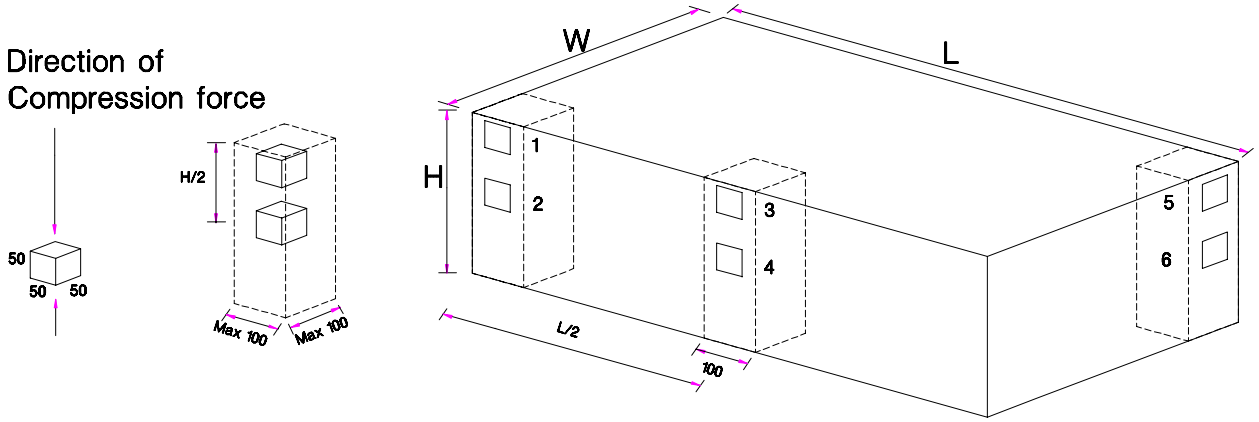

FIGURE 9.2A PROJ 24-11.doc

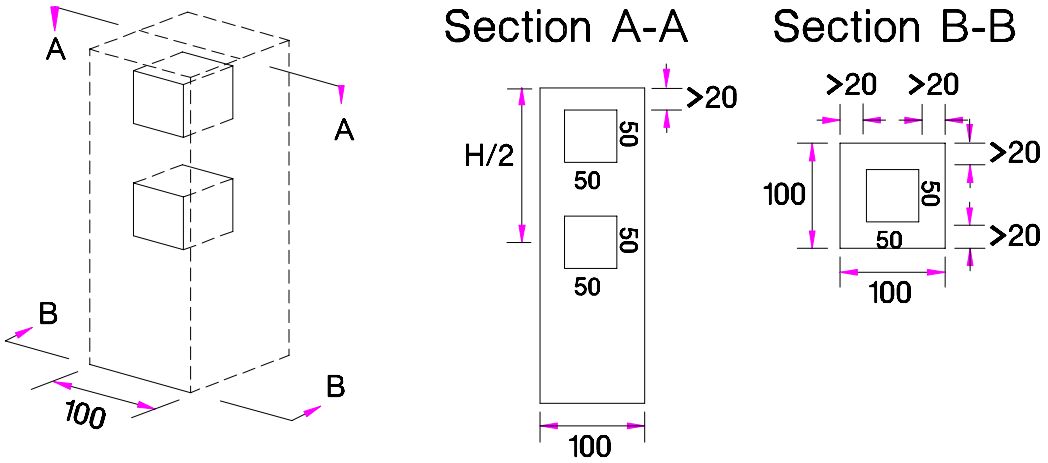

FIGURE 9.2B PROJ 24-11.doc

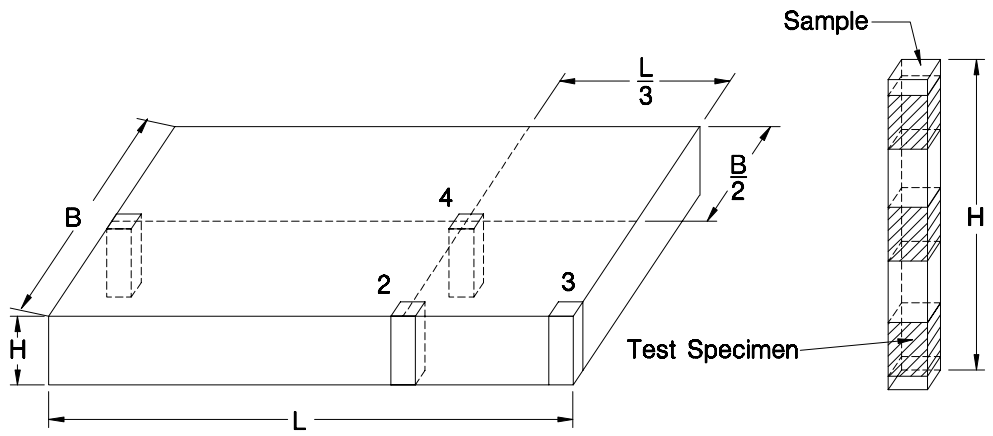

FIGURE 9.3 PROJ 24-11.doc

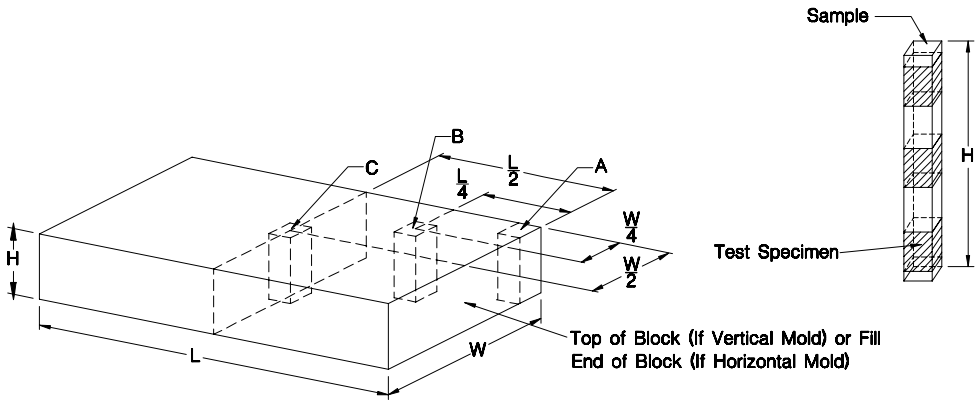

FIGURE 9.4 PROJ 24-11.doc

Material Designation		Minimum Allowable Density, kg/m^3 (lbf/ft^3)	
AASHTO (proposed)	**ASTM C 578**	**Each Block as a Whole**	**Any Test MQC/MQA Specimen**
EPS40	I	16 (1.0)	15 (0.90)
EPS50	VIII	20 (1.25)	18 (1.15)
EPS70	II	24 (1.5)	22 (1.35)
EPS100	IX	32 (2.0)	29 (1.80)

Material Designation	Dry Density, kg/m^3 (lbf/ft^3)	Compressive Strength, kPa (lbs/in^2)	Flexural Strength, kPa (lbs/in^2)	Elastic Limit Stress, kPa (lbs/in^2)	Initial Tangent Young's Modulus, MPa (lbs/in^2)
EPS40	15 (0.90)	69 (10)	173 (25)	40 (5.8)	4 (580)
EPS50	18 (1.15)	90 (13)	208 (30)	50 (7.2)	5 (725)
EPS70	22 (1.35)	104 (15)	276 (40)	70 (10.1)	7 (1015)
EPS100	29 (1.80)	173 (25)	345 (50)	100 (14.5)	10 (1450)

Phase	Sub-phase	Start of Phase	Description	Requirements	Possible Actions
I	None	Prior to shipment to the project site	Pre-certification of the molder	**Approved third-party certification:** Molder will • Identify the organization providing this service. • Provide detailed information as to the procedure and tests used by this organization to verify the molder's compliance with the specific requirements of this specification. • Provide written certification that all EPS blocks supplied to the project will meet the requirements specified in the project specifications. **No approved third-party certification:** • Contractor shall deliver a minimum of three full-size EPS blocks for each AASHTO EPS-block geofoam type to be used on the project to a location specified by the owner's agent. • Owner's agent will weigh, measure, sample and test a random number of blocks. Sampling and testing protocol will be the same as for Phase IIc MQA. • Molder should submit a letter stating that all EPS blocks supplied for the project are warranted to meet specification requirements and what MQC measures they employ.	• Acceptance of the molder's third-party certification by the owner's agent will waive the need for pre-construction product submittal and testing. • No EPS blocks shall be shipped to the project until such time as all parts of Phase I MQA have been completed.

II	IIa	As the EPS blocks are delivered to the project site	On-site visual inspection of each block delivered to the project site to check for damage as well as visually verify the labeled information on each block	**Approved third-party certification:** • Each truckload. Owner's agent should inventory each and every block. **No approved third-party certification:** • Each truckload. Owner's agent should inventory each and every block.	• Any blocks with significant physical damage or not meeting specifications will be rejected on the spot and placed in an area separate from those blocks that are accepted or marked "unacceptable" and returned to the supplier.

II	IIb	As the EPS blocks are delivered to the project site	On-site verification that the minimum block dry density as well as the physical tolerances meet specifications	**Approved third-party certification:** • Each truckload. Initially, only one block per load. **No approved third-party certification:** • Each truckload. Each block for the first load then at least one block per load for subsequent truckloads.	• If the selected block meets specifications with respect to its size and shape, and the mass agrees with that marked on the block, no further checking of the load for these parameters is required and the shipment is approved conditionally until the Phase IIc test results verify that the blocks meet specifications. • If the selected block does not meet specification, then other blocks in the truckload should be checked and none used until the additional checking has determined what blocks are unsatisfactory. • At the completion of this subphase, the construction contractor should be conditionally (until the Phase IIc test results verify that the blocks meet specifications) allowed to proceed with installing blocks.

II	IIc	As the EPS blocks are delivered to the project site	Confirming the EPS engineering design parameters related to stiffness as well as the quality control strength parameters	**Approved third-party certification:** • Discretion of owner's CQA agent. For example, can be omitted entirely on a small project, can perform testing only at the beginning of a project, or can be done on an ongoing basis. **No approved third-party certification:** • Performed on all projects throughout the entire duration of the project • For each AASHTO EPS-block geofoam type at least one block will be selected for sampling from the first truckload. • Additional blocks may be selected at a rate of sampling not exceeding one sample for every 250 cubic metres (325 cubic yards) • Sampling to be performed per the locations indicated in Figure 9.4. • Lab. tests should be performed to check for compliance with the parameters shown in Table 9.2 to include the elastic-limit stress, initial tangent Young's modulus, compressive strength, and flexural strength.	• Portions of sampled blocks that are not damaged or otherwise compromised by the sampling can be used as desired by the contractor. • If unsatisfactory test results are obtained, the contractor may be directed to remove potentially defective EPS blocks and replace them with blocks of acceptable quality at no additional expense to the owner.

II	IId	As the EPS blocks are placed	As-built drawing(s)	• Owner's agent with the cooperation of the contractor will prepare as-built drawing(s) as well as perform additional record keeping to document the location of all EPS blocks placed for the project.	

Note: A truckload of EPS blocks is intended to mean either a full length box- or flat-bed trailer of typical dimensions, i.e., approximately 12 m (40 ft) or more in length, fully loaded with EPS blocks. The volume of EPS in such a truckload would typically be on the order of 50 to 100 m^3 (65 to 130 yd^3).

CHAPTER **10**

TYPICAL DESIGN DETAILS FOR EPS-BLOCK EMBANKMENTS

Contents

INTRODUCTION

The main objective of this report is to facilitate the use of EPS-block geofoam in roadway applications. To accomplish this objective a provisional design guideline for roadway embankments is presented in Appendix B of this report. However, to complete this objective a material and construction standard as well as construction drawings need to be presented so the design engineer can distribute the EPS-block geofoam design for bidding and construction. An appropriate material and construction standard for geofoam embankments is included in Appendix C. As a result, the remaining aspect to facilitate the use of geofoam in roadway embankments is to provide designers with typical construction drawings and details to aid preparation of bid and construction documents. This chapter presents typical construction details for traditional, i.e., trapezoidal (see Figure 3.4(a)) geofoam roadway embankments and vertical EPS embankments or walls (see Figure 3.4(b)). The construction details presented in this chapter

were obtained from actual geofoam construction drawings from projects throughout the United States and can be used as a guide for developing site-specific drawings or details. The details presented relate to a variety of geofoam issues, such as, configuration of the EPS blocks, inclusion of utilities and roadway hardware, construction of a load distribution slab over the EPS, and anchoring of the EPS blocks to resist hydrostatic uplift. In some cases the figures that have been reproduced use either all Système International d'Unités (SI) or all inch-pound (I-P) units. Those figures have not been revised to show both sets of units. However, Appendix F presents factors that can be used to convert between SI and I-P units.

An important aspect of constructing a geofoam embankment is preparation of the foundation soil prior to block placement. No detail illustrating this important point was located so it is described before presenting the details. Before placement of the EPS blocks, the foundation soil should be prepared to facilitate placement and alignment of the blocks. This is sometimes difficult with soft foundation soil because the soil can displace as construction personnel traverse the site. Therefore, the alignment of the blocks should be identified prior to placement and a working platform consisting of soil or a geosynthetic may be required. This preparation is also required for earthen embankments and should not increase the cost of the geofoam embankment.

DESIGN DETAILS FOR TRAPEZOIDAL EPS EMBANKMENTS

Figure 10.1 presents a typical design cross-section for a roadway embankment consisting of only EPS-block geofoam construction over peat. This cross-section was obtained from the reconstruction of Indiana State Route 109 in Noble County (*1*), which is described in detail in Chapter 11. It can be seen that the blocks are overlain by an aggregate subbase and a flexible pavement system. Figure 10.2 presents a design cross-section for a roadway embankment that utilized both EPS-block geofoam and on-site earth material. This cross-section was obtained from the construction of an emergency escape ramp for Highway H-3 on the Island of Oahu in Hawaii (*2*). This case history is also described in more detail in Chapter 11. This cross-section

illustrates that use of EPS-block geofoam above on-site basalt tunnel mine spoil that is geosynthetically reinforced to increase stability. This cross-section shows that geofoam can be used with on-site material to produce a cost-effective design for roadway embankments.

Figure 10.1. Trapezoidal geofoam embankment detail (*1*).

Figure 10.2. Trapezoidal embankment using geofoam and on-site material (*2*).

DESIGN DETAILS FOR VERTICAL EPS WALLS

Figure 10.3 presents a typical design detail for a vertical roadway embankment consisting of only EPS-block geofoam. This detail was obtained from the Interstate-15 Corridor Reconstruction in Salt Lake City, Utah and was prepared by the Utah Department of Transportation (*3*). The detail shows a number of important aspects for construction of vertical EPS walls including the excavation of the existing ground to form a base for the geofoam wall and prevent frost heave, installation of a drainage blanket under the geofoam blocks, and placement of the geofoam blocks against a precast wall panel. This detail also illustrates the use of a geomembrane to protect the geofoam from hydrocarbon spills and a concrete pavement system above the granular subbase. Other important details in Figure 10.3 include a storm drain and flowable backfill to seal around the storm drain pipe, the inclusion of a traffic barrier (see Figure 10.4) and a concrete load distribution slab over the geofoam (see Figure 10.4). Figure 10.4 presents a detail for the anchoring of the traffic barrier to the precast wall panels and construction of a concrete load distribution slab over the EPS. It can be seen that the load distribution slab consists of No. 19 steel reinforcing bars at a spacing of 254 mm (10 in.). Figure 10.5 presents typical details for fabrication of the precast concrete wall panels for the vertical EPS wall with options for reinforced concrete and prestressed concrete panels. Figure 10.5 also presents a typical detail for the joints of the wall panels.

Figure 10.3. Construction detail for a vertical EPS wall (*3*).

Figure 10.4. Detail for traffic barrier and load distribution slab(*4*).

Figure 10.5. Detail for precast concrete wall panels for a vertical EPS wall (*5*).

DESIGN DETAILS FOR BRIDGE ABUTMENTS

This section of Chapter 10 presents construction details for the use of geofoam in bridge abutments. This is an important application of geofoam and involves drawings for both the embankment/abutment interface and the pavement system overlying the geofoam. Figure 10.6 presents a typical design detail for a pile supported bridge abutment from the Interstate-15 Corridor Reconstruction in Salt Lake City, Utah (*6*). It can be seen that the geofoam is trimmed and placed around the cylindrical piles after pile driving so a small void is left between the pile and geofoam. This also illustrates the inclusion of a geomembrane and concrete load distribution slab over the geofoam. Figure 10.7 presents a typical design detail for a geofoam supported bridge abutment from the bridge rehabilitation project over the Shoshone River near Yellowstone Park in Wyoming. This detail was prepared by the Wyoming Department of Transportation (*7*) and is discussed in more detail in Chapter 11. Detail A in Figure 10.7 illustrates the joint system between the approach slab and bridge abutment. Figure 10.8 illustrates the design of the bridge approach pavement system for the Shoshone River project. Cross-section C-C illustrates the pavement system at the bridge/abutment interface, which consists of a concrete pavement at the bridge/abutment interface. Cross-section B-B illustrates the pavement system at a distance of approximately 610 mm (24 in.) behind the abutment, which includes an asphalt overlay on the concrete pavement. Figure 10.8 also includes a cross-section of the geofoam embankment parallel to the abutment whereas Figure 10.7 presents a cross-section of the embankment perpendicular to the abutment.

Figure 10. 6. Detail for geofoam embankment with a pile-supported bridge abutment (*6*).

Figure 10.7. Detail for geofoam backfill behind a bridge abutment (*7*).

Figure 10.8. Detail of bridge approach pavement system over geofoam (*8*).

UTILITY AND ROADWAY HARDWARE DETAILS

A major consideration in roadway embankments is the inclusion of utilities in a geofoam embankment and the installation of roadway hardware, such as guardrails, on top of a geofoam

embankment. These features are illustrated using a four-lane state roadway (143rd Street) in Orland Park, Illinois and the drawings were prepared by the Illinois Department of Transportation (*9-11*). Figure 10.9 presents a cross-section through the Orland Park geofoam embankment, which illustrates the location of a storm drain and a guardrail system on the right side of the roadway. The storm drain is located near the centerline of the roadway and consists of a discontinuity in the geofoam for placement of the pipe and trench backfill. Figure 10.10 presents a detail of the drainage pipe installation and it can be seen that the pipe is underlain by one EPS-block. This block was inserted into the native soil to counter balance or offset the weight of the trench backfill material placed around the drainage pipe to reduce differential settlement of the embankment. After placement of the pipe above the EPS block, the discontinuity in the geofoam was backfilled with a granular material. Figure 10.11 presents a detail for the installation of the guardrail system on top of the Orland Park geofoam embankment. It can be seen that the guardrail post is inserted into a concrete foundation that was constructed above the geofoam to provide the necessary impact resistance. Figure 10.12 presents a photograph that depicts the placement of geofoam around a manhole in a different Orland Park geofoam project (131st Street). The EPS blocks where cut in the field to fit around the manhole pipe and some of the trimmings of EPS are visible near the manhole. Finally, Figure 10.13 illustrates the use of geofoam to support a sidewalk that was undergoing large settlement due to subsidence of a peat layer underlying the soil embankment and displacement of the peat into the lake on the right hand side of the photograph. The sidewalk is adjacent to Washington State Route 516 and the case history is referred to as the Lake Meridian settlement repair in Chapter 11.

Figure 10.9. Cross-section through geofoam embankment containing a storm drain and guardrail (*9*).

Figure 10.10. Detail of storm drain pipe in geofoam embankment (*10*).

Figure 10.11. Detail for guardrail on top of geofoam embankment (*11*).

Figure 10.12. Photograph of geofoam placement around a manhole.

Figure 10.13. Photograph of geofoam used to support a sidewalk on top of an earthen embankment (Washington State Dept. of Transportation).

DESIGN DETAILS FOR PROTECTIVE LOAD DISTRIBUTION SLAB

The uncertainties that are usually associated with inclusion of a load distribution slab warrant a separate section for this topic even though it is mentioned above. Figure 10.4 presents a detail for the construction of a concrete load distribution slab over and EPS embankment for the Interstate 15 project near Salt Lake City (*4*). It can be seen that the load distribution slab consists of No. 19 steel reinforcing bars at a spacing of 254 mm (10 in.) and the slab is placed directly over the EPS blocks.

A load distribution slab is only required if Step 14 (load bearing analysis) and Step 15 (pavement system design) of the EPS-block geofoam design procedure shown in Figure 3.3 indicates that a slab is required to distribute vehicle stresses to suitable levels or to reduce the thickness and cost of the pavement. As indicated in Chapter 4, a load distribution slab represents a significant cost on a project and can range from 20 to 30 percent of the total project cost. Additional concerns with a load distribution slab include the potential for sliding of the slab during an earthquake, potential for ponding of water within the pavement system, and the increased potential for differential icing and solar heating. However, a load distribution slab will typically be required to support heavy traffic loads or high-volume traffic such as encountered on interstate highways. A slab is also typically required when a vertical embankment is used to support the upper part of the exterior facing system and to provide anchorage for various highway hardware such as safety barriers, signage, and lighting. Alternate separation layers that can be considered include a geogrid, geocell with soil or PCC fill, and soil cement.

ANCHORING DETAILS FOR HYDROSTATIC UPLIFT

Figure 10.14 presents a cross-section for a pile-supported pavement in Japan that utilized an anchoring system to prevent hydrostatic uplift of the EPS-block geofoam (*12*). An anchoring system was required because the overburden applied to the EPS was insufficient to prevent uplift

of the blocks if they were subjected to the design water level acting on a side of the embankment. Also shown in Figure 10.14 is a detail of the anchor extending through the load distribution slab overlying the geofoam.

Figure 10.14. Anchoring system used to prevent hydrostatic uplift (flotation) of EPS-block geofoam (*12*).

INSTALLATION OF EPS-BLOCK GEOFOAM

Figure 10.15 presents an overview of installation of EPS-block geofoam for the 131st Street project in Orland Park, Illinois. The project involves a residential street and the geofoam was used to construct a roadway embankment over a soft clay deposit. Figure 10.16 presents a close-up photograph of the geofoam placement. This photograph illustrates the use of metal connectors between the EPS blocks and the close contact of the individual blocks after placement.

Figure 10.15. Photograph of geofoam placement for a residential street.

Figure 10.16. Photograph of metal connectors between geofoam blocks.

REFERENCES

1. Zaheer, M. A., "Experimental Feature Study The Use of Expanded Polystyrene (EPS) in Pavement Rehabilitation S.R. 109 in Noble County, Indiana." Indiana Department of Transportation Materials and Tests Division, Indianapolis (1999) 17 pp.
2. Mimura, C. S., and Kimura, S. A., "A Lightweight Solution." *Geosynthetics '95 Conference (1995: Nashville, Tenn.) Conference Proceedings,* Nashville, Tenn., Vol. I (1995) pp. 39-51.
3. "Typical Section Geofoam (EPS) Wall." *I-15 Corridor Reconstruction, Elev.-Geofoam Wall (8 m - 11 m), Corridor Standard Plan,* Utah Dept. of Transportation (1998) pp. CS-77.
4. "Load Distribution Slab Restraint Section." *I-15 Corridor Reconstruction, Elev.-Geofoam Wall (8 m - 11 m), Corridor Standard Plan,* Utah Dept. of Transportation (1998) pp. CS-80.
5. "Precast Wall Panel." *I-15 Corridor Reconstruction, Elev.-Geofoam Wall (8 m - 11 m), Corridor Standard Plan,* Utah Dept. of Transportation (1998) pp. CS-44.
6. "Typical Geofoam Section at Bridge Abutments." *I-15 Corridor Reconstruction, Elev.-Geofoam Wall (8 m - 11 m), Corridor Standard Plan,* Utah Dept. of Transportation (1998) pp. CS-50.
7. "Section A-A (Abut No. 1)." *Approach Slab No. 1 Details, Bridge Rehabilitation Bridge Over N.F. Shoshone River US 14,16,20 (P-31), KP 51.50 (MP 32.01),* Wyoming Dept. of Transportation (1997) pp. Sheet 9.
8. "Section B-B, C-C, D-D." *Approach Slab No. 1 Details, Bridge Rehabilitation Bridge Over N.F. Shoshone River US 14,16,20 (P-31), KP 51.50 (MP 32.01),* Wyoming Dept. of Transportation (1997) pp. Sheet 10.

9. "Sta. 77+00 to 81+00." *143rd Street Expanded Polystyrene Foam Typical Sections and Details,* Illinois Dept. of Transportation (1998) pp. Sheet 25B.
10. "EPS Layout Beneath Storm Sewer." *143rd Street Expanded Polystyrene Foam Typical Sections and Details,* Illinois Dept. of Transportation (1998) pp. Sheet 25D.
11. "SPB Guardrail Type A. Special." *143rd Street Expanded Polystyrene Foam Typical Sections and Details,* Illinois Dept. of Transportation (1998) pp. Sheet 25D.
12. Ninomiya, K., and Ikeda, M., "Design & construction of EPS method which surfacing and uses anchor for prevention." *International Symposium on EPS Construction Method (EPS Tokyo '96),* Tokyo, (1996) pp. 162-167.

EXPANDED POLYSTYRENE FILL

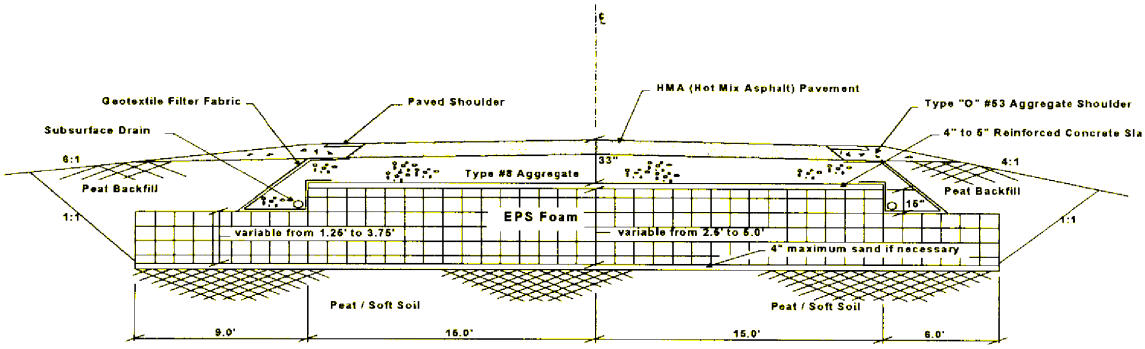

FIGURE 10.1 PROJ 24-11.doc

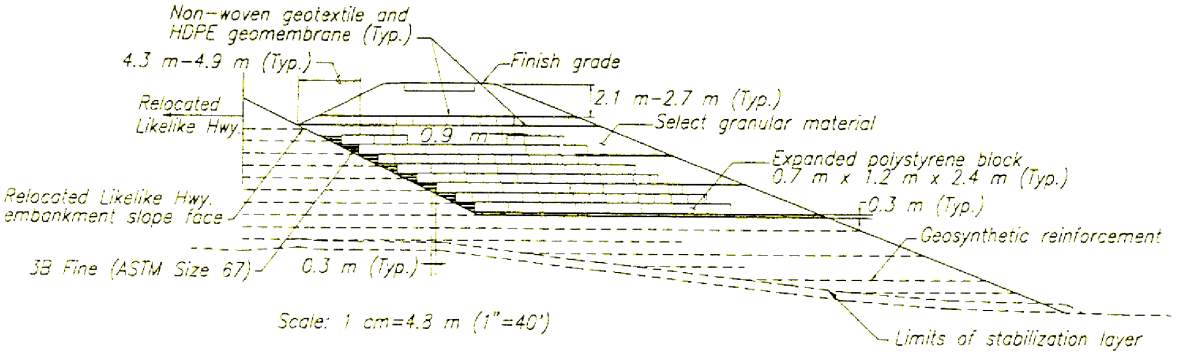

FIGURE 10.2 PROJ 24-11.doc

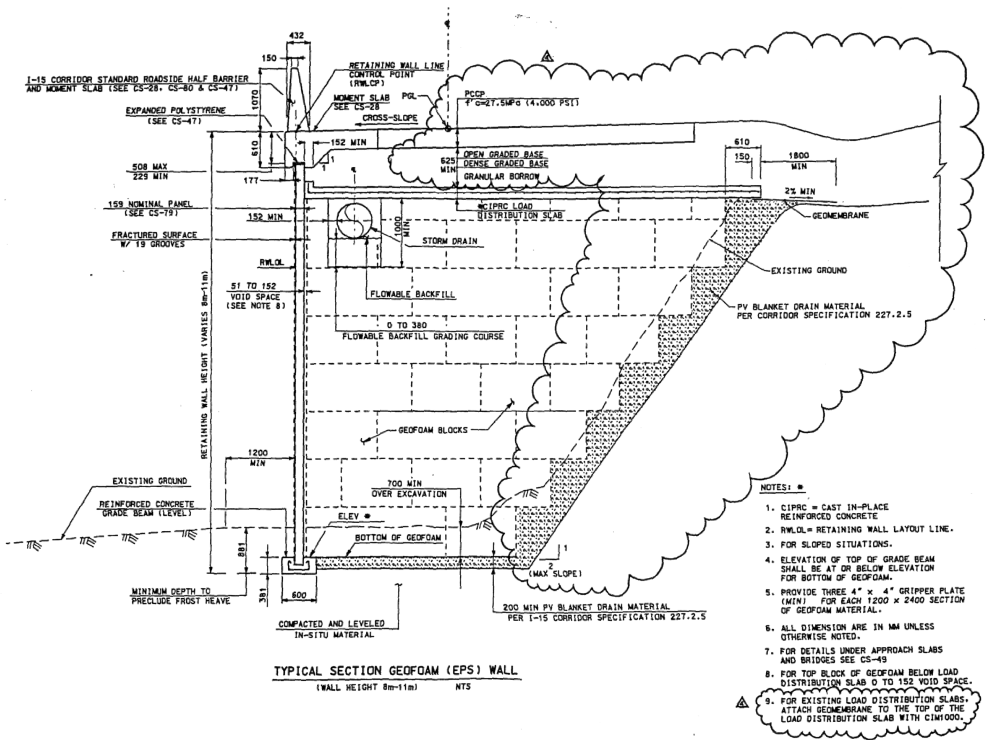

TYPICAL SECTION GEOFOAM (EPS) WALL

(WALL HEIGHT 8m-11m) NTS

FIGURE 10.3 PROJ 24-11.doc

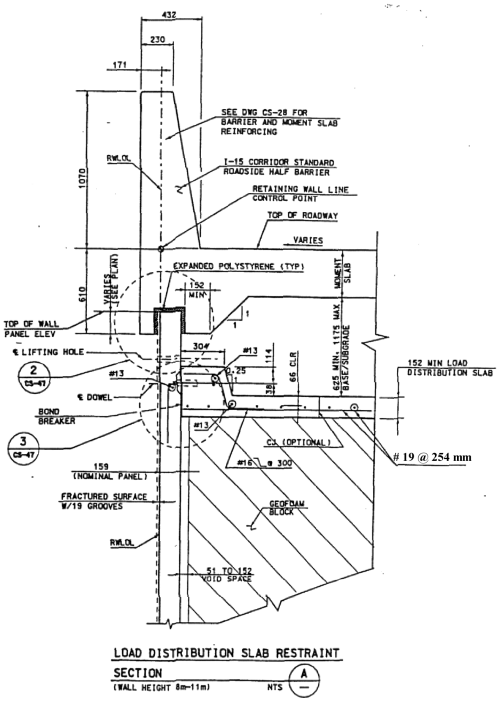

LOAD DISTRIBUTION SLAB RESTRAINT SECTION (A)

(WALL HEIGHT 8m-11m) NTS

NOTES:

1. LOAD DISTRIBUTION SLAB DESIGNED FOR HS-20 LOADING.
2. WHEEL LOADS ARE NOT PERMITTED WITHIN 1500 OF FREE EDGE OF LOAD DISTRIBUTION SLAB PRIOR TO PLACING PCCP SLAB.
3. LIFTING HOLES TO BE DRY PACKED.
4. ALL DIMENSION ARE IN MM UNLESS OTHERWISE NOTED.
5. SEE CS-28 FOR MOMENT SLAB REINFORCING.
6. FOR DETAILS UNDER APPROACH SLABS AND BRIDGES SEE CS-49.
7. TRANSVERSE CONSTRUCTION JOINTS ARE ALLOWED IN THE LOAD DISTRIBUTION SLAB AT THE OPTION OF THE CONTRACTOR.
8. ALL CRACKS OVER 0.5 MM SHALL BE SEALED WITH A HIGH MOLECULAR WEIGHT METHYL METHACRYLATE SEALANT (TRANSPO T-70 OR EQUAL).
9. CONCRETE SHALL BE CLASS AA(AE) EXCEPT AS MODIFIED FOR f'c=27.5 MPa (4,000 PSI). NO CONSTRUCTION LOADS SHALL BE PERMITTED ON THE LOAD DISTRIBUTION SLAB UNTIL AFTER 7 DAYS OF CURING.

FIGURE 10.4 PROJ 24-11.doc

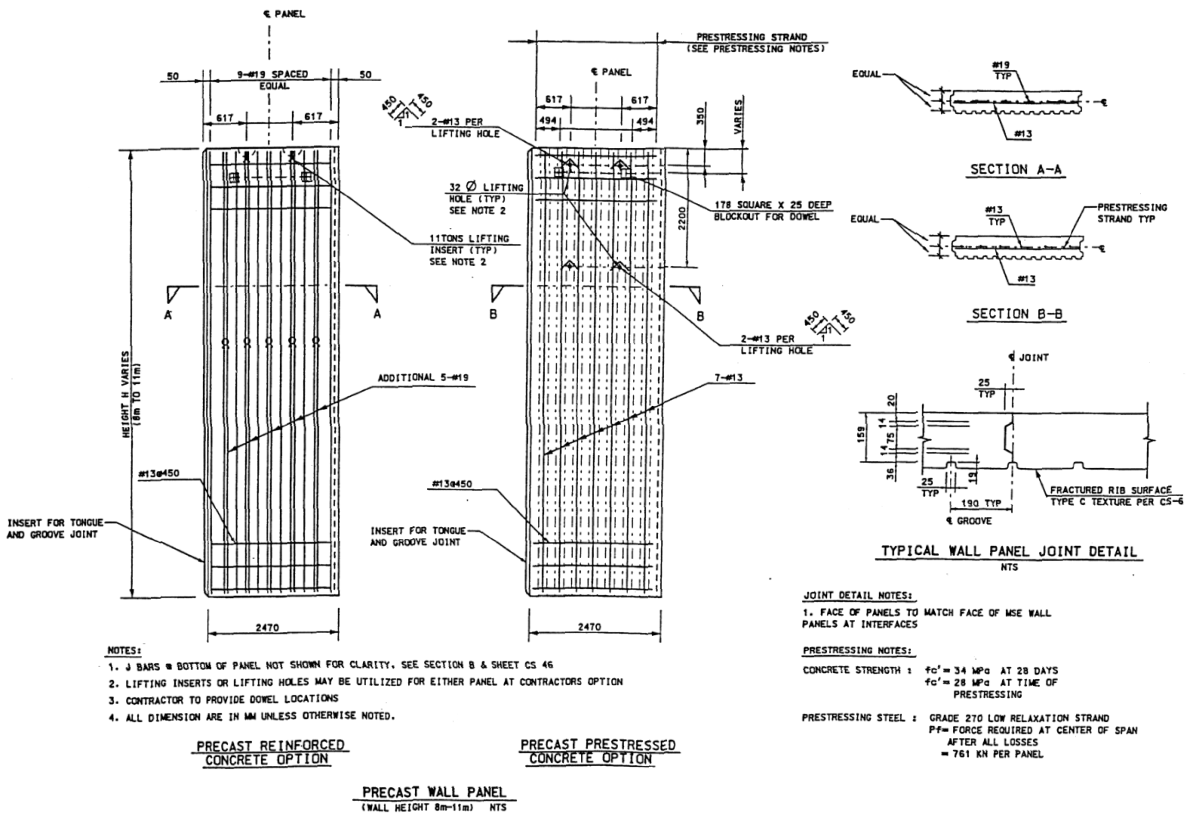

FIGURE 10.5 PROJ 24-11.doc

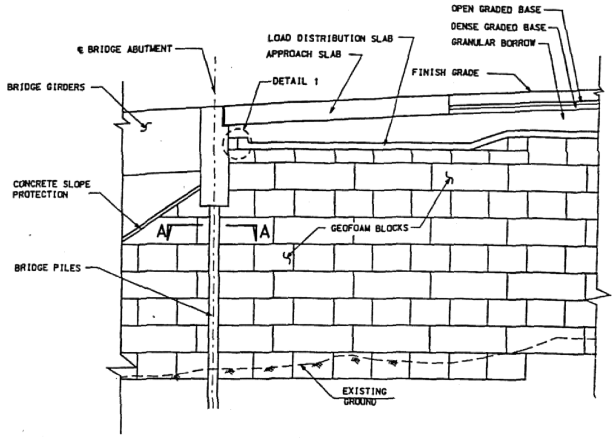

TYPICAL GEOFOAM SECTION AT BRIDGE ABUTMENTS
NOT TO SCALE

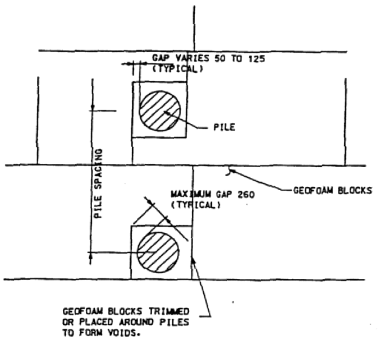

SECTION A-A
NOT TO SCALE

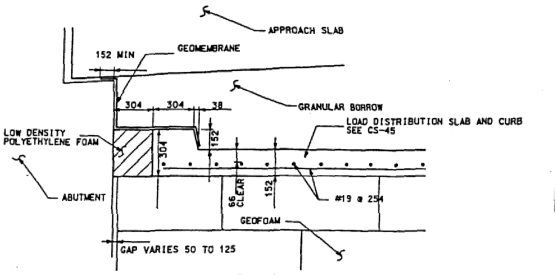

DETAIL 1
NOT TO SCALE

NOTES:
1) ALL DIMENSIONS IN MILLIMETERS UNLESS OTHERWISE INDICATED.
2) FOR LOAD DISTRIBUTION SLAB DRAINAGE, SEE PLANS AND CS-53.

FIGURE 10.6 PROJ 24-11.doc

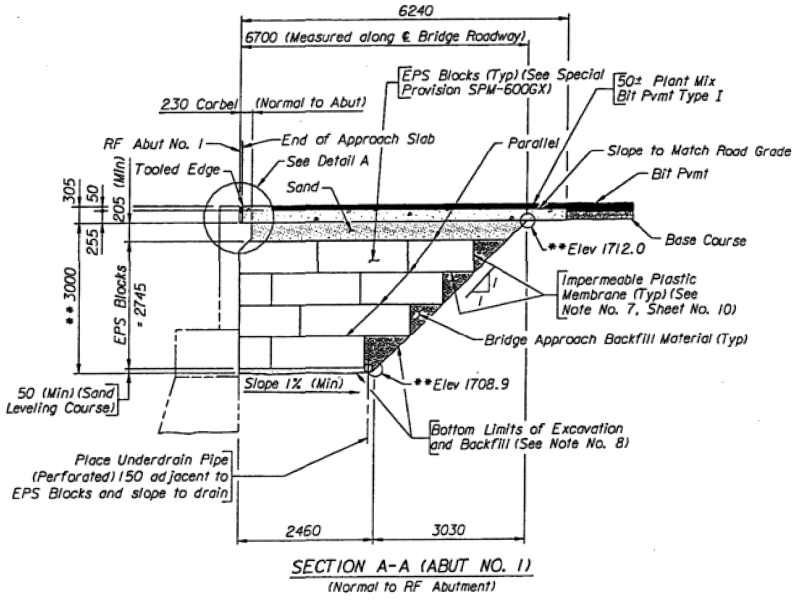

SECTION A-A (ABUT NO. 1)
(Normal to RF Abutment)

Note: 1) All reinforcing steel shall be coated.
2) For Sections B-B and C-C, see Sheet No. 10.
3) For Bill of Reinforcement see Sheet No. 10.
4) Place 13ASI bars parallel with ℄ Bridge Roadway.
5) The perforated underdrain pipe shall be wrapped with a layer of Geotextile Drainage and Filtration.
6) Dimensions and elevations preceded by a double asterisk (**) are measured at centerline bridge roadway.
7) For Settlement Plate Details, see Sheet No. 10.
8) The entire bottom of the excavation, including that portion under the perforated underdrain pipe and the exposed soil sides of the excavation, shall be lined with a layer of separation fabric prior to placement of sand leveling course.

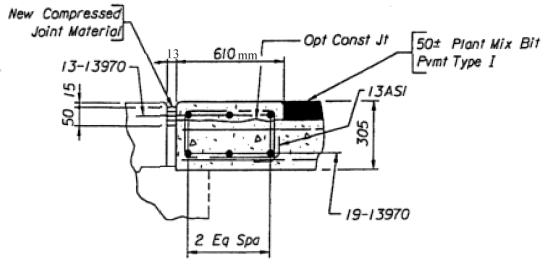

DETAIL A

FIGURE 10.7 PROJ 24-11.doc

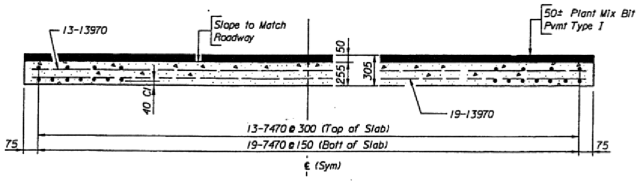

SECTION B-B

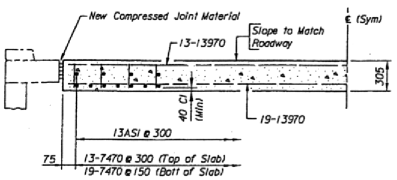

HALF SECTION C-C

BILL OF REINFORCEMENT		
Location	Mark	Number Req'd
Abutment No. 1	13ASI	39
	13-7470	39
	13-13970	22
	19-7470	77
	19-13970	22

BENDING DIAGRAM

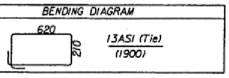

Note:
1) Underdrain Pipe (Perforated) 150 mm shall be capped at high end.
2) For location of Sections B-B and C-C, see Sheet No. 9.
3) The reinforcing steel fabricator shall prefix all approach slab bar marks with numeral 2 at Abutment No. 1.
4) The perforated underdrain pipe shall be wrapped with a layer of Geotextile Drainage and Filtration.
5) All reinforcing steel shall be coated.
6) For location of Settlement Plates, see Sheet No. 9.
7) All sides and the top of the EPS backfill shall be covered with a layer of Impermeable Plastic Membrane prior to backfilling next to and over the blocks.
8) Steel rods shall be field cut so that the top of the rod is 40 mm below the top of the asphalt.
9) Std Pipes shall be field cut so that the bottom of the pipe is 100 mm± above the Steel Settlement Plate.

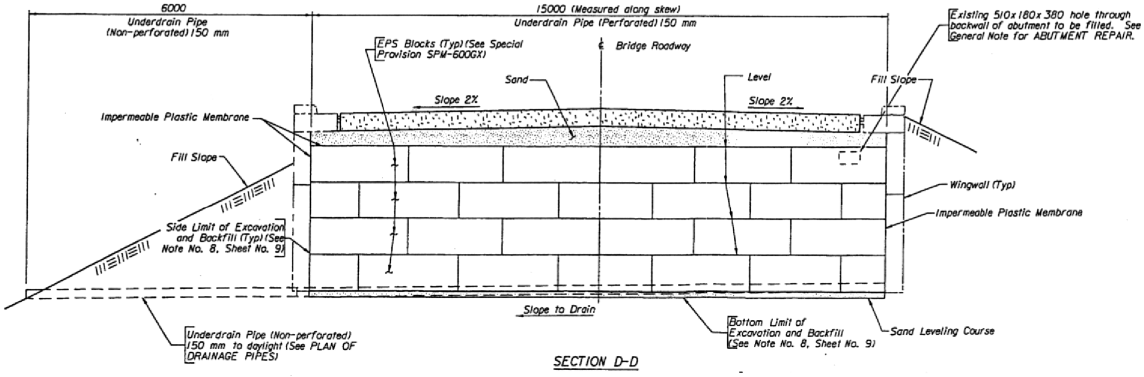

SECTION D-D

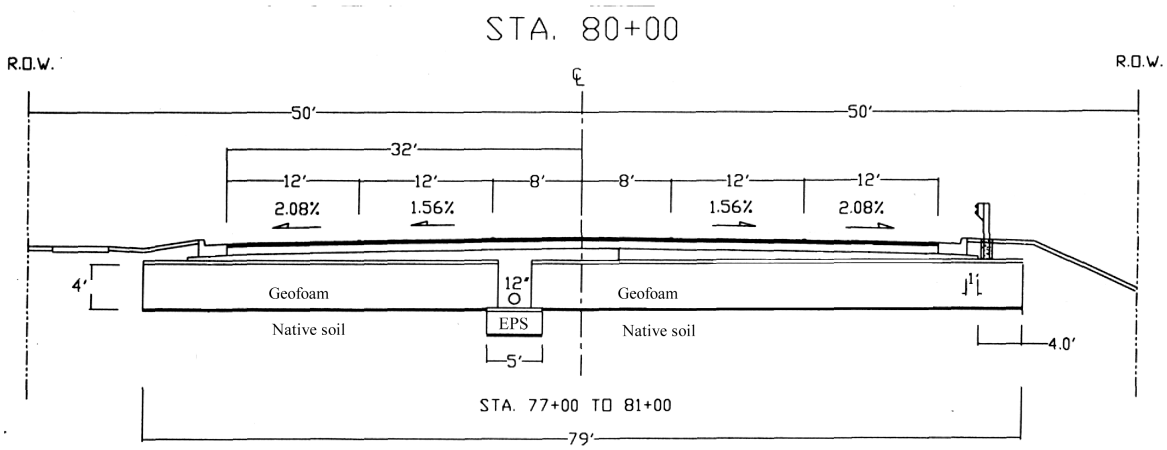

FIGURE 10.9 PROJ 24-11.doc

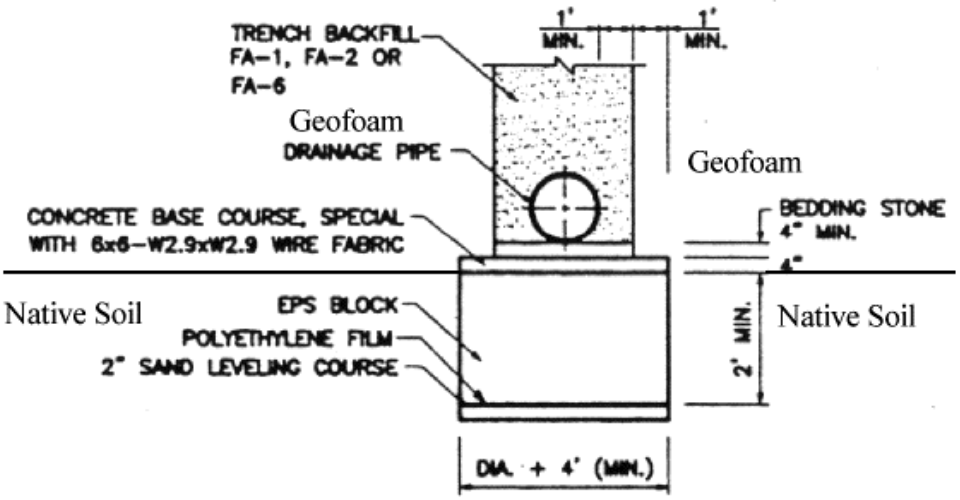

TYPICAL SECTION

EPS LAYOUT BENEATH STORM SEWER
(WITHIN EPS FILL SYSTEM)

FIGURE 10.10 PROJ 24-11.doc

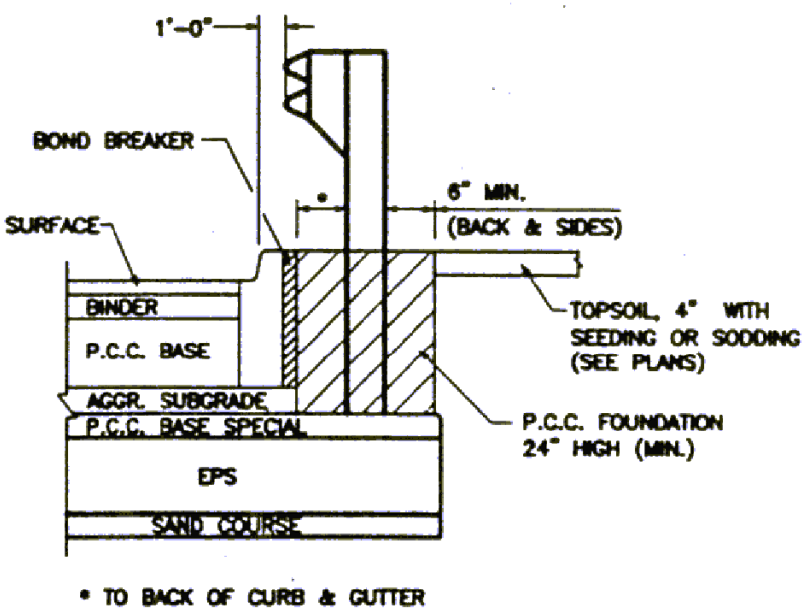

SPB GUARDRAIL, TYPE A, SPECIAL
(● EPS LOCATION W/GUARDRAIL)

FIGURE 10.11 PROJ 24-11.doc


4 1'99

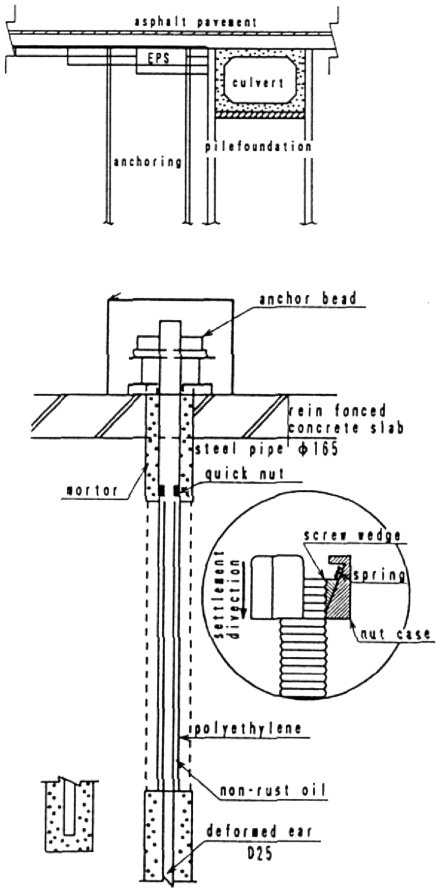

FIGURE 10.14 PROJ 24-11.doc

FIGURE 10.16 PROJ 24-11.doc

CHAPTER **11**

CASE HISTORIES

Contents

INTRODUCTION

The following case histories are presented to provide examples of cost-effective and successful EPS-block geofoam projects completed in the United States (U.S.). Although the focus of this report is limited to stand-alone embankments that have a transverse (cross-sectional) geometry such that the two sides are more or less of equal height (see Figure 3.4), several case histories involving hillside (side-hill) fills (see Figure 3.5) are also presented because these case histories provide useful cost or construction data that are applicable to traditional embankment geometries. In addition, in practice there is usually little or no separation made in the discussion of lightweight fills that utilize EPS-block geofoam. Chapter 12 presents an analysis of the cost data presented in these case histories and a comparison with other soft soil construction techniques. The summary at the end of this chapter summarizes the benefits of geofoam and the placement rates observed in these case histories. These placement rates are important because they can be compared with soil fill placement rates to estimate the decrease in construction time with the use of geofoam and facilitate bidding by contractors that are not familiar with geofoam placement. Finally, the case histories presented in this chapter are intentionally limited to the United States to reflect U.S. construction pricing and practices. Of course, there are many international geofoam case histories that are referred to throughout the report. In some cases the figures that have been reproduced use either all Système International d'Unités (SI) or all inch-pound (I-P) units. These figures have not been revised to show both sets of units. However, Appendix F presents factors that can be used to convert between SI and I-P units.

HAWAII: HIGHWAY H-3 (LIKELIKE HIGHWAY) EMERGENCY ESCAPE RAMP FOR THE KANEOHE INTERCHANGE, ISLAND OF OAHU

This case history involves the construction of a 12 to 21 m (39 to 69 ft) high vehicle emergency escape ramp for the Likelike Highway on the island of Oahu, Hawaii. Project information for this case history was obtained from (*1*). The purpose of the vehicle emergency escape ramp is to provide an escape route in the event that vehicles experience brake failure as

they descend from the tunnel exit at an elevation of about 213.4 m (700 ft) to an elevation of 39.6 m (130 ft) at the intersection with the Kahekili Highway. The downslope grade of the Likelike Highway is six percent.

The lower elevation portions of the ramp are underlain by approximately 6.1 m (20 ft) of very soft organic silt with natural water contents ranging from 80 to 120 percent. Undrained shear strengths ranged from 9.6 to 19.2 kPa (200 to 400 lbs/ft^2). The upper elevation portions of the site consist of soft to medium stiff clayey silt with natural water contents ranging from 60 to 80 percent and standard penetration values ranging from 2 to 8 blows per 0.30 metre (2 to 8 blows per foot). Undrained shear strengths obtained from unconsolidated undrained triaxial compression tests ranged from 38.3 to 105.3 kPa (800 to 2,200 lbs/ft^2). The water level was at the ground surface.

The original embankment was to be constructed of geotextile reinforced tunnel spoil material or select granular material. However, due to the presence of very soft organic silt in the lower portion of the ramp, this embankment design would have required time for consolidation to occur and to prevent a slope failure. Alternatives for construction of the ramp included relocation, concrete supported structure on deep foundations, in-situ stabilization of the existing soils, and lightweight fill. Lightweight fill was selected because the contractor could continue to construct the embankment thereby preventing delays to the project. The types of lightweight fills that the project team considered included volcanic cinder (unit weight of 11.8 kN/m^3 or 75 lbf/ft^3), lightweight concrete geofoam (unit weight of 3.9 to 4.7 kN/m^3 or 25 to 30 lbf/ft^3), and EPS-block geofoam (unit weight of 0.2 to 0.3 kN/m^3 or 1.25 to 2 lbf/ft^3). Although all three lightweight fill materials had similar costs, the volcanic cinder option was not used because it was heavier than EPS and lightweight concrete. The project team selected EPS based on discussions with suppliers of both products, availability of materials, and available construction methods.

EPS-block geofoam with a minimum specified density of 20 kg/m^3 (1.25 lbf/ft^3) was utilized for only a portion of the embankment. The bottom of the embankment below the geofoam

consisted of 0.6 to 1.5 m (2 to 5 ft) of clean gravel which served as a stabilizing layer for construction activities and as a drainage blanket for surface water and water discharged by the vertical strip drains installed to accelerate consolidation of the foundation soils. An approximate 4.6 m (15 ft) layer of geotextile reinforced basalt tunnel spoil was placed above the stabilization layer between June and November 1993. A 0.3 m (1 ft) thick gravel drainage blanket layer was placed above the reinforced basalt rock and underlying the first layer of geofoam blocks. Figure 11.1 presents a design cross-section of the roadway embankment.

Approximately 13,470 m^3 (17,618 yd^3) of EPS (6,450 blocks, each 700 by 1,200 by 2,400 mm or 28 by 47 by 94 in.) were placed from early December 1993 to mid February 1994. If it is assumed that EPS block placement started on December 1, 1993 and was completed on February 14, 1994, the number of work days is 54 days if weekends are not included and 76 days if weekend days are included. Based on this assumption, the production rate for EPS block placement can be estimated to be between 175 and 250 m^3 (229 to 327 yd^3) per day or 85 to 120 blocks per day. The placement of EPS fill was not greatly affected by rainy weather. At Sta. 9+55 the geofoam thickness was approximately 6.7 m (22 ft).

A 410 g/m^2 (12 oz/yd^2) non-woven polypropylene geotextile overlying a 60 mil thick textured high density polyethylene geomembrane was placed after every three layers of geofoam blocks. The purpose of the geomembrane was to protect the EPS blocks from any potential damage from a petroleum spill and the purpose of the geotextile was to reduce EPS damage from construction operations including the placement of 2.1 to 2.7 m (6.9 to 8.9 ft) of select granular fill over the geofoam. Placement of the select granular fill was completed by March 1994. Construction of the entire embankment was completed within 14 months.

Sixteen settlement gauges were installed as part of the embankment monitoring system following placement of the initial stabilization layer. Settlement measurements obtained during construction ranged from 305 to 1,650 mm (12 to 65 in.) for embankment heights ranging from 4.6 to 12.2 m (15 to 40 ft), respectively. Most of this settlement occurred during the placement of

the granular stabilization layer, reinforced basalt rock, and gravel drainage blanket layer that were placed below the geofoam. These granular layers contributed to approximately 1.2 m (3.9 ft) of the 1.4 m (4.6 ft) of settlement that occurred at Sta. 9+55 during construction. The entire embankment height at Sta. 9+55 was 12.3 m (40 ft).

The use of geofoam in the revised embankment design was successful because the embankment was completed ahead of the anticipated completion date and the use of geofoam significantly reduced ground settlement to tolerable levels and increased stability of the embankment (*1*).

Figure 11.1. Trapezoidal embankment using geofoam and on-site material (*1*).

INDIANA: STATE ROUTE 109, NOBLE COUNTY

The Indiana Department of Transportation (DOT) reconstructed 335.3 m (1,100 ft) of Route 109 using EPS blocks with a density of 24 kg/m^3 (1.5 lbf/ft^3) (*2*). The roadway consists of two 3.7 m (12 ft) lanes with two 0.9 m (3 ft) shoulders for a total width of 9.1 m (30 ft). The foundation soil along the roadway consists of peat that extends to a maximum depth of 11.6 m (38 ft). Prior to reconstruction, continuous maintenance of the roadway had been required due to settlement of the embankment that was resulting in horizontal movement of the roadway and associated shear cracking of the pavement. In 1994, the side slopes were flattened but additional pavement cracking occurred and the Indiana DOT had to close the roadway to traffic. Remedial treatment procedures that the Indiana DOT considered included total removal and replacement of the peat with conventional fill material, soil modification, and partial removal and replacement with a lightweight fill material. The Indiana DOT decided to partially remove the peat to a maximum depth of 2.1 m (6.8 ft) and replace it and the embankment with EPS-block geofoam.

The EPS embankment section consisted of a 102 mm (4 in.) maximum layer of sand, 380 to 1,520 mm (15 to 60 in.) layer of EPS blocks, 100 to 125 mm (4 to 5 in) thick reinforced concrete slab, 406 mm (16 in.) layer of No. 8 stone, and a 330 mm (13 in.) layer of an asphalt cement wearing surface. A 150 mm (6 in.) drain, wrapped in a geotextile, was placed at a depth

of 1.22 m (4 ft) below the pavement surface on both sides of the embankment. The pavement section design included sufficient dead weight to offset the hydrostatic uplift pressures from the 100 year flood. EPS block dimensions of 1.2 by 1.0 by 4.9 m (4 by 3.3 by 16 ft) were used. Figure 11.2 presents a design cross-section for the roadway embankment.

Table 11.1 presents the construction schedule summary of the project. The total roadway reconstruction lasted 48 working days. The placement of the required 4,708 m^3 (6,157 yd^3) of EPS blocks was completed in only 11 days. This is a placement rate of about 428 m^3 (560 yd^3) per day. New Holland Model No. 553 skid-steer loaders were used to transport the EPS blocks to the edge of the fill and a dolly was then used to carry the blocks to the required location.

Figure 11.2. Trapezoidal geofoam embankment detail (*2*).

Table 11.1. Construction Schedule Summary for State Route 109, Noble County, Indiana (*2*).

A cost comparison between the EPS embankment option that was used and the total removal and replacement of the peat is included in Table 11.2. As shown in Table 11.2, the estimated cost of the removal and replacement option would have been $339,617 (about 28 percent) more than the EPS embankment option. Additional benefits of using EPS over a total removal and replacement (TRR) option that are not included in the cost comparison include: a shorter construction time than that required for the TRR procedure, no dewatering which was probably necessary for the TRR procedure, less pavement maintenance than that required with the TRR procedure due to settlement that may have occurred within the proposed 11.6 m (38 ft) thick soil fill, no cost of sheet piles or additional right of way that would have been required for the TRR procedure, and completion before winter so no construction stoppages which might have occurred with the TRR option because EPS can be placed in most weather conditions. Neglecting these benefits results in a volumetric cost of the EPS ($86/$m^3$ or $66/$yd^3$) exceeding the cost of TRR ($12/$m^3$ or $9/$yd^3$) as shown in Table 11.2. However, it is clear that DOTS are recognizing

these tangible benefits, e.g., reduced construction time, because EPS was selected over TRR and the total cost is 28 percent less than the TRR option.

Settlements measured forty-three months after pavement placement were between 0.05 and 0.09 m (0.18 and 0.29 ft). Pavement performance parameters were also measured. A Pavement Condition Rating of 94.5 indicated that the pavement was in the excellent range. The International Roughness Index of 89 also indicated that the pavement was in the excellent range. Rutting measured was approximately 1 mm (0.04 in.) which is minor. In summary, the closed roadway was able to open quicker, for less cost, and will probably remain open longer than a soil embankment because geofoam was used.

Table 11.2. Cost Comparison Between EPS and Removal/ Replacement Alternatives for State Route 109, Noble County, Indiana (*2*).

NEW YORK: STATE ROUTE 23A, TOWN OF JEWETT, GREENE COUNTY

This case history involves the use of EPS-block geofoam to stabilize a roadway embankment on an unstable slope and is presented because cost information is available from (*3,4*). The site is located in a mountain valley and slopes downwards from north to south. Based on the results of two borings performed on both sides of the roadway, the subsurface soils at the centerline of the roadway consist of about 1.5 m (5 ft) of gravelly silt fill. The underlying native soils consist of approximately 4.3 m (14 ft) of layered clayey silt and silty clay overlying 10.7 m (35 ft) of clayey silt. The water table was located at a depth of 2.44 m (8 ft) in the clayey silt and silty clay or approximately 4.0 m (13 ft) below the pavement surface. Figure 11.3 presents a profile of the all soil embankment and subsurface soils

A 91.4 m (300 ft) section of Route 23A became unstable after the roadway was reconstructed in 1966. These movements resulted in a continuous maintenance problem and traffic hazard. In 1979, horizontal drains were installed to lower the groundwater table. However, slope movements continued. Lateral movements measured over a period of 14 years after the drains were installed totaled 203.2 mm (8 in.). Inclinometer data indicated that the failure surface

was about 11 to 12.2 m (36 to 40 ft) below the roadway surface which corresponds to the clayey silt layer. Figures 11.4 and 11.5 present a plan and profile view of the scarp, respectively. Consequently, in 1994, the New York State DOT (NYSDOT) evaluated the following remedial measures: soil removal and replacement with EPS blocks (weight reduction) and installing drainage, placement of a berm at the toe of the slope, use of a shear key, relocation of the roadway uphill away from the failure zone, lowering the grade and installing stone columns, and soil nailing. The NYSDOT selected the weight reduction and drainage option because it considered the other alternatives impractical due to limitations imposed by the site and its environment and/or considered the other alternatives too costly.

Figure 11.3. Profile of all soil embankment and subsurface soils (*3*).

Figure 11.4. Plan view of scarp (*3*).

Figure 11.5. Profile of failure surface (*3*).

Figure 11.6 presents a cross-section of the EPS-block geofoam embankment. Sheeting was required to support the excavation during soil removal and replacement due to the depth of soil removal required and the need to maintain one lane of traffic opened at all times adjacent to the excavation. The EPS-block geofoam fill system was designed against hydrostatic uplift because Schoharie Creek is located on the south side of the slope. Based on the 100-year flood, the depth of geofoam that could be used was limited to 4.6 m (15 ft). A subsurface drainage system was placed below the geofoam to lower the groundwater table and to maintain a positive drainage path. The drainage system consisted of a 0.61 m (2 ft) thick layer of graded crushed stone with a network of 152.4 mm (6 in.) diameter perforated polyethylene drainage pipes embedded in the stone. Both the stone and pipes are exposed on the embankment-slope face. The crushed stone also provided a working platform and a level surface for the placement of the geofoam blocks.

Figure 11.6. Profile of EPS-block geofoam embankment (*3*).

The EPS blocks were placed in mid-November 1995 and all construction was completed in January 1996. The blocks, which had dimensions of 0.61 by 1.22 by 2.44 m (2 by 4 by 8 ft), were delivered to the site on flatbed trailers. About 76.5 m^3 (100 yd^3) of blocks arrived per truckload. Blocks were unloaded by two laborers and carried and placed by four persons. The average placement rate was 1 hr to unload and place a trailer load of 40 blocks. This is a placement rate of 76.5 m^3 (100 yd^3) per hour or about 382.5 m^3 (500 yd^3) per day. Two metal barbed inter-block connector plates were placed on each block. One plate was placed in the center and the second plate was placed near an edge to approximate a 1.22 m (4 ft) grid pattern. A 101.6 mm (4 in.) thick reinforced concrete slab was placed over the geofoam. A minimum of 0.61 m (2 ft) of subbase material consisting of graded crushed-stone subbase was placed over the concrete cap. This minimum thickness of subbase material was based on the Norwegian experience to minimize potential problems of differential pavement icing. A supplemental measure utilized by the NYSDOT to minimize differential icing included the use of a subbase material with 25 to 60 percent passing the 6.35 mm (1/4-in.) sieve to provide a high heat-sink capacity. The pavement consisted of 228.6 mm (9 in.) of asphalt concrete.

The quantity of EPS fill that was initially estimated was 3,115.7 m^3 (4,075 yd^3). The bid price for the EPS block was $85.01 per m^3 ($65 per yd^3). However, only 2,817.6 m^3 (3,685 yd^3) of geofoam was used because the sheeting was driven 0.61 m (2 ft) off-line toward the excavation. In order to compensate for the reduced amount of soil removed, additional soil fill was placed along the toe of the slope. The removal of 2,817.6 m^3 (3,685 yd^3) of soil and replacement with geofoam resulted in a net reduction of driving weight of about 5,352.5 Mg (5,900 tons) and an increase in factor of safety of 1.0 to over 1.5.

No significant movements have been recorded in slope inclinometers between the end of construction and December 1998. Piezometers installed within the crushed stone drainage blanket below the geofoam have indicated no pore pressure buildup since installation in November 1995. The NYSDOT is obtaining readings twice a year during wet periods of the year to monitor pore

pressure buildup that may indicate that the drainage blanket is clogged and thus serve as an early warning of rising water table which may cause uplift of the geofoam. No differential icing during the winter nor pavement deterioration, due to slight temperature increases that have been recorded by thermistors in the subbase during the summers, have been observed between the end of construction and December 1998.

UTAH: I-15 RECONSTRUCTION

The design-build contractor utilized various soil improvement techniques as part of the I-15 reconstruction in Salt Lake County, Utah. These techniques included prefabricated vertical drains (PVD), lime-cement columns (LCC), EPS-block geofoam, embankment surcharging, geotextile reinforced slopes, and mechanically stabilized earth (MSE) walls (*5*). The I-15 construction, includes a total of 27 km (17 mi) of highway reconstruction and 142 rebuilt or new bridge structures at a cost of $1.59 billion and was scheduled to be completed by July 15, 2001 (*6*). The project involves replacing the existing six- lane highway with a 12-lane highway. The use of a design-build contractor has allowed the use of these soil improvement techniques, which had not been used by the Utah DOT (*6*).

The subsurface soils along the I-15 construction consist of soft clays with low undrained shear strength and high compressibility (*7*). Settlements of up to 1.5 m (5 ft) were estimated in certain embankment sections with the use of conventional borrow material (*7*). Staged construction using MSE walls are being utilized in areas of large settlement. However, geofoam is being used as an alternative to MSE walls in certain locations to minimize settlement damage to buried utility lines that underlie the proposed embankment (*5*). Where geofoam is used, settlement of less than a few centimeters (1 in.) is expected (*5*). The benefits of using geofoam in utility corridors include the cost and time savings associated with utility replacement and service interruption if damage occurs due to settlement and cost of not having to relocate the utility (*5*).

The secondary use of geofoam has been as an alternative to granular backfill for MSE walls that are 10 to 14 m (33 to 46 ft) high due to stability concerns, scheduling problems, and/or

geometry constraints (*5*). A typical MSE wall requires about 6 months of construction and observation time before the rigid pavement can be placed (*5*). This time includes foundation preparation, prefabricated vertical drain installation, wall construction, and surcharging. A vertical "geofoam wall" system with an exterior tilt-up panel facing can be constructed in 1 month. This time includes minor foundation preparation, geofoam placement, tilt-up panel wall placement, and a reinforced concrete slab placement on top of the geofoam. Approximately 100,000 m^3 (130,795 yd^3) of EPS-block geofoam will be used as part of the I-15 reconstruction (*8*). Figures 11.7 through 11.9 present typical construction details for the geofoam walls.

Because the I-15 project is a design-build project, a cost breakdown was not reported to the Utah DOT. However, based on discussions with the contractor, the Utah DOT provided the following approximate cost information (*9*). The cost of EPS block is about \$65 per m^3 (\$50 per yd^3) and \$75 per m^3 (\$57 per yd^3) for a system without and with a facia wall, respectively. Thus, the facia wall system can be estimated at \$10 per m^3 (\$7 per yd^3). The reinforced concrete slab being utilized above the EPS blocks is about \$55 per m^2 (\$5 per ft^2) for a typical 150 mm (6 in.) slab. Placement rates ranged from approximately 200 blocks per day for one crew for one shift to 350 blocks per day for two shifts (*9*). This corresponds to a placement rate of 470 m^3 (615 yd^3) for one shift and 940 m^3 (1,230 yd^3) for two shifts per day based on a block size of 0.8 m × 1.2 m × 4.9 m (2.6 ft × 4 ft × 16 ft). A crew is defined as four laborers and a foreman. Various soil improvement techniques in addition to the use of EPS-block geofoam were utilized as part of the I-15 reconstruction. Cost information on these alternate methods is presented in Chapter 12.

In (*9*), it is reported that the cost of the tilt-up-panel-facia wall is approximately \$200 per m^2 (\$19 per yd^2). The cost for non-geofoam MSE walls are about \$335 per m^2 (\$31 per ft^2) of wall face (*10*). This includes a cost for the prefabricated vertical drains of about \$35 per m^2 (\$3 per ft^2) of wall face. The cost of the prefabricated vertical drains is based on an average width of embankment treatment of 16 m per m (52.5 ft per 3.3 ft) of wall, prefabricated vertical drain

installation depth of 25 m (82 ft), rectangular drain spacing of 2 m (6.6 ft) or 4.5 drains per lineal m of wall (1.4 drains per ft), a typical 8 m (26 ft) high MSE wall, and a cost of $2.50 per lineal m ($0.76 per lineal ft) of drain installed.

Figure 11.7. Construction detail for a vertical EPS wall (*11*).

Figure 11.8. Detail for traffic barrier and load distribution slab (*12*).

Figure 11.9 Detail for precast concrete wall panels for a vertical EPS wall (*13*)

Lime-cement columns (LCCs) were utilized to support an MSE wall Number SS-01. LCCs were utilized because of concerns about a potential slope failure into an adjacent commercial property due to the extreme height of the fill, accelerated construction schedule, and the close proximity of the Utah DOT right-of-way to the face of the wall (*5*). Wall heights ranged from 10 to 12.5 m (32 to 41 ft). A surcharge of 3 m (9.8 ft) was placed above the top of the finished wall to pre-compress the soils beneath the tips of the columns so the differential settlement criteria established for the roadway could be satisfied (*14*). Columns of about 22 m (72 ft) in length and 600 to 800 mm (24 to 32 in.) in diameter were used. The wall face is supported by LCC panels that consist of overlapping 800 mm (32in.) columns spaced at 2 m (6.6 ft) center-to-center spacings. These panels extend 2 m (6.6 ft) in front and 2 m (6.6 ft) behind the wall (*14*). The fill behind the walls are supported on 600 mm (24 in.) individual columns placed in a rectangular spacing of between 1 m (3.3 ft) and 1.2 m (3.9 ft). As the I-15 project progressed, the contractor decided not to utilize LCC because of concerns about adequate installation production rates (*5*).

The reported cost of the LCC support system is $30 per m ($9 per ft) and that on average this would suggest a cost of $60 per m^3 ($46 per yd^3) (*15*). It is indicated in (*14*) that LCC costs ranged from $45 to $65 per m^3 ($34 to 50 per yd^3) of column. The cost of LCC depends on the spacing of the columns needed for stabilization. The LCC process did not result in spoils being brought up to the ground surface so no costs associated with spoil disposal were incurred. Settlement on the order of 100 mm (3.9 in.), which is about one-tenth of the normal settlement

experienced for MSE walls placed on untreated soil, has been reported for the LLC support system (*5*).

WASHINGTON: STATE ROUTE 516 - LAKE MERIDIAN SETTLEMENT REPAIR, KING COUNTY

This project utilized a vertical EPS-block embankment with a treated wood face to reconstruct a portion of an embankment that was experiencing settlement problems. Project information was obtained from the Washington State DOT (WSDOT). In 1993, the WSDOT performed a widening program of SR 516 from 132nd Ave. SE to 160th Ave. SE. The project is located approximately 40 miles southeast of the city of Seattle. The initial design consisted of raising the north shoulder by about 305 to 457 mm (12 to 18 in.) and placing 457 to 914 mm (18 to 36 in.) of new fill on the existing slope. In order to accommodate the eastbound (north side of the embankment) traffic during bridge construction on the westbound side (south side of the embankment), the WSDOT widened the existing north shoulder by about 0.6 to 1.2 m (2 to 4 ft) with quarry spalls. This shoulder widening changed the existing embankment slopes from an existing 1.5H:1V to 2H:1V. Movement was observed in the westbound lane soon after placement of the new rip-rap fill on the existing slope. The WSDOT estimated that settlement on the order of 76 to 102 mm (3 to 4 in.) occurred from the time the rip-rap was placed in April 1993 to mid June 1993 when a monitoring program was initiated. Vertical and horizontal movements of 33 mm and 25 mm (1.3 and 1 in.), respectively, were measured between June and September 1993.

The geotechnical report dated November 12, 1993 (*16*) indicates that the movements were likely caused by embankment settlement and lateral displacement into the underlying and adjacent peat and possibly from vibrations induced by pile driving and traffic. The WSDOT considered five alternatives for stabilizing the embankment. These options included continued monitoring, removing some of the rip-rap and constructing a reinforced fill embankment, retaining the fill embankment with sheet piles or soldier piles along the north edge of the slope,

constructing a structural boardwalk for the sidewalk, and constructing a half bridge on the north side of the roadway.

The monitoring approach was selected in the anticipation that movements would decrease to acceptable levels with time. A concrete sidewalk was constructed along the north side of the embankment. However, up to 0.10 m (0.33 ft) of vertical and 0.11 m (0.36 ft) of lateral movement was measured from July 1994 to February 1995 in the sidewalls. A memorandum dated May 3, 1995 (*17*) indicates that vertical and lateral displacements of 0.21 m (0.68 ft) and 0.25 m (0.82 ft), respectively, had occurred between Sta. 152+00 to 153+50 and vertical and lateral displacements of 30 mm (0.1 ft) and 46 mm (0.15 ft) had occurred in the remainder of the sidewalk between Sta. 149+50 and 154+00. There was concern that the sidewalk would become unsafe and if future movements occurred at the same rate, the roadway pavement and the underlying water lines would become distressed.

The WSDOT decided to replace a portion of the earth embankment with EPS blocks. Figure 11.10 shows the typical elevation and plan view of the EPS block repairs. Block sizes of 0.76 by 1.22 by 2.44 m (2.5 by 4 by 8 ft) were utilized. Two types of EPS embankment sections were used. Repairs from Sta. 152+00 to 154+00 consist of the first layer of EPS blocks extending 1.83 m (6 ft) horizontally from the facing system and Sta. 149+50 to 152+00 consist of the first layer of EPS blocks extending 1.22 m (4 ft) horizontally from the facing system. The second layer of EPS in both sections extends 2.44 m (8 ft) horizontally from the wall face. A 510 mm (2 in.) layer of sand was placed below the EPS blocks as a leveling layer in all locations. A 0.15 m (6 in.) concrete cap was placed on top of the EPS. A minimum of 2 timber fasteners per block was specified between blocks.

The facing system for the vertical wall consists of 92 by 92 mm (4 by 4 in.) treated wood posts spaced at 1.8 m (6 ft) center-to-center and extending 0.76m (2.5 ft) below the proposed subgrade level. Treated wood lagging (40 by 143 mm or 2 by 6 in.) was placed horizontally between the vertical posts. Figure 11.11 presents a photograph of the treated wood facing system.

The wood facing was placed before the EPS blocks and the EPS blocks were subsequently placed against the wood facing. Pea gravel meeting the gradation requirements of AASHTO No. 8 coarse aggregate was used to backfill the void between the wall of the cut and the EPS blocks. The lowest bid price for the 410.6 m^3 (537 yd^3) of EPS blocks was $105.94 per m^3 ($81 per yd^3). Although some lateral and vertical movement occurred during the February 28, 2001 Nisqually earthquake, the EPS embankment did not sustain any damage. Figures 11.12 and 11.13 present photographs of the embankment during construction and after the completion of construction, respectively.

Figure 11.10. Details of EPS-block vertical-faced fill used for the S.R. 516 repair in King County, Washington (Washington State Department of Transportation).

Figure 11.11. Photograph of treated wood facing system (Washington State Department of Transportation).

Figure 11.12. Photograph of geofoam used to support a sidewalk on top of an earthen embankment (Washington State Dept. of Transportation).

Figure 11.13. Photograph of completed EPS-block geofoam fill (Washington State Department of Transportation).

WISCONSIN: BAYFIELD COUNTY TRUNK HIGHWAY A

This case history involves the use of EPS-block geofoam as a hillside fill to repair a slow-moving landslide that had persisted for over 20 years (*18*). The Bayfield County Trunk Highway A in northern Wisconsin was 45 m (148 ft) wide and had a slope of approximately 14 degrees in the landslide area. The height of the embankment was 5 m (16 ft). The glaciolacustrine soils below the embankment consist of very soft, highly plastic clays and silts. The failure surface identified by an inclinometer is 6.1 m (20 ft) below grade and sliding was occurring in the soft, highly plastic clays and silts. The roadway was frequently patched due to the occurrence of tension and lateral shear cracks that developed within the asphalt pavement.

In addition to the lightweight fill alternative, excavation of the soils within the slide mass and replacement with granular fill was also considered. However, the total excavation alternative was not selected because it would require excavation below the groundwater level and temporarily closing the highway. Soil from the head of the slide was removed and replaced with EPS-block geofoam. The geofoam had a density of 24 kg/m^3 (1.5 lbf/ft^3) and dimensions of 0.81 by 1.22 by 2.44 m (2.7 by 4 by 8 ft). Three layers of EPS blocks were used. A drainage blanket consisting of 0.3 m (1 ft) of free-draining sand conforming to Wisconsin Department of Transportation Section 209, Grade 1 and a system of 200 mm (8 in.) diameter slotted plastic pipe was placed below the EPS blocks. The drain pipes were placed parallel to the road at the back of the excavation as well as transverse to the road at 15 m (50 ft) intervals. The transverse pipes extended from the parallel pipe at the back of the excavation to the embankment face. An impermeable membrane was placed on top of the geofoam as protection against petroleum spills. The top of the geofoam was kept at a depth of 1.5 m (4.9 ft) below the final pavement surface to minimize the potential for differential icing conditions. The fill placed over the EPS blocks and the sides of the embankment consists of free-draining sand. The installed cost of the EPS block was \$61.50 per m^3 (\$47.00 per yd^3). EPS-block geofoam was also used to remediate two other landslides along Bayfield County Trunk Highway A but cost information is not available for these applications.

WYOMING: MOORCRAFT BRIDGE, CROOK COUNTY

EPS-block geofoam was used as fill for both approaches for the Moorcraft bridge located along I-90 in Crook County, Wyoming in the summer of 1993. Project information was supplied by the Wyoming DOT and also obtained from (*19*). Two layers of EPS blocks with a density of 24 kg/m^3 (1.5 lbf/ft^3) were placed overlying a thin layer of 25 to 50 mm (1 to 2 in.) of crushed rock and pea gravel on the east and west abutments, respectively (*19*). Figure 11.14 presents a photograph of the EPS-block geofoam blocks used. The bottom EPS layer extended 10.4 m (34 ft) horizontally from the abutment and the upper EPS layer extended 10.7 m (35 ft)

from the abutment, about 3 m (10 ft) beyond the approach slab. A polyethylene geomembrane was placed on top of the geofoam to protect against petroleum spills. A 305 mm (12 in.) layer of sand was placed between the concrete approach slab and the geomembrane. The approach slab extended 7.6 m (25 ft) from the abutment and had a thickness of 3 m (1 ft) and a width of 12.5 m (41 ft). An asphalt cement pavement was placed on top of the concrete slab. Rings of barbed wire 100 mm (4 in.) in diameter were used as inter-block fasteners because the timber fasteners did not arrive on time (*19*).

Figure 11.14. Photograph of EPS-block geofoam used for the Moorcraft bridge approach (Wyoming Department of Transportation).

The main objective of the project was to reduce the differential settlement occurring at the abutment/embankment interface which had to be annually leveled. The initial project design consisted of a MSE wall approach fill. The approach design was subsequently changed to EPS block geofoam for the purpose of providing a full scale instrumental field test to obtain technical data on the use of EPS as bridge approach fill and facilitate future use by the DOT (*19*). The Wyoming DOT estimated the cost for the MSE wall approach fill design to be $58,696 while the cost of the EPS block approach fill option was $79,732, or $21,036 (28 percent) more than the original MSE wall option. This cost includes $37,000 for material and labor for the EPS blocks, geomembrane, sand base, as well as labor to drill holes in the abutment for monitoring instrumentation. Because this was one of the first EPS-block bridge approach projects in Wyoming, the higher cost of the EPS-block alternative could be attributed to the lack of familiarity by local contractors and probably did not consider the full benefits of the ease and speed of EPS-block placement and the possible placement of EPS blocks in adverse weather conditions. A cost comparison between the EPS-block and MSE systems is included in Table 11.3. A total of 377 m^3 (493 yd^3) of EPS blocks were utilized of which 65 m^3 (85 yd^3) were donated by the supplier. MSE walls had been utilized by the Wyoming DOT for over five years. The estimated volumetric costs for the EPS and MSE walls are $17.30 and $9.60 per m^3 of wall.

Table 11.3. **Cost Comparison Between EPS and MSE Approaches for the Moorcraft Bridge Structure.**

WYOMING: BRIDGE REHABILITATION, N.F. SHOSHONE RIVER

This project involved the rehabilitation of approaches to a bridge over the N.F. Shoshone River in Wyoming. Project information was provided by the Wyoming DOT (Wyoming DOT Project No. 031-1[68]) . The actual date of construction was estimated to be between 1997 and 1999. Two types of bridge approach fills were used below the approach slabs. One approach fill consists of EPS block geofoam and the other consists of an MSE wall (*20*). The bridge abutments are skewed approximately 55 degrees from the centerline of the bridge roadway. Both approach slabs have a surface area of 88 m^2 (947 ft^2) and a corresponding width of 6.24 m (20 ft) as measured normal to the abutment or 55 degrees from the roadway centerline. Both approach slabs consist of a 255 mm (10 in.) thick concrete slab and an overlying 50 mm (2 in.) thick bituminous pavement layer.

The depth of the EPS block approach fill system is 3 m (9.8 ft) at the centerline of the bridge roadway and includes 50 mm (2 in.) of sand below the EPS blocks, 2.7 m (9 ft) of EPS blocks and 205 mm (8 in.) of sand at the top of the blocks. The fill extends 2.5 m (8 ft) horizontally from the abutment and then slopes at 1(H):1(V). The density of EPS blocks used is 24 kg/m^3 (1.5 lbf/ft^3). The depth of the MSE wall approach system is 2.65 m (8.7 ft) at the centerline of the bridge roadway. The fill extends 3 m (9.8 ft) horizontally from the abutment then slopes at 1.8(H): 1(V) for a horizontal distance of 3.24 m (10.6 ft) as measured from the bottom of the fill and 1(H):1(V) for the remaining horizontal distance of 750 mm (30 in.). Figures 11.15 and 11.16 present details of the EPS-block geofoam bridge approach.

Figure 11.15. Detail for geofoam backfill behind the bridge abutment (*23*).

Figure 11.16. Detail of bridge approach pavement system over geofoam (*24*).

Table 11.4 provides a summary of the bridge approach costs for the EPS and MSE alternatives. The estimated volumetric costs for the EPS and MSE walls are $202 and $100 per

m³ ($154 and $76 per yd^3) of wall. Although the cost of using an EPS approach fill is $9,330 (32 percent) higher than the MSE wall, the EPS block approach fill system was used on one side because of its speed of construction and because of its lightweight properties (*21*). The higher cost of the EPS approach alternative may have been due to unfamiliarity of the EPS construction procedure by local contractors (*22*).

OTHER CASES AND STATE DOT EXPERIENCES

Connecticut

The Connecticut DOT recently awarded a contract to construct an embankment that involves placing expanded-shale aggregate over EPS-block geofoam. The cost of the EPS-block geofoam will be $98.09 per m^3 ($75 per yd^3) and the cost of the expanded shale aggregate will be $13.08 per m^3 ($10 per yd^3) . These unit prices include placement.

Table 11.4. Cost Comparison Between EPS and FRS Approaches for the N.F. Shoshone Bridge Structure.

Illinois

Based on information obtained from the Illinois DOT several problems occurred during construction on an embankment that utilized EPS-block geofoam as lightweight fill. The embankment is a four-lane state roadway (143rd Street) in Orland Park, Illinois. The embankment consists of about 1.22 m (4 ft) of geofoam in the inner lanes (part of the roadway that was reconstructed) and 1.52 m (5 ft) of geofoam in the outer lanes (new widened area). The project began in 1999 and was to be completed in 2000. A total of approximately 15,291 m^3 (20,000 yd^3) of EPS blocks were to be used in the embankment. The placement rate for the first phase of the project was approximately 313 m^3 per day (410 yd^3 per day). The first problem encountered involved the initial shipment of EPS blocks not meeting the specified density of 24 kg/m^3 (1.5 lbf/ft^3). The second problem involved hydrostatic uplift of part of the geofoam embankment during a heavy rainfall. A crack developed in the concrete cap, which was already in-place when uplift occurred, along the 1.22 to 1.52 m (4 to 5 ft) geofoam thickness transition line. Pumping

costs associated with providing temporary dewatering during construction to minimize the potential for uplift re-occurring was greater than anticipated. Figure 11.17 presents a cross-section of the EPS-block geofoam roadway and Figures 11.18 and 11.19 present details of the storm drain pipe and guardrail used with the EPS-block geofoam roadway embankment.

Figure 11.17. Cross-section through geofoam embankment containing a storm drain and guardrail (*25*).

Figure 11.18. Detail of storm drain pipe in geofoam embankment (*26*).

Figure 11.19. Detail for guardrail on top of geofoam embankment (*27*).

Maine

Based on a personal communication with the Maine DOT in 1999, the cost provided by a manufacturer for only geofoam blocks that were proposed for an embankment project was $57.21 per m^3 ($43.74 per yd^3) (*28*). This unit cost is a freight-on-board (FOB) site unit price and does not include placement.

Michigan

Table 11.5 below is a summary of the bids obtained from the Michigan DOT in 1999 for two embankment projects. No further project information was supplied. These projects involve the use of EPS-block geofoam for both bridge approaches and embankments. This data indicates a volumetric cost for the EPS embankment of $220 per m^3 ($168 per yd^3) in Project 1 and $1,160 per m^3 ($887 per yd^3) in Project 2. This large difference in volumetric cost in the same state illustrates the importance of obtaining site specific cost estimates.

Table 11.5. Unit Bid Prices for EPS Projects in Michigan.

City of Issaquah, Washington

Approximately, 1,835 m^3 (2,400 yd^3) of EPS-block geofoam was used for an approach fill on a bridge replacement project in 1995. The city of Issaquah is approximately 15 miles southeast of the city of Seattle. EPS was used instead of a surcharge procedure with prefabricated vertical drains because the use of EPS was cost competitive and the bridge approaches could be

constructed within one construction season as opposed two construction seasons for the surcharge option. The cost of the EPS block was \$59 per m^3 (\$45 per yd^3) and \$72 per m^3 (\$55 per yd^3) installed. Thus, the EPS installation cost was about \$13 per m^3 (\$10 per yd^3). Figures 11.20 through 11.22 provide photographs showing the placement of the EPS-blocks, concrete separation layer, and utilities. Although the bridge approach embankments settled approximately 50 mm (2 in.) because of liquefaction of the foundation soils, the bridge approaches did not experience damage due to any shifting of the blocks during the February 28, 2001 Nisqually earthquake. Nearby roadways that did not include EPS experienced more damage.

Figure 11.20. Placement of EPS blocks (City of Issaquah, WA).

Figure 11.21. Placement of concrete separation layer over the EPS blocks (City of Issaquah, WA).

Figure 11.22 Placement of utilities on top of sand base overlying the EPS blocks (City of Issaquah, WA)

SUMMARY

This chapter of the report presents case histories of geofoam usage in transportation applications that can be utilized to assess whether or not the proposed use is similar to prior uses. These case histories illustrate the many intangible or non-quantifiable benefits of geofoam that result in DOTs selecting geofoam over less costly and more traditional techniques. Some of these benefits include reduced placement time which is illustrated in Table 11.6 that presents observed geofoam placement rates, placement in adverse weather conditions, decreased maintenance costs because of smaller differential settlements, reduced lateral stress on bridge approach abutments, use of a vertical embankment which reduces right-of-way requirements, negligible impact on underlying utility corridors, excellent seismic behavior, elimination of surcharging and/or staged construction, excellent durability.

Table 11.6. Summary of Placement Rates of EPS-Block Geofoam in Embankment and Slope Repair Projects.

REFERENCES

1. Mimura, C. S., and Kimura, S. A., "A Lightweight Solution." *Geosynthetics '95 Conference (1995: Nashville, Tenn.) Conference Proceedings,* Nashville, Tenn., Vol. I (1995) pp. 39-51.
2. Zaheer, M. A., "Experimental Feature Study The Use of Expanded Polystyrene (EPS) in Pavement Rehabilitation S.R. 109 in Noble County, Indiana." Indiana Department of Transportation Materials and Tests Division, Indianapolis (1999) 17 pp.
3. Jutkofsky, W. S., "Geofoam Stabilization of an Embankment Slope, A Case Study of Route 23A in the Town of Jewett, Greene County." Geotechnical Engineering Bureau, New York State Department of Transportation, Albany (1998) 42 pp.
4. Jutkofsky, W. S., Sung, J. T., and Negussey, D., "Stabilization of an Embankment Slope with Geofoam." *Transportation Research Record 1736,* Transportation Research Board, Washington, D.C. (2000) pp. 94-102.
5. Bartlett, S. F., "Research Initiatives for Monitoring Long Term Performance of I-15 Embankments, Salt Lake City, Utah." *Proceedings of the 34th Symposium on Engineering Geology and Geotechnical Engineering,* Utah State University, Logan, Utah, (1999) pp. 54-67.
6. Warne, T. R., and Downs, D. G., "All Eyes on I-15." *Civil Engineering*, Vol. 69, No. 10 (October 1999) pp. 42-47.
7. Gunalan, K. N., Lee, T. S., and Sakhai, S., "Stage 1 Geotechnical Studies for Interstate 15 Reconstruction Project, Salt Lake County, Utah." *Proceedings: Fourth International Conference on Case Histories in Geotechnical Engineering,* St. Louis, Missouri, (March 9-12, 1998) pp. 458-468.
8. Negussey, D., "Putting Polystyrene to Work." *Civil Engineering*, Vol. 68, No. 3 (March 1998) pp. 65-67.
9. Bartlett, S., Negussey, D., Kimble, M., and Sheeley, M., "Use of Geofoam as Super-Lightweight Fill for I-15 Reconstruction (Paper Pre-Print)." *Transportation Research Record 1736,* Transportation Research Board, Washington, D.C. (2000) .
10. Bartlett, S. F., Personal Communication,7 October 1999.
11. "Typical Section Geofoam (EPS) Wall." *I-15 Corridor Reconstruction, Elev.-Geofoam Wall (8 m - 11 m), Corridor Standard Plan,* Utah Dept. of Transportation (1998) pp. CS-77.
12. "Load Distribution Slab Restraint Section." *I-15 Corridor Reconstruction, Elev.-Geofoam Wall (8 m - 11 m), Corridor Standard Plan,* Utah Dept. of Transportation (1998) pp. CS-80.
13. "Precast Wall Panel." *I-15 Corridor Reconstruction, Elev.-Geofoam Wall (8 m - 11 m), Corridor Standard Plan,* Utah Dept. of Transportation (1998) pp. CS-44.
14. Esrig, M. I., and Kenna, P. E. M., "Lime Cement Column Ground Stabilization for I 15 in Salt Lake City." *Proceedings of the 34th Symposium on Engineering Geology and Geotechnical Engineering,* Utah State University, Logan, Utah, (April 28-30, 1999) pp. 29-52.
15. Elias, V., Welsh, J., Warren, J., and Lukas, R., "Ground Improvement Technical Summaries." *Publication No. FHWA-SA-98-086,* 2 Vols, U.S. Department of Tranportation, Federal Highway Administration, Washington, D.C. (1999) .

16. "Report Supplemental Geotechnical Engineering Services Area G-SR 516 Roadway Improvements King County, Washington, For Washington State Department of Transportation." GeoEngineers, Inc., Redmond, WA (1993) 23 pp.
17. Allen, T. M., and Jenkins, D. V., Memorandum to R.Q. Anderson and T. Hamstra , SR-516, C.S. 1738, OL-2297, Lake Meridian Embankment Settlement Repair, Expanded Polystyrene (EPS) Fill,3 May 1993.
18. Reuter, G., and Rutz, J., "A lightweight solution for landslide stabilization." *Geotechnical Fabrics Report*, Vol. 18, No. 7 (September 2000) pp. 42-43.
19. Preber, T., and Bang, S., "Field Application and Instrumentation of Expanded Polystyrene Blocks as Bridge Backfill." *Proceedings of the 1995 Annual Symposium on Engineering Geology & Geotechnical Engineering (No. 31),* Logan, Utah, (1995) pp. 84-102.
20. Price, J. T., and Sherman, W. F., "Geotextiles Eliminate Approach Slab Settlement." *Public Works*, (January 1986) pp. 58-59.
21. Hager, G. M., Personal Communication,8 November 1999.
22. Fulton, K., Personal Communication, 27 August 1999.
23. "Section A-A (Abut No. 1)." *Approach Slab No. 1 Details, Bridge Rehabilitation Bridge Over N.F. Shoshone River US 14,16,20 (P-31), KP 51.50 (MP 32.01),* Wyoming Dept. of Transportation (1997) pp. Sheet 9.
24. "Section B-B, C-C, D-D." *Approach Slab No. 1 Details, Bridge Rehabilitation Bridge Over N.F. Shoshone River US 14,16,20 (P-31), KP 51.50 (MP 32.01),* Wyoming Dept. of Transportation (1997) pp. Sheet 10.
25. "Sta. 77+00 to 81+00." *143rd Street Expanded Polystyrene Foam Typical Sections and Details,* Illinois Dept. of Transportation (1998) pp. Sheet 25B.
26. "EPS Layout Beneath Storm Sewer." *143rd Street Expanded Polystyrene Foam Typical Sections and Details,* Illinois Dept. of Transportation (1998) pp. Sheet 25D.
27. "SPB Guardrail Type A. Special." *143rd Street Expanded Polystyrene Foam Typical Sections and Details,* Illinois Dept. of Transportation (1998) pp. Sheet 25D.
28. Breskin, K., Personal Communication,30 November 1999.

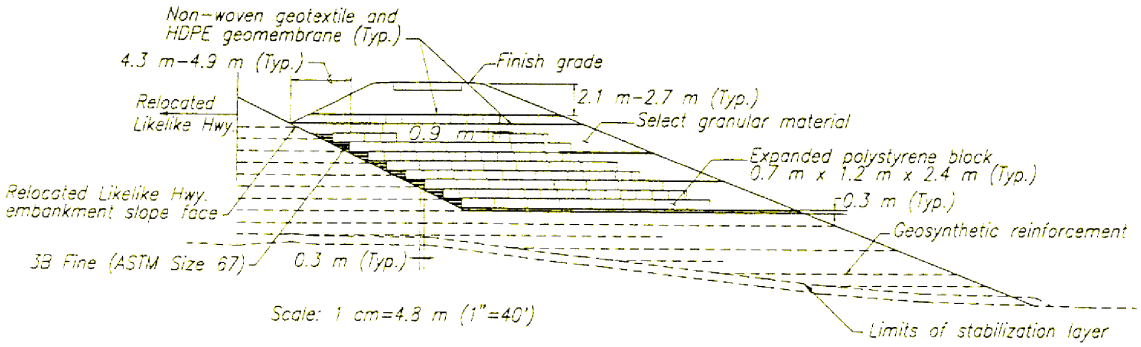

FIGURE 11.1 PROJ 24-11m.doc

EXPANDED POLYSTYRENE FILL

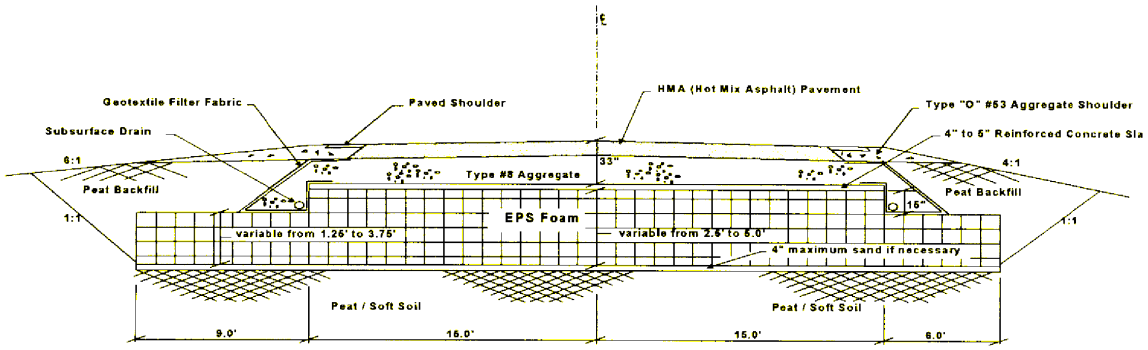

FIGURE 11.2 PROJ 24-11m.doc

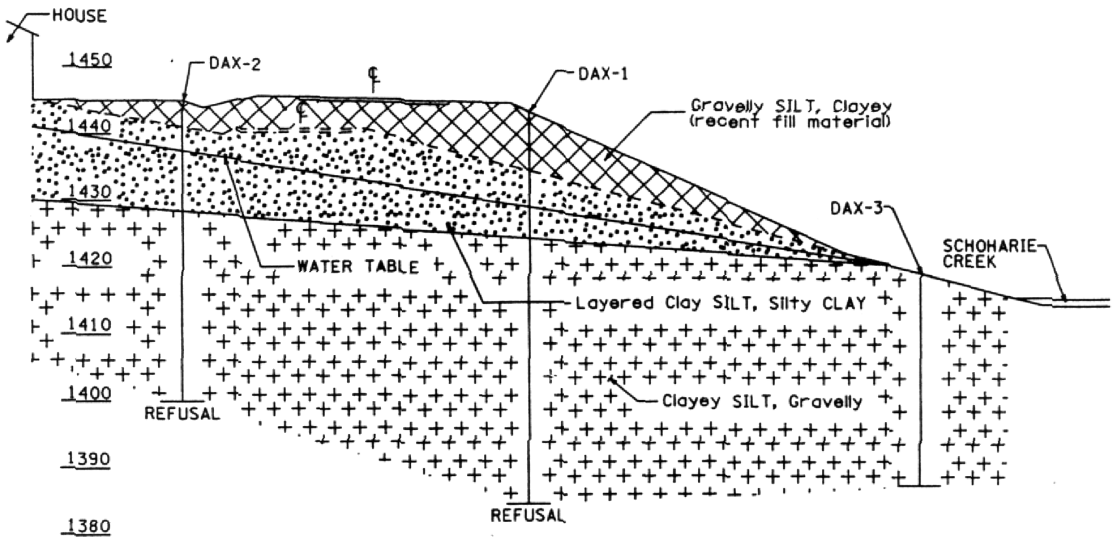

FIGURE 11.3 PROJ 24-11m.doc

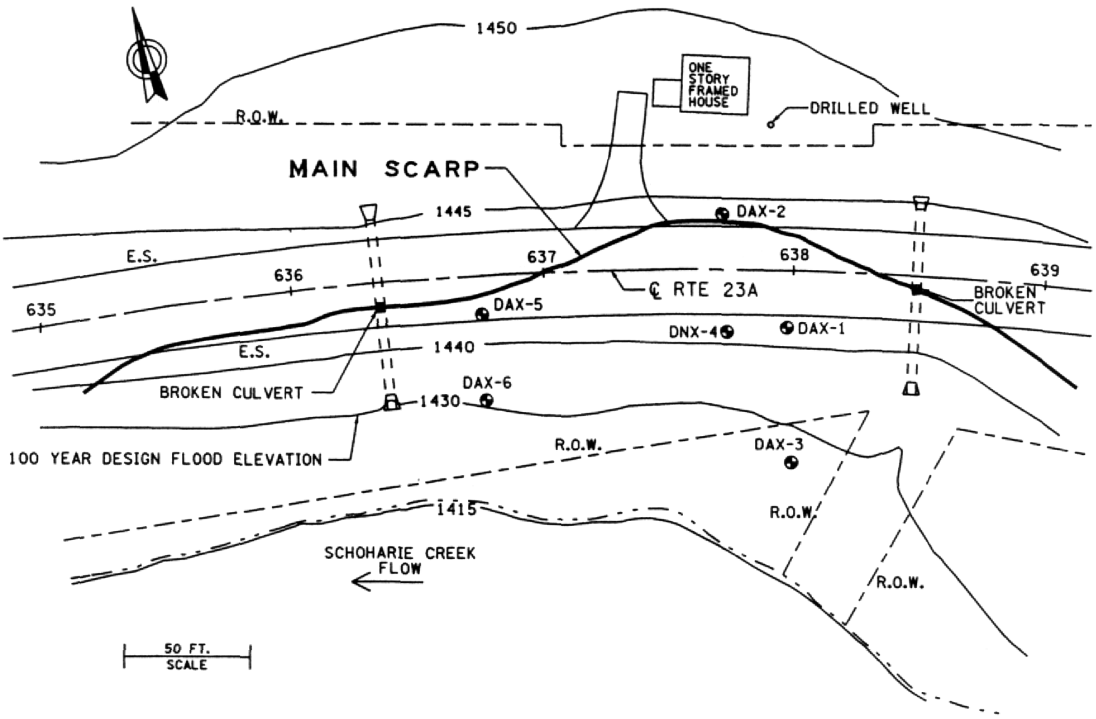

FIGURE 11.4 PROJ 24-11m.doc

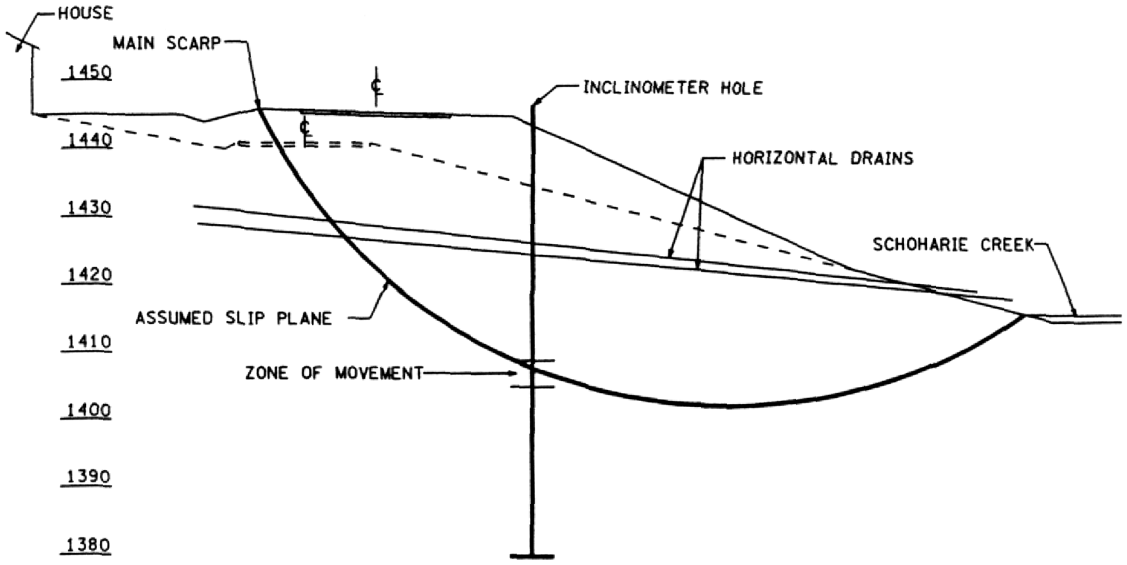

FIGURE 11.5 PROJ 24-11m.doc

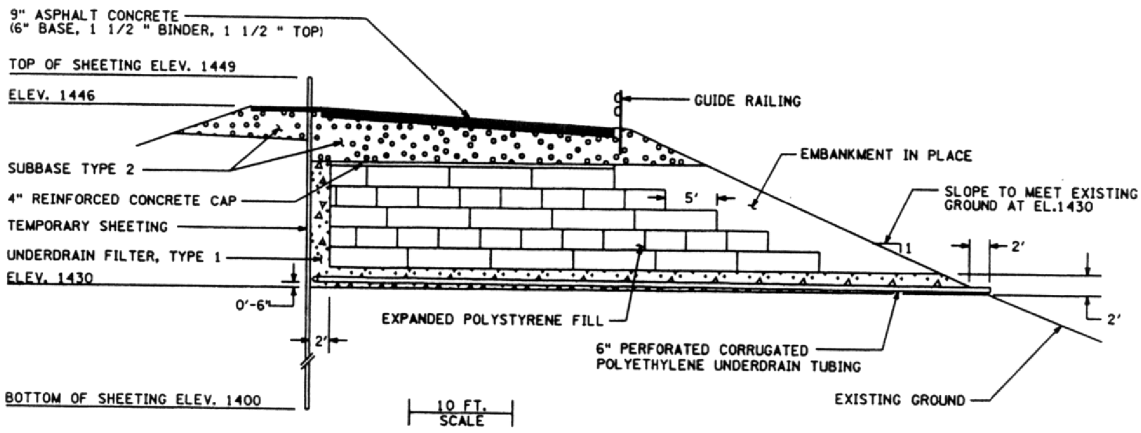

FIGURE 11.6 PROJ 24-11m.doc

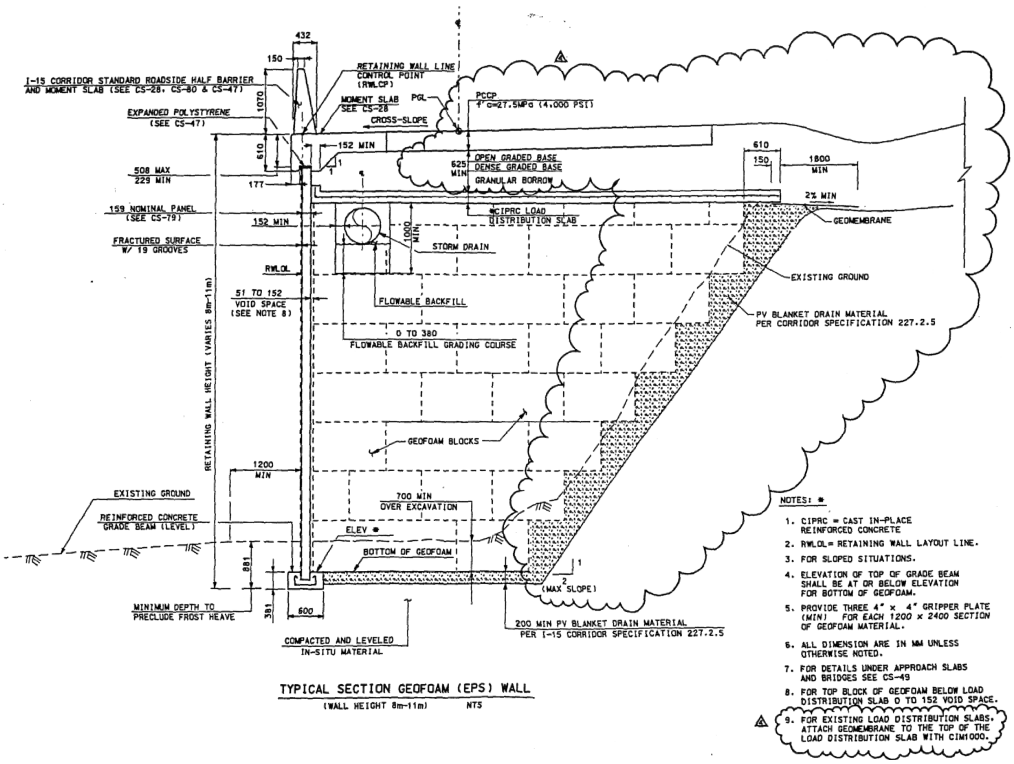

TYPICAL SECTION GEOFOAM (EPS) WALL

(WALL HEIGHT 8m-11m) NTS

FIGURE 11.7 PROJ 24-11m.doc

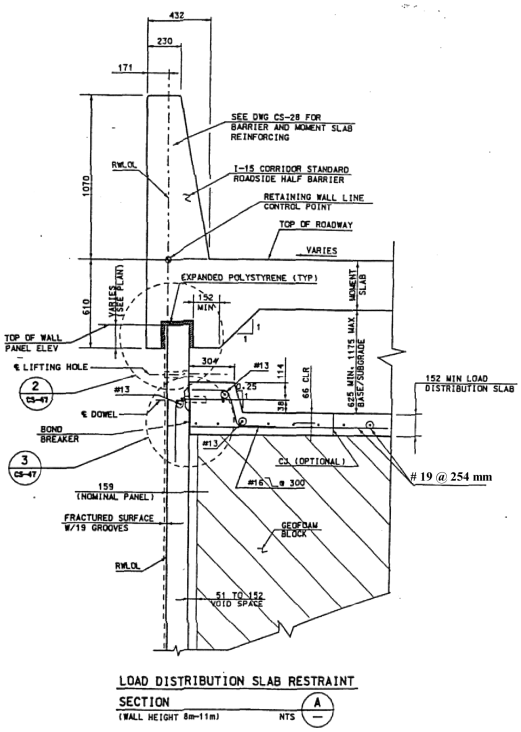

NOTES:

1. LOAD DISTRIBUTION SLAB DESIGNED FOR HS-20 LOADING.
2. WHEEL LOADS ARE NOT PERMITTED WITHIN 1500 OF FREE EDGE OF LOAD DISTRIBUTION SLAB PRIOR TO PLACING PCCP SLAB.
3. LIFTING HOLES TO BE DRY PACKED.
4. ALL DIMENSION ARE IN MM UNLESS OTHERWISE NOTED.
5. SEE CS-28 FOR MOMENT SLAB REINFORCING.
6. FOR DETAILS UNDER APPROACH SLABS AND BRIDGES SEE CS-49.
7. TRANSVERSE CONSTRUCTION JOINTS ARE ALLOWED IN THE LOAD DISTRIBUTION SLAB AT THE OPTION OF THE CONTRACTOR.
8. ALL CRACKS OVER 0.5 MM SHALL BE SEALED WITH A HIGH MOLECULAR WEIGHT METHYL METHACRYLATE SEALANT (TRANSPO T-70 OR EQUAL).
9. CONCRETE SHALL BE CLASS AA(AE) EXCEPT AS MODIFIED FOR f'c=27.5 MPa (4,000 PSI). NO CONSTRUCTION LOADS SHALL BE PERMITTED ON THE LOAD DISTRIBUTION SLAB UNTIL AFTER 7 DAYS OF CURING.

FIGURE 11.8 PROJ 24-11m.doc

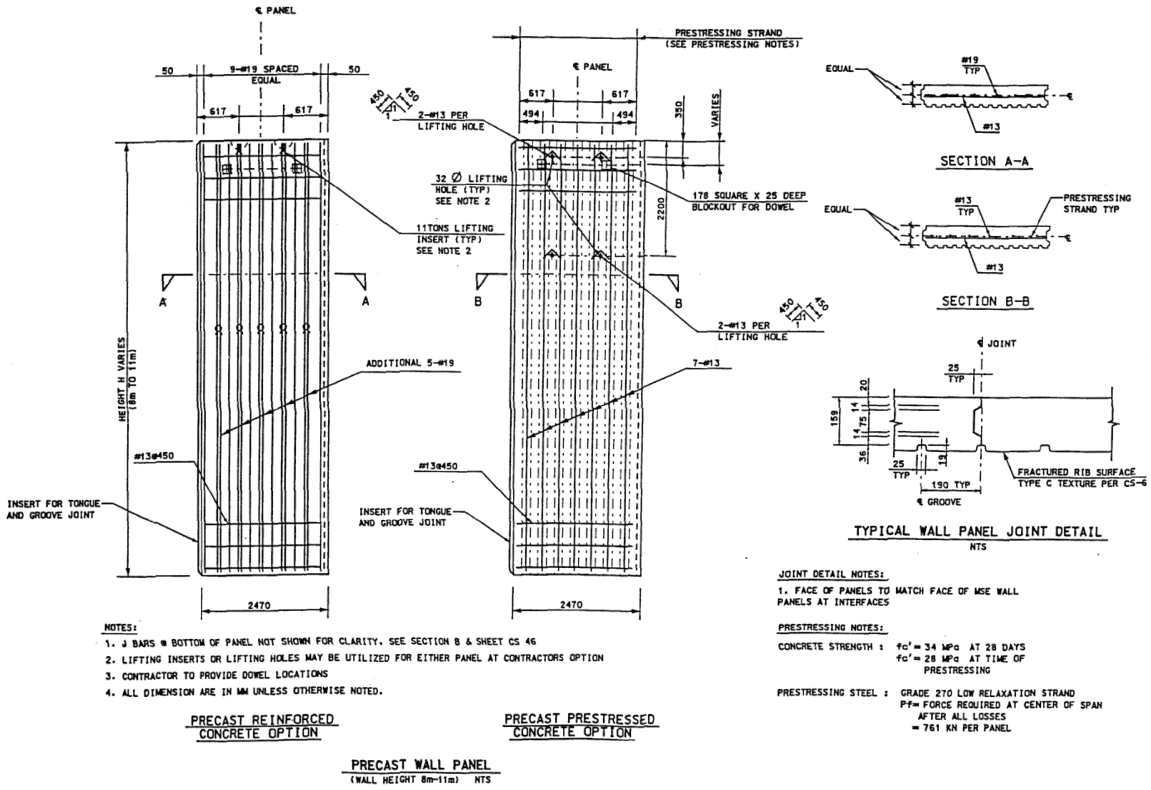

NOTES:

1. J BARS @ BOTTOM OF PANEL NOT SHOWN FOR CLARITY. SEE SECTION B & SHEET CS 46
2. LIFTING INSERTS OR LIFTING HOLES MAY BE UTILIZED FOR EITHER PANEL AT CONTRACTORS OPTION
3. CONTRACTOR TO PROVIDE DOWEL LOCATIONS
4. ALL DIMENSION ARE IN MM UNLESS OTHERWISE NOTED.

PRECAST REINFORCED CONCRETE OPTION

PRECAST PRESTRESSED CONCRETE OPTION

PRECAST WALL PANEL
(WALL HEIGHT 8m-11m) NTS

JOINT DETAIL NOTES:

1. FACE OF PANELS TO MATCH FACE OF MSE WALL PANELS AT INTERFACES

PRESTRESSING NOTES:

CONCRETE STRENGTH : $f_c' = 34$ MPa AT 28 DAYS
$f_c' = 28$ MPa AT TIME OF PRESTRESSING

PRESTRESSING STEEL : GRADE 270 LOW RELAXATION STRAND
Pf= FORCE REQUIRED AT CENTER OF SPAN AFTER ALL LOSSES
= 761 KN PER PANEL

FIGURE 11.9 PROJ 24-11m.doc

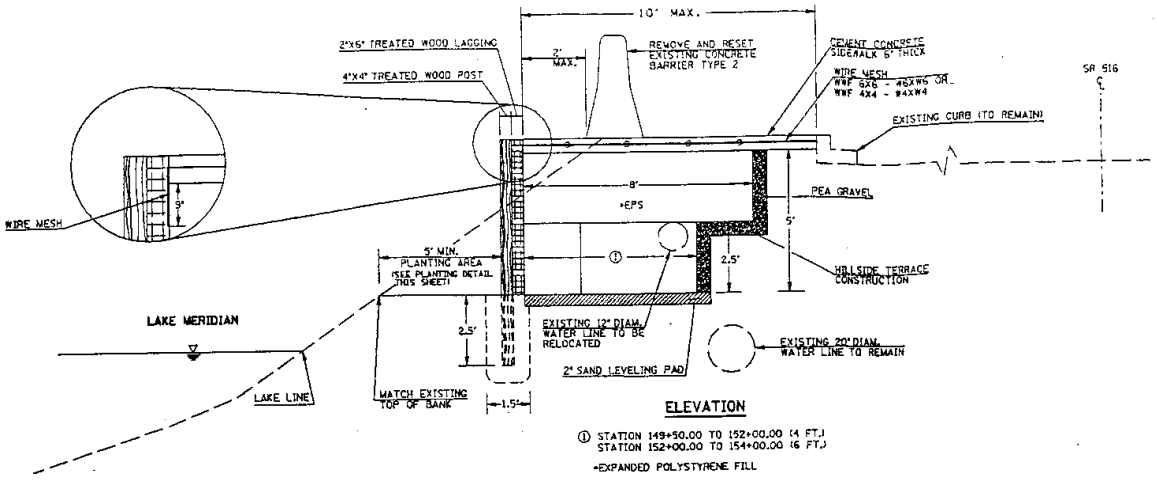

(a) Elevation view.

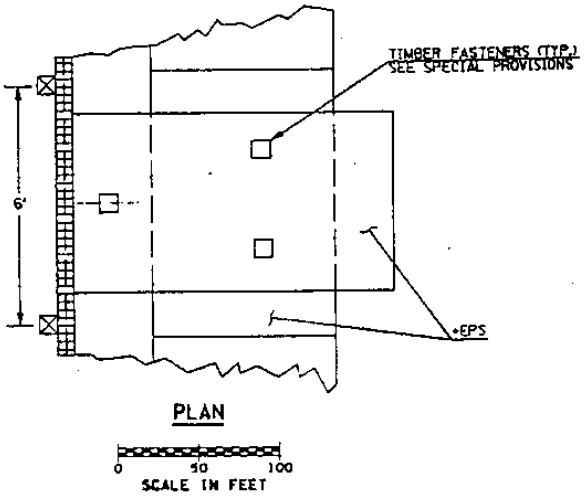

(b) Plan view

FIGURE 11.10 PROJ 24-11m.doc

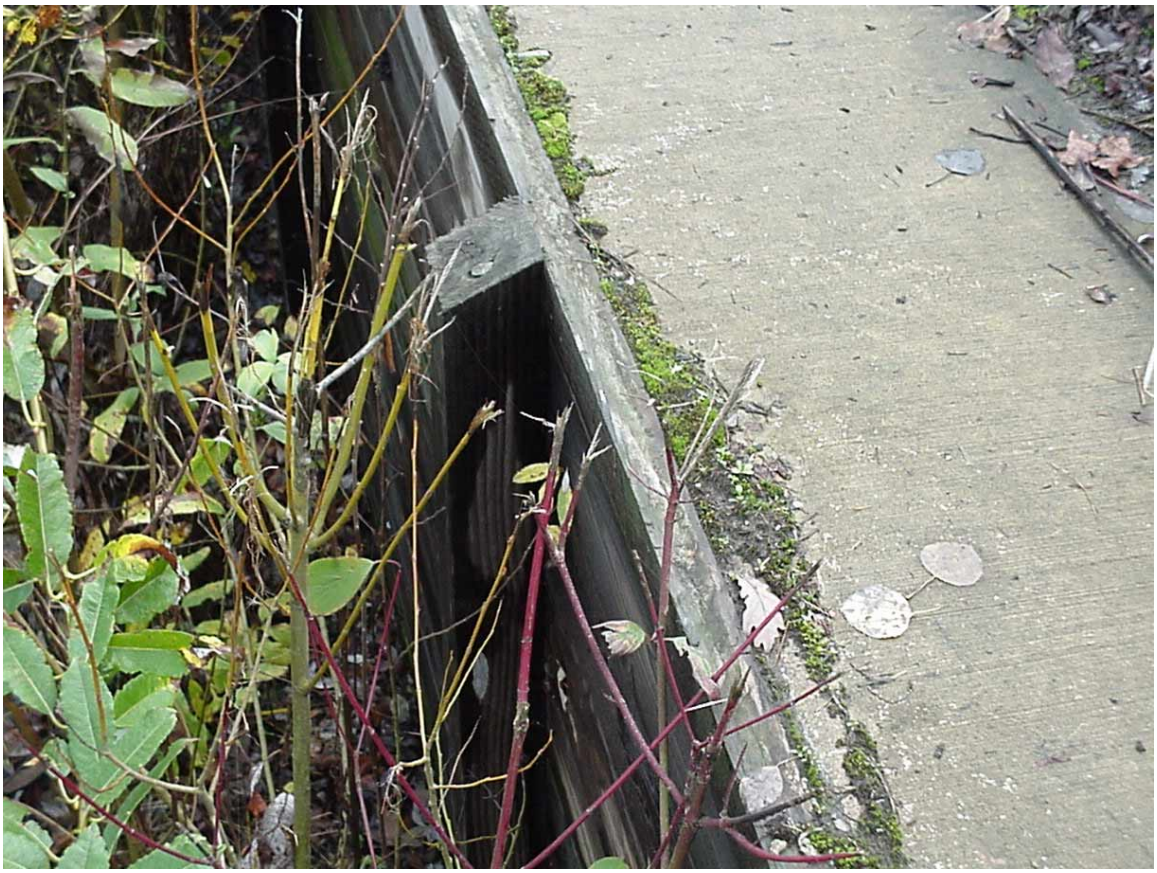

FIGURE 11.11 PROJ 24-11m.doc

FIGURE 11.12 PROJ 24-11m.doc

FIGURE 11.13 PROJ 24-11m.doc

FIGURE 11.14 PROJ 24-11m.doc

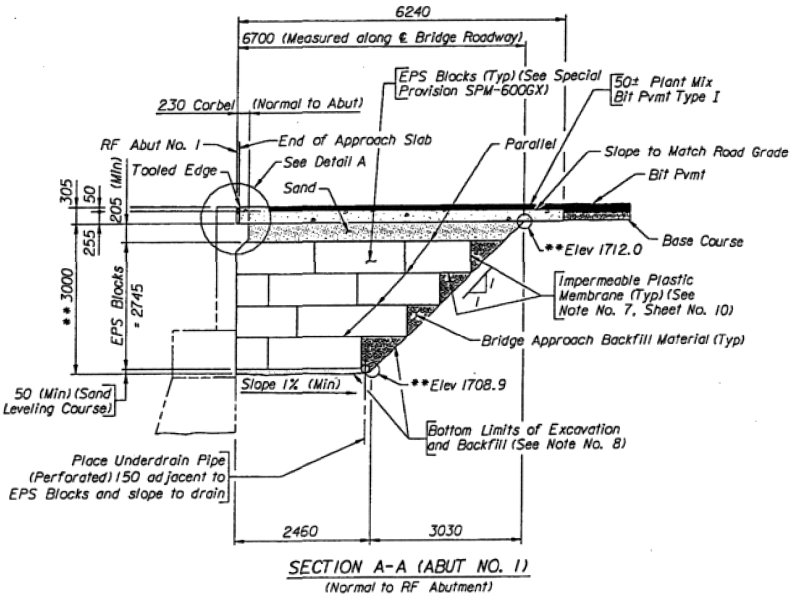

SECTION A-A (ABUT NO. 1)
(Normal to RF Abutment)

Note: 1) All reinforcing steel shall be coated.
2) For Sections B-B and C-C, see Sheet No. 10.
3) For Bill of Reinforcement see Sheet No. 10.
4) Place 13ASI bars parallel with ℄ Bridge Roadway.
5) The perforated underdrain pipe shall be wrapped with a layer of Geotextile Drainage and Filtration.
6) Dimensions and elevations preceded by a double asterisk (**) are measured at centerline bridge roadway.
7) For Settlement Plate Details, see Sheet No. 10.
8) The entire bottom of the excavation, including that portion under the perforated underdrain pipe and the exposed soil sides of the excavation, shall be lined with a layer of separation fabric prior to placement of sand leveling course.

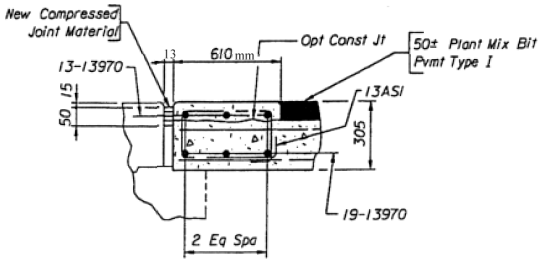

DETAIL A

FIGURE 11.15 PROJ 24-11m.doc

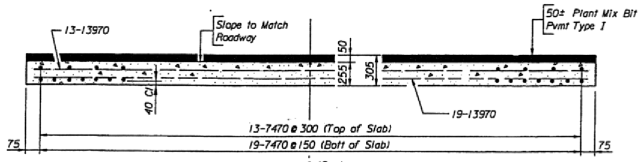

SECTION B-B

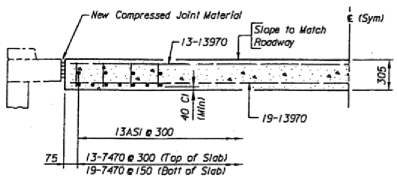

HALF SECTION C-C

BILL OF REINFORCEMENT		
Location	Mark	Number Req'd
Abutment No. 1	13ASI	39
	13-7470	39
	13-13970	22
	19-7470	77
	19-13970	22

BENDING DIAGRAM

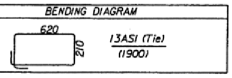

Note:
1) Underdrain Pipe (Perforated) 150 mm shall be capped at high end.
2) For location of Sections B-B and C-C, see Sheet No. 9.
3) The reinforcing steel fabricator shall prefix all approach slab bar marks with numeral 2 at Abutment No. 1.
4) The perforated underdrain pipe shall be wrapped with a layer of Geotextile Drainage and Filtration.
5) All reinforcing steel shall be coated.
6) For location of Settlement Plates, see Sheet No. 9.
7) All sides and the top of the EPS backfill shall be covered with a layer of Impermeable Plastic Membrane prior to backfilling next to and over the blocks.
8) Steel rods shall be field cut so that the top of the rod is 40 mm below the top of the asphalt.
9) Std Pipes shall be field cut so that the bottom of the pipe is 100 mm± above the Steel Settlement Plate.

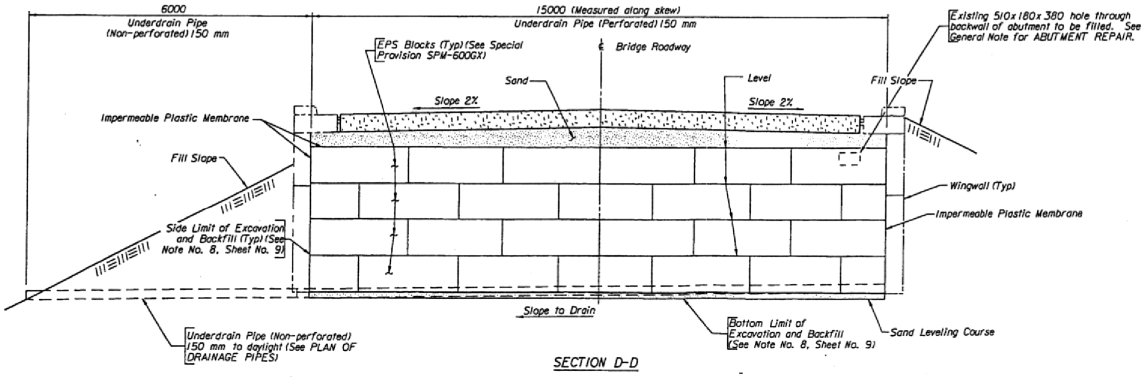

SECTION D-D

FIGURE 11.16 PROJ 24-11m.doc

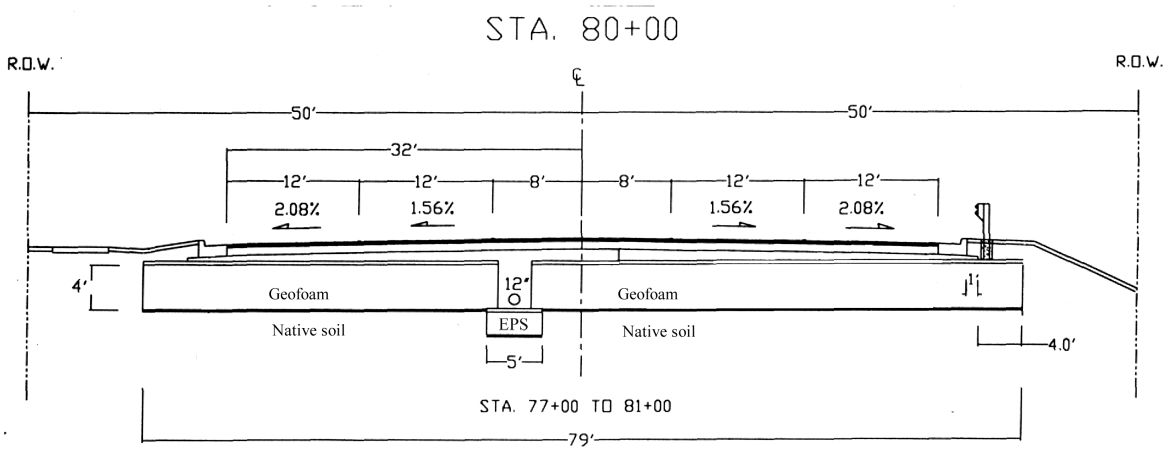

FIGURE 11.17 PROJ 24-11m.doc

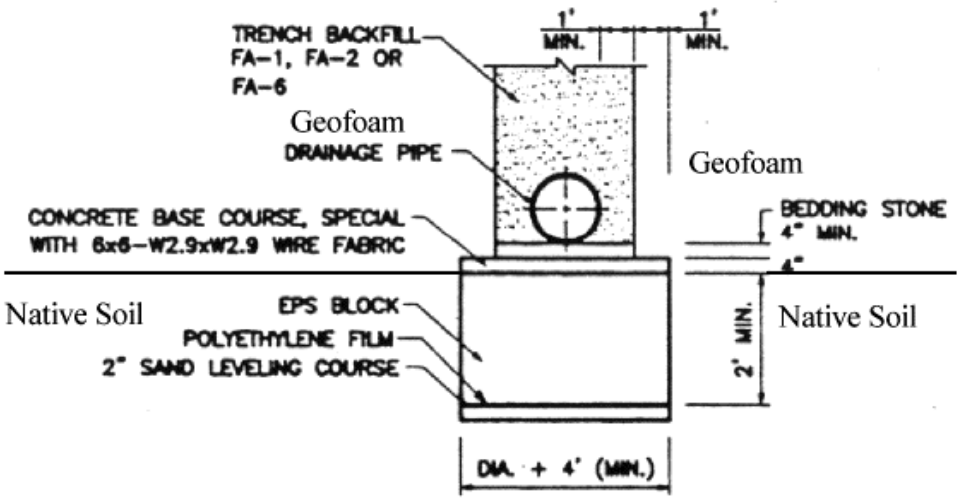

TYPICAL SECTION

EPS LAYOUT BENEATH STORM SEWER
(WITHIN EPS FILL SYSTEM)

FIGURE 11.18 PROJ 24-11m.doc

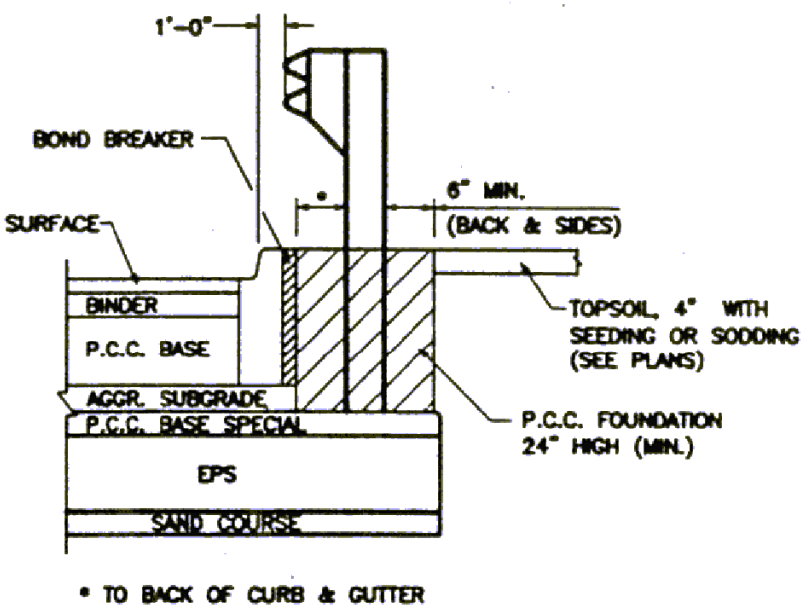

SPB GUARDRAIL, TYPE A, SPECIAL
(● EPS LOCATION W/GUARDRAIL)

FIGURE 11.20 PROJ 24-11m.doc

FIGURE 11.21 PROJ 24-11m.doc

FIGURE 11.22 PROJ 24-11m.doc

Activities	**Dates**
Excavation	10/11/95 to 10/26/95
EPS Placement	10/11/95 to 10/26/95
Concrete Slab Placement	10/23/95 to 10/27/95
No. 8 Aggregate Placement	11/2/95 to 11/8/95
Asphalt Base, Binder & Surface	11/22/95 to 11/29/95
Road Opened to Traffic	12/15/95

Items	EPS Embankment (Plan)				Total Removal & Replacement (Option)			
	Quantity	Unit	Unit Cost in U.S. Dollars	Cost in U.S. Dollars	Quantity	Unit	Unit Cost in U.S. Dollars	Cost in U.S. Dollars
Common Excavation	2,318.9 (3,033)	m^3 (yd^3)	$5.23 ($4.00)	$12,132	2,318.9 (3,033)	m^3 (yd^3)	$5.23 ($4.00)	$12,132
Peat Excavation	7,703.7 (10,076)	m^3 (yd^3)	$5.23 ($4.00)	$40,304	77,256.7 (101,048)	m^3 (yd^3)	$5.23 ($4.00)	$404,192
Borrow Fill	0	0	$0	$0	81,119.3 (106,100*)	m^3 (yd^3)	$6.54 ($5.00)	$530,500
Concrete Slab	3,066.1 (3,667)	m^2 (yd^2)	$40.66 ($34.00)	$124,678	0	0	$0	$0
EPS Block	4,708 (6,157)	m^3 (yd^3)	$86.58 ($66.20)	$407,593	0	0	$0	$0
Compacted Crushed Aggregate No. 8 Stone	1,360.8 (1,500)	Mg (ton)	$16.53 ($15.00)	$22,500	0	0	$0	$0
Total Cost				$607,207				$946,824

Notes: -The unit cost of peat excavation does not include cost for wet excavation, excavation using dredge line, peat disposal, etc. However, if this cost is added to the peat excavation then the cost of total removal and replacement option will be higher.

-* To estimate the fill volume, 5% is added to the volume of cut.

- Borrow fill is sand fill.

ITEM	UNIT	UNIT COST	QUANTITIES for MSE Wall	QUANTITIES for EPS Wall	MSE COST	EPS COST
Misc.Force Account Work	-	-	-	-	$15,000	$37,000
Dry Excavation	m^3 (yd^3)	15.70 (12.00)	1,192.7 (1,560)	1,529.1 (2,000)	$18,720	$24,000
Bridge Approach Backfill	m^3 (yd^3)	20.93 (16.00)	856.3 (1,120)	642.2 (840)	$17,920	$13,440
Bridge Approach Fill Reinforcing Fabric	m^2 (yd^2)	1.67 (1.40)	4,214.1 (5,040)	3,160.6 (3,780)	$7,056	$5,292
TOTAL					$58,696	$79,732

	EPS Block Approach Costs			MSE Approach Costs		
Item	Quantity	Unit Cost	Cost	Quantity	Unit Cost	Cost
Dry Excavation	210 m³ (275 yd^3)	$18.00 ($13.76)	$3,780	230 m³ (300 yd^3)	$18.00 ($13.76)	$4,140
Bridge Approach Backfill Material	20 m³ (26 yd^3)	$30.00 ($22.94)	$600	210 m³ (275 yd^3)	$30.00 ($22.94)	$6,300
Geotextile for Foundation Separation	110 m² (132 yd^2)	$6.75 ($5.64)	$742	0	0	$0
Geotextile for MSE	0	0	$0	850 m³ (1112 yd^3)	$1.75 ($1.34)	$1,487
Expanded Polystyrene Blocks	146 m³ (191 yd^3)	$104.00 ($79.52)	$15,184	0	0	$0
HDPE Geomembrane	200 m² (239 yd^2)	$4.50 ($3.76)	$900	0	0	$0
Reinforced Concrete Approach Slab	88 m² (105 yd^2)	$96.00 ($80.27)	$8,448	88 m² (105 yd^2)	$96.00 ($80.27)	$8,448
Underdrain Pipe (Perforated) 150 mm	6 m (20 ft)	$34.50 ($10.52)	$207	4.5 m (15 ft)	$34.50 ($10.52)	$155
Underdrain Pipe (Non-Perforated) 150 mm	15 m (49 ft)	$31.00 ($9.45)	$465	15 m (49 ft)	$31.00 ($9.45)	$465
		Total Cost =	$30,326		Total Cost =	$20,995

Project	Quantity of EPS $m^3(yd^3)$	Bid A Unit Price $/$m^3$($/yd^3)	Bid A Total Bid $	Bid B Unit Price $/$m^3$($/yd^3)	Bid B Total Price $
1	1,052 (1,376)	52.50 (40.14)	1,960,244	43.00 (32.88)	2,202,666
2	4,919 (6,434)	58.50 (44.73)	5,696,731	50.00 (38.23)	5,970,269

Project	Application	Placement Rate of EPS-Block Geofoam per Day
Hawaii	Embankment	175 – 250 m^3 (229 – 327 yd^3)
Indiana	Embankment	428 m^3 (560 yd^3)
New York	Slope Repair	382 – 383 m^3 (500 yd^3)
Utah I-15	Embankment	470 m^3 (615 yd^3)
Illinois	Embankment	313 m^3 (410 yd^3)

CHAPTER **12**

ECONOMIC ANALYSIS

Contents

INTRODUCTION

The goal of design and construction of highway embankments over soft ground is to provide an adequate transportation facility at the lowest overall life-cycle cost (*1*). Life-cycle

costs include design costs, construction costs, right-of-way costs, routine maintenance costs, periodic maintenance and rehabilitation costs, operating costs, accident costs, and users' cost (*1*). Additionally, performance and safety (e.g., pavement smoothness, foundation stability during construction, tolerable postconstruction total and differential settlements, hazards caused by maintenance operations and potential failures), inconvenience (e.g., costs to the public resulting from closing a roadway or traffic lanes for maintenance), environmental aspects, and aesthetic aspects should also be included in a life-cycle cost analysis (*1*). When all of these factors are evaluated, an alternative with a higher initial material or total cost, e.g. geofoam, may prove to be the best alternative.

Benefits of utilizing an EPS-block geofoam embankment or wall include: (1) ease and speed of construction, (2) placement in adverse weather conditions, (3) possible elimination of the need for surcharging and staged construction, (4) decreased maintenance costs as a result of less settlement from the low density of EPS-block geofoam, (5) alleviation of the need to acquire additional right-of-way to construct flatter embankment slopes because of the low density of EPS-block and/or the use of a vertical embankment, (6) reduction of lateral stress on bridge approach abutments, (7) excellent durability, (8) construction without utility relocation, and (9) excellent seismic behavior.

In a removal and replacement situation without surcharging, the use of geofoam may result in cost savings compared to other types of lightweight fill materials and conventional fill materials because the density of geofoam is $1/10^{th}$ to $1/30^{th}$ of the density of foamed concrete, $1/55^{th}$ to $1/145^{th}$ of the in-place density of boiler slag, and $1/100^{th}$ of the density of conventional granular fill material. The lower density of geofoam will have advantages over other types of lightweight fills in certain applications such as in embankment construction over existing utility corridors as occurred in the I-15 project in Utah (*2*). The low density of geofoam is also beneficial because seismic inertial force is proportional to the mass of the embankment. Thus, the lower

density of geofoam may alleviate the costs of soft soil removal and the possible need for an excavation support system, excavation widening, and temporary dewatering.

There is a limited amount of published information related to economic assessments made explicitly for EPS-block geofoam versus other design alternatives in road embankments on soft ground. Therefore, to address the issue of economic analysis, this chapter presents the available information for EPS-block geofoam projects and compares it to cost information for other design alternatives.

BACKGROUND

Comparison of various design alternatives requires that an economic analysis such as a life-cycle or cost-benefit analysis be performed. A cost-benefit analysis considers the intangible consequences or impacts of an alternative in addition to the tangible costs and benefits. These intangible consequences may be required to perform an adequate cost comparison. An overview of a cost-benefit analysis is presented in (*3*).

An approach for incorporating the intangible benefits into a life-cycle or cost-benefit analysis involves trying to quantify these benefits. For example, the benefit of reduced construction time can be quantified by estimating the value that travelers place on travel-time savings during periods of heavy congestion and incorporating the benefit into a life-cycle or cost-benefit analysis as discussed in (*4*). Based on traveler input from a survey performed for the State Route (S.R.) 91 corridor in Orange and Riverside Counties in Southern California, it was determined that the value that travelers place on total travel time varied from $2.64/hour for a household annual income of $15,000 to $8.05/hour for a household annual income of $95,000 (*4*).

Reduced construction time is also important if soft ground treatment is unanticipated during the construction phase or if the section of roadway or bridge approach that is to be treated affects the critical path of the construction schedule. Remedial treatment procedures such as stabilization by preloading may require several months to more than a year to complete. Maintenance and construction costs often increase as the time available for construction decreases

(*5*). Therefore, some of the least costly but more-time consuming techniques have become less attractive in recent years because of shorter project times, tighter schedules, and the need to maintain traffic (*5*). Consequently, soft ground treatment technologies such as the use of lightweight fills have taken on an increasing role in the construction of roadway embankments. The typically higher unit cost of some types of lightweight fill materials (a "negative" cited in (*5*) which was prepared in the late 1980s) is usually offset by savings when all of the project costs are considered. This greater use of lightweight fills in recent years is reflected in their inclusion in the FHWA Demonstration Project 116 (*6*).

This chapter summarizes cost data related to projects that have utilized or considered EPS-block geofoam versus other lightweight fill materials and ground improvement methods for roadway embankments on soft ground. This cost data summary along with the placement rates observed on geofoam projects in Table 11.6 are useful for performing an economic analysis of various alternatives. These placement rates can be used by contractors with little or no geofoam experience to develop reasonable bid packages instead of speculating on production rates, which usually result in an overestimate.

SCOPE

An important aspect of the research was to quantify the economic advantages of using EPS-block geofoam as a design alternative compared to other lightweight fill materials and traditional alternatives such as soil fill with ground improvement techniques (prefabricated vertical drains, geosynthetic reinforcement) or a structurally supported roadway. A brief summary of soft ground treatment alternatives available for the construction of embankments and bridge approaches and the results of a questionnaire distributed during this study relating to cost issues are presented. Cost-benefit data are tabulated for geofoam and alternative designs, where available, for each case history. Additionally, cost aspects of reinforced concrete caps over the geofoam are presented.

RESEARCH APPROACH

Because of limited published cost data for geofoam embankments, various strategies were employed to obtain cost comparison data:

- Cost information was solicited via a geofoam usage questionnaire (see Appendix A).
- Several Midwestern DOTs (Illinois, Indiana and Michigan) were contacted in an effort to obtain cost data. These states were chosen both for their proximity to the University of Illinois and their use of EPS-block geofoam technology for road construction.
- Personal contacts were made with individuals suggested in the usage questionnaire replies that indicated a knowledge of cost data.
- DOTs, companies, and individuals referenced in relevant geofoam technical literature were contacted.

- Cost data presented in the draft manual for the FHWA Demonstration Project No. 116 (*6*) and the National Cooperative Highway Research Program (N.C.H.R.P.) Synthesis No. 147 (*5*) were utilized.

SOFT GROUND TREATMENT ALTERNATIVES

A summary of various alternatives for treatment of problem foundations for highway embankments that have been used in the United States can be found in (*5*). These alternatives are also summarized in Table 12.1.

Various categories have been used to classify lightweight fills. Categories used in (*6*) include lightweight fill materials with compressive strength (geofoam, foamed concrete) and granular lightweight fills (wood fiber, blast furnace slag, fly ash, boiler slag, expanded clay or shale, shredded tires). Lightweight fill categories used in (*7*) include artificial fills (foam plastics and foamed concrete) and waste materials (shredded tires and wood chips). Lightweight fills are separated in (*8*) as traditional light material (wastes from the timber industry such as sawdust and bark, wastes from the production of building blocks of cellular concrete, and expanded clay aggregate) and superlight fill (EPS-expanded polystyrene block).

Table 12.1. Problem Foundation Treatment Alternatives (*5*).

Characteristics and Limitations of Lightweight Fill Materials

There is a significant range in material costs, engineering properties, and construction costs for various lightweight fills. The use of lightweight fill materials for embankments as an alternative to ground improvement increased during the 1990s. Although there are many reasons for this, two that appear to be among the more significant are:

- overall time for construction is typically much shorter when lightweight fills are used and
- the fact that lightweight fills produce relatively small undrained (initial) and consolidation settlements. Large undrained (initial) and consolidation settlements during construction may negatively affect adjacent existing roads, bridges,

buildings, utilities, etc. However, the use of lightweight fill materials will have no affect on the magnitude and time-dependent behavior of creep ("secondary consolidation") settlements but these settlements are significantly smaller than undrained (initial) and consolidation settlements. Creep is a function of the geometry and properties of the underlying soft soil subgrade only, and is thus independent of the external stresses applied to the subgrade. Of course, soil fill will also induce creep settlements.

Cost comparisons between different types of lightweight fills should be made on the price per cubic meter ($/yd^3) because of the wide variation of densities between the various lightweight fill materials (*6*). Equation (12.1) below is recommended in (*6*) for converting costs in dollars per ton to dollars per cubic meter:

dollars per ton x density in kg/m^3 x (1 ton/910 kg) = dollars per m^3. **(12.1)**

Geofoam blocks may also be priced in dollars per board foot (1 ft by 1 ft by 1 in) so conversion to dollars per cubic meter can be achieved using Equation (12.2) below:

dollars per board feet x (1 foot/ 0.305 m) x (1 inch/ 2.54 cm)(100 cm/1 m) =

dollars per m^3. **(12.2)**

Table 12.2 provides a general summary of lightweight fill material costs. As indicated in Table 12.2, lightweight fill material costs vary considerably. Factors that influence costs of utilizing the various types of lightweight fills include quantity required for the project, transportation costs, availability of materials, contractor's experience with the product, placement or compaction costs, and specialty items that may be required (*6,9*). Additionally the cost of using some waste fills will be dependent on the availability of state rebate programs.

Although some waste materials such as sawdust, bark, shells, cinders, slag, flyash, and bottom ash may be almost free at the source, transportation costs alone have made the use of some waste lightweight fill material uneconomical (*5*). The quantity required of a specified

lightweight fill type may not be available from just one vendor or source. In a project that used approximately 6,400 Mg (7,050 ton) of shredded tires as lightweight fill, four different vendors were required because no single vendor could provide the full quantity needed (*10*). The vendors were located about 240 to 440 km (150 to 275 mi) from the site, which resulted in a range of transportation costs.

A summary of the responses to the geofoam usage questionnaire are included in Appendix A. Questions B1, B2, and B3 of the questionnaire yielded information on costs associated with geofoam projects. Bid prices provided in the questionnaire replies varied widely and ranged from \$39.00 to \$98.00 per m^3 (\$30.00 to \$75.00 per yd^3) (see Table A.2 in Appendix A). These bid prices include material, transportation, placement, and contractor profit. The questionnaire responses show that the placement costs range from 35 to 45 percent of the unit bid price for geofoam. For example, if the unit bid price for geofoam, which includes material and labor, is \$70.00 per m^3 (\$53.52 per yd^3), the placement costs will range from \$24.50 to \$31.50 per m^3 (\$18.75 to \$24.10 per yd^3). However, another respondent indicates that placement costs range from about \$13.00 to \$20.00 per m^3 (\$10.00 to \$15.00 per yd^3) not including contractor profit.

In summary, the placement cost of EPS-block geofoam in roadway embankments can be assumed to range from \$13.00 to \$31.50 per m^3 (\$10.00 to \$24.10 per yd^3). This large range is probably caused by a large range in site conditions and contractor experience with geofoam. Items that were identified by the replies to have a significant impact on the overall cost of an EPS-block geofoam embankment or bridge approach are a reinforced-concrete capping slab, a facing system in the case of vertical geofoam fills, the cost of providing temporary dewatering during construction to prevent buoyancy of the geofoam from runoff that may accumulate in the excavation, the potential for a permanent drainage system, and the cost of lack of familiarity by local contractors with constructing a geofoam embankment which can result in over pricing of the geofoam alternative in the bid phase.

Table 12.2. Costs for Various Lightweight Fill Materials(*6*).

Placement and compaction costs can be higher for some types of lightweight fills than for conventional soil fill. For example, flyash and boiler slag are moisture sensitive and therefore, moisture control is critical for proper compaction of flyash and boiler slag. Proper compaction of shredded tires may require a greater number of compactor passes than for conventional soil fill (*6*). Of course, geofoam does not require moisture and compaction control, which allows placement in adverse conditions. Additionally, adverse weather conditions typically do not affect placement rates of geofoam. Therefore, the higher material cost of EPS-block geofoam may be offset by lower installation costs. The difference between loose and compacted density of some lightweight fill materials should be considered in the transportation and placement costs.

The wire strands exposed from tire shreds may puncture tires on construction equipment and prevent haul trucks from being routed over the fill (*10*). Thus the placement procedure for tire shreds may require additional measures to minimize the puncture hazard to construction equipment. These measures can result in extra placement costs. In addition, the thickness of shredded tires should be limited to 3 m (10 feet) to prevent spontaneous combustion fires.

The placement rate of foamed concrete may be slower than for EPS-block geofoam. Foamed concrete placement lifts are limited to depths of 0.6 m (2 ft) to minimize the presence of voids next to structures or formwork and to minimize the development of excessive heat of hydration which can negatively affect the foamed concrete air void content (*9*). Additionally, a 12-hr waiting period is required prior to the placement of subsequent foamed concrete lifts (*9*). The placement rates for geofoam embankments projects vary from 175m^3 (229 yd^3) to 428 m^3 (560 yd^3) per day as shown in Table 11.6.

The use of some types of lightweight fills may require the use of specialty items such as geotextiles, geomembranes, drainage blankets, and soil cover (*6*). The costs associated with the use of specialty items will depend on the specific lightweight fill embankment or bridge approach

design and these costs are not included in Table 12.2. For example, a geomembrane has been used to protect EPS-block geofoam from hydrocarbon spills.

An example of a project in which an item that could not be easily quantified but had an impact on the selection of a construction alternative is demonstrated by the new Charter Oak Bridge project in Hartford, CT. The bridge opened to traffic in August 1991 (*12*). Although an earthen embankment with a toe berm placed in the river was the most economical solution of the stabilization alternatives considered, it was rejected because of the delays associated with the time required to obtain environmental permits (*12*). The lightweight fill alternative consisting of expanded-shale aggregate, which cost an additional $2 million in construction compared with the conventional earth fill/berm/surcharge design, was used to construct the east approach. A total of 62,730 m^3 (82,050 yd^3) of lightweight fill was utilized. As indicated in Chapter 11, the cost of the EPS-block geofoam on one bridge approach for the N.F. Shoshone River Bridge Rehabilitation project was higher than the mechanically stabilized earth wall alternative, but the Wyoming DOT utilized geofoam because of its greater speed of construction and placement in adverse conditions. EPS-block geofoam was placed in utility corridors as part of the I-15 reconstruction project in Utah because of the potential cost and time savings associated with not having to re-locate utilities or repair utilities that were left in place and damaged by foundation settlement and the accompanying service interruption (*13*). In summary, geofoam provides a number of intangible benefits such as not requiring an environmental permit, greater speed of construction, placement in adverse conditions, long-term durability, consistent material properties, and no utility replacement that should be considered in the design and selection process.

Comparison of Lightweight Fill Material Properties

Most lightweight fills have favorable Mohr-Coulomb shear strength properties (i.e., cohesion and angle of internal friction) which may increase the internal stability of an embankment and increase the overall global stability of the embankment (*6*). Additionally, EPS-block geofoam and foamed concrete have low Poisson's ratio and low density resulting in

reduced lateral stresses applied to walls compared to conventional soils. Manufactured materials such as EPS-block geofoam and foamed concrete also have more uniform and consistent material properties than waste materials.

EPS-block geofoam, foamed concrete, expanded shale and clay, flyash, boiler slag, and air cooled slag have a compressibility and elasticity similar to natural soil and consequently these materials will behave under static and dynamic loads similar to conventional earth materials (*14*). However, shredded tires and wood fiber fills have a higher compressibility than conventional compacted soils (*6*). Thus, this higher compressibility must be considered in the pavement design. Settlements on the order of 10 to 15 percent have been observed in various shredded tire embankment projects (*15*). In the U.S. Route 42 project near Roseburg, Oregon, the shredded tire embankment (*10*) compressed 15 percent of its initial height between January and September 1991. This compression included compression due to the soil cap, aggregate base, and pavement surcharges as well as 3 months of traffic (*15*). The results of the settlement plate data indicate that a correlation existed between the thickness of shredded tire fill and compression measured. Although the use of shredded tires and wood fiber as lightweight fill may not result in intolerable settlement due to consolidation of the underlying soft foundation soil, a staged construction procedure, consisting of placing the pavement at a later date, may be required to allow for some settlement of the tire shreds or wood fibers to occur.

Shredded tires and wood fiber fills have a larger resiliency than geofoam and conventional compacted soils. Thus, this higher resiliency must be considered in the design and an appropriate soil cover must be placed over these materials to reduce the resiliency. A soil cover of at least 1m (3.3 ft) thick is typically placed over these materials (*6*). A 15.2 m (50 ft) section of embankment constructed as part of a landslide repair project on U.S. Route 42 near Roseburg, Oregon experienced cracking and rutting because the soil cap was only 0.5 to 0.6 m (1.5 to 2 ft) thick instead of the required 1.0 m (3.3 ft) (*10*). Thus, a thick soil cap is typically required over tire fills in order to increase the confining pressure and should be included in the

cost estimate. This resiliency also may limit the type of pavement used over shredded tires and wood fiber fills to a flexible pavement type. Falling weight deflectometer (FWD) tests were performed as part of the U.S. Route 42 project near Roseburg, Oregon after the aggregate base was placed, after the first lift of asphalt pavement was placed, and after the final asphalt pavement lift was placed (*10*). The results of the deflectometer tests performed after the first lift of asphalt pavement was placed resulted in the addition of 5.1 cm (2 in.) of asphalt pavement as part of the second lift. Thus, the total thickness of pavement is 25.4 cm (10 in.). Based on the results of the deflectometer tests, it was concluded that the shredded tire fill represented a softer subgrade than the in-situ subgrade.

Favorable construction aspects of EPS-block geofoam embankments include possible placement in adverse weather conditions and the ease and speed of construction. Placement of EPS fill is not greatly affected by rainy weather (*16*) nor by cool temperatures as was demonstrated by the Route 23A case history in Greene County, New York (*17*). The use of conventional earth fill as well as some types of lightweight fills such as fly ash and boiler slag require favorable weather conditions to achieve proper compaction because these materials are moisture sensitive.

Limitations to the use of some lightweight materials include difficulty in placing and handling such as fly ash when it is too dry or wet (*6*). Shredded tires may also be difficult to place because of their resiliency under compaction equipment. Sawdust and bark are difficult to compact (*15*). Other limitations of some lightweight fill materials include the need to incorporate protective measures to maintain good durability, to minimize leachate into the surrounding environment, and to maintain suitable geothermal properties.

Lightweight fill materials need to be protected to maintain good durability (*6*). The surface of EPS-block geofoam must be covered for protection against long-term ultraviolet radiation. If desired measures can also be taken to protect the EPS blocks from potential liquid petroleum hydrocarbon (gasoline, diesel fuel/heating oil) spills and damage from insect

infestation. Sufficient cover must be maintained over fly ash embankments to minimize erosion of the side slopes. A potential problem associated with sawdust and bark are that they are biodegradable and need to be encapsulated by a soil cover to minimize deterioration of the outer part of the wood fiber embankment with time (*15*).

Some lightweight fill materials must incorporate measures to minimize leachate that some lightweight fill materials may produce (*6*). Sawdust and bark require treatment to prevent groundwater pollution (*15*). Slags, cinders, and fly ash leachates may adversely affect groundwater quality or the structures in the vicinity of the waste material fill (*15*). Leachate of metals and hydrocarbons is a possible concern with using tire shreds. However, field study reports have shown that shredded automobile tires are not a hazardous material because the parameters of concern do not generally exceed the EP toxicity and Toxicity Characteristic Leaching Procedure (TCLP) criteria (*15*).

Most lightweight fill materials have geothermal properties that are different from soil (*6*). Problems with accelerated deterioration of flexible pavements or differential icing may occur if adequate design methods are not used. Potential combustible nature of tires is a concern with the use of shredded tires in roadway embankments and caution is required during construction to avoid any fire in tires that are stockpiled or already placed in the embankment (*15*). In general, the thickness of shredded tires should be limited to 3 m (10 ft) to prevent fires. A suitable thickness of protective earth cover is typically required on the top and side slopes of tire embankments. As with any plastic material, geofoam is flammable (*14*). Fire concerns with EPS-block geofoam can be alleviated by the addition of flame-retardant during the production of the geofoam blocks and adequate seasoning times as described in Chapter 9.

SUMMARY OF EPS-BLOCK GEOFOAM COST DATA

Table 12.3 summarizes cost data from the geofoam case histories in Chapter 11 and the usage questionnaire replies.

It can be seen from Table 12.3 that the unit cost for EPS-block geofoam varies widely and ranges from $39.00 to $104.00 per m^3 ($30.00 to $80.00 per yd^3) including transportation and placement costs. In (*6*) it is indicated that the cost ranges from $35.00 to $65.00 per m^3 ($26.00 to $50.00 per yd^3) FOB (freight on board) at the plant. The EPS Molders Association provided the cost data shown in Table 12.4 in a letter dated 10 April 2001. The material cost is a function of geofoam density but ordering more than one density should not affect the price significantly beyond the cost of the higher density material. The results of the usage questionnaire indicate that placement costs range from 35 to 45 percent of the unit bid price for geofoam. Based on the I-15 project in Utah, the cost of a fascia wall system is about $10.00 per m^3 ($7.00 per yd^3) (*2*).

A summary of costs associated with utilizing a reinforced concrete cap slab as a separation material between the pavement system and the EPS blocks is included in Table 12.5. As indicated in this table, the cost of a reinforced cap is relatively high and can range from 20 to 30 percent of the total project cost.

Table 12.3. Summary of EPS-Block Geofoam Embankment Costs.

Table 12.4. Geofoam material costs from EPS Molders Association based on 2000 business conditions.

Table 12.5. Summary of Reinforced PCC Separation Slab Costs.

Table 12.6 presents a list of all of the costs that could be incurred on a geofoam embankment project. This list is comprehensive and thus not all items will be required on a project. However, the large number of costs provides some insight to why the cost of EPS-block geofoam embankments ranges from $39.00 to $104.00 per m^3 ($30.00 to $79.52 per yd^3) including transportation and placement. Many of the costs in Table 12.6 are also incurred on embankment projects that do not utilize geofoam. It can be seen that Table 12.6 subdivides the costs into manufacturing costs, design detail costs, and construction costs.

Table 12.6. Potential Costs Associated with an EPS-Block Geofoam Project.

Cost data does not exist in published literature that allows a cost breakdown to account for all of the items listed in Table 12.6. Additionally, cost information that the various DOTs provided during this study are based on unit prices that include both material and installation. Thus, a cost breakdown of separate items such as manufacturing, transportation, placement, flame and insect retardant, and connection plates could not be performed during this study. However, based on the literature search, some general conclusions can be made regarding several geofoam cost issues.

- Design optimization requires an iterative analysis that considers the interaction between the three major components of the embankment or bridge approach (foundation soil, fill mass, and pavement system) to achieve a technically acceptable design at the lowest overall cost. An example of this interaction is the pavement system thickness which affects both the internal and external embankment stability by affecting the applied surcharge at the top of the embankment.
- The selection of an appropriate cross-sectional geometry as well as selection of the volume and density of EPS block should be carefully considered during the design process. For example, the use of a fill geometry with vertical sides as opposed to the more-traditional sloped-side geometry will provide the following advantages and disadvantages:
  - The volume of fill material, especially of the EPS blocks, is minimized, which reduces both material cost and construction time.
  - The footprint of the embankment and concomitant right-of-way acquisition is minimized, which can have cost, environmental potential, and other benefits.
  - The cost of covering the vertical faces of the EPS blocks with some type of structural material (which can impart a significant concentrated vertical force on the soft subgrade) as well as the need for a PCC slab on top of the EPS blocks (for anchorage of road hardware) may offset some of the savings of using vertical sides. Shotcrete is often the

least expensive facing alternative when architectural concerns are minimal or non-existent. When a more-attractive finish is desired, full-height precast PCC panels are used most often and can impart a significant cost.

  - Because EPS-block geofoam is typically more expensive than soil on a cost-per-unit-volume basis for the material alone, it is desirable to optimize the design to minimize the volume of EPS used yet still satisfy settlement and stability criteria. The selection of an appropriate EPS block density must also be optimized because the cost of EPS block increases with increasing density. For example, an EPS block with an overall average density of 32 kg/m^3 (2.0 lbf/ft^3) would use twice as much raw material as an EPS block with an overall average density of 16 kg/m^3 (1.0 lbf/ft^3) . In the U.S., raw material cost accounts for one half or more of the manufacturing cost of an EPS block so the impact of EPS density on project costs can be significant as shown in Table 12.4.

- End users should be aware of the fact that purchasing EPS-block geofoam through a distributor, as opposed to purchasing directly from a local block molder, generally results in a greater unit cost for the product because of distributor markup for overhead and profit. In many cases, there is no value added by a distributor.
- Specification of an insect deterrent will, in most parts of the U.S., restrict the number of molders that can supply a project. Because of this lack of competition and the inherent cost of the additive, the unit cost of the EPS blocks can be significantly higher.
- The routine use of mechanical connectors should be avoided because, while not technically detrimental, the connectors add a significant cost to a project.
- Typically, site preparation cannot be achieved by mechanical equipment alone so some manual labor will be required to achieve a reasonably planar ("smooth") subgrade surface prior to the placement of the first block layer.

- Where possible, it is desirable to try to use EPS blocks in their full as-molded size, assuming that the blocks meet certain dimensional quality criteria for straightness, etc. Although it is possible to factory cut a seasoned block into a smaller size, such cutting can add significantly to the unit cost of the final EPS-block geofoam product.

Summary of Foundation Improvement Cost Data

A lack of cost comparison data between EPS-block geofoam and various ground improvement techniques exists in the published literature. However, foundation improvement techniques are generally more expensive and more uncertain than the use of geofoam or another lightweight fill. Cost data on foundation improvement techniques are included here to provide a convenient means of performing a general cost comparison between the use of geofoam and various ground improvement techniques. The cost information for ground improvement techniques was obtained from (*6*).

Prefabricated Vertical Drains

Prefabricated vertical drains (PVDs), also referred to as wick drains, are used to accelerate consolidation of soft saturated compressible soils under load (preloading and/or surcharging). The main benefit of using PVDs with a surcharge compared to only using a surcharge include decreasing the time required for completion of settlement and final construction, which increases the rate of strength gain and associated increase in stability of the underlying soft soils (*6*). Limitations of using PVDs include the time required for consolidation to occur even with PVDs and the magnitude of secondary compression settlements are not reduced by the use of PVDs. Table 12.7 provides typical price ranges for PVDs. A mobilization and demobilization charge of $8,000 to $10,000 is typically added to these prices.

Table 12.7. **Typical Prefabricated Vertical Drain Unit Prices (*6*).**

Vibro-Compaction

The typical price per linear meter of vibro-compaction is approximately $15/m ($13.72/yd) when no backfill is placed around the probe and $25/m ($7.62/ft) when granular

backfill is added (*6*). The cost of the backfill will vary depending on the location of the project. A mobilization and demobilization cost of $15,000 per piece of installation equipment should also be added to the project cost.

Soil Nailing

Based on review of historical bid data compiled under FHWA-SA-96-069, the average bid price determined in (*6*) is approximately $380/m^2 ($318/yd^2) of wall. This is the average price for a soil nailed wall with a cast-in-place wall facing without a complicated architectural treatment. Architectural finishes on the facing augment the cost by $30/m^2 ($25/yd^2) of wall. Precast panel or timber faced walls average $600/ m^2 ($502/yd^2).

Stone Columns

The minimum cost of vibro-replacement stone column installation with readily available backfill material is $45 per linear metre ($13.72 per linear feet) and a dry vibro-displacement stone column starts at $60 per linear metre ($18.29 per linear feet) (*6*). Vibro-concrete columns raise the minimum cost of the column to $75 per metre ($22.87 per linear feet). Mobilization and demobilization costs approximately $15,000 per piece of installation equipment. The material cost of the stone backfill is a major component of the project and can account for over 40 percent of the estimated cost of stone column installation.

Soil Mixing

Based on deep soil mixing cost data from over a dozen projects completed in the last decade in the United States, soil mixing costs range from $100 to $150 per cubic metre ($76.50 to $115 per cubic yard) of volume treated (*6*). Mobilization and demobilization costs are about $100,000.

The cost of the first lime-cement column project in the U.S. for the I-15 project in Salt Lake City is $30 per linear metre ($9.00 per linear feet). On average this is about $60 per cubic metre ($45.00 per cubic yard) or about one-half the cost of deep soil mixing construction.

However, this project was implemented under a design-build contract and therefore detailed cost information is not readily available.

Mechanically Stabilized Earth (MSE) Walls

The typical total cost for MSE walls range from $160 to $300 per m^2 ($134 to $251 per yd^2) of face. The cost of the system is a function of wall height and the cost of the select fill. Bid prices for the I-94 project constructed in the City of St. Paul, MN indicates that the bid cost was $270 per square metre ($226 per square yard) installed for an MSE wall with dry cast segmental blocks facing units and a bid price of $409 per square metre ($342 per square yard) for cast-in-place concrete walls. In general, the use of MSE walls results in savings on the order of 25 to 50 percent and possibly more in comparison with a conventional reinforced concrete retaining structure, especially when the latter is supported on a deep foundation system. The low bid price for an MSE wall with precast concrete facing units for the US 23 (I-18 Extension) Unicoi County Tennessee was $313/$m^2$ ($262/$yd^2$). This price included the placement and compaction of the select fill within the reinforced soil zone. The average erection rate was 60 square meters per day (646 square feet per day).

For segmental pre-cast concrete faced MSE wall structures, the cost of the wall in terms of its principal components can be estimated as 20 to 30 percent of the total cost for erection of panels and contractors profit, 20 to 30 percent of total cost for reinforcing materials, 25 to 30 percent of total cost for facing system, and 35 to 40 percent of total cost for backfill materials including placement where the fill is a select granular fill from an off-site borrow source. The cost of excavation which may be somewhat greater than for other wall systems also needs to be considered. An approximate cost comparison between MSE walls and EPS-block geofoam is provided in the Utah I-15 reconstruction case history in Chapter 11.

SUMMARY

The case histories presented in Chapter 11 and summarized in this chapter reveal that EPS-block geofoam is cost competitive with other options for embankment and wall applications

even though the blocks have a higher material cost than soil fill material. The case histories show a cost of geofoam and MSE walls of $39 to $104 per m^3 ($30.00 to $80.00 per yd^3) and $100 to $300 per m^3 ($76.00 to $230.00 per yd^3) of wall face, respectively. The case histories show a cost of a trapezoidal geofoam embankment and a removal and replacement soil embankment of $13 to $220 per m^3 ($10 to $169 per yd^3) and $9 to $13 per m^3 ($7 to $10 per yd^3), respectively. The typical range of a trapezoidal geofoam embankment is $13 to $31.50 per m^3 ($10 to $24 per yd^3). In summary, vertical geofoam embankments are extremely cost-effective because they are more cost-effective than MSE walls, which are usually 25 to 50 percent more cost-effective than conventional reinforced concrete retaining structures. By comparison, trapezoidal embankments made of geofoam versus soil appear to be less favorable on a cost basis because the intangible benefits of using geofoam are not adequately reflected. These intangible benefits include shorter construction time because of faster placement rates, reduced utility relocation, or reduced maintenance costs. However, the low end of the cost of geofoam is in agreement with a soil embankment ($13 per m^3 ($10 per yd^3)), which suggests that if a knowledgeable contractor is available, geofoam is a cost-effective alternative to soil fill. The wide range of EPS-block walls and embankments that have been constructed indicate that a number of factors contribute to the cost of geofoam structures including material, site preparation, and contractor familiarity with geofoam. Thus, site specific cost estimates should be developed before comparing EPS-block solutions to more traditional solutions.

REFERENCES

1. Ceran, T., and Newman, R. B., "Maintenance Considerations in Highway Design." *NCHRP Report 349,* Transportation Research Board, Washington, D.C. (1992) 81 pp.
2. Bartlett, S., Negussey, D., Kimble, M., and Sheeley, M., "Use of Geofoam as Super-Lightweight Fill for I-15 Reconstruction (Paper Pre-Print)." *Transportation Research Record 1736,* Transportation Research Board, Washington, D.C. (2000) .
3. Campbell, B., and Humphrey, T. F., "Methods of Cost-Effectiveness Analysis for Highway Projects." *NCHRP Synthesis 142,* Transportation Research Board, Washington, D.C. (1988) 22 pp.
4. Small, K. A., Noland, R., Chu, X., and Lewis, D., "Valuation of Travel-Time Savings and Predictability in Congested Conditions for Highway User-Cost Estimation." *NCHRP Report 431,* Transportation Research Board, Washington, D.C. (1999) 74 pp.

5. Holtz, R. D., "Treatment of Problem Foundations for Highway Embankments." *NCHRP Synthesis 147,* Transportation Research Board, Washington, D.C. (1989) 72 pp.
6. Elias, V., Welsh, J., Warren, J., and Lukas, R., "Ground Improvement Technical Summaries." *Publication No. FHWA-SA-98-086,* 2 Vols, U.S. Department of Tranportation, Federal Highway Administration, Washington, D.C. (1999) .
7. Monahan, E. J., *Construction of Fills*, 2nd ed., John Wiley & Sons, Inc., New York, N.Y. (1994) 265 pp.
8. Flaate, K., "The (Geo) Technique of Superlight Materials." *The Art and Science of Geotechnical Engineering At the Dawn of the Twenty-First Century: A Volume Honoring Ralph B. Peck,* E. J. Cording, W. J. Hall, J. D. Haltiwanger, J. A.J. Hendron, and G. Mesri, eds., Prentice Hall, Englewood Cliffs, N.J. (1989) pp. 193-205.
9. Harbuck, D. I., "Lightweight Foamed Concrete Fill." *Transportation Research Record 1422,* Transportation Research Board, Washington, D.C. (1993) pp. 21-28.
10. Upton, R. J., and Machan, G., "Use of Shredded Tires for Lightweight Fill." *Transportation Research Record 1422,* Transportation Research Board, Washington, D.C. (1993) pp. 36-45.
11. "Processed Blast Furnace slag, The All-Purpose Construction Aggregate." *Bulletin No. 188-1,* National Slag Association (1988) .
12. Dugan, J. P., "Lightweight Fill Solutions to Settlement and Stability Problems on Charter Oak Bridge Project, Hartford, Connecticut." *Transportation Research Record 1422,* Transportation Research Board, Washington, D.C. (1993) pp. 18-20.
13. Bartlett, S. F., "Research Initiatives for Monitoring Long Term Performance of I-15 Embankments, Salt Lake City, Utah." *Proceedings of the 34th Symposium on Engineering Geology and Geotechnical Engineering,* Utah State University, Logan, Utah, (1999) pp. 54-67.
14. Horvath, J. S., *Geofoam Geosynthetic*, , Horvath Engineering, P.C., Scarsdale, NY (1995) 229 pp.
15. Ahmed, I., and Lovell, C. W., "Rubber Soils as Lightweight Fill." *Transportation Research Record 1422,* Transportation Research Board, Washington, D.C. (1993) pp. 61-70.
16. Mimura, C. S., and Kimura, S. A., "A Lightweight Solution." *Geosynthetics '95 Conference (1995: Nashville, Tenn.) Conference Proceedings,* Nashville, Tenn., Vol. I (1995) pp. 39-51.
17. Jutkofsky, W. S., "Geofoam Stabilization of an Embankment Slope, A Case Study of Route 23A in the Town of Jewett, Greene County." Geotechnical Engineering Bureau, New York State Department of Transportation, Albany (1998) 42 pp.

Method	Variations of Method
Berms; flatter slopes	
Reduced-stress method	Lightweight Fill: bark, sawdust, peat, fuel ash, slag, cinders, scrap cellular concrete, low-density cellular concrete, expanded clay or shale (lightweight aggregate), expanded polystyrene, shells.
Pile-supported roadway	
Removal of problem materials and replacement by suitable fill	Complete excavation, partial excavation, displacement of soft materials by embankment weight assisted by controlled excavation, displacement by blasting.
Stabilization of soft-foundation materials by consolidation	By surcharge only, by surcharge combined with vertical drains, by surcharge combined with pressure relief wells or vertical drains along toe of fill.
Consolidation with paving delayed (stage construction)	Before paving, permit consolidation to occur under normal embankment loading without surcharge, accept postconstruction settlements.
Chemical alteration and stabilization	Lime and cement columns, grouting and injections, electro-osmosis, thermal, freezing, organic.
Physical alteration and stabilization; densification	Dynamic compaction, blasting, vibrocompaction and vibroreplacement, sand compaction piles, stone columns, water.
Reinforcement	Geotextiles and geogrids, fascines, Wager short-sheet piles, anchors, root piles.

Lightweight Fill Type	Range in Density/Unit Weight, kg/m^3 (lbf/ft^3)(*4*)	Range in Specific Gravity	Approximate Cost, $/m^3 ($/yd^3)	Source of Costs
EPS (expanded polystyrene)-block geofoam	12 to 32 (0.75 to 2.0)	0.01 to 0.03	35.00 - 65.00 (26.76 - 49.70)(2)	Supplier
Foamed portland-cement concrete geofoam	335 to 770 (21 to 48)	0.3 to 0.8	65.00 - 95.00 (49.70 - 72.63)(3)	Supplier, (*9*)
Wood Fiber	550 to 960 (34 to 60)	0.6 to 1.0	12.00 - 20.00 (9.17 - 15.29)(1)	(*11*)
Shredded tires	600 to 900 (38 to 56)	0.6 to 0.9	20.00 - 30.00 (15.29 - 22.94)(1)	(*10*)
Expanded shales and clays	600 to 1,040 (38 to 65)	0.6 to 1.0	40.00 - 55.00 (30.58 - 42.05)(2)	Supplier, (*9*)
Boiler slag	1,000 to 1,750 (62 to 109)	1.0 to 1.8	3.00 - 4.00 (2.29 - 3.06)(2)	Supplier
Air cooled blast furnace slag	1,100 to 1,500 (69 to 94)	1.1 to 1.5	7.50 - 9.00 (5.73 - 6.88)(2)	Supplier
Expanded blast furnace slag	Not provided	Not provided	15.00 - 20.00 (11.47 - 15.29)(2)	Supplier
Fly ash	1,120 to 1,440 (70 to 90)	1.1 to 1.4	15.00 - 21.00 (11.47 - 16.06)(2)	Supplier

Notes: These prices correspond to projects completed in 1993 - 1994. Current costs may differ due to inflation.

(1) Price includes transportation cost.

(2) FOB (freight on board) at the manufacturing site. Transportation costs should be added to this price.

(3) Mixed at job site using pumps to inject foaming agents into concrete grout mix.

(4) Lightweight fill materials typically are characterized in the U.S.A. using the quantity of unit weight with I-P units. Therefore, the dual unit system of density in SI units of kg/m^3 and unit weight in I-P units of lbf/ft^3 is used in this table.

Date	Location of Project	Project Type	Quantity of EPS-Block m^3 (yd^3)	Unit Cost of EPS-Block \$/m^3 (\$/yd^3) (1)	Approximate Placement Rate m^3/day (yd^3/day)	Contract Value \$
1993	Wyoming	Bridge Approach	377 (493)	39.00 - 72.00 (30.00-55.00) (2)	-	79,732
1993-1994	Hawaii	Embankment	13,470 (17,618)	-	175-250 (229-327)	-
1995	Indiana	Embankment	4,708 (6,157)	86.58 (66.20)	428 (560)	607,207
1995	New York	Slope	3,116 (4,075)	85.01 (65.00)	382 (500)	-
1995	Washington	Bridge Approach	1,835 (2,400)	72.00 (55.00)	-	-
1995 ±	Washington	Embankment	411 (537)	105.94 (81.00)	-	-
1997-1999 ±	Wyoming	Bridge Approach	146 (191)	104.00 (79.52)	-	30,326
1999 ±	Connecticut	Embankment	321 (420)	98.00 (75.00)	-	-
1999 ±	Maine	Embankment	-	57.21 (43.74) FOB Site		
1999 ±	Michigan	Embankment	1,052 (1,376)	52.50/ 43.00 (40.14/32.88) (3)	-	1,960,245/ 2,202,667
1999 ±	Michigan	Embankment	4,919 (6,434)	58.50/ 50.00 (44.73/38.23) (3)	-	5,696,732/ 5,970,269
1999 ±	Utah	Vertical Embankment	-	65.00 (50.00) (w/o facing wall) 75.00 (57.00) (with facing wall)	470 (615)	-
1999	Illinois	Embankment	15,291 (20,000)	-	313 (410)	-
1999	Wisconsin	Slope	-	61.50 (47.00)	-	-

Notes:
- Data not available.
(1) Unit cost of EPS blocks includes transportation and placement unless indicated otherwise.
(2)From usage questionnaire reply.
(3)The lowest two bid values are reported.

	Density, kg/m³ (lbf/ft³)			
	16 (1.0)	20 (1.25)	24 (1.50)	32 (2.00)
Typical price range for flame retardant foam (Based on 2000 business conditions)	$35.31-$49.70 per m^3 ($27-$38 per yd^3)	$51.01-$54.93 per m^3 ($39-$42 per yd^3)	$60.17-$74.55 per m^3 ($46-$57 per yd^3)	$77.17-$88.94 per m^3 ($59-$68 per yd^3)
Impact of volume	Generally a reduction of 10-25%, volume not quantified			
Cutting or trimming blocks to size	Up to 10% depending upon extent required			
Third party certification, if required	0-10% depending upon level of certification			

Date	Location of Project	Thickness cm (in.)	Area m^2 (yd^2)	Unit Cost \$/ m^2 (\$/yd^2)	Total Cost of Concrete Cap	Total Cost of Concrete Cap as a Percentage of Total Contract Value
1997-1999 ±	Wyoming	25.5 (10)	88 (105)	96.00 (80.27)	$8,448.00	28%
1999 ±	Utah	15.24 (6)	-	55.00 (46.00)	-	-
1995	Indiana	10.2 - 12.7 (4-5)	3,066 (3,667)	40.66 (34.00)	$124,678.00	21%

MANUFACTURING COSTS:
1. Raw material price 1.1 Flame retardant chemicals 1.2 Use of low-VOC expandable polystyrene 1.3 Shipping from raw material supplier to molder 1.4 Subjective marketing factors 2. Density 2.1 Cost of blocks with increasing density. 2.2 Use of only one density versus using different product densities on the same project. 3. Manufacturer's cost 3.1 Direct purchase from molder 3.2 Purchase from a distributor 4. Shop drawings 5. Complexity of factory cut of blocks 6. Insecticide 7. Transportation from molder to job site 8. Overall project volume 9. Project schedule
DESIGN DETAIL COSTS:
1. Use of connector plates 2. Geometeric complexities of block layout 3. Wall facing system for vertical-faced embankment or soil cover for slope-sided embankment 4. Pavement system 4.1 Separation/stiffening material 5. Permanent drainage system 6. Other specialty items such as geotextiles and geomembranes
CONSTRUCTION COSTS:
1. On-site handling and storage 2. Subgrade preparation 2.1 Smooth, free of large objects, reasonably dry, leveling layer (if required) 3. Use of connector plates 4. Field cutting and block placement 5. Number of different density blocks 6. Season of year construction takes place 7. Misc. project constraints 7.1 Hours allowed 7.2 Days allowed 7.3 Relationship of geofoam work to other components 8. Temporary dewatering 9. Wall facing system for vertical-faced embankment or soil cover for sloped-sided embankment 10. Pavement system 10.1 Separation/stiffening material 11. Permanent drainage system 12. Other specialty items such as geotextiles and geomembranes

Site Category	Size Range m (ft)	Unit Price Range
Small	3,000 to 10,000 (9,843 to 32,808)	$2.25 to $4.00 per m ($0.69 to $1.22 per ft)
Medium	10,000 to 50,000 (32,808 to 164,042)	$1.60 to $2.50 per m ($0.49 to $0.76 per ft)
Large	50,000 and greater (164,042 and greater)	$1.20 to $2.00 per m ($0.37 to $0.61 per ft)

CHAPTER **13**

FUTURE RESEARCH AND DEVELOPMENT

Contents

GENERAL

Although this report presents a comprehensive design methodology for geofoam and EPS-block geofoam has been successfully used as lightweight fill, this NCHRP study did identify three main areas where further research would enhance the current state of knowledge of geofoam. These areas can be divided into material properties, analyses, and general conceptual issues. The recommendations included herein are primarily based on literature reviewed prior to April 2000.

MATERIAL PROPERTIES

Issues related to geofoam material properties that require further study are:

- Determining the minimum time required for seasoning EPS blocks to outgas the blowing agent to an acceptable level.
- Quantifying interface friction angles for EPS/EPS interfaces at large displacements and displacement reversals for use in static and seismic internal stability analyses.
- Quantifying interface friction angles for EPS/dissimilar materials, such as a variety of widely used geotextiles and geomembranes.

- Comparison of the stress-strain behavior of full-size EPS blocks versus small test specimens routinely used in practice for engineering property and quality control/assurance testing.
- Development of a laboratory test procedure to define the small-strain stiffness of EPS blocks.
- Development of an accurate small-strain creep model so creep strains can be reliably estimated for lightweight fills. This should include correlations between laboratory and in-situ creep data.
- Development of a non-invasive testing device such as a sonic-wave device for routine on-site evaluation of the average density, initial tangent Young's modulus of an EPS block, and, if possible, average elastic-limit stress.
- Development of a standardized manufacturing quality assurance (MQA) procedure for EPS blocks to provide greater guidance to end users. Additionally, development and passage of an ASTM standard that is specific to the use of geofoam in geotechnical applications. The provisional AASHTO specification presented herein can serve as the framework for development of the ASTM standard.
- Development of reliable correlations between Young's modulus as measured in small laboratory test specimens and the behavior of full-size EPS blocks in situ.

ANALYTICAL ISSUES

Analytical issues requiring further research using numerical modeling, physical testing, and/or observation of full-scale structures are:

- Determine whether an external slope stability failure induces failure through individual EPS blocks or whether the blocks remain intact and displace as

individual elements as a result of the slope instability. This is important for the modeling of geofoam embankments in slope stability analyses. This would also include a consideration of how an EPS-block geofoam embankment behaves under large and rapid settlements such as associated with seismic liquefaction.

- Develop a more realistic procedure for evaluating the potential for basal translation (sliding) due to wind loading especially under Atlantic hurricane conditions that can affect the east coast of the U.S. This is required because the current procedure is conservative because it treats a trapezoidal embankment as a vertical embankment and thus the wind is assumed to act on a vertical face instead of a sloped embankment. An evaluation of the applicability of roof design shapes and procedures to side-sloped EPS-block geofoam embankments is recommended. This assessment would also consider whether the current AASHTO or ANSI/ASCE 7-95 code values for wind loading are appropriate for use in routine design practice.

- Determining the effectiveness of using geogrid or geocell reinforcement in the unbound layer(s) of a pavement system above a geofoam fill.

- Quantifying the effects of significant changes in ground water level, and the concomitant buoyancy of EPS blocks. In particular, development of strategies for securing the EPS blocks that do not rely on gravity loads, such as vertical ground anchors. Alternatively, evaluating the effectiveness of open-cell geosynthetic lightweight fills (termed geocombs) in synergistic combination with EPS geofoam to resist buoyancy.

- Development of a procedure to determine the types of pavement materials and thicknesses of such materials that are required over the EPS blocks to minimize the potential for differential icing of the pavement surface over the EPS. Such a

procedure may require the development of a rational method for quantifying the amount of heat energy (BTUs or joules) required from a pavement system to prevent differential icing. This would replace the current empirical methodology that is difficult to implement in routine design practice.

- A more detailed assessment of the potential for flexible pavement deterioration over the EPS due to solar heating and development of a procedure to determine the types of pavement materials and thicknesses of such materials that are required to minimize the potential for solar heating deterioration.

- Develop a better understanding of the seismic behavior of EPS-block geofoam fills, particularly their interaction with bridge abutments.

- A detailed assessment of the interaction between the thermally stable geofoam mass and integral-abutment bridges (also known as jointless bridges, integral bridge abutments, and U-frame bridges) that undergo complex combined rotation and translation due to seasonal thermal changes.

- Develop a rational methodology for determining when mechanical connectors, e.g., barbed plates, are required between EPS blocks, as well as a methodology for selecting the number and placement location. In addition, development of a new connector that can be copied and reproduced inexpensively to reduce the cost of using mechanical connectors instead of the proprietary designs currently available. Recent Japanese research indicates that the effectiveness of barbed-plate connectors is limited especially under seismic loading because it involves strain reversals and accumulated cyclic strains.

- Investigation of the seismic behavior of relatively tall and slender EPS-block geofoam fills is needed to assess the rocking mode of behavior. This mode of

behavior has been observed in recent full-scale shake-table tests performed in Japan.

CONCEPTUAL ISSUES

Two conceptual issues that require further consideration are:

- Revise the design methodology presented herein for EPS-block geofoam in roadway embankments to utilize Load and Resistance Factor Design (LFRD) instead of Allowable Stress Design (ASD). This may be desirable given the use of LFRD in other AASHTO codes. However, a review of (*1*) suggests that there are still some difficulties in using LFRD for non-foundation geotechnical elements, such as earth retaining structures and earthworks, and thus the provisional design guidelines included herein are based on the traditional ASD methodology.
- Develop standardized design details for facing systems (shotcrete, precast panels or blocks, EIFS coating, etc.) for geofoam walls.

REFERENCES

1. Goble, G., "Geotechnical Related Development and Implementation of Load and Resistance Factor (LRFD) Methods, *NCHRP Synthesis of Highway Practice 276*." Transportation Research Board, Washington, D.C. (1999) 69 pp.

APPENDIX A
GEOFOAM USAGE SURVEY: QUESTIONNAIRE

APPENDIX A

GEOFOAM USAGE SURVEY: QUESTIONNAIRE

Contents

A.1. INTRODUCTION

A geofoam usage survey was conducted via a questionnaire developed by the project team to obtain case history information, cost data, design details and other geofoam related information. The final draft version of the questionnaire was submitted to NCHRP via postal mail on September 11, 1999 for the required review and approval. Notice of approval of the submitted draft version was received from NCHRP on October 1, 1999.

Distribution of the questionnaire began in early October 1999. Questionnaires were mailed to the designated TRB representative in of each of the 50 states as well as the District of Columbia and Commonwealth of Puerto Rico for distribution to the appropriate local Department of Transportation (DOT) representative. Questionnaires were also sent to the EPS Molders Association (EPSMA) in Crofton, Maryland for distribution to their members as well as to attendees at the American Society of Civil Engineers continuing education seminar titled "Designing with Geofoam Geosynthetic" that was held in Randolph, Massachusetts on October 14-15, 1999. The questionnaire was mentioned on the Internet via the now defunct Geofoam WWW Site™ (<www.geofoam.org>).

Because recipients of the questionnaire were encouraged to copy and distribute it further to interested colleagues, clients, and customers, a 3.5" computer diskette containing the questionnaire document file in Microsoft Word 97 format was included with each paper copy of

the questionnaire that was distributed. As a result, it is not possible to state exactly how many copies were actually distributed.

The official deadline date for responses was November 30, 1999. A copy of the questionnaire is included in this appendix. A summary and synthesis of the survey replies follows the copy of the questionnaire in the appendix.

A.2. COPY OF SURVEY

Geofoam Usage Survey

National Cooperative Highway Research Program (NCHRP) Contract No. HR 24-11

"Guidelines for Geofoam Applications in Embankment Projects"

Introduction

Geofoam is the generic term for any closed-cell foam material used in a geotechnical application. Geofoam is now recognized as a category of geosynthetic materials and related products in the same way as geotextiles, geomembranes and geogrids.

Many different types of foams have been used in geofoam applications over the years, with the first documented applications dating back to the mid 1960s. While several materials have performed satisfactorily in geofoam applications, block-molded expanded polystyrene (EPS block) emerged long ago as the material of choice in most applications for both technical and cost reasons.

EPS-block geofoam can be used for several geosynthetic functions or roles. One of the most widely used to date is as lightweight fill material beneath roads. The first documented project for this was the reconstruction of the Flom Bridge approach embankment in Norway in 1972. Thus the use of EPS-block geofoam as a lightweight fill for road construction represents a mature, not experimental, technology with almost 30 years of proven, successful use. This includes numerous projects in the U.S.A. for all types of roads, including those built to Interstate standards.

Although EPS-block geofoam for road construction is a well-established technology, it is currently underutilized in U.S. practice. To increase usage in the future, the National Research

Council through its Transportation Research Board has recently funded a research team (John S. Horvath, Ph.D., P.E. and Dov Leshchinsky, Ph.D.) led by Timothy D. Stark, Ph.D., P.E. at the University of Illinois at Urbana-Champaign to conduct a two-year project. The primary goal of this project is to develop practical and practice-oriented design guidelines and specifications in AASHTO format to facilitate the use of EPS-block geofoam as a lightweight fill in road embankments and bridge approach fills over soft ground. It is anticipated that these documents will encourage engineers to consider design alternatives incorporating EPS-block geofoam more in the future than they have in the past.

In keeping with the practice-oriented nature of this project, outside input is being solicited from, and peer review of the project documents will be undertaken by, all three groups that have a major influence on projects involving the use of EPS-block geofoam for road construction:

- design engineers acting on behalf of an agency having jurisdiction over roads,
- molders (manufacturers) and distributors of EPS-block geofoam, and
- construction contractors who build roads.

An important part of this outreach is a survey on geofoam usage to obtain input from members of each of these three groups. The attached two-part questionnaire is the primary component of this survey. Thus your completion of this questionnaire is crucial to helping us produce deliverables that are as responsive as possible to the needs of all concerned. Please complete only one questionnaire per organization or company and return your completed questionnaire no later than November 30, 1999 so your input can be included in the final report. A disk of the questionnaire in Word 97 format is also provided for your convenience. Thank you in advance for your cooperation and assistance in completing this questionnaire. Please note that all replies will be held in confidence to the maximum extent allowed by law. Only anonymous summarized results will appear in project reports.

Agency or Company Information

Date: _____

Agency or Company: _____

Name of Person Preparing Questionnaire: _____

Title of Person Preparing Questionnaire: _____

Postal Mail Address: _____

_____

_____

_____

City: _____

State: _____

Zip Code: _____

Telephone Number: _____

Telefax Number: _____

E-mail address: _____

Please return the completed questionnaire no later than November 30, 1999 to Mr. David Arellano, P.E., Graduate Research Assistant:

- by postal mail: David Arellano
  University of Illinois
  Department of Civil and Environmental Engineering
  Newmark Civil Engineering Laboratory
  205 North Mathews Avenue
  Urbana, IL 61801-2352
- by telefax: (217) 333-9464

Any questions concerning this questionnaire should be directed to Mr. David Arellano, P.E.:

- by e-mail: darellan@students.uiuc.edu

- by telephone: (217) 333-6940

Part A

The purpose of this part is to help us identify extreme opinions, i.e. the perceived best and worst, of EPS-block geofoam technology from the viewpoint of those in practice. If you require additional space for any answer, please use a separate sheet or the back of the sheet.

Question A1: Which category best describes the agency or company you represent:

design engineer [ ]

EPS molder [ ]

geofoam distributor [ ]

construction contractor [ ]

Question A2: Has the agency or company that you represent ever specified, supplied or installed EPS-block geofoam in a lightweight fill for any type of road?

No [ ] **>>> Please go to Question A3a below.**

Yes [ ] **>>> Please go to Question A3b below.**

Question A3a: If the answer to Question A2 was "No", what is the primary reason why not?

_____

_____

_____

_____

End of survey. Thank you for participating.

Question A3b: If the answer to Question A2 was "Yes", please proceed with the remainder of the questionnaire.

A3bi: To help us understand what is the primary benefit of using EPS-block geofoam so that we can develop this aspect to the fullest, what is the primary positive reason for using this material in road applications?

A3bii: To help us understand what aspect(s) of EPS-block geofoam most need improvement, what is the primary negative aspect or issue that you can state about this material in road applications? (Note: Exclude cost of the geofoam material itself.)

Please proceed to Part B on following page.

Part B

The purpose of this part is to provide us with information that is useful to some of the specific goals of this project.

Question B1: When developing a cost estimate for a design alternative involving EPS-block geofoam for road construction, what one aspect or factor related to the geofoam do you feel the most uncertain or unsure about? This will help us identify those issues requiring the greatest study to help reduce this uncertainty in the future.

Question B2: Other than the cost of the geofoam material itself, what item(s) that are related to geofoam (e.g. a reinforced-concrete capping slab, metal inter-block connectors, special site preparation) has your agency or company found to have significant impact on the overall cost of

a design alternative involving EPS-block geofoam in road construction? This will help us identify those items that need to be closely evaluated for the purpose of optimization or possibly even elimination in design in order to minimize overall project cost.

Question B3: Given that there are many factors that influence productivity for placing EPS blocks on a job site, from your experience what is the range of placement costs in dollars-per-cubic-yard or -cubic- meter basis?

Question B4: Concerning the geofoam specification used on your most recent project:

B4i: What was the source (e.g. State or County Department of Transportation Standard/Provisional Specification, in-house specification, provided by EPS molder or distributor)?

B4ii: What one item in, or aspect of, the specification were you least satisfied or comfortable with and would like to have more information on or knowledge about to improve?

Question B5: If you ever used EPS-block geofoam from a supplier, or if you are a supplier, who offers third-party certification for the manufactured quality of EPS block:

B5i: Do you rely solely on this or do you still do supplemental random sampling and testing of the EPS after it is delivered to the job site?

B5ii: Have you ever had a problem (such as, but not limited to, material not conforming) with third-party certification? If you did experience a problem, describe the problem and offer suggestions to prevent this problem in the future.

Question B6: Overall, what one item would you like us to consider or include in the NCHRP project documents that would be of greatest use to you in designing, supplying or installing EPS-block geofoam for road construction?

Question B7: Do you have any of the following supporting documentation that you think may be helpful to us in achieving the research objectives and that you would be willing to provide (we will contact you for follow up)? Please check all those items that apply:

Plans [ ], Specifications [ ], Design reports [ ], Cost estimates and comparisons [ ], Field instrumentation/Performance data [ ], Photographs [ ].

End of survey. Please feel free to provide any additional comments on a separate sheet.

Thank you for participating.

A.3. SUMMARY OF RESULTS

The questionnaire is divided into two parts: Parts A and B. The purpose of Part A was to identify extreme opinions, i.e. the perceived best and worst, of EPS-block geofoam technology from the viewpoint of those in practice. The purpose of Part B was to provide us with information that would be useful to some of the specific goals of this project. A total of thirty-four questionnaire replies were received by November 30, 1999. One survey was received after the November 30, 1999 deadline and also reviewed. Seven questionnaires were received via e-mail, eight by telefax, and the remaining twenty were received via postal mail. The format for the summary of replies consists of restatement of the question, a summary of replies provided by each respondent, and a synopsis of all the responses except for Questions A1 and A2. The replies to these two questions are presented in a slightly different format.

PART A

Question A1: Which category best describes the agency or company you represent:

design engineer [ ]

EPS molder [ ]

geofoam distributor [ ]

construction contractor [ ].

Replies to A1:

Twenty-six responses were received from state DOTs, seven replies were obtained from EPS molders, one reply was received from a contractor, and one from an engineering consultant. Table A.1 provides a summary of state DOTs that responded to the questionnaire. The term agency is used in this summary to include all types of respondents.

Table A.1. Summary of State DOTs that Responded to the Questionnaire

Question A2: Has the agency or company that you represent ever specified, supplied or installed EPS-block geofoam in a lightweight fill for any type of road?

No [ ] >>> Please go to Question A3a below.

Yes [ ] >>> Please go to Question A3b below.

Synopsis of Replies to A2:

Twelve of the thirty-five agencies that replied indicated their agency had specified, supplied, or installed EPS-block geofoam as a lightweight fill for road applications.

Question A3a: If the answer to Question A2 was "No", what is the primary reason why not?

Replies to A3a:

1. On a few occasions, we have used similar material for insulating, cushioning, etc. purposes , but not yet for lightweight fill. Primary reason is lack of familiarity until few years ago, and since then not having a good project match which we also felt justified the high cost of geofoam as we understand it. (IA DOT)

2. Although Delaware does have soft soil conditions in certain areas, the potential problems associated with these soils are mitigated by more conventional methods such as prefabricated vertical drains, surcharging, etc. (DE DOT)
3. Our focus is primarily packaging applications. Have not pursued geofoam market. (molder)
4. It has been considered but the cost has been greater than viable alternatives. (MT DOT)
5. Lack of opportunity. We have lightweight fill applications but we use wood chips where they have been less costly than foam. (OR DOT)
6. In areas of very soft soils, DOTD (Department of Transportation and Development) extends the bridge as to reduce the fill height of the approach embankment as much as possible. The settlement is mitigated by long (80+ ft) pile supported approach slabs are then built with decreasing pile lengths from the bridge abutment. In areas where higher fills are acceptable, wick drains are used to accelerate the settlement. To date, geofoam has not been used on a DOTD project-other lightweight aggregates have been used in the past. The technology has not yet been explored mainly due to the conservative approach of government agencies to trying something new compared to the traditional methods of addressing the problem. (LA DOT)
7. Unfamiliarity. Have used in compressible inclusion applications. (consultant)
8. Never heard of geofoam. (SCDOT)
9. There have not been any block geofoam jobs in our immediate trading area. (molder)
10. Not knowing how the cost compares to soil embankment fill. Not knowing how to design. Not knowing what the specifications need to be. Not knowing about the past performance and history. (NV DOT)
11. Not a current market emphasis. (molder)
12. No job was available at our cost. We were too high priced. (molder)

13. We have placed geofoam on the pre-approved materials list for a lightweight fill. However, the Geotechnical Branch does not specify the type of lightweight fill to be used on a project. (KY DOT)
14. In the situation where we utilized lightweight embankment, the site was a tidal area and there was a good potential for floods which would totally submerge the lightweight embankment. This would have resulted in buoyancy problems if we would have used Geofoam in the embankment. We will be considering geofoam on future projects if lightweight material is needed and if it is cost competitive with other solutions. (GA DOT)
15. As a supplier we have not yet had a job for road construction. (molder)
16. Not familiar with the product. High cost. (ID DOT)
17. Have not had a project in recent past that is applicable. (OH DOT)
18. This is a relatively new technology for us and for our state DOT We are planning to devote additional resources in 2000 toward educating the Texas DOT on this system. While we have not participated in any road embankment projects, we have provided EPS for lightweight fill in under-slab applications. (molder)
19. We have looked/analyzed applications but did not specify due to high cost and lack of geotechnical strength properties of the material. There appears to be no easy way to determine Phi-angle of product, and no values have been published. (WI DOT)
20. Limited knowledge of EPS-block geofoam and limited areas where application of this technology would be beneficial. We believe other options are less expensive but no product representative has ever visited the state. (NE DOT)
21. Expensive-other alternatives cheaper. Pending contract with Colorado DOT includes geofoam. (construction contractor)

Synopsis of Replies to A3a:

The primary reasons that agencies have not specified, supplied, or installed EPS-block geofoam as a lightweight fill for any road type are perceived high cost and lack of familiarity

with using EPS-blocks. More conventional treatment methods such as surcharging with prefabricated vertical drains and use of a bridge structure are preferred by some agencies over EPS-block geofoam. Other types of lightweight fills such as wood chips and lightweight aggregates have been used by several of the agencies that responded. Some agencies have not used EPS-block because of concerns with buoyancy. Molders' primary reasons for not supplying EPS-block is the lack of EPS-block projects in their vicinity, the EPS-block market is not a primary emphasis, or they have not actively pursued this market.

The purpose of this report is to provide a comprehensive document that provides both state-of-the-art knowledge and state-of-practice design guidance for engineers. The availability of this report will encourage wider as well as more consistent use of EPS-block geofoam in road embankments. In order to alleviate the high cost perception associated with the use of EPS-block goefoam, Chapter 12 provides an economic analysis of EPS-block geofoam embankments.

Question A3b: If the answer to Question A2 was "Yes", please proceed with the remainder of the questionnaire.

A3bi: To help us understand what is the primary benefit of using EPS-block geofoam so that we can develop this aspect to the fullest, what is the primary positive reason for using this material in road applications?

Replies to A3bi:

1. To reduce net load of fill/embankment over soft compressible materials. (CT DOT)
2. To lessen the added weight on existing soils or reduce pressure behind existing abutments. (MI DOT)
3. Quick, it works, solves problem. (molder)
4. Lightweight combined with high strength. (WA DOT)
5. Reduce embankment load on weak basement material or slide susceptible soils. (CO DOT)
6. Speed of construction = cost savings, rigid nature. (WY DOT)
7. Lightweight fill and compressible inclusion to reduce lateral earth pressures. (KS DOT)

8. Reduction in load applied to weak subgrade soils (lightweight fill). (IN DOT)
9. As a superlight weight fill used to reduce settlement and undercut in soft soil deposit. (IL DOT)
10. Weight credit. (MN DOT)
11. Settlement mitigation for buried utilities. (UT DOT)
12. Lightweight fill. (construction contractor)
13. Use as a lightweight fill in landslide treatment, improving stability and eliminating settlement problems of roadway embankments placed over soft soils. (NY DOT)

Synopsis of Replies to A3bi:

The primary positive reasons for using EPS-block geofoam in road applications indicated by the respondents are (1) its low density minimizes settlement and slope instability, (2) reduced lateral stress behind abutments, (3) fast placement rate which reduces construction time, and (4) reduced stress and consequently settlement over existing utilities. These benefits were included in the economic analysis chapter, Chapter 12.

A3bii: To help us understand what aspect(s) of EPS-block geofoam most need improvement, what is the primary negative aspect or issue that you can state about this material in road applications? (Note: Exclude cost of the geofoam material itself.)

Replies to A3bii:

1. EPS's low density makes its use difficult below the water table. Specific dewatering requirements may be needed in such situations. (CT DOT)
2. A good test method for determining compressive strength at 1% strain and examples showing applied loads that are less than that strain. (MI DOT)
3. Lack of knowledge, technical info., lack of experience. (molder)
4. (1) Surface capping requirements (i.e. reinforced concrete), (2) buoyancy-if used in areas with high ground water/flooding, and (3) facing requirements if blocks are placed vertically. (WA DOT)

5. No other problem but cost. (CO DOT)
6. Cost and availability. Cost/cu. yd. or Cost/cu. m. (WY DOT)
7. Geofoam distributor does not necessarily provide unequivocal data about their product in design phase. (KS DOT)
8. Uniform density and protection from dissolution in gasoline. (IN DOT)
9. Uncertainty regarding long-term durability, performance, flotation, and fire hazard. Placement of EPS blocks requires no standing water in excavation which mandates dewatering. (IL DOT)
10. I was going to say cost and the engineering means nothing without making the costs come out ok. Next I would say insulation or R value contributing to differential icing. Third, the minimum amount of cover needed to eliminate rutting when a concrete cap is not used with respect to both paved and unpaved cases. (MN DOT)
11. Susceptibility to chemical attack by petroleum and petroleum based fuels. (UT DOT)
12. Hydrocarbon attack, durability. (construction contractor)
13. Differential icing on roadway surface and overheating the asphalt concrete pavement section in winter and summer season, respectively, resulting from the insulating nature of geofoam blocks. (NY DOT)

Synopsis of Replies to A3bii:

In addition to providing a synopsis of the replies, the appropriate chapter number within the report that adresses these negative aspects is provided in parenthesis. The primary negative aspect that the respondents mentioned was susceptibility to hydrocarbon attack (Chapter 2 and 4). The next frequent reply was buoyancy below the water table (Chapter 3, 5, and 6, The respondents also mentioned the following additional negative aspects: difficulty in determining temporary dewatering requirements during construction to prevent buoyancy problems, general lack of knowledge with using EPS-block geofoam, lack of information regarding capping requirements such as the need for a reinforced concrete cap (Chapter 6), lack of information to

design against differential icing (Chapter 4), lack of information about facing requirements if a vertical embankment is used, density uniformity on blocks obtained at the site (Chapter 9), fire susceptibility (Chapter 2, 8, and 9), material may not be readily available, and lack of a good test method for determining compressive strength (Chapter 2).

PART B

Question B1: When developing a cost estimate for a design alternative involving EPS-block geofoam for road construction, what one aspect or factor related to the geofoam do you feel the most uncertain or unsure about? This will help us identify those issues requiring the greatest study to help reduce this uncertainty in the future.

Replies to B1:

1. Labor cost. (CT DOT)
2. Manufacturing cost (MI DOT)
3. Cost of placement. (molder)
4. Added value as a result of opening the highway to traffic earlier. The use of geofoam over very soft compressible soils may not require the need of pre-fabricated wick drains/surcharges/stage construction/time delays. Using geofoam may result completing the project in significantly less time. What value can we assign to this time savings? (WA DOT)
5. None (CO DOT)
6. Stability (solvents) and flame resistance. (WY DOT)
7. Testing frequency and product quality control (KS DOT)
8. Transportation costs, Installation costs. (consultant)
9. Cost of installation. The contractor over-bids the cost of placing EPS blocks because he doesn't know how easy it is. (IN DOT)
10. Specific engineering concerns such as compressive strength requirements and block size requirements (molder)
11. Uncertainty regarding the need for dewatering during construction. (IL DOT)

12. Same response as A3Bii second and third items. I would say insulation or R value contributing to differential icing. The minimum amount of cover needed to eliminate rutting when a concrete cap is not used with respect to both paved and unpaved cases. (MN DOT)
13. The thickness and reinforcing requirements for the reinforced-concrete capping slab. (UT DOT)
14. Long-term settlement in-place. (construction contractor)
15. In treating unstable slopes with geofoam blocks, a proper modeling of EPS blocks in slope stability analyses is currently not available. Other issues include design thickness of subbase material over the geofoam for different climate regions and alternatives to the use of concrete slab for traffic load distribution or petroleum spill protection. (NY DOT)

Synopsis of Replies to B1:

In addition to providing a synopsis of the replies, the appropriate chapter number within the report that addresses these uncertainties is provided in parentheses. The responses to this question are diverse. Some of the direct cost issues that the respondents indicated include manufacturing cost, transportation cost, and placement cost (Chapter 12). Some construction related items include the uncertainty in predicting temporary dewatering requirements during construction, the value of opening a highway to traffic quicker by using EPS-blocks versus traditional soft ground treatment methods such as surcharging or staged construction, and the uncertainty in the recommended requirements as part of a construction quality control (CQC) and construction quality assurance (CQA) program (Chapter 8 and 9). Some durability issues that were raised include the need for flame-retardant (Chapter 2, 8, and 9) and protection requirements against petroleum hydrocarbons (Chapter 2 and 4). A performance issue that was raised includes prediction of long-term settlement (Chapter 5). Design issues include the minimum amount of cover required to prevent pavement distress and to protect against differential icing if a reinforced concrete cap is not used (Chapter 4). Thickness and reinforcement requirements of a reinforced

concrete slab if a concrete cap is used (Chapter 6). The issue of block size requirements was also raised (Chapter 2).

Question B2: Other than the cost of the geofoam material itself, what item(s) that are related to geofoam (e.g., a reinforced-concrete capping slab, metal inter-block connectors, special site preparation) has your agency or company found to have significant impact on the overall cost of a design alternative involving EPS-block geofoam in road construction? This will help us identify those items that need to be closely evaluated for the purpose of optimization or possibly even elimination in design in order to minimize overall project cost.

Replies to B2:

1. Special site preparation. (CT DOT)
2. Concrete cap. (molder)
3. Horizontal capping slab and vertical facing requirements. Seismic requirements (is there a concern for anchoring the geofoam) when placed in a very seismically active area. (WA DOT).
4. Capping and drainage. (CO DOT)
5. Speed of construction, user familiarity. (WY DOT)
6. Uncertainty on part of contractors. (KS DOT)
7. Longevity. (HNTB Corp.)
8. (1) Reinforced concrete cap slab. (2) The contractor over-bids the cost of placing the EPS blocks because he doesn't know how easy it is. (3) Site preparation for the first lift. (IN DOT)
9. Dewatering the excavation was the most unexpected added cost to the project, since the EPS blocks required no standing water. (IL DOT)
10. The reinforced and or unreinforced concrete cap. (MN DOT)
11. Reinforced concrete slab, fascia wall. (UT DOT)
12. Cost of ground nails to stabilize excavation and eliminate horizontal loading on geofoam wall. (construction contractor)

13. Special site preparation, especially in areas with a high water table. (NY DOT)

Synopsis of Replies to B2:

Items found to have a significant impact on the overall cost include reinforced-concrete capping slab, unfamiliarity by construction contractors resulting in over pricing, special site preparation such as temporary dewatering, and facing systems in the case of vertical-faced fills. Other items mentioned include the cost of a permanent drainage system, seismic design, and earth retention to prevent horizontal loading on the EPS-block fill system when used in a side-hill fill application. One aspect that was indicated as reducing cost is the speed of construction when using an EPS-block fill system. These cost issues were included in the economic analysis chapter, Chapter 12.

Question B3: Given that there are many factors that influence productivity for placing EPS blocks on a job site, from your experience what is the range of placement costs in dollars-per-cubic-yard or -cubic- metre basis?

Replies to B3:

1. Our only experience with EPS has been on a small job (420 CY), below the water table, requiring special site preparation. The unit price given by the contractor (installed) was $75/CY. This price was much higher than for lightweight fill (5,810 CY) at ($10/CY). The lightweight fill was placed over the EPS. (CT DOT)
2. $52.50 - $58.50 per cubic meter. (MI DOT)
3. No idea (molder)
4. I believe placement costs are between 35% and 45% of the unit bid cost. For example-$60 cubic yard unit bid-(knowing the manufacturer's costs)-$21 to $27 would be the placement costs.
5. No experience (CO DOT)
6. $30-$55/ cu yd (WY DOT)
7. This information is isolated from us. (KS DOT)

8. Don't know. (consultant)
9. One contractor bid a job at $66 per cubic yard (material + labor), and another contractor bid at $50/per cubic yard (big variation). (IN DOT)
10. $10-$15, not including mark-up (profit). (IL DOT)
11. Our bid item is for furnished and installed so I do not have a breakdown on this cost. It should be easily under $1.00/cu. Yd. (MN DOT)
12. $65.00/cu m (geofoam without fascia wall), $75.00/cu m (geofoam with fascia wall). (UT DOT)
13. Not sure yet. (construction contractor)
14. Bid price on the only NYSDOT project was $65/cy in 1996. (NY DOT)

Synopsis of Replies to B3:

A summary of the responses to question B3 is included in Table A.2. Additional cost information is presented in Chapter 12.

Table A.2. Summary of EPS-Block Geofoam Prices

As shown above, placement prices range from $39.00 to $98.00 per m^3. These costs include material, transportation, placement, and contractor profit. The use of a fascia wall adds about $10.00 per m^3.

One respondent indicated that placement costs are approximately 35% to 45% of the unit bid cost and another respondent indicated that placement costs range from about $13.00 to $20.00 per m^3 not including contractor profit.

Question B4: Concerning the geofoam specification used on your most recent project:

B4i: What was the source (e.g., State or County Department of Transportation Standard/Provisional Specification, in-house specification, provided by EPS molder or distributor)?

Replies to B4i:

1. Specification provided by consultant. (CT DOT)

2. Ours. (MI DOT)
3. DOT(State), manufacturer, engineer. (molder)
4. I adopted a specification developed by the Colorado DOT. (WA DOT)
5. Other DOTs. (CO DOT)
6. WY DOT Geology/Bridge Program. (WY DOT)
7. Specification developed by us. (KSDOT)
8. We developed the specification in-house. (IN DOT)
9. Provided by the geotechnical consultant. (IL DOT).
10. Combination of sources: Dr. Horvath's book, industry, visiting Norwegian Engineers, other states, and in-house. (MN DOT)
11. Design-build team with consultation with EPS molder and his technical representative. (UT DOT)
12. Colorado DOT Special Provisions. (construction contractor)
13. State DOT, technical papers published by Norwegian researchers, in-house development, and EPS molder. (NY DOT)

Synopsis of Replies to B4i:

The primary source of a geofoam specification is other state DOT's specification or an in-house developed specification. However, some of the responses also included consultants and EPS molders. Based on the responses received, some of the state DOTs that have standard/provisional specifications include CO, IN, KS, MI, NY, WA, and WY. A provisional combined material, product, and constructin standard covering EPS-block geofoam in road applications is provided in Appendix C.

B4ii: What one item in, or aspect of, the specification were you least satisfied or comfortable with and would like to have more information on or knowledge about to improve?

Replies to B4ii:

1. The construction contract that included the specification was recently awarded and construction activity has not taken place. We have no comment at this time. (CT DOT)
2. Relationship between stress-strain and density. Need more background material. (MI DOT)
3. Recycle content in EPS Block. (molder)
4. Quality control-our specification relied upon manufacturers quality control. Should we require 3rd party lab testing. How may tests for a given volume of geofoam-what to test for/physical sample size used in tests etc. (WA DOT)
5. Density, strength, and creep. (CO DOT)
6. Relied only on supplier certification. (WY DOT)
7. Sampling frequency (KS DOT)
8. Use of polyethylene sheets underneath the EPS. (IN DOT)
9. Specifications should clearly define the method of anti-floatation procedure, in the event water enters the excavation. Also, a minimum amount of dewatering should be specified as incidental, beyond and above which the contractor would be compensated on a cost-plus basis. (IL DOT)
10. Long-term creep performance. (UT DOT)
11. Chemical barrier-an "impermeable geomembrane. (construction contractor)
12. Physical Properties - Water Absorption. (NY DOT)

Synopsis of Replies to B4ii:

Four items were mentioned more than once in the replies. One concern is relying only on supplier certification for material acceptance. Should third-party certification be required? Third-party certification is addressed in Chapter 9. Another concern is not knowing what types of tests to perform as part of a construction quality control (CQC) and construction quality assurance (CQA) program as well as the frequency of these tests. Test requirements are presented in Chapter 9. The other two concerns mentioned more than once involve the lack of understanding

between the relationship of density and compressive strength and the long term creep performance of EPS. These two concerns are addressed in Chapter 2 and 9.

The following items are indicated once in the replies: physical properties such as water absorption, the need for polyethylene sheets underneath the EPS, chemical barrier requirements over the EPS, and the amount of recycled EPS allowable.

Several concerns related to protection of the blocks during construction were also indicated. One concern is not specifying in the specifications the method of antiflotation procedure(s) to use in the event that water enters the excavation. One respondent suggested that a minimum amount of temporary dewatering should be specified as incidental.

Question B5: If you ever used EPS-block geofoam from a supplier, or if you are a supplier, who offers third-party certification for the manufactured quality of EPS block:

B5i: Do you rely solely on this or do you still do supplemental random sampling and testing of the EPS after it is delivered to the job site?

Replies to B5i:

1. Approval of the product may be by certification accepted by the Engineer, written approval of the Engineer, or prior test and or inspection by the Department. (CT DOT)
2. We do random sampling at job site. Density and 1% strain compression tests. (MI DOT)
3. Rely solely on 3rd party certification. (molder)
4. Our specification allowed owner testing-we would only test material delivered to the project, if based on visual inspection (shape/weight appearance), the material appears it would/may not meet specifications. (WA DOT)
5. On-site testing is still done. (CO DOT)
6. Rely on supplier certification. (WY DOT)
7. We do supplemental sampling and testing. (KS DOT)
8. We require manufacturer to submit samples to our laboratory in Materials and Tests Division. Additional on-site sampling and testing at the discretion of the project engineer. (IN DOT)

9. No third party was involved. The resident engineer conducted random sampling. (IL DOT)
10. We do random supplemental QA testing. (MN DOT)
11. Minimal random sampling. (UT DOT)
12. We would still perform on-site density check. (NY DOT)

Synopsis of Replies to B5i:

Nine of the twelve responses indicated that random sampling and testing is performed after the EPS is delivered to the job site. Of these, one response indicated that the manufacturer was required to submit samples to the state DOT laboratory. Sampling and testing procedures for EPS blocks are presented in Chapter 9.

B5ii: Have you ever had a problem (such as, but not limited to, material not conforming) with third-party certification? If you did experience a problem, describe the problem and offer suggestions to prevent this problem in the future.

Replies to B5ii:

1. No experience to date. (CT DOT)
2. Third party reports do not include 1% strain test. We use our own results. (MI DOT)
3. No. (molder)
4. No. (WA DOT)
5. Not to my knowledge. (CO DOT)
6. No. (WY DOT)
7. No. (KS DOT)
8. No. (IN DOT)
9. Not applicable (no third-party). However, there was the problem of the EPS blocks not meeting the weight requirement, but was corrected later. (IL DOT)
10. No problems. (MN DOT)
11. No. (UT DOT)

12. Yes, density of blocks varied considerably in one particular tractor trailer load with some blocks not meeting density criterion. Contractor had to weigh each block in order to salvage the load. This situation was brought to the attention of the manufacturer. Tighter quality control at the manufacturing plant was exercised. (NY DOT)

Synopsis of Replies to B5ii:

Nine of the twelve responses indicate that no problems with third-party certification have been experienced. Two of the respondents indicate that problems with third-party certification include the EPS blocks not meeting the density requirements. One response mentioned that the problem with third-party certification is that the compressive stress at 1% strain test results were not provided with the certifications. Third-party certification is addressed in Chapter 9.

Question B6: Overall, what one item would you like us to consider or include in the NCHRP project documents that would be of greatest use to you in designing, supplying or installing EPS-block geofoam for road construction?

Replies to B6:

1. No comment. (CT DOT)
2. A general design layout drawing for EPS under a roadway built on an Embankment. (MI DOT)
3. Cost factors vs. conventional methods. (molder)
4. Capping and facing requirements. Also look at overall stability modeling (block/rotational???), geofoam strength used in this analyses. (WA DOT)
5. Installation secrets. (WY DOT)
6. Suggested specification, next a design guide approved by FHWA. (KS DOT)
7. Is there a way to eliminate the concrete cap on EPS blocks so as to minimize the overall installation cost? (IN DOT)
8. Cross-sections should be checked for short-term (during construction) and long-term buoyancy of the entire system. (IL DOT)

9. Amount of cover for the different geofoam densities. (MN DOT)
10. Typical design details and specifications. (UT DOT)
11. Required thickness of subbase material overlying the geofoam to eliminate the phenomena of both differential icing of the roadway pavement surface in the cold season and overheating the pavement section in the warm season. (NY DOT)

Synopsis of Replies to B6:

In addition to providing a synopsis of the replies, the appropriate chapter number within the report that addresses these items is provided in parenthesis. The predominant item indicated that should be included in the NCHRP report is capping requirements to support stresses generated by traffic loads (Chapter 6), to prevent differential icing and overheating for the various geofoam densities (Chapter 4), and to include alternatives to a reinforced concrete slab (Chapter 4). Other suggested items include general design drawing details (Chapter 10), a design guide that includes slope stability analyses with recommended strength for the EPS (Chapter 5 and 6), facing requirements (Chapter 5), recommended specification (Chapter 9 and Appendix C), installation procedures to include addressing the potential short-term buoyancy problem (Chapter 8), and cost comparisons of the EPS alternative with other soft ground treatment procedures (Chapter 12).

Question B7: Do you have any of the following supporting documentation that you think may be helpful to us in achieving the research objectives and that you would be willing to provide (we will contact you for follow up)? Please check all those items that apply:

Plans [ ], Specifications [ ], Design reports [ ], Cost estimates and comparisons [ ], Field instrumentation/Performance data [ ], Photographs [ ].

Replies to B7:

A summary of the responses to B7 is included in Table A.3.

Table A.3. Summary of Replies to Question B7

Synopsis of Replies to B7:

Ten respondents indicate that they have construction plans, specifications, design reports, cost information, field instrumentation data, or photographs.

AR	MI
CO	MN
CT	MT
DE	NE
GA	NV
HI	NY
IA	OH
ID	OR
IL	SC
IN	UT
KS	WA
KY	WI
LA	WY

STATE	YEAR	QUANTITY m^3 (yd^3)	Bid Price in U.S. \$/ m^3 (\$/yd^3)
CT	1999	321.1 (420)	98.00 (75.00)
IN	1995	4,707.6 (6,157)	65.00 – 87.00 (50.00-66.00)
MI	-	-	52.50 – 58.50 (40.15-44.73)
NY	1996	3,115.7 (4,075)	85.00 (65.00)
UT	-	-	65.00 (Note 1) (50.00)
UT	-	-	75.00 (Note 2) (57.00)
WY	-	-	39.00 – 72.00 (30.00-55.00)

Note 1: Without fascia wall.
Note 2: With fascia wall.

Agency or Company	Plans	Specifications	Design Reports	Cost Estimates and Comparisons	Field Instrumentation /Performance Data	Photographs
CTDOT		X				
MIDOT		X		X		
MOLDER			X		X	X
WADOT	X	X	X	X		X
WYDOT	X	X		X	X	X
KSDOT	X	X				
INDOT	X	X		X	X	X
ILDOT	X	X	X	X		X
UTDOT	X	X	X	X	X	X
NYDOT	X	X	X		X	X

APPENDIX B
PROVISIONAL DESIGN GUIDELINE

Appendix B is not published here in. However, it is being published separately as NCHRP Report 529. To view this report online, go to http://www4.trb.org/trb/onlinepubs.nsf/web/crp and click on "National Cooperative Highway Research Program" under "Project Reports."

APPENDIX C
RECOMMENDED EPS-BLOCK GEOFORM STANDARD FOR LIGHTWEIGHT FILL IN ROAD EMBANKMENTS AND BRIDGE APPROACH FILLS ON SOFT GROUND

Appendix C is not published here in. However, it is being published separately as NCHRP Report 529. To view this report online, go to http://www4.trb.org/trb/onlinepubs.nsf/web/crp and click on "National Cooperative Highway Research Program" under "Project Reports."

APPENDIX D
BIBLIOGRAPHY

APPENDIX **D**

BIBLIOGRAPHY

Contents

D.1 INTRODUCTION

A bibliography of publications deemed relevant to the specific goals of the overall project that were obtained and reviewed are contained in this Appendix. This bibliography is based primarily on literature reviewed prior to April 2000. It is intended that this bibliography serve not only as documentation for this project but as a resource for future related research by others. Note that the entries in this bibliography are divided into three broad categories:

- Publications of an overall general and descriptive nature.
- Publications that focus on the engineering properties of block-molded EPS, whether in general or explicitly for geofoam applications.
- Publications that focus on the use of EPS-block geofoam for applications that involve the function of lightweight fill. Because of the size of this category and the specific needs of this project, this section was further subdivided into:
  - publications of a general nature (typically case histories),

- publications that contain design manuals or guidelines developed previously by others, and
- known U.S. patents (both expired and active).

In addition, a wide variety of manufacturer's literature from around the world was obtained and reviewed as general background information for this study. However, this literature is neither listed herein nor cited in this report as it was collectively judged to have little permanent scientific value.

In addition to the geofoam-related publications documented in this Appendix, a number of miscellaneous publications were found. These publications are cited where appropriate throughout this report.

D.2 GENERAL

Baker, A., editorial. *Geosynthetics World*, Geosynthetics Publications, Ltd., U.K., Vol. 5, No. 2 (1995) p. 3.

Baker, A., "Feature: EPS Geofoam Geosynthetic". *Geosynthetics World*, Vol. 5, No. 2 (1995), p. 5.

Baker, A., "Foam Foundations: Why On Earth Not?". *Shell Chemicals Europe Magazine*, No. 4 (1995) pp. 9-12.

Bergstrom, T., editorial letter. *Civil Engineering*, American Society of Civil Engineers, Reston, Va., U.S.A., Vol. 68, No. 11 (1998) p. 8.

Beinbrech, G. and Hohwiller, F., “Polstergründungen Hartschaum aus Styropor® Als Deformations- und Polsterschicht”. *Tiefbau*, Germany (1998).

Bhatia, S. K., "From the Editor's Corner". *Geotechnical News*, BiTech Publishers Ltd., Richmond, B.C., Canada, Vol. 14, No. 2 (1996) p. 24.

"Construyen Puentes con Bases de Espuma". *El Llanquihue*, No. 34088, Puerto Montt, Chile (1997), p. A9.

"EPS". Expanded Polystyrol Construction Method Development Organization, Tokyo, Japan (1993) 310 pp. (in Japanese).

"EDO - The 10th Anniversary". EPS Construction Method Development Organization, Tokyo, Japan (1996) 50 pp. (in Japanese).

"EPS in de GWW; Voor Zettingsvrije Onderhoudsarme Toepassingen". Stybenex, Zaltbommel, The Netherlands (undated) 32 pp.

"Geofoam Building Wide Acceptance". *Newsline*, EPS Molders Association, Crofton, Md., U.S.A., Vol. 1, No. 1 (1998) pp. 1 and 4.

Horvath, J. S., "The Case for an Additional Function". *IGS News*, International Geotextile Society, Vol. 7, No. 3 (1991) pp. 17-18.

Horvath, J. S., "'Lite' Products Come of Age; New Developments in Geosynthetics". *Standardization News*, American Society for Testing and Materials, Philadelphia, Pa., U.S.A., Vol. 20, No. 9 (1992) pp. 50-53.

Horvath, J. S., "Dark, No Sugar: A Well-Known Material Enters the Geosynthetic Mainstream". *Geotechnical Fabrics Report*, Industrial Fabrics Association International, St. Paul, Minn., U.S.A., Vol. 10, No. 7 (1992) pp. 18-23.

Horvath, J. S., "Geofoam Geosynthetics: An Overview of the Past and Future". *Geosynthetics World*, Geosynthetics Publications, Ltd., U.K., Vol. 3, No. 1 (1993), pp. 15-17 with corrections in Vol. 4, No. 1 (1993), p. 31.

Horvath, J. S., corrections to "Geofoam Geosynthetics: An Overview of the Past and Future". *Geosynthetics World*, Geosynthetics Publications, Ltd., U.K., Vol. 4, No. 1 (1993), p. 31.

Horvath, J. S., "Computer Software for Load-Deformation and Geothermal Analyses in Problems Involving Geosynthetics". *Geotextiles and Geomembranes*, Elsevier Science Ltd., London, U.K., Vol. 12, No. 5 (1993) pp. 425-433.

Horvath, J. S., "Geosynthetics in Residential Construction". *Building Research Journal*, Building Research Council, University of Illinois, Champaign, Ill., U.S.A., Vol. 3, No. 1 (1994) pp. 67-68.

Horvath, J. S., "Geosynthetics in Residential Construction". *Geotechnical Fabrics Report*, Industrial Fabrics Association International, St. Paul, Minn., U.S.A., Vol. 12, No. 3 (1994) pp. 22-23.

Horvath, J. S. (ed.), "Proceedings; International Geotechnical Symposium on Polystyrene Foam in Below-Grade Applications; March 30, 1994; Honolulu, Hawaii, U.S.A.", *Research Report No. CE/GE-94-1*, Manhattan College, Bronx, N.Y., U.S.A. (1994).

Horvath, J. S., “Development of the North American Market for Rigid Cellular Polystyrene as Geofoam Geosynthetic”. Horvath Engineering, P.C., Scarsdale, N.Y., U.S.A. (1994).

Horvath, J. S., “Development of the North American Market for Rigid Cellular Polystyrene as Geofoam Geosynthetic - Addendum No. 1”. Horvath Engineering, P.C., Scarsdale, N.Y., U.S.A. (1994).

Horvath, J. S., "'Lite' Products Come of Age; New Developments in Geosynthetics". *Standardization News*, special issue published jointly by the American Society for Testing and Materials and Chinese Association for Standardization (1994) pp. 26-29 (in Chinese).

Horvath, J. S., “Geofoam Geosynthetic”. Horvath Engineering, P.C., Scarsdale, N.Y., U.S.A. (1995) 229 pp.

Horvath, J. S., feature interview. *Geosynthetics World*, Geosynthetics Publications, Ltd., U.K., Vol. 5, No. 4 (1995) pp. 12-15.

Horvath, J. S., "EPS Geofoam: New Products and Marketing Trends". *Geotechnical Fabrics Report*, Industrial Fabrics Association International, St. Paul, Minn., U.S.A., Vol. 13, No. 6 (1995) pp. 22-26.

Horvath, J. S., “Development of the North American Market for Rigid Cellular Polystyrene as Geofoam Geosynthetic - Addendum No. 2”. Horvath Engineering, P.C., Scarsdale, N.Y., U.S.A. (1996).

Horvath, J. S., "Geofoam Developments in North America". *Geotechnical News*, BiTech Publishers Ltd., Richmond, B.C., Canada, Vol. 14, No. 2 (1996) pp. 25-29.

Horvath, J. S., ”Geofoam Geosynthetic: Past, Present, and Future”. *Electronic Journal of Geotechnical Engineering*, Vol. 1. No. 1 (1996).

Horvath, J. S., "Geofoam Conference Draws 320 Attendees to Tokyo". *Geotechnical Fabrics Report*, Industrial Fabrics Association International, St. Paul, Minn., U.S.A., Vol. 15, No. 1 (1997) pp. 11-12.

Horvath, J. S., "Special Issue on Geofoam: Overview and Summary". *Geotextiles and Geomembranes*, Elsevier Science Ltd., London, U.K., Vol. 15, Nos. 1-3 (1997) pp. 1-3.

Horvath, J. S. “Geofoam Geosynthetic: Past, Present, and Future”. Paper prepared for presentation at the EPS Molders Association Second Annual Meeting, Chicago, Ill., U.S.A. (1997).

Horvath, J. S., "International Symposium on Geofoam". *IGS News*, International Geosynthetics Society, Vol. 13, No. 1 (1997) p. 17.

Horvath, J. S., "Lectures in South America". *IGS News*, International Geosynthetics Society, Vol. 13, No. 1 (1997) p. 17.

Horvath, J. S., “Geofoam Geosynthetic: Past, Present, and Future”. Paper prepared for presentation at the ACF Environmental Design Seminar on Geosynthetic Technologies, Timonium, Md., U.S.A. (1997).

Horvath, J. S., “Geofoam Geosynthetic: Past, Present, and Future”. Paper prepared for presentation at the ACF Environmental Design Seminar on Geosynthetic Technologies, King of Prussia, Pa., U.S.A. (1997).

Horvath, J. S., “Geofoam Geosynthetic: Past, Present, and Future”. Paper prepared for presentation to the State of Delaware Department of Transportation, Dover, Del., U.S.A. (1997).

Horvath, J. S., “Geofoam Geosynthetic: An Assessment of the North American Market”. Notes prepared for distribution to attendees at a confidential presentation to industry, U.S.A. (1997).

Horvath, J. S., “Geofoam Geosynthetic: Past, Present, and Future”. Paper prepared for distribution to participants at the Fourth Professor Training Course for Geosynthetics, Auburn University, Auburn, Ala., U.S.A. (1997).

Horvath, J. S., “Geofoam Geosynthetic: An Overview of the Past, Present, and Future”. Paper prepared for distribution at the Premier Industries, Inc./Insulfoam Division and Polar Supply Company, Inc. Seminar on Design Issues Related to Geofoam in Arctic Applications, Fairbanks, Ak., U.S.A. (1997).

Horvath, J. S., “Geofoam Geosynthetic: An Overview of the Past, Present, and Future”. Paper prepared for distribution at the Premier Industries, Inc./Insulfoam Division and Polar Supply Company, Inc. Seminar on Design Issues Related to Geofoam in Arctic Applications, Anchorage, Ak., U.S.A. (1997).

Horvath, J. S., “Geofoam Geosynthetic: An Overview of the Past, Present, and Future”. Paper prepared for distribution at the Manhattan College Civil Engineering Day, Bronx, N.Y., U.S.A. (1997).

Horvath, J. S., "Geofoam Activities: Projects in South America and a New WWW URL". *IGS News*, International Geosynthetics Society, Vol. 13, No. 3 (1998) pp. 9-10.

Horvath, J. S., editorial letter. *Civil Engineering*, American Society of Civil Engineers, Reston, Va., U.S.A., Vol. 68, No. 6 (1998) p. 33.

Horvath, J. S., “Designing with Geofoam Geosynthetic”. Notes prepared for participants at an American Society of Civil Engineers continuing education seminar, Atlanta, Ga., U.S.A. (1999).

Horvath, J. S., “Designing with Geofoam Geosynthetic”. Notes prepared for participants at an American Society of Civil Engineers continuing education seminar, South San Francisco, Calif., U.S.A. (1999).

Horvath, J. S., “Lessons Learned from Failures Involving Geofoam in Roads and Embankments". *Research Report No. CE/GE-99-1*, Manhattan College, Bronx, N.Y., U.S.A. (1999).

Horvath, J. S., “Technical Issues for Designing with and Marketing EPS Geofoam”. Notes prepared for distribution to attendees at a confidential presentation to industry, U.S.A. (1999).

Horvath, J. S., “Designing with Geofoam Geosynthetic”. Notes prepared for participants at the Polyfoam Packers Corporation/American Society of Civil Engineers continuing education seminar, Glenview, Ill., U.S.A. (1999).

Horvath, J. S., “Geofoam Geosynthetic: An Overview of the Past and Present, and a View into the Future”. Paper prepared for distribution to participants at the Effective Roadway Design and Maintenance with Geosynthetics short course, University of Wisconsin - Madison, Department of Engineering Professional Development, Madison, Wis., U.S.A. (1999).

Horvath, J. S., “Geofoam Geosynthetic: An Overview of the Past and Present, and a View into the Future”. Paper prepared for distribution to participants at the Effective Engineering Approaches for Construction with Geosynthetics on Soft Soils and Waste Materials short course, University of Wisconsin - Madison, Department of Engineering Professional Development, Madison, Wis., U.S.A. (1999).

Horvath, J. S., “Designing with Geofoam Geosynthetic”. Notes prepared for participants at the American Society of Civil Engineers/Branch River Foam Plastics, Inc. continuing education seminar, Randolph, Mass., U.S.A. (1999).

Koerner, R. M., "Progress in Geosynthetics". *Proceedings - Geosynthetics 95*, Industrial Fabrics Association International, St. Paul, Minn., U.S.A. (1995) pp. 1-11.

Koerner, R. M., “Designing with Geosynthetics”. Prentice Hall, Upper Saddle River, N.J., U.S.A., 4th edition (1998).

Koerner, R. M. and Soong, T.-Y., “The Evolution of Geosynthetics”. *Civil Engineering*, American Society of Civil Engineers, Reston, Va., U.S.A., Vol. 67, No. 7 (1997) pp. 62-64.

Leaversuch, R. D., "EPS Foam Builds New Roles in Construction Sector". *Modern Plastics* (1994).

Mits, T. C., editorial letter. *Civil Engineering*, American Society of Civil Engineers, Reston, Va., U.S.A., Vol. 68, No. 7 (1998) p. 37.

Negussey, D., "Properties & Applications of Geofoam". Society of the Plastics Industry, Inc., Washington, D.C., U.S.A. (1996) 22 pp.

Negussey, D., "Putting Polystyrene to Work". *Civil Engineering*, American Society of Civil Engineers, Reston, Va., U.S.A., Vol. 68, No. 3 (1998) pp. 65-67.

Negussey, D., editorial letter. *Civil Engineering*, American Society of Civil Engineers, Reston, Va., U.S.A., Vol. 68, No. 11 (1998) pp. 8-9.

"PS-Hardschuim voor Weg- en Waterbouw". Stybenex: Vereniging van Fabrikanten van PS-Hardschuim, Enschede, The Netherlands (undated).

"Quarter Century Experience Gains Recognition for 'Geofoams'". *Plastics in Building Construction*, Vol. 17, No. 6 (1993) p. 8.

"Revolucionará la Ingenieria Civil". *El Constructor*, Montevideo, Uruguay (1996) p. 31.

Tsukamoto, H., "Technical Exchange with Overseas". In *EDO - The 10th Anniversary*, EPS Construction Method Development Organization, Tokyo, Japan (1996) 7 pp.

"The Final Report of International Symposium on EPS Construction Method". EPS Construction Method Development Organization, Tokyo, Japan (undated) 161 pp. (in English and Japanese).

"Una Espuma Resistente y Ecológia para Suelos Blandos o Anegadizos". *La Nueva Construccion*, No. 2, Buenos Aires, Argentina (1997) pp. 44-47.

Williams, M. F. and Williams, B. L., "Standards Development for Exterior Insulation and Finish Systems (EIFS)". *Standardization News*, American Society for Testing and Materials, Philadelphia, Pa., U.S.A., Vol. 20, No. 11 (1992) pp. 54-61.

D.3 MATERIAL PROPERTIES AND CONSTITUTIVE MODELING

Athanasopoulos, G. A., Pelekis, P. C. and Xenaki, V. C., "Dynamic Properties of EPS Geofoam: An Experimental Investigation". *Geosynthetics International*, Industrial Fabrics Association International, Roseville, Minn., U.S.A., Vol. 6, No. 3 (1999) pp. 171-194.

Bartholomew, C. L., "An Investigation of the Usage of Recycled Polystyrene Foam (EPS)". Research report submitted to ARCO Chemical Company, Widener University, Department of Civil Engineering, West Chester, Pa., U.S.A. (1992).

Bartlett, P. A. Letter report to unnamed customer, ARCO Chemical Company, Newtown Square, Pa., U.S.A., September 11 (1986).

Bartlett, P. A., "Expanded Polystyrene Scrap Recovery & Recycling". Report, ARCO Chemical Company (undated).

Coughanour, R. B., "Pentane Issue". Presentation at the 16th Annual SPI Expanded Polystyrene Division Conference, San Diego, Calif., U.S.A. (1988).

Duškov, M., "Materials Research on Expanded Polystyrene Foam (EPS)". Research report, Delft University of Technology, Delft, The Netherlands (1993).

Duškov, M., "Materials Research on Expanded Polystyrene Foam (EPS)". *Report No. 7-94-211-2*, Delft University of Technology, Delft, The Netherlands (1994).

Duškov, M., "Materials Research on EPS20 and EPS15 Under Representative Conditions in Pavement Structures". *Geotextiles and Geomembranes*, Elsevier Science Ltd., London, U.K., Vol. 15, Nos. 1-3 (1997) pp. 147-181.

Eriksson, L. and Tränk, R., "Properties of Expanded Polystyrene - Laboratory Experiments". In *Expanded Polystyrene as Light Fill Material; Technical Visit around Stockholm - June 19, 1991*, Swedish Geotechnical Institute, Linköping, Sweden (1991).

Horvath, J. S., discussion of "A Comparison of Some Engineering Properties of EPS to Soils" by D. Negussey and M. Jahanandish, preprint paper No. 930216. Transportation Research Board 72nd Annual Meeting, Washington, D.C., U.S.A. (1993).

Horvath, J. S., "Expanded Polystyrene (EPS) Properties for Geotechnical Engineering Applications". Preprint paper, International Geotechnical Symposium on Polystyrene Foam in Below-Grade Applications, Honolulu, Hawaii, U.S.A. (1994).

Horvath, J. S., "Expanded Polystyrene (EPS) Properties for Geotechnical Engineering Applications". In "Proceedings; International Geotechnical Symposium on Polystyrene Foam in Below-Grade Applications; March 30, 1994; Honolulu, Hawaii, U.S.A.", *Research Report No. CE/GE-94-1*, J. S. Horvath (ed.), Manhattan College, Bronx, N.Y., U.S.A. (1994).

Horvath, J. S., "Expanded Polystyrene (EPS) Geofoam: An Introduction to Material Behavior". *Geotextiles and Geomembranes*, Elsevier Science Ltd., London, U.K., Vol. 13, No. 4 (1994) pp. 263-280.

Horvath, J. S., "The Compressive Strength of Geofoam Materials: What Does It Really Mean?". Paper prepared for distribution at the Premier Industries, Inc./Insulfoam Division and Polar Supply Company, Inc. Seminar on Design Issues Related to Geofoam in Arctic Applications, Fairbanks, Ak., U.S.A. (1997).

Horvath, J. S., "Constitutive Modeling of the Stress-Strain-Time Behavior of Geosynthetics Using the Findley Equation: General Theory and Application to EPS-Block Geofoam". Paper prepared for distribution at the Premier Industries, Inc./Insulfoam Division and Polar Supply Company, Inc. Seminar on Design Issues Related to Geofoam in Arctic Applications, Fairbanks, Ak., U.S.A. (1997).

Horvath, J. S., "The Thermal Behavior of Geofoam Materials: What Do We Really Know?". Paper prepared for distribution at the Premier Industries, Inc./Insulfoam Division and Polar Supply Company, Inc. Seminar on Design Issues Related to Geofoam in Arctic Applications, Fairbanks, Ak., U.S.A. (1997).

Horvath, J. S., "The Compressive Strength of Geofoam Materials: What Does It Really Mean?". Paper prepared for distribution at the Premier Industries, Inc./Insulfoam Division and Polar Supply Company, Inc. Seminar on Design Issues Related to Geofoam in Arctic Applications, Anchorage, Ak., U.S.A. (1997).

Horvath, J. S. "Constitutive Modeling of the Stress-Strain-Time Behavior of Geosynthetics Using the Findley Equation: General Theory and Application to EPS-Block Geofoam". Paper prepared for distribution at the Premier Industries, Inc./Insulfoam Division and Polar Supply Company, Inc. Seminar on Design Issues Related to Geofoam in Arctic Applications, Anchorage, Ak., U.S.A. (1997).

Horvath, J. S. "The Thermal Behavior of Geofoam Materials: What Do We Really Know?". Paper prepared for distribution at the Premier Industries, Inc./Insulfoam Division and Polar Supply Company, Inc. Seminar on Design Issues Related to Geofoam in Arctic Applications, Anchorage, Ak., U.S.A. (1997).

Horvath, J. S., "Mathematical Modeling of the Stress-Strain-Time Behavior of Geosynthetics Using the Findley Equation: General Theory and Application to EPS-Block Geofoam". *Research Report No. CE/GE-98-3*, Manhattan College, Bronx, N.Y., U.S.A. (1998).

Järvelä, P., Sarlin, J., Järvelä, P. and Törmälä, P., "A New Method to Measure the Fusion Strength between Expanded Polystyrene (EPS) beads". *Journal of Materials Science*, Vol. 21 (1986) pp. 3139-3142.

Magnan, J.-P. and Serratrice, J.-F., "Propriétés Mécaniques du Polystyrène Expansé pour ses Applications en Remblai Routier". *Bulletin liaison Laboratoire Ponts et Chaussées*, 164, Laboratoire Central Ponts et Chaussées, Paris, France (1989) pp. 25-31.

Makiuchi, K. and Minegishi, K., "Compressive and Frictional Characteristics of Lightweight Fill Material EPS". *Twenty-Third National Conference of the Japanese Society of Soil Mechanics and Foundation Engineering* (1987) pp. 1975-1976 (in Japanese).

Makiuchi, K. and Minegishi, K., "Deformational Characteristics of Light Fill Material EPS under Repetitive Loads". *Twenty-Fourth National Conference of the Japanese Society of Soil Mechanics and Foundation Engineering* (1988) pp. 41-42 (in Japanese).

Makiuchi, K. and Minegishi, K., "Yielding Characteristics of Lightweight Fill Material EPS Subjected to Compressive Stresses". *Twenty-Fifth National Conference of the Japanese Society of Soil Mechanics and Foundation Engineering* (1989) pp. 2115-2116 (in Japanese).

McAffee, R. P., "Geofoam as Lightweight Embankment Fill". Senior-project report submitted to the University of New Brunswick, Fredericton, N.B., Canada (1993).

Negussey, D. and Jahanandish, M., "A Comparison of Some Engineering Properties of EPS to Soils". Preprint paper No. 930216, Transportation Research Board 72nd Annual Meeting, Washington, D.C., U.S.A. (1993).

Preber, T., Bang, S., Chung, Y. and Cho, Y., "Behavior of Expanded Polystyrene Blocks". *Transportation Research Record No. 1462*, Transportation Research Board, Washington, D.C., U.S.A. (1994) pp. 36-46.

Sarlin, J., Järvelä, P., Järvelä, P. and Törmälä, P., "The Inhomogeneity Inside a Block of Expanded Polystyrene (EPS)". *Plastics and Rubber Processing and Applications*, Vol. 6, No. 1 (1986) pp. 43-49.

Throne, J. L., "Thermoplastic Foams". Sherwood Publishers, Hinckley, Ohio, U.S.A. (1996).

Yasuda, Y., Murata, O. and Tateyama, M., "Repeated Load Test of Lightweight Fill Materials EPS". *Twenty-Fourth National Conference of the Japanese Society of Soil Mechanics and Foundation Engineering* (1988) pp. 45-46 (in Japanese).

D.4 LIGHTWEIGHT FILL APPLICATIONS

D.4.1 General

Aabøe, R., "Norwegian Roads on Foam Fill". Norwegian Road Research Laboratory, Oslo, Norway (undated).

Aabøe, R., "Plastic Foam in Road Embankments". *Våre Veger*, Norway (1981).

Aabøe, R., "Plastic Foam in Road Embankments". *Ground Engineering*, Thomas Telford Ltd., London, U.K., Vol. 19, No. 1 (1986) pp. 30-31.

Aabøe, R., "13 Years of Experience with EPS as a Lightweight Fill Material in Road Embankments". *Publication No. 61*, Norwegian Road Research Laboratory, Oslo, Norway (1987) pp. 21-27.

Aabøe, R., "Euroroad E18 in Vestfold". *Proceedings of the June 21, 1991 Seminar on the Use of EPS in Road Construction*, Norwegian Road Research Laboratory, Oslo, Norway (1991).

Aabøe, R., "Deformasjonsegenskaper og Spenningsforhold i Fyllinger av EPS". *Intern raport Nr. 1645*, Norwegian Road Research Laboratory, Oslo, Norway (1993) 22 pp.

Aoyama, N., "Earth Pressure Test of Retaining Wall Using EPS as Backfilling Material". *The Foundation Engineering and Equipment*, Vol. 18 (1990) pp. 21-25 (in Japanese).

Arai, N., Yokoyama, M. and Tamura, H., "EPS Embankment in Construction Road for 32 Ton Dump Trucks at Gassan Dam". *Proceedings of the International Symposium on EPS Construction Method (EPS Tokyo '96)*, EPS Construction Method Development Organization, Tokyo, Japan (1996) pp. 129-139.

Bang, S., Preber, T. and Cho, Y., "Evaluation of Expanded Polystyrene Block Bridge Backfill by Finite Element Method of Analysis". *Proceedings of the 31st Annual Geological and Geotechnical Symposium*, J. A. Caliendo (ed.), Utah State University, Logan, Utah, U.S.A. (1995) pp. 96-102.

Bartlett, S. F., "Research Initiatives for Monitoring Long Term Performance of I-15 Embankments, Salt Lake City, Utah". *Proceedings of the 34th Symposium on Engineering Geology & Geotechnical Engineering*, J. A. Bay (ed.), Utah State University, U.S.A. (1999) pp. 54-67.

Beinbrech, G., “Current Status of Geofoam Construction Method in Germany”. *Proceedings of the International Symposium on EPS Construction Method (EPS Tokyo ‘96)*, EPS Construction Method Development Organization, Tokyo, Japan (1996) pp. 117-127.

Beinbrech, G. and Hillman, R., "EPS in Road Construction - Current Situation in Germany”. *Geotextiles and Geomembranes*, Elsevier Science Ltd., London, U.K., Vol. 15, Nos. 1-3 (1997) pp. 39-57.

Briaud, J.-L., James, R. W. and Hoffman, S. B. "Settlement of Bridge Approaches (The Bump at the End of the Bridge)". *Synthesis of Highway Practice 234*, National Academy Press, Washington, D.C., U.S.A. (1997) 75 pp.

Bull-Wasser, R., "EPS - Hartschaum als Baustoff für Straßen". *Berichte der Bundesanstalt für Straßenwesen - Straßenbau Heft S4*, Bundesanstalt für Straßenwesen, Bergisch Gladbach, Germany (1993).

Carlsten, P., "Vertical Wall Made from Expanded Polystyrene - An Alternative to a Conventional Retaining Wall". In *Expanded Polystyrene as Light Fill Material; Technical Visit around Stockholm - June 19, 1991*, Swedish Geotechnical Institute, Linköping, Sweden (1991).

Chang, Y. C., “The Numerical Analysis and Field Measurement of EPS Embankment”. *Proceedings of the International Symposium on EPS Construction Method (EPS Tokyo ‘96)*, EPS Construction Method Development Organization, Tokyo, Japan (1996) pp. 149-160.

Cho, S. D., Kim, J. M., Woo, J. Y. and Choi, J. D., “Behavior of Vertical Wall System Using EPS Blocks”. *Proceedings of the International Symposium on EPS Construction Method (EPS Tokyo ‘96)*, EPS Construction Method Development Organization, Tokyo, Japan (1996) pp. 169-177.

Coleman, T. A., "Polystyrene Foam is Competitive, Lightweight Fill". *Civil Engineering*, American Society of Civil Engineers, New York, N.Y., U.S.A., Vol. 44, No. 2 (1974) pp. 68-69.

"Composite Modules Make Golf Green Float". *ENR*, December 3 (1990) p. 20.

Corbet, S. P. and Mobbs, C. J., “EPS Fill in the Dovercourt Bypass Embankment”. *Proceedings of the International Symposium on EPS Construction Method (EPS Tokyo ‘96)*, EPS Construction Method Development Organization, Tokyo, Japan (1996) pp. 141-148.

Crawford, C. B., Fannin, R. J. and Kern, C. B., "Embankment Failures at Vernon, British Columbia". *Canadian Geotechnical Journal*, Vol. 32, No. 2 (1995) pp. 271-284.

Dahlberg, R. G. and Refsdal, G., "Polystyrene Foam for Lightweight Road Embankments". *Proceedings of the PIARC XVIth World Road Congress*, Permanent International Association of Road Congresses (1979).

Dahlberg, R. G. and Refsdal, G., "Polystyrene Foam for Lightweight Road Embankments". *Publication No. 53*, Norwegian Road Research Laboratory, Oslo, Norway (1981) pp. 27-33.

Dorp, T., “Building on EPS Geofoam in the ‘Low-Lands’ - Experience in The Netherlands”. *Proceedings of the International Symposium on EPS Construction Method (EPS Tokyo ‘96)*, EPS Construction Method Development Organization, Tokyo, Japan (1996) pp. 59-69.

Duškov, M., "Use of Expanded Polystyrene Foam (EPS) in Flexible Pavements on Poor Subgrades". *Proceedings of the International Conference on Geotechnical Engineering for Coastal Development - Theory and Practice*, Yokohama, Japan (1991) pp. 783-788.

Duškov, M., "Influence of an EPS Sub-Base on the Pavement Structure's Behaviour". *Proceedings of the International Conference on Geotechnical Engineering for Coastal Development - Theory and Practice*, Yokohama, Japan (1991) p. 1163.

Duškov, M., "Measurements on Concrete Block Pavement Structures with an EPS Sub-Base". Research report, Delft University of Technology, Delft, The Netherlands (1993).

Duškov, M., "DIANA Non-Linear Analysis of Pavement Structures with an EPS Sub-Base Under Static Loading". *Report No. 7-94-211-3*, Delft University of Technology, Delft, The Netherlands (1994).

Duškov, M., "Measurements on Concrete Block Pavement Structures with an EPS Sub-Base". *Report No. 7-94-211-4*, Delft University of Technology, Delft, The Netherlands (1994).

Duškov, M., "Measurements on a Flexible Pavement Structure with an EPS Sub-Base". *Report No. 7-94-211-5*, Delft University of Technology, Delft, The Netherlands (1994).

Duškov, M., "EPS as a Light Weight Sub-Base Material in Pavement Structures; Final Report". *Report No. 7-94-211-6*, Delft University of Technology, Delft, The Netherlands (1994).

Duškov, M., "Asphalt Test Pavements with a Sub-Base of Expanded Polystyrene (EPS) Geofoam". *Geosynthetics World*, Geosynthetics Publications, Ltd., U.K., Vol. 5, No. 2 (1995) pp. 5-9.

Duškov, M., "Case Study of a Flexible Pavement Structure with the EPS Geofoam Sub-Base". *Proceedings of the First European Geosynthetics Conference - EuroGeo 1*, A. A. Balkema, Rotterdam, The Netherlands (1996) pp. 287-294.

Duškov, M., "3-D Finite Element Analyses of Pavement Structures with an EPS Geofoam Sub-Base". *Proceedings of the International Symposium on EPS Construction Method (EPS Tokyo '96)*, EPS Construction Method Development Organization, Tokyo, Japan (1996) pp. 47-57.

Duškov, M., "EPS as a Light-Weight Sub-Base Material in Pavement Structures". Doctor of Engineering thesis, Delft University of Technology, Delft, The Netherlands, 1st ed. (1997).

Duškov, M., "EPS as a Light-Weight Sub-Base Material in Pavement Structures". Doctor of Engineering thesis, Delft University of Technology, Delft, The Netherlands, 2nd ed. (1998).

Duškov, M., "Measurements on a Flexible Pavement Structure with an EPS Geofoam Sub-Base". *Geotextiles and Geomembranes*, Elsevier Science Ltd., London, U.K., Vol. 15, Nos. 1-3 (1997) pp. 5-27.

Duškov, M. and Bull-Wasser, R., "Analysis of Asphalt Test Pavements with a Sub-Base of Expanded Polystyrene Foam". *Proceedings of the 7th International Conference on Asphalt Pavements - Design, Construction and Performance*, Vol. III, Nottingham (1992) pp. 96-109.

Duškov, M., Houben, L. J. M. and Scarpas, A., "Response Investigation and Design Guidelines for Asphalt Pavements with an EPS Geofoam Sub-Base". *Proceedings of the Sixth International Conference on Geosynthetics*, R. K. Rowe (ed.), Industrial Fabrics Association International, Roseville, Minn., U.S.A. (1998) pp. 993-998.

Duškov, M. and Scarpas, A., "Three-Dimensional Finite Element Analysis of Flexible Pavements with an (Open Joint in the) EPS Sub-Base". *Geotextiles and Geomembranes*, Elsevier Science Ltd., London, U.K., Vol. 15, Nos. 1-3 (1997) pp. 29-38.

Ekström, A. and Tränk, R., "Plastic Foam in Road Embankments - Two Case Histories from Sweden". In *Expanded Polystyrene as Light Fill Material; Technical Visit around Stockholm - June 19, 1991*, Swedish Geotechnical Institute, Linköping, Sweden (1991).

Elander, P., "Access Embankment to a Bridge on Soft Clay - An Example of Design with Expanded Polystyrene". In *Expanded Polystyrene as Light Fill Material; Technical Visit around Stockholm - June 19, 1991*, Swedish Geotechnical Institute, Linköping, Sweden (1991).

"EPS Foam Keeps Building Foundation From Shifting". *Modern Plastic International*, Lausanne, Switzerland, No. 9 (1991).

Eriksson, L., "Kungsängsleden - Light Fill Embankment with Expanded Polystyrene". In *Expanded Polystyrene as Light Fill Material; Technical Visit around Stockholm - June 19, 1991*, Swedish Geotechnical Institute, Linköping, Sweden (1991).

"Example of Construction of Upright Retaining Walls on a Slope". *Technical Reports of Construction Method Using Expanded Polystyrol*, Expanded Polystyrol Construction Method Development Organization, Tokyo, Japan (1991).

"Example of Implementation at a Station". *Technical Reports of Construction Method Using Expanded Polystyrol*, Expanded Polystyrol Construction Method Development Method, Tokyo, Japan (1991).

"Execution of Consolidation Settlement Reducing Construction Method on the Poor Ground Using Expanded Polystyrol". *Technical Reports of Construction Method Using Expanded Polystyrol*, Expanded Polystyrol Construction Method Development Method, Tokyo, Japan (undated).

"Expanded Polystyrene is Economic Filler". *Highways* (1991).

"Fahrbahn-Setzung Begrenzt; Emder Pilotprojekt: Polystyrol-Teile für Autobahnbau Eingesetzt". *Ostfriesen-Zeitung*, Germany, 29 March (1995) p. 12.

"Fillmaster Used in Bridge Abutments". *Highways and Transportation*, June (1991) p. 15.

Flaate, K., "The (Geo)Technique of Superlight Materials". In *The Art and Science of Geotechnical Engineering at the Dawn of the Twenty-First Century - A Volume Honoring Ralph B. Peck*, E. J. Cording, W. J. Hall, J. D. Haltiwanger, A. J. Hendron, Jr., and G. Mesri (eds.), Prentice-Hall, Englewood Cliffs, N.J., U.S.A. (1989) pp. 193-205.

"Founded on Foam". *World Highways/Routes du Monde*, Route One Publishing Ltd., U.K., Vol. 1, No. 1 (1991) pp. 37-38.

Frydenlund, T. E., "Superlight Fill Materials". *Publication No. 60*, Norwegian Road Research Laboratory, Oslo, Norway (1986) pp. 11-14.

Frydenlund, T. E., "Soft Ground Problems". *Publication No. 61*, Norwegian Road Research Laboratory, Oslo, Norway (1987) pp. 7-12.

Frydenlund, T. E., "Expanded Polystyrene - A Lighter Way Across Soft Ground". *Internal Report No. 1502*, Norwegian Road Research Laboratory, Oslo, Norway (1991).

Frydenlund, T. E., "Standardization Activities within CEN". *Proceedings of the June 21, 1991 Seminar on the Use of EPS in Road Construction*, Norwegian Road Research Laboratory, Oslo, Norway (1991).

Frydenlund, T. E., "Railway Underpass at Bøle". *Proceedings of the June 21, 1991 Seminar on the Use of EPS in Road Construction*, Norwegian Road Research Laboratory, Oslo, Norway (1991).

Frydenlund, T. E. and Aabøe, R., "Expanded Polystyrene - A Superlight Fill Material". *Proceedings of the International Geotechnical Symposium on Theory and Practice of Earth Reinforcement; Fukuoka, Japan*, A. A. Balkema, Rotterdam, The Netherlands (1988) pp. 383-388.

Frydenlund, T. E. and Aabøe, R., "A Challenging Concept in Road Construction - Superlight Fill Materials". *Nordic Road & Transport Research*, Vol. 1, No. 2 (1989) pp. 18-21.

Frydenlund, T. E. and Aabøe, R., "Expanded Polystyrene - A Lighter Way Across Soft Ground". Preprint paper, *Proceedings of the XIII International Conference on Soil Mechanics and Foundation Engineering*, New Delhi, India (1994).

Frydenlund, T. E. and Aabøe, R., "Expanded Polystyrene - A Lighter Way Across Soft Ground". *Proceedings of the XIII International Conference on Soil Mechanics and Foundation Engineering*, Vol. 3, A. A. Balkema, Rotterdam, The Netherlands (1994) pp. 1287-1292.

Frydenlund, T. E. and Aabøe, R., "Expanded Polystyrene - A Lighter Way Across Soft Ground". *Internal Report No. 1662*, Norwegian Road Research Laboratory, Oslo, Norway (1994) 6 pp.

Frydenlund, T. E. and Aabøe, R., "Expanded Polystyrene - A Lighter Way Across Soft Ground". Preprint paper, International Geotechnical Symposium on Polystyrene Foam in Below-Grade Applications, Honolulu, Hawaii, U.S.A. (1994).

Frydenlund, T. E. and Aabøe, R., "Expanded Polystyrene - A Lighter Way Across Soft Ground". *Proceedings; International Geotechnical Symposium on Polystyrene Foam in Below-Grade Applications; March 30, 1994; Honolulu, Hawaii, U.S.A.; Research Report No. CE/GE-94-1*, J. S. Horvath (ed.), Manhattan College, Bronx, N.Y., U.S.A. (1994).

Frydenlund, T. E. and Aabøe, R., “Expanded Polystyrene - The Light Solution”. *Proceedings of the International Symposium on EPS Construction Method (EPS Tokyo ‘96)*, EPS Construction Method Development Organization, Tokyo, Japan (1996) pp. 31-46.

"Geotechnical Engineering in the Twenty-First Century". *ISSMFE News*, International Society for Soil Mechanics and Foundation Engineering, Vol. 16, No. 1 (1989) p. 2.

"Great Yarmouth Bridge Abutment Uses Polystyrene as Lightweight Fill". *Ground Engineering*, Thomas Telford Ltd., London, U.K., Vol. 19, No. 1 (1986) pp. 20-23.

"Ground Improvement & Filling with EPS". *Geosynthetics World*, Geosynthetics Publications, Ltd., U.K., Vol. 5, No. 2 (1995) p. 13.

Hagen, E., "New Highway No. 181 at Eidsvoll - Use of Expanded Polystyrene in Two Embankments". *Proceedings of the June 21, 1991 Seminar on the Use of EPS in Road Construction*, Norwegian Road Research Laboratory, Oslo, Norway (1991).

Hartlén, J., "Pressure Berms, Soil Replacement and Lightweight Fills". *Proceedings of the 3rd International Geotechnical Seminar*, Nanyang Technological Institute, Singapore (1985) pp. 101-111.

Hasegawa, N., Shinozaki, W. and Marui, E., "Method of Reducing the Vertical Earth Pressure in Retaining Wall Using Expanded Polystyrol". *Technical Reports of Construction Method Using Expanded Polystyrol*, Expanded Polystyrol Construction Method Development Method, Tokyo, Japan (undated).

Hatanaka, S., Nishiyama, S., Shimada, T. and Kusakabe, Y., "Use of EPS Blocks for Landslide Countermeasure". *Tsuchi-to-Kiso (Soils and Foundations)*, Japanese Society of Soil Mechanics and Foundation Engineering, Tokyo, Japan, Vol. 39, No. 4 (1991); in Japanese; English abstract in *Soils and Foundations*, Japanese Society of Soil Mechanics and Foundation Engineering, Tokyo, Japan, Vol. 31, No. 2 (1991).

Higuchi, Y., "EPS Construction Method". *The Foundation Engineering and Equipment*, Vol. 18 (1990) pp. 10-20 (in Japanese).

Hillman, R., "Research Projects on EPS in Germany - Material Behavior and Full Scale Model Studies". *Proceedings of the International Symposium on EPS Construction Method (EPS Tokyo '96)*, EPS Construction Method Development Organization, Tokyo, Japan (1996) pp. 105-115.

Himeno, K., "Temperature Distributions in Pavement Structure". *Proceedings of the International Conference on Geotechnical Engineering for Coastal Development - Theory and Practice*, Yokohama, Japan (1991) p. 1164.

Hohwiller, F., "EPS-Hartschaum als Leichtbaustoff im Straßenunterbau". *Straßen und Tiefbau*, Vol. 45, No. 1/2 (1991) pp. 10-17.

Holtz, R. D., "Treatment of Problem Foundations for Highway Embankments". *National Cooperative Highway Research Program Synthesis of Highway Practice 147*, Transportation Research Board, Washington, D.C., U.S.A. (1989).

Horbay, J. F., "Polystyrene Foam". In *Lightweight Fills for Embankment Construction*, Bachelor's degree thesis, Lakehead University, Canada (1984).

Horvath, J. S. Editorial letter, *Geotechnical Fabrics Report*, Industrial Fabrics Association International, St. Paul, Minn., U.S.A., Vol. 11, No. 5 (1993) pp. 8-9.

Horvath, J. S., discussion of "Weight-Credit Foundation Construction Using Artificial Fills" by E. J. Monahan, *Transportation Research Record No. 1422*, Transportation Research Board, Washington, D.C., U.S.A. (1993) pp. 4-5.

Horvath, J. S., "Can Geosynthetic Reinforcement Prove Useful in a 'Modified Dutch' Pavement System?". *Geosynthetics World*, Geosynthetics Publications, Ltd., U.K., Vol. 5, No. 2 (1995) p. 12.

Horvath, J. S., editorial letter. *ASCE News*, American Society of Civil Engineers, New York, N.Y., U.S.A. (1995).

Horvath, J. S., “Geofoam: A Lighter Alternative in Earthwork”. *Land and Water*, Fort Dodge, Ia., U.S.A., Vol. 40, No. 4 (1996) pp. 18-20.

Hotta, H., Nishi, T. and Kuroda, S., “Report of Results of Assessments of Damage to EPS Embankments Caused by Earthquakes”. *Proceedings of the International Symposium on EPS Construction Method (EPS Tokyo ‘96)*, EPS Construction Method Development Organization, Tokyo, Japan (1996) pp. 307-318.

Hotta, H., Nishi, T. and Tadatsu, T., "Dynamic Deformation Property of Expanded Polystyrene". *Twenty-Sixth National Conference of the Japanese Society of Soil Mechanics and Foundation Engineering*, Vol. 2 (1991) pp. 2225-2226 (in Japanese).

Ishihara, K., Kurihara, T., Tatsumi, O., Mae, Y. and Abe, M., “Application of EPS Construction Method to a Level Joint on Abutment”. *Proceedings of the International Symposium on EPS Construction Method (EPS Tokyo ‘96)*, EPS Construction Method Development Organization, Tokyo, Japan (1996) pp. 275-285.

Ishihara, K., Matsumoto, K. and Kato, T., “A Large EPS Embankment to Prevent from Lateral Flow Caused by Weak Subsoil”. *Proceedings of the International Symposium on EPS Construction Method (EPS Tokyo ‘96)*, EPS Construction Method Development Organization, Tokyo, Japan (1996) pp. 297-305.

Jutkofsky, W. S., “Geofoam Stabilization of an Embankment Slope; A Case Study of Route 23A in the Town of Jewett, Greene County”. Report, New York State Department of Transportation, Geotechnical Engineering Bureau, Albany, N. Y., U. S. A. (1998) 42 pp.

Kanai, M. and Kamato, Y., "Use of EPS (Expanded Polystyrene) Material in Embankment Remedy on a Steep Slope". *Tsuchi-to-Kiso (Soils and Foundations)*, Japanese Society of Soil Mechanics and Foundation Engineering, Tokyo, Japan, Vol. 39, No. 8 (1991); in Japanese; English abstract in *Soils and Foundations*, Japanese Society of Soil Mechanics and Foundation Engineering, Tokyo, Japan, Vol. 31, No. 3 (1991).

Koga, Y., Koseki, J. and Shimazu, T., "Shaking Table Test and Finite Element Analysis on Seismic Behavior of Expanded Polystyrol Embankment". *Civil Engineering Journal*, Vol. 33-8 (1991) pp. 56-61 (in Japanese).

Kuroda, S., Hotta, H. and Yamazaki, F., “Simulation of Shaking Table Test for EPS Embankment Model by Distinct Element Method”. *Proceedings of the International Symposium on EPS Construction Method (EPS Tokyo ‘96)*, EPS Construction Method Development Organization, Tokyo, Japan (1996) pp. 83-92.

Kurose, M. and Tanaka, T., “EPS Block with H or C Shape Cross Section for Embankment”. *Proceedings of the International Symposium on EPS Construction Method (EPS Tokyo ‘96)*, EPS Construction Method Development Organization, Tokyo, Japan (1996) pp. 189-199.

Kutara, K., Aoyama, N. and Takeuchi, T., "Use of New Super-Lightweight Material for Embankments". *Annual Report of the Public Works Research Institute*, Japan (1988).

Kutara, K., Aoyama, N. and Takeuchi, T., "Horizontal Pressure by EPS Used as Back Filling Behind Structures". *Proceedings of the 24th Japan National Conference on Soil Mechanics and Foundation Engineering* (1989) pp. 65-66.

Kutara, K., Aoyama, N. and Takeuchi, T., "Earth Pressure Test of Retaining Wall Using EPS As Backfilling Material". *Technical Reports of Construction Method Using Expanded Polystyrol*, Expanded Polystyrol Construction Method Development Method, Tokyo, Japan (1989).

Kutara, K., Aoyama, N., Takeuchi, T. and Takechi, O., "Experiments on Application of Expanded Polystyrol to Light Fill Materials". *The Foundation Engineering and Equipment*, Vol. 17 (1989) pp. 49-54 (in Japanese).

Kutara, K. and Fujino, T., "Use of Expanded Polystyrol and Corrugated Steel Pipes for Lightweight Road Embankments in Japan". *Annual Report of Roads*, Japan Road Association (1988).

Kyuraku, K., Aoyama, N. and Takeuchi, T., "Behavior of Polystyrene Foam When Subjected to Traffic Loads". *17th Japan Road Association Conference* (undated).

“Landslides; Investigation and Mitigation”. *Special Report 247*, Transportation Research Board, Washington, D.C., U.S.A. (1996) 673 pp.

"Large Scale Implementation of EPS Construction Method". *Technical Reports of Construction Method Using Expanded Polystyrol*, Expanded Polystyrol Construction Method Development Method, Tokyo, Japan (1989).

"Largest Rooftop Park Built on Foam". *Civil Engineering*, American Society of Civil Engineers, New York, N.Y., U.S.A., Vol. 63, No. 6 (1993) p. 86.

“Lightweight Fill Cuts Plaza Load”. *Ground Engineering*, Thomas Telford Ltd., London, U.K., Vol. 31, No. 2 (1998) p. 12.

“Lightweight Fill Brings Rail Line Back to Speed”. *Ground Engineering*, Thomas Telford Ltd., London, U.K., Vol. 31, No. 10 (1998) p. 15.

MacElroy, A., "Founded on Foam". *Esso Magazine*, No. 114 (undated) pp. 10-13.

MacMaster, J. B. and Wrong, G. A., "The Role of Extruded Expanded Polystyrene in Ontario's Provincial Transportation System". *Transportation Research Record No. 1146*, Transportation Research Board, Washington, D.C., U.S.A. (1987) pp. 10-22.

Magnan, J.-P., "Recommandations pour L´Utilisation de Polystyrene Expanse en Remblai Routier". Laboratoire Central Ponts et Chaussées, France (1989) 20 pp.

Magnan, J.-P., "Methods to Reduce the Settlement of Embankments on Soft Clay: A Review". *Vertical and Horizontal Deformations of Foundations and Embankments*, A. T. Yeung and G. Y. Félio (eds.), American Society of Civil Engineers, New York, N.Y., U.S.A. (1994) pp. 77-91.

Matsuda, T., Ugai, K. and Gose, S., "Application of EPS to Backfill of Abutment for Earth Pressure Reduction". *Proceedings of the International Symposium on EPS Construction Method (EPS Tokyo '96)*, EPS Construction Method Development Organization, Tokyo, Japan (1996) pp. 327-332.

Matsumoto, K., Kato, T. and Ishihara, K., "Countermeasures for the Lateral Displacement of Piles in Soft Clay". *Proceedings of GEOCOAST '91: International Conference on Geotechnical Engineering for Coastal Development - Theory and Practice*, Yokohama, Japan (1991).

McElhinney, A. H. and Sanders, R. L., "A47 Great Yarmouth Western Bypass: Use and Performance of Polystyrene Fill". *Contractor Report No. 296*, Transport and Road Research Laboratory, Crowthorne, Berkshire, U.K. (1992) 26 pp.

Miki, G., “EPS Construction Method in Japan”. *Proceedings of the International Symposium on EPS Construction Method (EPS Tokyo ‘96)*, EPS Construction Method Development Organization, Tokyo, Japan (1996) pp. 1-7.

Miki, G., “Ten Year History of EPS Method in Japan and Its Future Challenges”. *Proceedings of the International Symposium on EPS Construction Method (EPS Tokyo ‘96)*, EPS Construction Method Development Organization, Tokyo, Japan (1996) pp. 394-411.

Miki, G., Sagawa, Y., Takagi, H. and Tsukamoto, H., "Performance of Full Scale Road Embankment with Expanded Polystyrol". *The Foundation Engineering and Equipment*, Vol. 17 (1989) pp. 55-60 (in Japanese).

Miki, G. and Tsukamoto, H., "Behaviour of EPS Embankment in a Scale of Actual Banking by Using EPS Construction Method". *Technical Reports of Construction Method Using Expanded Polystyrol*, Expanded Polystyrol Construction Method Development Method, Tokyo, Japan (undated).

Miki, H., “An Overview of Lightweight Banking Technology in Japan”. *Proceedings of the International Symposium on EPS Construction Method (EPS Tokyo ‘96)*, EPS Construction Method Development Organization, Tokyo, Japan (1996) pp. 9-30.

Mimura, C. S. and Kimura, S. A., "A Lightweight Solution". *Proceedings - Geosynthetics '95*, Industrial Fabrics Association International, St. Paul, Minn., U.S.A. (1995) pp. 39-51.

Miyamoto, Y., Duan, M., Iwasaki, S., Deto, H. and Fujiwara, T., “Fundamental Study on Continuous Footing Made with EPS Styrofoam”. *Proceedings of the International Symposium on EPS Construction Method (EPS Tokyo ‘96)*, EPS Construction Method Development Organization, Tokyo, Japan (1996) pp. 349-359.

Mohamad, E. B., “History of EPS as Embankment Fill in Malaysia under PIC and Its Future”. *Proceedings of the International Symposium on EPS Construction Method (EPS Tokyo ‘96)*, EPS Construction Method Development Organization, Tokyo, Japan (1996) pp. 257-264.

Momoi, T. and Kokusho, T., “Evaluation of Bearing Properties of EPS Subgrade”. *Proceedings of the International Symposium on EPS Construction Method (EPS Tokyo ‘96)*, EPS Construction Method Development Organization, Tokyo, Japan (1996) pp. 93-103.

Monahan, E. J., "Weight-Credit Foundation Construction Using Foam Plastic as Fill". Notes distributed at a lecture sponsored by the American Society of Civil Engineers Metropolitan Section, New York, N.Y., U.S.A. (undated).

Monahan, E. J., "Weight-Credit Foundation Construction Using Foam Plastic as Fill". *New Horizons in Construction Materials; Volume I*, H.-Y. Fang (ed.), Envo Publishing Company, Inc., Lehigh Valley, Pa., U.S.A. (1976) pp. 199-210.

Monahan, E. J., “Construction of and on Compacted Fills”. John Wiley & Sons, New York, N.Y., U.S.A. (1986).

Monahan, E. J., "Weight-Credit Foundation Construction Using Artificial Fills". Preprint paper No. 930157, Transportation Research Board 72nd Annual Meeting, Washington, D.C., U.S.A. (1993).

Monahan, E. J., editorial letter. *Geotechnical Fabrics Report*, Industrial Fabrics Association International, St. Paul, Minn., U.S.A., Vol. 11, No. 3 (1993) p. 4.

Monahan, E. J., "Weight-Credit Foundation Construction Using Artificial Fills". *Transportation Research Record No. 1422*, Transportation Research Board, Washington, D.C., U.S.A. (1993) pp. 1-4.

Monahan, E. J., closure to "Weight-Credit Foundation Construction Using Artificial Fills". *Transportation Research Record No. 1422*, Transportation Research Board, Washington, D.C., U.S.A. (1993) pp. 5-6.

Monahan, E. J., editorial letter. *ASCE News*, American Society of Civil Engineers, New York, N.Y., U.S.A., May (1995).

Murata, O., Yasuda, Y., Tateyama, M. and Kikuchi, T., "Study on the Cyclic Loading Test and the Resonant Test of the Test Embankment Made by Using EPS on the Soft Ground". *Twenty-Fourth National Conference of the Japanese Society of Soil Mechanics and Foundation Engineering*, Vol. 1 (1988) pp. 53-56 (in Japanese).

Murata, O., Yasuda, Y., Tateyama, T., Hatinohe, Y. and Ohishi, M., "A Case Study of the Test Embankment by Using EPS (Expanded Polystyrol Construction Method) on the Soft Ground". *Twenty-Fourth National Conference of the Japanese Society of Soil Mechanics and Foundation Engineering* (1988) pp. 49-50 (in Japanese).

Myhre, Ø., "EPS - Material Specifications". *Publication No. 61*, Norwegian Road Research Laboratory, Oslo, Norway (1987) pp. 13-16.

Negussey, D., "Geofoam - A Super Light Weight Synthetic Geomaterial". *Geotechnical News*, BiTech Publishers Ltd., Richmond, B.C., Canada, Vol. 11, No. 1 (1993) p. 35.

Negussey, D. and Sun, M. C., "Reducing Lateral Pressure by Geofoam (EPS) Substitution". *Proceedings of the International Symposium on EPS Construction Method (EPS Tokyo '96)*, EPS Construction Method Development Organization, Tokyo, Japan (1996) pp. 201-211.

Ninomiya, K. and Ikeda, M., "Design & Construction of EPS Method Which Surfacing and Uses Anchor for Prevention". *Proceedings of the International Symposium on EPS Construction Method (EPS Tokyo '96)*, EPS Construction Method Development Organization, Tokyo, Japan (1996) pp. 161-167.

Nishi, T., Hotta, H. and Kuroda, S., "Feedback to Design Based on Results of Field Observations of EPS Embankments". *Proceedings of the International Symposium on EPS Construction Method (EPS Tokyo '96)*, EPS Construction Method Development Organization, Tokyo, Japan (1996) pp. 319-325.

Nishimura, S., Hayashi, M., Nakagawa, Y., Tanabe, S. and Matsumoto, K., “EPS Method Applied as a Countermeasure for Lateral Displacement of Soft Clay Ground Due to Embankment Work”. *Proceedings of the International Symposium on EPS Construction Method (EPS Tokyo ‘96)*, EPS Construction Method Development Organization, Tokyo, Japan (1996) pp. 287-295.

Nishizawa, T., Tsuji, K., Kiyota, Y., Oda, K. and Narikiyo, S., “EPS Vertical Wall Structure Back Fill at an Existing Sewage Treatment Plant”. *Proceedings of the International Symposium on EPS Construction Method (EPS Tokyo ‘96)*, EPS Construction Method Development Organization, Tokyo, Japan (1996) pp. 333-341.

Nomaguchi, A., “Studies on Earthquake Resisting Performance of EPS Embankment”. *Proceedings of the International Symposium on EPS Construction Method (EPS Tokyo ‘96)*, EPS Construction Method Development Organization, Tokyo, Japan (1996) pp. 382-393.

"Norway Banks on Foam". *International Construction*, Vol. 19 (1980) pp. 36-37.

Nystrom, J., "Geofoam Takes a New Tack". *Geotechnical Fabrics Report*, Industrial Fabrics Association International, Roseville, Minn., U.S.A., September (1999) pp. 40-41.

Ojima, K., Okazawa, Y., Matsunawa, I., Kitada, I., Tsuchiya, M., Yamaji, H. and Kojima, K., “Use of EPS in the Foundations of an Emergency Staircase of an Overpass”. *Proceedings of the International Symposium on EPS Construction Method (EPS Tokyo ‘96)*, EPS Construction Method Development Organization, Tokyo, Japan (1996) pp. 343-347.

"Plastic Roadbeds". *Newsweek*, December 15 (1980) p. 3.

"Plastics Replace Subsoil". *ENR*, April 27 (1989) p. 17.

"Polystyrene as Lightweight Fill: Norway and Yarmouth". *Road Engineering Intelligence & Research*, Vol. 13, No. 14 (1986) p. 3.

"Polystyrene Block for Building Bridges". *Highways*, September (1989) p. 14.

"Polystyrene Blocks Support Sinking Roadway". *Civil Engineering*, American Society of Civil Engineers, New York, N.Y., U.S.A., Vol. 64, No. 10 (1994) p. 86.

"Polystyrene Blocks Take Load on Soft Ground". *Highways*, November (1987).

"Polystyrene Fill Lightens Slope". *Highway & Heavy Construction*, U.S.A., Vol. 132, No. 12 (1989) p. 77.

"Polystyrene Foam Eases the Burden at Syracuse Mall". *Civil Engineering*, American Society of Civil Engineers, New York, N.Y., U.S.A., Vol. 61, No. 10 (1991) pp. 84.

"Polystyrene-Stabilized". *Contractors Market Center* (1989).

"Polystyrol Roads Introduced in Japan". *International Roads Federation*, May (1989).

"Potential of EPS Blocks in Construction". *Road Engineering Intelligence & Research*, July-August (1990) p. 8.

Preber, T. and Bang, S., "Field Application and Instrumentation of Expanded Polystyrene Blocks as Bridge Backfill". *Proceedings of the 31st Annual Geological and Geotechnical Symposium*, J. A. Caliendo (ed.), Utah State University, Logan, Utah, U.S.A. (1995) pp. 84-95.

Ramstedt, T. and Pettersson, L., "Cellplast som Lättfyllning i Vägbankar". *Document No. 1990:49*, Vägverket - Serviceavdelningen Väg- och Brokonstruktion, Sektionen för geoteknik, Ånge, Sweden (1990).

Refsdal, G., "Plastic Foam - From Frost Protection to Road Embankments". *The Northern Engineer*, Vol. 17, No. 3 (1985) pp. 16-19.

Refsdal, G., "EPS - Design Considerations". *Publication No. 61*, Norwegian Road Research Laboratory, Oslo, Norway (1987) pp. 17-20.

Refsdal, G., "Future Trends for EPS Use". *Publication No. 61*, Norwegian Road Research Laboratory, Oslo, Norway (1987) pp. 29-32.

Robbins, J., "Light Answer". *New Civil Engineer*, No. 1018, Thomas Telford Ltd., London, U.K., November 5 (1992) p. 24.

Rygg, N. O. and Sørlie, A., "Polystyrene Foam for Lightweight Road Embankment". *Proceedings of the Xth International Conference on Soil Mechanics and Foundation Engineering*, Vol. 2, A. A. Balkema (1981) pp. 247-252.

Sanders, R. L., “United Kingdom Design and Construction Experience with EPS”. *Proceedings of the International Symposium on EPS Construction Method (EPS Tokyo ‘96)*, EPS Construction Method Development Organization, Tokyo, Japan (1996) pp. 235-246.

Scheidegger, F., "Strassenbauten in Weichen Böden". *Schweizer Baublatt No. 97/Autostrasse No. 8*, 6 December (1977).

"Shop Aground". *NCE Roads Supplement*, Institution of Civil Engineers, U.K., June (1994) pp. 41-43.

Skuggedal, H. and Aabøe, R., "Temporary Overpass Bridge Founded on Expanded Polystyrene". *Proceedings of the 10th European Conference on Soil Mechanics and Foundation Engineering*, Vol. 2, Florence, Italy (1991) pp. 559-561.

Skuggedal, H. and Aabøe, R., "Temporary Overpass Bridge Founded on Expanded Polystyrene". *Proceedings of the June 21, 1991 Seminar on the Use of EPS in Road Construction*, Norwegian Road Research Laboratory, Oslo, Norway (1991).

Skuggedal, H. and Aabøe, R., "Temporary Overpass Bridge Abutments Founded on Fills of Expanded Polystyrene". *Nordic Road & Transport Research*, No. 2 (1991) pp. 20-23.

Sørlie, A., "Polystyrene Foam for Lightweight Road Embankments". *Proceedings of the XVIth World Road Congress*, Vienna, Austria (1979).

Stewart, J. P., Lacy, H. S. and Ladd, C. C., "Settlement of Large Mat on Deep Compressible Soil". *Vertical and Horizontal Deformations of Foundations and Embankments*, A. T. Yeung and G. Y. Félio (eds.), American Society of Civil Engineers, New York, N.Y., U.S.A. (1994) pp. 842-859.

Stewart, J. P., Pitulej, K. H. and Lacy, H. S., "Large Mat on Deep Compressible Soil". *Design and Performance of Mat Foundations - State-of-the-Art Review*, E. J. Ulrich (ed.),, American Concrete Institute, Detroit, Mich., U.S.A. (1995) pp. 245-264.

"Straßen Unterbau aus Hartschaum Bewährt Sich". *Straßen und Tiefbau*, Vol. 40, No. 6 (1986) p. 35.

Suzuki, Y., Nishimura, A. and Kuno, T., “Design and Construction of Road Embankment of Steep Hillside by EPS”. *Proceedings of the International Symposium on EPS Construction Method (EPS Tokyo ‘96)*, EPS Construction Method Development Organization, Tokyo, Japan (1996) pp. 265-273.

Takahara, T. and Miura, K., "Mechanical Characteristics of EPS Block Fill and Its Simulation by DEM and FEM". *Soils and Foundations*, Japanese Geotechnical Society, Tokyo, Japan, Vol. 38, No. 1 (1998) pp. 97-110.

Takahashi, Y., Hachinohe, Y., Marui, E. and Shinozaki, W., "Behavior of Upright Wall Using Expanded Polystyrol". *Technical Reports of Construction Method Using Expanded Polystyrol*, Expanded Polystyrol Construction Method Development Method, Tokyo, Japan (undated).

Tamura, C., "Dynamic Stability of EPS Block Structures". *The Foundation Engineering and Equipment*, Vol. 18, No. 12 (1990) pp. 26-30 (in Japanese).

Tamura, C., Konagai, K., Toi, Y. and Shibano, N., "Fundamental Study on Dynamic Stability of Expanded Polystyrol Block Structure - Part 1". *Journal of Institute of Industrial Science*, University of Tokyo, Japan, Vol. 41, No. 9 (1989) pp. 41-44 (in Japanese).

Tateyama, M., Murata, O. and Katanoda, T., "Application of EPS to Railway Road". *The Foundation Engineering and Equipment*, Vol. 18, No. 12 (1990) pp. 31-39 (in Japanese).

"Test Work of EPS Construction Method on National Road Route 1 Numazu By-Pass Road". Expanded Polystyrol Construction Method Development Method, Tokyo, Japan (undated).

Toi, Y., Shibano, N., Tamura, C. and Konagai, K., "Fundamental Study on Dynamic Stability of Expanded Polystyrol Block Structures - Part 2: Numerical Simulation". *Journal of Institute of Industrial Science*, University of Tokyo, Japan, Vol. 41, No. 9 (1989) pp. 45-48 (in Japanese).

Tränk, R., "Road E18, Enköping - Balsta; Active Design Using Lime Columns and EPS". *Expanded Polystyrene as Light Fill Material; Technical Visit around Stockholm - June 19, 1991*, Swedish Geotechnical Institute, Linköping, Sweden (1991).

Tsukamoto, H., “Slope Stabilization by the EPS Method and Its Applications”. *Proceedings of the International Symposium on EPS Construction Method (EPS Tokyo ‘96)*, EPS Construction Method Development Organization, Tokyo, Japan (1996) pp. 362-380.

Untitled preprint report by Expanded Polystyrol Construction Method Development Organization, Tokyo, Japan for the International Geotechnical Symposium on Polystyrene Foam in Below-Grade Applications held in Honolulu, Hawaii, U.S.A. (1994) 75 pp.

Untitled report by Expanded Polystyrol Construction Method Development Organization, Tokyo, Japan, *Proceedings; International Geotechnical Symposium on Polystyrene Foam in Below-Grade Applications; March 30, 1994; Honolulu, Hawaii, U.S.A.; Research Report No. CE/GE-94-1*, J. S. Horvath (ed.), Manhattan College, Bronx, N.Y., U.S.A. (1994).

Untitled case history volume for EPS-block geofoam and XPS geofoam used in lightweight fill applications, distributed at the International Symposium on EPS Construction Method (EPS Tokyo '96). EPS Construction Method Development Organization, Tokyo, Japan (undated) 61 pp. (in Japanese with English photo and figure captions).

"Use of EPS Blocks for Landslide Countermeasure". *Technical Reports of Construction Method Using Expanded Polystyrol*, Expanded Polystyrol Construction Method Development Method, Tokyo, Japan (1991).

van Dorp, T., "Expanded Polystyrene Foam as Light Fill and Foundation Material in Road Structures". Preprint paper, *The International Congress on Expanded Polystyrene: Expanded Polystyrene - Present and Future*, Milan, Italy (1988).

Wajima Public Works Bureau, "EPS Construction Method in Landslide Zone". *Technical Reports of Construction Method Using Expanded Polystyrol*, Expanded Polystyrol Construction Method Development Method, Tokyo, Japan (1989).

Wano, S., Oniki, K. and Hayakawa, H., “Prevention of Deformation of a Bridge Abutment Using the EPS Method and Its Effectiveness”. *Proceedings of the International Symposium on EPS Construction Method (EPS Tokyo ‘96)*, EPS Construction Method Development Organization, Tokyo, Japan (1996) pp. 179-187.

Widholm, P., “On Firm Footings; Expanded Polystyrene Supports Road, Supermarket”. *Midwest Construction Magazine*, August (1998).

Yamada, K., Sugimoto, M., Ogawa, S., Hotta, H. and Kuroda, S., "Vibration Characteristics of EPS Embankment Behind Abutment - Simulation Analysis". *Twenty-Seventh National Conference of the Japanese Society of Soil Mechanics and Foundation Engineering*, Vol. 2 (1992) pp. 2533-2534 (in Japanese).

Yamanaka, O., Onuki, T., Katsurada, H., Kitada, I., Kashima, K., Takamoto, A. and Maruoka, M., “Use of Vertical Wall-Type EPS Elevated Filling (H=15m) for Bridge Abutment Back Fill”. *Proceedings of the International Symposium on EPS Construction Method (EPS Tokyo ‘96)*, EPS Construction Method Development Organization, Tokyo, Japan (1996) pp. 223-233.

Yamazaki, F., Ichida, M., Ohbo, N. and Katayama, T., "Earthquake Observation and Finite Element Analysis of an RC Retaining Wall with EPS Backfill". *Journal of Institute of Industrial Science*, University of Tokyo, Japan, Vol. 44, No. 8 (1992) pp. 28-34.

Yamazaki, F., Ohbo, N., Kuroda, S. and Katayama, T., "Seismic Behavior of an RC Retaining Wall with EPS Backfill Based on Earthquake Observation and Response Analysis". Report (1994) 12 pp. (in Japanese with English abstract).

Yeh, S.-T. and Gilmore, J. B., "Application of EPS for Slide Correction". *Stability and Performance of Slopes and Embankments - II*, R. B. Seed and R. W. Boulanger (eds.), American Society of Civil Engineers, New York, N.Y., U.S.A. (1992) pp. 1444-1456.

Yoshihara, S. and Kawasaki, H., "Buried EPS Form for Large Scale Concrete Abutment". *Proceedings of the International Symposium on EPS Construction Method (EPS Tokyo '96)*, EPS Construction Method Development Organization, Tokyo, Japan (1996) pp. 235-246.

D.5 Design Manuals

International (Permanent International Association of Road Congresses - PIARC)

"Matériaux Légers pour Remblais/Lightweight Filling Materials". *Document No. 12.02.B*, PIARC - World Road Association, La Defense, France (1997) pp. 160-209 (in English and French).

France

"Utilisation de Polystyrene Expanse en Remblai Routier; Guide Technique". Laboratoire Central Ponts et Chaussées/SETRA, France (1990) 18 pp.

Germany

"Code of Practice; Using Expanded Polystyrene for the Construction of Road Embankments". BASF AG, Ludwigshafen, Germany (1995) 14 pp.

"Merkblatt für die Verwendung von EPS-Hartschaumstoffen beim Bau von Straßendämmen". Forschungsgesellschaft für Straßen- und Verkehrswesen, Arbeitsgruppe Erd- und Grundbau, Köln, Deutschland (1995), 27 pp.

Japan

"Design and Construction Manual for Lightweight Fill with EPS". The Public Works Research Institute of Ministry of Construction and Construction Project Consultants, Inc., Japan (1992) Ch. 3 and 5.

Norway

"Expanded Polystyrene Used in Road Embankments - Design, Construction and Quality Assurance". *Form 482E*, Public Roads Administration, Road Research Laboratory, Oslo, Norway (1992) 4 pp.

"Guidelines on the Use of Plastic Foam in Road Embankment". Public Roads Administration, Road Research Laboratory, Oslo, Norway (1980) 2 pp.

"Material Requirements for Expanded Polystyrene Used in Road Embankments". *Form 483E*, Public Roads Administration, Road Research Laboratory, Oslo, Norway (1992) 2 pp.

"Quality control of expanded polystyrene used in road embankments". *Form 484E*, Public Roads Administration, Road Research Laboratory, Oslo, Norway (1992) 4 pp.

United States of America

Elias, V., Welsh, J., Warren, J. and Lukas, R., "Ground Improvement Technical Summaries; Volume I; Demonstration Project 116; Working Draft: September 1998". *Publication No. FHWA-SA-98-086*, U.S. Department of Transportation, Federal Highway Administration, Washington, D.C., U.S.A. (1998) Section 2.

United Kingdom of Great Britain and Northern Ireland

Sanders, R. L. and Seedhouse, R. L., "The Use of Polystyrene for Embankment Construction". *Contractor Report 356*, Transport Research Laboratory, Crowthorne, Berkshire,, U.K. (1994) 55 pp.

D.6 U.S. Patents

Devine, J. P. and Holmquest, J. H., "Expanded Polystyrene Lightweight Fill". *U.S. Patent No. 5,549,418* (1996).

Monahan, E. J., "Floating Foundation and Process Therefor". *U.S. Patent No. 3,626,702* (1971).

Monahan, E. J., "Novel Low Pressure Back-Fill and Process Therefor". *U.S. Patent No. 3,747,353* (1973).

Savoy, T., "Building Material, with Protection from Insects, Molds, and Fungi". *U.S. Patent No. 5,194,323* (1993).

Savoy, T., "Building Material, with Protection from Insects, Molds, and Fungi". *U.S. Patent No. 5,270,108* (1993).

APPENDIX E
GLOSSARY OF TERMS

APPENDIX **E**

GLOSSARY OF TERMS

Block Molding is the second step in the two-step manufacturing process of EPS-block geofoam whereby the pre-puff is placed into a mold which is essentially a closed steel box that is rectangular in shape and steam is injected into the sealed mold to resoften the polystyrene and further expand the pre-puff causing the pre-puff to fuse thermally.

Blowing Agent is the naturally occurring petroleum hydrocarbon, almost always pentane (Japan is the only known country where an alternative, butane, is used routinely) mixed in the raw material of expandable polystyrene.

Compressive Strength is a traditional material parameter of EPS that is defined as the compressive stress at some arbitrary strain level. There is no universal agreement as to what this arbitrary strain level is. However, it is typically defined at 10 percent strain.

Creep is the additional strain or deformation that occurs with time under an applied stress or load of constant magnitude.

Density Gradients are variations in density within an EPS block caused by the inherent variability in the EPS manufacturing process.

Differential icing is a condition that develops during cold temperatures whereby ice forms on the pavement surface overlying lightweight fills while the adjacent pavement underlain by natural soil is ice free.

Elastic Limit Stress is the compressive stress at 1 percent strain as measured in a standard rapid-loading compression test.

Expandable Polystyrene (EPS) is the raw material that is used to manufacture EPS-block geofoam. Expandable polystyrene consists of fine to medium sand-size spherical particles of solid polystyrene with a naturally occurring petroleum hydrocarbon, almost always

pentane (Japan is the only known country where an alternative, butane, is used routinely), mixed in as a *blowing agent*. EPS is sometimes referred to as *beads or resin*.

External (global) stability is one of the three primary design phases where consideration is given to how the overall embankment, which consists of the combined fill mass and overlying pavement system, interacts with the existing foundation soil.

Failure is the loss of function of an embankment due to the embankment loads exceeding the resistance of the embankment and foundation and/or postconstruction settlement exceeding the maximum acceptable deformation.

Fill mass is the portion of the embankment that primarily consists of EPS-block geofoam, although some amount of soil fill may also be used between the foundation soil and bottom of the EPS blocks, and the soil or structural cover placed on the sides of the EPS blocks. It is one of the three major components of an EPS-block geofoam embankment.

Foundation soil is the existing natural soil that will support the embankment and is one of the three major components of an EPS-block geofoam embankment. Also referred to as soil subgrade.

Fusion refers to the thermal fusion between pieces of prepuff (and regrind when used) that occurs during the second stage of manufacturing, which is known as final block molding.

Initial Tangent Young's Modulus is the slope of the initial (approximately) linear portion of the stress-strain curve in a standard rapid-loading compression test.

Mechanical inter-block connectors are typically prefabricated barbed metal plates placed along the horizontal interfaces between EPS blocks, when required, to supplement the inter-block friction and provide additional resistance against horizontal driving or imposed forces.

Modified expandable polystyrene is a type of modified resin that contains an inorganic, bromine-based flame retardant that is sometimes used in the manufacture of flame-retardant EPS blocks.

Molder is the manufacturer of expanded polystyrene blocks that buys the expandable polystyrene and, in a multi-stage process, transforms it into expanded polystyrene block.

Oxygen Index (OI) is the minimum relative proportion (expressed as a percent) of oxygen in some mixture of gases that is required to support continuous combustion. Flammability of a polymeric material such as polystyrene is often measured or expressed by its OI.

Pavement system includes all materials, bound and unbound, placed above the EPS blocks and is one of the three major components of an EPS-block geofoam embankment. Design of the pavement system is one of the three primary design phases.

Pre-Expansion is the first step in the two-step manufacturing process of EPS-block geofoam whereby the expandable polystyrene raw material is placed into a large container called a *pre-expander* and then heated with steam. The expanded spheres of polystyrene are sometimes referred to as *pre-puff*.

Pre-Puff is the expanded spheres of polystyrene that are formed by the pre-expansion manufacturing process of EPS-block geofoam.

Regrind is recycled in-plant scrap or post-consumer recycled expanded polystyrene material that is reused by grinding it up into pieces that are generally sand-size. A small percentage of regrind is sometimes mixed in with virgin pre-puff during the final block molding process.

Relaxation is the reduction in applied stress or load with time under a constant magnitude of strain or deformation.

Seasoning is the process of allowing the EPS block to stabilize thermally (dimensional changes of the block occur during cooling) and chemically (residual blowing agent remaining in the cells of the EPS outgasses and is replaced by air) after the block is released from the mold. The block also dries during this seasoning period as a relatively significant amount of water vapor and liquid (which can artificially increase the apparent density of the EPS)

that is condensed steam from molding remains in the block at the end of molding. Seasoning is also referred to as *aging and conditioning* in the EPS industry.

Separation layer is a material placed between the EPS blocks and the overlying pavement system or between the embankment fill mass and the foundation soil.

Serviceability limit state (SLS) is the state at which the deformation of the embankment exceeds the maximum acceptable deformation.

Solar heating is a condition that develops during warm temperatures whereby the pavement surface overlying lightweight fills is warmer than the adjacent pavement underlain by natural soil.

Ultimate limit state (ULS) is the state at which the resistance of the embankment to failure is less than or equal to the embankment loads producing failure.

Ultra light cellular structures (ULCS) are a type of lightweight fill, sometimes called geocomb, because of their honeycomb appearance in cross section, that is similar to geofoam but with an open-cell structure that can flood and drain, and thus will not float.

Yield Stress is the stress corresponding to the onset of yielding in a standard rapid-loading test. Sometimes referred to as "plastic stress" .

APPENDIX F
CONVERSION FACTORS

APPENDIX **F**

CONVERSION FACTORS

Contents

F.1 INTRODUCTION

Both the Système International d'Unités (SI) and inch-pound (I-P) units have been used in this report. SI units are shown first and I-P units are shown in parentheses within text. Numerous figures are included for use in design. Therefore, only SI units are provided in some of the figures to avoid duplication of figures. Additionally, in some cases figures have been reproduced that use either all SI or all I-P Units. These figures have not been revised to show both sets of units. The one exception to the dual SI and I-P unit usage involves the quantities of density and unit weight. Density is the mass per unit volume and has units of kg/m^3 ($slugs/ft^3$) and unit weight is the weight per unit volume and has units of kN/m^3 (lbf/ft^3). Although density is the preferred quantity in SI, unit weight is still the common quantity in geotechnical engineering practice. Therefore, the quantity of unit weight will be used herein except when referring to EPS-block geofoam. The geofoam manufacturing industry typically uses the quantity of density with the SI units of kg/m^3 but with the I-P quantity of unit weight with units of lbf/ft^3. Therefore, the same dual unit system of density in SI and unit weight in I-P units will be used when referring to EPS-block geofoam.

F.2 CONVERSION FACTORS FROM INCH-POUND UNITS (I-P UNITS) TO THE LE SYSTÈME INTERNATIONAL d'UNITÉS (SI UNITS)

Length:	1 ft	=	0.3048 m
	1 ft	=	30.48 cm
	1 ft	=	304.8 mm
	1 in.	=	0.0254 m
	1 in.	=	2.54 cm
	1 in.	=	25.4 mm
	1 yd	=	0.9144 m
	1 yd	=	91.44 cm
	1 yd	=	914.4 mm
	1 mi	=	1.61 km
Area:	1 ft^2	=	929.03×10^{-4} m^2
	1 ft^2	=	929.03 cm^2
	1 ft^2	=	929.03×10^2 mm^2
	1 in^2	=	6.452×10^{-4} m^2
	1 in^2	=	6.452 cm^2
	1 in^2	=	645.16 mm^2
	1 yd^2	=	836.1×10^{-3} m^2
	1 yd^2	=	8361 cm^2
	1 yd^2	=	8.361×10^5 mm^2
Volume:	1 ft^3	=	28.317×10^{-3} m^3
	1 ft^3	=	28.317 cm^3
	1 in^3	=	16.387×10^{-6} m^3
	1 in^3	=	16.387 cm^3

	1 yd^3	=	0.7646 m^3
	1 yd^3	=	7.646×10^5 cm^3
Force:	1 lb	=	4.448 N
	1 lb	=	4.448×10^{-3} kN
	1 lb	=	0.4536 kgf
	1 kip	=	4.448 kN
	1 U.S. ton	=	8.896 kN
	1 lb	=	0.4536×10^{-3} metric ton
	1 lb/ft	=	14.593 N/m
Stress, Pressure, Modulus of			
Elasticity:	1 lb/ft^2	=	47.88 Pa
	1 lb/ft^2	=	0.04788 kPa
	1 U.S. ton/ft^2	=	95.76 kPa
	1 kip/ft^2	=	47.88 kPa
	1 lb/in^2	=	6.895 kPa
Density:	1 $slug/ft^3$	=	16.018 kg/m^3
Unit Weight:	1 lbf/ft^3	=	0.1572 kN/m^3
	1 lbf/in^3	=	271.43 kN/m^3
Moment:	1 lb-ft	=	1.3558 N • m
	1 lb-in.	=	0.11298 N • m
Temperature:	1° F	=	use 5/9 (°F –32) to obtain °C

General Note:	1 mil	=	10^{-3} in.

F.3 CONVERSION FACTORS FROM THE LE SYSTÈME INTERNATIONAL d'UNITÉS (SI UNITS) TO INCH-POUND UNITS (I-P UNITS)

Length:	1 m	=	3.281 ft
	1 cm	=	3.281×10^{-2} ft
	1 mm	=	3.281×10^{-3} ft
	1 m	=	39.37 in.
	1 cm	=	0.3937 in.
	1 mm	=	0.03937 in.
	1 m	=	1.094 yd
	1 cm	=	0.01094 yd
	1 mm	=	1.094×10^{-3} yd
	1 km	=	0.621 mi
Area:	1 m^2	=	10.764 ft^2
	1 cm^2	=	10.764×10^{-4} ft^2
	1 mm^2	=	10.764×10^{-6} ft^2
	1 m^2	=	1550 in^2
	1 cm^2	=	0.155 in^2
	1 mm^2	=	0.155×10^{-2} in^2
	1 m^2	=	1.196 yd^2
	1 cm^2	=	1.196×10^{-4} yd^2
	1 mm^2	=	1.196×10^{-6} yd^2
Volume:	1 m^3	=	35.32 ft^3
	1 cm^3	=	35.32×10^{-4} ft^3
	1 m^3	=	61,023.4 in^3
	1 cm^3	=	0.061023 in^3

	1 m^3	=	1.308 yd^3
	1 cm^3	=	1.308×10^{-6} yd^3
Force:	1 N	=	0.2248 lb
	1 kN	=	224.8 lb
	1 kgf	=	2.2046 lb
	1 kN	=	0.2248 kip
	1 kN	=	0.1124 U.S. ton
	1 metric ton	=	2204.6 lb
	1 N/m	=	0.0685 lb/ft
Stress, Pressure, Modulus of Elasticity:			
	1 Pa	=	20.885×10^{-3} lb/ft^2
	1 kPa	=	20.885 lb/ft^2
	1 kPa	=	0.01044 U.S. ton/ft^2
	1 kPa	=	20.885×10^{-3} kip/ft^2
	1 kPa	=	0.145 lb/in^2
Density:	1 kg/m^3	=	0.0624 $slugs/ft^3$
Unit Weight:	1 kN/m^3	=	6.361 lbf/ft^3
	1 kN/m^3	=	0.003682 lbf/in^3
Moment:	1 N • m	=	0.7375 lb-ft
	1 N • m	=	8.851 lb-in.
Temperature:	1° C	=	use $9/5$ (°C) + 32 to obtain °F

General Note: 1 Pa = 1 N/m^2